UNIVERSITY OF LONDON THESIS

Degree phD Year 2007 Name of Author MARCUS ANTONIO WALTERS

SYNTHESIS OF A83586C/CITROPEPTIN HYBRID AND SYNTHETIC STUDIES TOWARD AZINOTHRICIN

By

MARCUS WALTERS

A thesis presented to the University of London in fulfilment of the requirements of the degree of Doctor of Philosophy

The Christopher Ingold Laboratories
Department of Chemistry
University College London

ProQuest LLC
789 East Eisenhower Parkway
P.O. Box 1346
Ann Arbor, MI 48106-1346

ABSTRACT

The Azinothricin family of cyclodepsipeptides are a class of antitumour antibiotics whose antitumour properties are attributed to their ability to selectively repress the expression of genes essential for the progression of the cell cycle from G1 to S phase. They have been shown to inhibit E2F transcription factors, which are critical regulators of mammalian cellular proliferation. This biological observation has made them a potentially important new therapeutic target for the control of proliferative diseases, such as cancer.

An asymmetric total synthesis of an A83586C-citropeptin hybrid is presented in this thesis, along with a synthetic route to the azinothricin cyclodepsipeptide. The A83586C-citropeptin hybrid will serve as a useful intracellular probe that will provide valuable insights into the mechanism of the antitumour action of this class, which may contribute to a greater understanding of cancer biology. The cyclodepsipeptide components of these molecules have been assembled *via* a [2+2+2]-fragment condensation strategy and a HATU-mediated macrolactamisation. In the case of the A83586C-citropeptin hybrid, a chemoselective coupling was performed between the fully elaborated N-hydroxybenzotriazole activated ester and the citropeptin cyclodepsipeptide. The approach is summarised below:

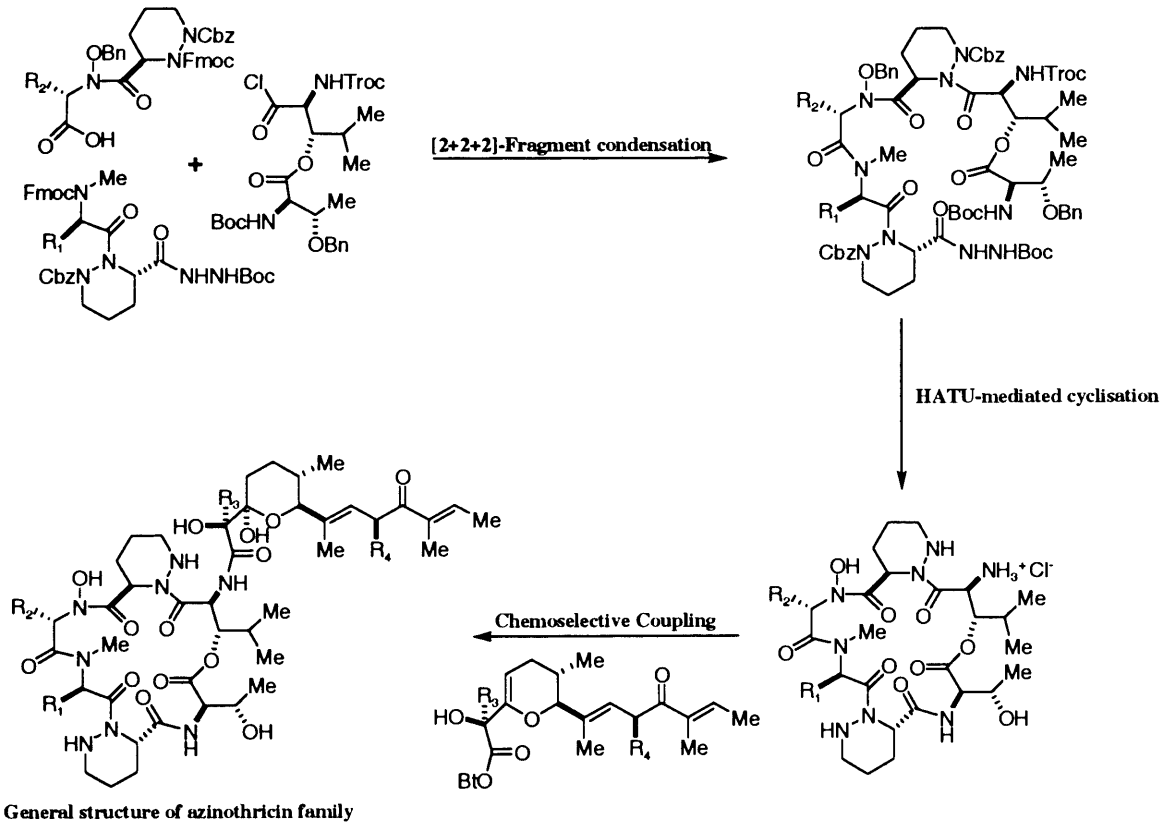

General structure of azinothricin family

'Nothing in life is to be feared, it is only to be understood'

ACKNOWLEDGEMENTS

Primarily I would like to express my sincere gratitude to Professor Karl Hale for his invaluable assistance and enthusiasm throughout the duration of my PhD; his eagerness to explain problems, and his willingness to accommodate you in his busy schedule will not be forgotten.

I would also like to thank a number of colleagues, both past and present, for their contributions toward a hard working, yet enjoyable, environment within the Hale group. I am especially grateful to Amandine, Guillame, Gurdeep, Gurpreet, John, Linos, Mark, Matthias, Maxine, Paschalis, Samuel, Shahid, Sven and Ying for all the good times over the past four years. I also want to give a special thanks to Dr Soraya Manaviazar for her support and maternal gestures; I thank you all.

I am entirely grateful to all the technical staff for their excellent assistance, namely Phil Hayes, Dave Knapp, Lisa Harris, Peter Mackie, John Hill and the late John Hughes. I want to give a personal thank you to Dr Abil Aliev, without whom the structural analysis for many of the complex molecules here within would have been virtually impossible.

Finally I am indebted to my family for their love, encouragement and support throughout my life. Upon the completion of this thesis Dad, poor health will prevent you from appreciating it, but I want to thank you for all your efforts throughout my life. I want to thank my grandmother and late grandfather for their love and support, without which, a higher education would have been impossible. To my little sister, Emma, your birth meant so much to me and I know times are currently hard for you, but I will always be there darling. My greatest thanks are to my mother; you have been an inspiration to me in so many ways, more than you will ever know. Your determination to persevere and succeed in the face of severe affliction has instilled a sense of determination within me, and has provided me with the motivation to successfully complete this work. You are always there when I need you and I dedicate this work to you.

ABBREVIATIONS

Chemistry

Alloc	allyloxycarbonyl
aq.	aqueous
Boc	*tert*-butyloxycarbonyl
Boc_2O	di-*tert*-butyl dicarbonate
BOP	benzotriazol-1-yloxy-tris(dimethylamino)-phosphonium hexafluorophosphate
BOP-Cl	bis(2-oxo-3-oxazolidinyl) phosphonic chloride
9-BBN	9-borobicyclo[3.3.1]nonane
Cbz	benzyloxycarbonyl
COSY	correlated spectroscopy
CSA	chlorosulfonic acid
DBAD	di-*tert*-butylazodicarboxylate
DBU	diazobicycloundecane
DCC	1,3-dicyclohexylcarbodiimide
DDQ	2,3-dichloro-5,6-dicyano-1,4-benzoquinone
DEC	diethyl carbonate
DEPT	distortionate enhancement of polarisation transfer
DET	diethyl tartrate
DIBAL or DIBAL-H	diisobutylaluminium hydride
DMAP	4-(dimethylamino)pyridine
DMDO	dimethyldioxirane
DMF	*N*,*N*-dimethylformamide
DMPU	1,3-dimethyl-3,4,5,6-tetrahydro-2[1H]-pyrimidinone
DMSO	dimethyl sulfoxide
DPPA	diphenylphosphoryl azide
EDCI	1-ethyl-3-(3-dimethylaminopropyl)carbodiimide
FAB HRMS	fast atom bombardment high resolution mass spectrometry
Fmoc	(9*H*-fluoren-9-ylmethoxy)carbonyl
Gly	glycine
HATU	*O*-(7-azabenzotriazol-1-yl)-*N*,*N*,*N*',*N*-tetramethyluronium hexafluorophosphate
HMBC	heteronuclear multiple-bond correlation
HMPA	hexamethyl phosporamide
HMQC	heteronuclear multiple-quantum coherence
HOBt	1-hydroxybenzotriazole
IR	Infra red spectroscopy

KHMDS	potassium hexamethyldisilasane
LDA	lithium diisopropylamide
MS	molecular sieves
NaHMDS	sodium hexamethyldisilasane
NBS	*N*-bromosuccinimide
NEM	*N*-ethyl morpholine
NMO	*N*-Methylmorpholine-*N*-oxide
NMR	nuclear magnetic resonance
NOESY	nuclear Overhauser effect spectroscopy
Oxone	potassium monopersulfate
PDC	pyridinium dichromate
PMB	4-methoxybenzyl
ppts	pyridinium *p*-toluene sulfonate
REDAL	sodium bis(2-methoxyethoxy)aluminium hydride
RT	room temperature
Sar	sarcosine
SO_3.Py	sulfur trioxide pyridine complex
TBAF	*tert*-butyl ammonium fluoride
TBDPS	*tert*-butyl diphenyl silyl (or diphenyl tertiary butyl silyl)
TBHP	*tert*-butyl hydroperoxide
TBS	*tert*-butyl dimethyl silyl
TFA	trifluoroacetic acid
THF	tetrahydrofuran
TLC	thin layer chromatography
Troc	trichloro-ethoxycarbonyl
TsOH	4-methyl benzenesulfonic acid

Biology

BALB	Bagg Albino – developed by H.J Bagg.
CDF_1 mice	a cross between female BALB/c x male DBA/2
CDKs	cyclin dependent kinases (a protein kinase involved in regulation of the cell cycle)
CDKIs	cyclin dependent kinase inhibitors (negatively regulate CDKs)
DNA	deoxyribonucleic acid
HCT116	human colon carcinoma cell lines (wild type p53 and p21)
HT29	human colonic adenocarcinoma cell lines
IC_{50}	median inhibition concentration (concentration that reduces the effect by 50%)

MIC	minimum inhibitory concentration (the lowest concentration of antibiotic, which inhibits the growth of the bacterium)
MTS	3-(4,5-dimethylthiazol-2-yl)-5-(3-carboxymethoxyphenyl)-2- (4-sulfophenyl)-2H-tetrazolium (used in assays with PMS)
Opn	osteopontin
PMS	phenazine methosulfate (used in assays with MTS)
RKO	colorectal cancer cell line that expresses wild-type p53
TCF4	transcription factor 4
T/C ratios	find efficacy of drugs by finding the ratio of tumour size in treated group to that of the control group (tumour size treated gp/tumour size control gp).
Wnt	the wnt signalling pathway is a network of proteins that has been implicated in embryogenesis and cancer. Wnt is a gene in the extensively studied Drosophila melanogaster, which, on damage, leads to a wingless phenotype.

TABLE OF CONTENTS

Page No

Chapter 1: THE AZINOTHRICIN FAMILY OF ANTITUMOUR ANTIBIOTICS AND RELATED MOLECULES

One of the great mysteries of cell biology remains the mechanism of information transfer, or signalling, within the cytoplasm and nucleus of the cell. Natural products that modulate these processes frequently offer unique insights into fundamental aspects of cell signal transduction and the means by which extracellular molecules influence intracellular events. The recent completion of the Human-Genome project has provided an outline map for further expeditions toward us gaining a complete understanding of how cellular processes operate at the molecular level.

Cancer is a major public health burden both in the United Kingdom and in other developed countries. Currently, one in three people will be diagnosed with cancer during their lifetime, and more than 270,000 new cases of cancer were registered in the UK in 2001.[1] Cancer still remains a partially understood affliction even today. A greater understanding of the biology surrounding this disease will undoubtedly allow the development of more suitable therapeutics in the future.

Natural product chemistry has long played an important role in the elucidation of biological mechanisms, and certain natural products have been uniquely suited for studying the mysterious workings of the cell; including cytoplasmic signal transduction, due to their interference with these processes. Cyclodepsipeptides, together with natural cyclic peptides, have been two classes of natural product that have proven especially useful in this regard. Cyclodepsipeptides are cyclic peptides that contain at least one ester linkage.[2] The diverse range of biological activities that they exhibit, their intriguing mechanisms of action, and their unusual chemical architectures have engendered considerable interest in this class of natural product in recent years. Many such molecules demonstrate antitumour, anti-inflammatory, antifungal, and immunosuppressant activities, and represent useful tools for research into the biological processes involved in cellular regulation.

The azinothricin family of antibiotics are characterised by a 19-membered cyclodepsipeptide core comprised of six amino acid units attached to a pyran hemiketal side chain. Their macrocyclic domains and complex side chains represent an enticing synthetic endeavour in their own right. However, in addition to this, their powerful antitumour properties and postulated mechanism of action make them synthetic targets of even greater distinction. The azinothricin family of antibiotics have been suggested to shut down the continually activated E2F/Rb pathway in many types of cancer cell. E2F transcription factors regulate the expression of a number of key genes that are essential for cell proliferation. The activity of these transcription factors is regulated through an association with the

retinoblastoma tumour suppresser protein (Rb) and other pocket proteins. Direct links are now being made between the loss of normal E2F-dependent transcriptional control and the development of cancer.[3] This finding therefore provides us with interesting targets for total synthesis; the advent of which could potentially expedite the future assembly of novel analogues of these biologically fascinating molecules.

1.1 ISOLATION AND STRUCTURE ELUCIDATION OF THE AZINOTHRICIN FAMILY OF ANTIBIOTICS

1.1.1 CORE FAMILY MEMBERS

The potent *in vitro* antibacterial activity of the culture filtrates from *Streptomyces* sp. X-14950 against Gram-positive bacteria attracted the attention of Hubert Maehr and co-workers at Hoffmann-La Roche in New Jersey in 1985. The active principle was isolated in crystalline form and identified as a novel cyclohexadepsipeptide antibiotic, designated azinothricin (**1**).[4] The chemical architecture of **1** was found to consist of a 19-membered cyclodepsipeptide ring, containing a single ester linkage, connected to hemiketal side chain. The cyclodepsipeptide core incorporated six amino acid units; *(2S,3S)*-3-hydroxyleucine, D-threonine, *N*-methyl-D-alanine, both L- and D-piperazic acids and *N*-hydroxy-*O*-methyl-L-serine (**Fig. 1**).

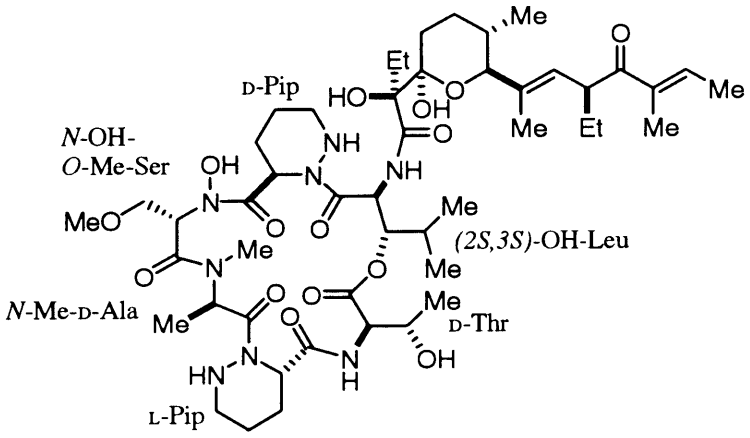

Azinothricin 1

Fig 1. Structure of azinothricin highlighting key structural components

It was observed that the *(2S,3S)*-3-hydroxyleucine moiety provided the ring-oxygen of the 19-membered lactone, as well as the amino group of the amide bond that connected the hemiketal side chain. The name given to the new antibiotic reflected the presence of the hydrazino groups of the piperazic acid moieties, which invite a comparison with the monamycin family of antibiotics.[5]

The structure of azinothricin was elucidated using a variety of NMR techniques (proton, carbon and dept), fast atom bombardment (FAB) mass spectrometry and X-ray crystallography.[4,6] The absolute configuration of azinothricin was based on the determination of the L-configuration of (2*S*,3*S*)-3-hydroxyleucine, following acid hydrolysis of the natural product; (2*S*,3*S*)-3-hydroxyleucine is a known constituent of the antibiotic telomycin.[7,8] The specific rotation of azinothricin was recorded as $[\alpha]_D$ + 117.65º (c 0.6, $CHCl_3$).

The next family member to be discovered was A83586C (**2**) by Tim Smitka and co-workers, at the Eli Lilly research laboratories in Indiana USA in 1998. It was isolated from fermentation broths of the Guam soil microorganism *Streptomyces karnatakensis*. This antibiotic also displayed potent Gram-positive activity, and X-ray crystallographic analysis showed that its structure closely resembled that of azinothricin (**Fig. 2**).[9] The absolute stereochemistry of A83586C was shown to be identical to that of azinothricin through the detection of D-threonine in the acid hydrolysate. The specific rotation of A83586C was very similar to that of azinothricin and was recorded as $[\alpha]_D$ +116.1º (c 0.2, $CHCl_3$). The structural analysis revealed that A83586C differs from azinothricin only in the presence of an *N*-hydroxy-L-alanine instead of the *N*-hydroxy-*O*-methyl-L-serine, and it having a methyl instead of an ethyl group at C(37)/C(38).

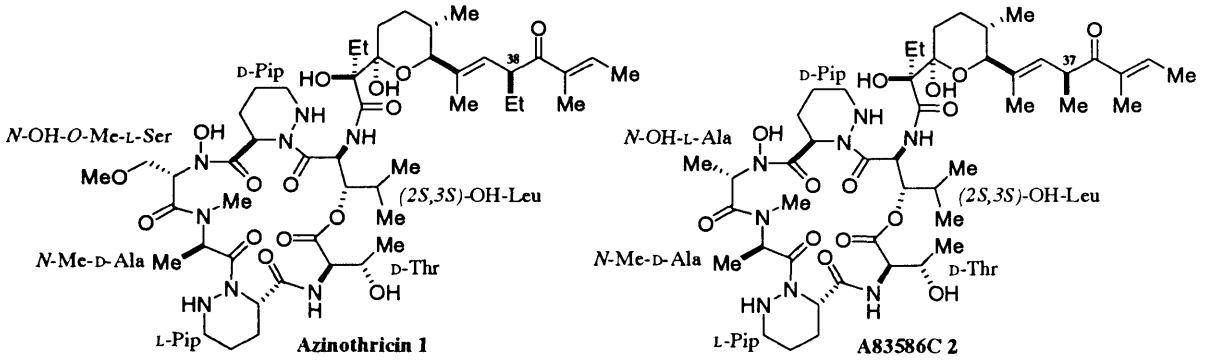

Fig 2. Structural comparisons of Azinothricin **1** and A83586C **2**.

Negative traits of these two antibiotics were that they demonstrated a high toxicity *in vivo* when administered at quite high drug concentrations (9.3 mg/kg/day). This factor prevented their clinical development as antibiotics and initially discouraged synthetic interest in members of this class.

The discovery of citropeptin **3**[10] in 1990 soon changed this situation, in arousing new interest in the azinothricin family of antibiotics. It was isolated from a soil sample collected in Brazil that was identified as a strain of *Streptomyces flavidovirens*, by Nakagawa and co-workers at the Kirin Brewery Co. Ltd in Tokyo. Citropeptin was shown to confer a 120% life extension on mice with P388 lymphocytic leukaemia when administered at the *non-lethal*

dosage of 2mg/kg/day. The structure of citropeptin was elucidated by NMR spectral analysis (^1H and ^{13}C) including a variety of 2D techniques (COSY, NOESY and HMBC).[10,11] Unfortunately however, the absolute stereochemistry of citropeptin was never determined, but it is presumed to be identical to that of azinothricin and A83586C due to its similar specific rotation ($[\alpha]_D$ +113º (c 0.5, $CHCl_3$)) and ^{13}C chemical shifts.[11] Like the previous two family members, citropeptin incorporates *(2S,3S)*-3-hydroxyleucine, D-threonine and L- and D-piperazic acid moieties in its cyclodepsipeptide skeleton (**Fig.3**). It differs from azinothricin slightly more than A83586C due to it having an *N*-methyl-D-leucine instead of an *N*-methyl-D-alanine, and it having a methyl instead of an ethyl group at both its C(33) and C(41) centres.

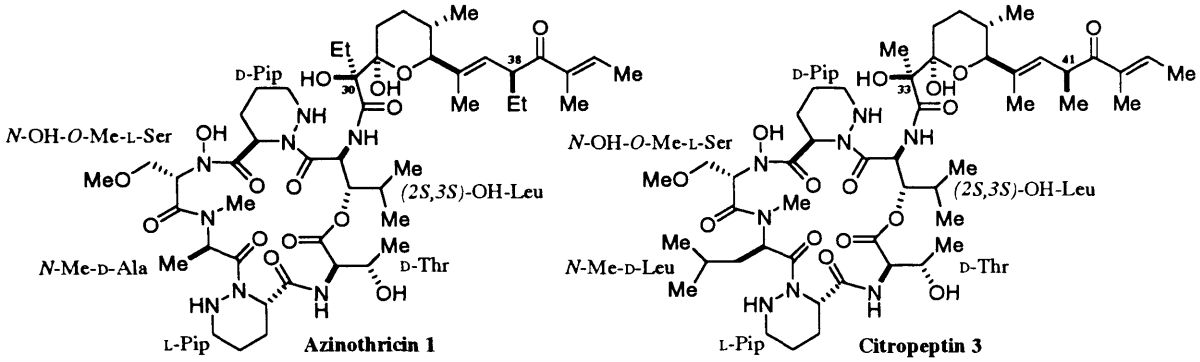

Fig 3. Structural comparisons of Azinothricin **1** and Citropeptin **3**.

The final and possibly most interesting core member of the azinothricin family was isolated from culture broths of *Streptomyces* sp. GE3 in 1997. This microorganism was obtained from a soil sample collected in the Shimane prefecture of Japan, and was found to produce a novel compound designated GE3[12] (**4**). GE3 displays potent cytotoxicity against a variety of human and mouse tumour cell lines with IC_{50} values ranging from 6 to 16 nM, and could reduce tumour size by 53%. A linear peptide was also isolated in addition to GE3 and was designated as GE3B, which was also biologically tested. GE3B showed no antimicrobial activity or cytotoxicity, suggesting that the cyclic structure was necessary for both activities of GE3. The structure of GE3 was elucidated using a wide range of 2D-NMR techniques. This led to a facile assignment of almost all the proton and carbon signals except the amide proton signal of the alanine unit.[13] GE3 was again shown to incorporate the now characteristic *(2S,3S)*-3-hydroxyleucine, D-threonine and L- and D-piperazic acid moieties into its cyclodepsipeptide skeleton (**Fig. 4**). However this molecule was structurally less comparable to azinothricin than its antecedent members. The cyclodepsipeptide core of GE3 represented a hybridized framework of A83586C and citropeptin incorporating a *N*-hydroxy-L-alanine and *N*-methyl-D-leucine into its skeleton as opposed to the *N*-hydroxy-*O*-methyl-L-serine and *N*-methyl-D-alanine units of azinothricin. The hemiketal side chain however, was identical to that of citropeptin in its possession of methyl groups at the C(32) and C(40) centres instead of the ethyl groups characteristic of azinothricin. The stereochemistry including the absolute configuration of GE3 was again assigned by

comparison with the founder members based upon similar specific rotation ($[\alpha]_D$ +111.5 º, c 0.08, $CHCl_3$) and ^{13}C chemical shifts.

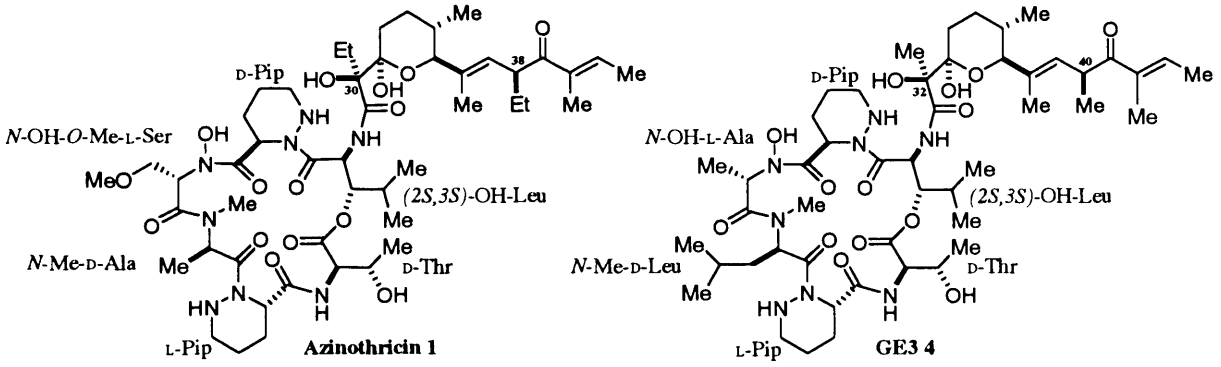

Fig 4. Structural comparisons of Azinothricin **1** and GE3 **4**.

1.1.2 STRUCTURALLY RELATED FAMILY MEMBERS

There are other structurally related molecules that have been isolated that vary more greatly in structure than their aforementioned counterparts but which are still related to this antibiotic class. Of this affiliated group, the molecule that bears the closest resemblance to azinothricin is L-156,602 (**5**). This molecule was extracted from cultures of *Streptomyces* MA-6348 that were isolated from a plant rhizosphere soil sample obtained from a Japanese garden.[14] The structure of L-156,602, including the absolute stereochemistry, was elucidated using a variety of 2D-NMR techniques and X-ray crystallography. The NMR evidence indicated that L-156,602 had a structure analogous to previous azinothricin family members but significant differences were noted (**Fig. 5**). Again the characteristic 19-membered cyclodepsipeptide skeleton was present containing both *(2S,3S)*-3-hydroxyleucine and the L- and D-piperazic acid moieties. However the D-threonine, *N*-methyl-D-alanine and *N*-hydroxy-*O*-methyl-L-serine residues of azinothricin were now all replaced by an *N*-hydroxy-D-alanine, a glycine and an *N*-hydroxy-L-alanine respectively. The C(26) quaternary centre of L-156,602 was also reminiscent of citropeptin (C(33)) and GE3 (C(32)), where a methyl group replaced the ethyl group common to azinothricin and A83586C. In addition to this, the hemiketal side chain of L-156,602 was considerably simplified. Notably an alkyl side chain at C(30) replaced the methyl substituent common to all previous family members and a methyl group conspicuously replaced the acyl side chain that was conjugated to the hemiketal ring (at C(31)). Despite these differences, the corresponding asymmetric centres of all these compounds had identical absolute stereochemistries.[14]

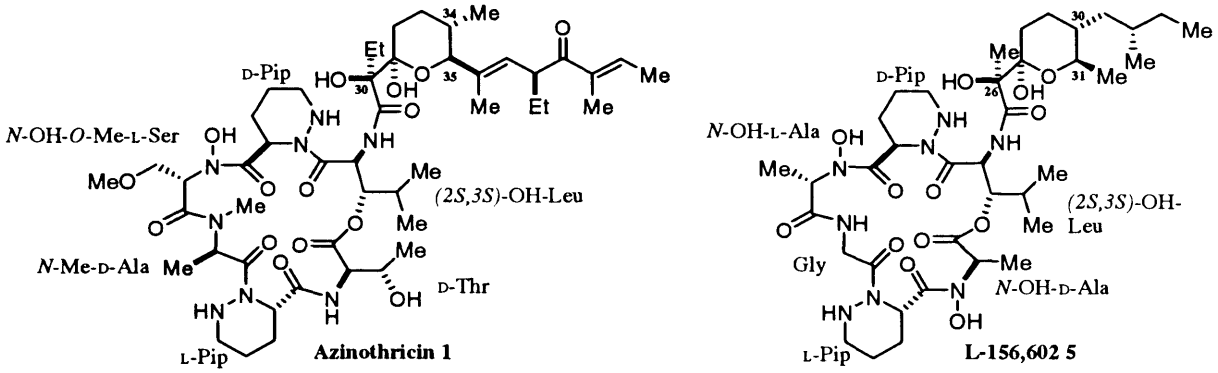

Fig 5. Structural comparisons of Azinothricin **1** and L-156,602 **5**.

The next molecule to be discovered having a close structural affinity with azinothricin and L-156,602 was variapeptin (**6**).[15] It was isolated from culture K2919, a strain of *Streptomyces variabilis*, obtained from a soil sample collected in Bosque, Brazil. Similar structure elucidation techniques were employed to those used for citropeptin,[11] and it was discovered that variapeptin was a novel cyclodepsipeptide related to azinothricin/L-156,602. Again variapeptin incorporated the three signature amino acid units of the azinothricin family within its cyclodepsipeptide core; namely, *(2S,3S)*-3-hydroxyleucine and the D- and L-piperazic acid moieties (**Fig. 6**). By way of contrast however, in variapeptin the D-threonine, *N*-methyl-D-alanine and *N*-hydroxy-*O*-methyl-L-serine residues of azinothricin are all replaced respectively with D-serine, *N*-methyl-D-phenylalanine and *N*-hydroxy-L-alanine units. Again the hemiketal side chain of variapeptin was very different to that of azinothricin; however it seems to be identical to that of L-156,602, it having the same distinguishing features. The absolute stereochemistry of variapeptin is again unknown but is presumed to be identical to that of azinothricin and L-156,602 due to similar specific rotations ($[\alpha]_D$ +128 º, c 0.5, MeOH) and ^{13}C chemical shifts.

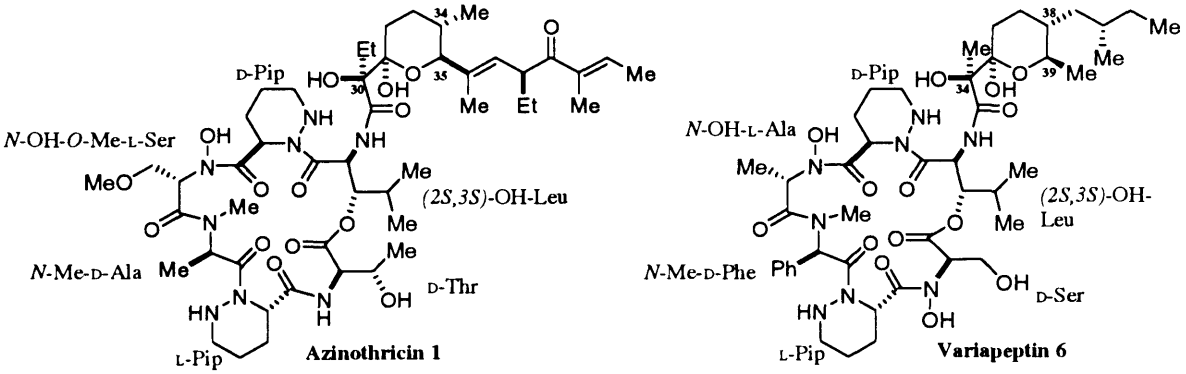

Fig 6. Structural comparisons of Azinothricin **1** and Variapeptin **6**.

The final member of this sub-group that was isolated in 1993 was verucopeptin (**7**). It was obtained from fermentation broths of *Actinomadura verrucosospora* Q886-2 collected

from a soil sample originating from Batangas in the Philippines.[16] The majority of research on this antibiotic was carried out by Koko Sugawara and co-workers at the Bristol-Myers Squibb Research Institute in Tokyo, Japan.[17,18] The structure of verucopeptin was elucidated by a wide variety of spectroscopic and chemical degradation experiments,[18] and was shown to be structurally related to the azinothricin family (**Fig. 7**). Despite rigorous efforts, the relative and absolute stereochemistry of verucopeptin remains undetermined, and as a consequence, a variety of diastereomeric possibilities exist. Verucopeptin exhibits the greatest simplicity with respect to its cyclodepsipeptide core although its hemiketal side chain is actually more complex than other azinothricin family members. Again a 19-membered cyclodepsipeptide is present, with the *(2S,3S)*-3-hydroxyleucine/D-piperazic motif common to all family members. However, the L-piperazic acid moiety was replaced with a glycine unit and a *N*-hydroxyglycine and two sarcosine (*N*-methylglycine) units replaced the D-threonine, *N*-methyl-D-alanine and *N*-hydroxy-*O*-methyl-L-serine residues of azinothricin. It has an identical quaternary centre to that of GE3 and citropeptin, which occurs at C(23) in this molecule. If we observe the hemiketal side chain of verucopeptin, we can see that the methyl substituent common to all core members is replaced by an *O*-methoxy (C(27)) and the acyl side chain (C(28)) is extended by two carbons in length and is missing the α,β-unsaturated ketone.

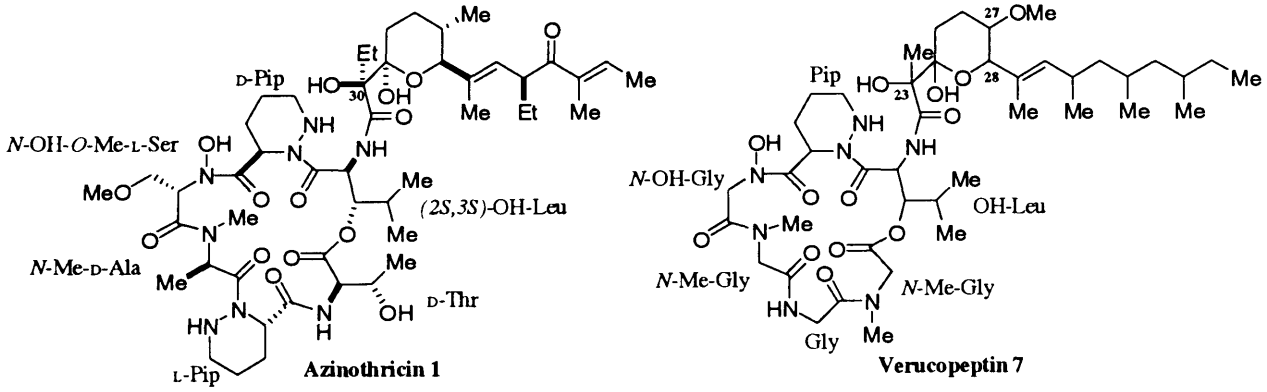

Fig 7. Structural comparisons of Azinothricin **[1]** and Verucopeptin **[7]**.

1.1.3 OTHER MEMBERS OF THE L-156,602 CLASS

During the course of a screening programme for new ionophoric compounds,[19] *Streptomyces aurantiacus* IMET 43917 was found to produce potent antibacterial antibiotics displaying high activity against *Bacillus subtilis* ATCC 663 and cytotoxic effects against L-929 fibroblast cells.[20] After structure elucidation[20] it was discovered that these compounds consisted of a 19-membered hexadepsipeptide ring with a hemiketal side chain and were structurally related to the azinothricin family of antibiotics. This new family of antibiotics were collectively named the aurantimycins **8(a)**, **(b)** and **(c)** and their structures are outlined below (**Fig.8**.)

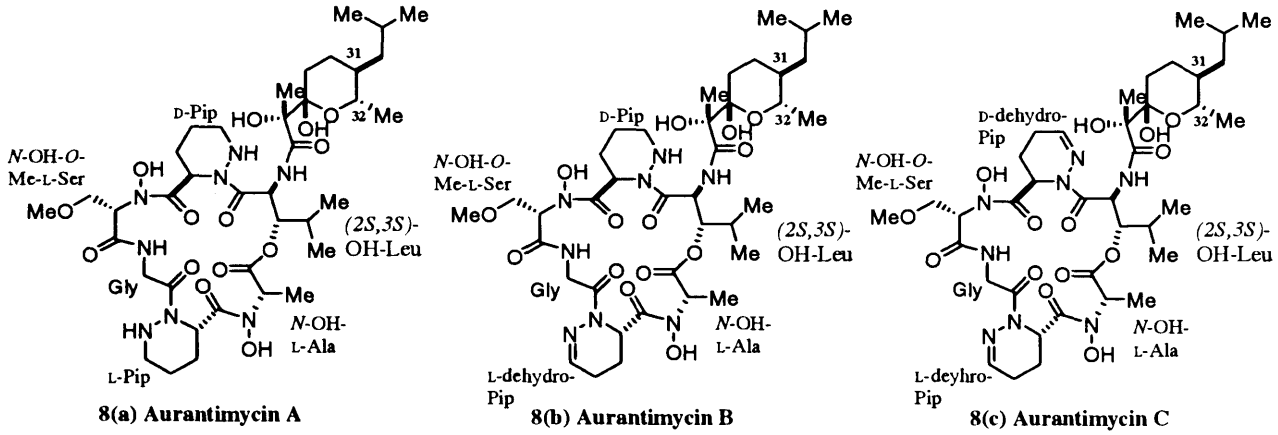

Fig 8. Structures of the Aurantimycin family

Again we can identify the characteristic 19-membered cyclodepsipeptide in these new molecules. However only aurantimycin A incorporates both the D- and L-piperazic acid moieties familiar to the azinothricin family. Aurantimycins B and C contained one and two dehydropiperazic acid moieties respectively. When compared with the azinothricin family members discussed in the previous subsection, the aurantimycins show significant differences in their hemiketal side chain. Within the aurantimycin family, the tetrahydropyranyl derivative 2-hydroxy-2-(2-hydroxy-5-isobutyryl-6-methyl-tetrahydropyran-2-yl)-propionic acid has inverted stereochemistry at its C(31) and C(32) stereocentres.

The penultimate molecule discussed in this section is that of the apoptosis-inducing agent Polyoxypeptin A (**9**).[21,22] The latter is a structurally novel cyclodepsipeptide metabolite that was isolated from culture broths of the *Streptomyces* species MK498-98F by Umezawa and co-workers at Keio University in Japan. Polyoxypeptin A was observed to induce programmed cell death in an apoptosis-resistant human pancreatic adenocarcinoma cell line (AsPC-1 cells) at the low drug concentration of 0.1 μg/mL.[23] Following structure elucidation[24] it was determined that **9** consisted of a novel 19-membered cyclodepsipeptide core and hemiketal side chain that had similarities to the azinothricin family (**Fig. 9**). The cyclodepsipeptide core was found to be comprised of six amino acid units, only three of which were common to the azinothricin family, namely *(2S,3S)*-3-hydroxyleucine, *N*-hydroxy-L-alanine and D-piperazic acid. The other three amino acids however, were anomalous; they were *N*-hydroxy-L-valine, the unique (2*S*,3*R*)-3-hydroxy-3-methylproline and 5-hydroxy-D-piperazic acid. The hemiketal side chain of **9** resembled that of L-156,602 and variapeptin; however, the only difference is the presence of an ethyl substituent compared to a methyl substituent at the C(37) stereocentre (methyl substituent at C(31) and C(39) centres of L-156,602 and variapeptin respectively).

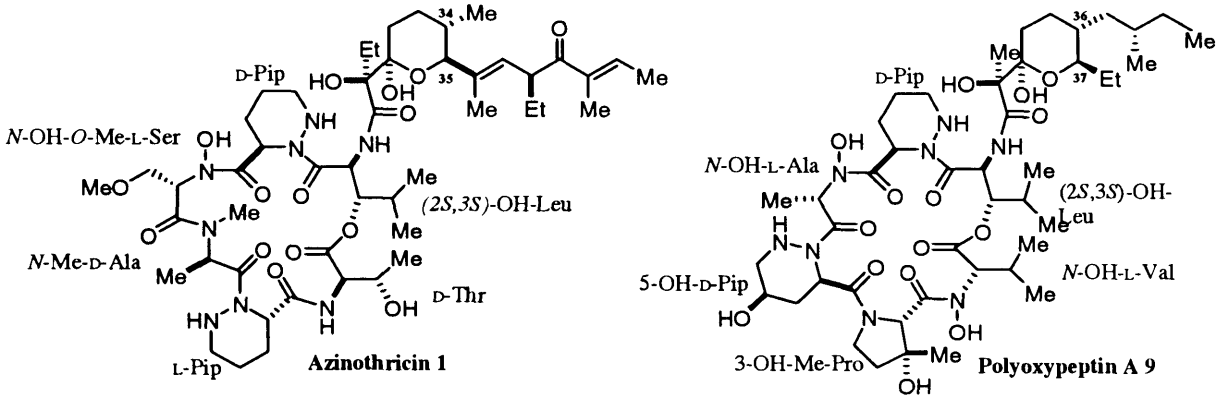

Fig 9. Structural comparisons of Azinothricin **1** and Polyoxypeptin A **9**.

The most recent discovery of an azinothricin related cyclodepsipeptide came with the isolation and characterisation of pipalamycin **10** in 2001.[25] Kazuo Umezawa and co-workers isolated this novel apoptosis-inducing cyclodepsipeptide from a culture filtrate of *Streptomyces* sp. ML297-90F8, during the course of their screening for apoptosis inducers in 2001. Following structure elucidation, using 2D NMR techniques and high-resolution mass spectrometry, it was established that pipalamycin was a member of the azinothricin family. It possessed a 19-membered cyclodepsipeptide that incorporated the characteristic 3-hydroxyleucine and piperazic acid moieties (**Fig. 10**). However the *N*-hydroxy-*O*-methyl-L-serine, *N*-methyl-D-alanine and D-threonine of the azinothricin core are substituted respectively by *N*-hydroxy alanine, glycine and alanine in pipalamycin. The hemiketal side chain of **10** is distinctly different to the core azinothricin family members, but reminiscent of the aurantimycins and polyoxypeptin. In terms of substituents, the C(26) and C(27) centres of pipalamycin are similar to the C(32)/(33) of polyoxypeptin and C(27)/(28) of the aurantimycins. Likewise the C(31) alkyl chain of pipalamycin is identical to the C(37) of polyoxypeptin, and the C(30) alkyl chain is reminiscent of the C(31) chain of the aurantimycins, it possessing the geminal methyl group; however, it does incorporate an extra carbon atom. At present **10** remains stereochemically undefined, hence the generic description of its amino acid subunits. Nevertheless, it is reasonable to assume that the piperazic acid and hydroxyleucine moieties have identical stereochemical configurations to those of the azinothricin family.

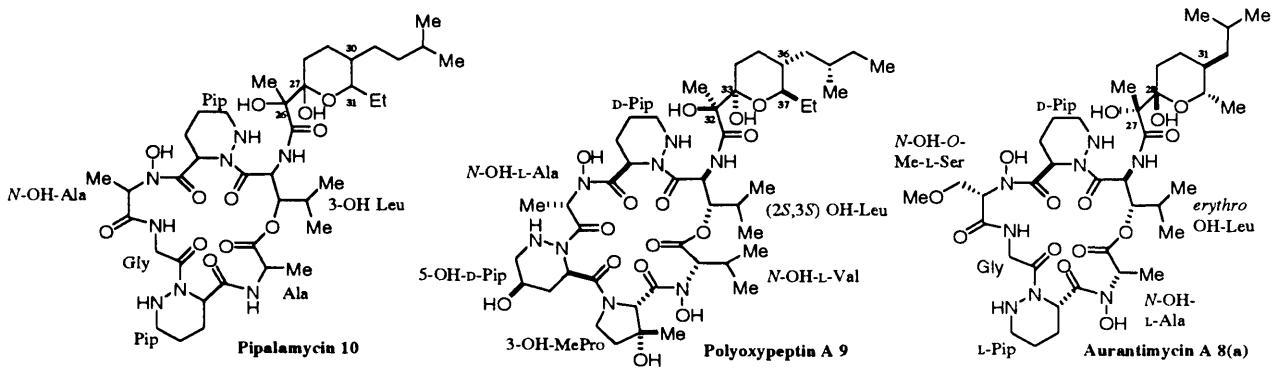

Fig 10. Structural comparisons of Pipalamycin **10**, Polyoxypeptin A **9** and Aurantimycin A **8(a)**.

It was shown that pipalamycin induced cell-death in AsPC-1 cells, *in vitro* at 0.3 μg/mL, and that it inhibited the proliferation of AsPC-1 cells after 3 days with an IC_{50} of 0.03 μg/mL. It also displayed antibacterial activity against Gram-positive bacteria with MIC values that ranged from 0.1 to 0.2 μg/mL.

1.2 DETAILED DISCUSSION OF THE BIOLOGICAL ACTIVITIES OF THE AZINOTHRICIN FAMILY OF ANTIBIOTICS

As already mentioned briefly, the azinothricin family of antibiotics all exhibit interesting antibacterial and antitumour properties; however, their high toxicity prevented their clinical development as antibacterial drugs. Both azinothricin and A83586C demonstrate potent Gram-positive activity *in vitro* and both display minimal activity against Gram-negative bacteria.[4,9] Azinothricin exhibited MIC values that ranged from 0.008 μg/mL to 0.063 μg/mL. A83586C had values in the range of 0.008 μg/mL to 0.006 μg/mL. A83586C also exhibited an IC_{50} of 0.0135 μg/mL against a human T-cell leukaemia line (CCRF-CEM cells).

Citropeptin was extremely cytotoxic against murine P388 leukaemia and B16 melanoma cells, with IC_{50} values of 0.02 μg/mL and 0.1 μg/mL respectively. When CDF_1 mice were inoculated with P388 leukaemia cells and treated intraperitoneally with citropeptin, administered at doses of 2 mg/kg/day, their survival periods were prolonged by 123% (T/C ratio = 123%). However when administered at doses of 4 mg/kg/day, citropeptin was shown to cause death by toxicity.[10]

GE3 has weak antibacterial effects, but has potent antitumour activity against human tumours both *in vivo* and *in vitro*. In this regard GE3 showed weak antibacterial activity against both Gram-positive and Gram-negative bacteria with MIC values that ranged from

10.4 μg/mL to 41.6 μg/mL.[12] It also demonstrated potent cytotoxicity against a range of human tumour cell lines (see Table below).

Human Tumour Cell Line	IC_{50} (nM)
HeLa S3 Cells	6
A431 Cells	16
Saos-2 Cells	3.6
Balb/3T3 Cells	7

Table 1. *In vitro* cytotoxicity of GE3

The *in vivo* antitumour effect of GE3, against a human tumour, was examined using a human xenograft mouse tumour model. When administered by a single intraperitoneal injection, GE3 showed significant antitumour activity against the PSN-1 human pancreatic carcinoma (T/C 0.47 – 53% reduction in tumour size) at a dose of 2 mg/kg. GE3 was active only when administered by single intraperitoneal injection and was inactive by consecutive injections.

Variapeptin displayed similar biological traits to azinothricin and A83586C in demonstrating very potent activity *in vitro* against Gram-positive bacteria but no activity against Gram-negative bacteria or fungi.[15] It also demonstrated *in vitro* activity against P388 leukaemia cells with an IC_{50} value 0.01 μg/mL, however, it was shown to be inactive *in vivo*. When variapeptin was administered intraperitoneally to mice with P388 lymphocytic leukaemia it was found to be inactive at the highest non-toxic dose, and toxic at 5 mg/kg.

Verucopeptin demonstrated weak antimicrobial activity; it was only marginally active against *Streptococcus faecalis and Bacillus subtilis* (MIC – 100 μg/mL) and showed no activity against other Gram-positive, Gram negative or anaerobic bacteria and fungi. Verucopeptin was also shown to inhibit DNA and RNA synthesis with IC_{50} values of 0.26 and 0.29 μg/mL respectively. The *in vitro* cytotoxicity of verucopeptin was examined against a range of tumour cells and the results are displayed in table 2. It can be seen that verucopeptin displayed relatively specific cytotoxicity against B16-F10 cells with an IC_{50} value that was substantially more potent than those against the other cells.

Human Tumour Cell Line	IC_{50} (μg/mL)
B16-F10 (murine melanoma)	0.004
P388 (murine lymphocytic leukaemia)	0.08
Moser (human colorectal carcinoma)	0.4
HCT-116 (human colon carcinoma)	0.04

Table 2. *In vitro* cytotoxicity of verucopeptin against murine and human tumour cells

The *in vivo* antitumour activity of verucopeptin was tested in experimental mouse tumour systems. Verucopeptin was intraperitoneally administered to the mice in structured treatment schedules. It demonstrated significant therapeutic activity against B16 melanoma prolonging the survival periods of the mice by up to 162 % (T/C – 146 ~ 162 %). Interestingly the compound exhibited no significant prolongation of life span in the P388 leukaemia system.

1.3 MODE OF CYTOTOXICITY OF THE AZINOTHRICIN FAMILY OF ANTIBIOTICS

Almost all of the azinothricin family of antibiotics exhibit potent cytotoxicity. However, the mechanism of cytotoxicity was essentially unknown until the discovery of GE3 in 1997.[12] Before then little had been described regarding their modes of anticancer action, although it had initially been proposed that their anticancer properties emanated from the inhibition of DNA and RNA synthesis in cells[17] and/or the inhibition of adhesion to extra-cellular matrix.[26] The mode of action of GE3 was elucidated by analysing its effect on cell cycle progression and on the expression of the cell cycle-related gene, cyclin A. It was discovered that GE3 inhibited cyclin A gene expression without repressing β-actin gene expression and consequently inhibit the progression of the cell cycle from G1 to S phase.[12] GE3 was also shown to prevent E2F transcription factors, the intracellular target of the retinoblastoma susceptibility (pRb) gene product, from binding to their recognition sequence.[27] This suggested that GE3 along with the other members of the azinothricin family exerted their cytotoxic effects by acting as inhibitors of E2F transcription factors.

Chapter 2: THE ROLE OF E2F TRANSCRIPTION FACTORS IN CELL CYCLE CONTROL AND CANCER

2.1 CANCER BIOLOGY

Cancer is a complex disease state that is characterised by the uncontrolled growth and spread of aberrant cells that invade and disrupt other tissues. Although cancer has become increasingly prominent as a disease in modern times, it is not a modern disease. Malignant tumours were described in the pictures and writings of many ancient civilisations including those of Asia and South America, and bone cancers (osteosarcomas) were diagnosed in a number of Egyptian Mummies. Today, cancer remains as one of the major causes of death in the developed nations - at least 1 in 5 of the population of Europe and North America can expect to die of cancer. World population growth and an increase in population age imply a progressive increase in the cancer burden – 15 million new cases and 10 million new deaths are expected in 2020, even if current rates remain unchanged.[28]

There are three main approaches to treating an established cancer - *surgical excision*, *irradiation* and *chemotherapy* - and the success of each of these remedies depends upon the type of tumour and the stage of its development. Chemotherapy is the main method of treatment for only a few cancers, but it is increasingly being used as an adjunct to surgery or irradiation for many types of tumour. However, chemotherapy presents many difficulties in biochemical terms, as cancer cells and normal cells are so similar in many respects that the drug can often act upon the healthy dividing cells of a patient and it has often proven extremely difficult to find general exploitable differences between both cell populations. In the last decade however, a prodigious advance in the comprehension of cellular proliferation has led to a better understanding of the biology of the cancer cell; this, in turn, is beginning to lead to new approaches being followed for the development of novel anticancer drugs.

2.1.1 DISTINGUISHING CHARACTERISTICS OF CANCER CELLS

There are four characteristics that distinguish cancer cells from normal mammalian cells and these are outlined below:

- **Uncontrolled Proliferation** - In cancer cells the cell cycle is disrupted and the proliferation of cancer cells are not controlled by the processes that normally regulate cell division and tissue growth.

- **Dedifferentiation and loss of function** - The multiplication of normal cells involves the division of stem cells of a particular tissue to give rise to daughter cells. The latter eventually differentiate to become the mature cells of the relevant tissue and carry out their programmed function. Cancer cells lose the ability to differentiate and, in general, poorly differentiated cancers multiply faster.
- **Invasiveness** – Generally speaking normal cells are not found outside their 'designated' tissue of origin. During differentiation and the growth of tissues and organs, normal cells develop certain spatial relationships with respect to one other and these are continually maintained by various localised tissue-specific survival factors. When a cell escapes these survival signals are lost and it undergoes apoptosis (programmed cell death). Cancer cells not only lose the restraints of viability in different locations, they also have the ability to secrete enzymes capable of breaking down the extra-cellular matrix enabling the cancer cells to enter other tissue sites.
- **Metastases** - Cancer cells that have the ability to metastasise have undergone a series of genetic changes, which alter their responses to the regulatory factors that control the tissue siting of normal cells. They now have conferred upon them the ability to exist 'extraterritorially' and as a consequence are able to reach other sites through blood vessels or the lymphatic system.

A normal cell develops into a cancer cell because of multiple mutations in its DNA. The development of cancer is a complex multistage process involving multiple genetic changes. The significant point concerning cancer cells is that their proliferation is not subject to the standard regulatory processes of normal mammalian cells.

2.2 THE MAMMALIAN CELL CYCLE

In discussing the main differences between the proliferation of normal cells and those of cancer cells, one needs to consider the cell cycle of dividing cells. The cell division cycle is an evolutionarily conserved process used by all eukaryotic cells to control growth and division.[29] The regulation of the cell cycle is mainly focussed upon two critical events: **the initiation of nuclear DNA synthesis (S Phase)** and **the initiation of mitosis (M Phase)**. It is a fundamental task of the cell cycle to ensure that DNA is faithfully replicated once (S-Phase) and that identical chromosomal copies are distributed equally between two daughter cells (mitosis) during the M phase.[30] In early embryonic cell cycles, the S and M phases are the only two phases present; however, in somatic cells two gap phases exist, which are termed **G1** (gap phase 1) and **G2** (gap phase2) respectively (**Fig. 11**). In the G1-phase, the cell prepares itself for DNA synthesis and checks the integrity of the DNA prior to it entering the S-phase. During the latter the cell responds to external signals, which if they are of a stimulatory nature, allow a full transition to the S-phase. However, in the absence of these

signals, or if growth inhibitory signals are present, the cell may exit the cell cycle and remain in a state of quiescence (termed **G0**).[31] The G1-phase is the most variable of the cell cycle phases and its length is the major determinant of the cell cycle time. In G2, the duplication of the genome has been completed and the cell prepares itself for mitosis (cell splits into two daughter cells – M phase).

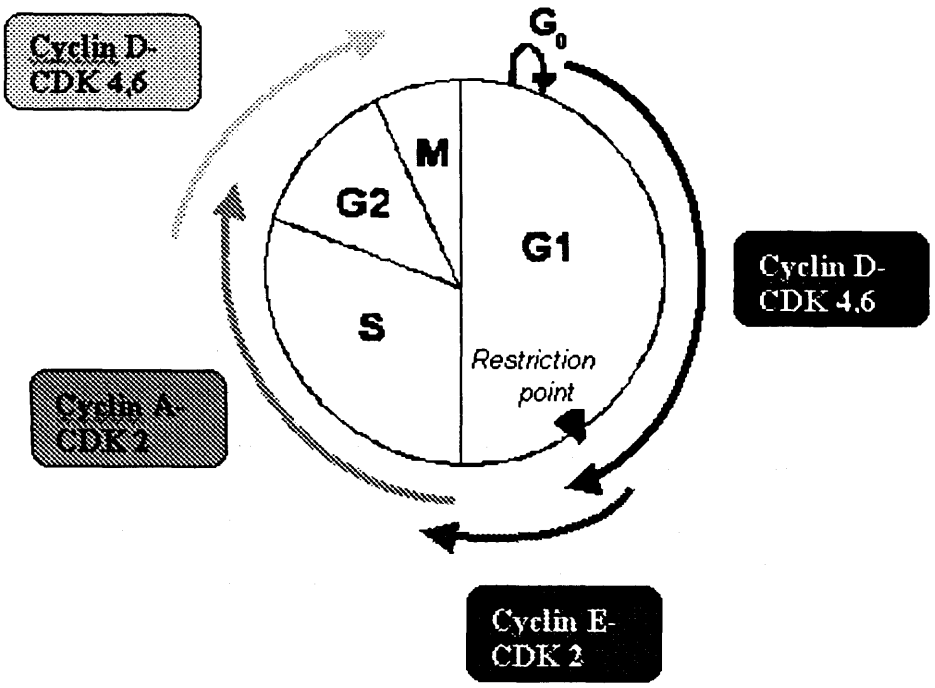

Fig 11. Diagram to show the four distinct phases of the cell cycle[31]

To ensure that the onset of one cell cycle phase is not initiated before the previous one has been completed, a number of checkpoints have evolved at which cell cycle progression will cease unless certain criteria are met.[32,33] These checkpoints provide adequate regions for the regulatory mechanisms that permit or prevent cell cycle progression to exert their effects and play an important role in maintaining the balance between old and new cells within an organism. A cell's commitment to replicate the genome and eventually divide has been assigned to an operationally defined period in late G1, known as the restriction point. It is widely believed that this checkpoint is analogous to START that has been operationally defined in experimental yeast.[33,34,35] It is at this point that the cell switches from its mitogen-dependent growth in early G1, to a largely growth factor-independent progression into, and beyond the S-phase. This is a highly regulated event that governs the integrity of the chromosomal DNA before the cells enter the S-phase. Once the cells have traversed the G1 restriction point they complete the whole cell cycle and divide into two daughter cells. There are other checkpoints that operate as surveillance systems to ensure the cellular environment is favourable for continued progression through the cell cycle. These will operate in the S-phase and limit the detrimental effects of DNA damage

enabling repair mechanisms to be activated.[36] An appreciation of restriction point control is central to our understanding of how, and why, cancer cells continuously cycle.

2.2.1 IMPORTANCE OF CYCLINS AND CYCLIN-DEPENDENT KINASES (CDKs) IN THE CELL CYCLE

One family of enzymes that play a key role in controlling cell cycle progression are the cyclin-dependent kinases (CDKs); these are protein complexes composed of a regulatory cyclin subunit and a catalytic partner and they act as the engine of the cell cycle.[37] These molecules work in conjunction with their substrate proteins and cyclin-dependent kinase inhibitors (CDKIs) in regulating the functions of the cell. The CDKs are expressed at similar levels throughout the cell cycle, but cannot function as active serine/threonine kinases on their own.[38] They are activated when bound to regulatory cyclins, which are expressed at different levels in different phases of the cell cycle, and are named as such due to these dramatic fluctuations in expression[39] (**Fig.12**). The cyclins form complexes with specific CDKs at distinct points within the cell cycle and phosphorylate phase-specific substrates, which induce the transcription of critical enzymes for DNA replication.[40,41] Passage through the restriction point and entry into the S-phase is controlled by CDKs that are sequentially regulated by cyclins D, E and A.

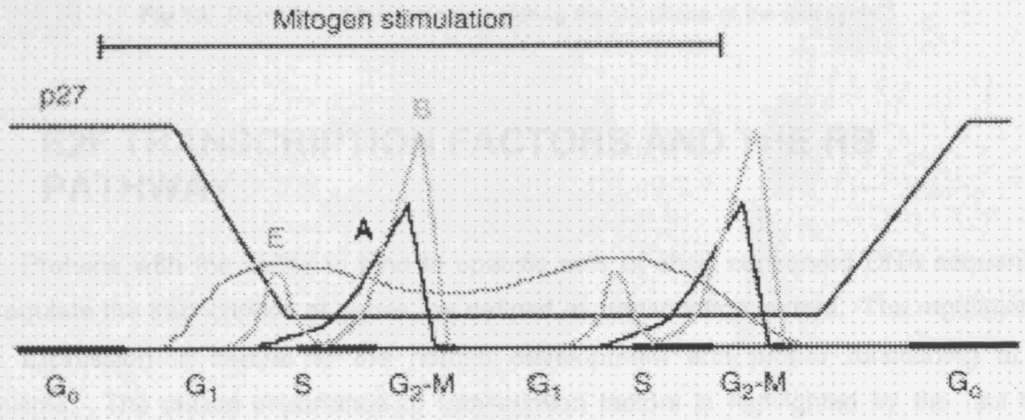

Fig 12. Fluctuations of cyclins and $p27^{KIP1}$ during the cell cycle. D-type Cyclins are expressed throughout the cycle in response to mitogen stimulation (period indicated by top bar)[42]

2.2.1.1 G1 CYCLINS AND CYCLIN-DEPENDENT KINASES

There are two classes of CDKs that function and drive the cell cycle through the G1-S transition and these are cyclin D- (early to late G1) and cyclin E- (late G1) dependent kinases.[43] The D-type cyclins (cyclin D1, D2 and D3) are expressed in a tissue specific

manner[44] and exclusively interact with catalytic partners CDK4 and CDK6;[45] both the synthesis of cyclin-D and its assembly with its catalytic partners depend highly upon mitogenic signals.[46] Mitogen withdrawal leads to cessation of cyclin-D synthesis and as a consequence the cells rapidly exit the cycle.[42] The active assembled holoenzymes (cyclin D/CDK 4/6 kinases) act by phosphorylating the retinoblastoma protein (pRB), which controls gene expression in conjunction with a family of heterodimeric transcription factors (**Fig. 13**). This family are collectively termed the E2F's[47] and they have the capacity to transactivate genes whose products are important for S-phase entry.[47,48]

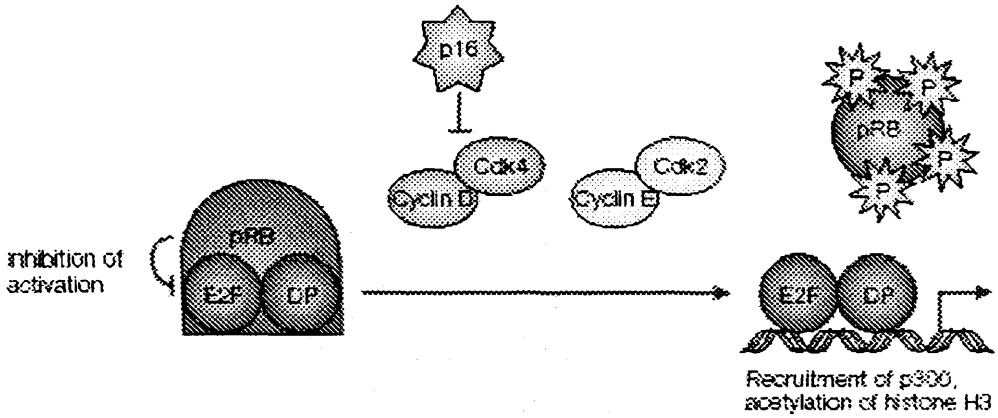

Fig 13. Depiction of the regulation during the G1 phase of the cell cycle[48]

2.3 E2F TRANSCRIPTION FACTORS AND THE RB PATHWAY

Proteins with the ability to bind to specific sets of short conserved DNA sequences and regulate the transcription of genes are defined as transcription factors. The regulation of gene expression is central to the normal development and proper functioning of all organisms. The critical importance of transcription factors is highlighted by the fact that mutations to the genes encoding them can result in a wide range of human diseases, most notably cancer.[49] The E2F family of transcription factors play a crucial role in the control of cell cycle progression, regulating the expression of genes required for the G1/S transition. Many E2Fs are modulated by multiple mechanisms including negative regulation by interaction with the Rb tumour suppressor protein (RB).

2.3.1 THE E2F FAMILY

E2F was initially identified in HeLa cells as the cellular factor activated by E1A and involved in the activation of the adenovirus E2 promoter,[50] hence its name (E2 Factor). The E2F binding site in the E2 promoter was identified as 'TTTCGCGC' and subsequent sites

were identified in a large number of cellular promoters.[51] Interestingly E2Fs can regulate their own activity directly[52] and now appear to play contrasting roles in transcriptional activation and repression, proliferation and apoptosis, tumour suppression and oncogenesis and possibly differentiation and DNA repair.[53] In mammals the E2F family consist of six identified members (E2F1 to E2F6) that can be placed into three groups based on differing homology (**Fig. 14**); along with their three heterodimeric partners (DP1 to DP3,[54] where DP2 and DP3 are alternatively spliced products of a single gene).[55] These heterodimeric proteins are of the basic helix-loop-helix class of transcription factors which recognise the consensus DNA sequence 'TTT(C/G)(C/G)CGC'.[56] Like other basic helix-loop-helix transcription factors, E2Fs bind DNA as dimers and, while E2F and DP homodimers can bind DNA, this binding is very weak compared to their heterodimeric form.[57] Each heterodimer contains one member of the E2F family and one member of the DP family of proteins.

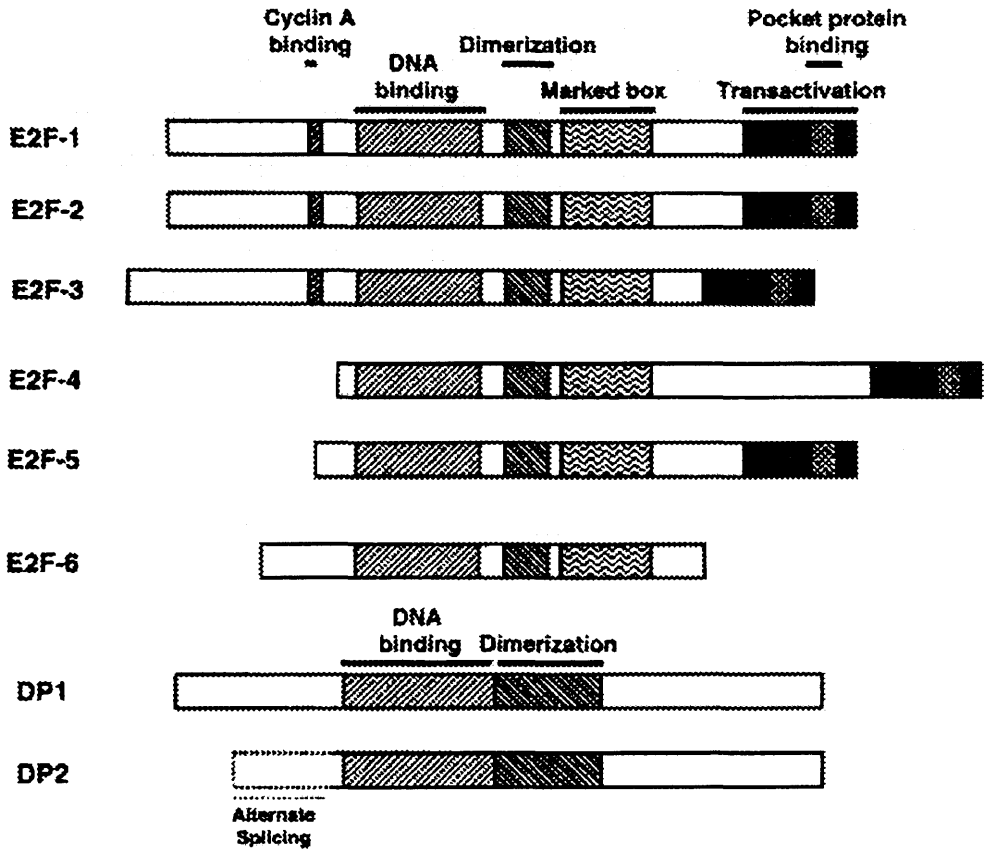

Fig 14. The E2F family of transcription factors[56]

All six E2F proteins have *N*-terminal DNA binding and dimerisation domains, followed by a conserved region termed the 'marked box', which can become involved in dimerisation and DNA bending.[57] Although the marked box motif is highly conserved between the different E2Fs, its function remains unknown. As we have depicted, E2Fs-1 to –3 differ from E2Fs-4 to –6 in the possession of an *N*-terminus in the DNA binding domain,

which binds to cyclin A. E2F-6 differs from the other family members in that it lacks the transactivation domain.[58] All members, except for E2F6, possess a *C*-terminal transactivation domain that is responsible for binding to the retinoblastoma family of tumour suppressors. [59] The exclusion of the transactivation/pocket protein-binding and cyclin A-binding domains of E2F-6 is not its only distinctive feature. E2F-6 has been identified as a transcriptional repressor from the identification of a transcriptionally repressive domain;[60] however, the precise nature of this repression remains to be elucidated. The E2F4 protein contains a stretch of consecutive serine residues between the marked box and the pocket protein binding domain that is not found in other E2F family members.[59,61] The DP1 and DP2 polypeptides contain DNA binding domains related to the E2F proteins but lack transcriptional activation domains or regions homologous to the pocket protein binding or marked box domains.[62] All E2F members can heterodimerise with both DP1 and DP2, allowing for the formation of at least 12 DNA-binding complexes. The complexity of E2F activity, as generated by the formation of a variety of heterodimeric protein complexes, suggests a complexity of function whereby the individual family members play distinct roles in cellular growth. E2F can also affect transcription through its ability to bind to other transcriptionally active factors such as pRb; this, in turn, provides additional levels of regulation by E2F.

2.3.2 THE pRb PATHWAY

The initial indication that E2F was involved in the control of cell proliferation came with its identification as a target for the product of the retinoblastoma tumour suppressor gene.[63] Studies on this interaction identified a pathway in which E2F activity was regulated through association with the retinoblastoma protein (pRb) and related pocket proteins.[64] The latter control cell proliferation, in part, through their ability to associate with the E2F transcription factors.[65]

The retinoblastoma protein is a member of a multigene family that contain two other identified members, namely p107 and p130 (**Table. 3 and Fig. 15**). They bind E2F through a structure termed the pocket (see **Fig. 14** above), which is comprised of non-contiguous regions near their *C*-terminus, and are collectively termed the pocket proteins. Pocket protein binding inhibits the transcriptional activation capacity of E2F factors by masking their transactivation domain thus blocking their ability to activate transcription. In some cases, they convert E2F factors to transcriptional repressors.[65,66]

"Pocket protein"	Cell cycle activity
pRb	G_0 and G_1
p107	S-phase
p130	G_0

Table 3. Pocket protein family members and associated cell cycle activities

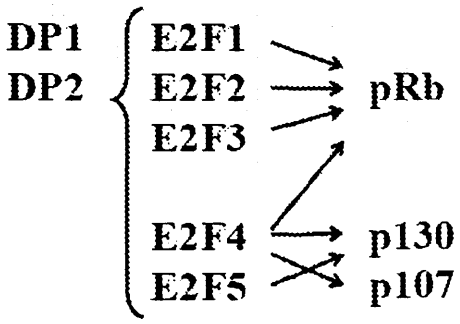

Fig 15. E2F family and associated pocket proteins

The pocket proteins differ in their ability to interact with different E2F family members; whereas pRb binds with high affinity to E2F-1, -2, -3 and sometimes E2F-4; p130 and p107 interact only with E2F-4 and –5.[67,68] Unlike the majority of E2F species, E2F-6 lacks a transactivation domain as well as a pocket protein binding epitope in its *C*-terminus, and so E2F/DP heterodimers act only as transcriptional repressors.[68] The mechanism of repression is either through competitive inhibition with other E2F species or through an active transcriptional repression domain located in the amino terminus of E2F-6.[68,69] The DP heterodimerisation partner does not appear to be involved in determining the binding specificity of E2F factors for the pocket proteins. However, DP factors do function in stabilising the interaction between E2F factors and the pocket proteins.[70,71]

E2F-dependent transcription during the cell cycle is mediated by phosphorylation of the pocket proteins. D-type cyclins modulate the function of Rb during the G1 phase of the cell cycle by activating associated cyclin-dependent kinases (CDK4 and CDK6), which in turn phosphorylate Rb.[72,73] In G0 and early G1, pocket proteins are hypophosphorylated (**Fig. 16**) and are able to interact with the E2Fs. Binding to the pocket protein masks the transactivation domain of E2F, and thus blocks the ability of E2F to activate transcription.

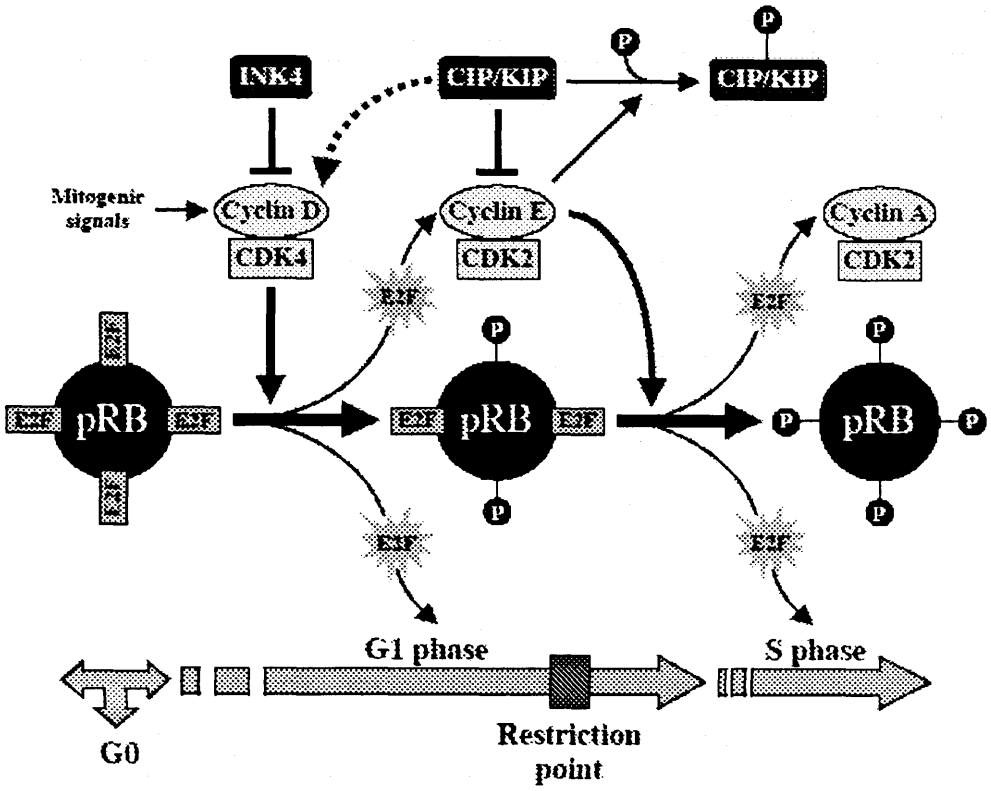

Fig 16. Scheme to depict the E2F/Rb pathway[31]

In mid G1, pRb is phosphorylated first by cyclin D/CDK4/6 and then by cyclin E/CDK2,[74] causing pRb to become hyperphosphorylated and thus no longer able to bind E2F. E2F is thus released from its inhibitory complexes, resulting in an accumulation of 'free' E2F and the activation of E2F-site containing genes in mid to late G1.[75] The p107 and p130 proteins have also been shown to be targets for G1 cyclin kinases, and like Rb, phosphorylation regulates their ability to associate with E2F.[76] Thus, through the regulation of E2F-pocket protein association, G1 cyclin kinases can regulate the expression of numerous genes required for S-phase entry.

2.3.2.1 CYCLIN-DEPENDENT KINASE INHIBITORS

Phosphorylation of pocket proteins is regulated by an array of cyclin-dependent kinase inhibitors (CDKIs), which are themselves regulated by a vast number of growth-regulated signals.[77] CDKIs negatively regulate the CDKs that drive the cell cycle through its different phases, by binding and inhibiting their function. CDKIs generally fall into two families; the CDK2-interacting protein/CDK-inhibitory protein (CIP/KIP) family, comprising $p21^{CIP1}$, $p27^{KIP1}$ and $p57^{KIP2}$ proteins;[78-80] and the inhibitor of CDK4 (INK4) family, which include $p16^{INK4A}$, $p15^{INK4B}$, $p18^{INK4C}$ and $p19^{INK4D}$.[81-84] Members of the CIP/KIP family are structurally unrelated to the INK4 family and, *in vitro* at least, show broad kinase specificity. Members of the CIP/KIP family are found associated with cyclin D-, E- and A- dependent kinases, and bind to both the cyclin and the CDK subunit of the complex. By possessing this

broad specificity for different cyclins and CDKs, they are able to act in different phases of the cell cycle.[42] In contrast, members of the INK4 family specifically bind to and inhibit the function of the cyclin D-dependent kinases, CDK4 and CDK6.[85]

THE CIP/KIP FAMILY

$p21^{CIP1}$ was the first member of this CDKI family to be identified and cloned.[86-89] This CDKI ($p21^{CIP1}$) directly interacts with the proliferating cell nuclear antigen and blocks its ability to activate DNA polymerase-δ.[90] This disrupts the function of DNA polymerase-δ in DNA replication,[91] but not in DNA repair. The interaction between PCNA and $p21^{CIP1}$ suggests a mechanism for balancing the action of the DNA replication and repair machinery's throughout the cell cycle. It was initially thought that members within this family inhibited the functioning of cyclin D-, cyclin E- and cyclin A-CDKs; however, later experiments showed that while the CIP/KIP proteins truly interact and inhibit the function of both cyclin E/CDK2 and cyclin A/CDK2 complexes, they do not inhibit the activity of cyclin D-dependent kinases.[92] Instead, binding of CIP/KIP proteins to the cyclin D/CDK4/6 complexes is necessary for their function as active serine/threonine kinases.[93] The CIP/KIP proteins therefore have dual roles in cell cycle regulation, serving as negative regulators of the cyclin E- and A-dependent kinases, but positive regulators of cyclin D/CDK4/6. In addition to phosphorylating and inactivating pRb, active cyclin D/CDK4/6 complexes also compete with cyclin E/CDK2 complexes for $p21^{CIP1}$ and $p27^{KIP1}$ molecules.[94] Cyclin E/CDK2 not only neutralises pRb by phosphorylation, but also inactivates $p27^{KIP1}$ by the same mechanism, leading to degradation of $p27^{KIP1}$ [95] and contributing to the irreversibility of progression through the G1 restriction point.

THE INK4-FAMILY

The INK4 inhibitors induce growth arrest by specifically targeting and inactivating CDK4 and CDK6;[96,97] their expression in normal tissues vary,[98] depending largely upon cell type and age.[99] The prototypic member of the family was identified as $p16^{INK4A}$; it was first discovered as a protein that specifically interacted with CDK4 in cells transformed with the SV40 virus.[81,100] The INK4-family form binary complexes with CDKs and block the ability of these to interact with both the D-type cyclins and the CIP/KIP proteins. $p16^{INK4A}$ is distinguished from its close relatives; $p15^{INK4B}$, $p18^{INK4C}$ and $p19^{INK4D}$, in its role as a potent tumour suppressor. They all have exon/intron structures, possess ankyrin-like motifs in their sequences, and all function as specific inhibitors of CDK4 and CDK6. By inhibiting D/CDK4 and D/CDK6 the INK4 family can prevent cells with functioning Rb from entering the S-phase, thereby arresting cells in the G1 phase of the cycle. The gene that encodes the p16 protein is located on chromosome 9p21 and this gene encodes another distinct protein in addition to $p16^{INK4A}$.[101] This alternative product from the INK4a locus has been identified as ARF ($p14^{ARF}$ in humans and $p19^{ARF}$ in mice) and these unique proteins (INK4a/ARF) intimately link the pRb and p53 tumour suppressor pathways.[102] The manner by which a single genetic locus encodes both $p16^{INK4A}$ and $p19^{ARF}$ is unprecedented in mammals. The

ARF product is a highly basic protein that localises to the nucleolus in cells,[103,104] it does not interact with any of the CDKs[105] but has the capacity, when induced or over expressed, to induce growth arrest. In contrast to the INK4 proteins, which induce G1 arrest in a pRb dependent manner, ARF causes cell cycle arrest in both G1 and G2, and is instead dependent on p53.[106,107]

INHIBITOR	DESCRIPTION
$p21^{CIP1}$, $p27^{KIP1}$	Inhibit Cyclin E/CDK2 Promote Cyclin D/CDK4,6
$p16^{INK4A}$, $p15^{INK4B}$ $p18^{INK4C}$, $p19^{INK4D}$	Inhibit Cyclin D/CDK4,6
Cyclin E	Targets itself for degradation

Table 4. CDKIs and their functions

2.3.3 E2F AND APOPTOSIS

In addition to modulation of cell growth and the cell cycle, effects on apoptosis also appear to be an important feature of E2F mediated growth regulation. Overexpression of E2F1 has been shown to overcome the inhibitory activities of Rb (and related family members)[108], $p16^{INK4a}$, $p21^{CIP1}$ and p27 [109,110] and lead to S-phase entry. E2F2 and E2F3 are also able to induce S-phase entry in serum-starved or $p16^{INK4a}$-overexpressing cells,[110,111] but to a lesser extent. The induction of S phase entry by E2F1 overexpression is accompanied by a p53-dependent induction of apoptosis,[112,113] and the overexpression of E2F1 induces the accumulation of p53 protein.[114,115] The p53 protein (tumour suppressor) is a transcription factor that functions in DNA-damaged checkpoint control, by causing cell cycle arrest.[116] A primary function of p53 is to act as a sequence-specific transcription factor,[117] and this is attributed to its capacity to limit proliferation. In normal circumstances the p53 protein remains in a latent state, but following genotoxic or other forms of cellular stress, post-transcriptional mechanisms result in an accumulation of the p53 protein, leading to cell cycle arrest or apoptosis, contributing to the suppression of the malignant disease.[118] Initially the function of p53 as a tumour suppressor was solely associated with DNA damage;[119] however p53 has also been linked to proliferation responses (response to E2F-1), and its levels oscillate during the cell cycle,[120] implying an intrinsic cell cycle regulatory control. Based on the finding that overexpression of other E2Fs could not induce apoptosis in serum-starved fibroblasts, it has been proposed that the induction of apoptosis is a property unique to E2F1;[111] however, this finding may be cell type-specific since E2F2 and, to a lesser extent E2F4, also display these properties.[121] The ability of E2F1 to induce apoptosis may be related to its unique ability to induce the accumulation of p53,[114,115] which may in turn be related to the ability of E2F1 to bind to Mdm2.[122] Mdm2 is a key target of p53

and acts as a feedback loop to limit the action of p53, both by inhibiting the transcriptional activation capacity of p53 and by catalysing its destruction.[123] Over expression of Mdm2 has been shown to inhibit apoptosis induced by E2F1[115] and implies that E2F1 may compete for Mdm2 binding, thus relieving the Mdm2-mediated degradation of p53. Evidence to support this emerged when it was discovered that Mdm2 could also bind to and inactivate pRb and functions as an E2F co-activator.[122,124] This further supports evidence that suggest p53 may perform as a checkpoint function during proliferation by monitoring E2F activity.

As with growth regulation by E2F, E2F-mediated apoptosis is regulated by pocket proteins. pRb can inhibit apoptosis in both p53-positive and p53-negative cells,[125] and loss of pRb is linked to both p53-dependent and p53-independent apoptotic defects in transgenic animals.[126,127] Loss of function by Rb and related family members can bypass p53-mediated G1 arrest,[128] but Rb loss induces E2F and p53-dependent apoptosis.[129] A direct connection between E2F1 and pRb in apoptosis is also supported by the finding that loss of E2F1 is able to significantly suppress abnormal apoptosis observed in RB knockout mouse embryos.[130] The ability of pRb to block E2F-mediated apoptosis presumably relies upon its masking of the E2F1 transactivation domain in cells where this domain is required. However, pRb mediated repression is likely to mediate this anti-apoptotic activity in cells, where the E2F1 transactivation domain is dispensable for induction of apoptosis. This demonstrates that the pRb and p53 pathways are physiologically linked and there is a direct connection between pRb, p53 and E2F.[114] As pRb constrains E2F functions, release from this control leads to p53 accumulation in proportion to E2F activity.

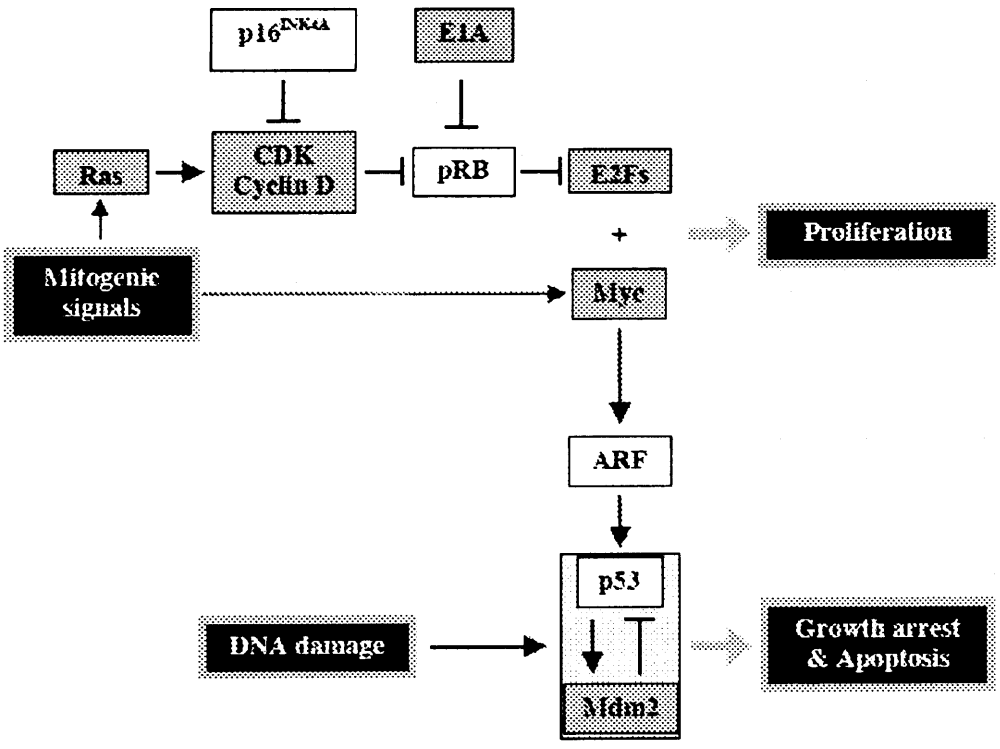

Fig 17. Diagram to show the association between E2F, pRb and p53, and their role in apoptosis[31]

2.3.3.1 THE ARF-p53 PATHWAY

The role of $p16^{INK4A}$ as an inhibitor of cyclin D-dependent kinases has already been discussed, however emerging evidence is providing valuable insights into the molecular circuitry through which $p19^{ARF}$ modulates p53 activity, as part of a checkpoint response to oncogenic hyperprofilerative signals. In short, mutational events that disable the $p16^{INK4A}$-cyclin D/CDK4-Rb pathway and enforce cell proliferation are counterbalanced by a p53-dependent apoptotic response that can eliminate incipient cancer cells. The ability of E2F to trigger p53-dependent cell suicide implies that a biochemical connection links their functions. Other cellular oncogenes, such as Myc also induce p-53 dependent apoptosis,[131] once again demonstrating that p53 is not only activated by DNA damage, but provides an 'oncogene checkpoint' function that guards cells against hyperproliferative signals. In addition to this, recent data has also suggested that $p19^{ARF}$ and p53 might function in the same biochemical pathway,[132] and it is in this setting that $p19^{ARF}$ plays a key role. ARF expression stabilises p53 and induces p53-responsive genes, Mdm2 among them. ARF can physically interact with Mdm2, and its binding blocks both Mdm2-induced p53 degradation and transactivational silencing.[104,133] ARF requires p53 to induce growth arrest, but the direct physical interactions among $p19^{ARF}$, p53 and Mdm2 in various binary and ternary complexes suggest that some p53 functions may reciprocally depend on ARF. Also over expression of the so-called immortalising oncogenes Myc and adenovirus E1A, including E2F1, can induce p53 through both ARF-dependent and ARF- independent pathways, but much higher levels of oncoprotein expression are required to activate p53 when ARF is absent.[132] Therefore, Myc, E1A and E2F1 trigger a p53-dependent oncogene checkpoint gated by ARF. The ability of ARF to sense hyperproliferative stimuli must be important in tumour surveillance, because ARF loss strongly predisposes to spontaneous cancer development and accelerates the frequency of tumour induction by irradiation or carcinogens.[134]

2.4 ROLE OF E2F AND THE Rb PATHWAY IN CANCER

In keeping with the central role of E2F in growth control, a network of overlapping mechanisms regulates E2F activity. The interplay between p53, pRb and E2F is highly complex; whether signals that induce E2F activity lead to cell growth or apoptosis will depend upon a fine balance of the effects on individual members of this pathway. There is much indirect evidence to suggest that the activation of E2F transcription factors, via alterations in the p16-cyclinD-Rb pathway, is a key event in the development of most human cancers. E2F transcription factors have emerged as central components of possibly the most frequently affected genetic pathway in human cancer[42] (**Fig. 18**). The pRb-family proteins are immediate regulators of E2F activity; other cellular proteins regulate the ability of pRb to bind to E2F, which in turn are regulated by another set of proteins. All of these

proteins comprise a linear genetic pathway that ultimately regulates E2F activity, and genetic alterations in most of the genes shown in this pathway are known to correlate with human malignancy.

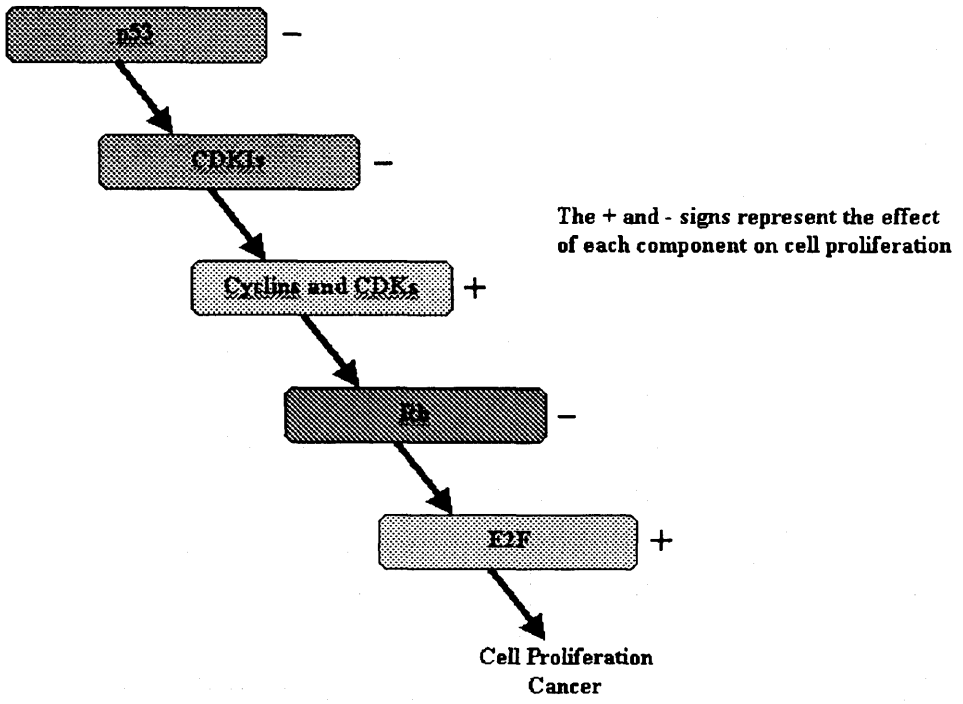

Fig 18. The E2F/pRb genetic pathway[144]

Mutations to members of the retinoblastoma gene family are common and frequently found in retinoblastomas and small cell lung carcinomas. Rb mutations are also found in non-small lung carcinomas, bladder, breast and prostrate carcinomas, leukaemias, malignant gliomas and many sarcomas.[135] Mutations that inactivate pRb would lead to increased levels of 'free' E2F and would result in increased transcription of target genes that are both activated and repressed by E2F.

Immediately upstream of the Rb gene in the pathway (**Fig. 18**) are the cyclin and CDK genes. Amplification of the cyclin D1 gene is frequently associated with head and neck squamous cell carcinomas, oesphophageal carcinomas, bladder and ductal breast cancers as well as hepatocellular carcinomas. Amplification of the CDK4 gene is also common in human sarcomas and gliomas.[136] Since cyclin/CDK kinases phosphorylate the pRb protein, which, in turn, regulates the levels of 'free' E2F, amplification of either the cyclin D1 or CDK/4 genes would reduce the levels of pRb *via* hyperphosphorylation, and thus result in an increased transcription of genes that are activated and repressed by E2F.

Upstream of the cyclins and CDKs in the pathway are the CDKIs. As we have already discussed (Chapter 2.3.2.1) p16 is a CDKI that binds to and directly inhibits CDK4

and CDK6 that heterodimerise with the D-type cyclins. It inhibits cyclin/CDK activity and therefore results in the hypophosphorylation of the pRb protein. Mutations in the p16 CDKI gene are probably the second most common mutation in human cancer, occurring in an estimated 20% - 30% of cases.[137] They are frequently found in leukaemias, anaplastic astrocytomas, mesotheliomas, biliary tract cancers, nasopharyngeal carcinomas, pancreatic carcinomas, oesophageal carcinomas, bladder and ovarian carcinomas and non-small cell lung cancers.[136] Loss of CDKI activity would result in hyperphosphorylation of pRb and an increase in the levels of 'free' E2F, thus an increase in transcription of target genes that are activated and repressed by E2F.

The most common mutation in human cancer, and one that is apparent in more than 50% of human tumours,[138] is that of the p53 tumour-suppressor protein which lies upstream from the CDKIs in the genetic pathway. The direct connection between E2F, pRb and p53, including the physiological association between the pRb and p53 pathways has already been discussed (Chapter 2.3.3).[111,114,115] Overexpression of E2F1 is accompanied by a p53-dependent induction of apoptosis and the accumulation of the p53 protein in proportion to E2F activity. Loss of p53 function and thus this apoptotic defence mechanism, could serve to allow the cell to progress through the cell cycle, thus facilitating proliferation. pRb can inhibit apoptosis in both p53-positive and p53-negative cells,[126] and loss of pRb is linked to both p53-dependent and p53-independent apoptotic defects in transgenic animals.[126,127] In addition to this p53 is an activator of p21 (an important CDKI) transcription; mutation of p53 could serve to reduce the levels of p21, thus increasing the levels of its corresponding cyclin/CDK kinases. This would result in hyperphosphorylation of pRb and increased levels of 'free' E2F, and thus an increase in transcription of target genes that are activated and repressed by E2F.

Additional evidence implicating E2F genes with the occurrence of cancer arises from experiments with mutant mice that lack functional E2F1.[139,140] These mice were reported to have an increased incidence of tumours, and suggests that in the absence of E2F1, genes that are normally repressed by E2F become active.[141] Other observations that correlate abnormalities in E2F genes or gene expression with human cancer were also made. It was discovered that amplification and overexpression of E2F1 was found in human HEL erythroleukaemia cells,[142] and that alterations in E2F4 were detected in colorectal cancers.[143] Although the interactions between components of the E2F genetic pathway are well established, additional interactions between pRb proteins and cellular transcription factors, other than E2F, may have some influence. The binding of some of these transcription factors is also regulated by phosphorylation of pRb and could also play a role in the regulation of cell proliferation and human cancer.[144]

E2F transcription factors play a key role in cell proliferation control by linking the activities of the cell cycle machinery, with the transcriptional regulation of genes whose products are required for S-phase entry and DNA synthesis. The E2F family appear to accomplish these diverse activities through the regulated expression of distinct E2F factors, and through their associations with a variety of cell cycle-regulatory proteins including pRb and p53. The retinoblastoma (Rb) and p53 genes are not essential for completion of the cell division cycle, but disruption of their functions is central to the life of most, if not all, cancer cells. The E2F family seem to represent central components of both the pRb and p53 pathways and a detailed understanding of these complex intrinsic relationships is beginning to emerge. Although much has been learned about the role of E2F in the regulation of cell growth and cell cycle progression, even more remains to be determined. These pathways provide important targets for molecular probes to enable further understanding of the mechanisms employed by mammalian cells for controlling cell cycle progression. It was with this in mind that the Hale group some years ago embarked on its synthetic work on the pRb, cyclin-D, E2F, cyclin-A regulatory A83586C/GE3/azinothricin/citropeptin class of molecules.

Chapter 3: PREVIOUS SYNTHETIC STUDIES TOWARD MEMBERS OF THE AZINOTHRICIN FAMILY

3.1 SYNTHESIS OF L-156,602

Following their isolation and structure determination of L-156,602 (**5**), Caldwell and Durette led a Merck team to the synthesis of an enantiomerically pure form of this chemically ornate molecule.[145,146] They originally envisaged the coupling of a protected linear cyclodepsipeptide amine **12** with the HOBt activated ester of pyran **11**. The piperazic acid nitrogens and *N*-OH groups of **12** were protected with benzyloxycarbonyl (Cbz) groups and *O*-benzyl ethers respectively, while the anomeric hydroxyl of **11** was masked as a methyl pyranoside (Scheme 1). Successful execution of the total synthesis was dependent on the judicious choice of protecting groups for the amino, carboxyl and hydroxyl functionalities of the various amino acids and peptide fragments along the proposed pathway.

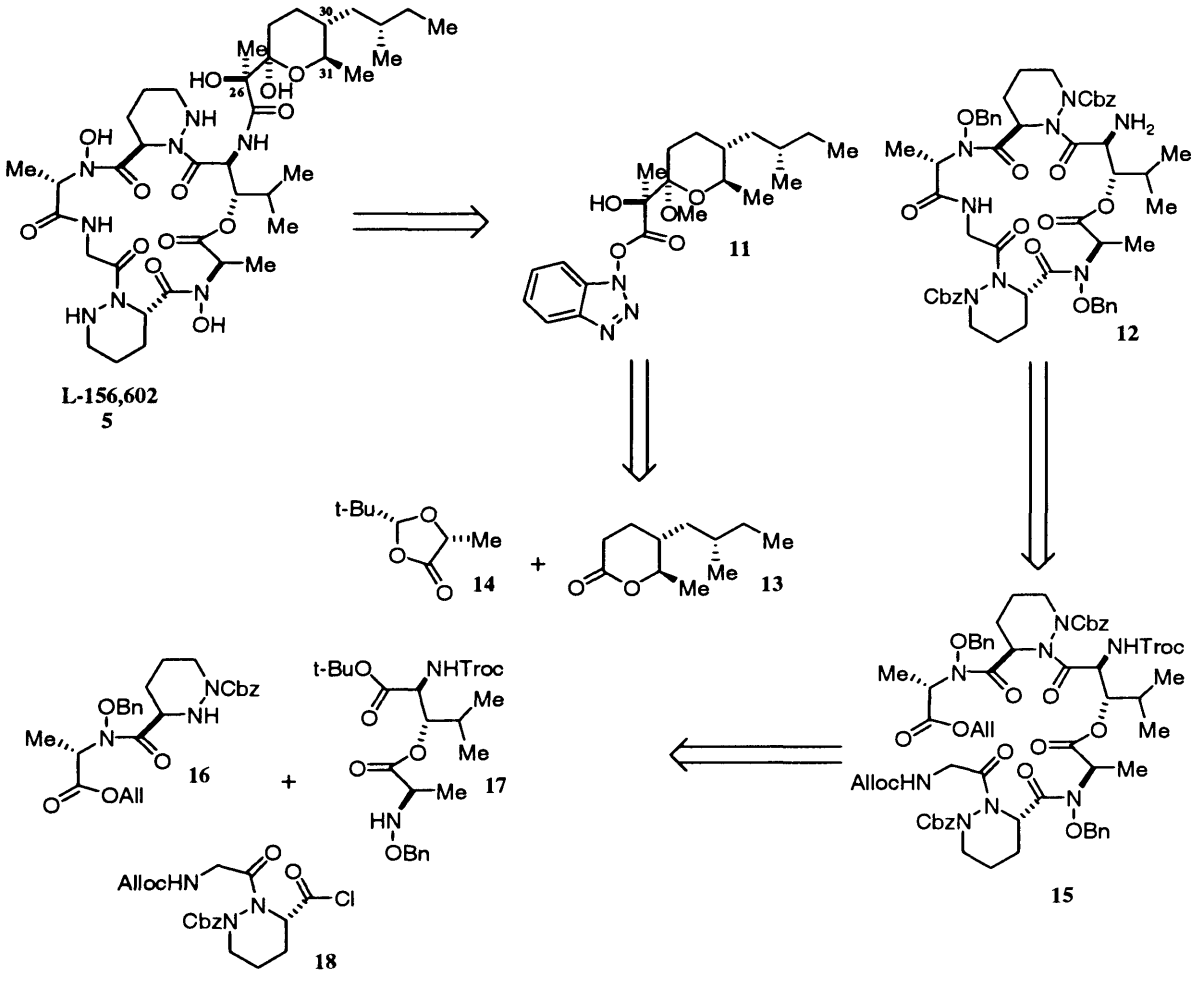

Scheme 1 Caldwell and Durette's original retrosynthetic analysis of L-156,602 **5**

The linkage selected to effect closure of the 19-membered cyclodepsipeptide ring in **12** was the peptide bond between the glycine and *N*-benzyloxy-L-alanine residues in **15**. This site presented the most nucleophilic and least sterically encumbered nitrogen available for the attack on the activated carbonyl group *via* the mixed phosphonic hydride method.[147] Their assembly strategy for the linear hexadepsipeptide **15** consisted of a [2+2+2] fragment condensation of the protected dipeptides **16**, **17** and **18**. They wanted to establish the depsipeptide linkage between the *N*-hydroxy-D-alanine and *(2S,3S)*-3-hydroxyleucine residues at an early stage. The configuration at the C(26) quaternary centre of activated ester **11** was defined with the chiral acetal **14**, developed by Seebach,[148] *via* an enantioselective Claisen condensation reaction and the accession of lactone **13** was accomplished using a Frater-Seebach alkylation.[149]

During their first synthetic attempt at gaining access to L-156,602, Caldwell and Durette successfully constructed the required linear hexadepsipeptide **15** and activated ester **11**. The *N*-terminal Alloc and *C*-terminal allyl ester groups were cleaved in a single step by palladium-catalysed hydrogenolysis using Bu_3SnH,[150] and ring closure was achieved by means of the mixed phosphonic anhydride method[147] to give the fully protected 19-membered cyclodepsipeptide **19** (Scheme 2). With the aim of connecting pyran **11**, the Troc group attached to the *(2S,3S)*-3-hydroxyleucine residue of cyclodepsipeptide **19** was cleaved with Zn/AcOH and the resulting crude amine **12** was reacted with the HOBt activated ester **11**. Unfortunately, none of the desired amide **20** was detected and the only product isolated was the 18-membered (ring contracted) cyclic peptide alcohol **21**, resulting from *O*- to *N*-acyl shift. Evidently an alternative approach had to be sought that delayed macrolactamisation until after the pyran moiety was connected to the *(2S,3S)*-3-hydroxyleucine nitrogen of an appropriately protected hexapeptide amine fragment.

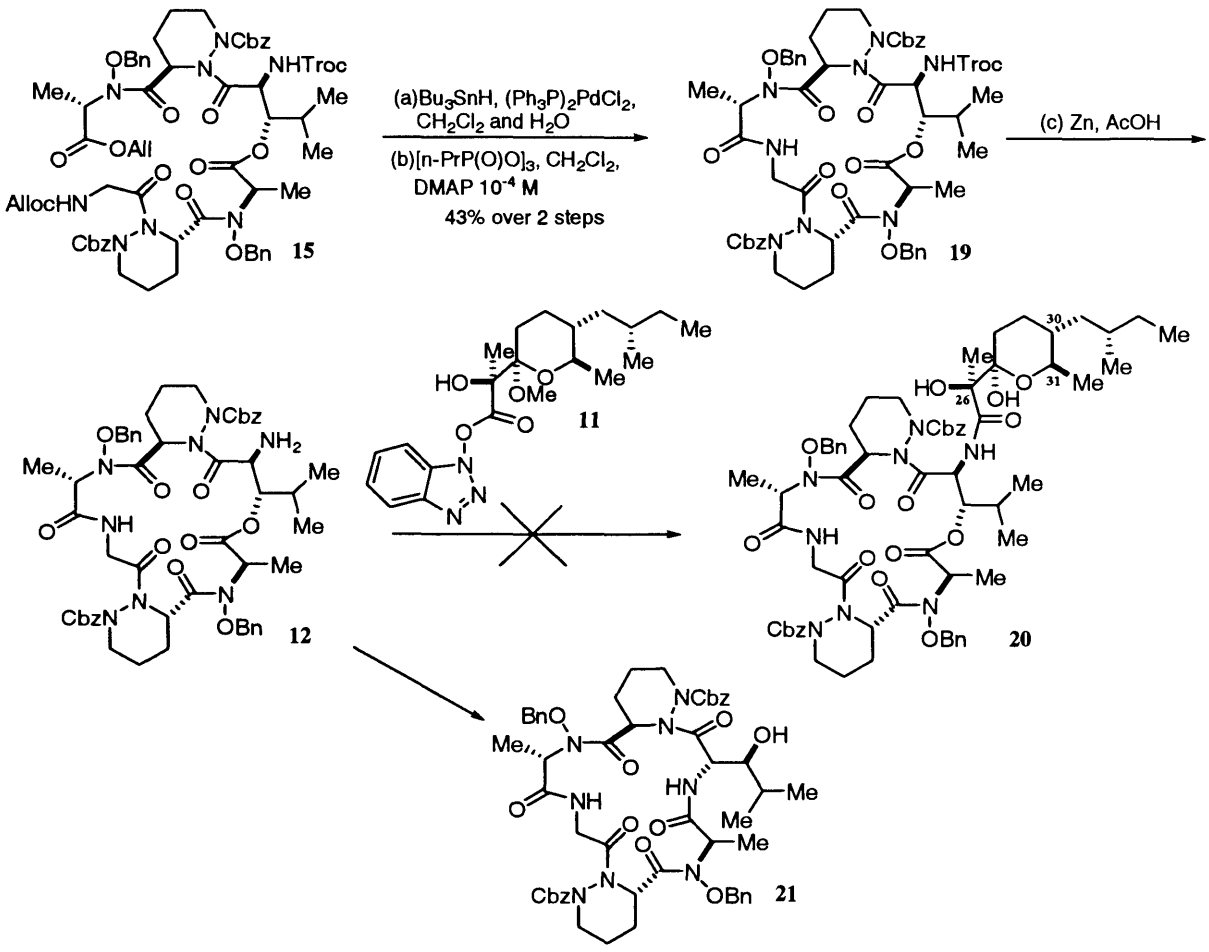

Scheme 2 Initial proposed end game towards L-156,602 **5**

The revised retrosynthetic strategy is shown in Scheme 3. The only difference between the newly devised strategy and that of the originally proposed route was that the C-14 side chain activated ester **11** would be coupled to the main skeletal core at an earlier stage. The reaction sequences for all the fragments required for the synthesis of the linear hexadepsipeptide **23** and the activated ester **11** remained unchanged. The rationale for this new approach was that to prevent the undesired *O*- to *N*-acyl shift, the *(2S,3S)*-3-hydroxyleucine residue of the linear hexadepsipeptide **23** would have to be capped with the pyran fragment prior to macrolactamisation, affording the pre-macrolactamisation precursor **22**. They then envisaged that the cyclisation of **22** would proceed without the occurrence of the undesired *O*- to *N*-acyl shift to provide the desired macrolactam **5**.

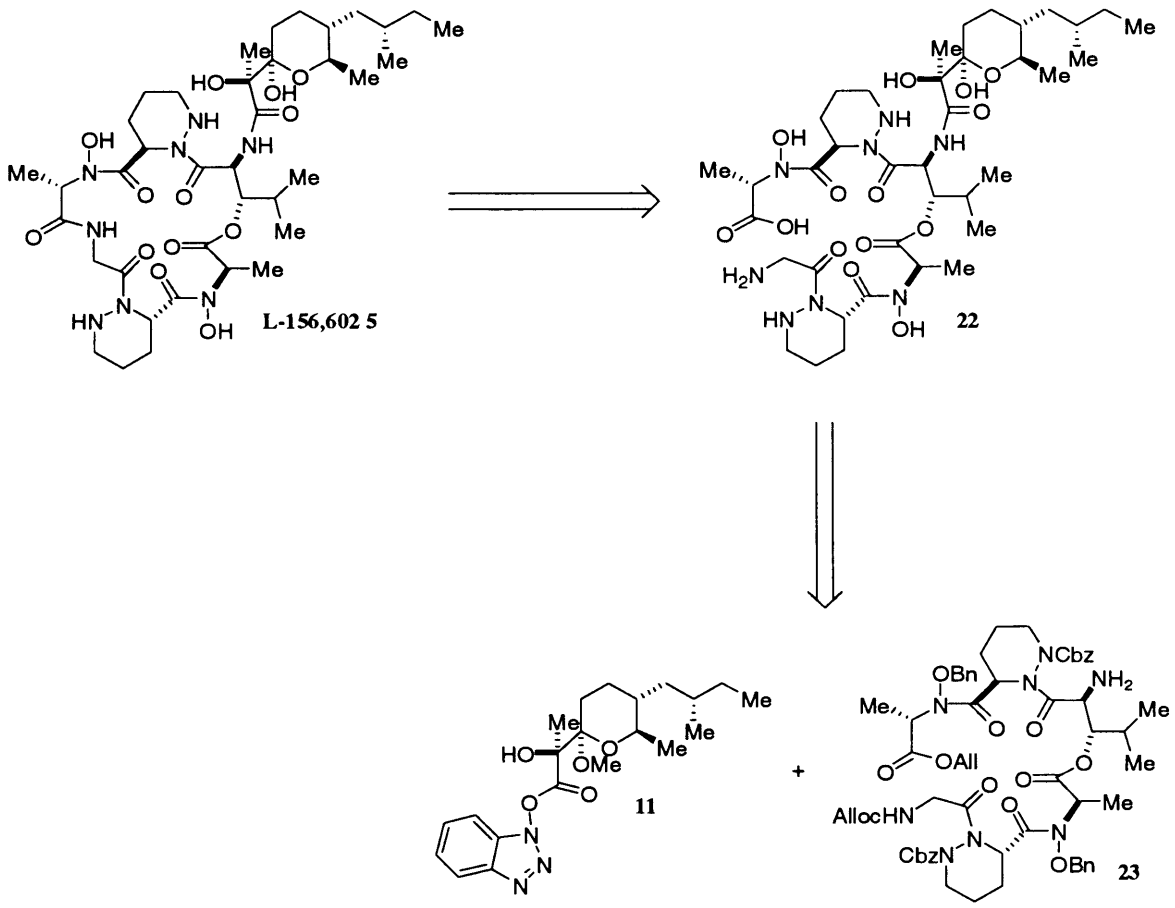

Scheme 3 Caldwell and Durette's revised retrosynthetic analysis of L-156,602 **5**

3.1.1 SYNTHESIS OF LINEAR HEXADEPSIPEPTIDE

As previously, Caldwell and Durette envisaged assembly of the requisite linear hexadepsipeptide fragment *via* a [2+2+2]-fragment condensation strategy. This would require the preparation of three protected dipeptide fragments **16**, **17** and **18** (Schemes 5, 8 and 6 respectively).

The enantiomeric Cbz-piperazic acid derivatives **29** (3*R*) and **30** (3*S*) were prepared by a route that exploited a Diels-Alder cycloaddition reaction between di-t-butylazodicarboxylate **25** and methyl-2,4-pentadienoate **24** (Scheme 4). Following hydrogenation of the double bond in the cycloadduct, saponification and quantitative trifluoroacetic acid-mediated deprotection of the Boc-protecting groups furnished the racemic piperazic acid trifluoroacetic acid salt **27** with a 61% overall yield from **24** and **25**. After preparation of the *N*(1)-Cbz-piperazic acid derivative **28**, an optical resolution performed with (+)- and (-)-ephedrines[151] to obtain **29** and **30** in 18% and 15% yields respectively.

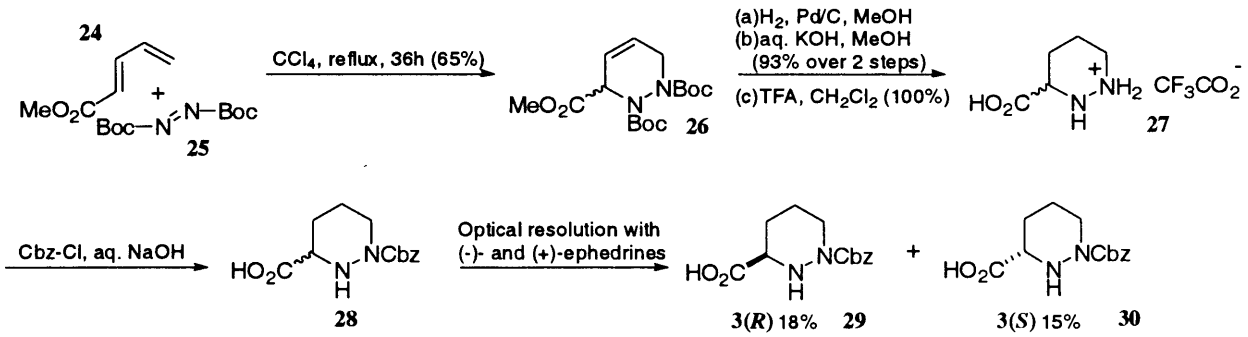

Scheme 4 Synthesis used in the Caldwell/Durette preparation of 3(*R*)-**29** and 3(*S*)-**30** piperazic Acids

Dipeptide **16** was prepared as shown in Scheme 5. Carpino Fmoc acid chloride technology[152] was used for effecting peptide bond formation due to the attenuated nucleophilicity of the *O*-benzylated hydroxamate nitrogen in **34**. Hydroxamic acid ester **34** was synthesised in three steps from commercially available (*R*)-methyl lactate **32** by *O*-triflate displacement with $BnONH_2$, ester hydrolysis with aq. NaOH and *O*-allylation with carbonyldiimidazole and allyl alcohol. The key Carpino acid chloride coupling between **31** and **34** proceeded smoothly delivering **16** in 62% overall yield for three steps following Fmoc deprotection with Et_2NH.

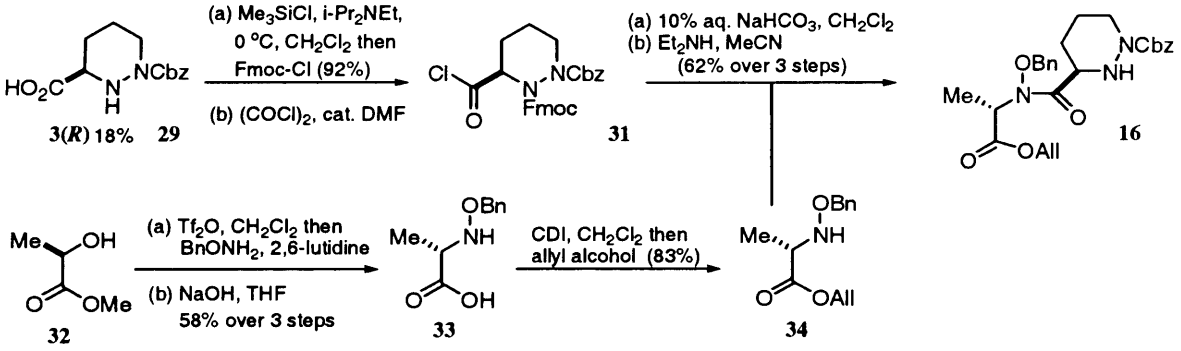

Scheme 5 Synthesis of the 3(*R*)-*N*-Cbz-piperazic-*N*-OBn-L-alanine dipeptide **16** of L-156,602

The Carpino biphasic acid chloride coupling methodology was also employed in the synthesis of dipeptide **18** (Scheme 6). The resolved (3*S*)-Cbz-piperazic acid **30** was protected as a t-butyl ester and then coupled *via* the Carpino method to the acid chloride of *N*-Alloc-glycine **35** to furnish dipeptide **36**. The latter was then converted to acid chloride **18** following cleavage of the t-butyl ester and treatment with oxalyl chloride.

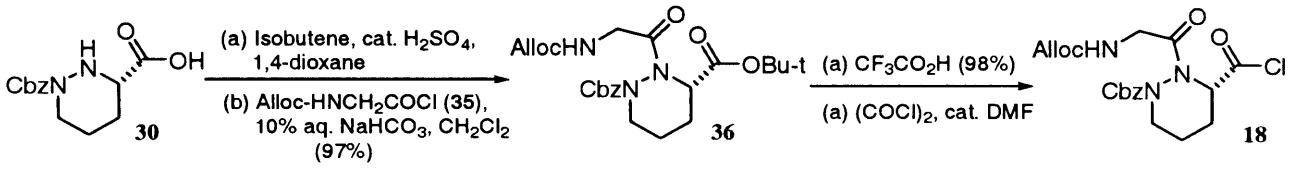

Scheme 6 Synthesis of the 3(*S*)-*N*-Cbz-piperazic-*N*-Alloc-glycine dipeptide **18** of L-156,602

The synthesis of depsipeptide **17** required construction of (2*S*,3*S*)-3-hydroxyleucine **41** which had previously been reported by Caldwell and Bondy.[153] Their 4-step sequence to **41** utilised Sharpless asymmetric epoxidation technology as a starting point on allylic alcohol **37**. Subsequent oxidation of epoxy alcohol **38** furnished epoxy acid **39**, which underwent regioselective nucleophilic ring opening with benzylamine to afford **40** in 66% yield. The *N*-benzyl protecting group was removed by hydrogenation over Pearlman's catalyst to yield (2*S*,3*S*)-3-hydroxyleucine **41** (89%).

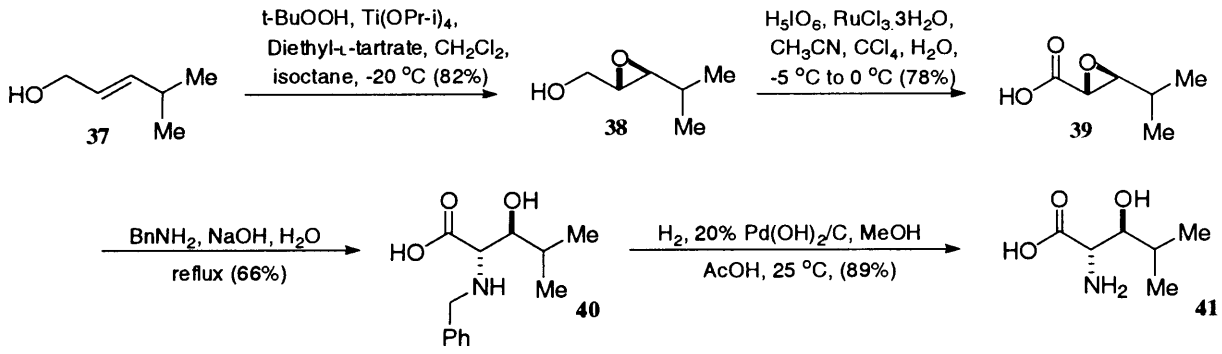

Scheme 7 Synthesis of (2*S*,3*S*)-3-hydroxyleucine **41**

With **41** now in hand, depsipeptide **17** was synthesised in a further 5 steps as depicted in Scheme 8. Following regioselective protection of **41**, the protected amino acid **42** was coupled with the *N*-hydroxybenzyl-D-alanine residue **44** exploiting 1,1-carbonyldiimidazole to afford depsipeptide **17** in 67% yield.

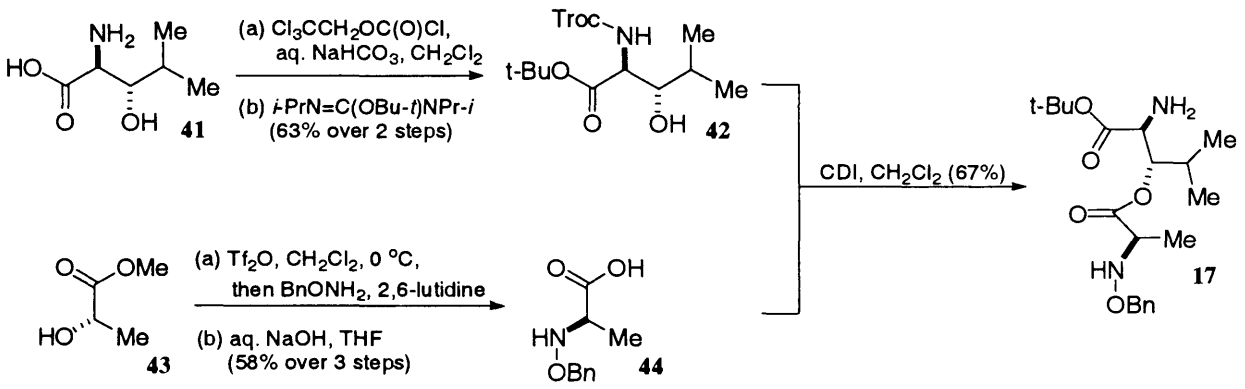

Scheme 8 Synthesis of depsipeptide fragment **17**

Protected linear hexadepsipeptide **15** (Scheme 9) was then assembled employing the [2+2+2] fragment condensation strategy discussed earlier. The synthesis commenced with a silver cyanide-mediated amidation between acid chloride **18** and partially protected depsipeptide **17** to furnish the first [2+2] tetrapeptide **45**. The *t*-butyl ester was removed with TFA, and the liberated acid converted to acid chloride **46**. A Carpino biphasic amidation between **46** and **16** then ensued to assemble the [4+2] protected linear hexadepsipeptide **15** and the Troc-urethane reductively excised with zinc dust to furnish the partially protected linear hexadepsipeptide **23**.

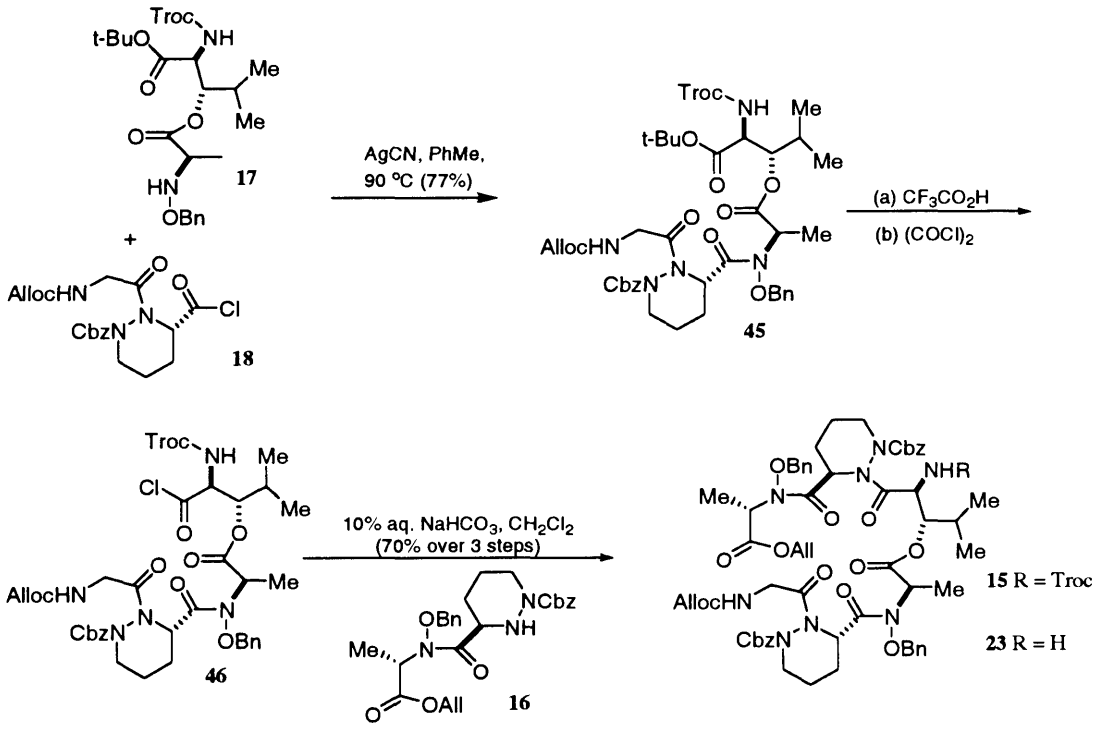

Scheme 9 Synthesis of partially protected linear hexadepsipeptide **23**

3.1.2 SYNTHESIS OF TETRAHYDROPYRAN ACTIVATED ESTER SIDE CHAIN OF L-156,602

The route to the tetrahydropyranylpropionate sector of L-156,602 (Scheme 10) was initiated with a diastereoselective Frater-Seebach alkylation reaction[148,149,154] between the enolate derived from methyl (*R*)-3-hydroxybutyrate **47** and (*S*)-1-iodo-2-methylbutane **48**, which furnished alcohol **49** in 46% yield. Protection of the secondary alcohol followed by ester reduction furnished primary alcohol **50** in 52% yield over 2 steps; this was then oxidised under Swern conditions to afford aldehyde **51**, which underwent a Wittig condensation to yield (*E*)-enoate **52**. Following hydrogenation and *O*-desilylation spontaneous lactamisation occurred to provide lactone **13**.

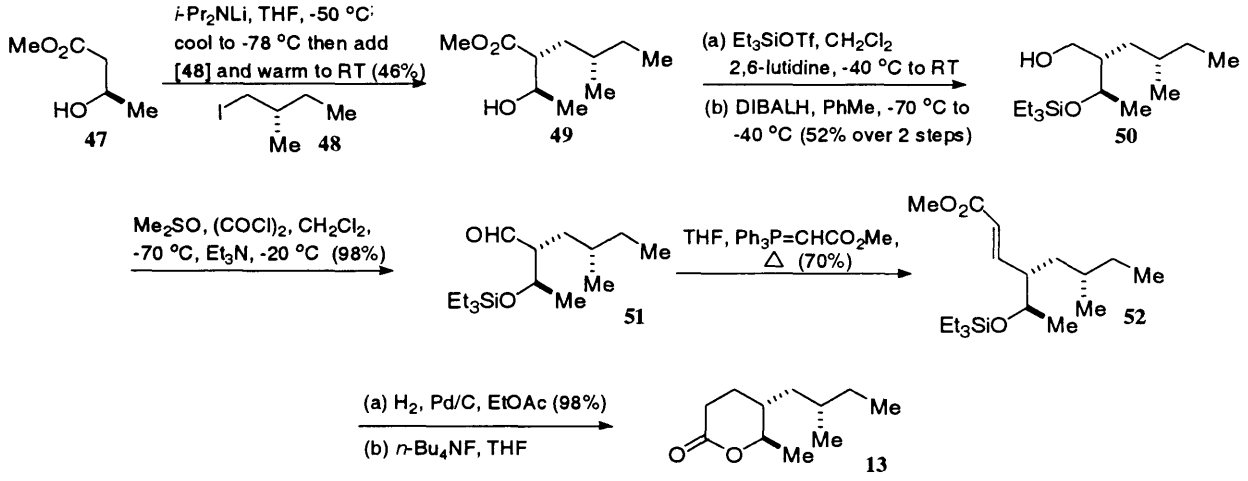

Scheme 10 Frater-Seebach approach to lactone intermediate **23**

A second attractive approach to the 11-carbon lactone **13** was also investigated that utilised diastereoselective reactions directed by the pinanediyldioxyboryl group[155] to establish both chiral centres in the lactone ring (Scheme 11). In this route, the Grignard reagent derived from (*S*)-1-bromo-2-methylbutane **53** was added to trimethylborate and the resulting boronic acid ester condensed with (1*R*,2*R*,3*R*,4*R*)-(-)-pinanediol to afford cyclic ester product **54**. This was then treated with dichloromethyllithium and the addition product was rearranged *in situ* under the influence of zinc chloride to furnish α-chloroboronate **55**. This, in turn, was treated with the Grignard reagent derived from 2-(2-bromoethyl)-1,3-dioxane to provide acetal **56** in 73% overall yield from **53**. Subsequent homologation with dichloromethyllithium and zinc chloride was followed by nucleophilic substitution of the resulting chloride **57** with methyllithium followed by treatment with zinc chloride to give substitution product **58** in 79% yield from intermediate **54**. Oxidation with basic hydrogen peroxide gave alcohol **59**, which was esterified with 4-bromobenzoic acid in the presence of DCC and 3-hydroxypropyl ester to give **60** in 91% yield. The resulting ester was then treated

with sodium hypochlorite in a mixture of aqueous acetone and acetic acid to furnish diester **61** in 68% yield, which underwent saponification with sodium hydroxide followed by an acid work up to afford lactone **13** in 87% yield.

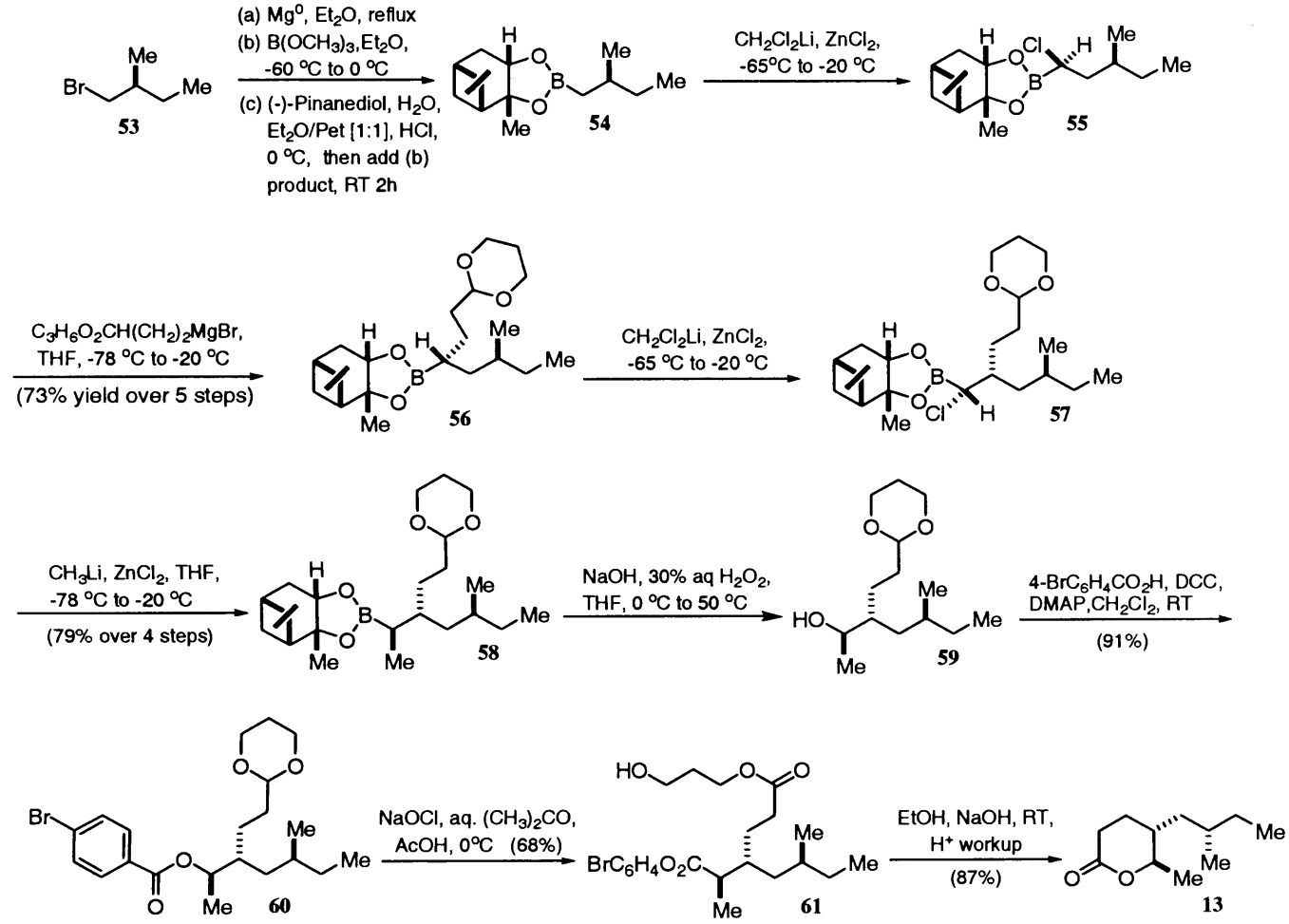

Scheme 11 Pinanediol boronic ester approach to lactone intermediate **23**

The remaining three carbon atoms of the tetrahydropyranylpropionate side chain were then introduced *via* a highly diastereoselective Claisen condensation with the lithium enolate of (2*R*,5*R*)-2-*t*-butyl-5-methyl-1,3-dioxolan-4-one **14** (Scheme 12). The desired addition product **63** was obtained as a single diastereoisomer in 75% yield accompanied by 16% of recovered lactone **13**. The methyl pyranoside was then formed *via* Fischer glycosidation to block the hemiketal functionality so as to prevent a retro-Claisen reaction from occurring during the base mediated cleavage of the lactone in **63**. This saponification step proved sluggish and the resulting acid was not sufficiently stable to allow isolation. They therefore deduced that the best method for cleaving the *t*-butyl-1,3-moiety was through transesterification with sodium methoxide in methanol (78% yield) followed by saponification with potassium hydroxide in ethanol to give the more stable potassium carboxylate salt **64**.

This salt was then taken on and treated with Castro's BOP reagent[156] to furnish the activated ester precursor **11** for coupling to the linear hexadepsipeptide **23**.

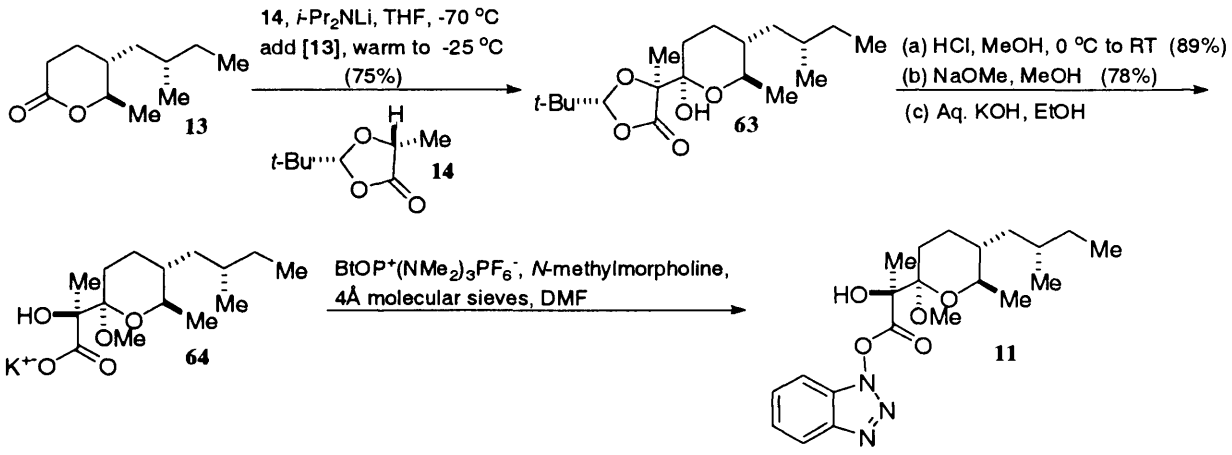

Scheme 12 Synthesis of activated ester **11**

3.1.3 L-156,602 ENDGAME STRATEGY

The total synthesis of L-156,602 was completed as illustrated in Scheme 13. The partially protected amine **23** underwent *N*-acylation with activated ester **11** in 56% yield over 2 steps from C-14 acid. In contrast to the results obtained with the cyclic amine **12**, the undesired *O*- to *N*-acyl shift was not observed during this revised strategy. The terminal allyl protecting groups were removed from **65** using Pd(0) and tri-*n*-butylstannane[150] to afford the macrolactamisation precursor **22**. This precursor in turn facilitated macrolactamisation, when *n*-propane phosphonic anhydride and DMAP[157] were used to close the 19-membered ring. The final step of the synthesis was accomplished by hydrogenolytic deprotection of the macrolactamisation product **66** to obtain L-156,602 **5** in 53% yield.

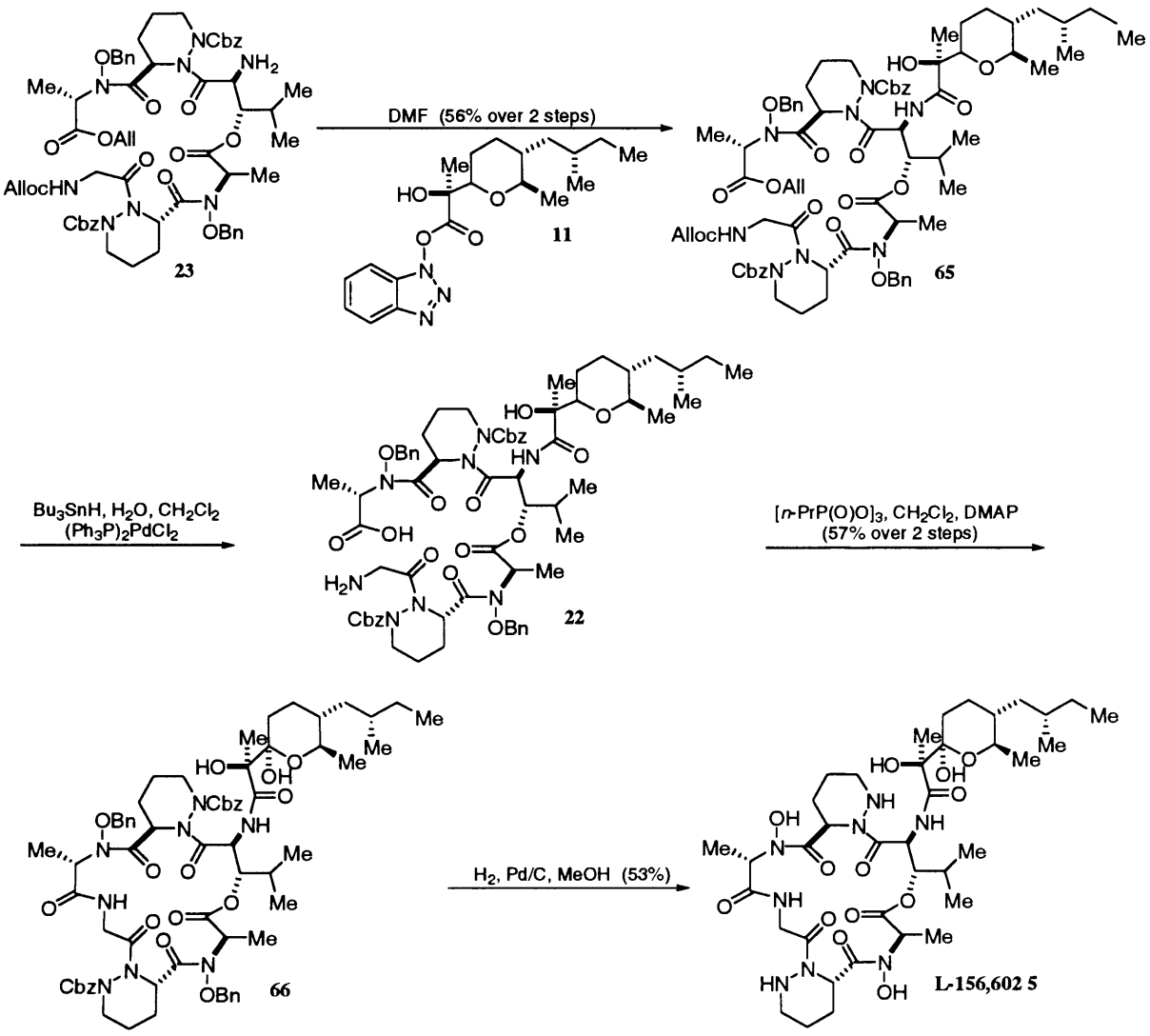

Scheme 13 L-156,602 **5** endgame strategy

3.2 SYNTHESIS OF A83586C

The first asymmetric total synthesis of A83586C (**2**) was accomplished by Hale and co-workers[158] at the Christopher Ingold Laboratories, University College London in 1997. Hale's initial unsuccessful strategy to A83586C was based upon the chemoselective coupling of **69** with **68**, ester hydrolysis and macrolactamisation to obtain **2**. However, all efforts to bring about this macrolactamisation were met with failure and alternative synthetic approaches were therefore considered. One possibility was predicted upon the successful union of the fully elaborated benzotriazole activated ester **68** with the hydrochloride salt of the fully deprotected cyclodepsipeptide **71** (Scheme 14). The resulting glycal **70** would then be chemoselectively hydrated under mild acidic conditions to afford the natural product **2**. The new strategy should again be based upon the highly chemoselective coupling of two

largely unprotected fragments. Such a deliberate avoidance of heteroatom protecting groups at the final stages were considered necessary due to the lability of the final target towards acids, bases, oxidants, many reducing protocols and a variety of strong nucleophiles.

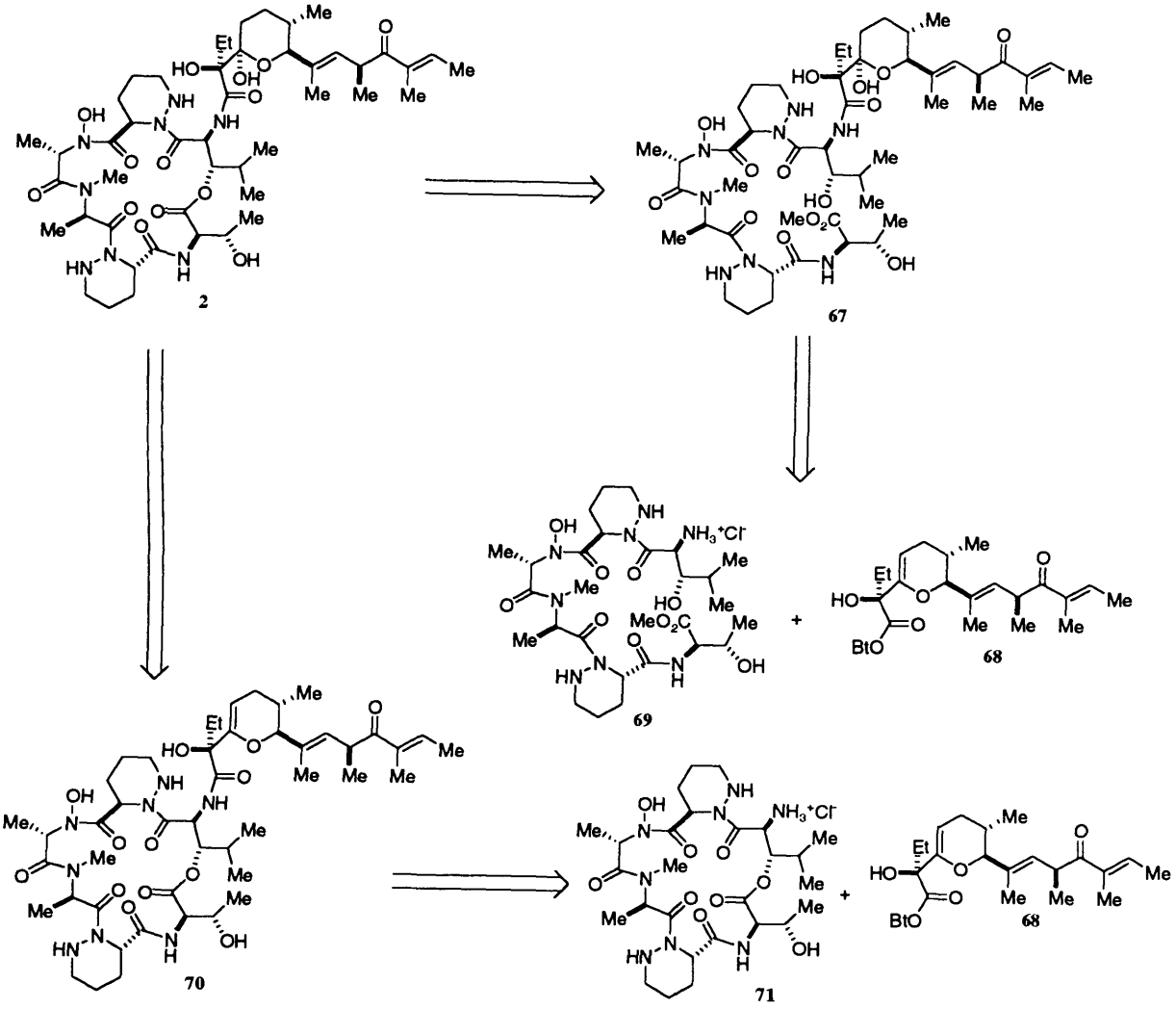

Scheme 14 Retrosynthetic analysis of A83586C **2**

3.2.1 SYNTHESIS OF THE TETRAHYDROPYRAN ACTVATED ESTER OFA83586C

Hale's retrosynthetic analysis of pyran **68** proposed its assembly from the intermediates **72**, **73** and **74**. Phenylsulfone **74** was assembled in six steps from enantiopure propionamide **75** (**Scheme 15**) utilising Evans asymmetric aldol chemistry[159] to install the two *syn* stereocentres and the (*E*)-trisubstituted alkene **77** in a single step. Removal of the chiral oxazolidinone from the aldol adduct was accomplished *via* transesterification and methyl ester reduction, which collectively provided the 1,3-diol **78**.

Selective thioetherification with tributylphosphine and phenyldisulfide then ensued, followed by *O*-silylation and Trost-Curran oxidation[160] with oxone to furnish the desired sulfone **74**; the complete the synthetic sequence proceeded in an overall yield of 50%.

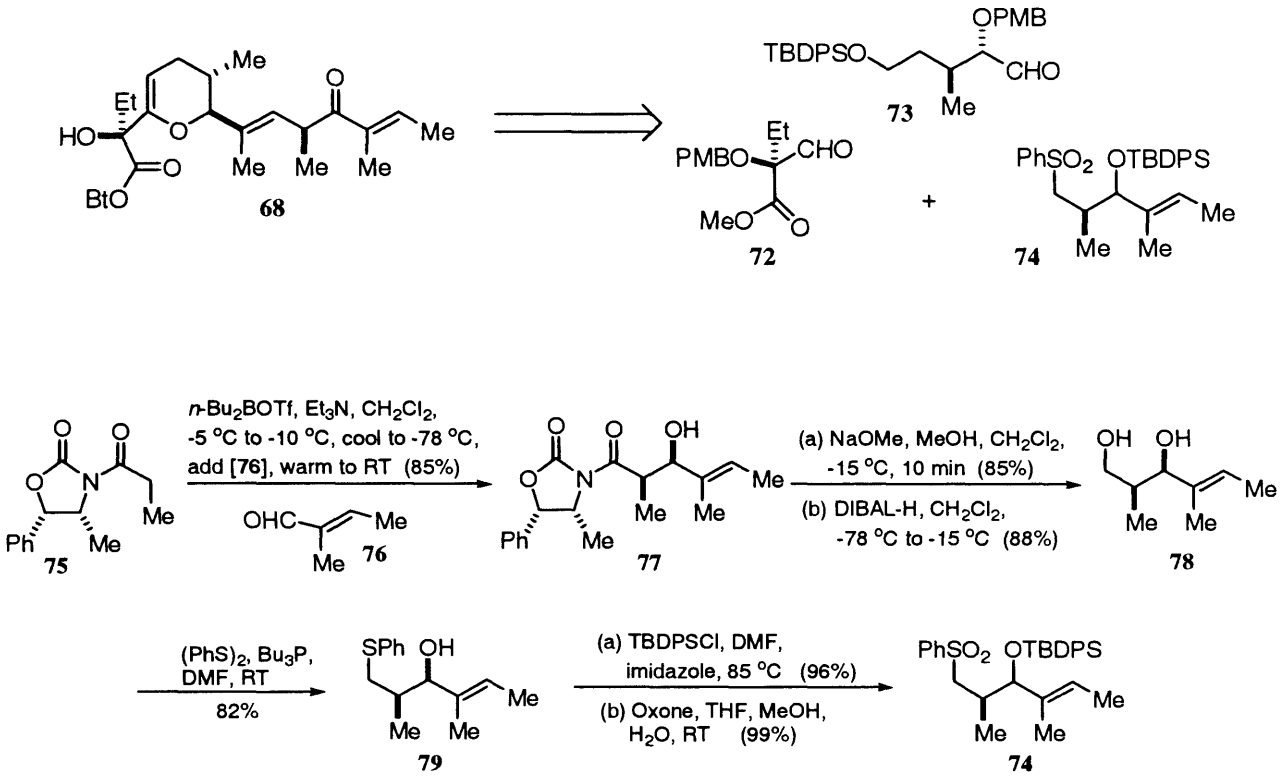

Scheme 15 Retrosynthetic analysis of activated ester **68** and synthesis of phenylsulfone **74**

During the synthesis of intermediate **73** (Scheme 16), efficient procurement of the *anti*-relationship that existed between the two adjacent stereocentres was considered the main priority. This was achieved by a chelation controlled epoxide ring opening reaction of the chiral 2,3-epoxy alcohol[161] **82** with trimethylaluminium, which proceeded with a 20:1 C3:C2 selectivity.[162] Epoxyalcohol **82** was synthesised by Sharpless asymmetric epoxidation (AE) of the allylic alcohol derived from propargylic alcohol **81**. The major 1,2-diol was thereafter protected as a *p*-methoxybenzylidene acetal **83**, and the latter reductively cleaved[163] to selectively protect the secondary alcohol as a *p*-methoxybenzyl ether. A Swern oxidation then ensued to furnish the desired aldehyde **73** in 83% yield.

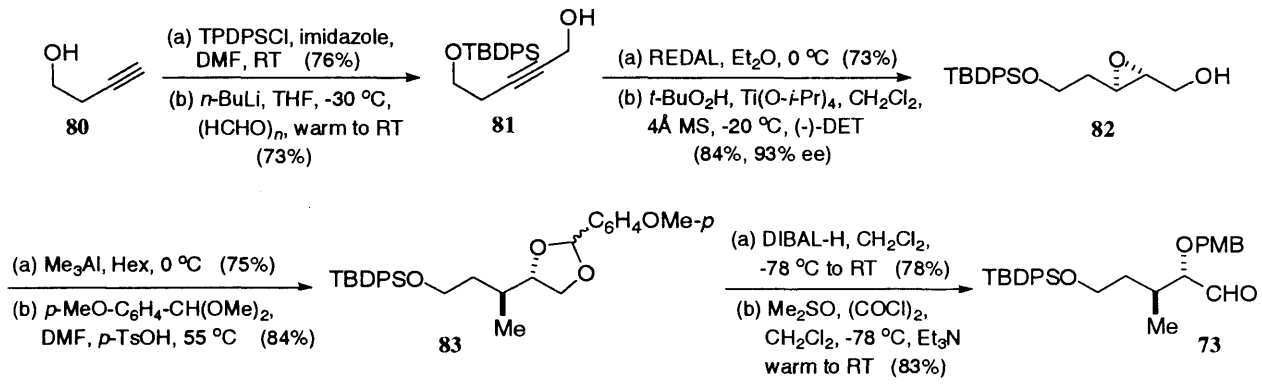

Scheme 16 Synthesis of aldehyde **73**

With the desired subtargets now in hand (**73** and **74**), unification was effected by metallation of **74** with *n*-BuLi and by nucleophilic addition to afford a diastereomeric mixture of β-hydroxysulfones **84** (Scheme 17), which were subjected to a Swern oxidation with trifluoroacetic anhydride and DMSO to provide ketone **85** in 92% yield. Desulfonylation of this β-ketosulfone mixture was accomplished *via* Smiths free-radical tri-*n*-butylstannane method[164] and afforded ketone **86** as a single diastereoisomer. The next step was to install the (*E*)-trisubstituted alkene moiety. Although conversion of **86** to the (*Z*)-enol triflate was successful, attempts at performing cross-couplings using Stille[165] and McMurry-Scott[166] protocols were unsuccessful. Access to alkene **87** was eventually achieved *via* a Grignard addition/$POCl_3$-pyridine-mediated dehydration tactic that resulted in a 2.6:1 mixture of desired **87**:1,1-disubstituted alkene. This mixture proved difficult to separate and was selectively *O*-desilylated at the primary position with HF-pyridine, which facilitated chromatographic separation of the two isomers to give **88** in 55% overall yield from ketone **86**. Following *O*-desilylation a thioetherification and an oxidation, furnished the desired sulfone **89** in very good yield.

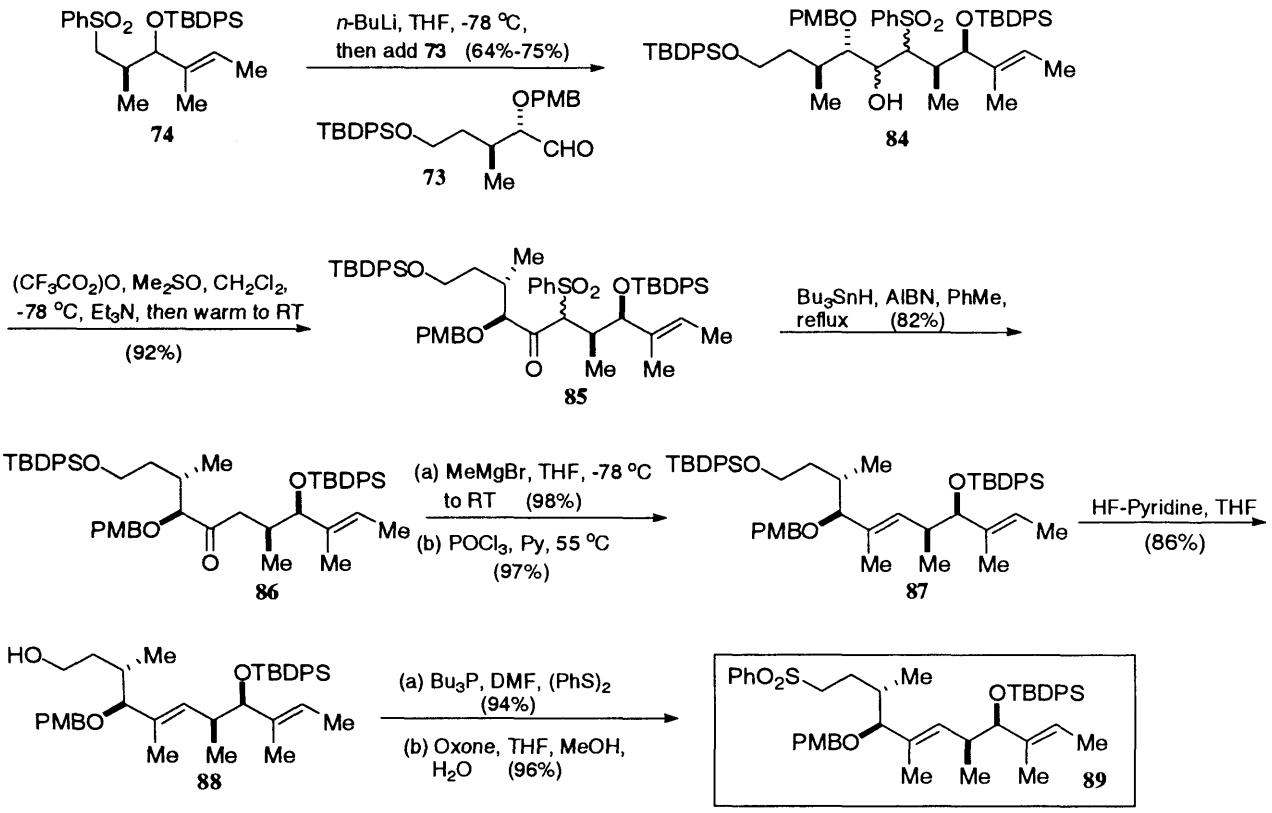

Scheme 17 Synthesis of phenylsulfone **89**

The route to the chiral β-aldehydo ester partner **72** (Scheme 18) commenced with a Sharpless catalytic asymmetric dihydroxylation reaction[167] on the 1,1-disubstituted alkene **90**, which delivered diol **91** in an admirable 99% yield and greater than 92% ee. Diol **91** was then protected as a *p*-methoxybenzylidene acetal **92**, reminiscent of the aldehyde **73** sequence, and a reductive cleavage was attempted with DIBAL to position the PMB group on the more hindered hydroxyl product. Unfortunately the reaction progressed with low regioselectivity, providing a 2:1 mixture of alcohols **93** and **94**. Fortunately these were easily separated from one another *via* SiO_2 flash chromatography. An oxidation-esterification sequence on **94** delivered methyl ester **95** in 64% yield over 2 steps, and this was followed by *O*-desilylation and a Swern oxidation to furnish the desired aldehyde **72**.

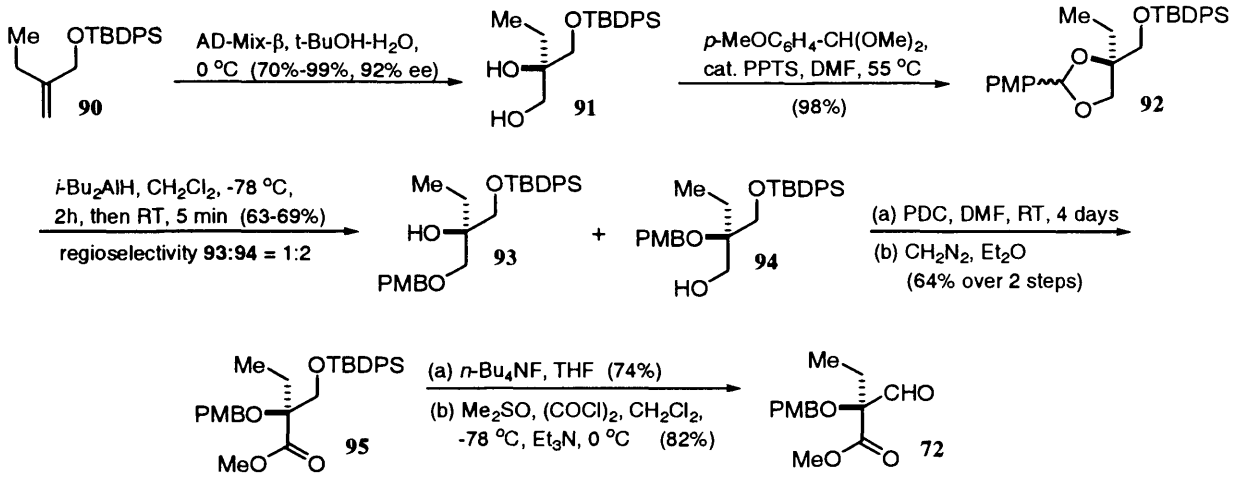

Scheme 18 Synthesis of aldehyde **72**

With all the necessary fragments in place, the final assembly of the A83586C tetrahydropyranyl side chain could commence (Scheme 19). Union of **89** and **72** was effected by adding the sulfone anion derived from **89** onto aldehyde **72** at low temperature. The ensuing mixture of β-hydroxysulfones **96** was then Swern oxidised and desulfonylated with the aluminium amalgam method of Corey-Chaykovsky[168] to afford ketone **97** essentially as a single diastereoisomer. Removal of the more electron-rich and less hindered secondary PMB ether was next achieved by treatment with a limited quantity of DDQ in ice-cold dichloromethane/H_2O. This provided an equilibrating three-component mixture: the linear δ-hydroxy ketone and the two α- and β-ring-closed hemiketals, which were subjected to a dehydrative ring-closure with methanol and PPTS to obtain glycal **98**. Following *O*-desilylation the methyl ester was then saponified to obtain acid **99**. The activated ester **68** was thereafter prepared by treatment with Castro's BOP reagent,[156] Swern oxidation and deprotection of the tertiary PMB ether with DDQ[169] in wet chloroform then provided the desired target. The last few steps of this sequence that were carried out in the presence of sensitive functionality are particularly noteworthy due to the range of selective chemistry. In this regard the esterification that was conducted in the presence of the secondary allylic alcohol, and the oxidation and deprotection sequence in the presence of the HOBT ester were especially pleasing.

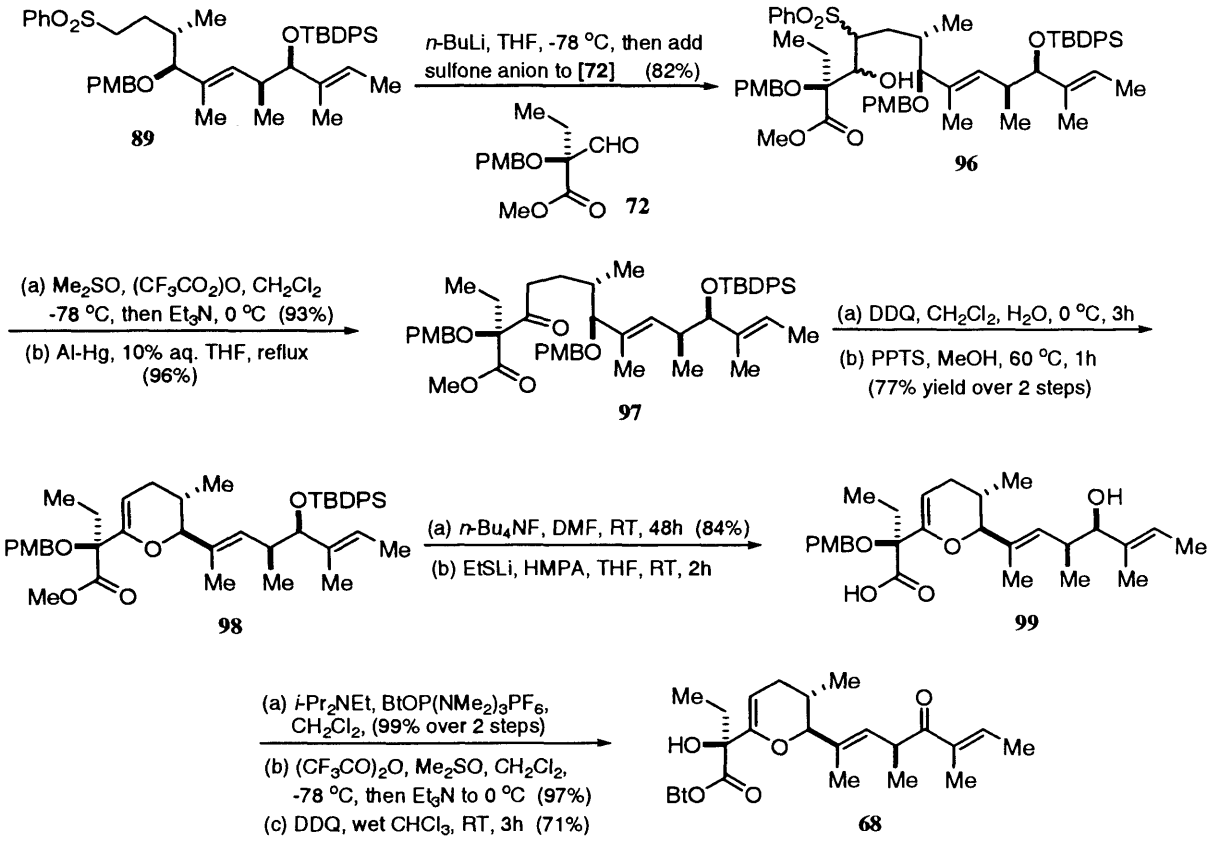

Scheme 19 Synthesis of A83586C activated ester **68**

3.2.2 SYNTHESIS OF THE CYCLODEPSIPEPTIDE HYDROCHLORIDE SALT OF A83586C

Hale's construction of the cyclodepsipeptide core of A83586C used a similar [2+2+2] fragment condensation tactic to the one employed by Durette in the synthesis of L-156,602 (Scheme 20). The cyclodepsipeptide ring of A83586C closely resembled that of L-156,602, with the presence of (3*S*)- (3*R*)-piperazic acid and (2*S*,3*S*)-3-hydroxyleucine moieties. However given all the difficulties associated with the Roche/Merck resolution methodology for obtaining the piz (piperazic acid) enantiomers, Hale considered it necessary to develop new methodology for accessing these fragments. In this regard Hale and co-workers introduced the tandem asymmetric hydrazination/nucleophilic cyclisation technology to access functionalised and nonfunctionalised homochiral piperazic acid derivatives.[170] This group also developed a new and more convenient procedure for preparing (2*S*,3*S*)-3-hydroxyleucine.[171]

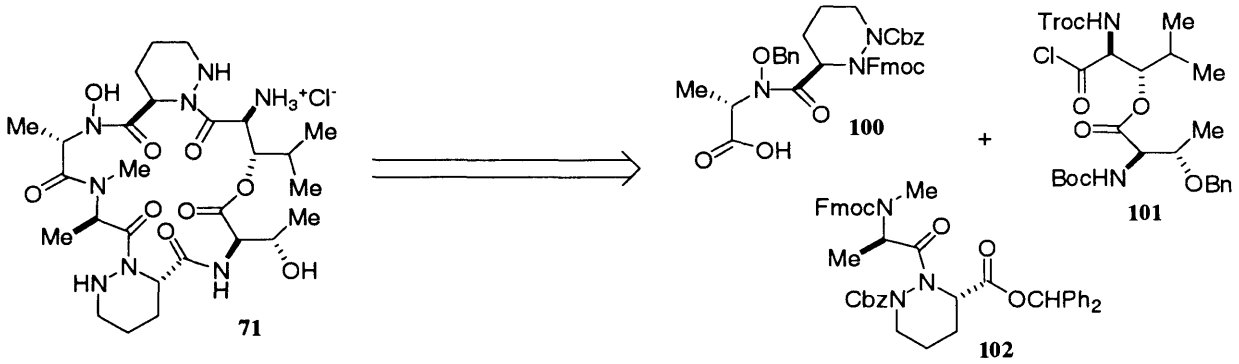

Scheme 20 Retrosynthetic analysis of the A83586C cyclodepsipeptide hydrochloride salt **71**

In the tandem electrophilic hydrazination/nucleophilic cyclisation protocol[169] a bromovaleric acid derivative was tethered onto an Evans chiral oxazolidinone **103** and an asymmetric electrophilic hydrazination[172] performed at low temperature. DMPU is then added to bring about a facile cyclisation reaction to obtain **104**.[169] The ring-closed product **104** was obtained with high overall efficiency, and its enantiomer **107** is also readily accessible by this approach. Hale and co-workers recommended that the crude product is hydrolysed by treatment with lithium hydroxide in aqueous THF and that the resulting crude acid has its Boc groups detached by treatment with anhydrous TFA. This furnishes the trifluoroacetic acid salts **105** and **108** in 68% yield from **104** and **107** respectively. In the case of **105**, it was then converted in three steps to the (3*R*)-*N*(1)-Cbz-*N*(2)Fmoc-piperazic acid chloride **31**, which was coupled with *N*-benzyloxy-L-alanine diphenylmethyl ester **109**, to afford deprotected dipeptide **100** after removal of the diphenylmethyl group.

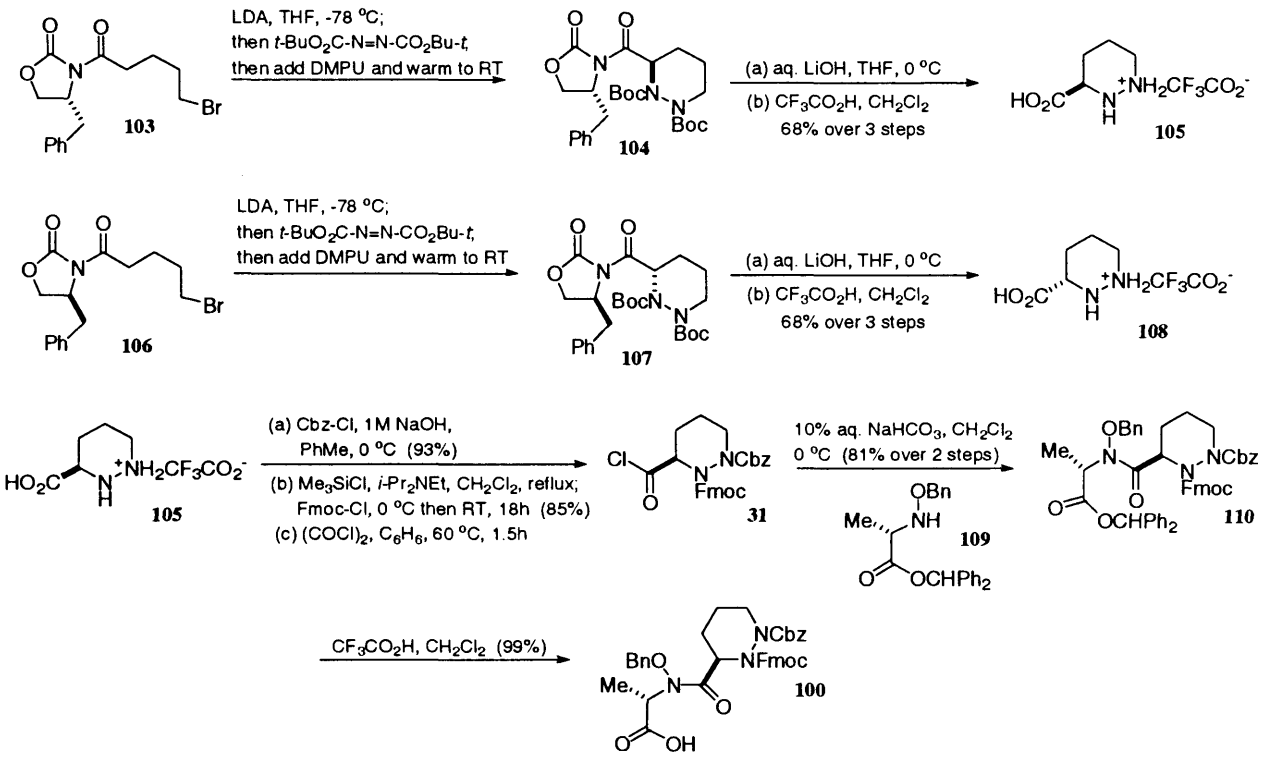

Scheme 21 Novel synthetic routes to the (3*R*)- 3(*S*)-piperazic acid trifluoroacetic acid salts **105** and **108** and synthesis of dipeptide **100**.

As well as allowing dipeptide **100** to be readily prepared, this method also allowed its dipeptide partner **114** to be readily synthesised (Scheme 22). Starting from known Fmoc-*N*-Me-D-alanine **111**, a silver cyanide-assisted coupling between the acid chloride derivative of **111** and **113** was applied to provide **102**. Acid chloride activation was again essential for the preparation of **102**, since activated ester and mixed anhydride methods both failed to mediate this particular amidation. At this stage, it was discovered that the Fmoc protecting group could not be liberated from **102** without it also causing exclusive formation of the diketopiperazine. To circumvent this problem, the diphenylmethyl ester group of **102** was replaced with a *tert*-butylcarbazide function,[173] which now permitted an efficient deprotection of the Fmoc group to obtain **114**. The [2+2] fragment condensation between **114** and **100** proceeded satisfactorily when the acid component was activated with BOP chloride to furnish **115** in 75% yield from **102**. Many activation protocols were examined before success was achieved using this reagent. To date this remains the only reagent that has successfully coupled **114** and **100**. Following Boc group removal and oxidation of the acyl hydrazine, with *N*-bromosuccinimide (NBS) in aqueous THF,[174] the resulting crude acid was esterified with diphenyldiazomethane and the Fmoc group excised to deliver **116**.

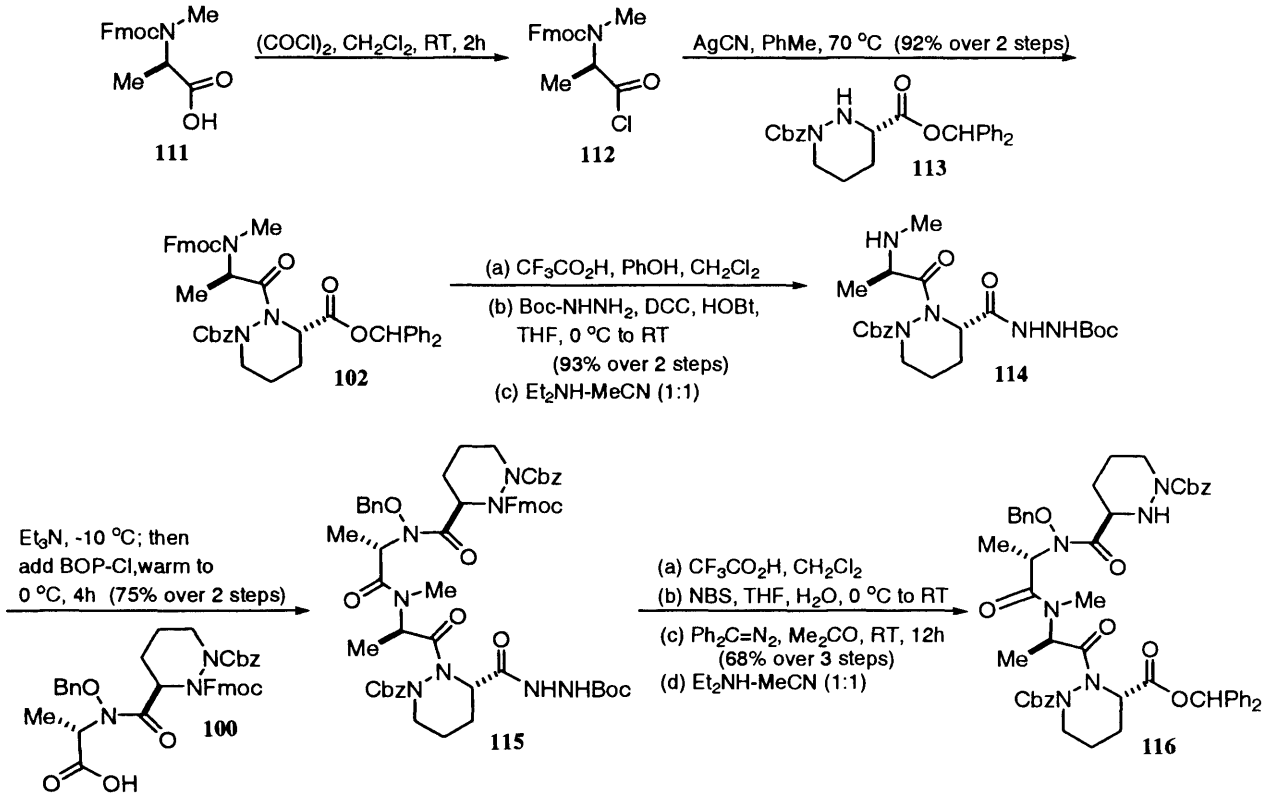

Scheme 22 Synthesis of tetrapeptide **116**

To access (2*S*,3*S*)-3-hydroxyleucine residue **41**, a Sharpless asymmetric dihydroxylation (AD)/cyclic sulphate opening with azide ion was used to install the *anti*-aminoalcohol motif (Scheme 23)[171]. Further functional group protection resulted in the Troc-protected *O*-allyl ester **120**. The depsipeptide linkage of **124** was forged through a DMAP-assisted DCC coupling between **120** and partially protected D-threonine **123**. Approximately 5-10% epimerisation was always encountered at the D-threonine unit, but since the reaction proceeded in high yield this was not essentially problematic. Palladium catalysed (Pd(0)) (Kunz-Waldmann) *O*-deallylation of **124** with morpholine and chlorination with oxalyl chloride subsequently provided the depsipeptide acid chloride **101**, which was used directly in the next step.

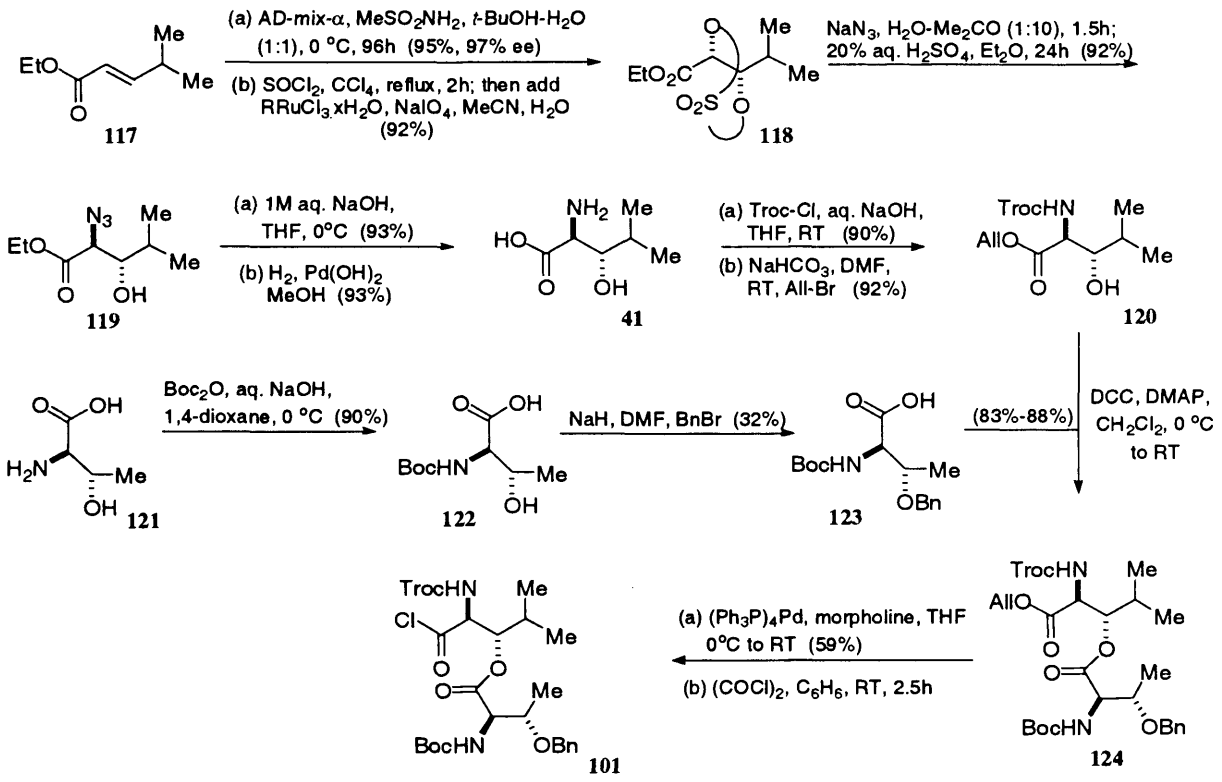

Scheme 23 New synthetic strategy to (2*S*,3*S*)-3-hydroxyleucine **41** and subsequent coupling to form depsipeptide **101**

The final stages of the A83586C endeavour involved the silver cyanide assisted amidation between **116** and **101**. This took place efficiently provided the reaction mixture was heated at 60°C for only two minutes (Scheme 24); prolonged heating invariably resulted in decomposition of **125**. The Troc group of **125** was thereafter removed with excess zinc in acetic acid[145] and the amine salt acylated with benzylchloroformate, to obtain **126** in 78% yield over the two steps. Mild acidolysis with TFA thereafter deprotected the Boc and diphenylmethyl ester protecting groups, and quantitatively furnished the key macrolactamisation precursor **127**. Following evaluation of a significant number of peptide coupling reagents for the instigation of the desired macrolactamisation, only Carpino's HATU system[175] delivered the desired product in 25-40% yield. Deprotection of this material was best accomplished by catalytic hydrogenation over Pd-C catalyst in methanolic HCl to furnish the globally deprotected cyclodepsipeptide **71**. One equivalent of acid was added to the reaction mixture to protonate the hydroxyleucine amine on its liberation, to prevent the occurrence of *O*- to *N*-acyl migration during this lengthy reaction. The final stages of the synthesis involved the rapid chemo- and regioselective coupling between **71** and **68** mediated by triethylamine, which furnished **70** in 31% overall yield from the protected macrolactam. The glycal unit of **70** was then coaxed into undergoing a very clean and highly regioselective hydration[158a,b] reaction in wet deuterated chloroform to deliver A83586C **2** in quantitative yield.

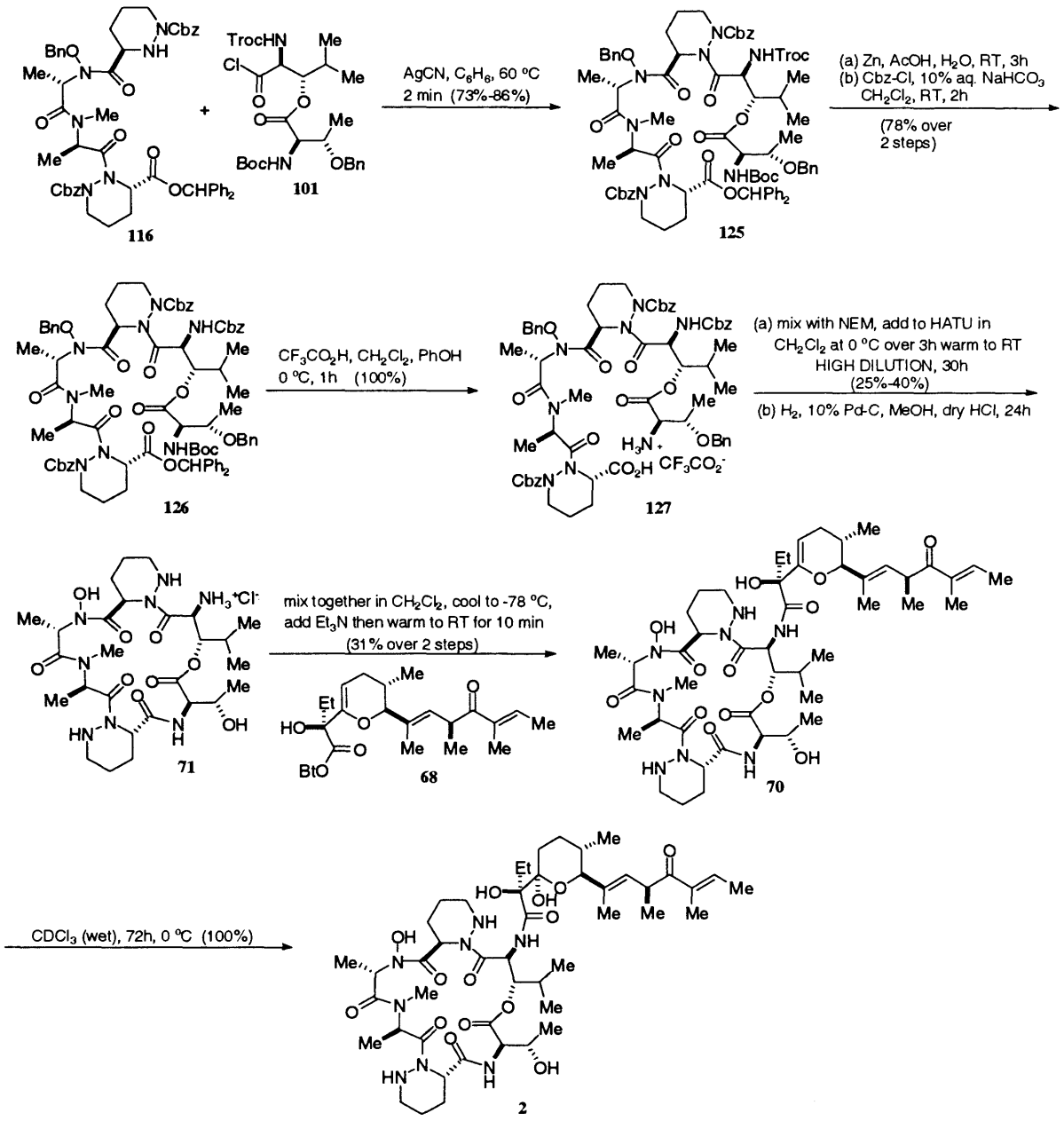

Scheme 24 Endgame strategy in the synthesis of A83586C **2**

3.2.3 TOTAL SYNTHESIS OF 4-*EPI*-A83586C

In an effort to improve the yield of the HATU[175]/NEM-mediated macrolactamisation depicted in Scheme 23, Hale and co-workers decided to evaluate the effects of BOP[156] and DMAP in this capacity[176] (Scheme 25). They discovered that rather than markedly enhancing the yield of the step, this new reagent partnership actually afforded an alternative major product **129** in 51% yield. Only a very small amount of **128** was present in the reaction mixture signifying a virtually complete epimerisation at the L-piperazic acid unit of **127**.

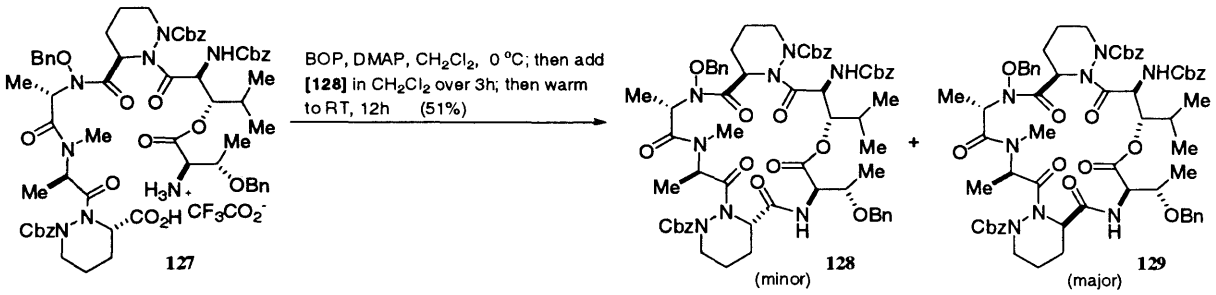

Scheme 25 Scheme to show the epimerisation at the L-piperazic acid unit of **127**

Hale and co-workers hypothesised that the enhanced basicity of DMAP, and the likely formation of acyl pyridinium intermediates, contribute to the readiness with which H(4) is abstracted and the ease of epimerisation. This chance observation enabled the Hale group to not only synthesise the desired A83586C **2** but to synthesise a novel analogue, 4-*epi*- A83586C **132** (Scheme 26) to be assessed for biological activity. Compound **129** was then globally deprotected by catalytic hydrogenation in methanolic HCl, and the resulting crude hydrochloride salt **130** was suspended in dry dichloromethane along with activated ester **68**, and the mixture cooled to -78°C, prior to the addition of triethylamine. This afforded 4-*epi*- A83586C **132** in 42% yield, and provided another interesting analogue for biological evaluation.

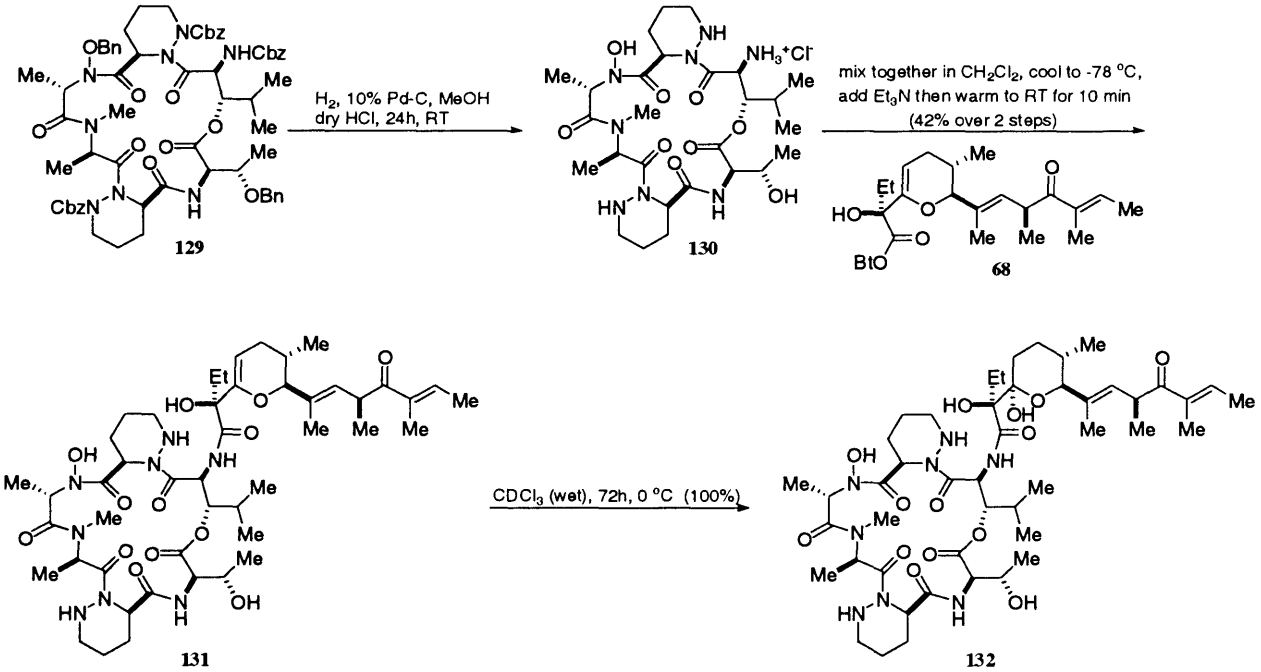

Scheme 26 Synthesis of 4-*epi*- A83586C **132**

While the BOP/DMAP mediated cyclisation served to markedly improve the overall yield of macrolactamisation from 25-40% to 70%, biological testing established that this epimerised analogue was much less potent as an antitumour drug than the parent A83586C. This served as a useful tool since the only difference between A83586C and its 4-*epi*-analogue is that the (3*S*)-piperazic acid moiety in A83586C is substituted with a (3*R*)-piperazic acid residue suggesting that variations in conformation in the cyclodepsipeptide core has very adverse effects on the antitumour potency. Detailed structural studies on **132** showed that the C(8)-carbonyl group adopts a *cis*-orientation relative to the piperazic acid N-NH bond, compared to its *trans* orientation in A83586C **2** (**Fig. 19**). These observations provided useful information to assist in the development of future analogues of the azinothricin family of antibiotics.

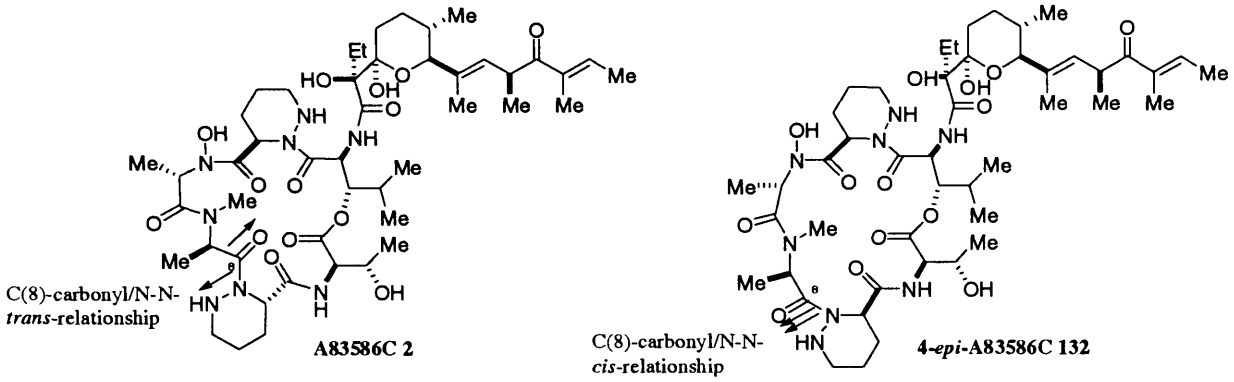

Fig. 19 Southern hemisphere conformational disparities between A83586C **2** and 4-*epi*-A83586C **133**

3.2.4 SYNTHESIS OF AN L-PROLINE MODIFIED MIMETIC OF A83586C

Following the synthesis of 4-*epi*- A83586C **132** and its consequent biological profile, Hale and co-workers sought to identify a more readily synthesised analogue of A83586C that had similar conformational properties and improved potency.[177] They chose to replace the (3*S*)-piperazic acid moiety with an L-proline derivative. Their choice of this candidate was guided by two factors:

1) Cyclisation at an active proline residue is usually free of racemisation risk.
2) (3*S*)-Piperazic acid had previously functioned as an effective mimic of L-proline in ACE-inhibitory drugs.[178]

The L-proline modified A83586C mimetic **133** (Scheme 27) was considered derivable from the chemoselective union of activated ester **68** and cyclodepsipeptide **134**, which in turn was to be synthesised from a [2+2+2] fragment condensation sequence involving **100**, **101** and **135**.

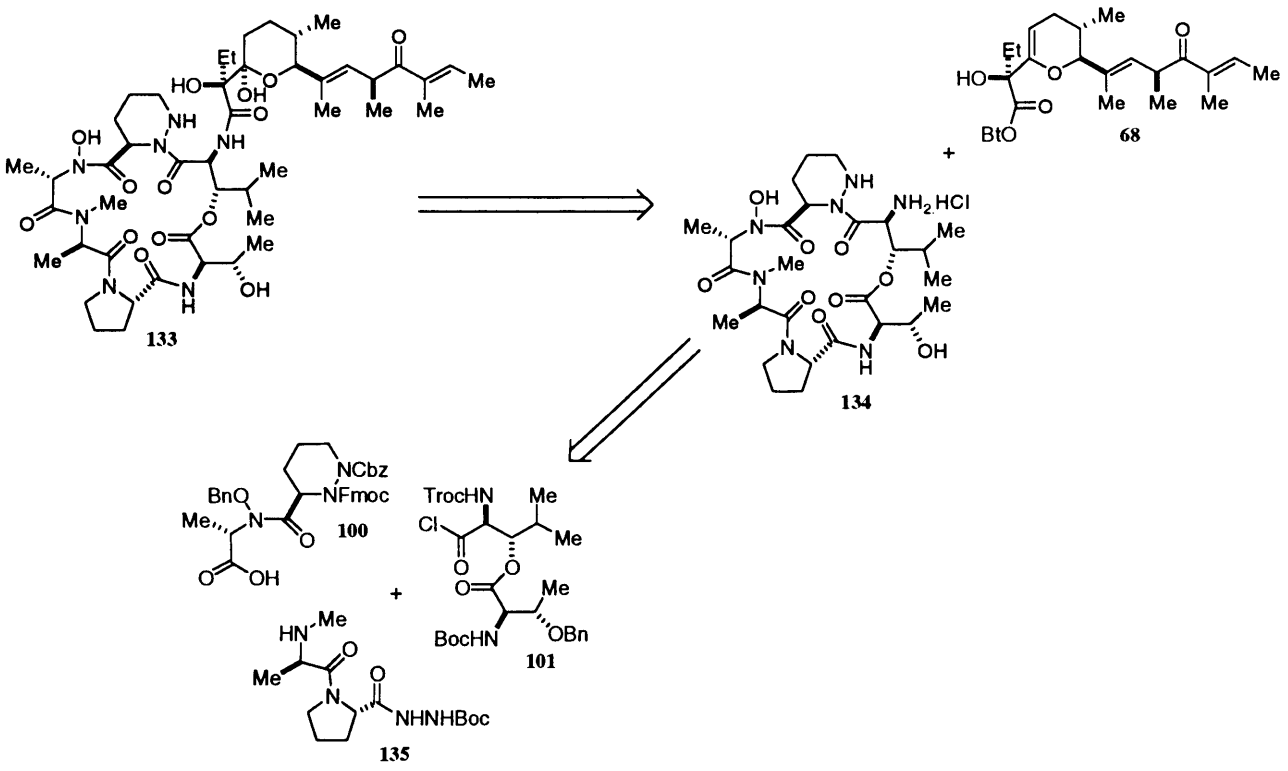

Scheme 27 Hale's retrosynthetic analysis of the L-proline mimetic of A83586C **133**

Fragments **68**, **100** and **101** were synthesised via the routes discussed in section 3.2.2; however dipeptide **135** was prepared from *N*(Cbz)- L-proline **136** (Scheme 28) by amidation with *tert*-butyl carbazate,[173] hydrogenolytic removal of the Cbz-group from **137** with a Pd/C catalyst, and a silver cyanide mediated coupling[146] with **112**. Removal of the Fmoc[179] protecting group from **138** subsequently procured **135**, and the coupling of dipeptides **135** and **100** proceeded smoothly when mediated by BOP-Cl and Et_3N, to furnish tetrapeptide **139** in 89% yield. Another Fmoc- deprotection then ensued and the subsequent silver cyanide mediated coupling of **140** with acid chloride **101** furnished the desired linear depsipeptide **141** in 73% yield. Conversion of the acyl-hydrazide of the L-proline residue to its corresponding acid by successive treatment with TFA and *N*-bromosuccinimide in aqueous THF, followed by macrolactamisation of *seco*-aminoacid **142** with HATU[175] under high dilution, afforded macrolactam **143** in 48% yield from **141**. Removal of the Troc protecting group of **143** with Zn in aqueous AcOH[180], followed by acylation with Cbz-Cl provided **144**, which was globally deprotected with Pd/C in methanolic HCl, to afford cyclodepsipeptide salt **134**. The synthesis was completed by the chemoselective coupling of

134 and **68**, in CH_2Cl_2 in the presence of Et_3N at −78 °C. After warming the reaction to room temperature, the A83586C- L-proline derivative **133** was isolated in a disappointing 17% yield.

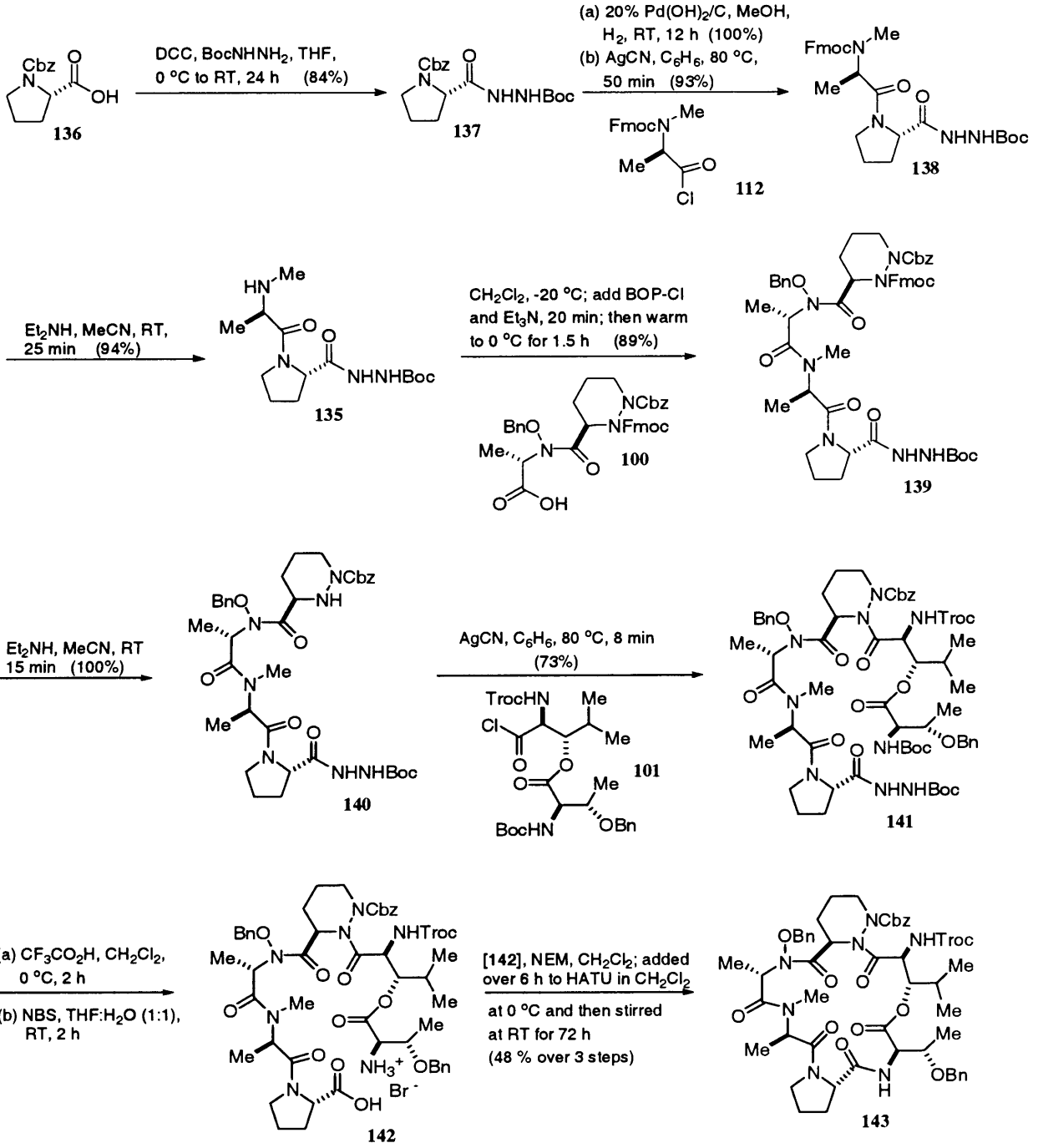

(Scheme Continued On Next Page)

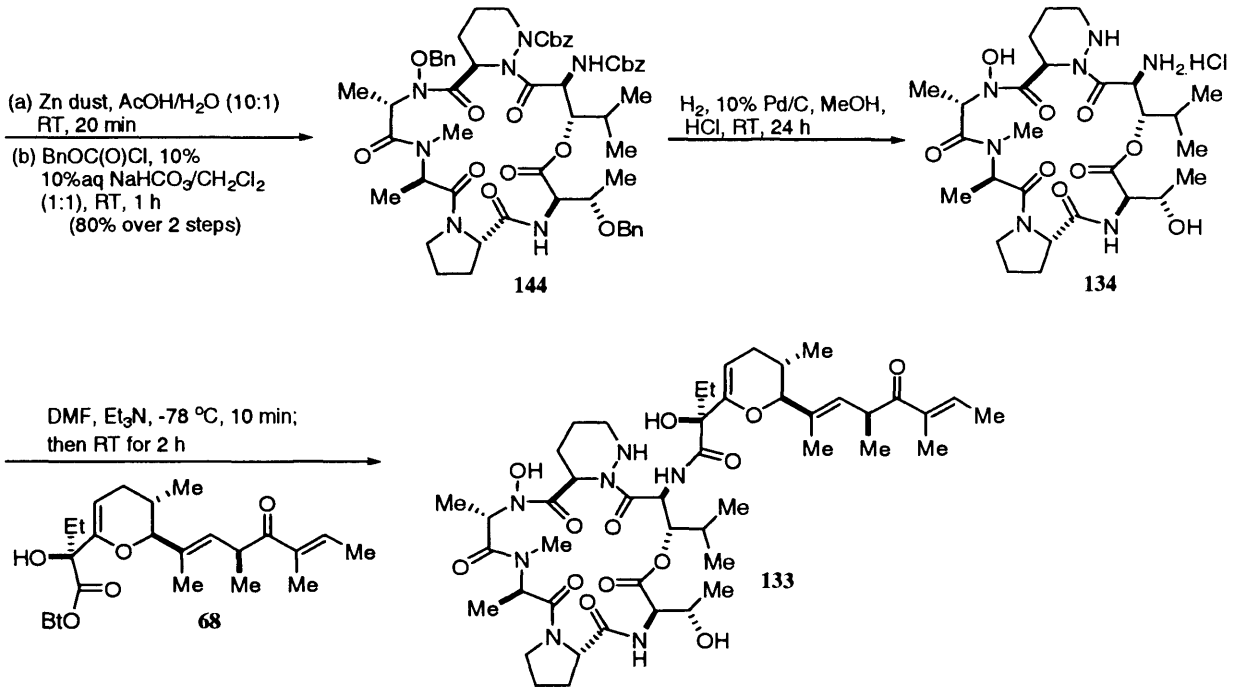

Scheme 28 Hale's route to the L-proline mimetic of A83586C **133**

3.3 SYNTHETIC STUDIES TOWARDS GE3

There have been no reported total syntheses of the antitumour antibiotic GE3 to date. However, the groups of Hale[181] and Hamada[182] have reported the first stereoselective syntheses of the respective cyclodepsipeptide **146** (Hale et al.) and tetrahydropyranyl **145** (Hamada et al.) fragments of GE3. Based on past synthetic approaches[145,146,158] one can envisage the end-game strategy for GE3 involving the chemoselective coupling of these two derived fragments.

3.3.1 SYNTHESIS OF THE GE3 TETRAHYDROPYRANYL SIDE CHAIN

The Hamada group[182] first reported the stereocontrolled synthesis of the acyl side chain segment of GE3 **4** in 2002, and their retrosynthetic strategy is depicted in Scheme 29. Disconnection between the acyl side chain and the cyclodepsipeptide fragment gave the C1-C14 segment **147** masked as an internal hemiacetal. This was then disconnected further at the C4-C5 bond to afford C1-C4 fragment **148** and C5-C14 fragment **149**. The quaternary centre in **148** was considered installable via Sharpless asymmetric dihydroxylation[167] technology on the tiglic ester **150**, and fragment **149** was to be constructed using the diastereoselective *syn* and *anti* aldol condensations with the respective Evans[159(a)] and Paterson[183] chiral auxiliaries.

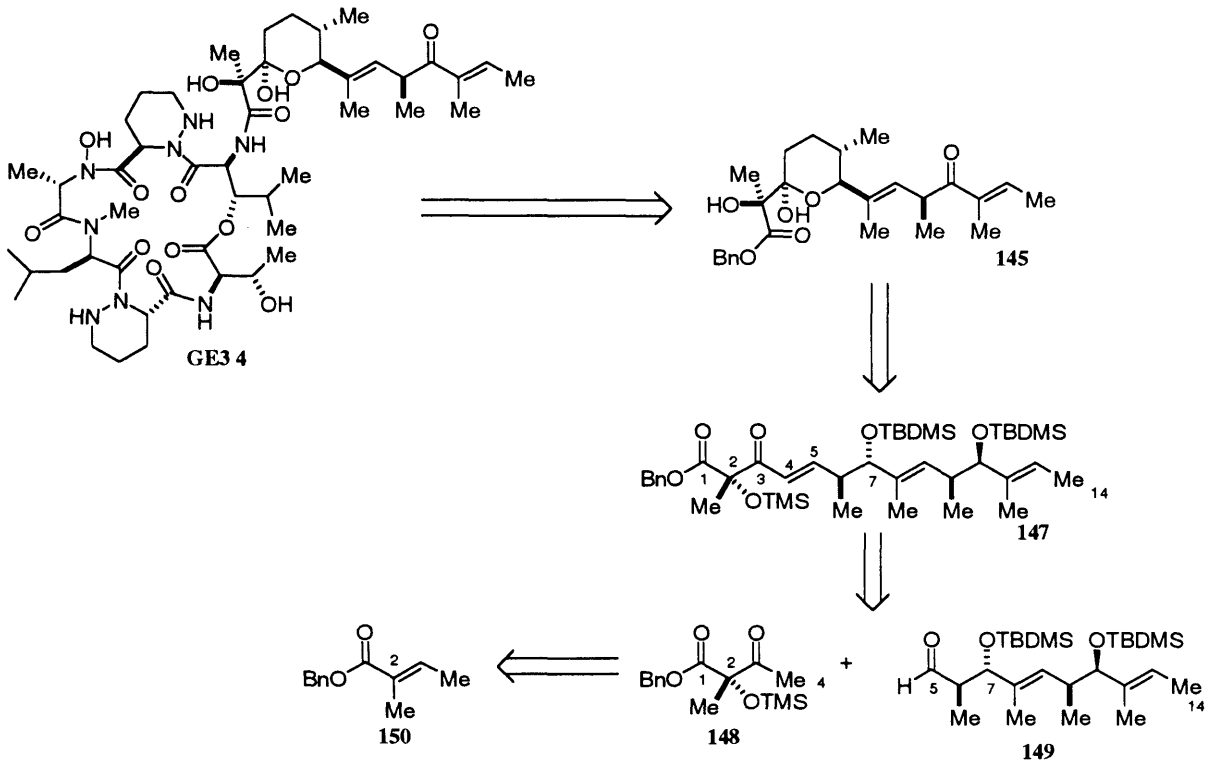

Scheme 29 Hamada's retrosynthetic approach to the acyl side chain of GE3 **145**

Hamada's expeditious route to fragment **148** is outlined in Scheme 30. The commercially available benzyl tiglate **150** underwent a Sharpless asymmetric dihydroxylation with AD-mix-β, and selective oxidation with sulphur trioxide-pyridine complex in DMSO to afford the ketone **151** in 96% yield. The route was completed with the protection of the tertiary alcohol of ketone **151** as a trimethylsilyl (TMS) ether in 94% yield.

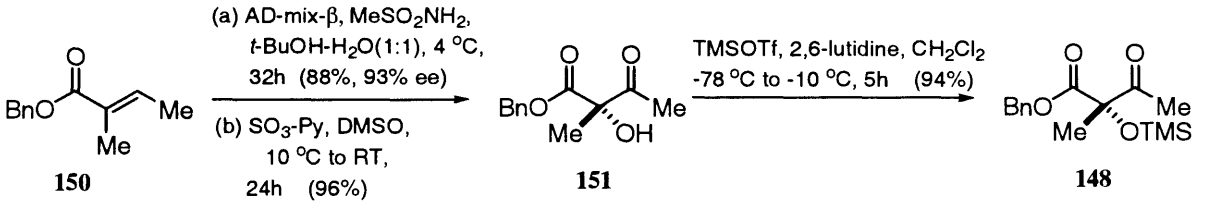

Scheme 30 Synthesis of Hamada's C1-C4 fragment **148** of GE3 acyl side chain

The synthesis of the C5-C14 fragment **149** was initiated by employing Evans aldol methodology[184] as depicted in Scheme 31. A *syn*-aldol condensation reaction was effected between the boron enolate derived from *N*-propionyl-2-oxazolidinone **152** and tiglic aldehyde **76** to give the diastereomerically pure adduct **153** in 48% yield. This unexpectedly low yield was improved by employing the use of a titanium enolate, which afforded the desired *syn*

adduct **153** along with its diastereomer in a 13:1 ratio and 92% yield. Protection of the resultant alcohol as a *tert*-butyldimethylsilyl ether and auxiliary cleavage with lithium ethanethiolate thereafter provided the thiol ester **154** in 85% yield. After the reduction of the thiol ester to an aldehyde according to Fukuyama's method,[185] a Wittig reaction with ethyl 2-(triphenylphosphoranyldiene) propionate gave the (*E*)-α,β-unsaturated ester **155** in 86% yield. Reduction of ester **155** with DIBAL and oxidation of the resulting allylic alcohol with active MnO_2[186] afforded aldehyde **156** in 94% yield. Paterson's *anti* aldol technology was then used to set the C(6) and C(7) stereocentres, this entailed performing a stereocontrolled condensation between **156** and the lactate-derived ketone **157**, via its dicyclohexylboronate. Compound **158** was formed as the sole product in 99% yield. Protection of the C(7) alcohol in **158** as a TBDMS ether followed by reduction of the carbonyl function with lithium aluminium hydride gave the *vic*-diol **159** in 82% yield. The route was completed via oxidative cleavage with sodium metaperiodate and furnished the desired fragment **149** in 93% yield.

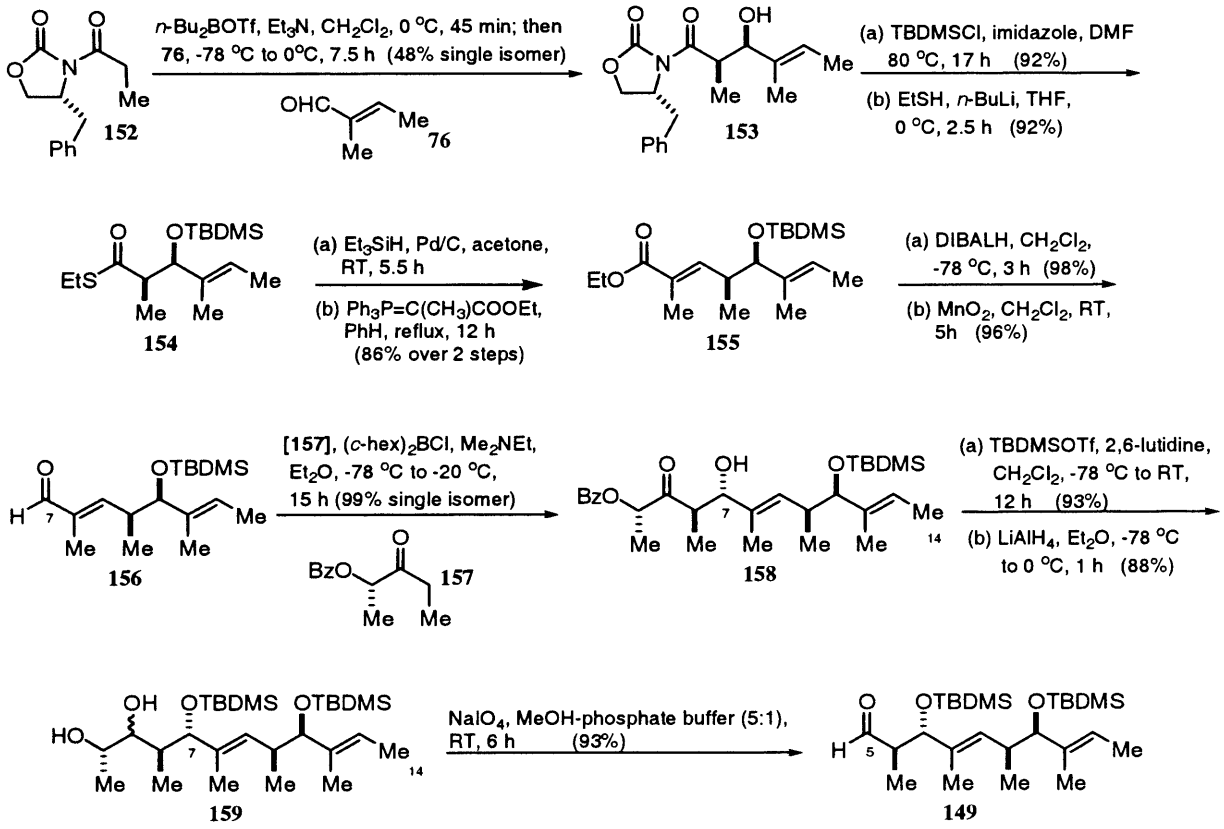

Scheme 31 Synthesis of Hamada's C5-C14 fragment **149** of GE3 acyl side chain

With key intermediates **148** and **149** now in hand, the synthesis of the target hemiacetal was completed in a further 5 steps (Scheme 32). Fragment coupling of **148** and **149** was achieved using an aldol condensation mediated by LDA-$ZnCl_2$ in THF;[187] a 4:1 mixture of aldol adducts **160** was obtained in 83% yield. Successive mesylation and elimination of the C5 hydroxy group, in the presence of excess triethylamine, provided the

desired (*E*)-α,β-unsaturated ketone **147** in moderate yields as a mixture with unreacted **160**. However, the use of Burgess reagent[188] as a dehydrating reagent afforded ketone **147** in good yield. Treatment of **147** with Stryker's reagent $[(Ph_3P)CuH]_6$[189] and subsequent deprotection of the TMS ether produced alcohol **161** in 54% yield. The synthesis was completed with the removal of the TBDMS ether and concurrent hemiacetal formation to furnish the GE3 acyl side chain **145** in 49% yield.

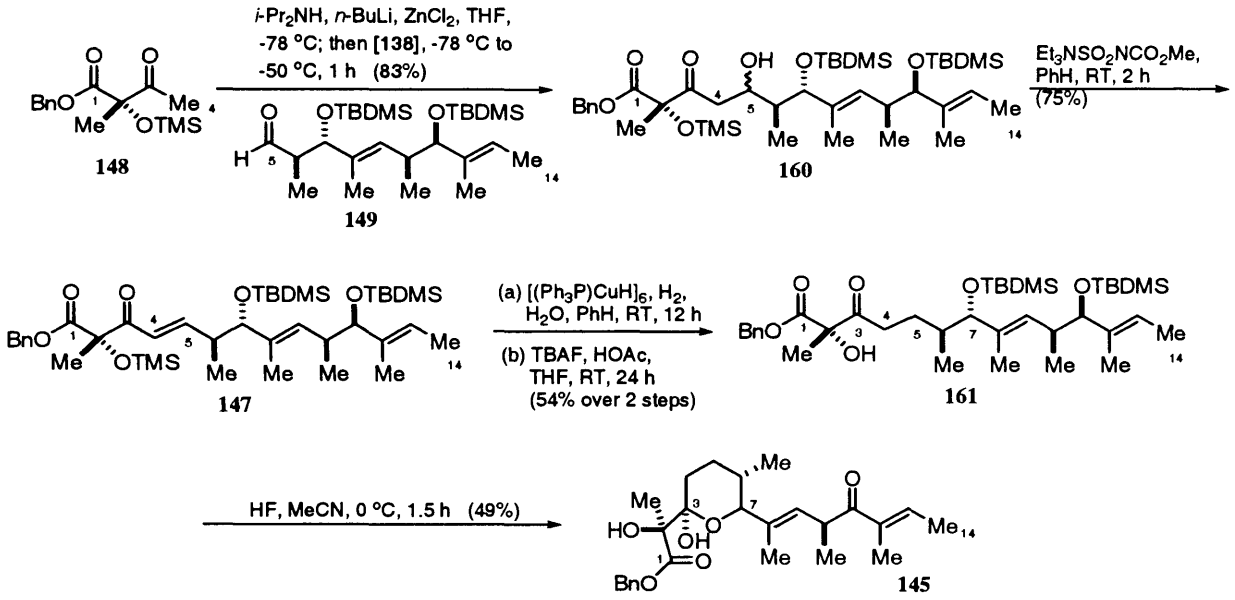

Scheme 32 Unification of fragments **148** and **149** and subsequent synthesis of the GE3 acyl side chain **145**

3.3.2 SYNTHESIS OF CYCLODEPSIPEPTIDE HYDROCHLORIDE SALT OF GE3

The Hale group[181] were the first to report a stereocontrolled synthesis of the cyclodepsipeptide core of GE3 **4** in 2002. Their retrosynthetic planning for GE3 (Scheme 33) was identical to that of A83586C, and was predicated upon the biogenetically inspired coupling of cyclodepsipeptide **146** with activated benzotriazole ester **162**. Likewise the assembly of cyclodepsipeptide **146** was predicated upon the tested [2+2+2] union of **100**, **101** and **163**.

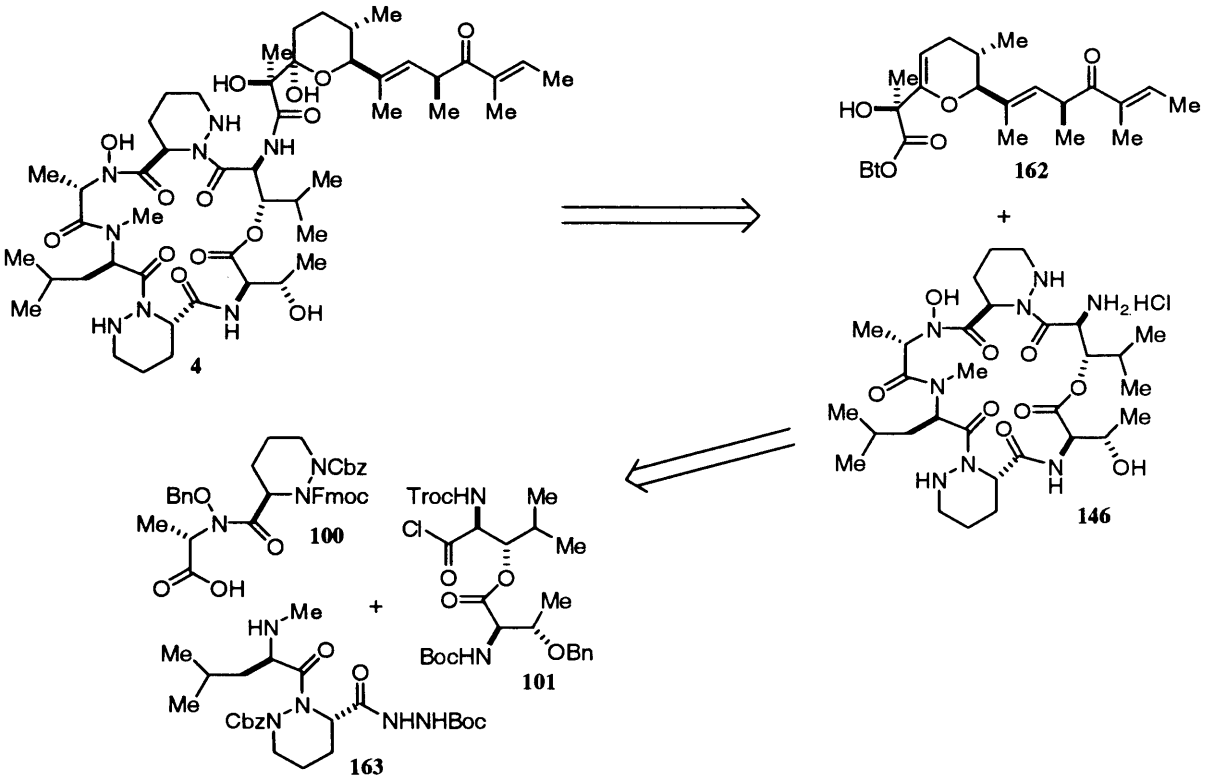

Scheme 33 Hale's retrosynthetic analysis of the GE3 antitumour antibiotic **4**

Since the relevant technology was available for the synthesis of dipeptides **100** and **101**, their attention was focussed upon the assembly of dipeptide **163**. The synthesis of **163** (Scheme 34) commenced from known (3*S*)-*N*(1)-Cbz-piperazic acid **30**. Compound **30** was directly converted to the acyl hydrazide **164** by treatment with *tert*-butyl carbazate, DCC and HOBt in THF, without any need for protecting the free NH. A silver cyanide-mediated chemoselective coupling was then effected between **165** and **167**. The latter was itself synthesised in four steps from the commercially available D-leucine **165** to afford **168** in 90% yield. Following Fmoc-excision, a wide variety of conditions were evaluated for effecting the desired [2+2] coupling between **163** and **100**. After much effort it was discovered that only the combination of BOP-Cl and collidine could mediate the successful union of these two fragments, and this regime afforded the tetrapeptide **169** in 66% yield. Significantly, the BOP-Cl/Et_3N coupling conditions that had previously worked so successfully in the A83586C venture failed in this system. After Fmoc-deprotection of the (3*R*)-piperazic acid residue for **169**, the final fragment condensation was attempted with **170**, and the previously prepared acid chloride **101** in the presence of AgCN, this desired [4+2] coupling proceeded in 65% yield. Following cleavage of the two Boc groups with TFA and oxidation of the liberated *N*-acyl hydrazine with NBS in aqueous THF, the amino acid cyclisation precursor **172** was obtained. A Carpino HATU-mediated cyclisation[175] was then implemented at high dilution in CH_2Cl_2; the desired macrolactam **173** was isolated in 40% yield over the three steps from **171**. Customary *N*-Troc to *N*-Cbz interchange followed next and greatly facilitated the final purification of **174**. The latter was then cleanly deprotected by catalytic hydrogenation under

mildly acidic conditions over 10% Pd/C to quantitatively furnish the desired cyclodepsipeptide hydrochloride salt **146**.

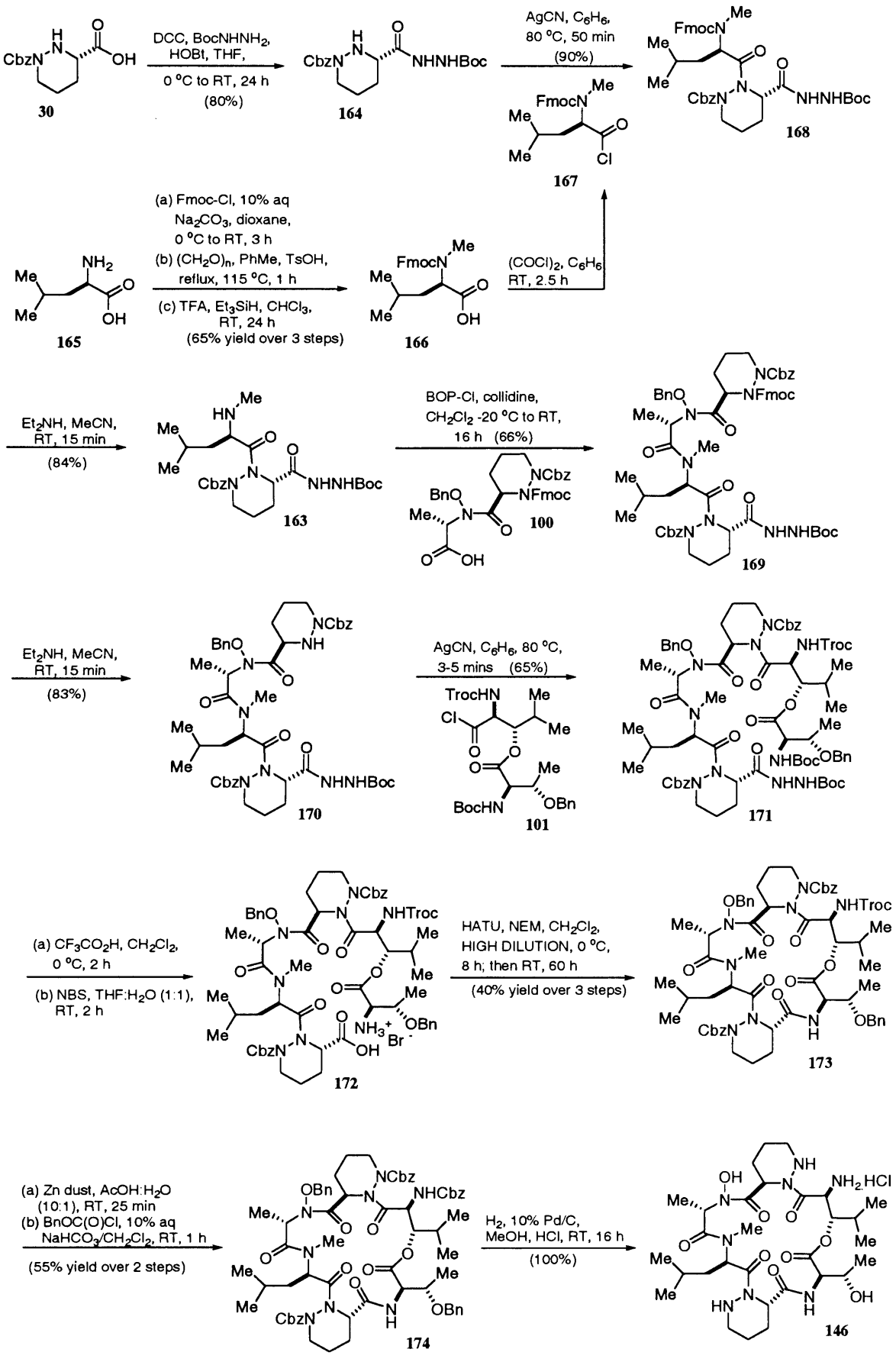

Scheme 34 Route to the cyclodepsipeptide hydrochloride salt of GE3 **146**

3.3.3 SYNTHESIS OF GE3/A83586C HYBRID ANTITUMOUR ANTIBIOTIC

With the technologies now in hand for the syntheses of the cyclodepsipeptide core of GE3 and the activated benzotriazole ester of A83586C, Hale and co-workers decided to attempt the synthesis of an A83586C/GE3 hybrid to evaluate its biological properties. Based upon the findings of 4-*epi*-A83586C, where conformational perturbations in the cyclodepsipeptide core all but eliminated biological potency, they thought it would be interesting to see how a hybrid of these two natural products affected the potency. The biological profiles of GE3 and A83586C were reported by Sakai et. al.[12] and Smitka et. al.[9] respectively, and Hale et al. wanted to see if a hybrid would have enhanced antitumour effects. During the final stages in the synthesis of L-156,602 Caldwell and Durette coupled the linear hexadepsipeptide **23** with the hydroxybenzotriazole ester **11** (Scheme 13 p. 39) in DMF[145], and the step proceeded with a 56% yield. Hale and Lazarides therefore decided to follow suit[190] and attempt the coupling between **146** and **68** in DMF with a reduced amount of Et_3N (2 equiv c.f. 11.2equiv) (Scheme 35). After purification and hydration in wet $CDCl_3$ they afforded the hybrid antitumour antibiotic **175** in 41% yield, providing another interesting molecule for biological evaluation.

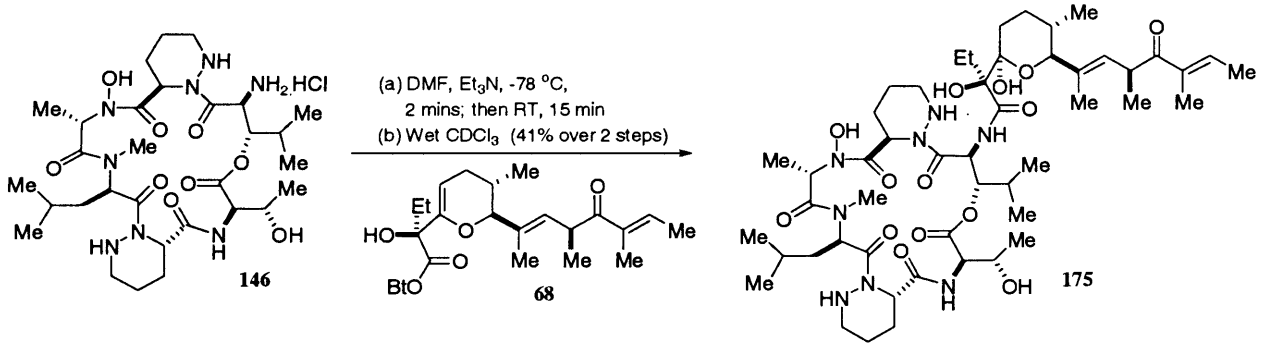

Scheme 35 Synthesis of GE3/A83586C hybrid antitumour antibiotic **175**

3.4 SYNTHETIC STUDIES TOWARDS VERUCOPEPTIN

The relative and absolute stereochemistry of verucopeptin remains undetermined and consequentially there are eight diasteromeric possibilities for the cyclodepsipeptide core of the molecule. Despite this Hale and co-workers sought to synthesise the cyclodepsipeptide sector of verucopeptin, based on the assumption that since verucopeptin is a member of the azinothricin class of natural products, its northern sector would contain (3*R*)-piz and (2S,3S)-3-hyroxyleucine residues.[191] Based on this conclusion Hale and co-workers reported the synthesis of the cyclodepsipeptide core of verucopeptin in 2001. From their previous

experiences with A83586C and its 4-*epi*-analogue they envisioned constructing the 19-membered linear hexadepsipeptide via a [2+2+2]-fragment condensation between **178**, **179**, and **180** (Scheme 36). This would furnish the cyclisation precursor **183**, which would then undergo macrolactamisation between its Gly and Sar termini and global deprotection to provide **177**. Although this was the originally conceived approach, they nevertheless chose to pass this strategy over in favour of a [3+3] fragment condensation strategy, as the latter would be more convergent.

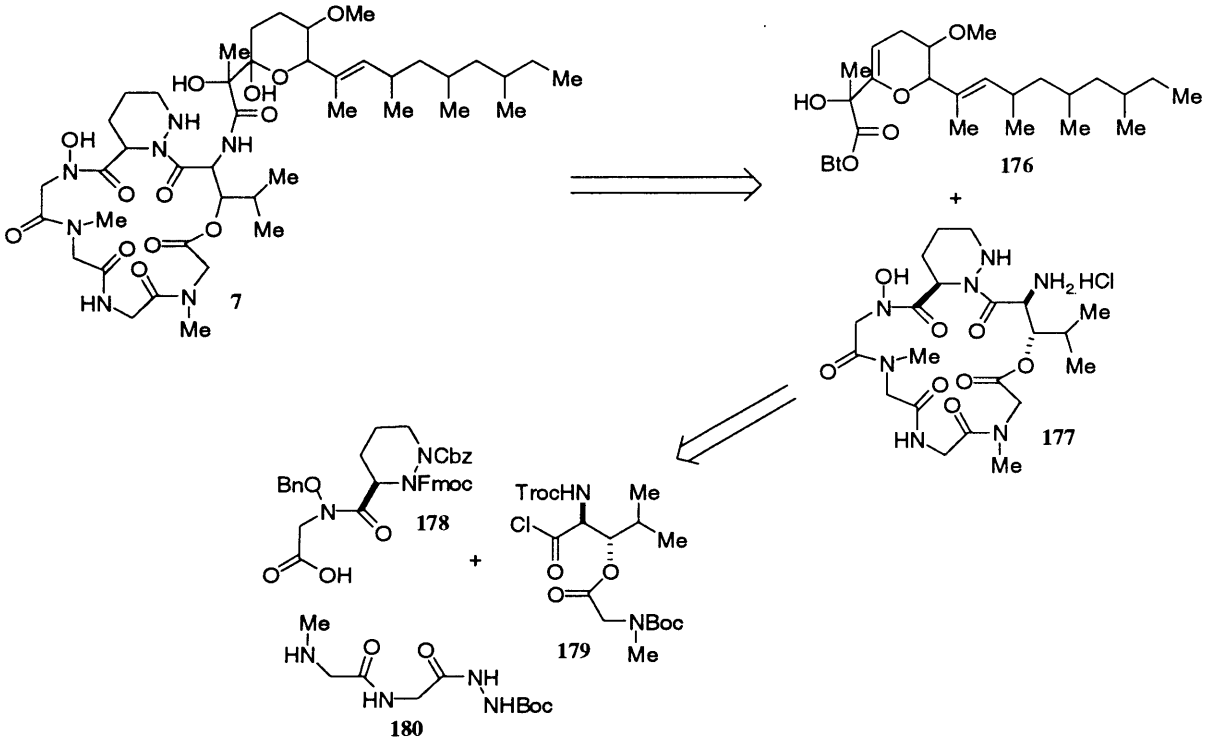

Scheme 36 Hale's retrosynthetic analysis of Verucopeptin **7**

3.4.1 SYNTHESIS OF THE CYCLODEPSIPEPTIDE HYDROCHLORIDE SALT OF VERUCOPEPTIN

With this in mind Hale's original synthetic strategy was to construct the macrolactamisation precursor **183** via a [3+3]-fragment condensation (Scheme 37) between tripeptides **181** and **182**. However, after a variety of attempts employing varied reaction conditions, no reaction was observed.[192] This prompted the group to revert to the familiar [2+2+2] technology utilised in the syntheses of A83586C, L-proline A83586C, GE3 and 4-*epi*-A83586C molecules.

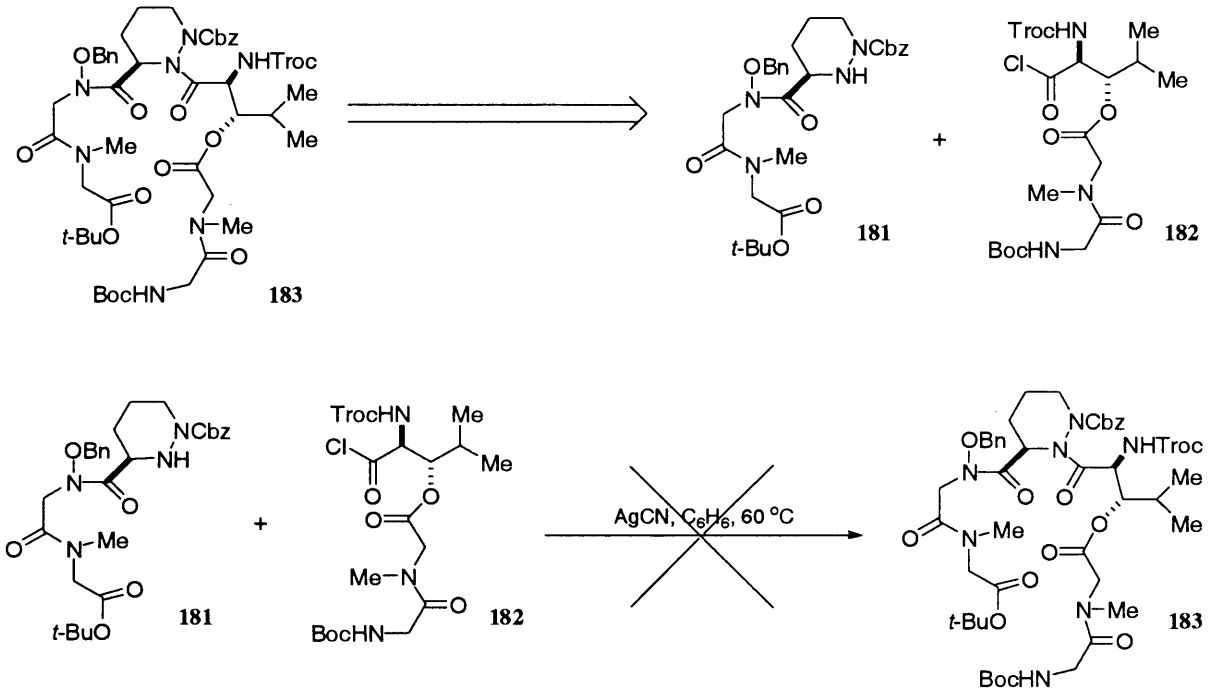

Scheme 37 Hale's original synthetic strategy towards the cyclodepsipeptide core of verucopeptin **7**

The verucopeptin cyclodepsipeptide synthetic venture commenced with the synthesis of dipeptide **181**, which required preparation of the protected hydroxamic acid **184**. This was synthesised according to the method of Kolasa and Chimiak[193] (Scheme 38). The acid functionality was temporarily protected as a diphenylmethyl ester,[195] and the free amine coupled to the known (3*R*)-piperazic acid chloride **31** under AgCN-assisted amidation conditions[145,158,176] in excellent yield. The diphenylmethyl ester group was then cleaved from **186** with TFA, to obtain acid **178** in 96% yield.

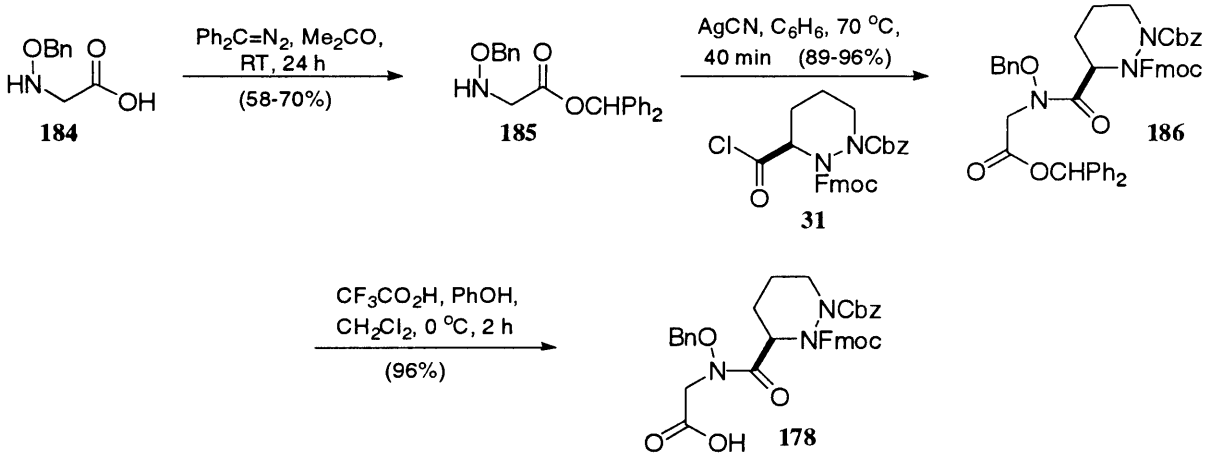

Scheme 38 Hale's synthetic route to dipeptide **178**

The next step of the synthesis was construction of dipeptide **180** (Scheme 39), which was achieved using standard DCC conditions[195] for the coupling of **187** and **188**. A *tert*-butyl carbazate group was selected to protect the Gly acid, as previous experience dictated that this was the most feasible group to avoid undesired diketopiperazine formation during Cbz removal (Sect. 3.2.2, p. 45). The Cbz group of **189** was cleaved via hydrogenolysis to quantitatively yield the tetrapeptide precursor **180**. With dipeptides **178** and **180** now in hand their union was effected with BOP-Cl[196] and triethylamine at low temperature. Following Fmoc-group removal with diethylamine in MeCN, tetrapeptide **191** was isolated in 87% yield.

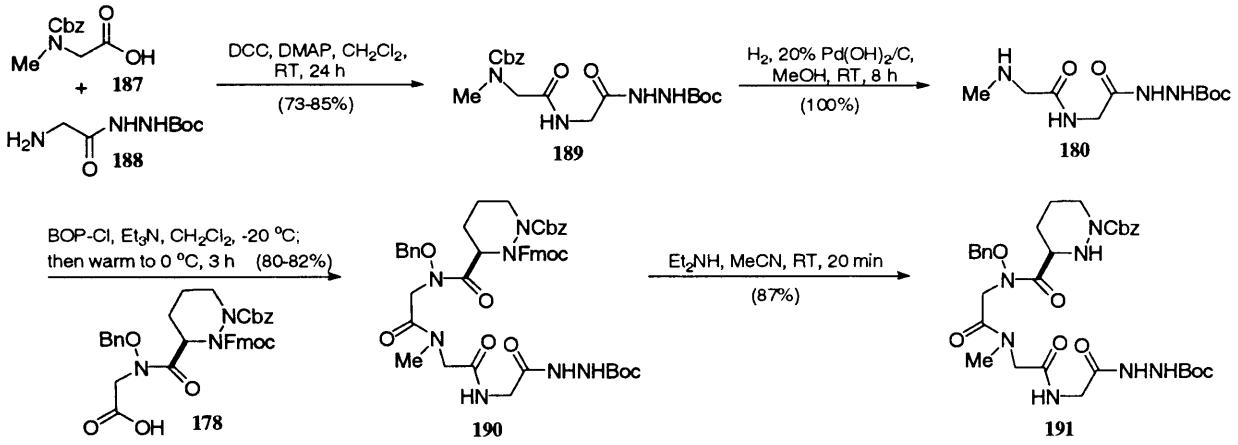

Scheme 39 Hale's synthetic route to dipeptide **180** and subsequent silver cyanide coupling to form tetrapeptide **191**

The final fragment to be synthesised was acid chloride **179**, which was prepared from the known amino acids **120** and **192** according to Scheme 40. This sequence proceeded with a DCC-DMAP mediated *O*-esterification, to obtain **193**, followed by a Kunz-Waldmann *O*-deallylation with Pd(0) and morpholine to unmask the acid, and a chlorination with oxalyl chloride in benzene to obtain **179**. The chemoselective union of **191** and **179** was effected by heating in benzene at 80 °C for 2-3 minutes in the presence of AgCN, to afford protected linear hexadepsipeptide **194** in very good yield. Treatment of **194** with TFA and chemoselective oxidation of the Gly hydrazide grouping (in the presence of the Sar amine), with *N*-bromosuccinimide in aqueous THF, provided the macrolactamisation precursor **195**, which cyclised in the presence of HATU[175] under conditions of high dilution to afford **196** in 67% yield from **194**. Detachment of the Troc-group was achieved with Zn dust in aqueous acetic acid, and was followed by protection with benzylchloroformate under classical Schotten-Baumann conditions in good yield. Global deprotection of **197** was then achieved via hydrogenolysis with Pd/C under mild acidic conditions; it quantitatively furnished the verucopeptin cyclodepsipeptide hydrochloride salt **177**.

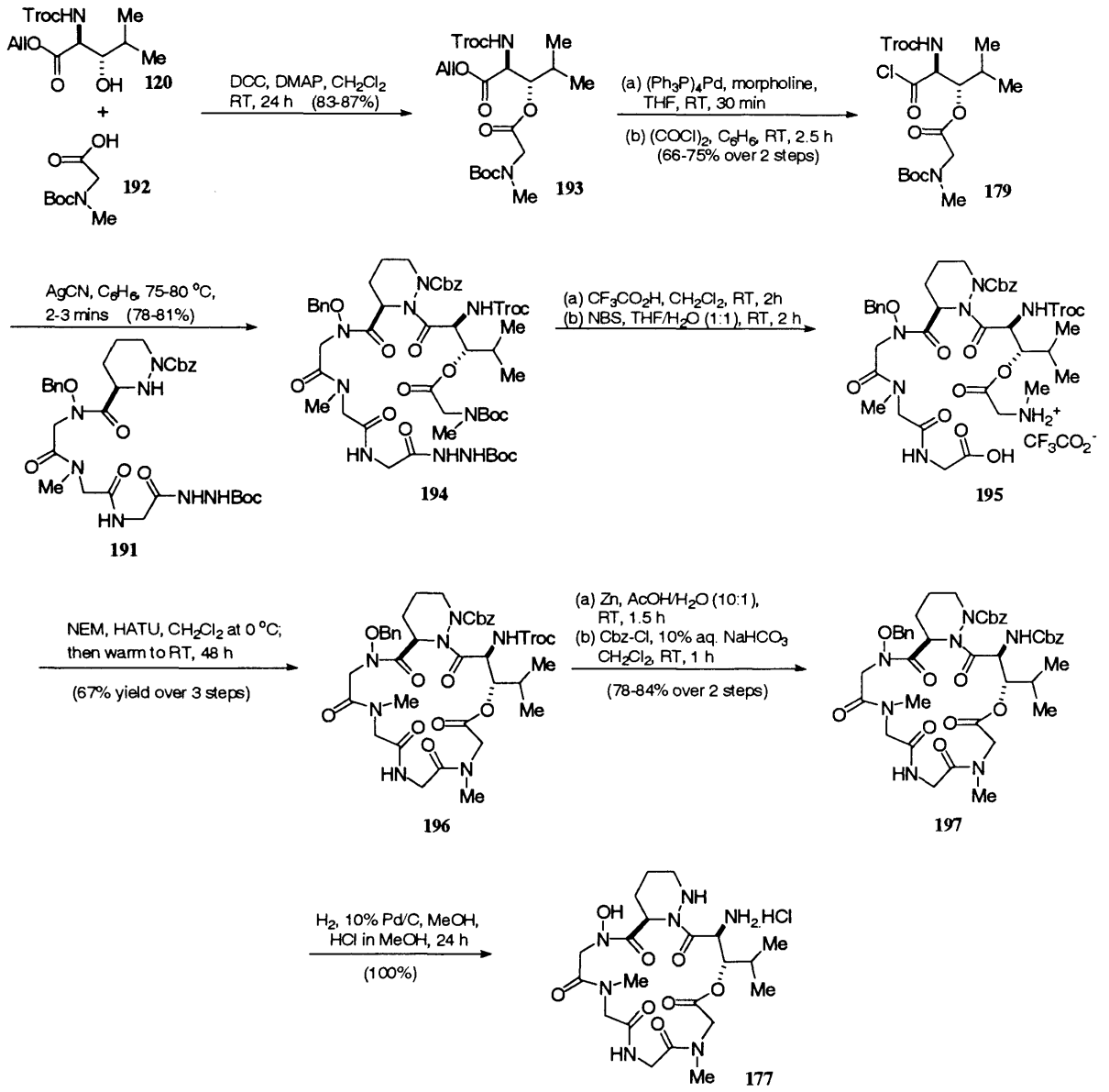

Scheme 40 Hale's endgame to the verucopeptin cyclodepsipeptide hydrochloride salt **177**

3.5 SYNTHETIC STUDIES TOWARDS POLYOXYPEPTIN A

Polyoxypeptin A **9** is a molecule that has not been fully synthesised to date. However, as with GE3 (p. 55), syntheses of various fragments have been fully achieved by a number of research groups. While the cyclodepsipeptide core of polyoxypeptin A has similarities to the azinothricin family, in terms of amino acid residues, there are also distinct differences between them. There are two amino acid residues present in polyoxypeptin A that are not present in any of the azinothricin family; these being the novel (2*S*,3*R*)-3-hydroxy-3-methylproline and (3*R*,5*R*)-5-hydroxypiperazic acid. The first stereoselective synthesis of (2*S*,3*R*)-3-hydroxy-3-methylproline was achieved by Kobayashi[197] and co-workers in 2001.

This was followed in 2002 by two more reported syntheses by Yao[198] and Hamada[199] respectively. Previous methods for obtaining (3*R*,5*R*)-5-hydroxypiperazic acid involved an uneconomical optical resolution of the racemate with quinine.[201] However, in 1998 Hale and co-workers[170(c)] devised an efficient enantiospecific synthesis of (3*R*,5*R*)-5-hydroxypiperazic acid and this was followed by Danishefsky[201] and co-workers in 2000. Syntheses of the acyl side chain of polyoxypeptin A have been accomplished by the groups of Kobayashi[202], Kurosu[203] and Yao[204] and we shall now discuss these in further detail.

3.5.1 SYNTHESIS OF THE ACYL SIDE CHAIN OF POLYOXYPEPTIN A

The acyl side chain of polyoxypeptin A **9** is very similar to that of L-156,602 **5**, the only distinguishing factor being the presence of an ethyl substituent at C-5 of the pyran in polyoxypeptin A compared with a methyl substituent at the same position in L-156,602 (**Fig. 20**).

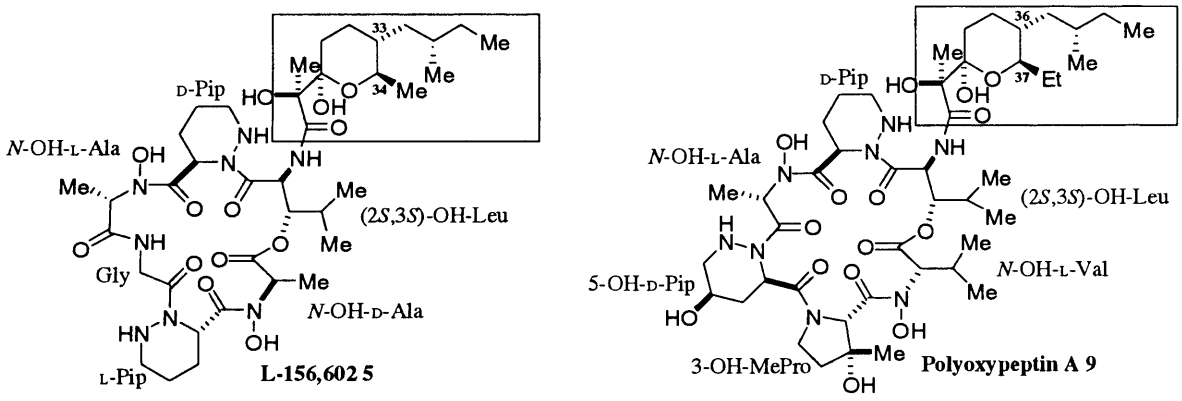

Fig. 20. Comparison of the lipophilic side chain structures of L-156,602 **5** and polyoxypeptin A **9**

Kobayashi and co-workers reported the first synthesis of the acyl side chain segment **199** of polyoxypeptin in 2000[202] based upon the Pd-catalysed hydrogenolysis of 4,5-epoxy-2-alkenoate **203**. Kobayashi's retrosynthetic analysis of the acyl side chain **199** is depicted below (Scheme 41). He envisioned the α,β-keto ester (C1-C3) moiety in **200**, including the quaternary centre at C2, being installed via the asymmetric dihydroxylation of trisubstituted olefin **201**; which, in turn, could be derived from unsaturated ester **202** by a conventional Wittig approach. Pd-catalysed hydrogenolysis methodology, devised in the group[205], could be employed to convert the (*Z*)-alkenyloxirane **203**, obtained from allylic alcohol **204** via epoxidation and a (*Z*)-selective Horner-Emmons reaction, into the requisite *anti*-isomer **202**.

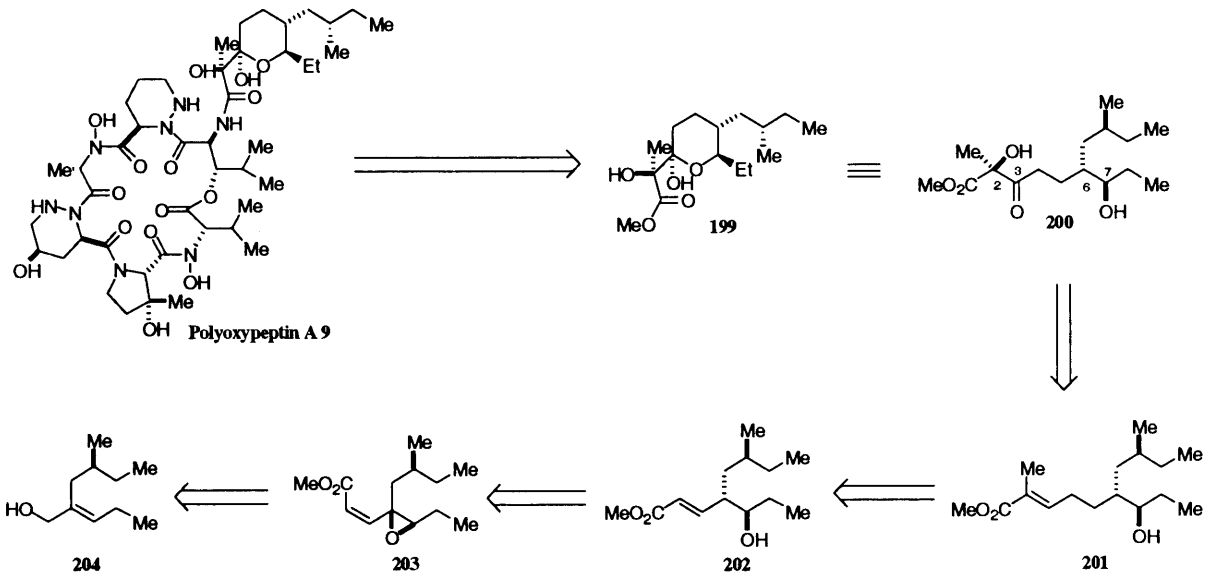

Scheme 41 Kobayashi's retrosynthetic analysis of the polyoxypeptin A acyl side chain **199**

Alkenyloxirane **203** was synthesised in nine steps from chiral alcohol **205**, which in turn, was readily prepared from L-(+)-isoleucine (Scheme 42) by a known procedure.[206] Alcohol **205** was transformed into phosphonium bromide **206**, and so-derived phosphonium ylide was acylated with methyl chloroformate and the resulting stabilised ylide reacted with propionaldehyde **207** to afford (*E*)-alkenoate **208** in 40% yield based on chloroformate. A DIBAL reduction was next effected and the resulting allylic alcohol **204** was subjected to Sharpless asymmetric epoxidation[207] using D-(-)-tartrate to provide the epoxyalcohol **209** in 75% yield (99% de). Oxidation of **209** under Swern conditions, and treatment of the resulting aldehyde reacted with the (*Z*)-selective phosphonate $[(CF_3CH_2O)_2P{=}OCH_2CO_2Me]$[208] afforded the desired (*Z*)-alkenyloxirane intermediate **203** in 81% yield from **209**.

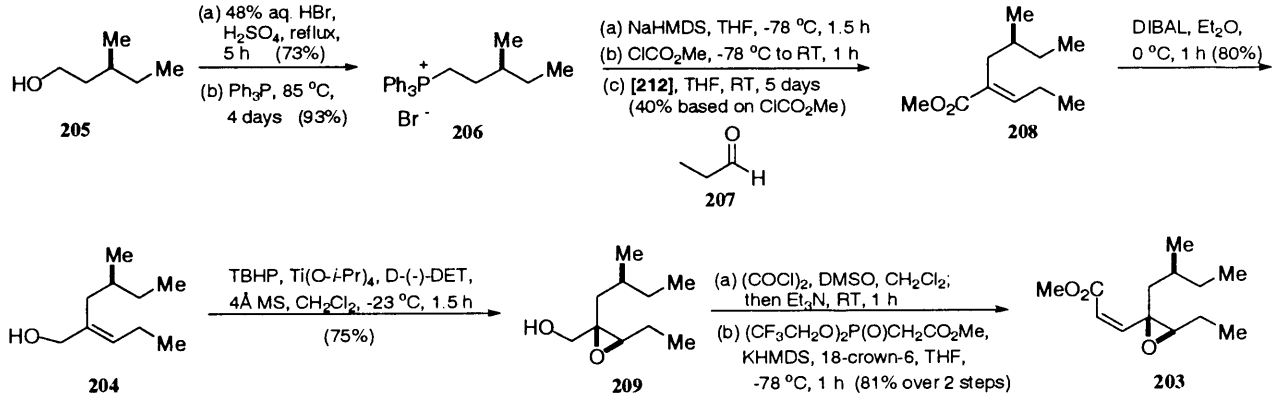

Scheme 42 Kobayashi's route to (*Z*)-alkenyloxirane **203**

The (*Z*)-alkenyloxirane **203** was then subjected to a modified stereospecific Pd-catalysed hydrogenolysis[205] in DMF at RT to obtain the desired *anti*-isomer **202** in 73% yield with high stereospecifity (*anti*:*syn*/96:4) (Scheme 43). Following protection of the alcohol as a TBDPS ether, the unsaturated ester **210** was reduced to alcohol **211** in high yield. Oxidation of **211** under Swern conditions, followed by a Wittig reaction on the resulting aldehyde with phosphorane afforded unsaturated ester **212** as a single stereoisomer. Sharpless asymmetric dihydroxylation with AD-mix-β on **212** now followed. The secondary hydroxyl of the resulting diol was thereafter oxidised with SO_3.Py. The synthesis of the acyl side chain **199** was completed by deprotection of the TBDPS-ether of **217** with HF-MeCN to afford **199** in 60% yield.

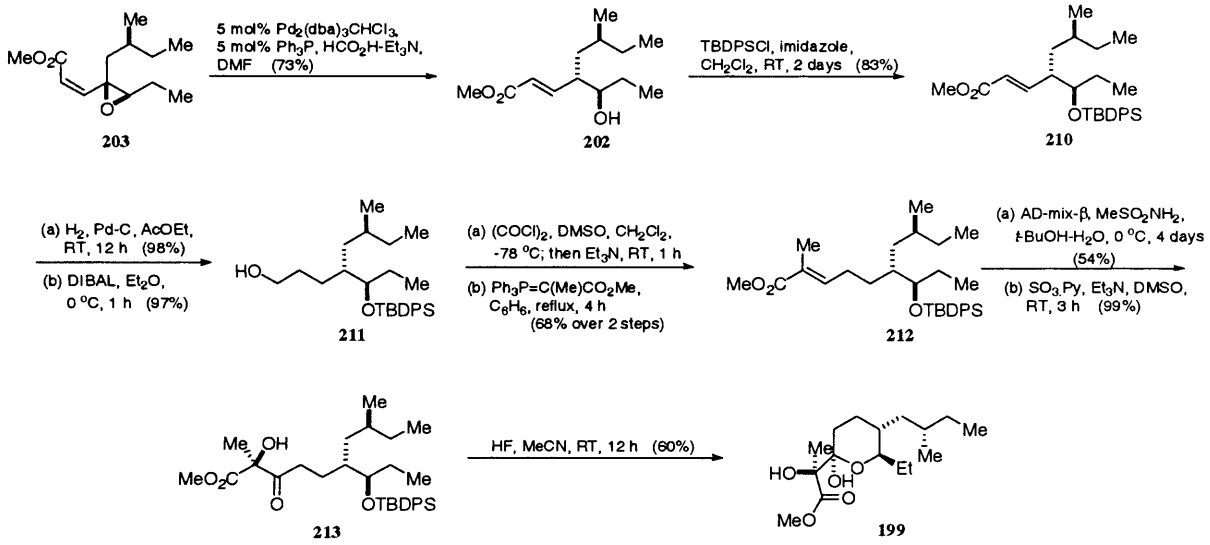

Scheme 43 Kobayashi's route from (*Z*)-alkenyloxirane **203** to the acyl side chain **199**

The groups of both Yao and Kurosu devised an approach to the lipophilic side chain of polyoxypeptin A based on methods adopted by Caldwell and co-workers in the synthesis of the corresponding fragment of L-156,602. They planned on accessing the acyl side chain **214** via a condensation between lactone **215** and Seebach's ester[148] **14**. They considered the latter process would offer the most efficient means of setting the tertiary hydroxyl stereogenic centre in **214**, and their retrosynthetic analysis is outlined below (Scheme 44).

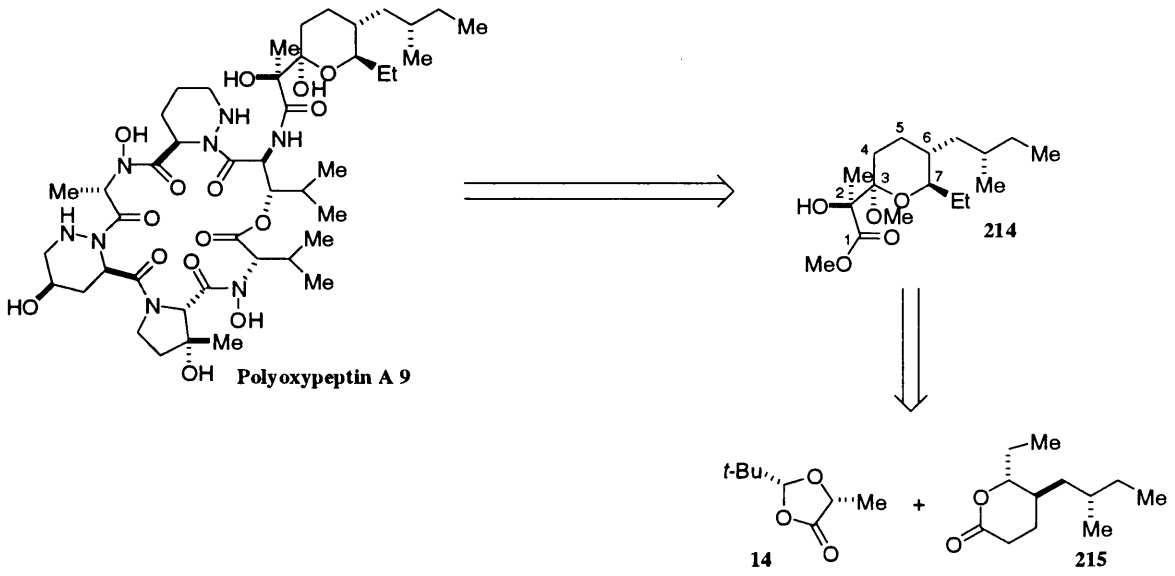

Scheme 44 Kuroso and Yao's retrosynthetic analysis of the acyl side chain of the polyoxypeptins

The route selected by Kurosu and co-workers[203] to access intermediate, lactone **215** utilised a highly diastereoselective *anti*-aldol reaction for setting the C(6) and C(7) stereocentres (Scheme 45). The synthesis commenced with the water-soluble carbodiimide/DMAP mediated *O*-esterification of alcohol **216** with the known chiral carboxylic acid **217**. The resulting ester **218** was then converted to the *E*-enolate. After transmetallation with Cp_2ZrCl_2 and aldolization with propionaldehyde **207** the *anti*-aldol adduct **220** was formed in 85-90% yield with 98% de. Protection of the resulting alcohol as a TBS ether and reductive cleavage of the chiral auxiliary yielded alcohol **221** in 95% yield. The primary alcohol was then activated as its tosylate and the latter reacted with the caesium methyl malonate anion at 70 °C in DMF to give **222**. The malonate adduct **222** was then transformed into lactone **215** in 90% yield through the intermediate lactone-carboxylic acid **223** by treatment with 80% AcOH at 90 °C. Using this sequence Kurosu was able to obtain **215** from **218** in 43% overall yield.

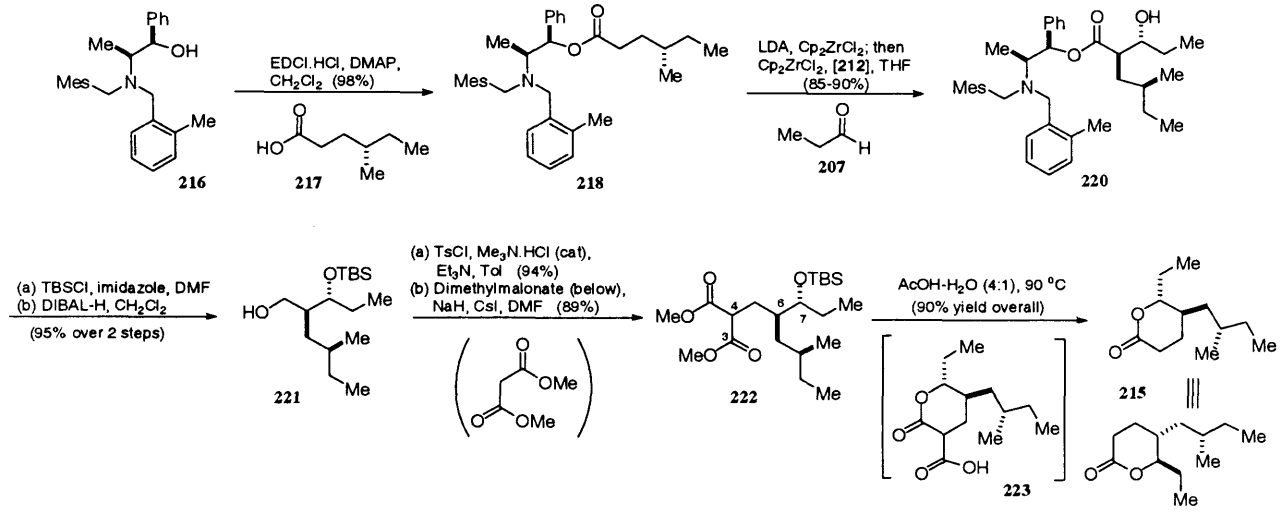

Scheme 45 Kuroso's route to key lactone intermediate **215**

With the desired lactone now in hand, Kurosu attempted to reproduce the highly diastereoselective Claisen condensation with the lithium enolate of **14**, as accomplished by Caldwell and co-workers,[146] to install the remaining three carbon atoms of the tetrahydropyranylpropionate side chain. Despite considerable effort they were unable to obtain the coupling product under the conditions described by Seebach,[148] and in order to facilitate the coupling reaction they had to convert lactone **215** into acyclic aldehyde **224** (Scheme 46). This was achieved over 4 steps via standard conditions and furnished the desired aldehyde **224** in 74% yield from **[220]**. Coupling of **224** with the lithium enolate of **14** generated at –100 to –95 °C, followed by a Swern oxidation provided the β-keto ester **225** in 65-80% yield over the two steps. Removal of the TBS protecting group with 49% HF in MeCN afforded the hemiketal, which was then transformed into mixed methyl ketal **226**. Subsequent transesterification of **226** with NaOMe in absolute methanol yielded the desired acyl side chain **214** in 95% yield.

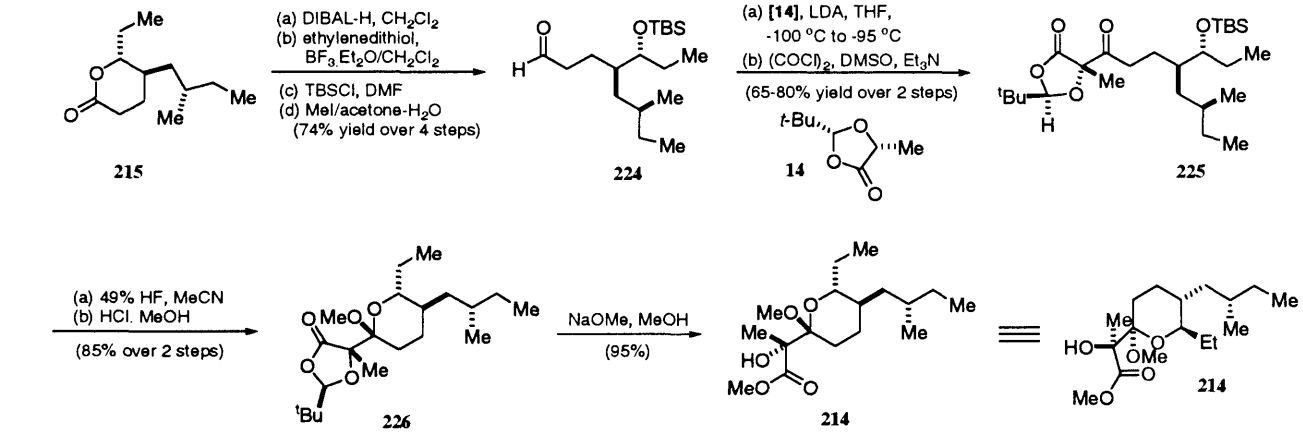

Scheme 46 Kuroso's route to desired acyl side chain **214** from lactone **215**

Yao's strategy for accessing lactone **215** commenced with the Sharpless asymmetric epoxidation[209] of *trans*-2-pentenol **227** using D-(-)-tartrate (Scheme 47) to afford epoxy alcohol **228** in 65 % yield and up to >99% ee following purification of its *p*-nitrobenzoate derivative and basic hydrolysis. Regioselective epoxide opening of **228** with the Grignard reagent derived from (*S*)-1-bromo-2-methylbutane in the presence of CuI at –30 °C gave 1,3-diol **229** in 60% yield, which was protected as an acetal using benzaldehyde dimethyl acetal. After reductive opening with DIBAL-H the primary alcohol **230** was obtained in 95% yield. Oxidation of **230** under Swern conditions, followed by the phosphonate carbanion addition of triethyl phosphonoacetate in the presence of NaH afforded the *trans*-α,β-unsaturated ester **231** in 82% yield. Hydrogenation with a catalytic amount of $Pd(OH)_2$ on charcoal resulted in both reduction of the double bond and removal of the *O*-benzyl protecting group, and was followed by treatment with 6N HCl on SiO_2 to access the desired lactone **215** in 96% yield. Unlike Kurosu, Yao and co-workers were able to achieve the introduction of the remaining three carbon atoms of the acyl side chain with the lithium enolate of Seebach's ester **14** in THF at –78 to –30 °C. It was observed that maximum yields of **232** were achieved when 2 equiv. of the lithium enolate of **14** were used and **232** was afforded in 76% yield as a single diastereoisomer. Treatment of **233** with methanolic HCl smoothly converted the hemiketal into the methyl pyranoside intermediate, and subsequent transesterification of the resulting dioxalanone with an excess of sodium methoxide furnished **214** in 70% yield for the step, and 15.5% overall yield.

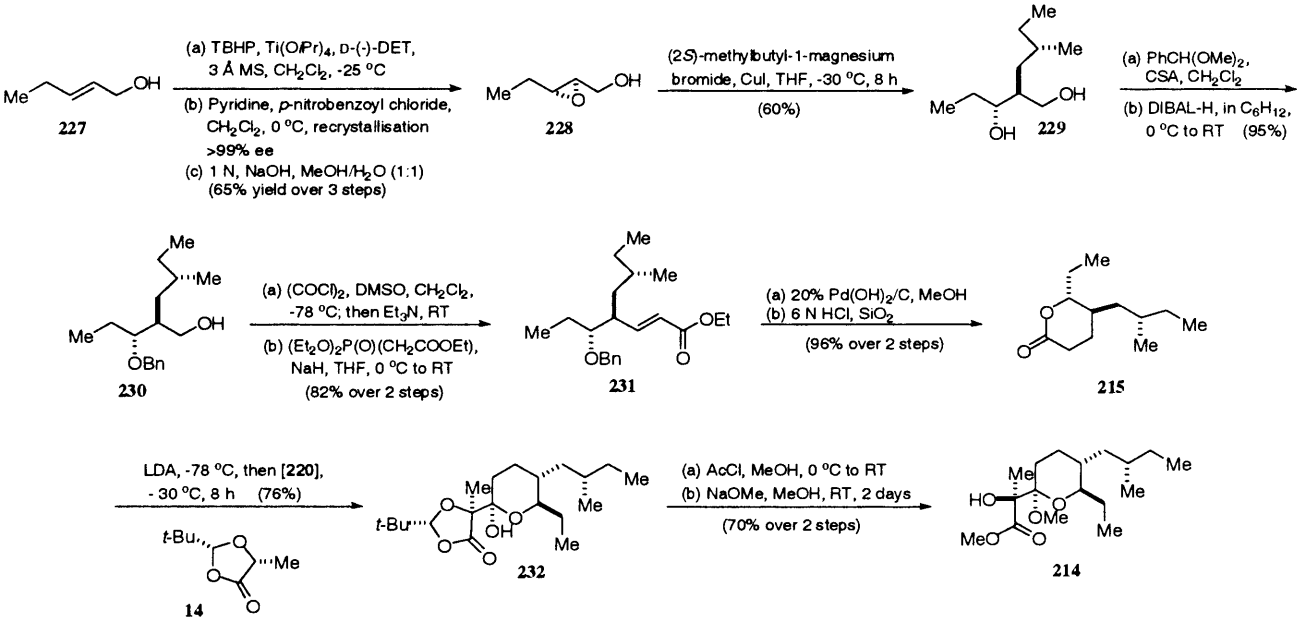

Scheme 47 Yao's route to desired acyl side chain **214**

A noteworthy observation (Scheme 48) made by Yao and co-workers was that on prolonged standing in $CDCl_3$, the methyl acetal **214** undergoes conversion to the semi-acetal **199** as reported by Kobayashi.[202]

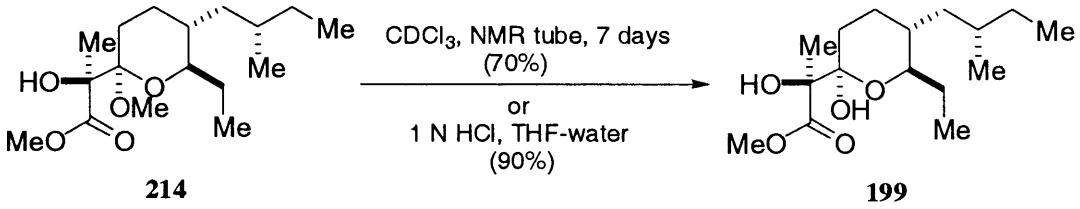

Scheme 48 Yao's observation. Conversion of methyl acetal **214** to semi-acetal **199**

3.5.2 SYNTHESIS OF (3*R*,5*R*)-5-HYDROXYPIPERAZIC ACID

The first enantiospecific total synthesis of a homochiral hexahydropyridazine was that of (3*S*, 5*S*)-5-hydroxypiperazic acid **233**, by Hale and co-workers in 1998[170(c)]. Their synthetic endeavour was encouraged by the presence of this molecule in the skeletal framework of monamycin D_1, and the limited methods for obtaining this amino acid residue. Their strategy again utilised the tandem electrophilic hydrazination and nucleophilic cyclisation technology that was so successfully exploited in their syntheses of homochiral piperazic acid[170] (Sect. 3.2.2, p. 47). Their synthesis commenced with the commercially available and inexpensive D-mannitol (Scheme 49), which underwent selective protection to provide the known D-mannitol derivative[210] **234**. Oxidative cleavage of diol **234**[210] with $Pb(OAc)_4$ in buffered CH_2Cl_2 provided aldehyde **235**, which readily participated in a Wittig-Horner olefination with known phosphonate **236**[211] under Roush-Masamune conditions[212] to afford the crystalline alkene **237** as a single geometric isomer. Treatment of **237** with 40% aq. HF in THF/MeCN detached the silyl protecting group and hydrogenation of the resulting alcohol in EtOAc over10% Pd/C chemoselectively reduced the olefin to provide alcohol **238** in good yield. Bromination of **238** then ensued, with PPh_3 and CBr_4 in dry THF at room temperature, to furnish **239** in 83% yield, and 71% overall yield from **234**. Treatment of bromide **239** with LDA in THF and hexanes at –78 °C, followed by the addition of DBAD and DMPU, facilitated the highly stereoselective hydrazination[172(b)] and tandem cyclisation[170] to provide **240** in 50-66% yield. A noteworthy observation of the Hale group was that unlike

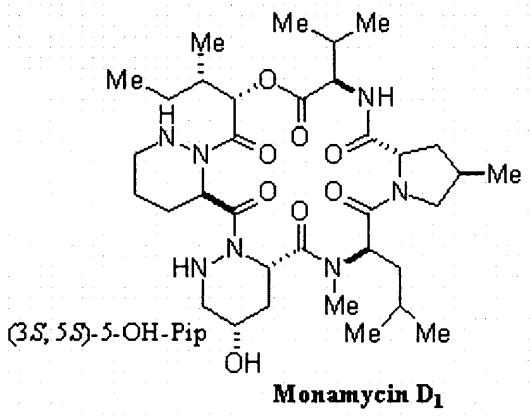

Monamycin D_1

the cyclisation of the aza anion derived from **106** (p. 47), the cyclisation of the anion derived from **239** was much slower, requiring a prolonged period at room temperature to reach completion; this caused some epimerisation at the newly installed stereocentre. The chiral auxiliary was then cleaved from **240** upon reaction with NaOMe in CH_2Cl_2 and methanol, at -30 °C to provide **241** in 93% yield. Following cleavage of the *O*-benzyl ether via catalytic hydrogenolysis with $Pd(OH)_2$ in methanol, temporary protection of the resulting alcohol as an *O*-acetate provided **242** in 89% yield. This protection was necessary to permit the clean and high yielding deprotection of the two Boc groups with TFA. Crude **243** was thereafter reacted with excess LiOH in THF/water at 0 °C to access the desired (3*S*,5*S*)-5-hydroxypiperazic acid **233**.

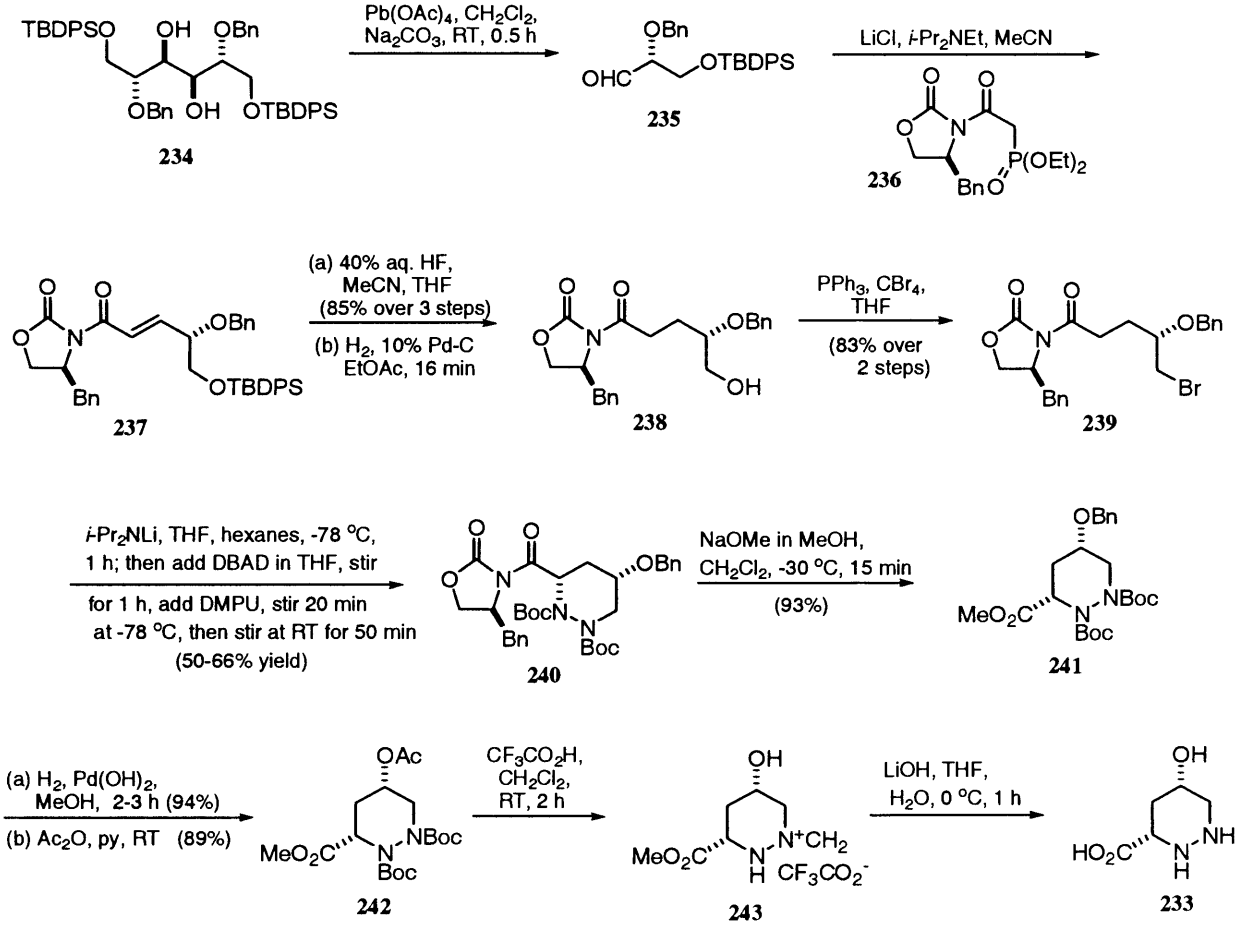

Scheme 49 Hale's enantiospecific synthesis of (3*S*,5*S*)-5-hydroxypiperazic acid **233**

In order to synthesise (3*R*,5*R*)-5-hydroxypiperazic acid, Hale et al. devised a new synthetic approach (Scheme 50), which also allowed the formation of (3*R*,5*S*)-5-chloropiperazic acid that, the latter is a key substituent of monamycins G_1 to I. The new synthesis commenced from known 2-*O*-benzyl-L-threose,[213] which is prepared from commercially available diethyl-L-tartrate **244**. Basically the diol in **244** is protected as a

benzylidene acetal; this is then reductively cleaved with AlH_3 to provide triol **245**. Oxidative cleavage of the 1,2-diol in **245**, followed by Wittig homologation with triethyl phosphonoacetate furnished the known 1,2-disubstituted alkene **246** in 76% yield. The primary alcohol of **246** was next protected as a TBDPS ether, and hydrolysis of the ester afforded the α,β-unsaturated acid **247**. Acid **247** was then converted to the mixed pivalic acid anhydride, which was added to the lithiated chiral auxiliary **251** to provide the enantiomeric partner of **237** (p. 73), **249**. The synthesis was completed following a route analogous to the one devised to obtain **233** from **237**. Thus **249** was converted to **250**; it was subjected to tandem hydrazination/nucleophilic cyclisation to give **251** and the latter was taken through to **252**. Following *O*-desilylation and chlorination with Ph_3P/CCl_4 in MeCN, the desired chloride **253** was obtained. The (3*R*, 5*S*)-5-chloropiperazic acid salt **254** was thereafter obtained by Boc-deprotection and saponification.

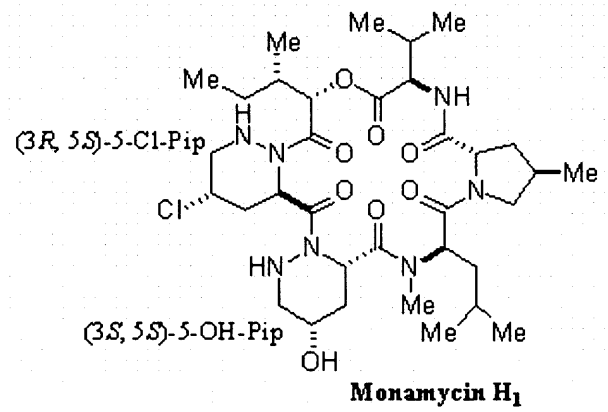

Monamycin H_1

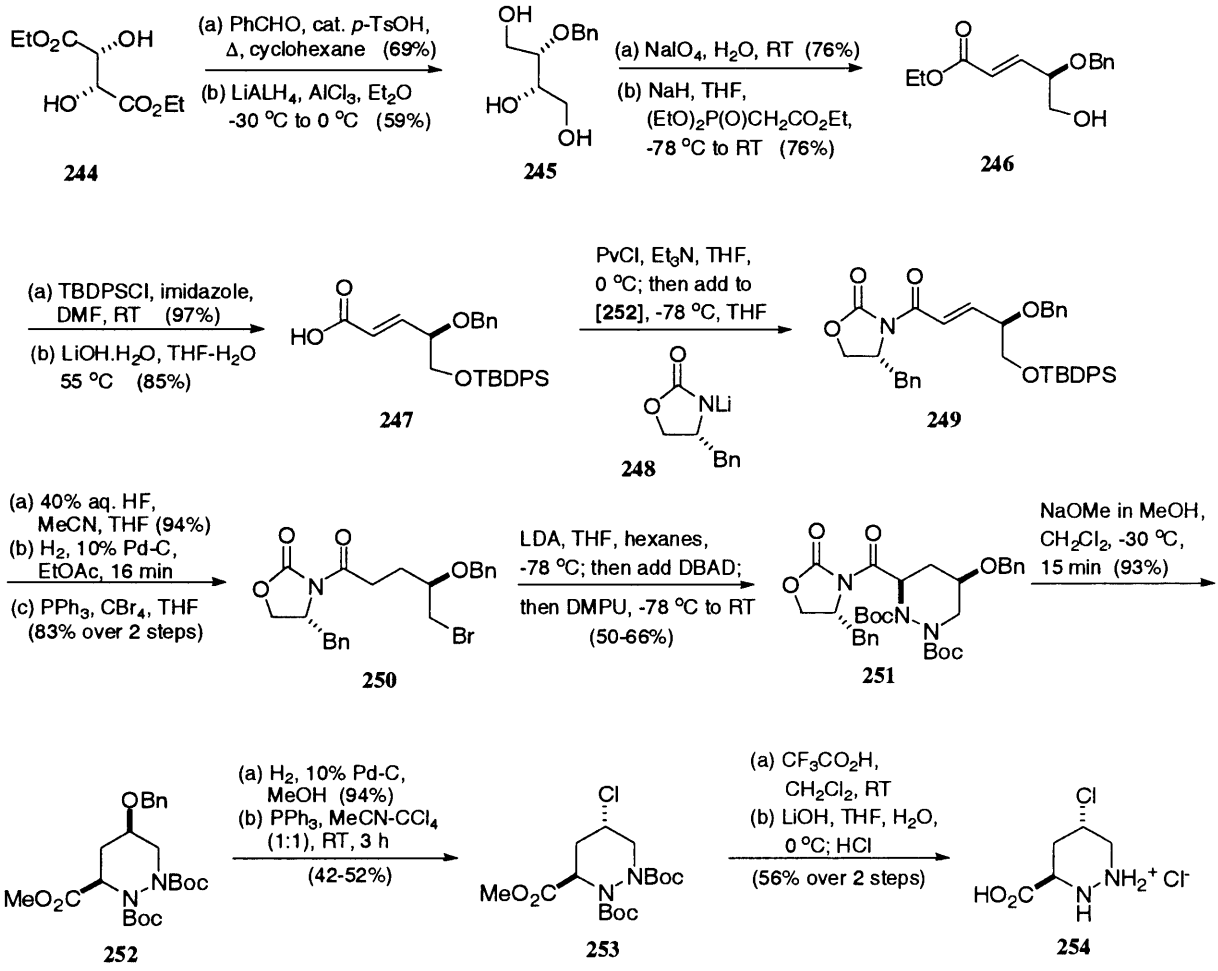

Scheme 50 Hale's enantiospecific synthesis of (3*R*,5*S*)-5-chloropiperazic acid salt **254**

Danishefsky and Kamenecka have also published a route to (3*R*,5*R*)-5-hydroxypiperazic acid **264**. Their synthesis, which first appeared in 1998,[201] was motivated by the presence of this moiety in the antitumour natural product natural product himastatin.[214] Conceptually Danishefsky also uses electrophilic hydrazination and nucleophilic cyclisation to build up **264**. The Danishefsky group devised two separate routes to (3*R*,5*R*)-5-hydroxypiperazic acid; one starting from D-glutamic acid, the other using an Evans hydrazination and diastereoselective bromolactonisation. *R*-Dihydro-5-(*p*-tolylsulfonyloxymethyl)-2(3*H*)-furanone **256** (Scheme 51) was synthesised in three steps from D-glutamic acid.[215] Advancement of **256** to the known epoxy ester[216] was followed by opening with LiBr and AcOH to provide hydroxyl ester **257**. The resulting alcohol **257** was protected as a TBS ether and hydrazination of **258** with DBAD provided fully protected amino esters **259** and **260** after separation. The former underwent nucleophilic cyclisation in the presence of NaH to furnish piperazic esters **260** and **261**. Removal of the Boc groups from **260** and selective protection of the more nucleophilic nitrogen with a Troc, gave amino ester **262** that was quantitatively hydrolysed with LiOH to afford protected (3*R*,5*R*)-5-hydroxypiperazic acid **265**. The *trans*-ester was also converted into desired acid **265**, via alcohol **263**, and the *cis*-piperazic acid lactone **264**.

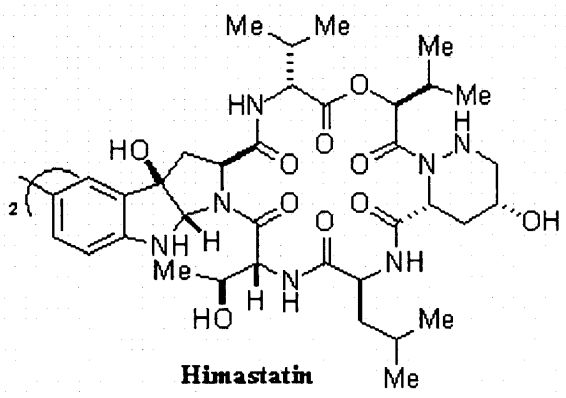

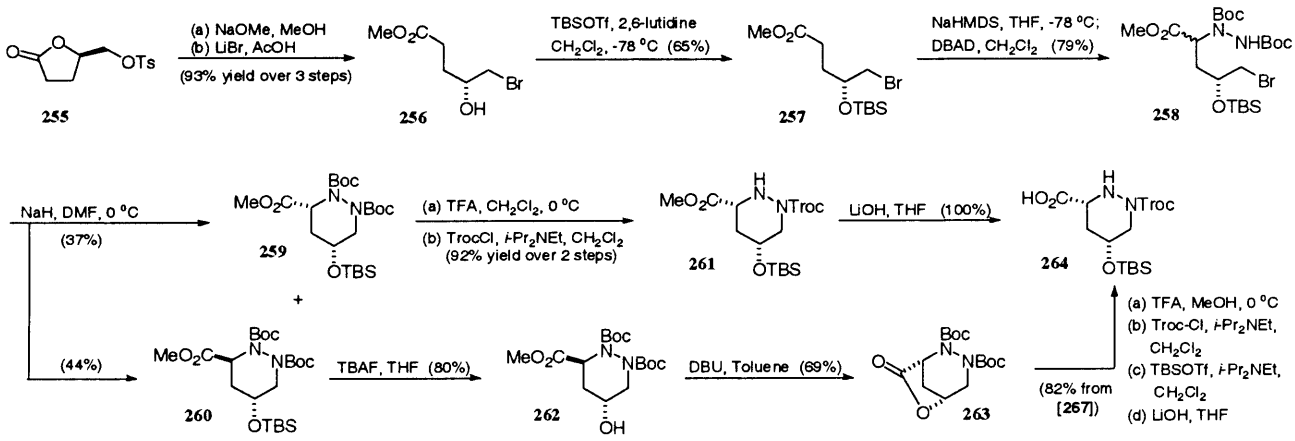

Scheme 51 Danishefsky's enantioselective synthesis of partially protected (3*R*,5*R*)-5-hydroxypiperazic acid **264** from D-glutamic acid

Their second stereoselective route to 5-hydroxypiperazic acid **264** utilised acyloxazolidinone **265**, previously prepared by Hale et al.[170(c)] (Scheme 52). Cleavage of the

Evans auxiliary from **265** followed by bromolactonisation of the resultant acid **266**, gave **267** and **268** in a ratio of 4.5:1. The bromine function of **267** was displaced upon deprotonation of N1 to provide lactone **263** that was converted into **264** using the strategy shown above (Scheme 51).

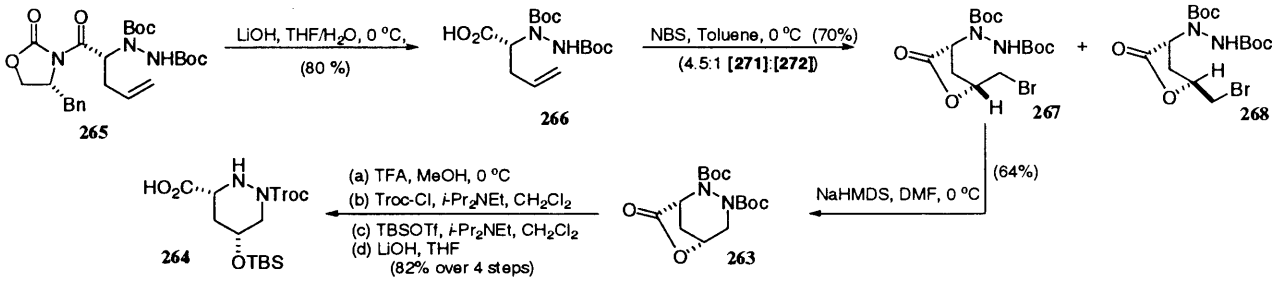

Scheme 52 Danishefsky's enantioselective synthesis of partially protected (3*R*,5*R*)-5- hydroxypiperazic acid **264** via Evans amination and diastereoselective bromolactonisation

3.5.3 SYNTHESIS OF (2*S*,3*R*)-3-HYDROXY-3-METHYLPROLINE

The first stereoselective synthesis of (2*S*,3*R*)-3-hydroxy-3-methylproline **269** was achieved by Kobayashi and co-workers in 2001,[197] and involved a palladium-catalysed cyclisation as the key step. The strategy for their synthesis is outlined below (Scheme 53) and involves an unprecedented pyrrolidine formation via a palladium-catalysed cyclisation of alkenyloxirane **271**, which in turn could be prepared via the asymmetric epoxidation[207] of geraniol **273**.

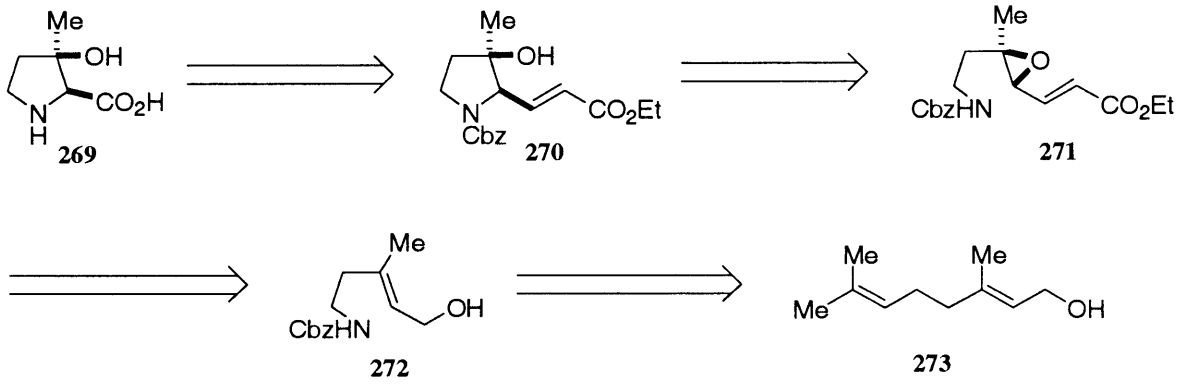

Scheme 53 Kobayashi's retrosynthetic strategy towards (2*S*,3*R*)-3-hydroxy-3-methylproline **269**

Known aldehyde **274** was readily prepared from geraniol in three steps[217] (Scheme 54) and was oxidised to carboxylic acid **275**, which was subjected to a modified Curtius rearrangement using $(PhO)_2P(O)N_3$ (DPPA). After heating the acyl azide in benzyl alcohol/C_6H_6 at reflux for 22 h, *O*-deacetylation provided allylic alcohol **272** in 67% yield from

275. Sharpless asymmetric epoxidation[207] with D-(-)-tartrate was then executed upon **272**, to afford epoxyalcohol **276** in 55% yield with 97% ee. Oxidation of alcohol **276** under Swern conditions and reaction of the resulting aldehyde with triethyl phosphonoacetate provided the desired precursor **271** in 58% yield from **276**. The key Pd-catalysed cyclisation step on **271** was then implemented and a mixture of pyrrolidine derivatives **270** and **277** was obtained in 74% yield in a favourable ratio. Ozonolytic cleavage of the double bond of this mixture afforded **278** and **279**, which were separable by chromatography. Pinnick oxidation of aldehyde **278** provided protected amino acid **280**. The synthesis was completed by deprotection of the benzyloxycarbonyl (Cbz) group, which quantitatively afforded (2*S*,3*R*)-3-hydroxy-3-methylproline **269**.

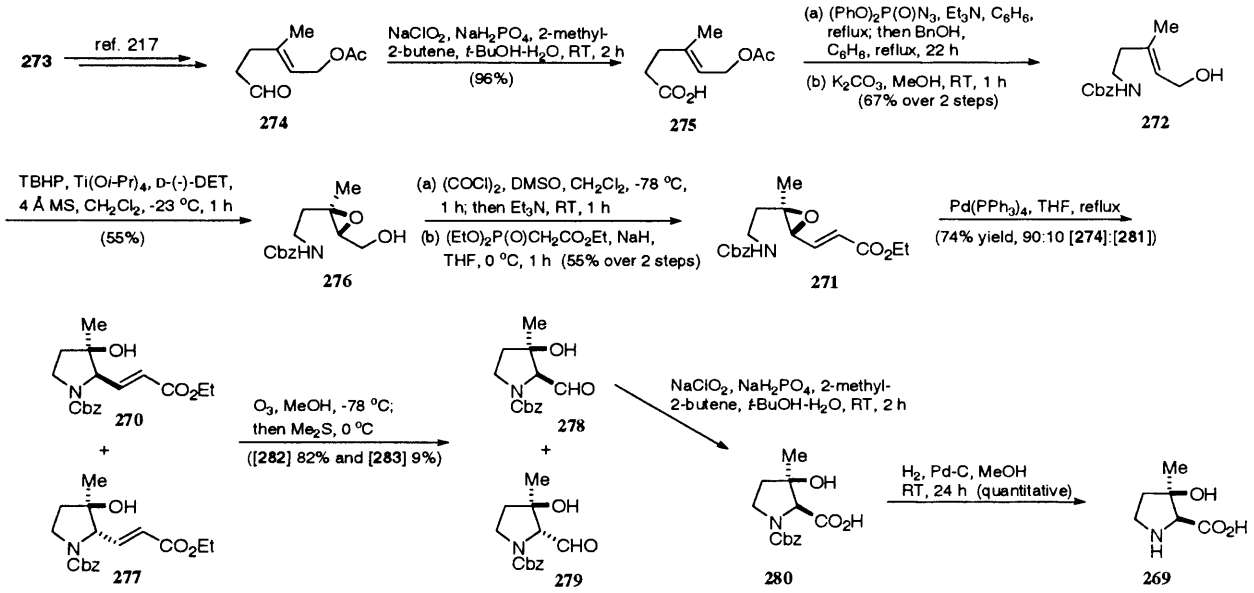

Scheme 54 Kobayashi's synthetic route to (2*S*,3*R*)-3-hydroxy-3-methylproline **269**

Another enantioselective synthesis of (2*S*,3*R*)-3-hydroxy-3-methylproline **269** was achieved by Yao and co-workers in 2002.[198] Their strategy involved a Sharpless AD[218] on the trisubstituted olefin **283** and a regioselective opening of a cyclic sulphate with NaN_3 followed by intramolecular ring-closure used for pyrollidine assembly; their sequence is depicted below (Scheme 55). Commercially available 3-butyn-1-ol **281** was protected as a benzyl ether and treated with *n*-BuLi to give the lithium acetylide. *C*-acylation with methyl chloroformate thereafter furnished the acetylene **282** in 85% yield. Addition of Me_2CuLi to **282** in THF[219] afforded the (2*Z*)-α,β-unsaturated ester **283** in 89% yield. Sharpless asymmetric dihydroxylation[218] of **283** using AD-mix-α thereafter gave diol **284** in 90% yield and 95.5% ee. Cyclic sulphate formation on **284**, using Et_3N and $SOCl_2$ in CH_2Cl_2 and *in situ* ruthenium (III) chloride catalysed oxidation provided cyclic sulphate **285** in 90% yield over the two steps. Reaction of the cyclic sulphate **285** with sodium azide, followed by hydrolysis

of the sulphate salt afforded the α-azido-β-hydroxy ester **286** as the sole product in 86% yield. Hydrogenolysis of the azido group in the presence of catalytic Pd-C (10%) and Boc_2O in EtOAc followed by removal of the benzyl group with $Pd(OH)_2$-C (20%) in MeOH afforded diol **287** and lactone **288** in 72% and 23% yields respectively. Lactone **288** was quantitatively converted into **287** by alkaline hydrolysis and esterification with diazomethane, and **287** was subsequently treated with MsCl and Et_3N in CH_2Cl_2 to give the desired pyrrolidine **289** in 91% yield. Deprotection of the methoxyester and Boc groups was achieved with LiOH and TFA respectively and the resulting crude acid treated with Dowex (50 x 2), eluting with 2 N $NH_3.H_2O$, to furnish (2*S*,3*R*)-3-hydroxy-3-methylproline **269** in 97% yield as a crystalline solid.

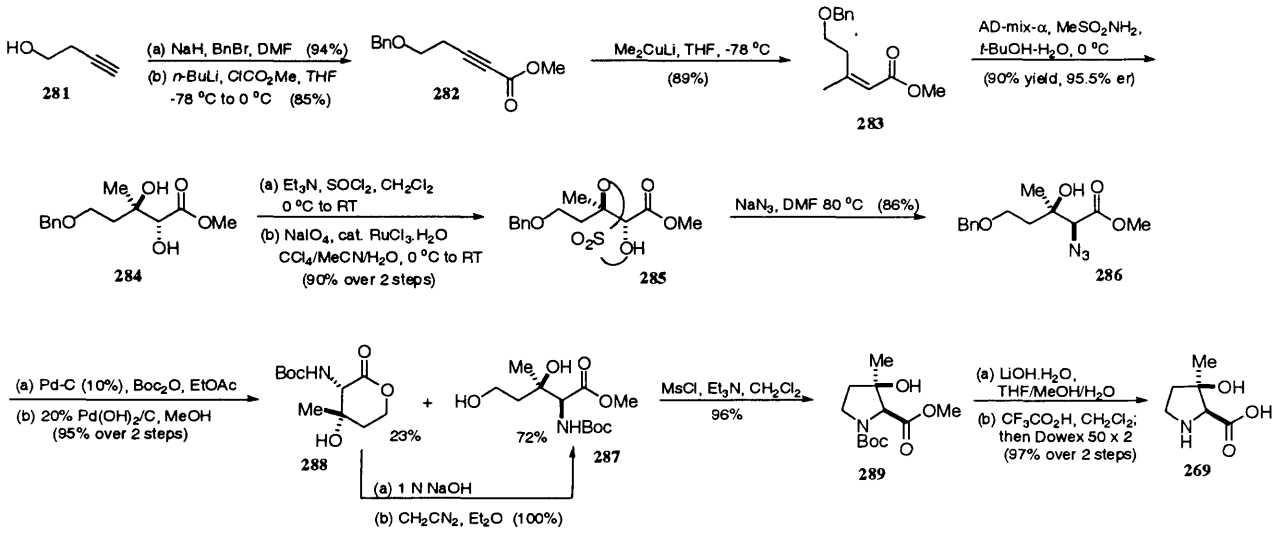

Scheme 55 Yao's synthetic route to (2*S*,3*R*)-3-hydroxy-3-methylproline **269**

Another stereoselective synthesis of (2*S*,3*R*)-3-hydroxy-3-methylproline **269** was reported by Hamada and co-workers in 2002,[199] which utilised a SmI_2-mediated diastereoselective cyclisation as a key step. Hamada's retrosynthetic strategy for accessing (2*S*,3*R*)-3-hydroxy-3-methylproline **269** is outlined below (Scheme 56). They envisioned constructing the asymmetric quaternary centre at C(3) by a diastereoselective cyclisation on **290** with SmI_2. The latter, in turn, could be readily derived from (2*S*,3*R*) threonine **291**.

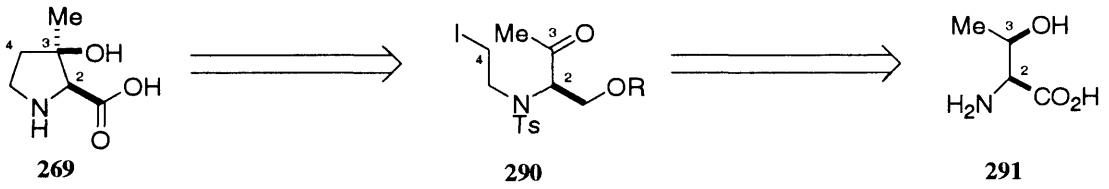

Scheme 56 Hamada's retrosynthetic strategy towards (2*S*,3*R*)-3-hydroxy-3-methylproline **269**

Their synthesis commenced with the preparation of tosylamide **292** in 81% yield over 4 steps (Scheme 57) from standard manipulations on **291**. *N*-Allylation of **292** provided alkene **293** in 96% yield. Oxidative cleavage of the olefin in **293** with OsO_4-NMO followed by treatment with $NaIO_4$ and subsequent reduction of the aldehyde functionality gave alcohol **294** in quantitative yield. Iodination of **294** with iodine and triphenylphosphine, in the presence of imidazole, provided iodoalkane **295** in 97% yield. Following acid catalysed removal of the isopropylidene acetal, a selective protection of the primary alcohol in **296** as a TBDPS ether and a subsequent Dess-Martin periodinane[220] oxidation of the secondary alcohol quantitatively furnished iodoketone **297**. Removal of the TBDPS protecting group with aq. HF/MeCN provided alcohol **298** in 86% yield, which was treated with SmI_2 in THF-HMPA (10:1) at low temperature to exclusively afford (97:3) **299** in 75% yield. The synthesis of (2*S*,3*R*)-3-hydroxy-3-methylproline **269** was completed by the selective oxidation of the primary alcohol of **299** to the carboxylic acid and subsequent deprotection of the tosyl group. This sequence furnished **269** in 91% yield without epimerisation.

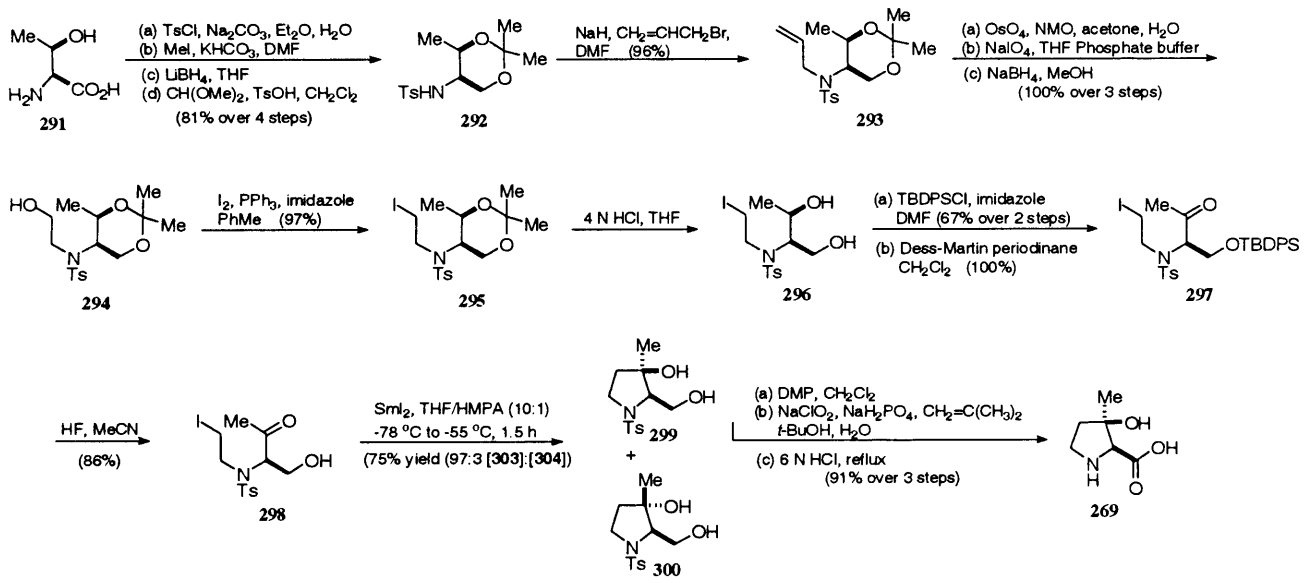

Scheme 57 Hamada's synthetic route to (2*S*,3*R*)-3-hydroxy-3-methylproline **269**

Chapter 4: RESULTS AND DISCUSSION

The azinothricin family of antibiotics, if they were to become widely available, could provide valuable insights into the cellular mechanisms that control the onset of many mammalian cancers. It has been suggested that molecules of this class exert their therapeutic effects by preventing E2F transcription factors from binding to their recognition sequence, thus inhibiting transcriptional activity.[12,27] However, there has never been any supporting biological information to confirm how these molecules chemically interact with these biological targets to elicit their antitumour effects. Do they simply bind to the E2F/DP heterodimer, or do they bind to the individual E2F or DP components and prevent heterodimerisation, thereby preventing transcription? Do they bind to the recognition sequence themselves, rather like E2F/DP transcription factors, but without the ability to cause conformational changes or bends in the DNA necessary to initiate transcription? A further hypothesis is that they prevent transcriptional co-activators such as the CREB binding protein from being recruited to the E2F/DP complex. Clearly, many possibilities exist that need examining in more detail, and access to molecules of the azinothricin class could aid such investigations. It has already been discussed that the fate of mammalian cells depends upon the highly complex interplay between E2F, pRb and p53. Molecules that serve as probes of these cellular pathways could significantly improve our understanding of the intricate mechanisms of the mammalian cell.

The remarkable potency of this family of antibiotics in combating human tumours has been tarnished somewhat by their significant toxicity (even lethality) at high dosages. Nevertheless hopes still remain that an analogue might be identified that has improved pharmacological effects. Previous biological experiments have already established that an intact cyclodepsipeptide core is an essential feature of these molecules, since the linear peptide form of GE3 (GE3B) is devoid of antitumour activity. The tetrahydropyranyl side chain is also an essential component, as our own biological experiments on the A83586C cyclodepsipeptide hydrochloride salt have revealed that it lacks antitumour activity. Observations from the synthesis of *epi*-A83586C have further demonstrated that significant structural deviations to the conformation of the cyclodepsipeptide core can have adverse effects on antitumour potency. With this knowledge, we therefore felt that if we could establish the essential structural features of these molecules required for optimum antitumour activity, then we might be able to diminish, or even eliminate, their toxicities by excluding the toxic components from their skeletal framework. In light of these factors our group initiated a total synthesis programme on the azinothricin family of antibiotics, with the sole purpose of preparing novel analogues that could:

1) Elucidate the mechanism of antitumour action within human cancer cells, and provide more conclusive information about the biological activity of members of this class.
2) Identify the toxic components of this class and establish whether toxicity might be eliminated without diminishing potency.
3) To identify the actual biological receptors/drug targets of molecules of this class.

The exciting biological profile of citropeptin captured our attention, as it was shown to confer a 120% life extension on mice with P388 leukaemia, when administered at 2mg/kg/day. It also possessed a novel *N*-hydroxy-*O*-methyl-L-serine residue. We thought that it would be interesting to synthesise the cyclodepsipeptide core (**Fig. 21**) of this molecule and couple it to the acyl side chain of A83586C, to observe what, if any, changes occur in its biological activity. Success in this venture would add yet another fascinating molecule of the azinothricin class, albeit a synthetic one, to our accomplishments in this area.

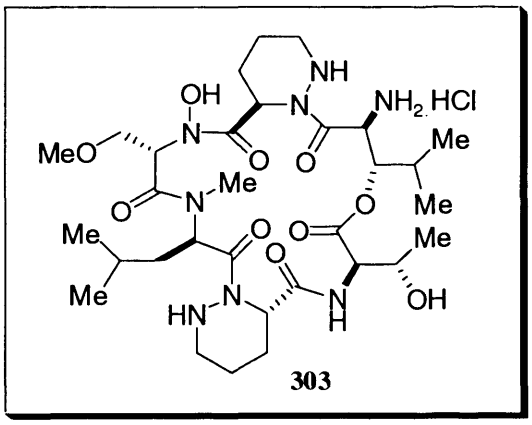

Fig. 21. Structure of the citropeptin cyclodepsipeptide target **303**

Since the synthesis of citropeptin would involve the synthesis of *N*-hydroxy-*O*-methyl-L-serine, we thought that it would be useful to also attempt the synthesis of the azinothricin cyclodepsipeptide core (**Fig. 22**), since this molecule also incorporates this fragment into its skeletal framework. This would provide us with yet another scaffold to couple to the A83586C acyl side chain, and various other more simplified pyrans, providing yet more analogues of this class of natural products for biological evaluation. It would also enable us to attempt the first asymmetric total synthesis of the founder member of this family of antibiotics, namely, azinothricin.

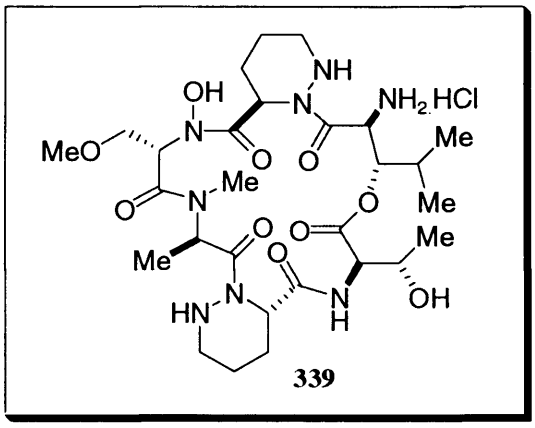

Fig. 22. Structure of the azinothricin cyclodepsipeptide target **339**

4.1 SYNTHETIC STUDIES ON THE CYCLODEPSIPEPTIDE CORE OF CITROPEPTIN

Although the cyclodepsipeptide core of citropeptin is markedly different to that of A83586C, it incorporates the (3*R*)- and (3*S*)- piperazic acid units [D- and L- respectively]; the (2*S*, 3*S*)-3-hydroxyleucine; and the (2*R*, 3*S*)-threonine [D-threonine] residues found in the A83586C structure. However, it also incorporates the *N*-methyl-D-leucine fragment common to GE3 and the novel *N*-hydroxy-*O*-methyl-L-serine unit within its skeletal frame. Our retrosynthetic analysis of citropeptin is outlined below (Scheme 58). We envisioned accessing the citropeptin skeleton **301** *via* a chemoselective union between the hydrochloride salt **303** and the pyranyl side chain **302**. We believed that the cyclodepsipeptide core **303** could be assembled in the same way as its predecessors, *via* a [2+2+2] fragment condensation between **304**, **163** and thereafter **101**. However a rather crucial new twist to the envisaged sequence to **303** was whether this strategy would work with dipeptide **304**. The synthesis of *N*-hydroxy-methoxy-L-serine had never previously been accomplished, and its coupling with other amino acids had never been attempted. Given that a single change in the amino-acid sequence can have dramatic consequences for a successful result, we thought it important to address this issue.

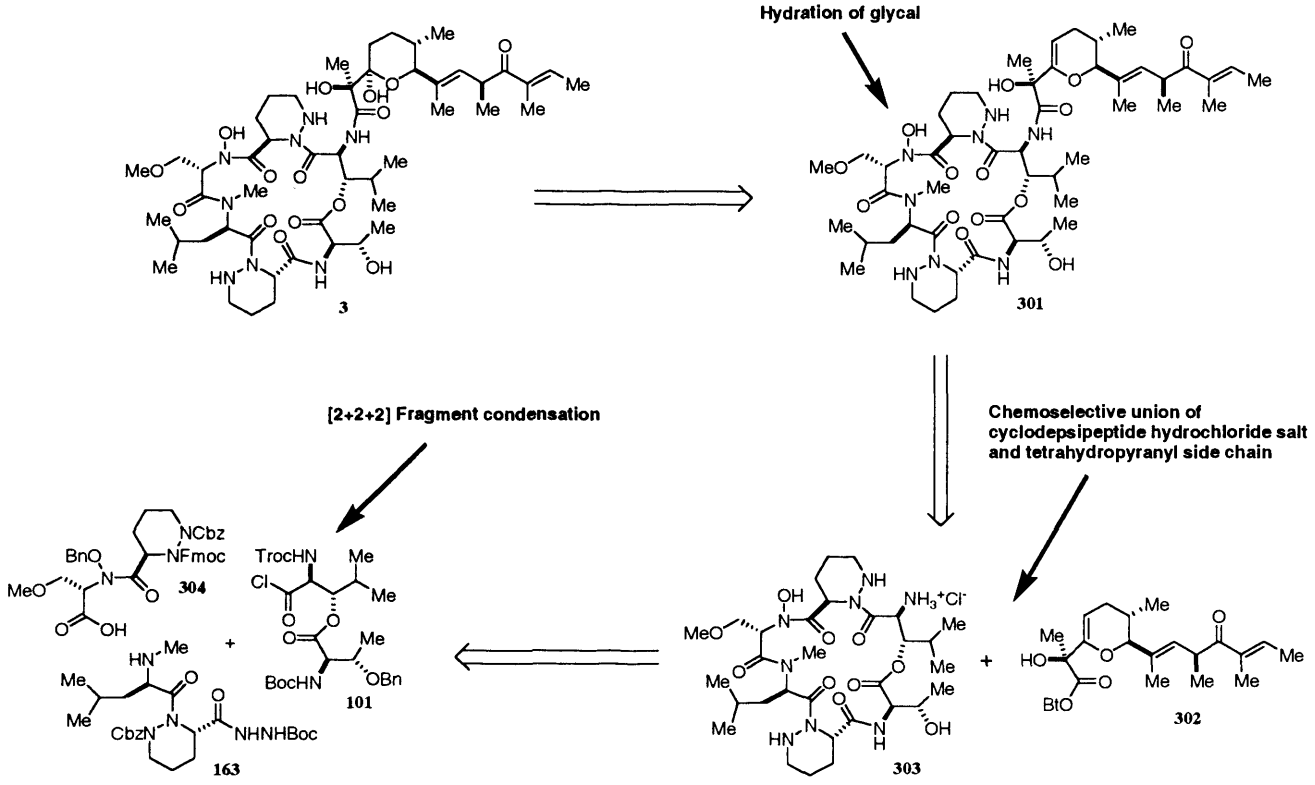

Scheme 58 Retrosynthetic analysis of citropeptin **3**

Our initial attention was therefore focused on the construction of dipeptide **304**, since the technology for accessing **101** and **163** had already been devised within our group during the syntheses of A83586C and GE3. Accordingly, we would then intersect with the methodology used in assembling the cyclodepsipeptide cores of the previously synthesised molecules to complete our synthesis.

4.1.1 STUDIES TOWARD THE SYNTHESIS OF *N*-HYDROXY-*O*-METHYL-L-SERINE

Our past cumulative experiences suggested that the dipeptide **304** would probably best be obtained from the coupling of partially protected piperazic acid chloride **31**, with the partially protected *N*-hydroxy-*O*-methyl-L-serine **305**. Our initial strategy for obtaining **305** centred on oxidising the *N*-Cbz-derivative of *O*-methoxy-L-serine methyl ester **308** with DMDO, and then attempting the *O*-benzylation of the resulting hydroxylamine. We thought that this approach would be the most efficient way of synthesising this fragment in sufficient quantities for gram-scale syntheses of various members of the azinothricin family. We initiated the proposed sequence *via* an *O*-methylation of **306** with trimethyloxonium tetrafluoroborate and proton sponge in CH_2Cl_2[221] with exclusion of light; this provided **308** in very good yields. The IR spectrum of **307** showed strong absorptions at 3331 cm^{-1} and 1690

cm^{-1}, characteristic of a secondary amide and saturated ester respectively. These were accompanied by secondary and tertiary C-H stretching absorptions, along with an *O*-CH_3 stretching absorption, in the region of 2813 – 2953 cm^{-1}. Further conformation of the structure of **307** was provided by its 500 MHz ^1H NMR spectrum in $CDCl_3$, where the *O*-methoxy singlet at δ 3.30 was also accompanied by the existing singlet of the methyl ester at δ 3.73. A major advantage of using an oxonium salt to bring about the desired alkylation was that it used much milder conditions than those necessary using more conventional alkyl halide based alkylation methods. As a consequence the stereochemistry of the asymmetric centre was not compromised. Removal of the carbobenzyloxy-protecting group was achieved by hydrogenation with Pd-C in methanol. Oxidation of the resulting amine **308** with 2,2-dimethyl dioxirane[222] was next attempted with little success (Scheme 59). The complications associated with this mode of oxidation of primary amines led us to rethink our strategy towards **305**. In the end we decided that the hydroxylamine functionality had to be introduced in protected form for the synthesis to be successful.

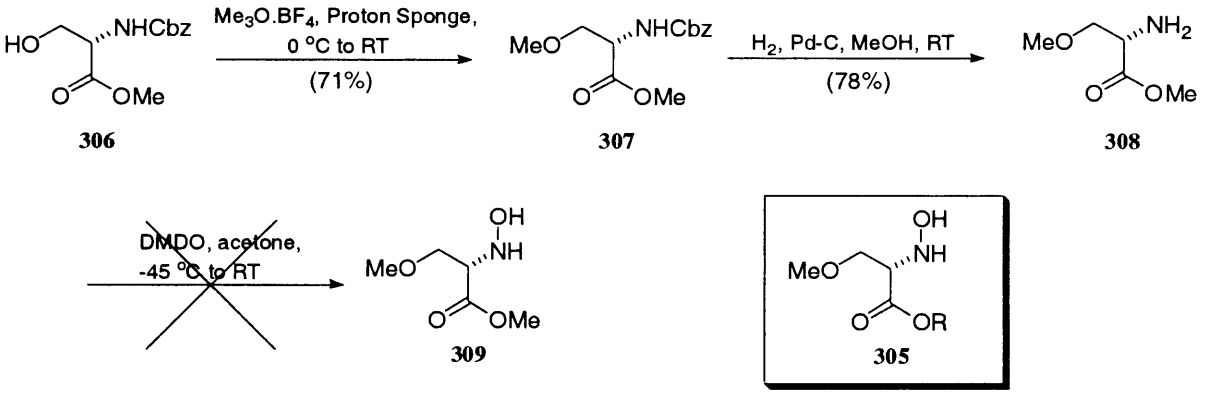

Scheme 59 Failed route to hydroxamic ester **309**

We believed that the *O*-benzyl derivative **310** of **305** would probably best fit our purposes, as this molecule could potentially be accessed from the relatively inexpensive and commercially available D-mannitol **311**, through a series of protecting group manipulations and an oxidative degradation. Specifically we envisioned converting D-mannitol **311** into acid **315**, which could thereafter be deprotected to access **312**. We believed that **305** could potentially be synthesised *via* an S_N2 reaction with *O*-benzyl-hydroxylamine on the *O*-triflate derived from alcohol **312**, to provide the desired hydroxamic ester **310** (Scheme 60).

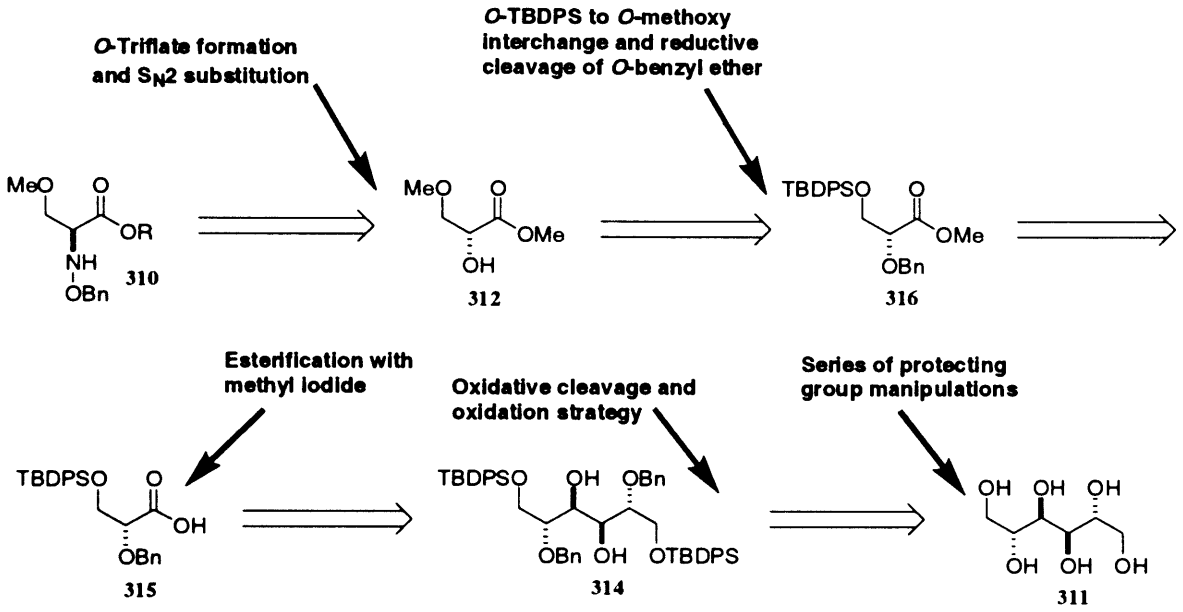

Scheme 60 Retrosynthetic approach to protected amino acid **310**

D-Mannitol was protected as its 1,3-4,6-di-*O*-benzylidene acetal, using benzaldehyde and catalytic conc. H_2SO_4 in DMF.[223] The reaction proceeded in 41% yield following an exhaustive work up with ice-cold saturated aq. potassium carbonate, hexanes and chloroform, to provide the desired diol as a white solid after recrystallisation from methanol/hexanes (Scheme 61). The NMR spectrum of this molecule was significantly simplified due to its C_2 centre of symmetry, and the singlet at δ 5.53 in the 500 MHz ^{1}H NMR spectrum in CD_3OD confirmed the presence of the benzylidene acetals (PhC<u>H</u>), as did the characteristic phenyl multiplets at δ 7.49 and 7.33 respectively. This assignment was supported by the strong sharp O-H stretch absorption at 3480 cm^{-1} and the medium C-H stretching absorptions at 2857, 2956 and 2979 cm^{-1} respectively indicative of the –O-CH-O- functionality.

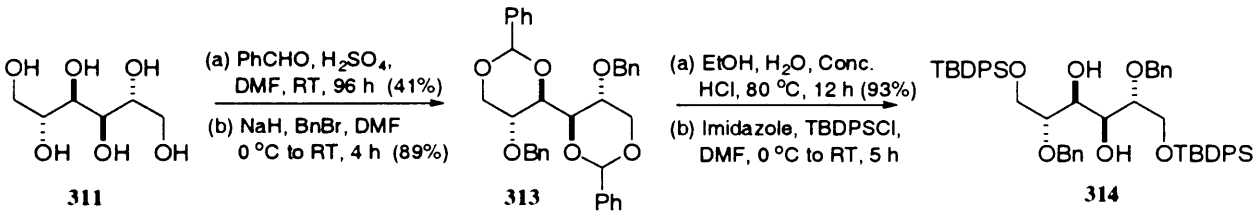

Scheme 61 Route to diol intermediate **314**

After *O*-benzylation with NaH and BnBr in DMF at room temperature, **313** was obtained as a white solid in 89% yield. The singlet of the benzylidene acetal shifted to δ 5.42 in the 500 MHz ^{1}H NMR spectrum of **313** in $CDCl_3$, and we observed twice as many carbon

peaks in the δ 120-140 region in the 125 MHz ^{13}C NMR spectrum. In addition to this, two benzylic methylene carbons were present at δ 69.5 and 72.1. The presence of two distorted AB doublets at δ 4.61 and 4.58 (J_{AB} = 11.8 Hz) (PhC$\underline{H}_2$) also supported the presence of the two new benzyl groups. Further evidence for this came from the IR spectra, where the strong O-H absorption was now absent and replaced with aryl-H stretches at 3063 and 3028 cm^{-1} respectively. Removal of the benzylidene acetals from **313** was best accomplished with conc. HCl in EtOH at 80 °C for 12h. A single product was formed according to TLC analysis, which was most conveniently purified by simple recrystallisation from EtOAc/hexanes to provide the desired tetrol as a fluffy white solid. The 500 MHz ^1H NMR of the tetrol in $CDCl_3$ showed that the number of aromatic protons in the region of δ 7.35 – 7.41 had halved, indicating a loss of a phenyl group. The singlet at δ 5.42 further confirmed that the benzylidene acetals had been removed. The presence of two broad singlets at δ 2.98 and 2.51 respectively, confirmed the presence of the four alcohol groups. Further analysis in CD_3OD at 500 MHz (no O*H* observed due to interchange) indicated the loss of one phenyl group. There were signals associated with the *O*-benzyl ethers that were present at δ 7.38 (d, *ortho*-Ph, J = 7.11 Hz), δ 7.29 (m, *meta*-Ph), δ 7.24 (m, *para*-Ph) and AB doublets at δ 4.73 and 4.60 respectively (J_{AB} = 11.3 Hz). Further confirmation of acetal removal was provided by in the IR spectrum of the tetrol, with the appearance of a somewhat broad O-H absorption that separated into three signals at 3474, 3383 and 3269 cm^{-1} respectively. After selective protection of both primary alcohols as TBDPS ethers with TBDPS-Cl and imidazole in anhydrous DMF, the known *vic*-diol **314** was obtained as a crude yellow oil that was taken on to the next reaction sequence without further purification. A broad medium OH stretching absorption at 3481 cm^{-1} in the IR spectrum of **314** confirmed that an OH was still present and this was accompanied by a strong absorption at 1111 cm^{-1} that is indicative of a Si-O stretch. Further confirmation was provided by 500 MHz ^1H NMR analysis in $CDCl_3$ where a broad OH singlet at δ 3.12 was present, which was accompanied by a *tert*-butyl singlet at δ 1.07, multiplets at δ 7.71 (4H, *ortho*-Ph-Si) and δ 7.34-7.46 (6H, *meta*- and *para*-Ph-Si); in addition to the multiplet at δ 7.29 that corresponded to the phenyl group of the *O*-benzyl ethers.

Oxidative cleavage of **314** was next effected with lead tetraacetate in CH_2Cl_2 (Scheme 62). The resulting aldehyde was not purified any further, but simply oxidised with PDC in aqueous DMF to furnish acid **315** in 75% yield for the three steps. The formation of the acid was indicated by the appearance of a brown streak on TLC with an R_f ~ 0.2 when eluted with EtOAc/hexanes (1:1) and stained with H_2SO_4/anisaldehyde. Success in the two-step oxidation was confirmed by the presence of a broad singlet at δ 10.28, in the 500 MHz ^1H NMR spectrum of **315** in $CDCl_3$ that was characteristic of an acid O$\underline{H}$. The signals for the *O*-TBDPS and *O*-benzyl protecting groups were also still present.

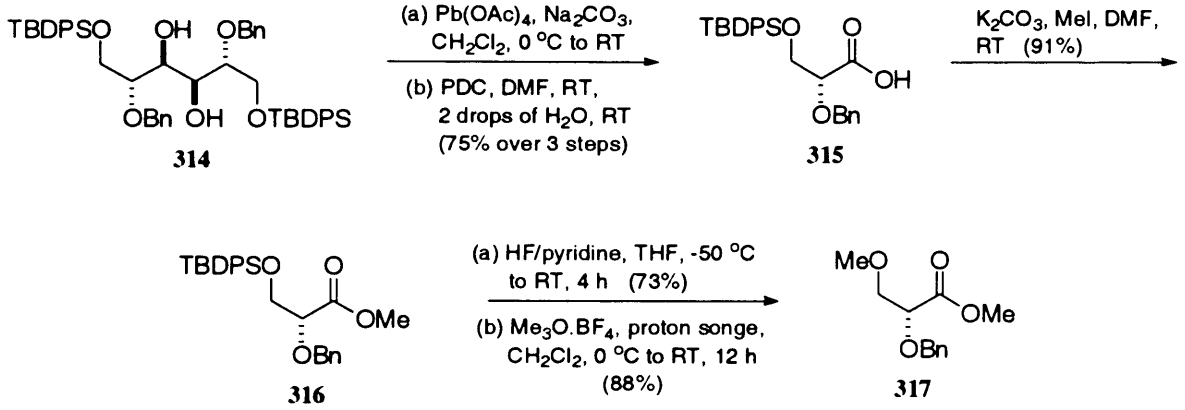

Scheme 62 Reaction sequence from **314** to methyl ester **317**

O-Methylation of **315** was most readily accomplished with potassium carbonate and methyl iodide in DMF at room temperature for 1 hour; methyl ester **316** was obtained in 91% yield. TLC analysis of the reaction mixture showed a faster-moving yellow spot (R_f ~ 0.8), when the plate was eluted with EtOAc/hexanes (2:1) and developed with anisaldehyde stain, which signified that the esterification had taken place. The 500 MHz ^{1}H NMR spectrum of **316** in $CDCl_3$ now showed a singlet at δ 3.83 corresponding to the methyl ester $OC\underline{H}_3$, and the $CO_2\underline{H}$ resonance previously present at δ 10.28 in **315** was now absent. Removal of the TBDPS protecting group was most readily accomplished with HF/pyridine solution in THF at RT for 4h. It was generally found optimal to initiate this reaction at –50 °C, and then warm to RT over 3 hours. Success in this reaction was confirmed by the absence of the characteristic 4H and 6H multiplets of the TBDPS group between δ 7.3 and δ 7.8, and the absence of the *t*-butyl resonance previously at δ 1.11 in **316**. Following treatment with trimethyloxonium tetrafluoroborate and Proton Sponge in CH_2Cl_2 (with the exclusion of light), methyl ether **317** was obtained in 88% yield. Successful etherification was confirmed by the appearance of an $OC\underline{H}_3$ singlet at δ 3.33 in the 500 MHz spectrum of **317** in $CDCl_3$, which was slightly more up field than the singlet for the methyl ester (δ 3.72), which was as one would expected.

Removal of the *O*-benzyl ether from **317** was accomplished by catalytic hydrogenation, at 1 atm, over a $Pd(OH)_2$ catalyst in MeOH for 18 hours (Scheme 63). Success in this reaction was confirmed by the 500 MHz ^{1}H NMR spectrum of **312** in $CDCl_3$, which now lacked the aromatic protons in the δ 7.21-7.28 region. Additionally, the characteristic AB doublets at δ 4.74 and 4.48 in **317** were also now absent, and an O*H*-resonance could now be observed at δ 3.19. Following *O*-triflation of **312** with Tf_2O and 2,6-lutidine at 0 °C for 40 mins in CH_2Cl_2, a solution of *O*-benzylhydroxylamine in CH_2Cl_2 was added dropwise to the mixture at -40 °C, and the cooling bath removed to allow the reaction

mixture to warm to ambient temperature over 2 hours; this provided the desired amine **319** in 71% yield. The latter method for preparing *O*-benzylated hydroxamic acid derivatives was first reported in 1988,[224] and was shown to be essentially racemisation free, leading to the expected products by clean S_N2 inversion at the *O*-triflate-leaving carbon atom. Previous work in our group and others, has confirmed the stereochemical outcome of such reactions and we were somewhat confident of a successful outcome here. The success of the reaction was confirmed by the 500 MHz ^{1}H NMR spectrum of **319** in $CDCl_3$ where the broad singlet previously observed at δ 3.19 in **312** was now absent; also the occurrence of aromatic multiplet signals in the region of δ 7.26-7.29 further confirmed the desired outcome. The presence of a singlet and broad singlet at δ 4.71 and δ 6.17 also proved the presence of the methylene AB system of the benzyl group and the NH respectively.

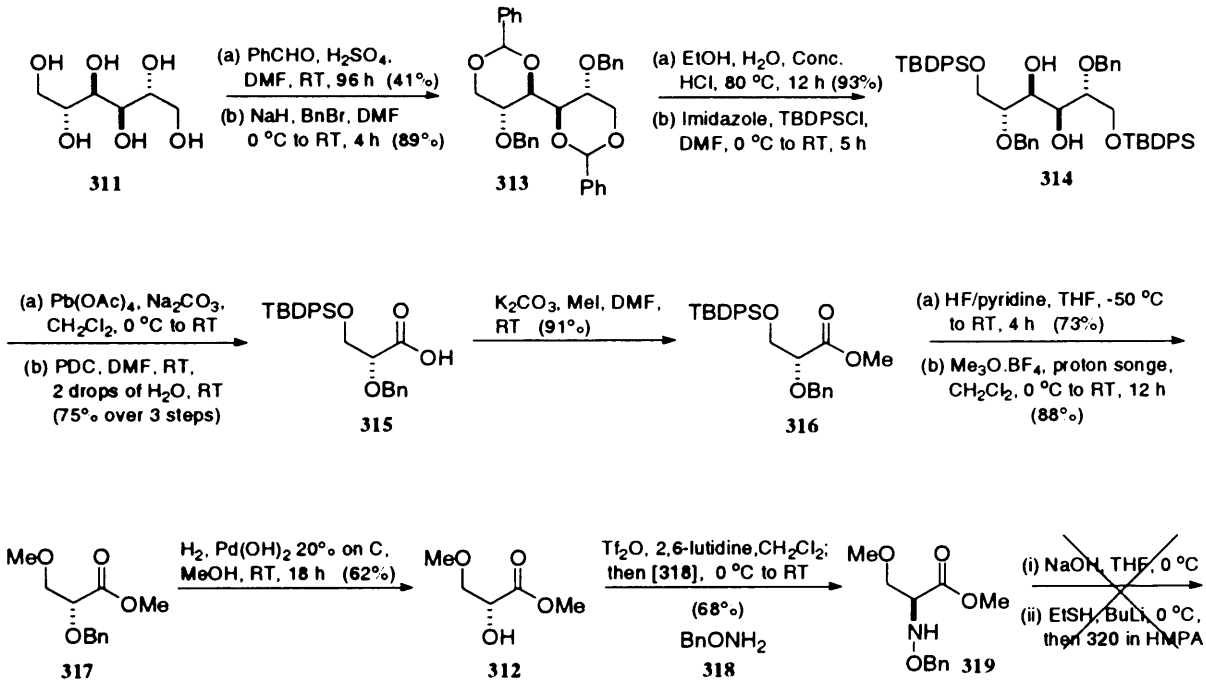

Scheme 63 Failed route to hydroxamic acid (Reaction Summary)

The saponification of **319** was attempted with both sodium hydroxide and lithium hydroxide in THF at 0 °C. However TLC analysis of these separate reactions revealed that a mixture of products was formed. Separation of these products proved futile and one can only assume that they occur due to loss of the labile methoxy or benzyloxy groups due to base-mediated abstraction of the α-proton (**Fig. 23**). Our use of LiSEt in HMPA also proved unsuccessful for obtention of the desired acid.

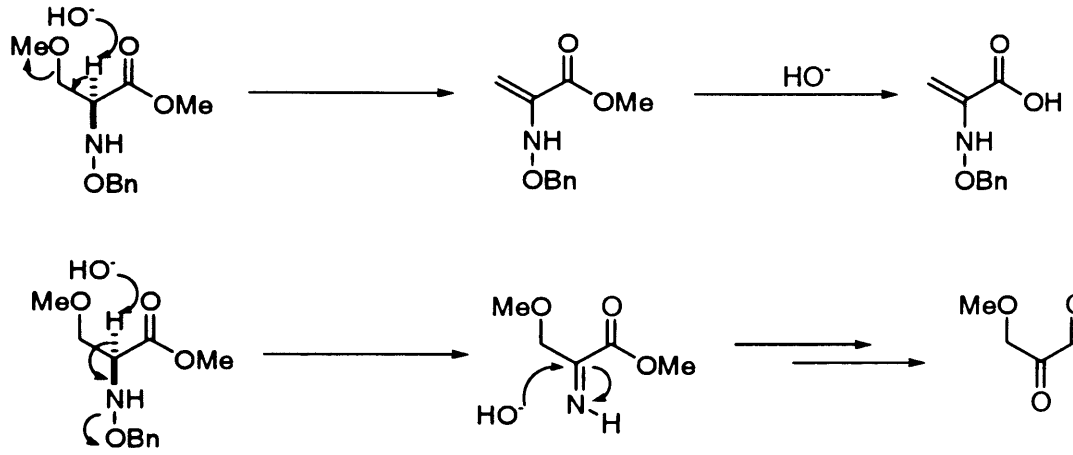

Fig. 23. Some possible decomposition pathways that might be operating during the base hydrolysis of **319**

In light of these failures we decided to review our protecting group strategy for this sequence of reactions. We wanted to deliberately avoid the use of an ester-protecting group that would require the use of strong base for its removal. We considered the use of an *O*-allyl ester as a possible alternative. The relatively mild conditions used to cleave *O*-allyl esters would make this an ideal choice for constructing the dipeptide acid **304** needed for our [2+2+2]-fragment condensation strategy to **303** (see Scheme 58). Given that it would probably be extremely difficult to selectively deprotect the *O*-benzyl ether by the current route, given the presence of an *O*-allyl ester, some further design modifications were considered necessary.

After considerable thought we decided to make the protected amino acid **328** our new subtarget, and we envisioned accessing it *via* the S_N2 strategy discussed earlier from alcohol **320**, where the acid functionality was now protected as an *O*-allyl ester. Alcohol **320** could potentially be derived from the vicinal diol **321** (Scheme 64), through a lead tetraacetate cleavage and a subsequent oxidation of the intermediary aldehyde to the desired acid **327**. Diol **321** could itself be obtained from (-)-diethyl-D-tartrate **322**, utilising methodology developed by Jäger and Wehner[213] for accessing 2-*O*-benzyl-D-glyceraldehyde.

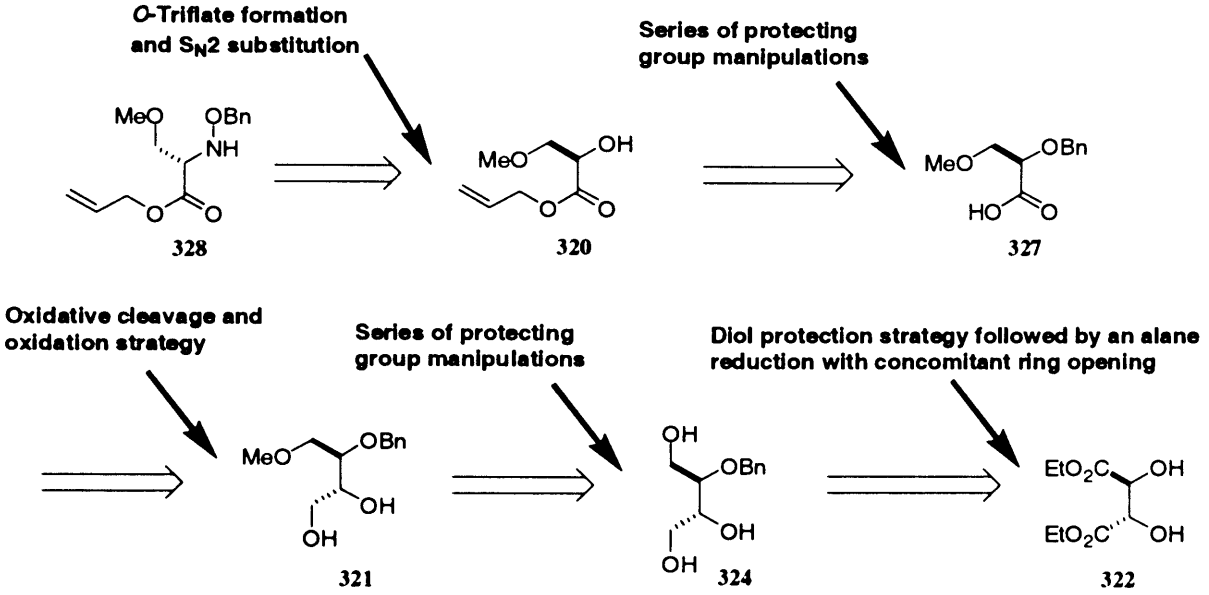

Scheme 64 Revised synthetic strategy to generic protected hydroxamic acid **310** (**328**)

The starting point for our synthesis of the orthogonally protected dipeptide **304** commenced with the protection of the vicinal diol in (-)-diethyl-D-tartrate **322** as the *O*-benzylidene acetal **323** (Scheme 65). Jäger recommends the use of benzaldehyde and *p*-toluenesulfonic acid in benzene under Dean-Stark conditions to effect this transformation and we therefore followed their published method to obtain this compound. The 500 MHz ^{1}H NMR spectrum of **323** in $CDCl_3$ matched with that reported in the literature[213]; the presence of the *O*-benzylidene acetal was confirmed by the presence of two large multiplets at δ 7.54 and 7.33 ppm respectively, representing the Ph group; and the singlet at δ 6.11 due to the acetal benzylic hydrogen.

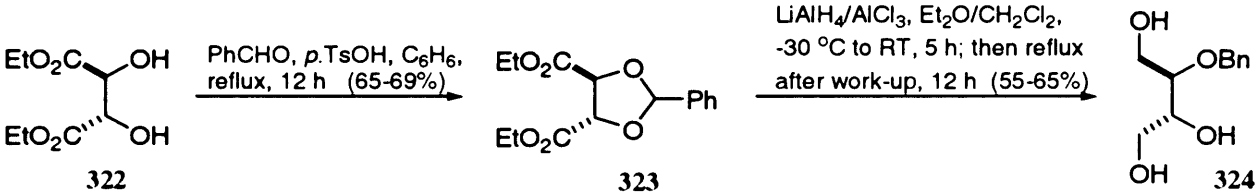

Scheme 65 Route to triol **324**

Concurrent reduction of the ester functionality in **323** and ring-opening of the *O*-benzylidene acetal was thereafter achieved using alane (AlH_3) generated from the $LiAlH_4/AlCl_3$ complex; it provided (+)-2-*O*-benzyl-D-threitol **324** in good yield. In the 500 MHz ^{1}H NMR-spectrum of **324** in $CDCl_3$, the loss of the two sets of ethyl ester signals at δ 1.21 and 1.26 (2 t, 6*H*, $CH_2C\underline{H}_3$), and δ 4.19 and 4.24 (2 q, 4*H*, $C\underline{H}_2CH_3$) in **323**, signified reduction of the ester functionality. The occurrence of three broad OH resonances at δ 2.62,

2.70 and 2.95 respectively, further confirmed a successful outcome. The presence of the characteristic multiplet at δ 7.32 and the occurrence of AB doublets at δ 4.56 and 4.68 (J_{AB} = 11.6 Hz), due to the C$\underline{H_2}$PH-group confirmed that the desired opening of the benzylidene acetal had occurred.

The vicinal diol in **324** was selectively protected as an *O*-isopropylidene acetal using 2,2-dimethoxypropane and *p*-TsOH in CH_2Cl_2. Although it is possible to form a 1,3-dioxane-type acetal in this protection, the 1,3-dioxolane is formed more rapidly due to it being a five-membered ring. Notwithstanding the 1,3-dioxolane being thermodynamically less stable than the 1,3-dioxane system, it nevertheless forms preferentially under these reaction conditions due to them being under kinetic, rather than thermodynamic, control. Evidence for the 1,3-dioxolane system in **325** was provided by the 125 MHz ^{13}C NMR spectrum in $CDCl_3$, which showed the acetal C-resonance at δ 109.2, which was in the expected region for a 1,3-dioxolane system. 1,3-Dioxane-type acetal C-atoms typically resonate at ~ δ 99 ppm. In addition there were two singlets at δ 1.34 and 1.41 respectively, in the 500 MHz ^1H NMR-spectrum in $CDCl_3$, due to the geminal methyl groups of the isopropylidene acetal. The IR-spectra for **325** also had a broad OH-stretching absorption at 3449 cm^{-1}.

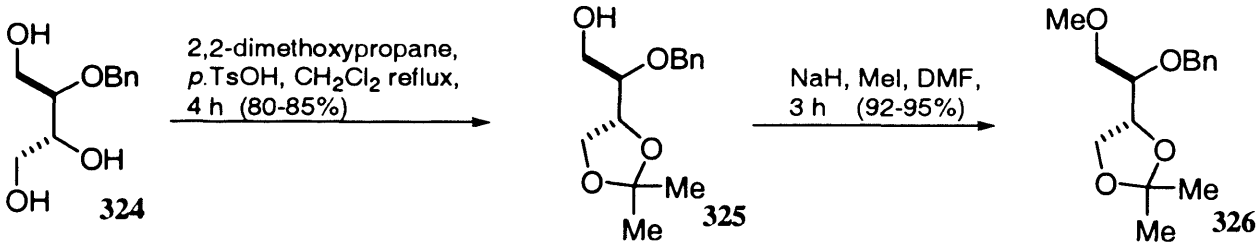

Scheme 66 Route from triol **324** to fully protected intermediate **326**

The next step in the synthesis was the *O*-methylation of the primary alcohol in **325** using sodium hydride and methyl iodide in DMF, which furnished **326** in excellent yields (92-95%). The etherification with MeI, was confirmed by the 500 MHz ^1H NMR-spectrum in $CDCl_3$, which showed the loss of the broad singlet at δ 2.64 in **325** and the appearance of a new 3*H* singlet at δ 3.30 in **326**, which corresponded to the newly introduced methoxy functionality. Further confirmation of the identity of **326** was provided by its IR spectrum, which no longer had a broad OH-stretch present.

Deprotection of the *O*-isopropylidene acetal was next effected with *p*-TsOH in MeOH and provided diol **321** in very good yields (88-92%). Diol **321** was thereafter converted into acid **327** in two steps by cleavage with buffered $Pb(OAc)_4$ and a Pinnick oxidation[225] of the resulting aldehyde. Our initial strategy for achieving this conversion had employed pyridinium dichromate for this oxidation. However this reaction proved somewhat tedious and difficult to work-up, and consistently led to rather poor yields of the desired acid. The Pinnick oxidation method was far superior in terms of work-up and product yield (76-

80%), and therefore was the protocol of choice for accessing **327**. Catalytic hydrogenation of the *O*-benzyl ether in **327** was next effected with Pearlmans' catalyst in MeOH at RT for 12 h. The resultant acid was now protected as an *O*-allyl ester, using allyl bromide in anhydrous DMF with potassium carbonate and Bu_4NI to provide **320** in good yields. These relatively mild conditions ensured that the acid was protected chemoselectively over the alcohol. The successful outcome of this reaction was confirmed by the 500 MHz ^1H NMR-spectrum of **320** in $CDCl_3$, which showed a downfield multiplet at δ 5.86 due to the more substituted vinylic proton of the allyl group. The presence of two doublets at δ 5.28 (J = 17.2 Hz) and 5.21 (J = 10.5 Hz), due to its *trans*- and *cis*- alkenic proton partners respectively, further indicated that the mono-alkylation had been successful. The presence of an alcohol and ester in **320** was confirmed by its IR-stretching absorptions at 3420 cm^{-1} (OH) and 1746 cm^{-1} (allyl ester C=O).

The synthesis of **328** was completed by subjecting **320** to an *O*-triflation with Tf_2O/2,6-lutidine and an *in situ* displacement of the so-derived *O*-triflate ester with $BnONH_2$ **318**, derived from commercially available *O*-benzylhydroxylamine hydrochloride, in a similar fashion to the route described earlier (p. 87); this provided the protected hydroxamic acid ester **328** in 66-69% yield. The appearance of inherently identical methylene protons at δ 4.72 and multiplets at δ 7.27-7.34 indicated the presence of the *O*-benzyl moiety. The presence of the allyl ester was confirmed by the presence of a multiplet at δ 5.90, and doublets at δ 5.32 (*trans*) and δ 5.23 (*cis*) representing the alkenic protons of the ester. The *O*-methoxy signal was also still intact and appeared at δ 3.30 in the spectrum. The IR spectrum of **328** also signified loss of the OH functionality (no broad peak at 3420 cm^{-1}) and the appearance of an NH absorption at 3266 cm^{-1} was also consistent with the desired S_N2 substitution.

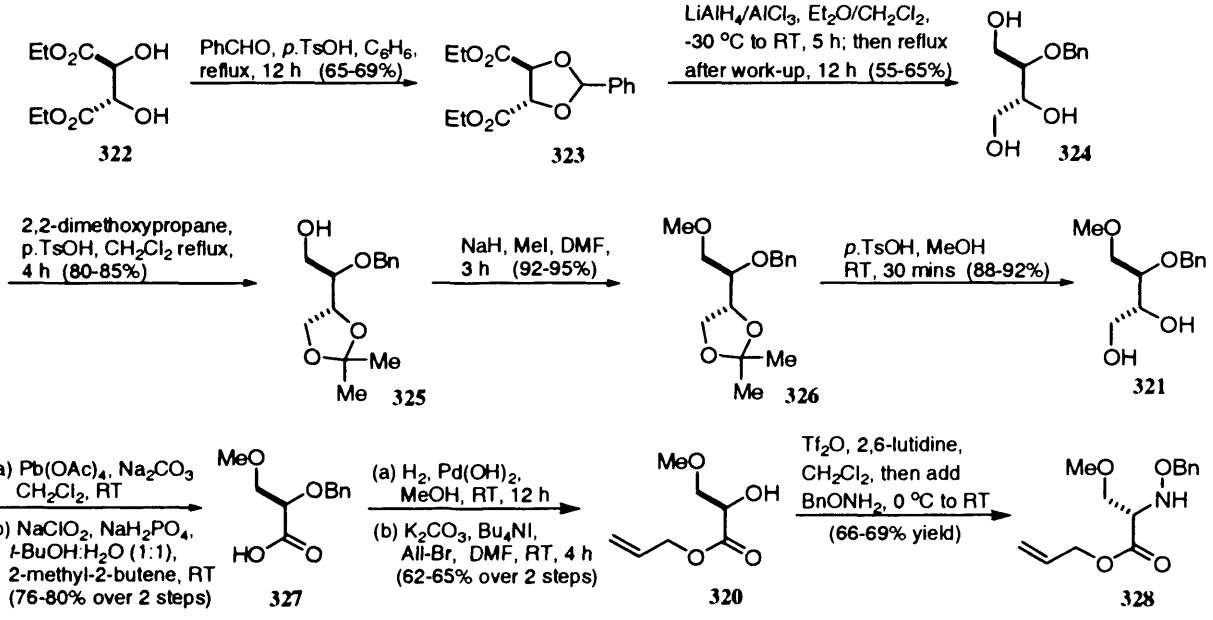

Scheme 67 Synthetic strategy to protected hydroxamic acid **328**

4.1.2 SYNTHESIS OF THE CYCLODEPSIPEPTIDE CORE OF CITROPEPTIN

Access to the orthogonally protected dipeptide **304** was achieved *via* a silver cyanide mediated coupling between **328** and the piperazic acid chloride derivative **31** and furnished the protected dipeptide **329** in 78-82% yield (Scheme 68). Use of acid chloride technology was very important at this stage due to the attenuated nucleophilicity of the hydroxamic acid ester **328**. The inductive electron-withdrawing effect of the more electronegative oxygen atom, serves to reduce the nucleophilicity of the adjacent nitrogen. Despite the complimentary activity of the α-effect, the interaction between the two lone pairs on adjacent heteroatoms, the bulky benzyl group only serves to hinder the nucleophilicity of the nitrogen atom. Fmoc-protected α-amino acid chlorides are highly reactive entities that couple efficiently to donors of low nucleophilicity. The silver cyanide is important as it encourages the displacement of the chloride ion by acting as a halogen-selective Lewis acid

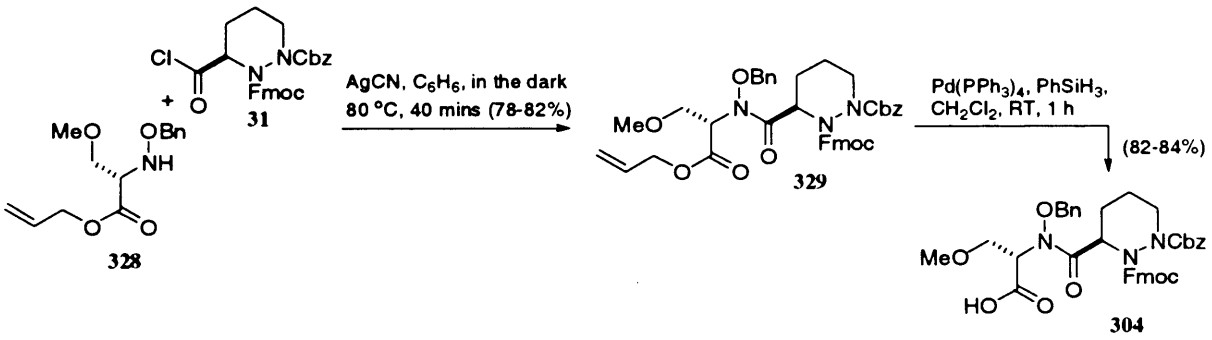

Scheme 68 Synthesis of dipeptide **304**

Despite the difficulty in assigning NMR spectroscopic data for these molecules, due to their rotameric nature, the structure of **329** was confirmed by 500 MHz ^{1}H NMR-spectroscopy in $CDCl_3$. The broad multiplet at δ 7.74 corresponded to protons 4 and 5 of the fluorene ring (**Fig. 24**), and this was accompanied by a large broad multiplet in the region of δ 7.14-7.60 that accounted for the other 16-aromatic signals. Further confirmation of the presence of the Fmoc-group was provided by the appearance of a signal at δ 4.34 (2*H*, *J* = 7.6 Hz) that signified the presence of the methylene protons of the Fmoc-protecting group. These were correlated by way of HMQC and DEPT to a peak in the ^{13}C NMR (125 MHz) at δ 68.8, which seems to be characteristic for signals of this kind. Signals were also identified in the 500 MHz ^{1}H NMR spectrum of **329** that corresponded to the presence of the methoxyserine unit. A multiplet at δ 5.89 corresponded to the vinylic proton of the allyl ester, and this was accompanied by its *cis*- and *trans*- partners at δ 5.25 (J = 11.3 Hz) and δ 5.32 (J = 17.2) respectively. Other signals that corresponded to the methoxyserine moiety in the 500 MHz ^{1}H NMR spectra included that for the *O*-methoxy protons at δ 3.31. At 298 K a pair of signals were observed that collectively accounted for 3-protons. The phenomenon is attributable to the existence of rotamers in **329**. Spectral analysis of this dipeptide was also

attempted at 363 K in toluene, however this technique only served to broaden the spectra further and was of little use. FAB HRMS confirmed our structural assignment, showing a $(M+Na)^+$ ion at *m/e* 756.28824 (Calcd. For: $C_{42}H_{43}N_3O_9Na$ $(M+Na)^+$: 756.38968).

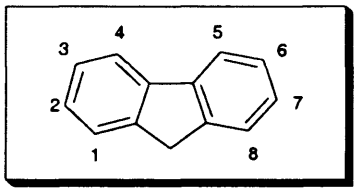

Fig.24. Numbering of fluorene protons

Following deallylation with $Pd(PPh_3)_4$ and phenylsilane in CH_2Cl_2 at room temperature, dipeptide **304** was isolated in very good yields (82-84%). Initial attempts to perform the Pd(0) catalysed deallylation step using both morpholine and *n*-tributyltin hydride as suitable allyl scavengers proved unsuccessful, with the latter affording the desired product accompanied with tin residues that were extremely difficult to remove. The relative ease of reaction and purification, accompanied by excellent yields, made the phenylsilane protocol the method of choice for this *O*-deallylation step. Following this *O*-deallylation, despite the spectra being broad, 500 MHz ^1H NMR analysis in $CDCl_3$, confirmed the loss of the vinylic multiplet at δ 5.89 and doublets at δ 5.25 and δ 5.32 respectively; these signals were replaced by a broad singlet at δ 8.11 that corresponded to the acidic O*H* proton of **304**. Yet again FAB HRMS confirmed our structural assignment, showing a $(M+Na)^+$ ion at *m/e* 716.25546 (Calcd. for $C_{39}H_{39}N_3O_9$ $(M+Na)^+$: *m/e* 716.35839).

Dipeptide **168** was obtained (Scheme 69) utilising an identical strategy to that used in the preparation of the cyclodepsipeptide core of GE3 (p. 60). It was synthesised *via* a silver cyanide-mediated coupling between **164** and **167**, which were derived from known (3*S*)-*N*(1)-Cbz-piperazic acid **30** and commercially available D-leucine **165** respectively. (3*S*)-*N*(1)-Cbz-Piperazic acid **30** was directly converted to its hydrazide derivative **164**, upon treatment with *tert*-butyl carbazate and DCC in the presence of HOBt in THF at 0 °C. Notably this reaction proceeds without the need for protection of the secondary amine in **30**. The product from this reaction stains yellow in anisaldehyde, and has an R_f ~ 0.4 when eluted with hexanes/EtOAc (1:1). The structure of **164** was confirmed by FAB HRMS, which contained a $(M+Na)^+$ ion at *m/e* 401.17963 (Calcd. For: $C_{18}H_{26}N_4O_5Na$ $(M+Na)^+$: 401.18008). An optical rotation was also taken and it correlated with previous recordings in our group $[\alpha]_D$ = -29.1° (*c* 0.268 CH_2Cl_2) compared with $[\alpha]_D$ = -26.1° (*c* 0.624 CH_2Cl_2) (p. 137 of ref 192).

The amine of **165** was protected with an Fmoc group using Fmoc-Cl in dioxane at 0 °C in the presence of aqueous Na_2CO_3. Extraction of the acidified aqueous layer with EtOAc

afforded the Fmoc protected amino acid as a white foam. The protected amine was then converted into its *N*-methyl derivative in two steps by successive treatment with: i) paraformaldehyde and catalytic *p*-TsOH and azeotropic removal of water; and ii) ionic reduction of the crude aminoacetal with TFA/Et_3SiH. The desired acid was obtained in 65% yield from **165**. The 500 MHz ^1H NMR spectrum of **168** in $CDCl_3$ was very broad due to its rotameric forms. However, we were able to distinguish the presence of the Fmoc-group due to a signal at δ 7.72 which signified protons 4 and 5 of the fluorene unit. In addition to this there was a large peak at δ 1.4 which was consistent with the presence of a tertiary butyl group. The fact that both these signals represent sections of the individual peptides, **164** and **167**, implied that their unification was successful. Our structural assignment was further confirmed by FAB HRMS, showing a $(M+H)^+$ ion at *m/e* 728.36661 (Calcd. for $C_{40}H_{49}N_5O_8$ $(M+H)^+$: *m/e* 728.36592).

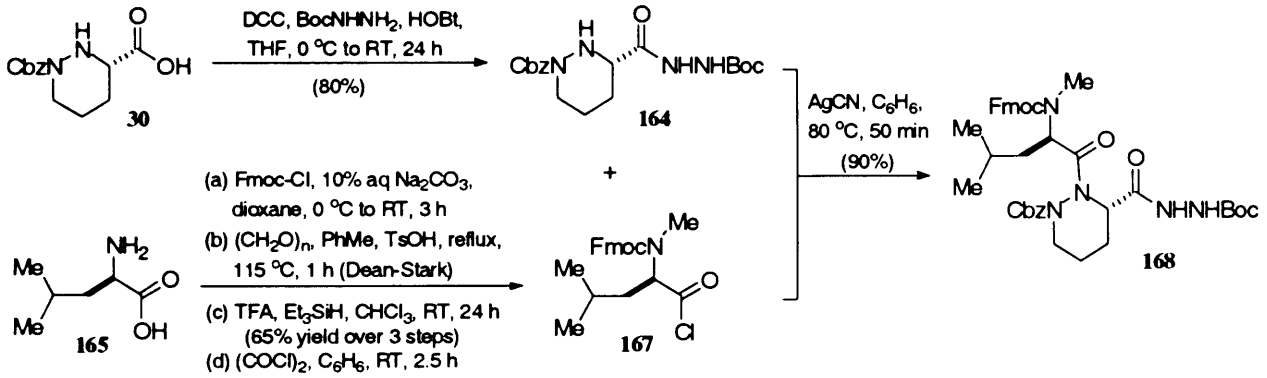

Scheme 69 Synthesis of dipeptide **168**

We again utilised a silver cyanide-mediated coupling strategy to provide dipeptide **168** in excellent yield. Once again resort to these conditions was found necessary due to the attenuated nucleophilicity of N(2) in an N(1) acylated α-hydrazino acid. The electron-withdrawing and steric hindrance effects of the acylated amine both serve to decrease the nucleophilicity of the adjacent heteroatom. We have already demonstrated that Fmoc-protected α-amino acid chlorides couple efficiently with donors of low nucleophilicity without racemisation; and the presence of AgCN is to act as a halogen selective Lewis acid (**Fig. 25**).

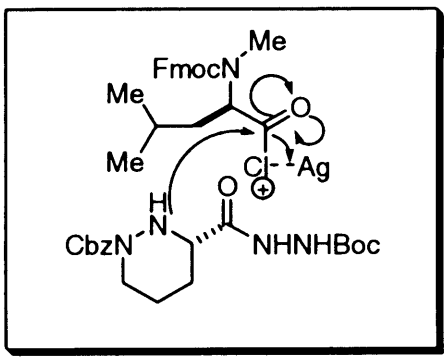

Fig.25. Proposed mechanism for the silver cyanide assisted coupling

Deprotection of **168** was achieved with diethylamine in acetonitrile, and provided the desired dipeptide **163** in excellent yields [90-94%] (Scheme 70). With the desired dipeptides now in hand, unification was achieved with BOP-Cl and Et_3N in CH_2Cl_2 at 0 °C; it afforded the tetrapeptide **330** as a white foam in good yields. The 500 MHz ^1H NMR spectra of **330** in $CDCl_3$ showed significant broadening of its resonances, it being unresolvable across a range of temperatures. We could however make out the presence of the Fmoc group, it giving rise to a broad signal at δ 7.72, which correspond to protons 4 and 5 of the fluorene ring. In addition to this, in the benzyl region, between δ 7.23-7.33, a broad signal is observed that accounted for 22 more protons and which is consistent with the number of aromatic signals we would expect if the coupling were successful. There was also a split signal at δ 3.25 which corresponded to the methoxy group of the serine residue, and a large peak at δ 1.4 which corresponded to the *tert*-butyl group of the carbazate functionality. This implied that the unification of **163** and **304** had been successful since signals corresponding to both dipeptides could be observed in the 500 MHz ^1H NMR spectrum of **330**. We mainly relied upon FAB HRMS to provide any conclusive information with regard to the success of the reaction. FAB HRMS confirmed our structural assignment, showing a $(M+Na)^+$ ion at *m/e* 1203.54049 (Calcd. for $C_{64}H_{76}N_8O_{14}$ $(M+Na)^+$: *m/e* 1203.53784).

Following another Fmoc excision, the resulting amine underwent a further silver cyanide mediated coupling with the previously prepared acid chloride **101** (Scheme 70), to provide hexadepsipeptide **331** very good yields (70-72%). Again, despite the 500 MHz ^1H NMR spectrum in $CDCl_3$ being very broad, the fluorene signal observed at δ 7.72 in **330** was no longer apparent, and its structure was further confirmed by FAB HRMS which showed a $(M+H)^+$ ion at *m/e* 1553.61423 (Calcd. for $C_{74}H_{99}N_{10}O_{20}Cl_3$ $(M+H)^+$: *m/e* 1553.61806).

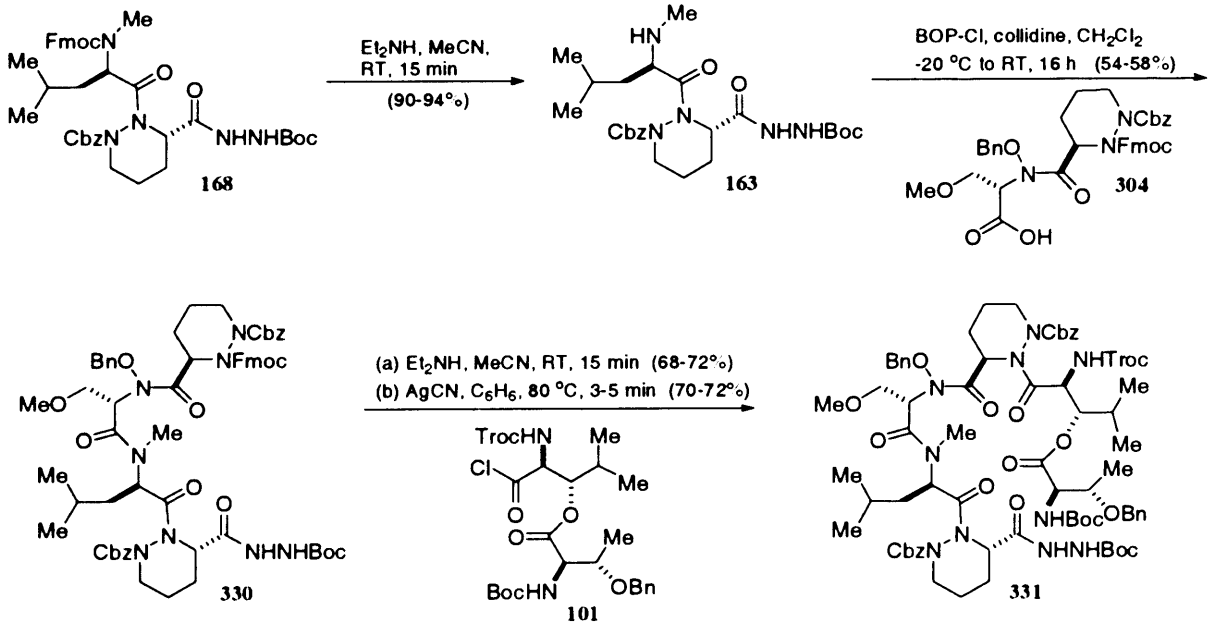

Scheme 70 Synthesis of hexadepsipeptide **331**

Hale and co-workers successfully avoided any undesired diketopiperazine formation during the synthesis of A83586C by replacing the then used diphenylmethylester-protecting group with its carbazate counterpart. However during the synthesis of citropeptin diketopiperazine formation was also observed, although not exclusively, demonstrating that protecting group interchange serves to merely mitigate the intramolecular cyclisation. The methodology used here (AgCN coupling) mirrored that employed during the syntheses of both A83586C and GE3, to achieve a similar [4+2] unification. We again have a similar situation to that encountered during the unification of **164** and **167**, where two electronegative atoms are adjacent to one another. The fact that one of the nitrogens is acylated only serves to exacerbate this problem, in having a greater electron withdrawing effect on its neighbouring atom and further decreasing its nucleophilicity (**Fig. 26**). In this instance the reaction proceeded in very good yield, to furnish the desired protected hexadepsipeptide **331** as a white foam. The products from these reactions appear as a streak on TLC and first impressions imply that you have obtained a mixture of products with different R_f values. Following careful flash chromatographic separation and analysis of different apparent fractions, it was subsequently concluded, from FAB HRMS and ^{1}H NMR spectroscopy, that each fraction represented an identical [4+2] product.

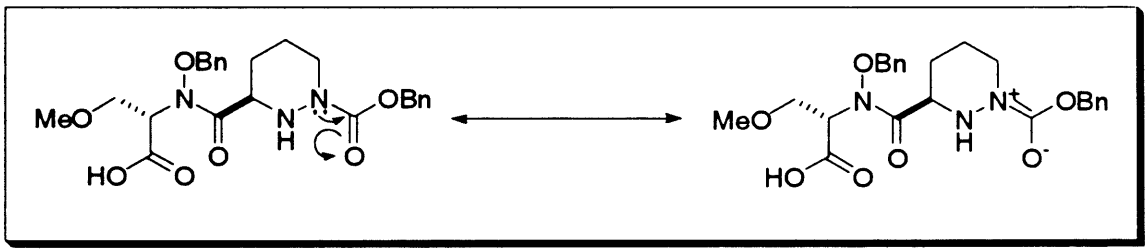

Fig.26. Diagram to show the attenuated nucleophilicity of the nitrogen atom

Following the removal of the Boc groups from **331**, with trifluoroacetic acid in CH_2Cl_2, and oxidation of the acyl hydrazine with NBS in THF, we obtained the macrolactamisation precursor **332** as an off white foam. Cyclisation was achieved in an identical fashion to that with A83586C and GE3, using the highly diluted Carpino-HATU system.[175] The desired macrolactam **333** was isolated in 42 % yield over three steps from **331**. The structure of **333** was confirmed by its FAB HRMS, which contained a $(M+Na)^+$ ion at *m/e* 1343.4551 (Calcd. For: $C_{64}H_{79}N_8O_{16}Cl_3Na$ $(M+Na)^+$: 1343.4577). Following the execution of this reaction sequence, the product appears as two UV active spots on TLC that stain golden brown in anisaldehyde, and have very similar R_f values (~ 0.4 when eluted with hexanes/EtOAc [1:1]). We decided to proceed with the *N*-Troc to *N*-Cbz interchange, using zinc dust in aqueous acetic acid, and benzylchloroformate and sodium bicarbonate in CH_2Cl_2, which facilitated the separation of these materials to afford **334** as the less polar (faster) product in 51% yield from **333** (N.B. 51% yield faster running material; 25% yield slower running material). The TLC of this reaction is a lot clearer than that of the initial

cyclisation when the Troc group is utilised for protecting the *(2S,3S)*-3-hydroxyleucine amine. The two spots were both UV active on TLC, and stained golden brown in anisaldehyde; however, their R_f values now differed considerably (R_f ~ 0.2 and 0.5 respectively). The structure of **334** was confirmed by FAB HRMS, which contained a $(M+Na)^+$ ion at *m/e* 1303.60663 (Calcd. For: $C_{64}H_{84}N_8O_{16}Na$ $(M+Na)^+$: 1303.6005) and strong band absorptions in the IR spectrum (KBr) at 1764 and 1728 cm^{-1} that were indicative of the cyclodepsipeptide ester linkage and secondary amide C=O absorptions. Also the IR spectrum (KBr) of **334** had a weak signal at 3341 cm^{-1} that represented the secondary amides N-H within the molecule.

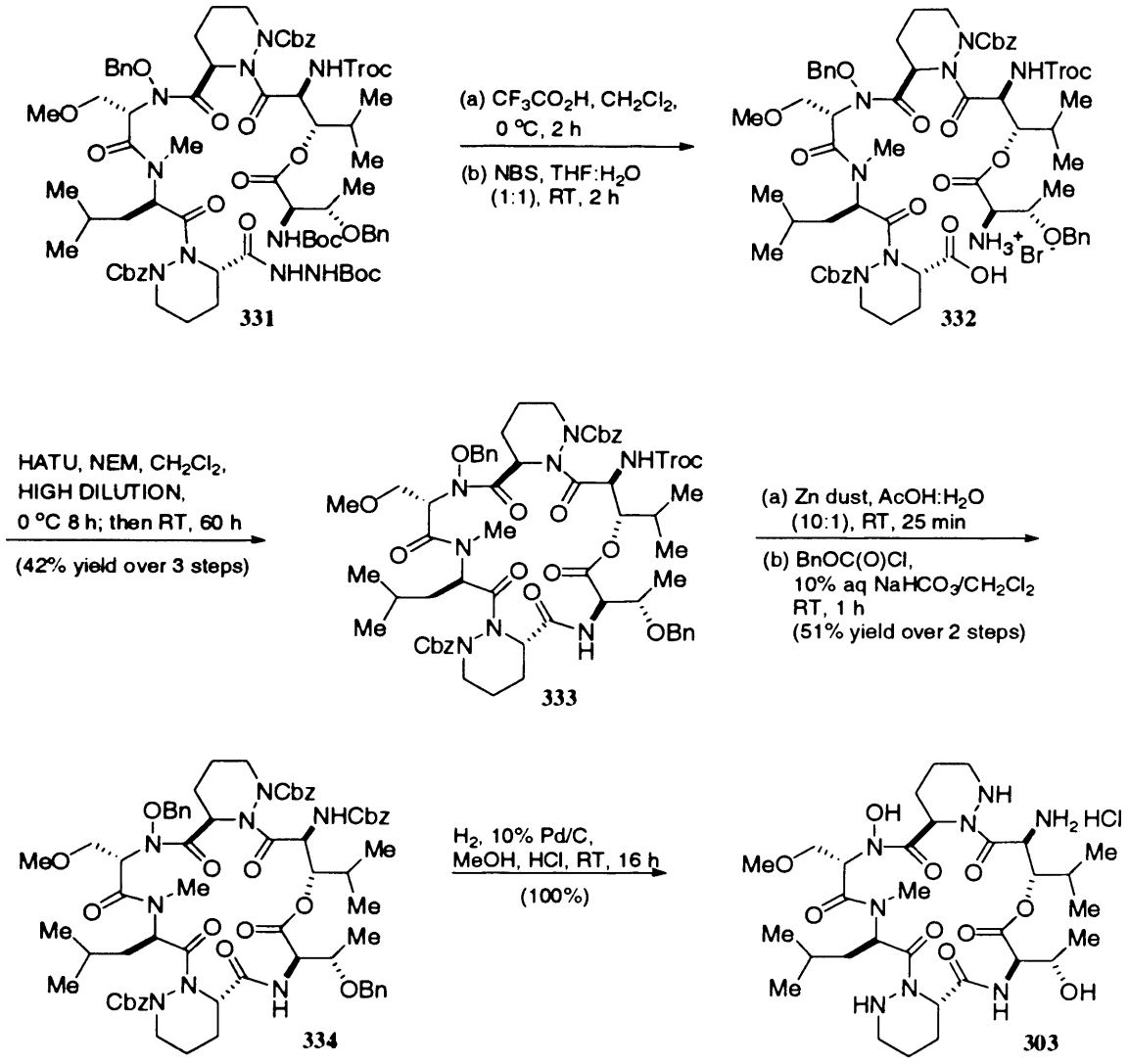

Scheme 71 Synthesis of citropeptin hydrochloride salt **303**

As is the case with all these polypeptides, conclusive NMR structure determination proved futile, due to the large number of rotamers in each system, and following each coupling the number of rotamers increased significantly, resulting in even broader and more uninformative spectra on each occasion. Various different solvents, across a range of temperatures, were utilised in the attempt to achieve more interpretable NMR spectra;

however, as the number of amide residues in the molecule increased, the quality of spectra adopted an inversely proportional relationship. Instead, we relied mainly upon mass spectrometry to provide useful information with regard to the identity of these highly complex molecules. Following FAB HRMS analysis it was deduced that these two isolated spots were in fact identical, however due to the experiences during the synthesis of A83586C and the limited information provided by mass spectra, we were uncertain if the slower running minor product was in fact an epimer, or whether we were witnessing similar chromatographically resolvable isomers to those observed by Caldwell, Durette and co-workers during the synthesis of L-156,602.[145] Access to the desired hydrochloride cyclodepsipeptide salt was achieved *via* the global deprotection of **334** (faster running material on TLC) with Pd-C, in methanolic HCl under H_2, to quantitatively provide the cyclodepsipeptide hydrochloride salt **303** as a white solid. Despite the removal of protecting groups diminishing the number of amide functionalities within the molecule, the 500 MHz ^{1}H NMR spectra were still very broad and difficult to interpret despite **303** being assessed in a variety of deuterated solvents across a range of temperatures. Again we relied upon accurate mass spectrometry to verify that we had actually synthesised the desired cyclodepsipeptide.

The structure of **303** was confirmed by its FAB HRMS, which contained a $(M+Na)^+$ ion at *m/e* 721.38597 (Calcd. For: $C_{31}H_{55}N_8O_{10}ClNa$ $(M+Na)^+$: 721.38551). Notwithstanding our removal of all protecting groups, and the ^{1}H NMR spectrum not being as broad, it nonetheless was equally as difficult to interpret. The IR (KBr) spectrum for **303** had very strong broad absorptions in the region of 2873 – 3280 cm^{-1}; these represent C-H stretches and the presence of secondary amides and amino salts. There were two additional strong absorption bands at 1733 and 1636 cm^{-1} that were consistent with the presence of the cyclodepsipeptide ester linkage and N-H bending of $-NH_3^+$ respectively.

4.2 FIRST GENERATION STRATEGY TO THE ACYL SIDE CHAIN OF A83586C

The route to the A83586C acyl side chain **68** had already been established within our group (chapter 3.2.1) and during the course of my research, I employed this developed methodology to synthesise this fragment. The first generation assembly of **68** focussed upon the unification of aldehyde **72** with sulfone **74**, and has already been discussed on pp. 40-45. I was provided with the coupled sulfone intermediate **89** and alcohol **335** by Dr Linos Lazarides of this group.[192] I converted **335** into aldehyde **72** by Swern oxidation, and then went on to couple it with sulfone **89**. The resulting β-hydroxysulfones **96** were subsequently converted into ketone **97** in 87% yield, using the methodology previously published on the A83586C synthesis[158] (Scheme 72).

The structure of **97** was confirmed by a range of NMR techniques. The 125 MHz ^{13}C NMR spectrum of **97** in $CDCl_3$, showed 39 peaks consistent with the number of distinctive carbon atoms in the molecule. Peaks at δ 208.1 and δ 169.8 corresponded to the ketone and ester moieties in the molecule respectively. Two further peaks at δ 159.2 and 158.8 represented the quaternary olefinic carbons within the molecule. The 125 MHz ^{13}C DEPT NMR also showed that there were 5 methylene signals at δ 68.9, 66.5, 36.3, 26.9 and 24.4; in addition to the 2 carbonyl and 2 quaternary peaks mentioned above there were a further 6 quaternary carbons at δ 136.8, 134.4, 134.1, 131.7, 131.0 and 129.7, and a total of 24 signals corresponding to the methine and methyl carbons of the molecule. Significant features in the ^1H NMR of **97** in $CDCl_3$ were two pairs of doublets at δ 7.70 (J = 6.5 Hz) and 7.63 (J = 6.6 Hz) respectively that were assigned to the aromatic groups of the *O*-TBPDS-ether. A quartet at δ 5.00 and doublet at δ 4.88 (J = 9.7), represented the vinylic protons in the chain, and these were accompanied by two methoxy singlets at δ 3.79 and 3.76, from the *O*-PMB groups, and another at δ 3.69 from the methyl ester. Another distinctive feature in the ^1H NMR spectrum of this molecule was the doublet at δ 3.05 (J = 9.6 Hz) which corresponded to the *H*-34 proton adjacent to the *O*-PMB ether. It was accompanied by a prominent singlet at δ 1.09 which represented the *t*-butyl functionality of the *O*-TBDPS ether.

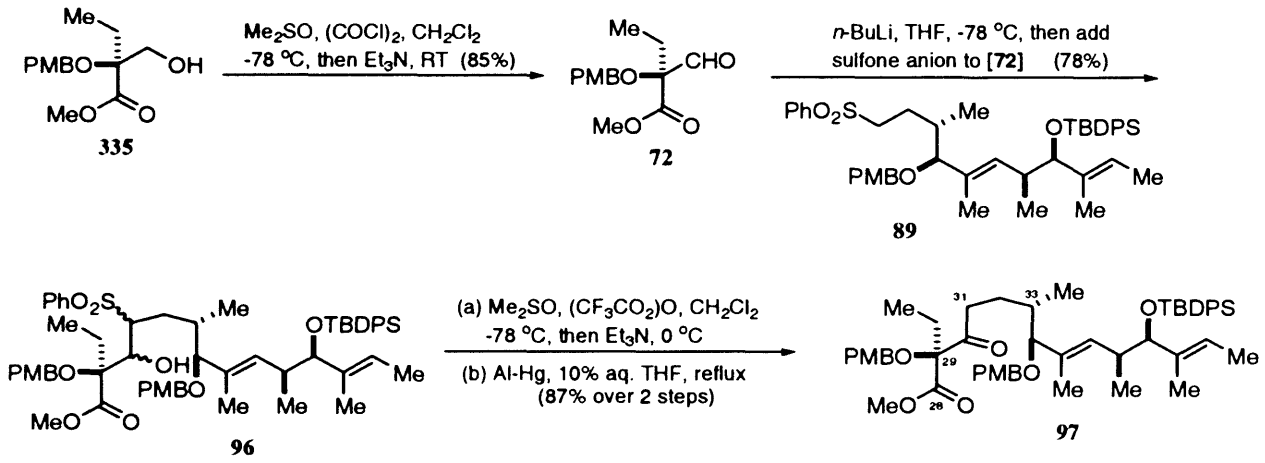

Scheme 72 First generation route to ester **97**

A chemoselective deprotection of the less hindered PMB ether in **97** then ensued and ring-closure was achieved with PPTS in MeOH, at 60 °C for 1 hour; this provided glycal **98** in 86% yield (Scheme 73). In the aromatic region of the 500 MHz ^1H NMR spectrum of **98** in $CDCl_3$, there was a reduction in the overall number of peaks, most notably the loss of two doublets from the spectra of **97** at δ 7.14 and δ 6.87, and the loss of a methoxy singlet which clearly indicated that one of the PMB groups had been lost. Further confirmation that cyclisation had been successful was apparent from loss of the ketone carbonyl peak at δ 208.1, and the shift of the *H*-34 doublet (J = 9.3 Hz) from δ 3.05 in **97** to δ 3.51 in **98**, consistent with the formation of the glycal. Completion of the desired pyran sector **68** was achieved in a further 5 steps from **98**, utilising identical technology to that used during the

A83586C first generation strategy. Removal of the *O*-TBDPS ether was achieved with *n*-butylammonium fluoride in DMF. The success of this reaction was confirmed by the 500 MHz ^{1}H NMR spectrum of **99** in $CDCl_3$, which showed a significant reduction in the number of peaks in the aromatic region of the spectra, with only the two doublets of the *O*-PMB ether remaining at δ 7.27 (J = 8.5 Hz) and δ 6.82 (J = 8.6 Hz) respectively. Further evidence of the deprotection tactic being successful was provided by the loss of the *t*-butyl singlet of the TBDPS, formerly at δ 1.05 in **98**, and the appearance of the *H*-38 signal as a doublet at δ 3.62 (J = 9.3Hz) in the resulting alcohol. This was further confirmed by the IR spectra of this molecule, which had a broad *O*H absorption at 3470 cm^{-1}. The desired activated ester **68** was then synthesised in a further 4 steps involving: saponification with EtSLi and HMPA in THF; esterification with Castro's BOP reagent;[156] Swern oxidation; and *O*-PMB deprotection with DDQ in wet $CHCl_3$, which provided **68** in 17% overall yield from **98**.

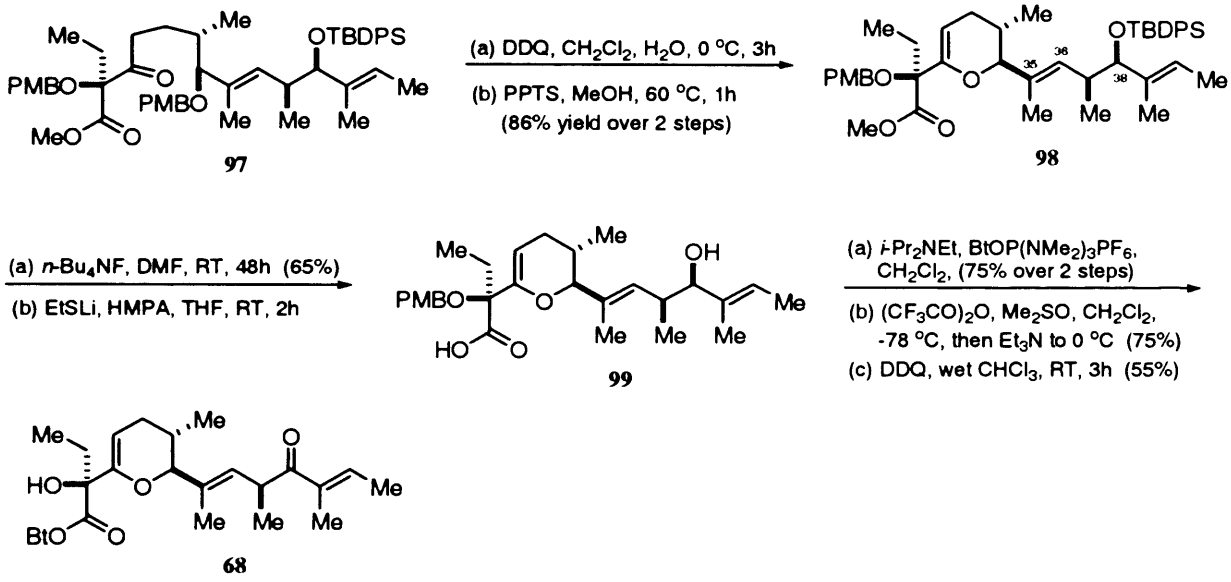

Scheme 73 First generation synthesis of A83586C acyl side chain **68**

4.3 SYNTHESIS OF A83586C/CITROPEPTIN HYBRID

In our hands we now had both the citropeptin cyclodepsipeptide hydrochloride salt **303** and the acyl side chain of A83586C **68**, and we could now proceed towards joining these two fragments with a view to accessing an interesting new synthetic molecule of the azinothricin class: the A83586C/citropeptin hybrid (Scheme 74). Previous success in the synthesis of an A83586C /GE3 hybrid within our group had already established that the original Et_3N/CH_2Cl_2 coupling conditions were not always the preferred conditions for achieving unification. As was the case, during the synthesis of the GE3/A83586C hybrid, we too reverted to the coupling strategy utilised by Caldwell, Durette and co-workers where DMF was used as the reaction solvent. We reduced the quantity of Et_3N to 2 equivalents,

made it up as a stock solution in DMF, and accordingly added it to 1 equivalent of both the citropeptin cyclodepsipeptide hydrochloride salt **303** and A83586C activated ester **68** at –78 °C. The mixture was stirred at –78 °C for 5 min and then allowed to reach ambient temperature whilst being closely monitored by TLC. To our great satisfaction this desired method afforded the A83586C/citropeptin hybrid **336** with the highest yield ever recorded within our group for this chemoselective coupling strategy. The hybrid molecule was obtained as a white solid following isolation *via* preparatory thin layer chromatography (20:1 CH_2Cl_2/MeOH multi-elution) and exposure to $CDCl_3$ for 36h, in a gratifying 63% yield. Using this procedure 180 mg of **336** was synthesised from 200 mg of **303** and 130 mg of **68**.

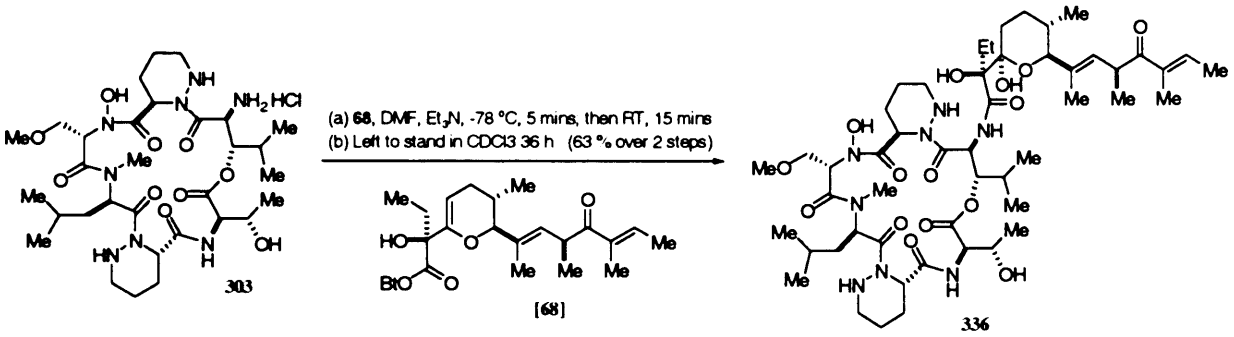

Scheme 74 Endgame strategy towards the synthesis of A83586C /citropeptin hybrid **336**

The structure of **336** was confirmed by NMR spectral analysis including a variety of 2D techniques and by FAB HRMS. The presence of the *N*-hydroxy proton was clearly evident in the 500 MHz ^{1}H NMR spectrum of **336** in $CDCl_3$, it appeared as a low-field singlet at δ 9.96. A peak that represented the methyl group (*N*-CH_3) of *N*-methyl-D-leucine was clearly visible as a singlet at δ 3.01, which was in close proximity to another singlet at δ 3.33 attributable to the *O*-methoxy group also present within the molecule. Beside these resonances, there were other distinctive peaks also present. For example, the doublet (J = 10.7 Hz) at δ 8.20 was attributable to the NH of hydroxyleucine; also apparent was a doublet of doublets at δ 5.38 that signified the C(28) proton adjacent to the ester linkage in D-threonine. Also two vinylic signals were observed at δ 5.59 and δ 6.73, as a doublet of doublets and a quartet respectively, and were shown to respectively correspond to the C(40) and C(44) vinylic protons. Another really discernable peak in the 500 MHz ^{1}H NMR spectrum of **336** in $CDCl_3$ was the multiplet at δ 4.04, which corresponded to the proton attached to C(41) that is adjacent to the ketone moiety in the acyl side chain of **336**.

The 125 MHz ^{13}C NMR spectrum of **336** in $CDCl_3$ showed 51 carbon signals, including a ketone peak at δ 203.0, a carbonyl ester linkage at δ 170.3 and six amide carbonyl signals at δ 169.5, 170.8, 171.3, 172.3, 173.6 and 175.3. Following ^{13}C DEPT analysis, it was observed that the molecule possessed 11 methylenes at δ 21.1, 21.4, 24.1,

24.4, 25.9, 27.3, 28.3, 36.6, 45.7, 47.9 and 68.4; accompanied by 4 quaternary carbons at δ 80.1, 99.6, 132.8 and 137.5 and 28 methine and methyl carbons.

Further conclusive evidence was obtained in the form of FAB HRMS, which contained a $(M+Na)^+$ ion at *m/e* 1072.24372 (Calcd. For: $C_{51}H_{84}N_8O_{15}Na$ $(M+Na)^+$: 1072.24735). In addition to this the IR spectrum (KBr) showed strong absorptions at 1634 and 1732 cm^{-1}, which were characteristic of the α,β-unsaturated ketone and cyclodepsipeptide ester linkage respectively. These were accompanied by a strong C-H stretch absorption at 2934 cm^{-1} and medium and weak signals at 3418 and 3280 cm^{-1} respectively, which are characteristic of secondary amides. The ^{13}C and ^1H NMR spectra of this hybrid molecule were extremely similar to those of the natural product components that make up its composition, and thus the spectral data is summarised overleaf.

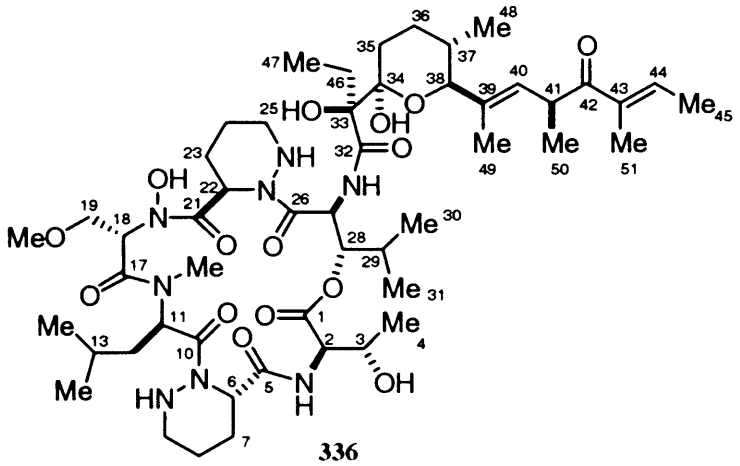

336

Fig. 27. Structural representation of **336** with Carbons numbered according to the system used by Nakagawa and co-workers[11]

Position	δ_C	δ_H	J_{H-H} (Hz)	Position	δ_C	δ_H	J_{H-H} (Hz)
Thr				25	45.7	3.13, 2.90-2.94 (m)	
1	170.3			25-*NH*		4.39	
2	56.3	4.50	8.5	**OH-Leu**			
3	64.8	4.75	5.5	26	170.8		
4	18.9	1.02	6.5	27	54.7	4.88	10.7
2-*NH*		6.17	8.5	28	78.5	5.38	10.7/2.2
3-*OH*		4.34-4.41		29	29.8	1.74	
Pip				30	19.4	0.68	6.9
5	169.5			31	14.9	0.79	6.9
6	52.3	5.16	5.8/2.0	27- *NH*		8.20	10.7
7	24.4	2.55, 1.69		**Side chain**			
8	21.4	1.55-1.62		32	175.3		
9	47.9	3.30, 2.55		33	80.1		
9- *NH*				34	99.6		
***N*-Me-Leu**				35	28.3		
10	172.3			36	27.3		
11	50.2	6.12-6.20		37	32.6		
12	36.6			38	82.2	3.94	10.2
13	24.7			39	132.8		
14	22.7	0.92	6.4	40	129.4	5.59	7.5/1.4
15	22.7	0.92	6.4	41	38.2	4.04	
16	29.2	3.01		42	203.0		
***N*-OH-*O*-Me-Ser**				43	137.5		
17	171.3			44	136.8	6.73	6.9/4.5
18	54.4	5.29	6.4/1.3	45	14.7	1.82	6.3
19	68.4	see experimental		46	25.9	1.99	13.9/6.3
20	59.1	3.33		47	8.2	0.81	7.5
18-*NOH*		9.96		48	17.62	0.67	6.5
Pip				49	12.0	1.55	1.4
21	173.6			50	19.5	1.09	6.97
22	51.5	4.88-4.93		51	11.4	1.74	1.2
23	24.1	2.21, 1.9-2.0		33-*OH*		2.91	
24	21.1	1.51-1.72		34-*OH*		6.25	

4.4 SYNTHESIS OF THE CYCLODEPSIPEPTIDE CORE OF AZINOTHRICIN

With the technology now established for synthesising multi-gram quantities of *N*-hydroxy-*O*-methyl-L-serine **328** and consequently dipeptide **304**, we were now well positioned to attempt the synthesis of the cyclodepsipeptide core of azinothricin (Scheme 75).

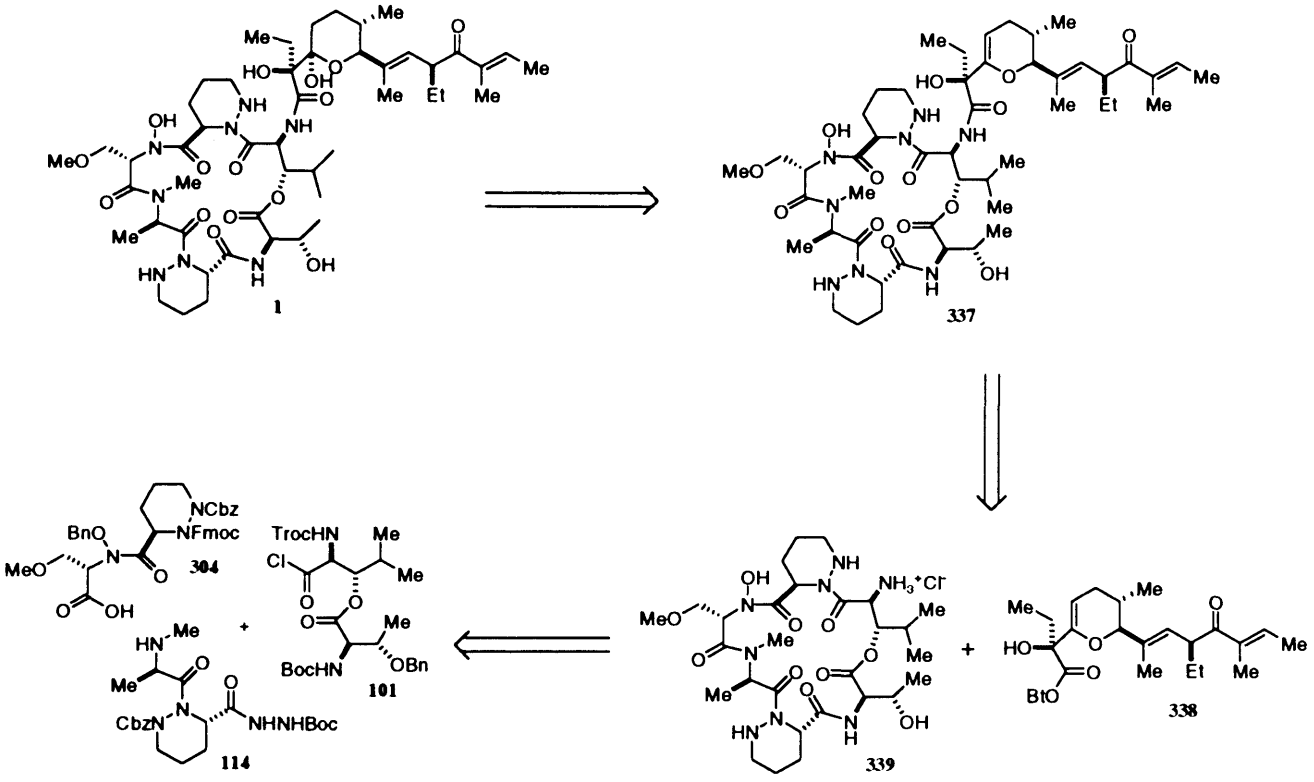

Scheme 75 Retrosynthetic analysis of azinothricin **1**

Dipeptide **114** was synthesised in a similar manner to that employed in the synthesis of A83586C. However, the protecting group strategy used was identical to that employed in the synthesis of the corresponding component in citropeptin (i.e. using a carbazate group opposed to a diphenyl methyl ester). The (3*S*)-*N*(1)-Cbz-piperazic acid derivative **30** was synthesised using identical technology to that employed during the syntheses of A83586C and GE3 (electrophilic hydrazination-nucleophilic cyclisation strategy), however during the synthesis of azinothricin we chose to employ an auxiliary derived from norephedrine, opposed to phenylalanine, to access **30** (Scheme 76). The reason we chose to employ the norephedrine derived auxiliary for this synthetic endeavour was that the intermediary products obtained were crystalline and relatively easy to purify, and its expediency enabled access to large quantities of **30**, thus facilitating the multi-gram synthesis of members of the azinothricin family. Despite the compromise in terms of enantiomeric purity with the

utilisation of the norephedrine-derived auxiliary, the comparative ease of the isolation and purification of intermediary products more than justified its employment.

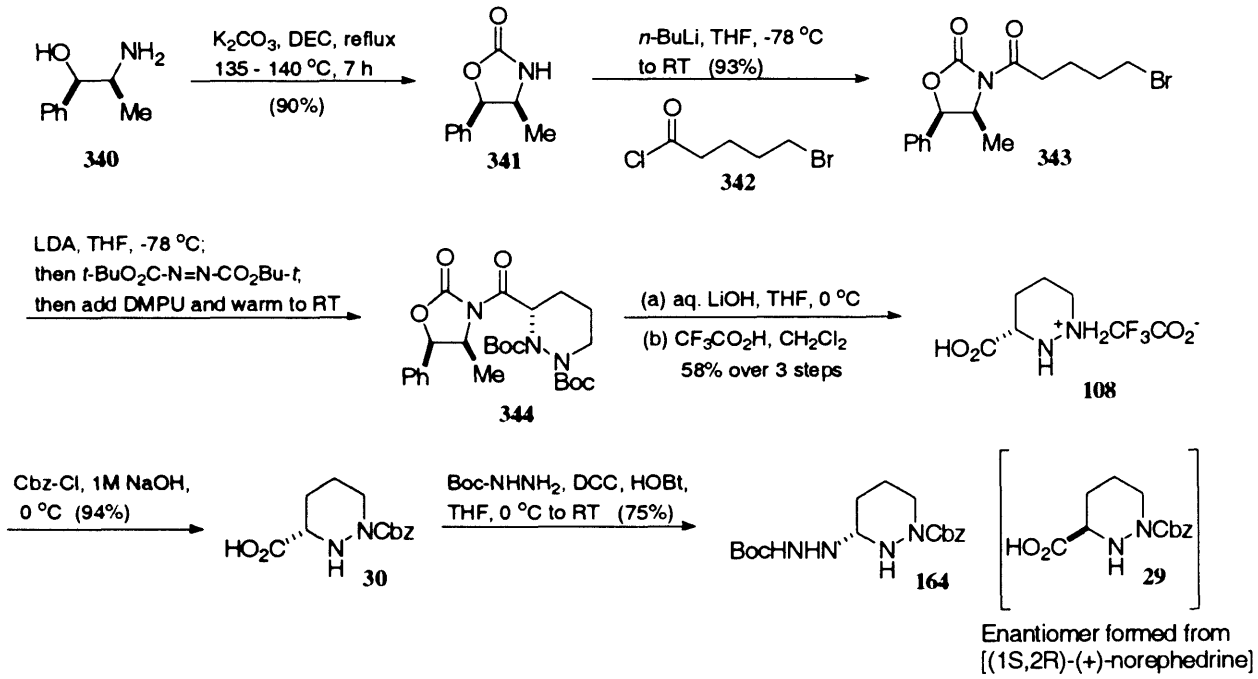

Scheme 76 Synthesis of partially protected piperazic acid **164** from norephedrine

(1*R*,2*S*)-(-)-norephedrine **340** was refluxed in diethyl dicarbonate with potassium carbonate to provide oxazolidinone **341**. This was then deprotonated with *n*-BuLi and reacted with the acid chloride **342**, derived from 5-bromovaleric acid, to furnish **343** in 93% yield. The same sequence of steps was performed upon the enantiomer of **340** [(1*S*,2*R*)-(+)-norephedrine **359**] to access (3*R*)-*N*(1)-Cbz piperazic acid **29**. With **343** in hand, we were now able to apply the tandem electrophilic hydrazination-nucleophilic cyclisation strategy devised by Hale and co-workers[170,172] during the synthesis of A83586C. **343** underwent an asymmetric electrophilic hydrazination[172] at low temperature, which was followed by an *in situ* formation of the cyclised product **344**, facilitated by DMPU. The ring-closed product **344** is obtained with high overall efficiency and is sufficient to be taken onto the next step without further purification. The chiral oxazolidinone is removed *via* hydrolysis with lithium hydroxide in aqueous THF and excision of the Boc protecting groups was achieved with anhydrous TFA to provide the trifluoroacetic acid salt **108** in 58% yield over the three steps from **344**. **108** was then converted into its Cbz-derivative following treatment with sodium hydroxide and benzyl chloroformate at 0 °C, and the resulting (3*S*)-*N*(1)-Cbz-piperazic acid moiety **30** was directly converted into the acyl hydrazide **164** in 75% yield, without the need for protection of the free amine. Confirmation of the structure of **30** was achieved using 500 MHz ^{1}H NMR spectroscopy in DMSO. The spectra in other deuterated solvents were quite broad and difficult to determine, this was still the case in DMSO at 298K. However, on

heating the sample to 343 K, we were able to resolve most of the peaks and heating further to 363 K did little to improve the spectra. At 298 K were able to observe a broad singlet at δ 12.71 that corresponded to the acidic proton of **30**. This broad peak was no longer observed on heating at 343 K, however a number of peaks were resolved and we were able to observe a multiplet at δ 7.39-7.27, and a singlet at δ 5.1 that represented the phenyl and geminal AB system of the Cbz-group protecting group respectively. Further confirmation of the structure of **30** was provided by FAB HRMS which contained a $(M+H)^+$ ion at *m/e* 265.11910 (Calcd. For: $C_{13}H_{16}N_2O_4$ $(M+H)^+$: 265.11883).

With the partially protected (3*S*)-*N*(1)-Cbz-piperazic acyl hydrazide **164** now in hand, dipeptide **114** was synthesised in a further two steps involving the silver cyanide-mediated coupling between **164** and acid chloride **112**[226] (Scheme 77), and the excision of the Fmoc-protecting group to furnish dipeptide **346**. **346** was synthesised in 92 % yield from the acid derivative of **112**, and its structure was confirmed by 500 MHz ^{1}H NMR spectroscopy in deuterated toluene at 373 K. When the same sample was observed in $CDCl_3$ at 273 K, the spectra was very broad due to its rotameric forms, heating at 373 K served to reduce these rotameric effects, however it did not totally eliminate them. In the ^{1}H NMR spectrum at 373 K there were two sets of doublets at δ 7.47 and δ 7.37 that were attributable to protons 4 and 5, and 1 and 8, of the fluorene ring respectively (see **Fig. 24.** p. 94). These are accompanied by a multiplet from δ 7.17- 6.91 that integrates to a further 9 protons and represent the remaining aromatic protons of the molecule. In addition to this there are two more significant distinguishable singlets at δ 2.74 and δ 1.29, which represented the *N*-methyl and *t*-butyl protons of **346** respectively. Further conclusive structural evidence was provided by FAB HRMS which showed a $(M+Na)^+$ ion at *m/e* 708.30240 (Calcd. For: $C_{37}H_{43}N_5O_8$ $(M+Na)^+$: *m/e* 708.30092).

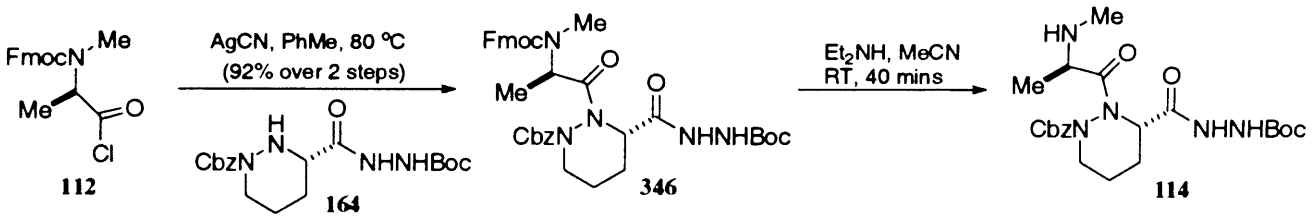

Scheme 77 Synthesis of tetrapeptide **114**

Dipeptide **114** was utilised without further purification, the main reason for this was to avoid diketopiperazine **345** formation. However, despite the use of the carbazate protecting group, a small amount of **345** was detected (Scheme 78). The observation of this cyclisation was more prominent during the synthesis of citropeptin. I think that this is due to the Thorpe-Ingold effect, where substituents on the ring increase the rate or equilibrium constant for ring-forming reactions. The greater the number of substituents, then the more

likely a cyclised product would be formed at equilibrium. This has clearly been demonstrated in this work where the presence of the geminal methyl group in citropeptin facilitated ring-formation at a faster rate than that of a single methyl group (azinothricin).

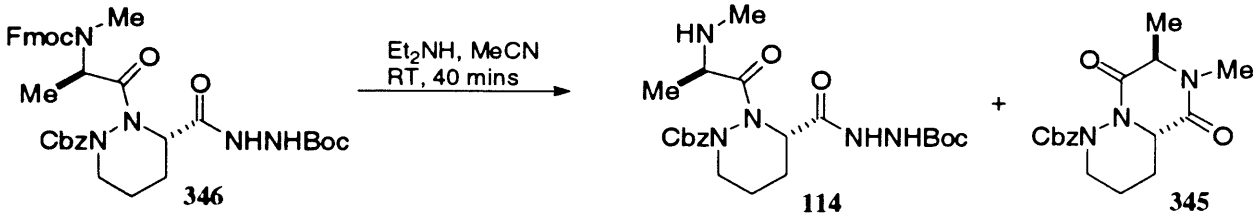

Scheme 78 Scheme demonstrates the undesired formation of the diketopiperazine **345**

It was decided to promptly tether the resulting free amine so as to avoid this undesired intramolecular cyclisation, and the [2+2] strategy proceeded with **304** in 55% yield over the two steps (Scheme 79). During this [2+2] sequence it was noticed that the yields obtained when collidine was used as the base were not as good as previous experiences (GE3 and citropeptin syntheses), however when we reverted back to the original system of BOP-Cl and Et_3N, used during the synthesis of A83586C, the reaction proceeded adequately providing the desired tetrapeptide **347** in the expected yields. The 500 MHz ^1H NMR spectrum of **347** in $CDCl_3$ was extremely broad and the use of dueterated toluene, at variable temperature, did little to improve this. The appearance of a peak at δ 7.73 was consistent with the signal for protons 4 and 5 of the fluorene ring (see p. 94) along with a broad multiplet in the region of δ 7.36-7.03, that integrated to approximately 21 protons, which is the expected number of aromatic signals for this molecule. In addition to these signals there are also two singlets at δ 3.26 and δ 1.42 that correspond to the *O*-methoxy and *t*-butyl moieties respectively. Due to the complex nature of these spectra the most reliable method of structure determination was FAB HRMS, and this provided a spectra for **347** with a $(M+Na)^+$ ion at *m/e* 1161.491967 (Calcd. for $C_{61}H_{70}N_8O_{14}$ $(M+Na)^+$: *m/e* 1161.49089).

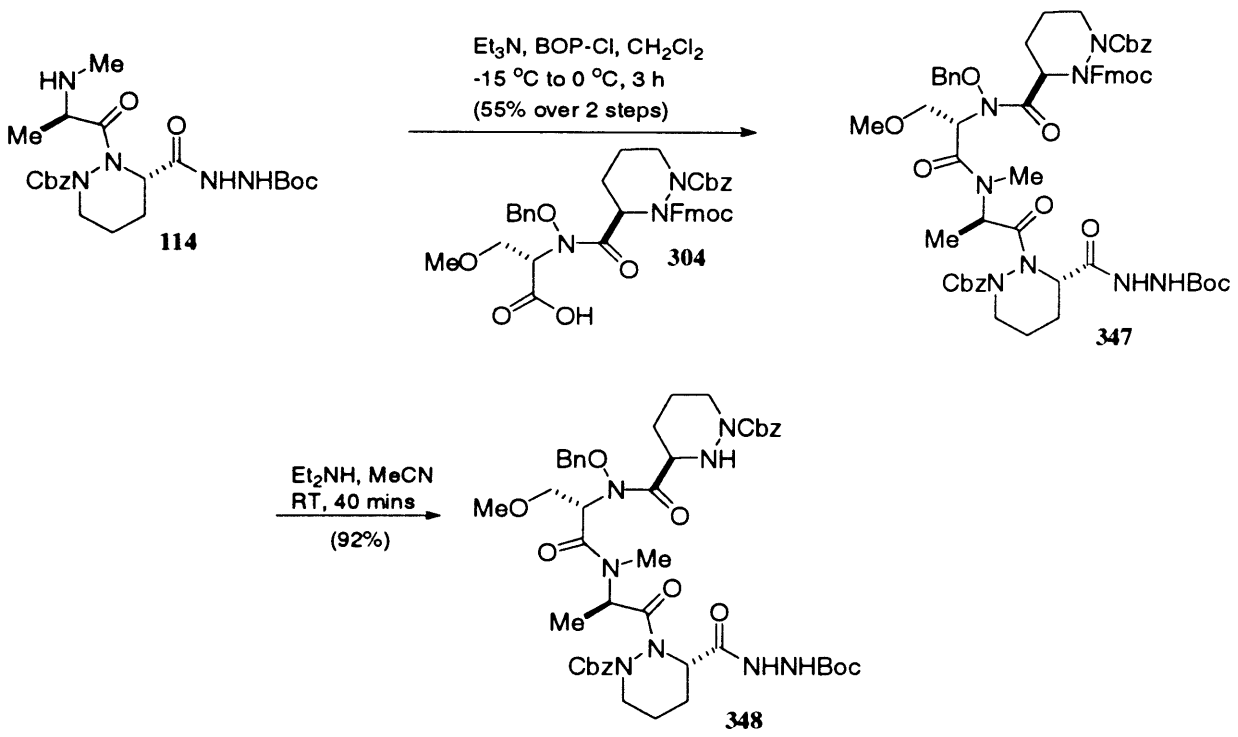

Scheme 79 Synthesis of tetrapeptide **348**

Following deprotection with diethylamine in acetonitrile, the stage was set for the [4+2] coupling between **348** and **101**, the synthesis to which has already been described in chapter 3.2.2 (p. 45). However, during the synthesis of the azinothricin cyclodepsipeptide core, there was a slight variation in our methods to access **101**. A significant problem with the original strategy used to obtain **101** was that we were only able to afford the partially protected D-threonine **123** in very poor yields (28-32%). We decided to utilise a tactic devised by a team at Jilin University in China,[227] here they used oxazaborolidinones for the selective side-chain protection of serine and threonine. Despite applying this somewhat tedious method (Scheme 80) we were able to synthesise the desired protected amino acid **123** in much-improved yields from D-threonine *via* its sodium salts. Partially protected amino acid **350** was synthesised in three steps from D-threonine in 70% yield. Its structure was confirmed by 500 MHz ^{1}H NMR spectroscopy, in deuterated methanol, where we observed the appearance of aromatic multiplets in the region of δ 7.24-7.26. In addition to this an AB system of doublets could be observed at δ 4.63 and δ 4.52 respectively, which corresponded to the geminal protons of the benzyl protecting group, indicating successful protection. Further confirmation of success in this reaction was provided by FAB HRMS which showed a $(M+H)^+$ ion at *m/e* 210.11296 (Calcd. for $C_{61}H_{70}N_8O_{14}$ $(M+H)^+$: *m/e* 210.11301). Access to **123** was then achieved in 70% yield using Boc-anhydride and aqueous sodium hydroxide in THF. Again the reaction was confirmed using 500MHz ^{1}H NMR spectroscopy in $CDCl_3$ where, in addition to the aromatic multiplets in the region of δ 7.23-7.35, we observed a

singlet at δ 1.44 consistent with *t*-butyl functionality. Also present were the geminal AB system of the benzyl-protecting group at δ 4.57 and δ 4.27 respectively, and a doublet at δ 1.24 that corresponded to the methyl group of **123**. We then continued with an identical strategy to that employed in previous constructions of this depsipeptide, which utilised a DCC/DMAP-mediated coupling and relevant protection strategies to afford depsipeptide **101**. The spectroscopic data for the acid derivative of **101** was in agreement with data collected from previous syntheses within our group.

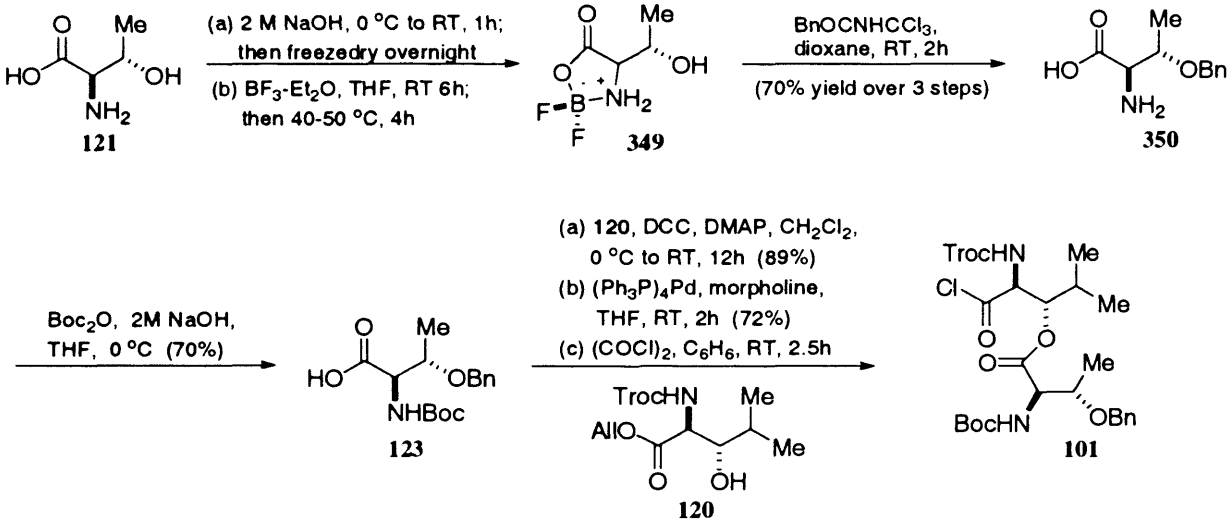

Scheme 80 Revised strategy to depsipeptide **101**

Unification of **348** and **101** was achieved using silver cyanide in benzene under reflux for under 2 mins (Scheme 81), monitored closely by TLC to afford the protected hexadepsipeptide **351**. As was the case for **347** (p 109), due to the broad appearance of the NMR spectra, the most informative method of spectroscopic analysis for **351** proved to be FAB HRMS, which showed a $(M+Na)^+$ ion at *m/e* 1533.55185 (Calcd. for $C_{71}H_{93}N_{10}O_{20}Cl_3$ $(M+Na)^+$: *m/e* 1533.55306).

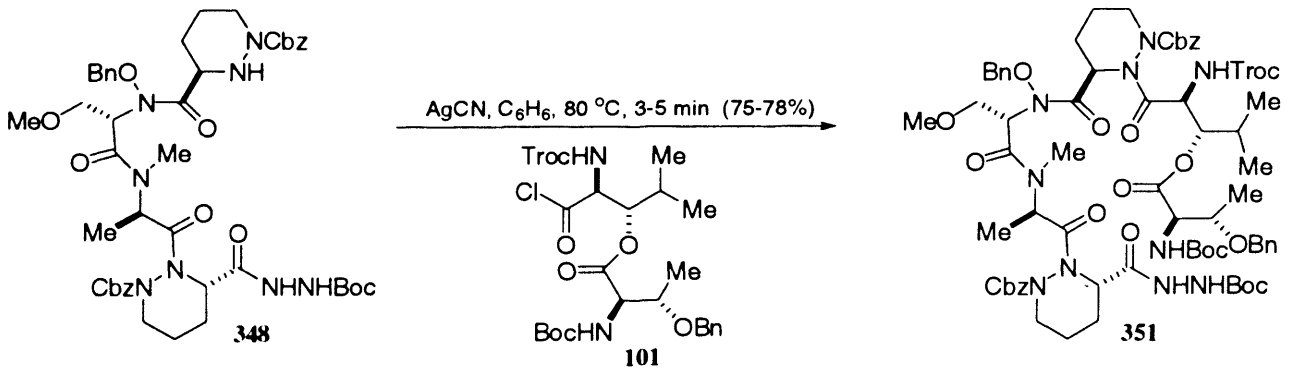

Scheme 81 Synthesis of fully protected hexadepsipeptide **351**

Similar to the [2+2] coupling step for this reaction, T.L.C analysis appeared to indicate two different products. Separation of the two materials *via* flash chromatography gave two products that were indistinguishable by NMR and mass spectrometry in a ratio of 2:1 (Slower running material (52%): faster running material (26%)). The materials were taken on separately, since any epimerisation would only become apparent after the cyclodepsipeptide had been coupled to the desired acyl side chain. In contrast to this however, Caldwell, Durette and co-workers[146] observed that on the cyclisation of the linear hexadepsipeptide, *via* the mixed phosphonic anhydride method, the desired cyclic hexadepsipeptide was obtained as a mixture of chromatographically resolvable isomers and following deprotection one product was obtained. What we observe on TLC at both the [2+2] and [4+2] coupling stages could very well be something similar to Caldwell and Durette, due to the number of amide bonds present, however caution has to be applied at such an advanced stage of the synthesis. Removal of the Boc groups then ensued with TFA in CH_2Cl_2 and this was followed by oxidation of the acyl hydrazine using NBS in aqueous THF (Scheme 82). This provided the macrolactamisation precursor **352**, which readily underwent cyclisation using Carpino's HATU system[175] to afford cyclic product **353** in 70% yield over the three steps from **351**. On observation of TLC, the product appeared as a golden streak, and the reaction was confirmed by way of FAB HRMS, which contained a $(M+Na)^+$ ion at *m/e* 1301.41146 (Calcd. For: $C_{61}H_{73}N_8O_{16}Cl_3Na$ $(M+Na)^+$: 1301.41076).

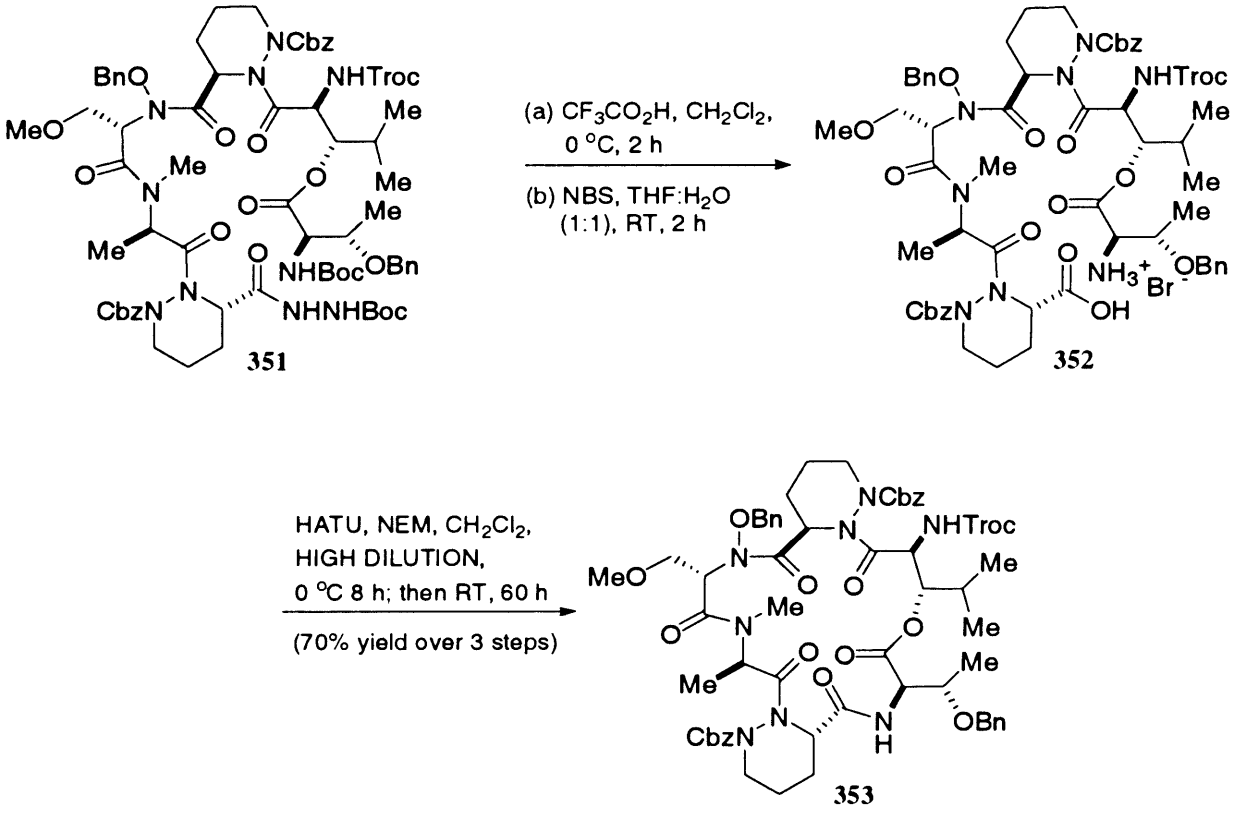

Scheme 82 Synthesis of fully protected cyclodepsipeptide **353**

Customary Troc to Cbz interchange then ensued, using zinc dust in aqueous acetic acid, followed by treatment of the resulting amine with 10% sodium bicarbonate and benzylchloroformate in CH_2Cl_2, to afford cyclic hexadepsipeptide **354** in 52-56% yield from **353** (On assumption that the faster running material is the desired product and the slower running material is the epimer. However if we establish that indeed both products are in fact the same compound, then the yield would obviously be improved). The spots of the azinothricin Cbz-protected analogue were somewhat closer on TLC than they were for its citropeptin counterpart. When eluted in 1:1 hexanes/EtOAc the ratio of R_f values for the two materials was approximately 1.5, compared with 2.5 in the case of the citropeptin cyclodepsipeptide. As was the case during the synthesis of citropeptin, both these materials stain golden brown on TLC when developed with anisaldehyde. Following FAB HRMS analysis it was determined that they were both identical in terms of molecular weight and composition and their FAB HRMS contained a $(M+Na)^+$ ion at *m/e* 1261.54225 (Calcd. For: $C_{66}H_{78}N_8O_{16}Na$ $(M+Na)^+$: 1261.54332).

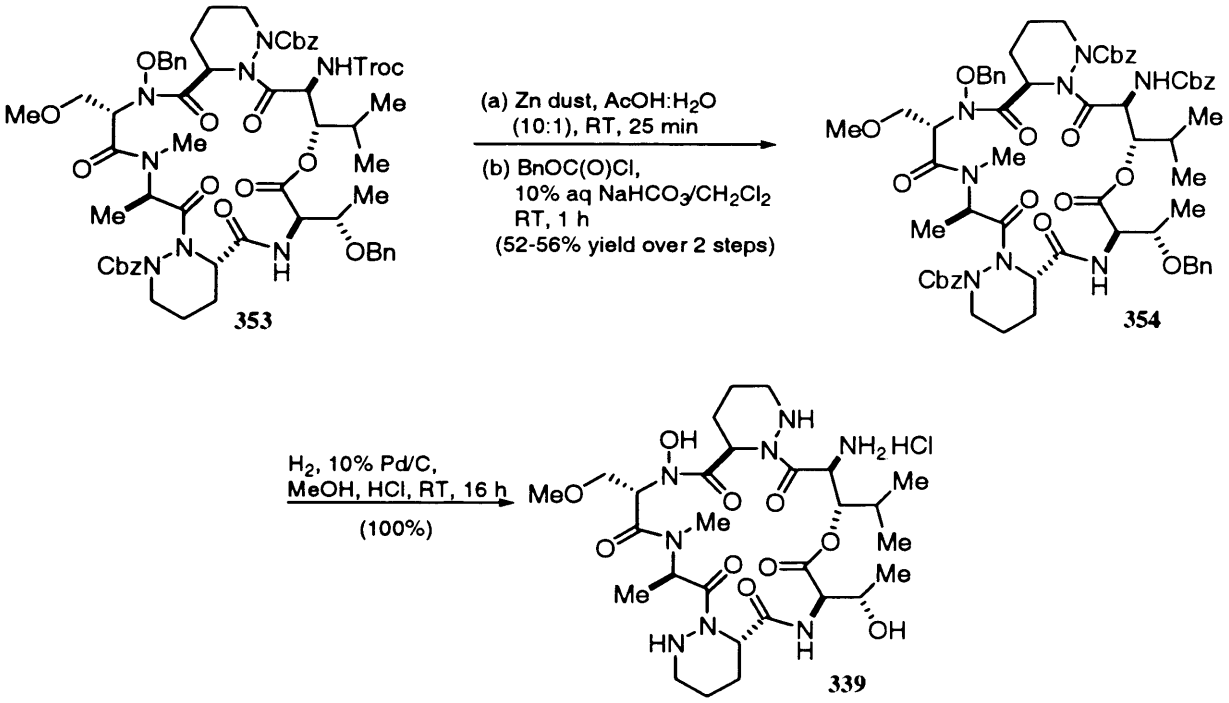

Scheme 83 Endgame synthesis of the azinothricin cyclodepsipeptide hydrochloride salt **339**

Following the HATU cyclisation, we are presented with what appears to be two inseparable spots on TLC, however following the Troc to Cbz interchange we are able to isolate these products and they were taken on separately to avoid any unnecessary contamination of the final product. We found that the ratio of the faster running material to the slower running material was approximately 3:1, however on observing the FAB HRMS both materials were indistinguishable. Once again this could be another representation of the conformational isomer phenomena observed by Caldwell and Durette. However, due to

the epimerisation at the (3*S*)-piperazic acid stereocentre encountered by Hale and co-workers, it was essential that all material was kept separate until conclusive evidence had been obtained. The desired cyclodepsipeptide hydrochloride salt **339** was quantitatively provided, following global deprotection under H_2 with Pd/C in methanolic HCl. The structure of **339** was confirmed by FAB HRMS, which contained an $(M+H)^+$ ion at *m/e* 657.35722 (Calcd. For: $C_{28}H_{49}N_8O_{10}H^+$ $(M+H)^+$: 657.35715). The IR (KBr) spectrum for **339** had very strong broad absorptions in the region of 2861–3280 cm^{-1}; these represent C-H stretches and the presence of secondary amides and amino salts. There are two additional strong absorption bands at 1746 and 1647 cm^{-1} that are consistent with the presence of the cyclodepsipeptide ester linkage and N-H bending of $-NH_3^+$ respectively.

4.5 SECOND GENERATION STRATEGY TOWARD THE ACYL SIDE CHAIN OF A83586C

As part of our effort to significantly improve the available technology to access these highly complex molecules we decided to revise the current route to the acyl side chains of these molecules. Our long-term goal within the Hale group is to synthesise these complex natural products and analogues on multi-gram scale within the laboratory. Since we have devised the necessary technology to accomplish this for the cyclodepsipeptide sectors of these molecules it became significantly important to achieve similar success for the synthesis of the acyl side chain. In order for us to realise our ambitions it was essential to develop a second-generation strategy towards the acyl side chains of these molecules.

Given that the Julia coupling between sulfone **89** and aldehyde **72**, and the subsequent ring-closure to the glycal **98**, are now a well established and robust processes[158(a),(b),176,177], we decided to maintain this sequence and focus solely upon the synthesis of the sulfone **89**. During the synthesis of **89** (C(31) to C(47)) all efforts to incorporate the trisubstituted alkene using McMurry-Scott and Stille protocols proved futile. Instead Hale and co-workers employed an inferior Grignard addition/$POCl_3$-pyridine-mediated dehydration tactic to provide the desired trisubstituted alkene **89**. Unfortunately the latter was the predominant isomer of a 2.6:1 mixture with the 1,1-disubstituted alkene **355** (Scheme 84), and we realised that if we were to be successful in synthesising these molecules on a large scale, then this sequence needed to be revised.

*** Note: All carbon numberings from here on are with reference to the numbering of A83586C**

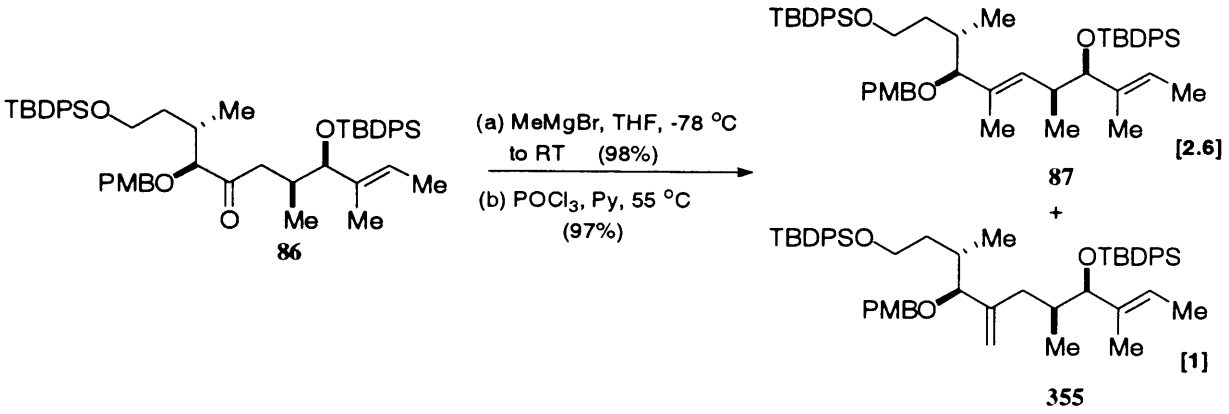

Scheme 84 Representation of the inferior Grignard addition/$POCl_3$-pyridine-mediated dehydration tactic used in the synthesis of the acyl side chain **68** of A83586C

Our strategy for the synthesis of the C(31)-C(47) fragment is outlined in Scheme 85 below. We envisioned that the construction of **89** could be achieved from terminal alkene **356**, using a hydroboration tactic followed by simple functional group interconversions. Alkene **356** could, in turn, be derived from α,β-unsaturated aldehyde **357**, utilising an asymmetric crotylation to conveniently install the C(33) and C(34) stereocentres. The (*E*)-geometry of the double bond in aldehyde **357** was envisioned to be constructed using a Wittig olefination and reduction sequence on aldehyde **358**, which in turn was to be created using a strategy that mirrors the tactic used during the synthesis A83586C, utilising a fully stereo-controlled Evans aldol reaction between *N*-propionyl oxazolidinone **75** and tiglic aldehyde **76**, to install the two stereocentres with a *syn*- relationship and the (*E*)-trisubstituted alkene in a single step.

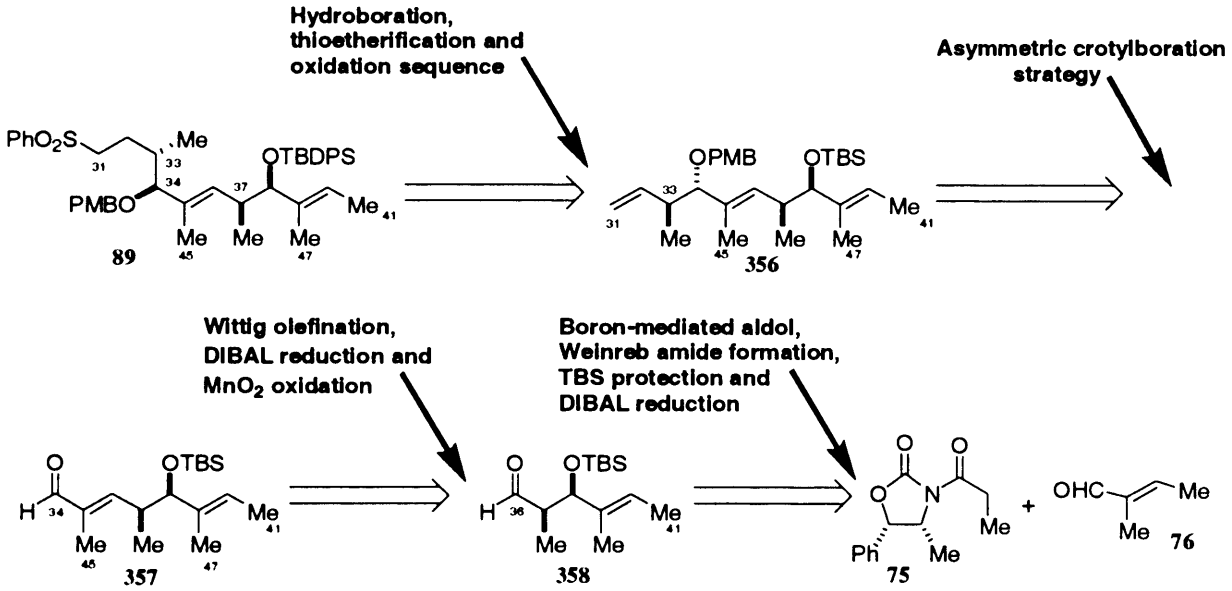

Scheme 85 Retrosynthetic analysis of the second-generation strategy towards the synthesis of sulfone **89**

4.6 IMPLEMENTING THE SECOND-GENERATION STRATEGY IN THE SYNTHESIS TOWARDS AZINOTHRICIN

Since we had already assembled the cyclodepsipeptide core of azinothricin in substantial quantities, we thought it wise to attempt the total synthesis of this founder-member natural product, adopting the revised second-generation synthetic strategy to sulfone **89**. The only difference between the acyl side chains of A83586C **68** and azinothricin **338** is the presence of an ethyl moiety at C(38), in the case of azinothricin compared with a methyl moiety at C(37) in the case of A83586C (**fig. 28.**).

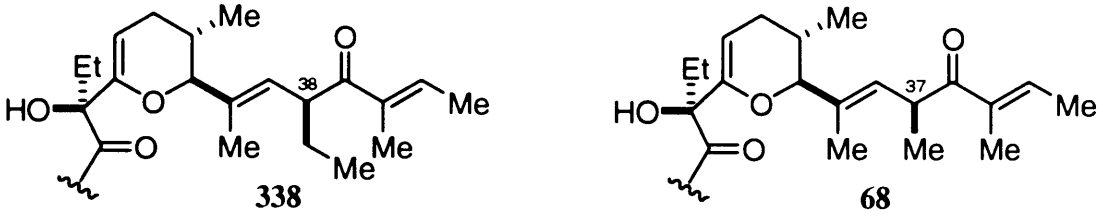

Fig. 28. Structural disparities between the acyl side chains of azinothricin **338** and A83586C **68**

Oxazolidinone **362** was synthesised in two steps from (1S,2R)-(+)-norephedrine **359** and butyryl chloride **361**, and the resulting amide underwent a boron-mediated Evans aldol reaction[159(a)] with tiglic aldehyde **76** to afford the *syn*-aldol **363** in 93% yield as a single diasteroisomer (Scheme 86). Transformation of this imide to the Weinreb amide was achieved by treatment with $AlMe_3$ and MeNH(OMe).HCl and the resulting alcohol **364** protected as a TBS ether to provide amide **365** in 80% yield. The structure of **364** was confirmed by 1D and 2D NMR analysis and IR spectroscopy. The 500 MHz ^{1}H NMR spectra of **364** in $CDCl_3$ contained a quartet at δ 5.36 (J = 6.7) that represented the C(40) vinylic proton of the molecule which was accompanied by two singlets at δ 3.51 and δ 2.99 that correspond to the methoxy and methyl groups of the Weinreb amide. The peak that corresponded to the *O*-methoxy group of the Weinreb amide was quite broad at the base due to an overlap with the signal that corresponds to the alcohol functionality. In addition to this there were three strong bands in the IR spectrum of **364**, a broad peak at 3418 cm^{-1}, from the O-H stretch, an overlapping series of peaks in the region 2822-2936 cm^{-1} and a C=O stretch at 1636 cm^{-1}. The *O*-TBS-protection was confirmed in the 500 MHz ^{1}H NMR spectrum of **365** in $CDCl_3$, by the appearance of three prominent singlets at δ 0.81, -0.03 and –0.11 that correspond to the *t*-butyl and methyl groups of the *O*-TBS ether respectively. This was further supported in the IR spectrum of **365** by the disappearance of the broad absorption at 3418 cm^{-1} in **364**. Our initial thoughts regarding this TBS protection strategy were somewhat reserved, since we wanted to be in a position to correlate the spectra of the 2nd generation sulfone, with that of the sulfone synthesised during the 1st generation strategy

(utilised TBDPS protection strategy during 1st generation synthesis). Despite this however, this was the most expedient option and we proceeded with this protection strategy toward completion of sulfone **376**.

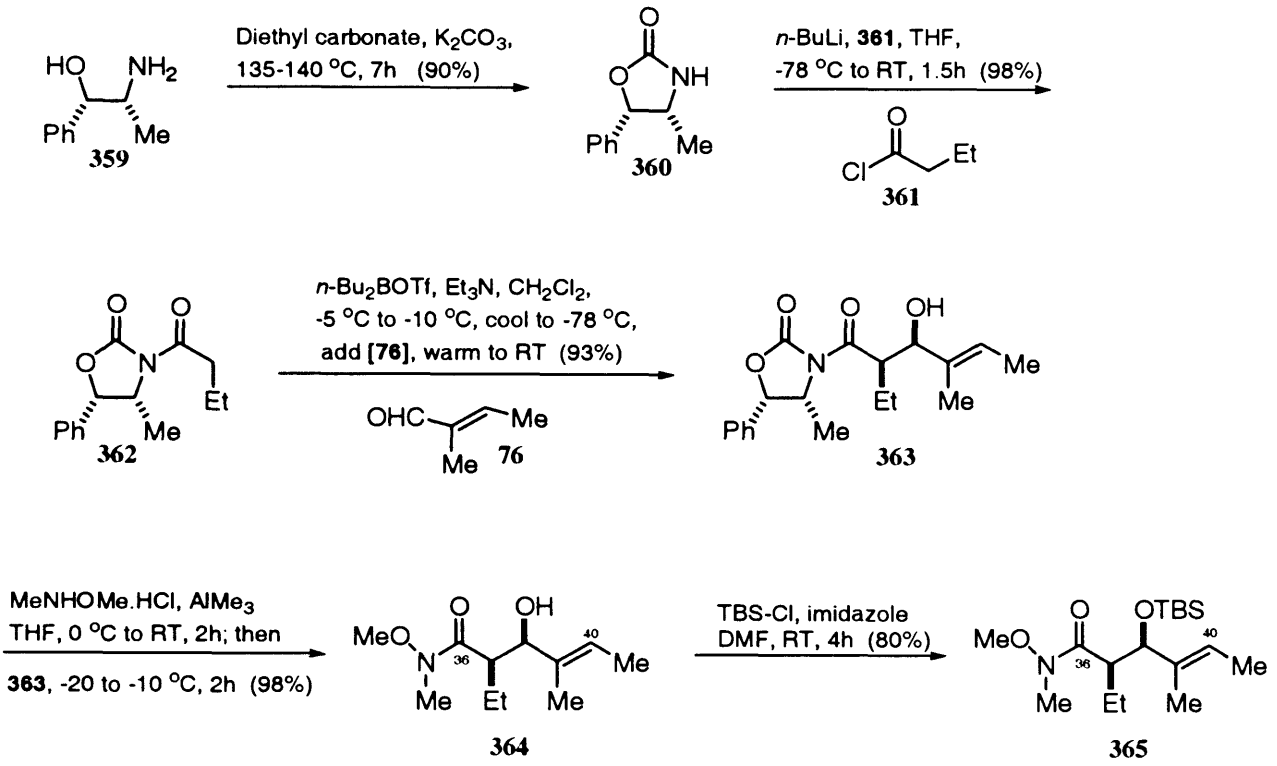

Scheme 86 Synthesis of TBS-protected alcohol **365**

Partial reduction of Weinreb amide **365** was accomplished with DIBAL-H in toluene at low temperature (Scheme 87) to provide aldehyde **366**. The success of the reaction was confirmed by the 500 MHz ^{1}H NMR spectrum of **366** in $CDCl_3$ which showed the loss of both the methyl and *O*-methoxy singlets at δ 3.02 δ 3.56 respectively, and the appearance of a doublet at δ 9.48 (J = 3.58) corresponding to the proton of the newly-formed aldehyde, which correlated with a peak at δ 204.1 in the 125 MHz ^{13}C NMR spectrum of **366**. In addition to this doublet the 500 MHz ^{1}H NMR spectrum of **366** in $CDCl_3$ also contained a quartet at δ 5.38 (J = 6.7) and a doublet at δ 4.16 (J = 7.4), which corresponded to the C(40) vinylic proton and the C(38) proton adjacent to the *O*-TBS ether. There were also singlets for the *O*-TBS ether present at δ 0.82 (9*H*), -0.22 (3*H*) and –0.08 (3*H*) respectively. Aldehyde **366** was thereafter subjected to a Wittig olefination with the stabilised (carbethoxyethylidene) triphenylphosphorane ylide **367** to furnish the (*E*)-α,β-unsaturated ester **368** in 80% yield. The structure of **368** was once again confirmed by 500 MHz ^{1}H NMR spectroscopy, with the ^{1}H NMR spectrum of **368** in $CDCl_3$ containing a doublet of doublets at δ 6.38 (J = 9.6, 1.4), a doublet at δ 1.79 (J = 1.4), a multiplet at δ 4.14 and a triplet at δ 1.25 (J = 7.1); all of which corresponded to protons from the newly introduced α,β-unsaturated ester. The 125 MHz ^{13}C NMR spectrum of **368** provided more evidence of this Wittig olefination with the presence of

a further 5 signals, which would be expected for this transformation, and one of them being a methylene carbon (from the ethyl ester). FAB HRMS for **368** was obtained which showed a $(M+H)^+$ ion at *m/e* 355.26599 (Calcd. for $C_{20}H_{38}O_3Si$: *m/e* 355.26683).

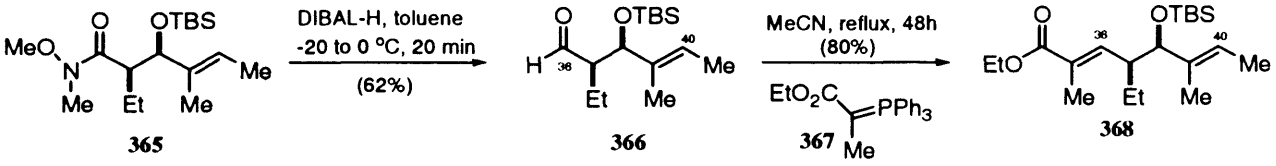

Scheme 87 Synthesis of α,β-unsaturated ester **368**

The resulting ester was reduced with DIBAL-H to provide allylic alcohol **369** in 94% yield. The 500 MHz ^{1}H NMR spectrum of **369** in $CDCl_3$ showed that the multiplet and triplet at δ 4.14 and δ 1.25 respectively in **368**, which corresponded to the ethyl ester, were no longer present. The appearance of a singlet at δ 3.92 that corresponded to the geminal allylic protons confirmed that the reduction had successfully occurred. In addition to this the carbonyl signal at δ 168.2 in the 125 MHz ^{13}C NMR spectrum of **368** was no longer present in **369**, which provided further confirmation of a successful reduction. Another interesting observation, which also assisted in confirming the loss of the ester functionality, was that the signals that corresponded to the two vinylic protons within the molecule (C(36) and C(40)) had now changed in terms of electron shift. The C(36) doublet of doublets that was further downfield (δ 6.38) than the C(40) quartet (δ 5.30) in **368** was now further up field in **369** appearing at δ 4.95 (J = 9.2, 1.2), while the quartet appeared at δ 5.23. This was obviously due to the loss of the electron-withdrawing ester moiety, which was exemplified by the conjugation of the molecule, which shifted the vinylic proton substantially further downfield. Allylic alcohol **369** was then oxidised with MnO_2, to provide the α,β-unsaturated aldehyde **370** in 78% yield. The loss of the singlet at δ 3.92 and subsequent appearance of a singlet at δ 9.35, in the 500 MHz ^{1}H NMR of **370** in $CDCl_3$, signified the conversion to the aldehyde and this was supported by the presence of a peak at δ 195.4 in the 125 MHz ^{13}C NMR spectra. Once again the C(36) vinylic doublet of doublets at δ 6.07 was further downfield than its C(40) counterpart quartet at δ 5.29. This is once again due to the reintroduction of this α,β-unsaturated system that serves to withdraw electron density from the tri-substituted olefin.

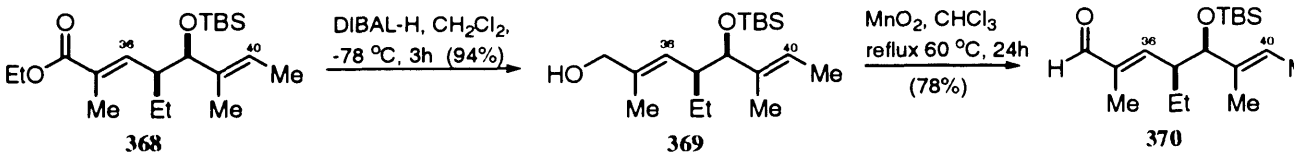

Scheme 88 Synthesis of α,β-unsaturated aldehyde **370**

Our next step was to devise a strategy that would allow exploitable access to terminal alkene **372**. The reaction of unsaturated aldehydes with chiral boronates is generally known to provide homoallylic alcohols in low to moderate enantioselectivity.[228] Nevertheless, we hoped that through careful optimisation of the reaction conditions we might be able to employ an asymmetric crotylboration strategy on **370** to set the C(33) and C(34) stereocentres in a single step. After significant experimentation, it was discovered that the Brown[229,230] asymmetric crotylboration protocol gave a mixture of products that seemed to resemble the four sets of possible diastereoisomers, and isolation of the (*S,S*)-homoallylic alcohol **372** was impossible. Attempts with the Roush[228,231] protocol however were more fruitful, the desired (*S,S*)-homoallylic alcohol **372** being isolable in 61% yield following SiO_2 chromatographic purification from an extremely modest 2.2:1 crude mixture of diastereoisomers (30% of other diastereoisomer). The presence of the terminal alkene in **372** was confirmed by 500 MHz ^{1}H NMR spectroscopy in $CDCl_3$, which showed that a successful crotylboration had proceeded through the appearance of a multiplet at δ 5.73 and two doublets at δ 5.10 (*J* = 17.1 Hz - *trans*) and δ 5.18 (*J* = 9.5 Hz - *cis*) respectively corresponding to the three protons of the terminal alkene. In addition, the appearance of a doublet at δ 3.61 (*J* = 8.1 Hz), a multiplet at δ 2.32 and a doublet at δ 0.89, each of which respectively represented the protons of C(34), C(33) and the methyl group attached to C(33), all confirm that the crotylboration strategy was successful. Other structural proof included the 125 MHz ^{13}C NMR spectrum of **372** in $CDCl_3$, and the absence of the carbonyl peak at δ 195.4 in **370** and the appearance of four new carbon signals at δ 115.8, 16.5, 41.6 and 141.1.

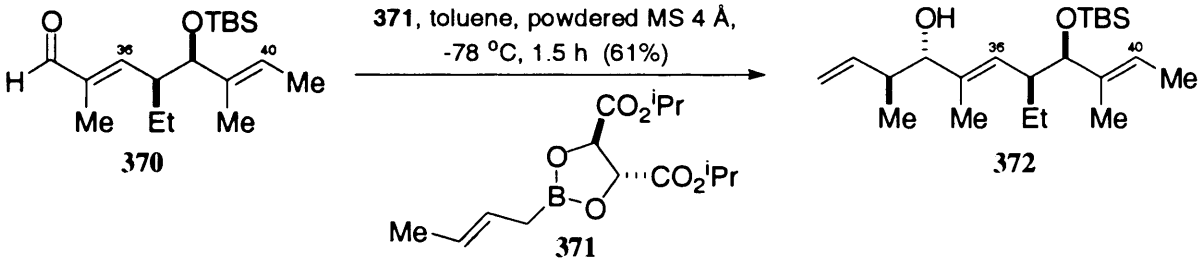

Scheme 89 Roush crotylboration strategy to **372**

Despite the somewhat disappointing selectivity, we proceeded with our planned strategy and protected the newly formed secondary hydroxyl as an *O*-PMB ether. The successful outcome of this reaction was confirmed by 500 MHz ^{1}H NMR spectroscopy in $CDCl_3$ where the presence of two aromatic doublets at δ 7.19 (*J* = 8.5 Hz) and δ 6.84 (*J* = 8.5 Hz), an AB system of doublets at δ 4.26 (*J* = 11.6 Hz) and δ 3.98 (*J* = 11.5 Hz), and an *O*-methoxy singlet at δ 3.78, all corroborated the introduction of the *O*-PMB ether. Due to the nature of unsaturation of **373**, we decided to employ a hydroboration strategy with Wilkinson's catalyst and catechol borane on the terminal alkene to obtain the alcohol **374**, which was difficult to separate from the boronate side products in the mixture. The resulting

alcohol was thus taken forward partially crude, and converted into the phenyl sulphide *via* thioetherification to provide **375** in 59% yield over the two steps. The structure of **375** was confirmed by ^{1}H NMR analysis in $CDCl_3$. The aromatic doublets of the *O*-PMB ether were evident at δ 7.14 (J = 8.6 Hz) and δ 6.82 (J = 8.6 Hz) and the aromatic carbons of the phenyl group were in the region of δ 7.20-7.33. The C(36) vinylic doublet and C(40) vinylic quartet were apparent at δ 4.87 (J = 10.5 Hz) and δ 5.31 (J = 6.7, 5.8 Hz) respectively and the triplet at δ 2.86 represented the geminal protons adjacent to the sulphur atom. In addition to this the *O*-TBS ether was still intact with singlets at δ 0.88, 0.04 and –0.04 that represented the *t*-butyl and methyl signals of the group respectively. Further structural confirmation was provided by FAB HRMS which showed a $(M+Na)^+$ ion at *m/e* 619.35996 (Calcd. for $C_{36}H_{56}O_3SSi$ $(M+Na)^+$: *m/e* 619.36169). Thioether **375** was then oxidised with oxone, in the hope that the desired sulfone **376** would be formed, but to our disappointment, we were only able to obtain a mixture of unidentified undesirable products. Interestingly however, it was noticed that the TBS group was lost during this step, a lot sooner than we had anticipated in our earlier reservations, and recourse of this protection strategy was necessary to accomplish this synthesis.

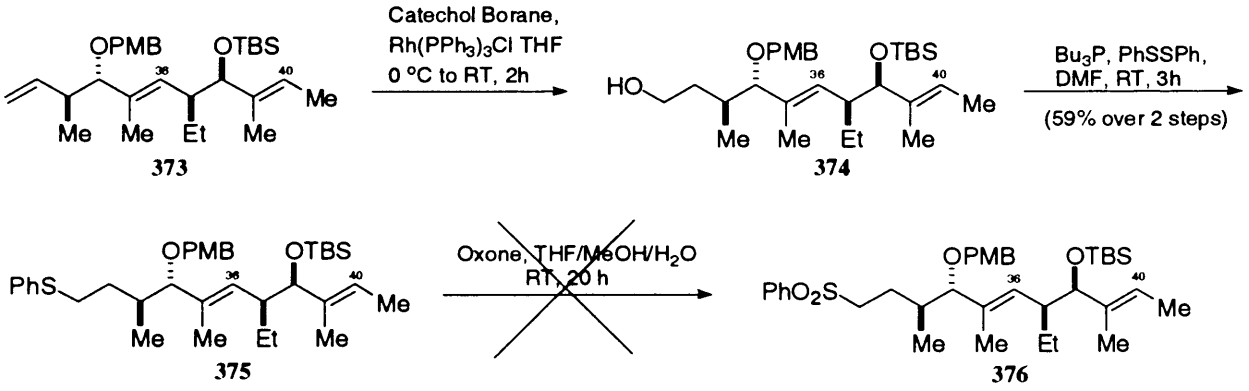

Scheme 90 Attempted synthesis of sulfone **376**

Following this setback we decided to revert to the seemingly more robust protection strategy that employed the use of the *O*-TBDPS ether in accomplishing the synthesis of our target. An advantage of using this protection strategy is that we would be able to unambiguously correlate the sulfone **385** of the newly devised strategy with that formed from the original route used by Hale and co-workers during the synthesis of A83586C. Weinreb amide **364** was protected as an *O*-TBDPS ether and an identical synthetic strategy to that employed for its TBS counterpart then ensued. Partial reduction of amide **377** provided aldehyde **378**, in 86% yield. The structure of **378** was confirmed by way of NMR spectroscopy by the appearance of a doublet at δ 9.57 (J = 3.3 Hz) in the 500 MHz ^{1}H NMR and a peak at δ 204.1 in the 125 MHz ^{13}C NMR spectra. The 500 MHz ^{1}H NMR spectra was very similar to that of **366** apart from slight variations in chemical shift that occur due to the

presence of a different protecting group (*O*-TBDPS - m at δ 7.32-7.68 and s at δ 1.06). Aldehyde **378** then underwent a Wittig olefination and DIBAL-H reduction sequence to afford allylic alcohol **379** in 79% yield. This reaction sequence was affirmed by the 500 MHz ^{1}H NMR spectrum of **379** in $CDCl_3$, by the appearance of the C(40) vinylic quartet at δ 5.01 and C(36) doublet of doublets at δ 4.85, the latter being introduced via the reduction. The geminal protons of the allylic alcohol were also shown by a singlet at δ 3.85, which had a doublet in close proximity at δ 3.87 (J = 7.4 Hz) that represented the proton adjacent to the *O*-TBDPS ether (C(38)). FAB HRMS of **379** showed a $(M+Na)^+$ ion at 459.26991 (Calcd. for $C_{28}H_{40}O_2Si$ $(M+Na)^+$: *m/e* 459.26951), which further confirmed a successful olefination-reduction sequence.

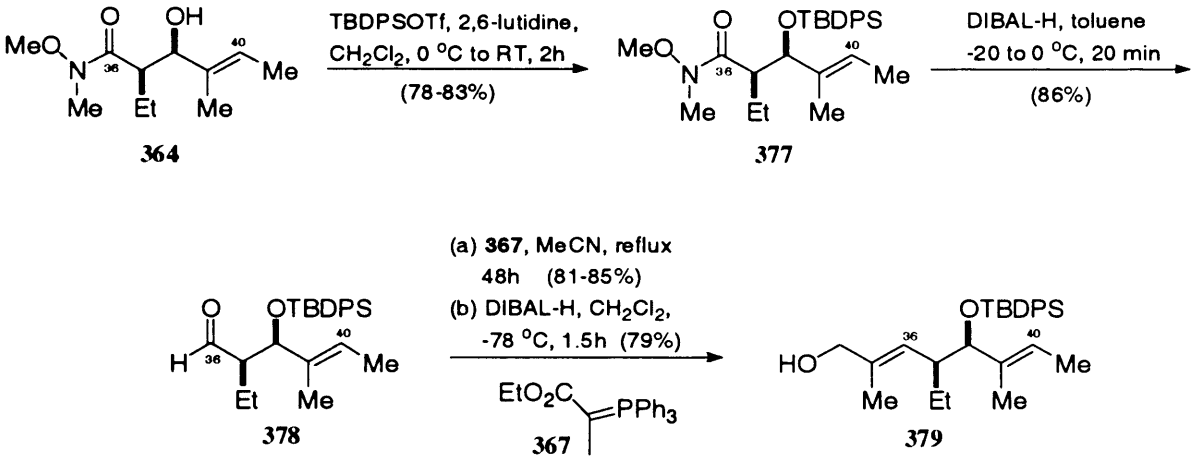

Scheme 91 Synthesis of allylic alcohol **379**

Oxidation of **379**, with MnO_2, provided α,β-unsaturated aldehyde **380**, the structure of which was confirmed by 500 MHz ^{1}H NMR spectroscopy in $CDCl_3$, which showed the loss of the singlet, which represented the geminal protons of the allylic alcohol, at δ 3.85 in **379** and the appearance of a singlet at δ 9.30 that corresponds to the proton of the aldehyde in **380**. Once again due to the α,β-unsaturated system, we witnessed the doublet of doublets of the C(36) vinylic proton move further downfield (δ 5.95) than the quartet for its counterpart at C(40) (δ 5.08). Further confirmation was provided by the 125 MHz ^{13}C NMR spectra in $CDCl_3$, by the appearance of a characteristic aldehyde peak at δ 195.5, and FAB HRMS which showed a $(M+Na)^+$ molecular ion at *m/e* 457.25250 (Calcd. for $C_{28}H_{38}O_2Si$ $(M+Na)^+$: *m/e* 457.25386). Aldehyde **380** then underwent crotylation, using Browns[229,230] chiral (*E*)-crotylboronate derived from (-)-pinene, to furnish (*S,S*) homoallylic alcohol **381** in 59% yield from a 2:1 mixture of diastereoisomers. Since this disappointing result mirrored that of our experiences with Roush'[228,231] asymmetric crotylboration protocol, we decided to use the latter in this capacity since we believed that this protocol could be conducted with greater ease than the Brown strategy, thus facilitating large scale synthesis and was shown to provide **381** in a slightly better ratio of 2.7:1. The structure of **381** was confirmed by NMR

analysis in $CDCl_3$ by the loss of the aldehyde peaks at δ 9.30 and δ 195.5, in the 500 MHz ^1H NMR and 125 MHz ^{13}C NMR respectively; and the subsequent appearance of a multiplet at δ 5.71, and doublets at δ 5.09 (*J* = 16.8 Hz - *trans*) and δ 5.06 (*J* = 10.3 Hz - *cis*), which correspond to the vinylic protons of the newly introduced terminal alkene. This was corroborated by the appearance of a further four carbon signals in the 125 MHz ^{13}C NMR in $CDCl_3$, at δ 141.1, 115.7, 41.4 and 16.6 respectively, and the appearance of a peak at $(M+H)^+$ 491.33251 (Calcd. for $C_{32}H_{46}O_2Si$ $(M+H)^+$: *m/e* 491.33451) in the FAB HRMS of **381**.

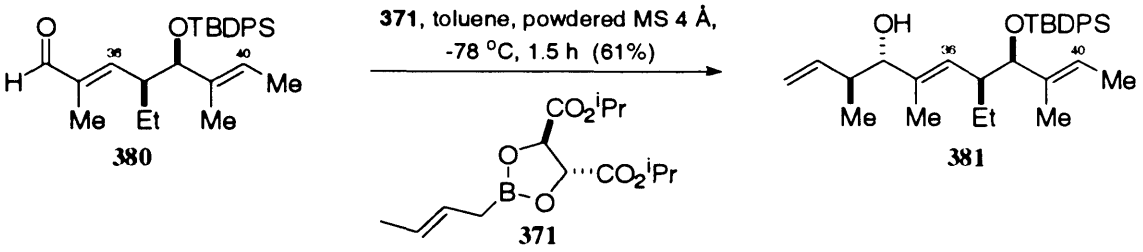

Scheme 92 Crotylboration strategy to **381**

Having negotiated the crotylboration step with only muted success the newly formed allylic alcohol **381** was protected as an *O*-PMB ether, using 0.02 M TfOH in ether with PMB-acetimidate. Efforts to achieve a similar result with PMB-acetimidate and PPTS in CH_2Cl_2 were proven to take substantially longer and provide the desired protected alcohol in an inferior yield, thus deeming the triflic acid method the one of choice. The success of the PMB protection was confirmed by the appearance of two aromatic doublets at δ 7.21 (J = 8.6 Hz) and δ 6.87 (J = 8.5 Hz), an AB doublet system at δ 4.28 (*J* = 11.5 Hz) and δ 3.98 (*J* = 11.6 Hz), and an *O*-methoxy singlet at δ 3.81 in the 500 MHz ^1H NMR of **382** in $CDCl_3$. The resulting triene **382** was then regioselectively hydroborated with catechol borane, unfortunately several attempts to achieve this hydroboration failed. We believed that this was probably due to the decomposition of the starting borane and decided to attempt this hydroboration step with 9-BBN instead. To our satisfaction the reaction proceeded smoothly to afford alcohol **383** in 79% yield (superior to the catechol borane method). The 500 MHz ^1H NMR spectrum of **383** in $CDCl_3$ showed loss of the vinylic multiplet and *cis*/*trans*-doublets at δ 5.92, 5.03 (*J* = 7.4 Hz) and 5.09 (*J* = 15.9 Hz) in **382** respectively. Instead the appearance of two broad multiplets at δ 3.62 and 3.54, in addition to another at δ 1.76 corresponded to the two pairs of geminal protons adjacent to the alcohol functionality. Alcohol **383** then underwent thioetherification with tri-*n*-butyl phosphine and diphenyl disulfide in DMF, to furnish phenyl sulphide **384** in 86% yield. The 500 MHz ^1H NMR spectrum of **384** in $CDCl_3$ was virtually identical to that of **383**, the only significant difference was that the broad multiplets at δ 3.62 and 3.54, which represented the geminal protons adjacent to the alcohol in **383**, had shifted to δ 2.83 in **384**, where they now appeared as a multiplet due to the adjacent sulphur atom. In addition to this there was in increase in the

number or aromatic protons in the spectra of **384**, consistent with the introduction of the phenylsulfide moiety.

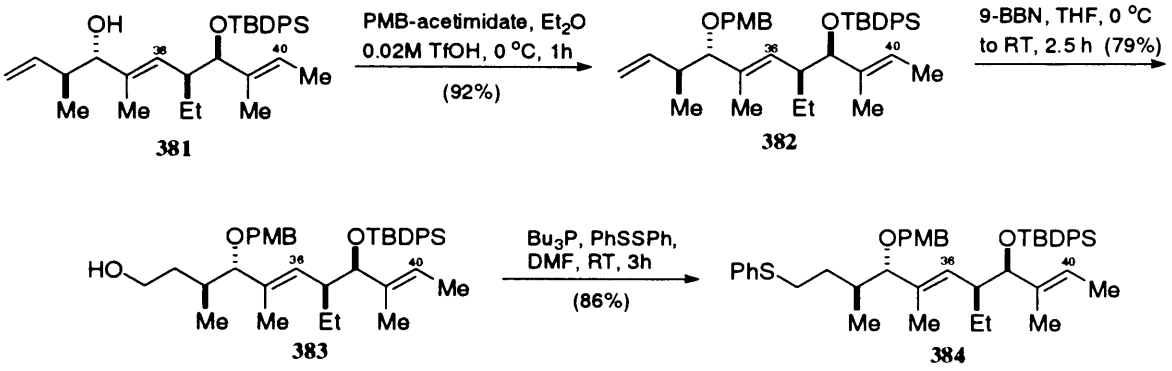

Scheme 93 Reaction sequence from (*S,S*) homoallylic alcohol **381** to phenylsulfide **384**

While attempting the oxidation of phenyl sulphide **384** with oxone in THF/MeOH/H_2O [1:1:1], we observed something quite strange. The TLC of the reaction mixture indicated complete conversion of the phenyl sulphide to what we believed was the desired sulfone **385**, however after isolation and purification of this product, the ^{1}H NMR spectra indicated that we in fact had a mixture of products. This was somewhat confusing and the only viable explanation was that this mixture, that was superimposable on TLC, was in fact the desired sulfone and the sulfoxide. We understood that this was an unusual phenomenon, as sulfoxides should be markedly more polar than their sulfone counterparts, however to understand this problem we decided to subject this mixture to the identical oxidation conditions. After isolation the product ^{1}H NMR demonstrated that we had reduced the ratio of this mixture from what initially appeared to be 1:1 to 2:1 (end of appendix). Following this observation we then subjected this mixture to a further oxidation under identical conditions and were bitterly disappointed on discovering the loss of the TBDPS group, and realised we were witnessing a similar problem to that encountered with its TBS counterpart **375**. The reaction was extremely difficult to follow, as the mixture of products seemed to have identical R_f values and no separation was witnessed despite multi-elution on TLC. We were extremely disappointed at this result and were subsequently unable to complete the synthesis of the desired acyl side chain **338**, due to significant time restraints.

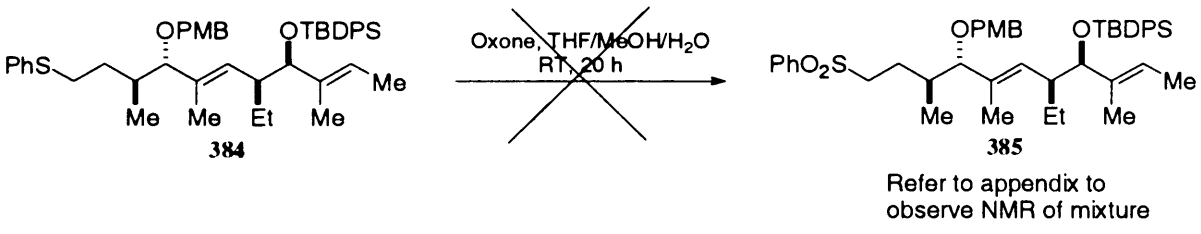

Scheme 94 Failed step towards sulfone **385**

Our disappointment at failing at this pivotal point was immeasurable, not only because we were unable to complete the synthesis of **338** and subsequently azinothricin, but also because it would have provided sufficient information regarding the syntheses of the cyclodepsipeptide cores of these molecules. The complex ^{1}H NMR spectra obtained from these cyclodepsipeptide cores is significantly improved when coupled with the acyl side chain. Analysis of these spectra would have demonstrated whether or not the different spots observed on TLC during the cyclisation sequences of these reactions were in fact epimers, or whether we were simply observing a similar phenomenon to Caldwell, Durette and co-workers with chromatographically resolvable isomers. In addition to this azinothricin is known to exist as a crystalline solid, thus we would have also been able to crystallographically analyse this molecule and provide more conclusive evidence regarding its synthesis and structure. Future work will certainly entail the completion of this synthetic strategy to afford **338** and its chemoselective coupling with the synthesised azinothricin cyclodepsipeptide core **339** to provide azinothricin in substantial quantities. In addition to this, the second-generation strategy can also be used for the synthesis of the A83586C acyl side chain to provide another interesting hybrid structure in the form of an azinothricin/A83586C hybrid. While I recognise that we have made a significant improvement to the accession of **385**, by reducing its linear sequence by 10 steps, there is also room for improvement. If the crotylation selectivity could be improved in any way, then this would be extremely beneficial to the synthesis of these complex natural products. Alternatively if a 3rd generation strategy could be devised that would improve the overall efficiency of this reaction sequence then this would be welcomed within our group, in obtaining a more practical expedient route to these interesting class of compounds.

Chapter 5: EVALUATION OF THE BIOLOGICAL PROPERTIES OF THE A83586C/CITROPEPTIN HYBRID

The A83586C/citropeptin hybrid **336** was sent for biological evaluation at Novartis Pharmaceuticals USA in New Jersey. It was screened alongside A83586C on a variety of human colorectal cancer cell lines and was shown to have a similar potency (Table 5). Their *in vitro* study used MTS assays to establish the tumour growth inhibition potency of these molecules. These assays use tetrazolium salts (MTS) and the electron coupling reagent phenazine methosulfate (PMS), and are based on the conversion of these salts (MTS) into a coloured formazan product that is soluble in tissue culture medium. MTS is chemically reduced by the mitochondrial activity of viable cells at 37 °C and the amount of formazan produced by dehydrogenase enzymes is directly proportional to the number of living cells in culture.

MTS IC_{50}, nM	RKO	HCT116	HT29
A83586C	18	40	46
336	18±4	47±4	50±13

Table 5. Comparison of the potencies of A83586C and **336** on a range of colorectal cancer cell lines

336 was next screened against A83586C, using MTS Top/Fop reporter assays for TCF4, and was shown to be more potent that A83586C (Table 6). The Top/Fop technique uses reporter constructs that contain three repeats of wild-type (TOP) or mutant (FOP) binding sites to determine the ratio of luciferase expression driven by TOP or FOP sequences. This assay demonstrated that **336** was selective against plasmids with mutant TCF4 (T/F = 3), and while the results are similar it can be seen that **336** was more potent than A83586C in this assay also.

MTS IC_{50}, nM	MTS	TCF4 Luc (Top/Fop)
A83586C	252±18	3
336	207+2	3

Table 6. Comparison of the potencies of A83586C and **336** on TCF4

The team at Novartis also conducted an in vivo experiment with **336**. They established that **336** was potent and non-toxic when administered at 1.25 mg/kg, however at 2.5 mg/kg **336**

was shown to be fatal for one of the four mice. It was also insoluble in water and DMSO was used, which is not ideal for *in vivo* studies.

To discover more about the biology this molecule, **336** was also sent to Dr Mohamed El-Tanani at the Institute of Clinical Science at Queens University in Belfast. A novel mechanistic observation was made when **336** was examined on various late stage components of the Wnt/APC/β-catenin cell-signalling pathway. This pathway is known to control cyclin D1 expression and is deregulated in many human cancers. They discovered that **336**, when administered at concentrations 10nM, is a powerful down-regulator of β-catenin and osteopontin (Opn) expression within the highly metastatic Rama 37-OPN breast cancer line; in addition to this **336** was also shown to upregulate TCF4. Osteopontin is an acidic glycophosphoprotein that is often overexpressed in tumours and promotes tumour cell dissemination and metastasis, through its interactions with the CD44 and integrin cell surface receptors [232]. High osteopontin levels are generally found in highly invasive metastatic tumours, and usually correlate with a poor prognosis for most cancer patients. The discovery that **336**, along with other members of this class, can function as powerful inhibitors of Opn expression is of great significance as it could emanate from a potent and simultaneous inhibition of the E2F and Wnt cell signalling pathways. These findings suggest that molecules of the azinothricin class will not only serve as useful probes of E2F and Wnt mediated messaging but will also provide valuable new insights into Opn mediated signalling within cancer cells. In particular, molecules of the azinothricin genre could potentially provide a more comprehensive understanding of Opn mediated metastasis, cell adhesion, invasion and migration; and could for the first time help validate the important link that we have established between osteopontin expression and E2F1 mediated gene transcription involving ribonucleotide reductase. In this regard, a number of groups have recently shown that Opn expression with metastatic cancer cells can be significantly modulated by the levels of ribonucleotide reductase (RR)[233], and since RR expression is known to be controlled by E2F1 mediated transcription, then a link between Opn and E2F1 would now appear to have been made.

As you can see there is much work to be done. However, preliminary biological results highlight the significance of these molecules in the quest for information regarding the cellular mechanisms of neoplastic entities. This study indicates the potential importance that molecules of the azinothricin class may have in providing a more thorough understanding of the world's deadliest malady.

Chapter 6: EXPERIMENTAL

Materials and Methods [234]

Reactions were carried out under a nitrogen atmosphere with freshly distilled solvents unless otherwise stated. Hexanes refer to the distillate fraction of petroleum spirit that is collected at 40-60 °C and was distilled prior to use. All solvents were reagent grade. Dichloromethane, chloroform, toluene, benzene and acetonitrile were distilled from calcium hydride under nitrogen. Diethyl ether and THF were distilled from sodium under nitrogen. All other reagents were used 'as supplied' from the manufacturer unless otherwise stated. Flash chromatography was carried out according to Still et al.[235] with Kiesel gel 60 40/60A (220-240 mesh) silica gel. Precoated silica gel plates (250 μm) with a fluorescent indicator (E. Merck) were used for analytical thin layer chromatography. The plates were initially examined under UV light and then developed with either a sulfuric acid stain [EtOH:H_2SO_4:*p*-$MeOC_6H_4CHO$ (95:4:1)] or phosphomolybdic acid stain unless otherwise stated. Concentrated *in vacuo* refers to the removal of solvents at < 45 °C on a Büchi rotary evaporator. ^1H NMR spectra were acquired at 500 MHz with a Brucker DRX 500 and ^{13}C NMR acquired at 125 MHz with a Brucker DRX 500. Chemical shifts are reported in δ-values relative to tetramethylsilane and all NMR spectra were recorded in deuterated solvents. All infrared spectra were recorded on either a Perkin-Elmer 1605 FT-IR spectrophotometer or Shimadzu FTIR-8700 spectrophotometer. High-resolution mass spectra were measured by the UCL Chemistry Department Mass Spectrometry Service on a VG Analytical 70S instrument. Optical rotations were measured on an Optical Activity, Polaar 2000 Automatic polarimeter. Melting points were measured on a Reichert melting point apparatus. Compounds **335** and **89** used in this synthesis were prepared by Dr Linos Lazarides, using our previous routes[192].

1,3-4,6-Di-*O*-benzylidene-D-mannitol

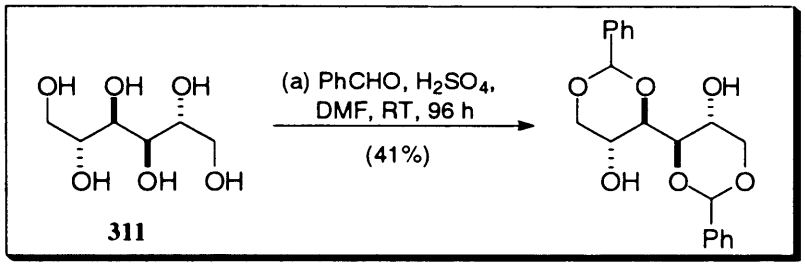

To a stirred suspension of D-mannitol **311** (100 g, 0.55 mol) in DMF (300 mL) at room temperature was added benzaldehyde (120 mL, 1.18 mol) followed by conc. H_2SO_4 (20 mL) and the reaction mixture left to stir for 96 hours. The reaction mixture was quenched *via* cautious addition of saturated $NaHCO_3$ solution and the mixture filtered. The off white residue was then washed with copious amounts of water and hexane, and the resulting pasty white product suspended in EtOAc (400 mL) and water (400 mL). The biphasic mixture was heated with stirring to ensure complete dissolution and the aqueous phase separated and extracted with EtOAc (3 x 200). The combined organic layers were then dried over $MgSO_4$, filtered and concentrated *in vacuo* to afford 1,3-4,6-Di-*O*-benzylidene-D-mannitol as a white solid (81.1 g, 41%).

The spectral data for this molecule corresponded with that in the literature[223].

1,3-4,6-Di-*O*-benzylidene-2,5-di-*O*-benzyl-D-mannitol 313

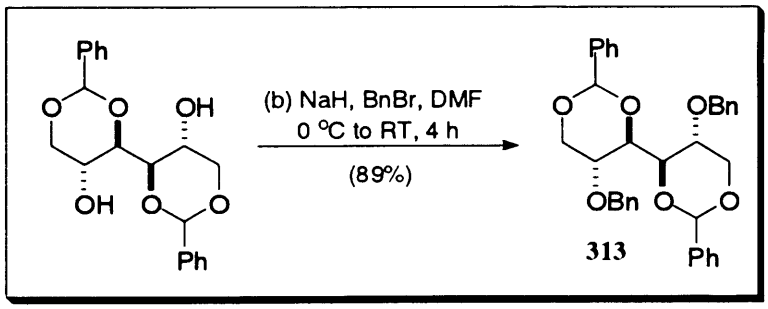

To a stirred solution of 1,3-4,6-Di-*O*-benzylidene-D-mannitol (48.25 g, 0.13 mol) in anhydrous DMF (650 mL) at 0 °C was added in two portions, NaH [60% dispersion] (32.31, 0.81 mol) and the reaction mixture allowed to stir at 0 °C for 30 mins. After this time had lapsed, BnBr (37 mL, 0.31 mol) was added dropwise to this pasty mixture and the reaction mixture allowed to

reach ambient temperature over 4 hours. The reaction mixture was diluted with Et_2O (300 mL) and the reaction cautiously quenched with H_2O. The ethereal layer was separated and the aqueous layer extracted further with Et_2O (2 x 500 mL). The combined ethereal layers were then washed with H_2O (2 x 200 mL), dried over $MgSO_4$, filtered and concentrated *in vacuo* to provide a cloudy oil. Hexane was then added to this crude material and a white solid crystallised out following trituration. The resultant solid was then recrystallised from Et_2O/hexane to afford **313** as a white solid (64.54 g, 89%).

The spectral data of this molecule corresponded with that in the literature[223].

2,5-Di-*O*-benzyl-D-mannitol

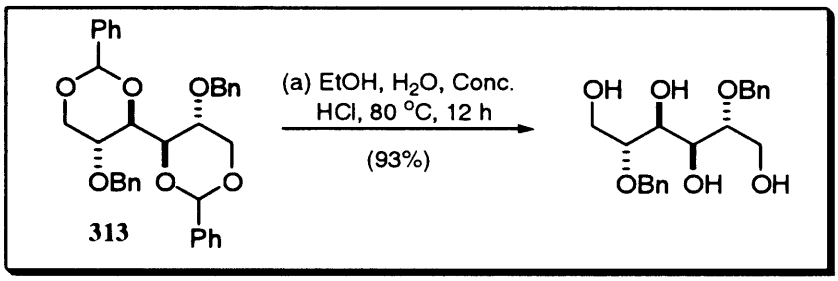

To a stirred suspension of **313** (62.71 g, 0.12 mol) in EtOH (1030 mL) was added at room temperature H_2O (210 mL) followed by slow addition of Conc. HCl (72 mL) *via* a Pasteur pipette and the resulting mixture heated at reflux (~ 80 °C) for 15 hours. The reaction mixture was then cooled to ambient temperature and neutralised with 20% aq. NaOH. The resulting solution was then concentrated *in vacuo* and the white solid residue dissolved in EtOAc (700 mL) and water (300 mL) added. The organic layer was separated and the aqueous layer extracted further with EtOAc (3 x 200 mL). The combined organic layers were then dried over $MgSO_4$, filtered, concentrated *in vacuo* to provide a solid residue that was suspended in Et_2O and filtered. This provided 2,5-Di-*O*-benzyl-D-mannitol as a white fluffy solid (39.24 g, 93%).

The spectral data of this molecule corresponded with that in the literature[223].

1,6-Di-*O*-TBDPS-2,5-di-*O*-benzyl-D-mannitol 314

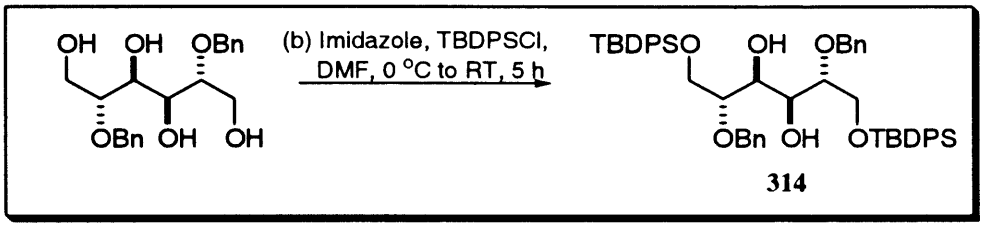

314

To a stirred solution of 2,5-Di-*O*-benzyl-D-mannitol (24.95 g, 68.84 mmol) in anhydrous DMF (105 mL) at 0 °C was added imidazole (21.09 g, 309.79 mmol) in a single portion, followed by dropwise addition of TBDPS-Cl (39.4 mL, 151.45 mmol) and the reaction mixture stirred at 0 °C for 30 mins before being allowed to reach ambient temperature over 4 hours. The reaction mixture was then diluted with Et_2O (500 mL) and washed with sat. aq. $NaHCO_3$. The organic layer was separated and the aqueous layer extracted further with Et_2O (3 x 200 mL). The combined ethereal layers were then dried over $MgSO_4$, filtered and concentrated *in vacuo* to provide a yellow oil that was sufficiently pure for the next step. **IR (neat)** 3482 (br m), 3070 (w), 2931 (s), 2890 (w), 1589 (w), 1471 (m), 1427 (m), 1391 (w), 1360 (w), 1329 (w), 1309 (w), 1265 (w), 1211 (w), 1188 (w), 1111 (s), 1058 (w), 1029 (w), 938 (w), 910 (w), 824 (m), 801 (w), 738 (s), 704 (s), 615 (m), 506 (s); **^{1}H NMR (500 MHz, $CDCl_3$, 298 K)** δ 7.73-7.70 (m, 4*H*, arom), 7.46-7.34 (m, 6*H*, arom), 7.31-7.27 (m, 5*H*, arom), 4.70 (d, *J* = 11.5 Hz, 1*H*, $OC\underline{H}_2Ph$), 4.56 (d, *J* = 11.5 Hz, 1*H*, $OC\underline{H}_2Ph$), 4.08 (d, *J* = 6.6 Hz, 1*H*, Bn*O*CHC<u>H</u>OH), 3.96 (dd, *J* = 6.4, 4.6 Hz, 1*H*, $C\underline{H}_2OSiPh_2{}^tBu$), 3.89 (dd, *J* = 5.9, 5.1 Hz, 1*H*, $C\underline{H}_2OSiPh_2{}^tBu$), 3.74 (m, 1*H*, BnOC<u>H</u>CHOH), 3.12 (br s, 1*H*, Bn*O*CHCHO<u>H</u>), 1.07 (s, 9*H*, $Ph_2SiC(C\underline{H}_3)_3$) [<u>Note</u>: the molecule has a C_2 centre of symmetry, double up the number of proton peaks for the total number of protons in the molecule]; **^{13}C NMR (125 MHz, $CDCl_3$, 298 K)** δ 138.3 (arom), 135.6 (arom), 133.1 (arom), 133.0 (arom), 128.3 (arom), 128.0 (arom), 127.9 (arom), 127.6 (arom), 80.5 (Bn*O*<u>C</u>HCHOH), 73.1 (*O*<u>C</u>H_2Ph), 69.8 (Bn*O*CH<u>C</u>HOH), 64.0 (<u>C</u>$H_2OSiPh_2{}^tBu$), 26.8 ($C(\underline{C}H_3)_3$), 19.1 ($\underline{C}(CH_3)_3$); **FAB HRMS** Calcd. for $C_{26}H_{30}O_4Si$: *m/e* 839.4163; Found: *m/e* 839.41356.

2-*O*-Benzyl-3-*O*-TBDPS-D-glyceraldehyde

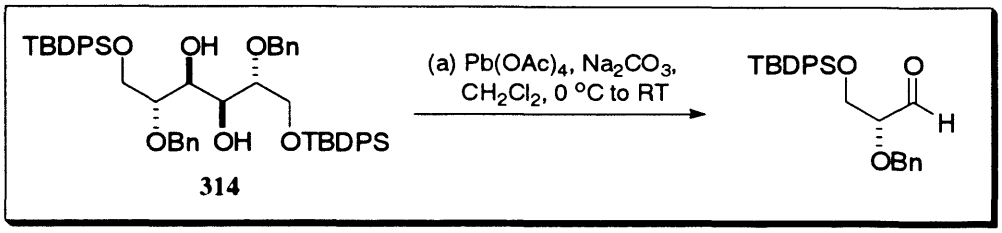

314

To a stirred solution of **314** (57.77 g, 68.84 mmol) in anhydrous CH_2Cl_2 (600 mL) at room temperature was added in single portions, Na_2CO_3 (14.59 g, 137.67 mmol) followed by $Pb(OAc)_4$ (33.57 g, 75.72 mmol) and the reaction mixture allowed to stir for 20 mins. The reaction mixture was then filtered through Celite, washing with copious quantities of CH_2Cl_2 and the resulting filtrate concentrated *in vacuo* to provide a crude pale yellow oil that was of sufficient purity for the next step.

2-*O*-Benzyl-3-*O*-TBDPS-D-glycerate 315

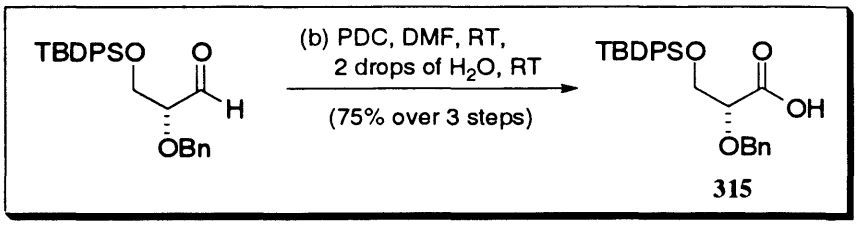

315

To a stirred solution of 3-*O*-TBDPS-2-*O*-benzyl-D-glyceraldehyde (57.64 g, 0.14 mol) in DMF (700 mL) at room temperature was added in a single portion PDC (103.6 g, 0.28 mol) followed by water (3-4 drops from pipette) and the reaction mixture allowed to stir for 15 hours. The mixture was then diluted with H_2O (300 mL) and extracted with Et_2O (4 x 400 mL) and the combine organic layers washed with H_2O (500 mL), dried over $MgSO_4$ and filtered. The orange coloured solution was then concentrated *in vacuo* and purified by SiO_2 flash chromatography using hexanes/EtOAc (4:1 to 2:1 to 1:1) to provide **315** as a yellow oil (22.44 g, 75% over 3 steps). **IR (neat)** 3031 (w), 2931 (m), 2857 (m) – with broad peak overlap, 1725 (m), 1472 (w), 1454 (w), 1427 (m), 1391 (w), 1361 (w), 1113 (s), 1058 (w), 1028 (w), 998 (w), 937 (w), 824 (m), 737 (m), 700 (s), 614 (m), 504 (m), 489 (w); **^{1}H NMR (500 MHz, $CDCl_3$, 298 K)** δ 10.28 (br s, 1*H*, $CO_2\underline{H}$), 7.68 (m, 4*H*, arom), 7.44-7.29 (m, 11*H*, arom), 4.74 (d, *J* = 11.8 Hz, 1*H*, $O\underline{CH_2}Ph$), 4.61 (d, *J* = 11.8 Hz, 1*H*, $O\underline{CH_2}Ph$), 4.14 (dd, *J* = 3.8, 0.8 Hz, 1*H*, $BnO\underline{CH}CO_2H$), 4.00 (m, 2*H*,

$C\underline{H}_2OSiPh_2{}^tBu$), 1.05 (s, 9*H*, $C(C\underline{H}_3)_3$); **^{13}C NMR (125 MHz, $CDCl_3$, 298 K)** δ 174.6 ($\underline{C}O_2H$), 136.8 (arom), 135.6 (arom), 132.8 (arom), 129.8 (arom), 128.5 (arom), 128.0 (arom), 128.0 (arom), 127.7 (arom), 78.7 ($BnO\underline{C}HCO_2H$), 72.6 ($O\underline{C}H_2Ph$), 64.2 ($\underline{C}H_2OSiPh_2{}^tBu$), 26.7 ($C(\underline{C}H_3)_3$), 19.2 ($\underline{C}(CH_3)_3$); **FAB HRMS** Calcd. for $C_{26}H_{30}O_4Si$ $(M+Na)^+$: *m/e* 457.18110; Found: *m/e* 457.18151.

2-*O*-Benzyl-3-*O*-TBDPS-propionic acid methyl ester 316

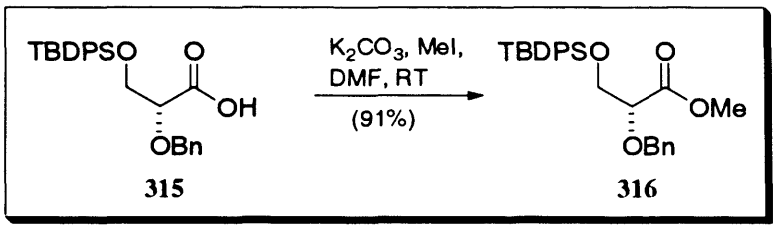

To a stirred solution of **315** (15 g, 34.51 mmol) in anhydrous DMF (300 mL) was added at room temperature K_2CO_3 (23.85, 172.57 mmol) followed by methyl iodide (21.5 mL, 345.15 mmol) and the reaction mixture stirred for 1 hour. The mixture was then diluted with H_2O (150 mL) and extracted with Et_2O (200 mL). Following further extraction of the aqueous layer with Et_2O (3 x 200 mL) the combined ethereal layers were washed with water (300 mL) and dried over $MgSO_4$. Following filtration the resulting solution was concentrated *in vacuo* and the resulting crude yellow oil was purified by SiO_2 flash chromatography using hexanes/EtOAc (7:1 to 5:1) to afford **316** as a pale yellow oil (14.09 g, 91%). **IR (neat)** 3071 (m), 3030 (m), 2932 (s), 2856 (s), 1960 (w), 1890 (w), 1755 (s), 1589 (m), 1497 (m), 1472 (s), 1454 (s), 1427 (s), 1391 (m), 1362 (m), 1259 (m), 1204 (s), 1113 (s), 1059 (m), 1028 (m), 1009 (m), 937 (w), 824 (s), 739 (s), 700 (s), 615 (s), 505 (s), 490 (s), 432 (w); **^{1}H NMR (500 MHz, $CDCl_3$, 298 K)** δ 7.46 (m, 4*H*, arom), 7.48-7.31 (m, 11*H*, arom), 4.82 (d, *J* = 11.9 Hz, 1*H*, $OC\underline{H}_2Ph$), 4.58 (d, *J* = 11.9 Hz, 1*H*, $OC\underline{H}_2Ph$), 4.21 (t, *J* = 5.1 Hz, 1*H*, $BnOC\underline{H}CO_2CH_3$), 4.03 (m, 2*H*, $C\underline{H}_2OSiPh_2{}^tBu$), 3.79 (s, 3*H*, $OC\underline{H}_3$), 1.11 (s, 9*H*, $C(C\underline{H}_3)_3$); **^{13}C NMR (125 MHz, $CDCl_3$, 298 K)** δ 171.2 ($\underline{C}O_2CH_3$), 137.4 (arom), 135.5 (arom), 133.0 (arom), 129.6 (arom), 128.3 (arom), 127.8 (arom), 127.7 (arom), 127.6 (arom), 79.2 ($BnO\underline{C}HCO_2CH_3$), 72.4 ($O\underline{C}H_2Ph$), 64.7 ($\underline{C}H_2OSiPh_2{}^tBu$), 51.8 ($O\underline{C}H_3$), 26.6 ($C(\underline{C}H_3)_3$), 19.1 ($\underline{C}(CH_3)_3$). **FAB HRMS** Calcd. for $C_{27}H_{32}O_4Si$ $(M+Na)^+$: *m/e* 471.19675; Found: *m/e* 471.19816.

2-*O*-Benzyl-3-hydroxy-propionic acid methyl ester

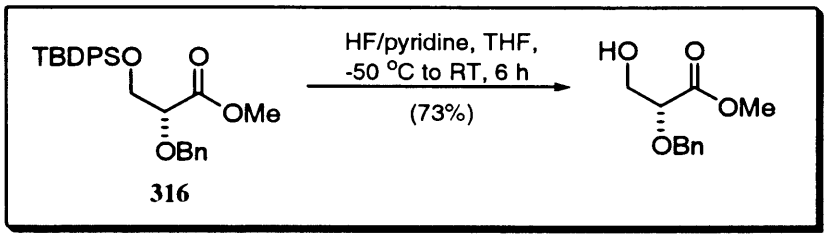

To a stirred solution of **316** (11.7 g, 26.08 mmol) in THF (250 mL) contained in a plastic container, was added dropwise at –50 °C, *via* a plastic syringe, a solution of HF/pyridine (39.12 mL, 39.12 mmol) and the reaction mixture allowed to reach ambient temperature over 6 hours. The mixture was quenched *via* the cautious addition of solid $NaHCO_3$ at –20 °C, followed by further addition of sat. aq. $NaHCO_3$ until effervescence subsides. The reaction mixture was then diluted with EtOAc (300 mL) and the organic layer extracted. The aqueous layer was then extracted further with EtOAc (3 x 200 mL) an the combined organic layers were dried over $MgSO_4$, filtered and concentrated *in vacuo*, to provide a crude yellow oil. This crude material was then purified by SiO_2 flash chromatography using hexanes/EtOAc (5:1 to 1:1) to afford the desired product as a yellow oil (4.02 g, 73%). **IR (neat)** 3435 (br s), 3063 (m), 2953 (s), 2878 (m), 1747 (s), 1636 (w), 1497 (m), 1456 (s), 1437 (s), 1398 (m), 1278 (s), 1209 (s), 1124 (s), 1051 (s), 912 (w), 885 (w), 853 (w), 804 (w), 743 (s), 700 (s), 610 (w), 463 (w); **^{1}H NMR (500 MHz, $CDCl_3$, 298 K)** δ 7.33-7.23 (m, 5*H*, arom), 4.73 (d, *J* = 11.5 Hz, 1*H*, *O*C$\underline{H}_2$Ph), 4.44 (d, *J* = 11.5 Hz, 1*H*, *O*C$\underline{H}_2$Ph), 4.02 (dd, *J* = 3.7, 1.8, 1*H*, Bn*O*C$\underline{H}$C$\underline{O}_2$C$\underline{H}_3$), 3.73-3.84 (br m, 2*H*, Bn*O*C$\underline{H}_2$OH), 3.69 (s, 3*H*, *O*C$\underline{H}_3$), 2.95 (br m, 1*H*, O$\underline{H}$); **^{13}C NMR (125 MHz, $CDCl_3$, 298 K)** δ 170.9 ($\underline{C}O_2CH_3$), 136.8 (arom), 128.2 (arom), 127.9 (arom), 127.7 (arom), 78.6 (Bn*O*$\underline{C}$HCO$_2$CH$_3$), 72.4 (*O*$\underline{C}$H$_2$Ph), 63.0 (Bn*O*$\underline{C}$H$_2$OH), 51.8 (*O*$\underline{C}$H$_3$). **FAB HRMS** Calcd. for $C_{11}H_{14}O_4$ $(M+H)^+$: *m/e* 211.09862; Found: *m/e* 211.09682.

2-*O*-Benzyl-3-*O*-methoxy-propionic acid methyl ester 317

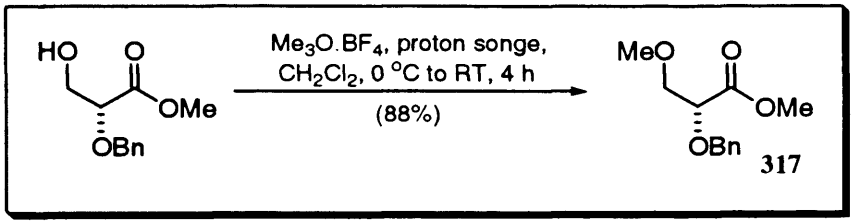

To a stirred solution of 2-*O*-benzyl-3-hydroxy-propionic acid methyl ester (3.5 g, 16.65 mmol) in anhydrous CH_2Cl_2 (150 mL) within a reaction vessel wrapped in aluminium foil was added at 0 °C, in a single portion, trimethyloxonium tetrafluoroborate (3.69 g, 24.97 mmol). The reactants were stirred at 0 °C for 5 mins, before Proton Sponge ® (5.35 g, 24.97 mmol) was added in a single portion. After stirring at 0 °C for 20 mins, the reaction mixture was stirred at room temperature for 4 hours. The mixture was then filtered through Celite, washed with copious amounts of CH_2Cl_2, and the resulting filtrate washed successively with 1 M aq. HCl (50 mL) and brine (50 mL). The organic material was then dried over $MgSO_4$, filtered and concentrated *in vacuo* to provide a pasty solid that was purified by SiO_2 flash chromatography using hexanes/EtOAc (5:1 to 3:1) to afford **317** as a yellow oil (3.28 g, 88%). **IR (neat)** 3031 (w), 2952 (s), 2894 (s), 1751 (s), 1498 (m), 1454 (s), 1436 (m), 1401 (w), 1383 (w), 1342 (w), 1272 (m), 1206 (s), 1116 (s), 1067 (m), 1028 (m), 973 (w), 912 (w), 852 (w), 803 (w), 742 (m), 699 (m), 611 (w), 458 (w); **^{1}H NMR (500 MHz, $CDCl_3$, 298 K)** δ 7.25-7.33 (m, 5*H*, arom), 4.74 (d, J = 11.9 Hz, 1*H*, $OC\underline{H}_2Ph$), 4.48 (d, J = 11.9 Hz, 1*H*, $OC\underline{H}_2Ph$), 4.11 (dd, J = 3.8, 1.5 Hz, 1*H*, $BnOC\underline{H}CO_2CH_3$), 3.72 (s, 3*H*, $CO_2C\underline{H}_3$), 3.66 (m, 2*H*, $BnOC\underline{H}_2OMe$), 3.33 (s, 3*H*, $CH_2OC\underline{H}_3$); **^{13}C NMR (125 MHz, $CDCl_3$, 298 K)** δ 170.8 ($\underline{C}O_2CH_3$), 137.0 (arom), 128.1 (arom), 127.8 (arom), 127.6 (arom), 77.6 ($BnO\underline{C}HCO_2CH_3$), 72.9 ($BnO\underline{C}H_2OCH_3$), 72.3 ($O\underline{C}H_2Ph$), 59.2 ($BnOCH_2O\underline{C}H_3$), 51.8 ($CO_2\underline{C}H_3$). **FAB HRMS** Calcd. for $C_{12}H_{16}O_4$: *m/e* 224.10485; Found: *m/e* 224.10412.

Diethyl (-)-2,3-*O*-benzylidene-D-tartrate 323

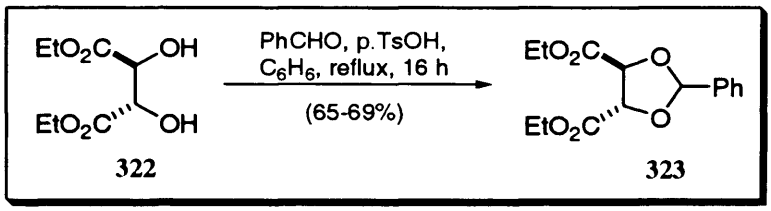

To a 1 L round bottomed flask, equipped with a Dean Stark trap, was successively added a solution of diethyl-D-tartrate (70 g, 0.34 mol)) in anhydrous benzene (300 mL), benzaldehyde (41.5 mL, 0.41 mol), and *p*-toluenesulfonic acid monohydrate (0.5 g). The resulting mixture was stirred under reflux, with the azeotropic removal of water, for 16 hours. Following cooling, the reaction mixture was concentrated *in vacuo* and the residual oil dissolved in Et_2O (700 mL). It was then washed with sat. aq. $KHCO_3$ (200 mL) followed by H_2O (2 x 200 mL). The ethereal layer was separated and dried over $MgSO_4$, filtered, and concentrated *in vacuo* to provide a crude yellow solid. This was then triturated with hexanes to afford **323** as off white crystals (65.94 g, 66%) following isolation by filtration.

The data for **323** were in agreement with those reported by Jäger and co-workers.[224]

(+)-2-*O*-Benzyl-D-threitol 324

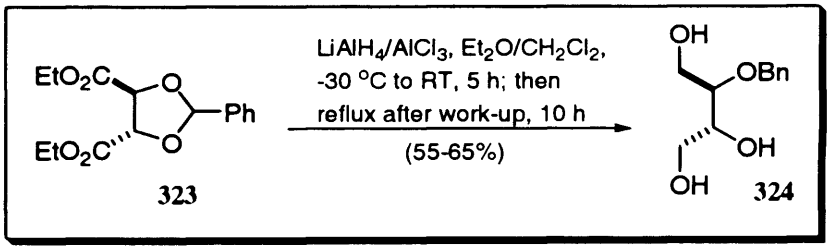

To a 2 L, three-necked round-bottomed flask, charged with $LiAlH_4$ (16 g, 0.42 mol), equipped with a pressure-equalising dropping funnel, mechanical stirrer and reflux condenser, connected to a nitrogen source (see **Fig. 29.**), was added anhydrous Et_2O (158 mL) and the vessel was cooled to –30 °C with vigorous stirring. An ice-cold solution of $AlCl_3$ (56.18 g, 0.42 mol) in anhydrous Et_2O (130 mL) was added dropwise over a 40-minute period at –30 °C, followed by rapid addition of anhydrous CH_2Cl_2 (130 mL), while the temperature is allowed to reach 0 °C. A solution of **323** (62 g, 0.21 mol) in anhydrous CH_2Cl_2 (130 mL) was added dropwise

at 0 °C over 30 minutes and the reaction mixture was allowed to reach ambient temperature, where it was maintained for 1 hour, and thereafter heated at reflux for an additional 2 hours. The mixture was then cooled to –20 °C, and quenched *via* the **cautious** addition of H_2O (18 mL), followed by a solution of KOH (30 g) in H_2O (45 mL), and finally by the addition of H_2O (18 mL). The resulting mixture was allowed to reach ambient temperature before being heated at reflux with THF (200 mL) for 10 hours (Note: Vigorous stirring is required throughout the reaction). The mixture was then cooled and filtered through Celite, and the inorganic precipitate was extracted with CH_2Cl_2 (500 mL) in a Soxhlet apparatus for three days. The filtrate and extracts were then combined and concentrated *in vacuo* and the resulting solid was recrystallised from CH_2Cl_2 to furnish white crystals (27.73 g, 62%) after drying over P_4O_{10} for 48 hours in a dessicator.

N.B. The $AlCl_3/Et_2O$ solution was made by adding solid $AlCl_3$ (56.18g, 0.42 mol) into ice cold anhydrous Et2O with stirring to ensure complete dissolution.

The data for **324** were in agreement with those reported by Jäger and co-workers.[224]

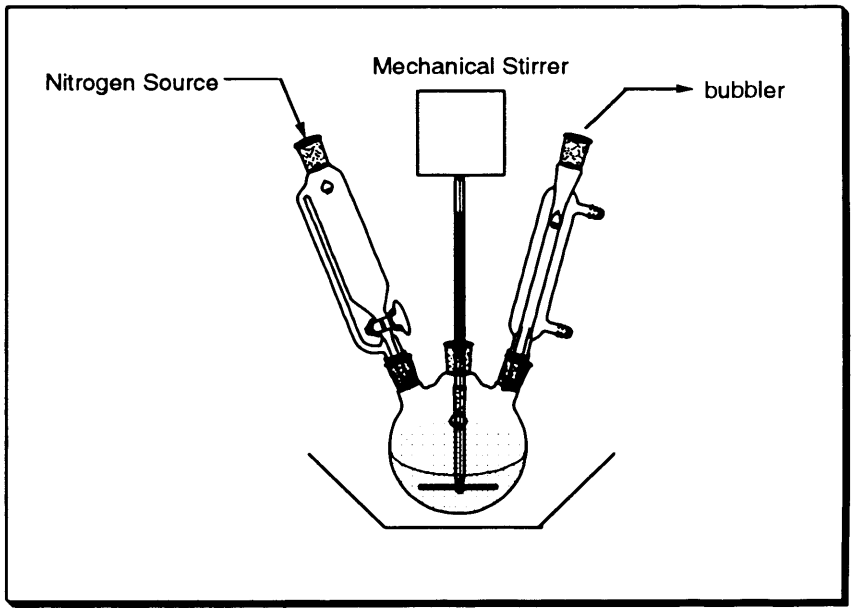

Fig. 29. Apparatus for the synthesis of (+)-2-*O*-Benzyl-D-threitol **324**

Note: If $LiAlH_4$ and $AlCl_3$ are not of high purity then use an excess of 10% of each to avoid obtaining a mixture of products from incomplete reduction.

(+)-2-*O*-Benzyl-3,4-*O*-isopropylidene-D-threitol 325

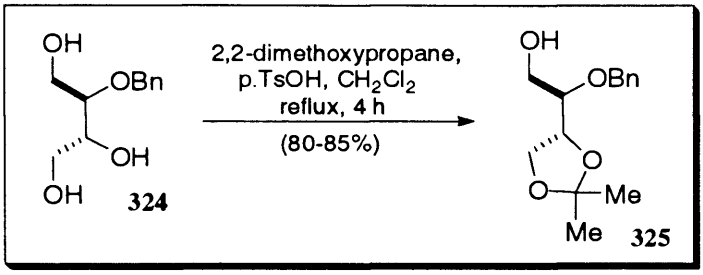

To a stirred solution of **324** (25 g, 0.12 mol) in anhydrous CH_2Cl_2 (600 mL) at room temperature was added in single portions, 2,2-dimethoxypropane (22 mL, 0.18 mol) and *p*-toluenesulfonic acid monohydrate (0.85 g), and the mixture was heated under reflux using a Soxhlet extractor containing 4 Å molecular sieves for 4 hours. The reaction mixture is then cooled to ambient temperature where it was washed with sat. aq. $NaHCO_3$ (200 mL), dried over $MgSO_4$, filtered, and concentrated *in vacuo* to obtain a yellow oil. The crude residue was purified by SiO_2 flash chromatography using hexanes/EtOAc (7:1 to 2:1) to afford **325** as a pale yellow oil (24.66 g, 83%). **$[\alpha]_D^{12}$** +18.1 ° (*c* 0.648, CH_2Cl_2); **IR (Neat)** 3449 (s), 2986 (s), 2883 (s), 1638 (w), 1497 (m), 1456 (s), 1371 (s), 1213 (s), 1028 (s), 854 (s), 795 (m), 739 (s), 698 (s), 606 (m), 513 (m); **^{1}H NMR (500 MHz, $CDCl_3$, 298 K)** δ 7.34-7.24 (m, 5*H*, Ph), 4.73 (d, *J* = 11.9 Hz, 1*H*, PhC<u>H</u>$_2$) 4.66 (d, *J* = 11.9 Hz, 1*H*, PhC<u>H</u>$_2$), 4.26 (apparent q, *J* = 6.7, 6.6, 6.3 Hz, 1*H*, C<u>H</u>OCH$_2$O), 3.97 (dd, *J* = 6.59, 1.79 Hz, 1*H*, CHOC<u>H</u>$_2$O), 3.76 (dd, *J* = 7.17, 1.18 Hz, 1*H*, CHOC<u>H</u>$_2$O), 3.70 (m, 1*H*, C<u>H</u>$_2$OHCHOBn), 3.56 (m, 1*H*, C<u>H</u>$_2$OHCHOBn), 3.50 (m, 1*H*, CH$_2$OHC<u>H</u>OBn), 2.64 (br s, 1*H*, O<u>H</u>), 1.41 (s, 3*H*, OCC<u>H</u>$_3$), 1.34 (s, 3*H*, OCC<u>H</u>$_3$); **^{13}C NMR (125 MHz, $CDCl_3$, 298 K)** δ 138.1 (<u>C</u> Ph), 128.3 (<u>C</u> Ph), 127.7 (<u>C</u> Ph), 127.6 (<u>C</u> Ph), 109.2 (O$_2$<u>C</u>(CH$_3$)$_2$), 79.2 (<u>C</u>H$_2$OHCHOBn) 76.4 (<u>C</u>HOCH$_2$O), 72.6 (Ph<u>C</u>H$_2$), 65.4 (CHO<u>C</u>H$_2$O), 61.5 (CH$_2$OH<u>C</u>HOBn), 26.2 (O$_2$C(<u>C</u>H$_3$)$_2$), 25.2 (O$_2$C(<u>C</u>H$_3$)$_2$); **FAB HRMS** Calcd. for $C_{14}H_{20}O_4$ (M+H)$^+$: *m/e* 253.14398; Found: *m/e* 253.14425.

(+)-*O*-Methoxy-2-*O*-benzyl-3,4-*O*-isopropylidene-D-threitol 326

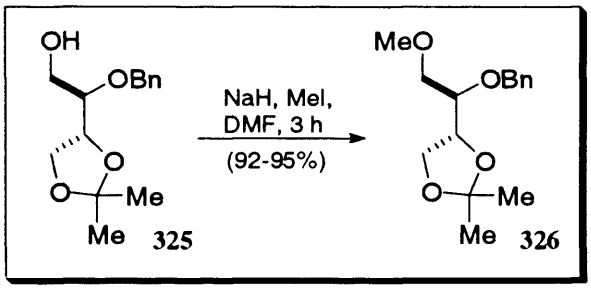

To a stirred solution of **325** (23.5 g, 93.1 mmol) in anhydrous DMF (300 mL) at room temperature was added in a single portion NaH (4.84 g, 121.08 mmol, [60% dispersion]) followed by MeI (7 mL, 111.77 mmol) and the reaction mixture was stirred at room temperature for 3 hours. The mixture was cooled to 0 °C and quenched *via* the cautious addition of H_2O (200 mL). Following extraction with Et_2O (3 x 300 mL), the combined ethereal layers were dried over $MgSO_4$, filtered, and concentrated *in vacuo* to provide a yellow oil that was purified by SiO_2 flash chromatography using hexanes/EtOAc (7:1 to 5:1) to afford **326** as a pale yellow oil (23.07 g, 93%). **$[\alpha]_D^{12}$** +2.7 ° (*c* 0.88, CH_2Cl_2); **IR (Neat)** 2985 (m), 2891 (m), 2813 (w), 1454 (m), 1380 (m), 1369 (m), 1255 (w), 1212 (m), 1101 (s), 1071 (s), 738 (m), 698 (m); **^{1}H NMR (500 MHz, $CDCl_3$, 298 K)** δ 7.35-7.21 (m, 5*H*, arom), 4.71 (d, *J* = 12.4 Hz, 1*H*, PhC$\underline{H}_2$), 4.67 (d, *J* = 12.5 Hz, 1*H*, PhC$\underline{H}_2$), 4.21 (apparent q, *J* = 6.6, 6.5 Hz, 1*H*, C$\underline{H}$OCH$_2$O), 3.94 (dd, *J* = 6.6 Hz, 1*H*, CHOC$\underline{H}_2$O), 3.74 (dd, *J* = 7.4, 0.725 Hz, 1*H*, CHOC$\underline{H}_2$O), 3.55 (apparent q, *J* = 5.6, 4.77 Hz, 1*H*, CH$_2$OHC$\underline{H}$OBn), 3.47 (distorted d, *J* = 4.9 Hz, 2*H*, C$\underline{H}_2$OHCHOBn), 3.30 (s, 3*H*, OC$\underline{H}_3$), 1.38 (s, 3*H*, OCC$\underline{H}_3$), 1.34 (s, 3*H*, OCC$\underline{H}_3$); **^{13}C NMR (125 MHz, $CDCl_3$, 298 K)** δ 138.5 (C Ph), 128.2 (C Ph), 127.8 (C Ph), 127.5 (C Ph), 109.1 ($O_2\underline{C}(CH_3)_2$), 78.1 (CH$_2$OH$\underline{C}$HOBn), 76.7 ($\underline{C}$HOCH$_2$O), 72.8 ($\underline{C}$H$_2$OHCHOBn), 72.8 (Ph$\underline{C}$H$_2$), 65.8 (CHO$\underline{C}$H$_2$O), 59.2 (O$\underline{C}$H$_3$), 26.4 ($O_2C(\underline{C}H_3)_2$), 25.4 ($O_2C(\underline{C}H_3)_2$); **FAB HRMS** Calcd. for $C_{15}H_{22}O_4$ $(M+H)^+$: *m/e* 267.15963; Found: *m/e* 267.16026.

(+)-*O*-Methoxy-2-*O*-benzyl-D-threitol 321

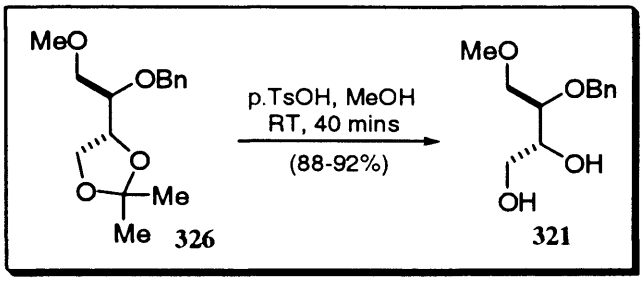

To a stirred solution of **326** (22 g, 82.60 mmol) in MeOH (500 mL) was added at room temperature and in a single portion p.TsOH (15g, 82.60 mmol) and the resulting solution stirred at room temperature for 40 mins. The reaction mixture was then concentrated *in vacuo* and diluted with CH_2Cl_2 (300 mL) and washed with sat. aq. $NaHCO_3$ (200 mL), extracting the aqueous layer further with EtOAc (2 x 200 mL). The combined organic layers were then dried over $MgSO_4$, filtered and concentrated *in vacuo* to provide a crude yellow oil that was purified by SiO_2 flash chromatography using hexanes/EtOAc (2:1 to 0:1) to afford **321** as a pale yellow oil (16.63 g, 89%). **$[\alpha]_D^{12}$** –35.0 ° (*c* 1.032, CH_2Cl_2); **IR (Neat)** 3362 (br s), 3063 (m), 3030 (m), 2880 (s), 2814 (m), 1958 (w), 1815 (w), 1605 (w), 1585 (w), 1497 (m), 1454 (s), 1398 (m), 1310 (m), 1196 (s), 1028 (s), 1001 (m), 959 (m), 920 (m), 872 (m), 820 (w), 739 (s), 700 (s), 604 (m), 465 (w); **^{1}H NMR (500 MHz, $CDCl_3$, 298 K)** δ 7.31-7.24 (m, 5*H*, arom), 4.70 (d, *J* = 11.6 Hz, 1*H*, PhC$\underline{H}_2$), 4.53 (d, *J* = 11.6 Hz, 1*H*, PhC$\underline{H}_2$), 3.73 (apparent q, *J* = 4.8 Hz, 1*H*, $CH_2OHC\underline{H}OBn$), 3.60 (d, *J* = 4.9 Hz, 2*H*, $C\underline{H}_2OHCHOBn$), 3.52-3.58 (m, 3*H*, $C\underline{H}_2OHCHOH$ and $CH_2OHC\underline{H}OH$), 3.32 (s, 3*H*, $OC\underline{H}_3$), 3.07 (s, 2*H*, 2 x O$\underline{H}$); **^{13}C NMR (125 MHz, $CDCl_3$, 298 K)** δ 137.9 ($\underline{C}$(Ph)), 128.3 ($\underline{C}$(Ph)), 127.8 ($\underline{C}$(Ph)), 127.7 ($\underline{C}$(Ph)), 78.0 ($CH_2OH\underline{C}HOH$), 72.6 (Ph$\underline{C}H_2$), 71.9 ($CH_2OH\underline{C}HOBn$), 71.9 ($\underline{C}H_2OHCHOH$), 63.3 ($\underline{C}H_2OHCHOBn$), 59.1 ($O\underline{C}H_3$); **FAB HRMS** Calcd. for $C_{12}H_{18}O_4$ $(M+H)^+$: *m/e* 227.12779; Found: *m/e* 227.12753.

2-*O*-Benzyl-3-*O*-methoxy-D-glyceraldehyde

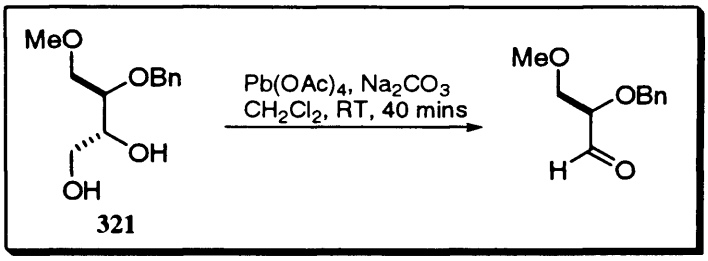

To a stirred solution of **321** (15 g, 66.29 mmol) in anhydrous CH_2Cl_2 (250 mL) at room temperature was added in single portions, Na_2CO_3 (14.05 g, 132.58 mmol) followed by $Pb(OAc)_4$ (32.33 g, 72.92 mmol). The reaction mixture was thereafter stirred at ambient temperature for 40 mins, before being diluted with CH_2Cl_2 (200 mL) and filtered through Celite. After washing the residual solids with copious amounts of CH_2Cl_2, the filtrate was concentrated *in vacuo* and the resultant aldehyde taken directly on to the next step without purification.

2-*O*-Benzyl-3-*O*-methoxy-D-glycerate 327

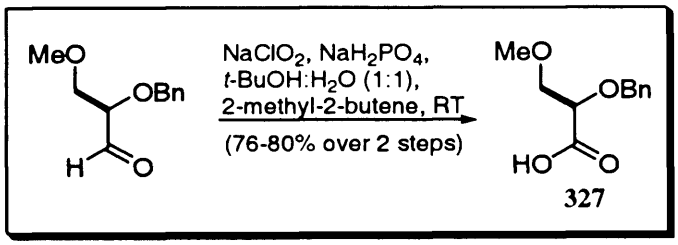

To a stirred solution of *O*-methoxy-2-*O*-benzyl-glyceraldehyde (12.88 g, 66.29 mmol) in ^tBuOH (580 mL) and 2-methyl-2-butene (255 mL) at room temperature was added in 3 portions over 5 minute intervals, a solution of $NaClO_2$ (17.99 g, 198.88 mmol), NaH_2PO_4 (23.86 g, 198.88 mmol) in H_2O (580 mL) and the mixture was stirred for 3 hours. The reaction mixture was then poured into a solution of sat. aq. NH_4Cl (300 mL) and extracted with CH_2Cl_2 (4 x 300 mL). The combined organic layers were then dried over $MgSO_4$, filtered, and concentrated *in vacuo* to provide **327** (10.87 g, 78% over 2 steps) as a clear oil following purification by SiO_2 flash chromatography using hexanes/EtOAc (2:1 to 0:1).

3-*O*-Methoxy-D-glycerate

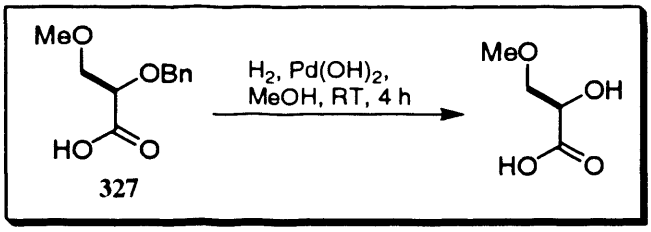

To a stirred solution of **327** (9.5 g, 45.19 mmol) in MeOH (200 mL) was added at RT, $Pd(OH)_2$ 20% on carbon (2.5 g), and the reaction vessel was purged with H_2 before being vigorously stirred for 4 hours. The mixture was filtered through Celite, and the filter pad washed with copious amounts of MeOH and EtOH (100 mL). The filtrate was then concentrated *in vacuo* to afford a crude colourless oil that was of sufficient purity for the next step.

(2R)-2-Hydroxy-3-*O*-methoxy-propionic acid allyl ester 320

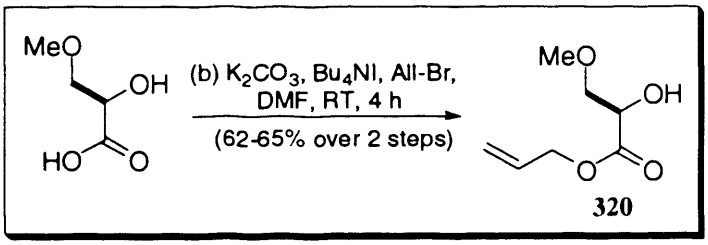

To a stirred solution of 3-*O*-methoxy-D-glycerate (5.43 g, 45.19 mmol) in anhydrous DMF (100 mL) was added in single portions at room temperature, K_2CO_3 (6.56 g, 47.45 mmol) followed by Bu_4NI (3.34 g, 9.03 mmol). Allyl bromide (16 mL, 180.75 mmol) was then added dropwise over 5 mins, and the reaction mixture allowed to stir at RT for 4 hours. The resulting solution was then diluted with H_2O (100 mL) and extracted with Et_2O (3 x 200 mL). The combined ethereal layers were then washed sequentially with 10% aq. HCl (50 mL), 5% aq. $NaHCO_3$ (50 mL) and brine (100 mL), dried over $MgSO_4$, filtered and concentrated *in vacuo*. The desired allyl ester **320** was obtained following purification of the crude residue by SiO_2 flash chromatography using hexanes/EtOAc (5:1 to 2:1 to 1:1). **320** was obtained as a pale yellow oil (4.63 g, 64%). $[\alpha]_D^{12}$ +3.51 ° (*c* 0.398, CH_2Cl_2); **IR (Neat)** 3420 (br s), 3088 (w), 2987 (w), 2933 (m), 2896 (m), 2828 (w), 1746 (s), 1649 (w), 1456 (m), 1419 (w), 1377 (w), 1196 (s), 1129 (s), 1112 (s), 1045 (m), 975 (m), 929 (m), 560 (w); **^{1}H NMR (500 MHz, $CDCl_3$, 298 K)** δ 5.87 (m, 1*H*, H5), 5.29 (d, *J* = 17.2 Hz, 1*H*, $CO_2CH_2CHCH_2$-*trans*), 5.21 (d, *J* = 10.5 Hz, 1*H*, $CO_2CH_2CHCH_2$-*cis*), 4.65 (m, 2*H*,

$CO_2C\underline{H}_2CHCH_2$), 4.28 (br s, 1*H*, C<u>H</u>OHCH$_2$OCH$_3$), 3.64 (m, 2*H*, CHOHC<u>H</u>$_2$OCH$_3$), 3.33 (s, 3*H*, OC<u>H</u>$_3$), 3.21 (br s, 1*H*, O<u>H</u>); **^{13}C NMR (125 MHz, $CDCl_3$, 298 K)** δ 172.2 (<u>C</u>O), 131.3 ($CO_2CH_2\underline{C}HCH_2$), 118.7 ($CO_2CH_2CH\underline{C}H_2$), 73.8 (CHOH<u>C</u>H$_2OCH_3$), 70.6 (<u>C</u>HOHCH$_2OCH_3$), 66.1 ($CO_2\underline{C}H_2CHCH_2$), 59.3 (O<u>C</u>H$_3$); **CI HRMS** Calcd. for $C_7H_{12}O_4$ $(M+H)^+$: ***m/e*** 161.08138; Found: ***m/e*** 161.08152.

O-Benzylhydroxylamine 318

To a stirred solution of *O*-Benzylhydroxylamine hydrochloride (12 g, 75.18 mmol) in MeOH (125 mL) was added at room temperature and in one portion Et_3N (11.5 mL, 82.70 mmol) and the reaction mixture stirred for 30 mins. After this time TLC indicated that the reaction was complete by the appearance of a bright yellow spot at R_F 0.4 (hexanes/EtOAc 2:1 – anisaldehyde) and the mixture was concentrated *in vacuo*. The resultant white solid residue was then suspended in Et_2O and filtered, washing the residue with copious quantities of Et_2O. The filtrate was then concentrated *in vacuo* to afford **318** as a clear oil, with a distinctive odour that was of sufficient purity for the next step.

N-*O*-Benzylhydroxy-*O*-methyl-L-serine allyl ester 328

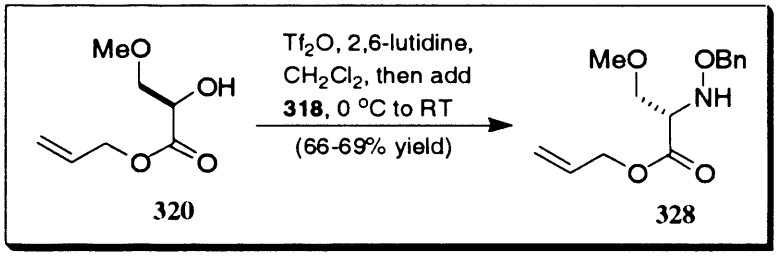

To a stirred solution of **320** (4.5 g, 28.10 mmol) in anhydrous CH_2Cl_2 (10 mL) at 0 °C was added dropwise freshly distilled Tf_2O (5.2 mL, 30.90 mmol) and the reaction mixture stirred at 0 °C for 15 mins. To this mixture was added dropwise 2,6-lutidine (3.9 mL, 33.71 mmol) while the temperature was maintained at 0 °C and the resultant mixture stirred at this temperature for a further 15 mins. A solution of **318** (6.92 g, 56.19 mmol) in anhydrous CH_2Cl_2 (20 mL) was then added dropwise into the reaction mixture and the mixture stirred at 0 °C for 20 mins before being allowed to reach ambient temperature over 2 hours. The reaction mixture was then diluted with CH_2Cl_2 (300 mL) and washed with H_2O (2 x 40 mL), 1 M HCl (2 x 40 mL) and brine (100 mL).

The organic layer was then dried over $MgSO_4$, filtered, concentrated *in vacuo* and purified by SiO_2 flash chromatography using hexanes/EtOAc (5:1 to 2:1) to afford **328** as a pale yellow oil (5.07 g, 68%). $[\alpha]_D^{12}$ -17.05 ° (*c* 0.616, CH_2Cl_2); **IR (Neat)** 3266 (w), 3031 (w), 2927 (m), 2881 (w), 2828 (w), 1740 (s), 1648 (w), 1498 (w), 1454 (m), 1382 (m), 1367 (m), 1331 (w), 1274 (m), 1199 (s), 1118 (s), 972 (m), 936 (m), 821 (w), 749 (m), 699 (m), 614 (w); **^{1}H NMR (500 MHz, $CDCl_3$, 298 K)** δ 7.34-7.27 (m, 5*H*, arom), 5.90 (m, 1*H*, $CO_2CH_2C\underline{H}CH_2$), 5.32 (d, *J* = 17.2 Hz, 1*H*, $CO_2CH_2CHC\underline{H}_2$-*trans*), 5.23 (d, *J* = 10.5 Hz, 1*H*, $CO_2CH_2CHC\underline{H}_2$-*cis*), 4.72 (s, 2*H*, $PhC\underline{H}_2$), 4.66 (m, 2*H*, $CO_2C\underline{H}_2CHCH_2$), 3.82 (apparent t, *J* = 5.1, 4.7, 1*H*, $NC\underline{H}CH_2OCH_3$), 3.60 (d, *J* = 5.1, 2*H*, $NCHC\underline{H}_2OCH_3$), 3.30 (s, 3*H*, $OC\underline{H}_3$); **^{13}C NMR (125 MHz, $CDCl_3$, 298 K)** δ 170.8 ($\underline{C}O_2CH_2CHCH_2$), 137.5 ($\underline{C}$Ph), 131.7 ($CO_2CH_2\underline{C}HCH_2$), 128.4 ($\underline{C}$Ph), 128.3 ($\underline{C}$Ph), 127.8 ($\underline{C}$Ph), 118.4 ($CO_2CH_2CH\underline{C}H_2$), 76.4 ($Ph\underline{C}H_2$), 70.2 ($NCH\underline{C}H_2OCH_3$), 65.6 ($CO_2\underline{C}H_2CHCH_2$), 63.7 ($N\underline{C}HCH_2OCH_3$) 59.9 ($O\underline{C}H_3$). **FAB HRMS** Calcd. for $C_{14}H_{19}NO_4$ $(M+Na)^+$: *m/e* 288.12117; Found: *m/e* 288.12169.

Synthesis of dipeptide 329

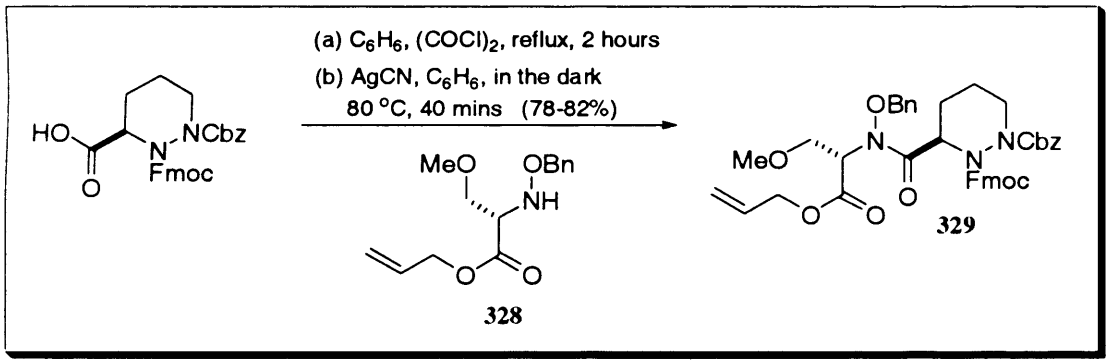

To the partially protected piperazic acid derivative of **29** (13.84 g, 28.45 mmol) in anhydrous C_6H_6 (52 mL) was added at room temperature and under N_2, $(COCl)_2$ (50 mL, 568.93 mmol) and the reaction mixture was heated at reflux for 2 hours. The reaction mixture was then concentrated *in vacuo* and the resulting mixture was co-evaporated with C_6H_6 (3 x 20 mL) to remove the excess $(COCl)_2$. To the resulting golden foam, was added at room temperature and under N_2, a solution of **328** (7.4 g, 27.89 mmol) in anhydrous C_6H_6 (52 mL), and the reaction vessel was covered in aluminium foil. AgCN (5.61 g, 41.84 mmol) was then added in a single portion and the vessel was connected to a reflux condenser. The reaction mixture was stirred at RT for 10 mins, before being heated at 80 °C for a further 40 mins. The reaction mixture was then cooled, diluted with CH_2Cl_2 (300 mL) and filtered through Celite, washing the flask and

residue with copious quantities of CH_2Cl_2. The filtrate was then concentrated *in vacuo* and purified by SiO_2 flash chromatography using hexanes/EtOAc (7:1 to 5:1 to 2:1) to afford **329** as a white foam (15.4 g, 75%). $[\alpha]_D^{12}$ –65.4 ° (*c* 0.46, CH_2Cl_2); **IR (Neat)** 3321 (br w), 2931 (w), 2894 (w), 1706 (s), 1498 (w), 1450 (m), 1410 (m), 1359 (w), 1256 (m), 1194 (m), 1095 (m), 1047 (w), 975 (w), 915 (w), 879 (w), 849 (w), 742 (m), 698 (m), 621 (w), 548 (w); **^{1}H NMR (500 MHz, $CDCl_3$, 298 K)** δ 7.74 (br d, *J* = 7.4 Hz, 2*H*, arom), 7.60-7.14 (m, 16*H*, arom), 5.89 (m, 1*H*, $CO_2CH_2C\underline{H}CH_2$), 5.60 (br s, 1*H*), 5.32 (d, *J* = 17.2, 1*H*, $CO_2CH_2CHC\underline{H}_2$-*trans*), 5.25 (d, *J* = 11.3, 1*H*, $CO_2CH_2CHC\underline{H}_2$-*cis*), 5.22 (br m, 2*H*), δ 5.05 (br m, 2*H*), 4.83 (br m, 1*H*), 4.63 (br d, *J* = 5.7, 2*H*, $CO_2C\underline{H}_2CHCH_2$), 4.34 (br d, *J* = 7.2, 2*H*, $NCO_2C\underline{H}_2$-Fluoro), 4.20 (br m, 1*H*), 3.99 (t, *J* = 7.2, 1*H*, $NC\underline{H}CH_2OCH_3$), 3.87 (br m, 2*H*, $NCHC\underline{H}_2OCH_3$), 3.31 (s, 3*H*, $NCHCH_2OC\underline{H}_3$), 2.94 (m, 1*H*), 2.17 (br m, 1*H*), 1.94 (m, 1*H*), 1.79 (br m, 1*H*), 1.45 (br m, 1*H*); **^{13}C NMR (125 MHz, $CDCl_3$, 298 K)** δ 172.3 ($\underline{C}O$), 167.9 ($\underline{C}O$), 155.7 ($\underline{C}O$), 154.2 ($\underline{C}O$), 143.8, 143.2, 141.2, 136.5, 134.3, 131.4, 129.4, 128.5, 128.4, 128.1, 127.7, 127.6, 127.0, 125.0, 119.9, 118.9, 78.6, 69.2 ($NCH\underline{C}H_2OCH_3$), 68.6 ($NCO_2\underline{C}H_2$-Fluoro), 67.5 ($CO_2CH_2CH\underline{C}H_2$), 66.1 ($CO_2\underline{C}H_2CHCH_2$), 62.1, 58.8 ($O\underline{C}H_3$), 49.8, 46.8 ($N\underline{C}HCH_2OCH_3$), 44.1, 24.3, 18.4 **FAB HRMS** Calcd. for $C_{42}H_{43}N_3O_9$ $(M+Na)^+$: *m/e* 756.38968; Found: *m/e* 756.28824.

Synthesis of acid 304 *via* deprotection of 329

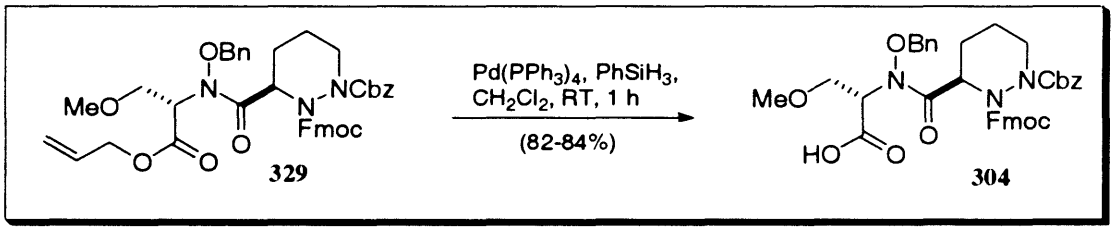

To a solution of **329** (15.17 g 20.67 mmol) in anhydrous CH_2Cl_2 (150 mL) was added, in one portion at room temperature and under N_2, $Pd(PPh_3)_4$ (0.48 g, 0.41 mmol) followed by phenylsilane (5.1 mL, 41.35 mmol) and the reaction mixture stirred for 1 hour. The reaction mixture became a dark, almost black, colour and was thereafter diluted with H_2O and extracted with CH_2Cl_2 (3 x 200 mL). The combined organic extracts were dried ($MgSO_4$), filtered, and concentrated *in vacuo* to provide a dark purple residue that was purified by SiO_2 flash chromatography using hexanes/EtOAc (2:1 to 0:1) to afford **329** as an off-white foam (13.2 g, 92%). $[\alpha]_D^{12}$ –16.4 ° (*c* 0.676, CH_2Cl_2); **IR (Neat)** 3438 (br w), 3033 (w), 2932 (w), 2895 (w), 1707 (s), 1497 (w), 1450 (m), 1413 (m), 1359 (w), 1257 (m), 1196 (m), 1096 (m), 1048 (w), 971 (w), 912 (w), 879 (w), 849 (w), 755 (m), 742 (m), 698 (m), 621 (w), 547 (w); **^{1}H NMR (500 MHz,**

$CDCl_3$, 298 K) δ 8.11 (br s, 1*H*, $CO_2\underline{H}$), 7.72 (br d, *J* = 7.5 Hz, 2*H*, arom) 7.55-7.13 (m, 16*H*, arom), 5.55 (br m, 1*H*) 5.20 (br m, 1*H*) 5.06 (br m, 2*H*), 4.89 (br s, 1*H*), 4.75 (br s, 1*H*), 4.60 (br m, 1*H*), 4.32 (br d, *J* = 7.8, 2*H*, $NCO_2C\underline{H}_2$-Fluoro), 4.17 (br m, 1*H*), 3.98 (apparent t, *J* = 7.1, 1*H*, $NC\underline{H}CH_2OCH_3$), 3.90 (apparent dd, *J* = 5.3, 4.9, 1*H*, $NCHC\underline{H}_2OCH_3$), 3.79 (br m, 1*H*, $NCHC\underline{H}_2OCH_3$), 3.29 (s, 3*H*, $OC\underline{H}_3$), 2.89 (br m, 1*H*), 2.13 (br m, 1*H*), 1.96 (br m, 1*H*), 1.81 (br m, 1*H*), 1.43 (br m, 1*H*); **^{13}C NMR (125 MHz, $CDCl_3$, 298 K)** δ 172.6, 171.4, 155.8, 155.3, 143.8, 141.2, 136.4, 135.8, 129.5, 128.9, 128.5, 128.2, 127.8, 127.1, 125.2, 125.0, 119.9, 78.7, 69.1 ($NCH\underline{C}H_2OCH_3$), 68.8, 68.3 ($NCO_2\underline{C}H_2$-Fluoro), 67.7, 62.2, 58.8 ($O\underline{C}H_3$), 50.1, 44.8 ($N\underline{C}HCH_2OCH_3$), 23.8, 18.8; **FAB HRMS** Calcd. for $C_{39}H_{39}N_3O_9$ $(M+Na)^+$: *m/e* 716.35839; Found: *m/e* 716.25546.

(3*S*)-*N*(1)-Carbobenzyloxy-piperazic acid 30

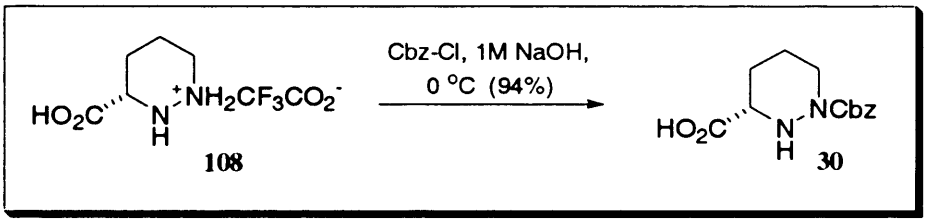

To a stirred solution of **108** (29.7 g, 0.12 mol) in 2 M NaOH (250 mL, 0.49 mol) at 0 °C was added benzyl chloroformate (18.2 mL, 0.13 mol) over 15 mins at 0 °C and the reactants were stirred for 2 hours at this temperature. The mixture was then diluted with H_2O (200 mL) and extracted with Et_2O (2 x 100 mL). The aqueous layer was then acidified to pH 2 with conc. HCl and cooled to 0 °C and this temperature maintained for 45 mins. The white solid precipitate that was formed was filtered and the residue washed with H_2O and hexanes. The white solid so obtained was then dried over P_2O_5 for two days under high vacuum in a dessicator to afford **30** as a white crystalline solid (30.22 g, 94%). $[\alpha]_D^{21}$ –44.2 ° (*c* 0.052, MeOH); M.p. = 149-152 °C; **IR (neat)** 3393 (br w), 3258 (s), 3010 (br s), 2946 (s), 2917 (s), 2857 (s), 1745 (s), 1683 (s), 1498 (s), 1454 (s), 1416 (s), 1358 (s), 1334 (m), 1296 (s), 1260 (s), 1236 (s), 1193 (s), 1140 (s), 1118 (s), 1080 (m), 1029 (m), 1014 (m), 1003 (m), 992 (m), 981 (m), 918 (m), 905 (m), 884 (w), 863 (w), 825 (w), 751 (s), 695 (s), 640 (w), 595 (s), 479 (m); **^{1}H NMR (500 MHz, DMSO, 298 K)** δ 12.71 (br s, 1*H*, $O\underline{H}$), δ 7.37-7.30 (m, 5*H*, arom), 5.07 (s, 2*H*, $PhC\underline{H}_2$), 3.80 (apparent d, *J* = 12.4 Hz, 1*H*, pip-$C\underline{H}_2$), 3.36 (m and br peak overlapping, 2*H*, $HO_2CC\underline{H}NH$ and $N\underline{H}$), 3.06 (br m, 1*H*, pip-$C\underline{H}_2$), 1.88 (m, 1*H*, pip-$C\underline{H}_2$), 1.67 (m, 1*H*, pip-$C\underline{H}_2$), 1.52 (m, 2*H*, pip-$C\underline{H}_2$); **^{13}C NMR (125**

MHz, DMSO, 413 K) δ 172.6 (CO), 155.1 (CO), 136.9 (PhC), 128.3 (PhC), 127.8 (PhC), 127.5 (PhC), 66.2 ($PhCH_2$), 57.8 (HO_2CCHNH), 44.0 (pip-CH_2), 27.0 (pip-CH_2), 22.9 (pip-CH_2); **FAB HRMS** Calcd. for $C_{13}H_{16}N_2O_4$ $(M+H)^+$: *m/e* 265.11883; Found: *m/e* 265.11910.

(3S)-*N*(1)-Carbobenzyloxy-piperazic acid *t*-butyl carbazate ester 164

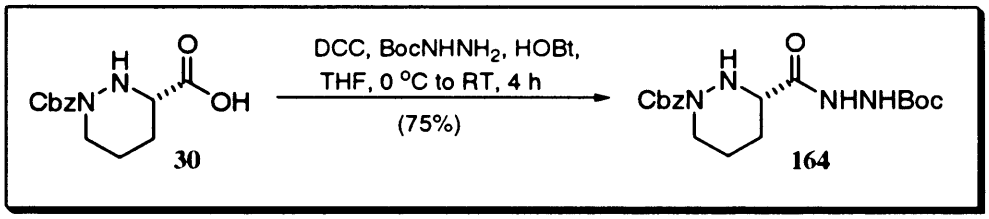

To a stirred solution of **30** (28.65 g, 0.11 mol) in anhydrous THF (285 mL) at 0 °C were successively added in single portions, *t*-butyl carbazate (14.61 g, 0.11 mol), HOBt (14.94 g, 0.11 mol) and DCC (22.82 g, 0.11 mol) and the reactants stirred at 0 °C for 30 mins before being allowed to warm to ambient temperature where it was maintained for 4 hours. The mixture was then diluted with Et_2O (600 mL) and filtered through Celite. The filtrate was then washed with 0.5 N aq. HCl (2 x 100 mL), sat. aq. $NaHCO_3$ (2 x 100 mL) and brine (100 mL). The ethereal layer was dried over $MgSO_4$, filtered and concentrated *in vacuo* to afford a crude clear oil that was purified by SiO_2 flash chromatography using hexanes/EtOAc (2:1 to 1:1) to afford **164** as a white foam (30.77 g, 75%). $[\alpha]_D^{21}$ –29.1 ° (*c* 0.268, CH_2Cl_2); **IR (neat)** 3277 (br m), 2934 (w), 2862 (w), 1686 (s), 1499 (m), 1458 (m), 1439 (m), 1406 (m), 1367 (m), 1244 (m), 1163 (m), 1128 (w), 1099 (w), 1013 (w), 872 (w), 735 (w), 698 (w); **^{1}H NMR (500 MHz, DMSO, 413 K)** δ 9.12 (br s, 1*H*, NH), 7.85 (br s, 1*H*, NH) 7.37-7.28 (br m, 5*H*, arom), 5.12 (s, 2*H*, $PhCH_2$), 4.81 (br s, 1*H* NH), 3.57-3.45 (br m, 3*H*), 1.87-1.80 (br m, 2*H*), 1.69 (m, 1*H*), 1.58 (m, 1*H*), 1.43 (s, 9*H*, $NCO_2C(CH_3)_3$); **^{13}C NMR (125 MHz, DMSO, 413 K)** δ 170.4 (CO), 155.3 (CO), 154.9 (CO), 137.0 (PhC), 128.2 (PhC), 127.5 (PhC), 127.4 (PhC), 79.5 ($C(CH_3)_3$), 66.7 ($PhCH_2$), 57.2 (NCHCON), 44.4 (pip-CH_2), 28.1 ($C(CH_3)_3$), 25.6 (pip-CH_2), 21.8 (pip-CH_2); **FAB HRMS** Calcd. for $C_{18}H_{26}N_4O_5$ $(M+Na)^+$: *m/e* 401.18008; Found: *m/e* 401.17963.

Synthesis of dipeptide 168

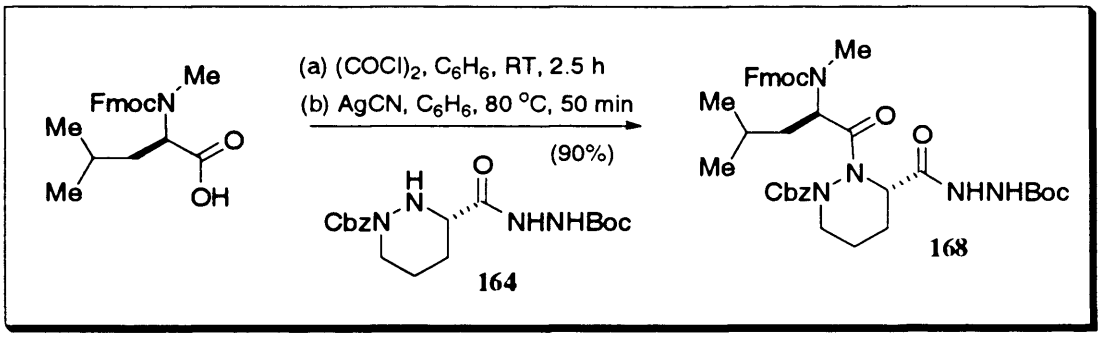

To a RT solution of the acid derivative of **167** (10.43 g, 28.41 mmol) in anhydrous CH_2Cl_2 (50 mL) under N_2 was added $(COCl)_2$ (50 mL, 568.14 mmol) in a single portion. After stirring for 2 hours, the reaction mixture was then concentrated *in vacuo* and the residue co-evaporated with C_6H_6 (3 x 20 mL) to remove the excess $(COCl)_2$. The resulting yellow foam **167** was then placed under high vacuum for 20 mins. To this yellow foam was added, at room temperature and under N_2, a solution of **164** (10.75 g, 28.41 mmol) in anhydrous C_6H_6 (100 mL) and the reaction vessel covered with aluminium foil. AgCN (5.71 g, 42.61 mmol) was then added in a single portion, and the reactants heated at 80 °C for 45 mins. The reaction mixture was then cooled and diluted with EtOAc (100 mL), filtered through Celite and the flask and residue washed with copious amounts of EtOAc. The filtrate was then concentrated *in vacuo* and purified by SiO_2 flash chromatography using hexanes/EtOAc (5:1 to 2:1) to afford **168** as a white foam (17.31 g, 84% yield over the 2 steps). **$[\alpha]_D^{12}$** +14.5 ° (*c* 0.662, CH_2Cl_2); **IR (neat)** 3289 (br w), 2957 (w), 2361 (w), 1698 (s), 1452 (m), 1405 (m), 1365 (m), 1247 (s), 1196 (m), 1160 (s), 1121 (w), 1044 (w), 912 (w), 759 (w), 737 (s), 700 (w); **^{1}H NMR (500 MHz, $CDCl_3$, 298 K)** δ 9.29 (br m, 1*H*, *N*H), 7.74 (br d, *J* = 7.5 Hz, 2*H*, arom), 7.56 (br d, *J* = 7.4, 2*H*, arom), 7.39-7.27 (br m, 9*H*, arom), 6.18 (br s, 1*H*, *N*H), 5.26-4.90 (br m, 3*H*) 4.81-4.69 (br m, 1*H*), 4.45 (br m, 1*H*), 4.21 (br m, 2*H*), 2.89 (s, 3*H*, *N*CH$_3$), 2.26-2.02 (br m, 1*H*), 1.73 (br m, 1*H*), 1.42 (br s, 12*H*, *N*CO$_2$C(CH$_3$)$_3$ [9*H*] + signal underneath [3H]), 0.94 (apparent d, *J* = 6.3, 2*H*, *N*MeCHCH$_2$CH(CH$_3$)$_2$), 0.91 (apparent d, *J* = 6.3, 2*H*, *N*MeCHCH$_2$CH(CH$_3$)$_2$), 0.74 (apparent d, *J* = 6.3, 2*H*, *N*MeCHCH$_2$CH(CH$_3$)$_2$); **^{13}C NMR (125 MHz, $CDCl_3$, 298 K)** δ 174.1 (CO), 168.1 (CO), 156.3 (CO), 154.8 (CO), 143.8, 141.3, 135.1, 129.9, 129.2, 128.9, 127.6, 127.0 125.0, 119.9, 81.1, 69.2, 67.5, 54.7, 52.1, 47.3, 46.9, 38.2, 29.2 (*N*CH$_3$), 28.1 (*N*CO$_2$C(CH$_3$)$_3$), 24.6, 23.9, 23.0 (*N*MeCHCH$_2$CH(CH$_3$)$_2$), 22.4, 20.0; **FAB HRMS** Calcd. for $C_{40}H_{49}N_5O_8$ $(M+H)^+$: *m/e* 728.36592; Found: *m/e* 728.36661.

Fmoc deprotection of 168

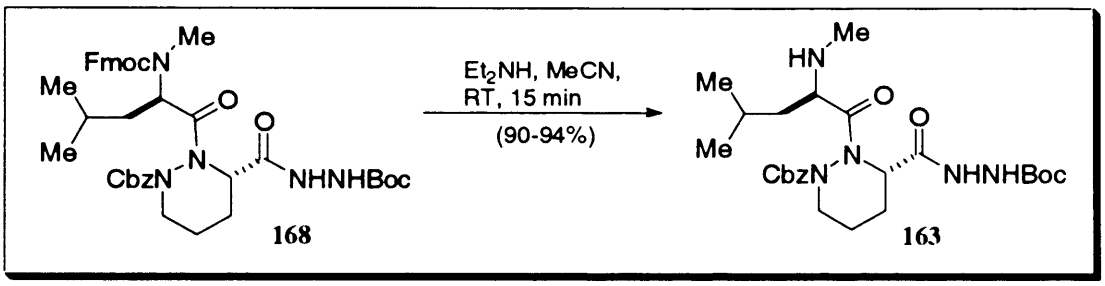

To a RT solution of **168** (17.25 g, 23.70 mmol) in anhydrous MeCN (200 mL) under N_2 was added, in one portion, diethylamine (105 mL, 948 mmol) and the reaction mixture was stirred for 40 mins. The reaction mixture was then concentrated *in vacuo* and co-evaporated with C_6H_6 (3 x 20 mL) to remove the excess diethylamine. The residue was then placed on a high vacuum pump and was of sufficient purity to be used directly for the next step. $[\alpha]_D^{12}$ -36.6 ° (*c* 0.59, CH_2Cl_2); **IR (Neat)**; 3303 (m), 3033 (w) 2957 (s), 2870 (m), 2804 (w), 1700 (s), 1455 (s), 1403 (s), 1366 (s), 1246 (s), 1195 (s), 1164 (s), 1118 (m), 1042 (m), 973 (w), 915 (m), 872 (w), 807 (w), 733 (s), 700 (m), 647 (w), 532 (w); **^{1}H NMR (500 MHz, $CDCl_3$, 298 K)** δ 9.22 (br s, 1*H*, *N*H), 7.33-7.29 (m, 5*H*, arom), 6.53 (br s, 1*H*, *N*H), 5.24 (br m, 1*H*, *N*$CO_2C\underline{H}_2$Ph), 5.10 (br d, *J* = 11.8, 1*H*, *N*$CO_2C\underline{H}_2$Ph), 4.31-4.20 (br m, 1*H*), 3.20-3.33 (br m, 1*H*), 3.09 (br t, *J* = 10.2, 1*H*), 2.36 (br s, 1*H*), 2.23 (s, 3*H*, *N*$C\underline{H}_3$), 2.00 (br s, 1*H*), 1.75 (br m, 3*H*), 1.51 (br m, 1*H*), 1.40 (s, 9*H*, *N*$CO_2C(C\underline{H}_3)_3$), 1.27 (m, 1*H*), 1.03 (br m, 1*H*), 0.83 (apparent d, *J* = 6.2, 4*H*, *N*MeCHCH_2CH$(C\underline{H}_3)_2$), 0.70 (br m, 4*H*, *N*MeCHCH_2CH$(C\underline{H}_3)_2$); **^{13}C NMR (125 MHz, $CDCl_3$, 298 K)** δ 178.4 (<u>C</u>O), 156.9 (<u>C</u>O), 154.9 (<u>C</u>O), 135.1 (arom), 129.3 (arom), 128.5 (arom), 128.4 (arom), 81.0, 69.3 (*N*$CO_2\underline{C}H_2$Ph), 58.0, 53.2, 46.6, 42.9, 34.9 (*N*$\underline{C}H_3$), 28.0 (*N*$CO_2C(\underline{C}H_3)_3$), 24.8 (*N*MeCH$CH_2CH(\underline{C}H_3)_2$), 23.5, 21.2, 20.3; **FAB HRMS** Calcd. for $C_{25}H_{39}N_5O_6$ $(M+H)^+$: *m/e* 506.29784; Found: *m/e* 506.29841.

<u>N.B</u>. The spectral data is taken from a purified sample of the above – purified by SiO_2 flash chromatography using hexanes/EtOAc (5:1 to 2:1 to 1:1).

[2 + 2] Coupling of 304 and 163 to tetrapeptide 330

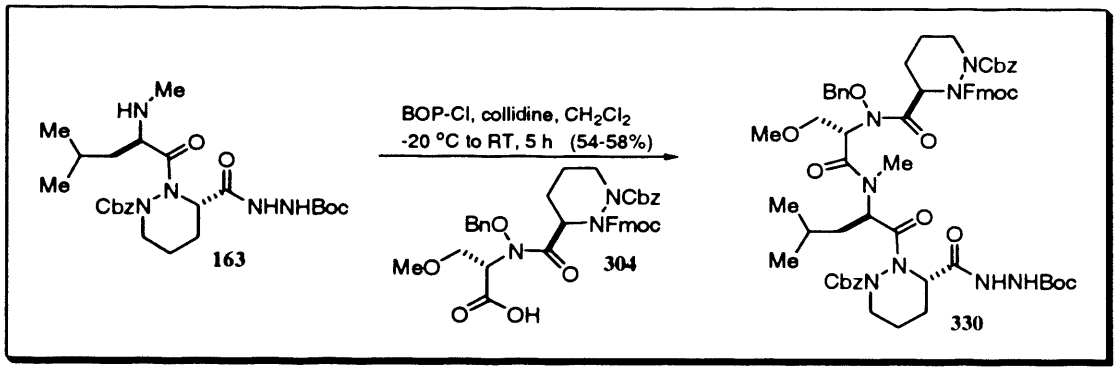

To a – 20 °C solution of **304** (12.44 g, 17.93 mmol) and crude **163** (9.52 g, 18.83 mmol) in anhydrous CH_2Cl_2 (70 mL) under N_2, was added distilled collidine (4.74 mL, 35.86 mmol) followed by BOP-Cl (5.48 g, 21.52 mmol) in one portion. The reaction mixture was stirred between –15 °C and 0 °C for 30 mins before being allowed to warm to RT, where it was stirred for 5 hours. The reaction mixture was diluted with EtOAc (300 mL) and washed with 1 N aq. HCl (2 x 50 mL), 5% aq. $NaHCO_3$ (2 x 50 mL) and brine (50 mL). The organic layer was then dried ($MgSO_4$), filtered and concentrated *in vacuo* to provide a yellow foam, which was purified by SiO_2 flash chromatography using hexanes/EtOAc (10:1 to 5:1 to 1:1) to afford **330** as a white foam (12.36 g, 58%). **$[\alpha]_D^{12}$** –60.1 ° (*c* 0.694, CH_2Cl_2); **IR (neat)** 3301 (br w), 2957 (w), 2361 (w), 1706 (s), 1497 (w), 1453 (m), 1414 (m), 1363 (m), 1291 (m), 1252 (m), 1195 (m), 1161 (w), 1124 (w), 1092 (w), 1049 (w), 1010 (w), 970 (w), 913 (w), 734 (s), 700 (w); **^{1}H NMR (500 MHz, $CDCl_3$, 298 K)** δ 7.71 (br m, 2*H*, arom), 7.51-7.15 (br m, ~ 21*H*, arom), 5.54 (br m, 2*H*), 5.22-4.60 (br m, ~ 8*H*), 4.29-3.89 (br m, ~ 6*H*), 3.59 (br m, 1*H*), 3.25 (br m, 3*H*, $OC\underline{H}_3$), 3.15-2.92 (br m, ~ 5*H*), 2.41-2.13 (br m, 2*H*), 1.88-1.66 (br m, ~ 6*H*), 1.41 (br m, ~ 13*H*), 0.92-0.68 (br m, ~ 7*H*); **^{13}C NMR (125 MHz, $CDCl_3$, 298 K)** δ 173.4, 169.1, 165.4, 155.8, 154.5, 143.9, 143.2, 141.2, 136.6, 135.5, 135.2, 134.3, 128.6, 128.4, 128.2, 127.9, 127.0, 125.1, 112.0, 81.2, 78.8, 68.7, 68.4, 67.6, 67.4, 60.5, 58.7 ($O\underline{C}H_3$), 57.3, 55.8, 50.1, 46.8, 45.3, 44.6, 44.0, 41.7, 37.7, 33.0, 30.0, 29.4, 28.1 ($CO_2C(\underline{C}H_3)_3$), 25.1, 24.7, 24.3, 23.1, 22.9, 22.5, 21.2, 20.0, 19.3, 18.4; **FAB HRMS** Calcd. for $C_{64}H_{76}N_8O_{14}$ $(M+Na)^+$: *m/e* 1203.53784; Found: *m/e* 1203.54049.

O-Benzyl-D-Threonine 350

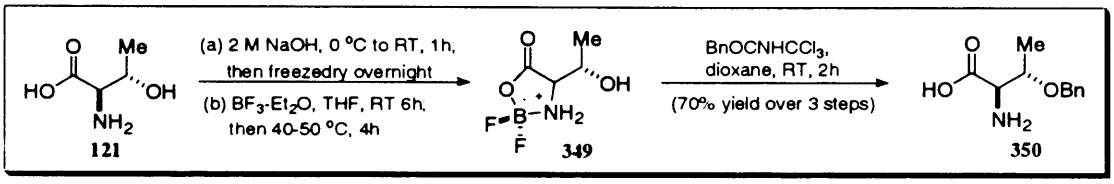

121 349 350

To D-threonine (10 g, 83.95 mmol) at 0°C in a 100 mL round bottom flask, was added 2 M aq. NaOH (50 mL). The reaction mixture was stirred for 15 mins at 0 °C and then allowed to reach ambient temperature where it was stirred for 1 hour. The reaction mixture was then put on a freeze dryer for 24 hours. The white solid that had formed was put on a rotary evaporator for 30 mins at 80 °C, and then suspended in anhydrous THF (120 mL). $BF_3.Et_2O$ (48 mL, 377.8 mmol) was added dropwise at RT, and the reaction mixture stirred vigorously for 6 hours at RT, and then heated between 40 °C and 50 °C for a further 4 hours. The resulting mixture was then concentrated *in vacuo* to form a white solid that at all times was protected from moisture. To this residual white solid, at room temperature, was added anhydrous dioxane (250 mL) and the mixture was stirred for 10 mins. Benzyl trichloroacetimidate (19 mL, 100.74 mmol) was then added dropwise over 15 mins and the reaction mixture was stirred at room temperature for 2 hours. Methanol (40 mL) was then added and stirring continued for a further 10 mins before 1 M aq. NaOH solution (250 mL) was added. The reactants were thereafter heated at 50 °C for an additional 30 mins, and concentrated *in vacuo*. The residue so obtained was dissolved in H_2O (600 mL) and washed with Et_2O (3 x 30 mL). The aqueous layer was adjusted to pH 6, with conc. HCl, and passed through a column containing Amberlite XAD-4 resin (~ 8 cm diameter, 20 cm length). The column was washed with H_2O and then H_2O/EtOH (2:1), the latter eluent containing the desired compound. The resulting solution was then concentrated *in vacuo* to provide a white solid (12.27 g, 70% over 3 steps). **FAB HRMS** Calcd. for $C_{11}H_{15}NO_3$ $(M+H)^+$: *m/e* 210.11301; Found: *m/e* 210.11296.

The spectral data obtained for **350** matched that in the literature[227]

N- Boc-*O*-Benzyl-D-Threonine 123

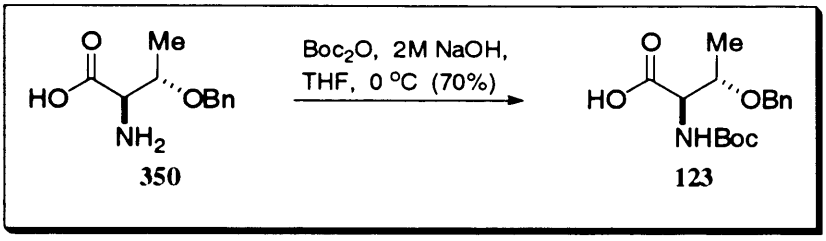

To a solution of **350** (9.62 g, 45.98 mmol) in THF (25 mL) at 0 °C was added 2 M NaOH (23 mL, 45.98 mmol) and the solution allowed to stir for 10 mins. Boc_2O (11.15 g, 51.08 mmol) was then added dropwise and the mixture was stirred at 0 °C for 4 hours. The reaction mixture was then extracted with Et_2O (2 x 50 mL) and the aqueous layer acidified to pH 2 with conc. HCl and extracted further with EtOAc (3 x 200 mL). The combined organic layers were then dried ($MgSO_4$), filtered and concentrated *in vacuo* to afford a crude yellow oil. This was then purified by SiO_2 flash chromatography using hexanes/EtOAc (5:1 to 2:1 to 0:1) to afford **123** as a viscous clear oil (9.91 g, 70%). **IR (neat)** 3443 (w), 2979 (m), 2933 (m), 1718 (s), 1504 (m), 1454 (m), 1394 (m), 1369 (m), 1345 (w), 1316 (w), 1253 (w), 1211 (w), 1164 (s), 1130 (w), 1099 (w), 1074 (m), 1027 (w), 999 (w), 914 (w), 856 (w), 776 (w), 735 (m), 899 (m), 676 (w), 611 (w), 462 (w); **^{1}H NMR (500 MHz, $CDCl_3$, 298 K)** δ 11.16 (br s, 1*H*, $CO_2\underline{H}$), 7.30-7.24 (br m, 5*H*, arom), 5.32 (d, *J* = 9.3 Hz, 1*H*, $N\underline{H}$), 4.57 (d, *J* = 11.6 Hz, 1*H*, $OC\underline{H}_2Ph$), 4.43 (d, *J* = 11.6 Hz, 1*H*, $OC\underline{H}_2Ph$), 4.36 (d, *J* = 8.9 Hz, 1*H*, $HO_2CC\underline{H}$), 4.17 (m, 1*H*, $HO_2CCHC\underline{H}CH_3$), 1.44 (s, 9*H*, $NO_2C(C\underline{H}_3)_3$), 1.24 (d, *J* = 6.3 Hz, 3*H*, $HO_2CCHCHC\underline{H}_3$); **^{13}C NMR (125 MHz, $CDCl_3$, 298 K)** δ 176.1 (CO), 156.2 (CO), 137.5 (arom), 128.4 (arom), 127.8 (arom), 127.7 (arom), 80.2 ($NO_2\underline{C}(CH_3)_3$), 74.3 ($HO_2CCH\underline{C}HCH_3$), 71.1 ($O\underline{C}H_2Ph$), 58.0 ($HO_2C\underline{C}H$), 28.3 ($NO_2C(\underline{C}H_3)_3$), 16.1($HO_2CCHCH\underline{C}H_3$); **FAB HRMS** Calcd. for $C_{16}H_{23}NO_5$ $(M+H)^+$: *m/e* 310.16544; Found: *m/e* 310.16685.

Fmoc-deprotection of 330

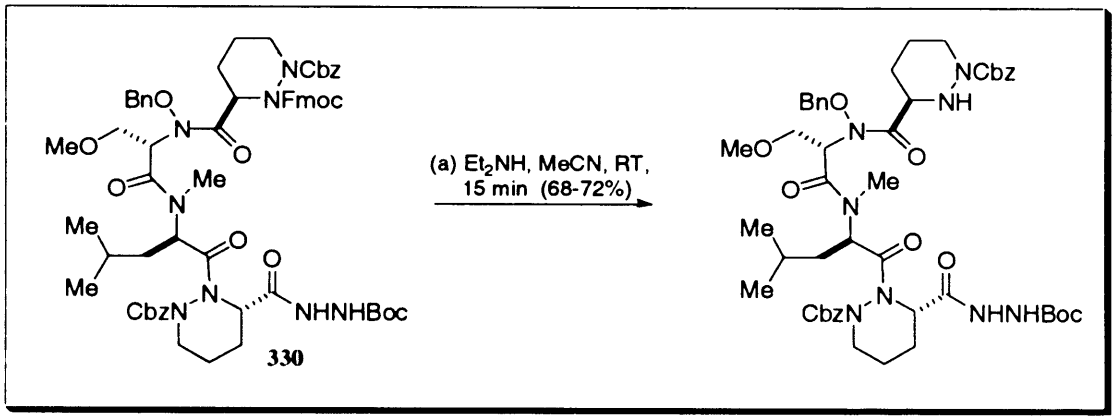

To a RT solution of **330** (12.26 g, 10.38 mmol) in anhydrous MeCN (100 mL) under N_2 was added diethylamine (43 mL, 415.13 mmol). The reaction mixture was stirred for 30 mins, diluted with EtOAc (50 mL), concentrated *in vacuo*, and the residue purified by SiO_2 flash chromatography using hexanes/EtOAc (2:1 to 1:1 to 0:1) to afford the desired amine as a white foam (6.9 g, 69%). **$[\alpha]_D^{12}$** –50.5 ° (*c* 0.422, CH_2Cl_2); **IR (neat)** 3287 (br w), 2956 (m), 1698 (s), 1498 (w), 1455 (m), 1404 (m), 1364 (m), 1259 (m), 1181 (m), 1123 (m), 1076 (w), 1039 (w), 1002 (w), 914 (w), 872 (w), 733 (m), 700 (m), 648 (w), 602 (w); **^{1}H NMR (500 MHz, $CDCl_3$, 298 K)** δ 7.38-7.24 (br m, 15*H*, arom), 5.49 (br m, 1*H*), 5.25-4.99 br m, 6*H*), 4.82 (br m, 1*H*), 4.20-3.87 (br m, ~ 5*H*), 3.81-3.50 (br m, ~ 4*H*), 3.44-3.10 (br m, 7*H*), 2.99-2.77 (br m, ~ 3*H*), 2.39-2.24 (br m, 1*H*), 2.01-1.39 (br m, ~ 19*H*), 0.98-0.67 (br m, ~ 5*H*); **^{13}C NMR (125 MHz, $CDCl_3$, 298 K)** δ 174.0, 169.2, 168.4, 156.7, 136.7, 136.1, 135.5, 134.3, 129.1, 128.7, 128.6, 128.5, 128.4, 128.2, 128.0, 78.9, 68.8, 68.4, 68.0, 67.3, 60.5, 59.3, 58.8, 57.6, 56.8, 56.0, 45.2, 43.2, 42.8, 41.8, 41.3, 32.9, 28.0, 27.5, 25.0, 24.3, 23.1, 21.3, 21.1, 20.0; **FAB HRMS** Calcd. for $C_{49}H_{66}N_8O_{12}$ $(M+H)^+$: *m/e* 959.48782; Found: *m/e* 959.49001.

Synthesis of linear hexadepsipeptide 331

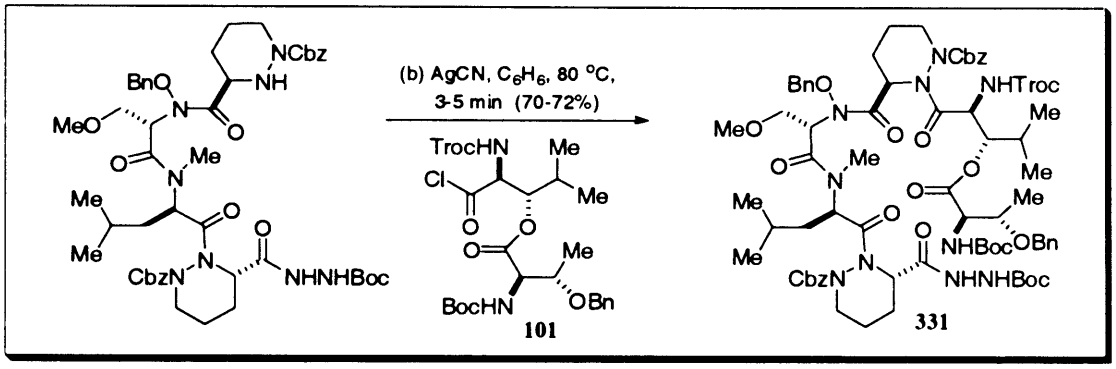

To a RT solution of the acid derivative of **101** (4.28 g, 6.97 mmol) in anhydrous C_6H_6 (21 mL) under N_2 was added, in one portion, $(COCl)_2$ (21 mL, 240.85 mmol), and the mixture was stirred for 2.5 hours. The excess $(COCl)_2$ was removed *in vacuo* and the residue co-evaporated with C_6H_6 (3 x 10 mL). The resulting golden oil was then placed under high vacuum pump for 20 mins to provide **101** as a golden foam. To this golden foam of **101** was added, at room temperature and under N_2, a solution of the deprotected product of **330** (6.6 g, 6.88 mmol) in C_6H_6 (65 mL). The reaction vessel was then covered in aluminium foil and AgCN (1.38 g, 10.32 mmol) was added. The reaction mixture was immersed into a pre-heated oil bath then at 80 °C for 3-5 mins, before being cooled, diluted with EtOAc (100 mL) and filtered through Celite, washing the flask and residue with copious amounts of EtOAc. The filtrate was then concentrated *in vacuo* and the resulting product purified by SiO_2 flash chromatography using hexanes/EtOAc (5:1 to 2:1 to 1:1) to afford the desired amine as a white foam (7.49 g, 70% over 2 steps). **$[\alpha]_D^{12}$** –60.2 ° (*c* 0.334, CH_2Cl_2); **IR (neat)** 3306 (br w), 2972 (w), 1737 (s), 1718 (s), 1674 (s), 1501 (m), 1455 (m), 1394 (m), 1366 (m), 1308 (w), 1247 (m), 1196 (w), 1162 (m), 1122 (w), 1096 (w), 1072 (w), 1047 (w), 995 (w), 914 (w), 872 (w), 822 (w), 733 (w), 699 (w), 648 (w), 621 (w), 568 (w); **^{1}H NMR (500 MHz, $CDCl_3$, 298 K)** δ 7.33-7.15 (br m, 20*H*, arom), 5.76 (br m, 1*H*), 5.69 (d, *J* = 9.4, 1*H*), 5.52-5.40 (br m, 1*H*), 5.28 (d, *J* = 9.4, 1*H*), 5.23-4.92 (br m, ~ 8*H*), 4.85-4.68 (br m, 1*H*), 4.61 (d, *J* = 12.0 Hz, 1*H*), 4.54-4.47 (br m, 2*H*), 4.43-4.36 (br m, 2*H*), 4.15-4.09 (br m, 2*H*), 3.89-3.45 (br m, 3*H*), 3.21 (distorted s, 3*H*, $OC\underline{H}_3$), 3.07 (br m, 2*H*), 2.83-2.75 (br m, 2*H*), 2.37-1.79 (br m, ~ 8*H*), 1.54-1.29 (br m, ~ 20*H*), 1.24-1.21 (br m, ~ 3*H*), 0.94-0.86 (br m, ~ 11*H*); **^{13}C NMR (125 MHz, $CDCl_3$, 298 K)** δ 171.7, 170.0, 156.3, 155.6, 154.5, 153.2, 137.7, 136.0, 135.2, 134.2, 130.0, 129.1, 128.5, 128.3, 128.2, 128.0, 127.8, 127.6, 127.5, 126.4, 95.2, 79.8, 78.9, 74.6, 74.2, 73.1, 70.4, 68.6, 68.1, 58.8 ($O\underline{C}H_3$), 58.2, 55.9, 51.1, 45.6, 37.6, 28.8, 28.3, 28.2 ($NCO_2C(\underline{C}H_3)_3$), 28.1 ($NCO_2C(\underline{C}H_3)_3$), 25.2, 25.0, 23.1, 21.1, 19.8, 17.2, 16.5, 16.2, 16.0; **FAB HRMS** Calcd. for $C_{74}H_{99}N_{10}O_{20}Cl_3(M+H)^+$: *m/e* 1553.61806; Found: *m/e* 1553.61423.

Synthesis of macrolactamisation precursor 332

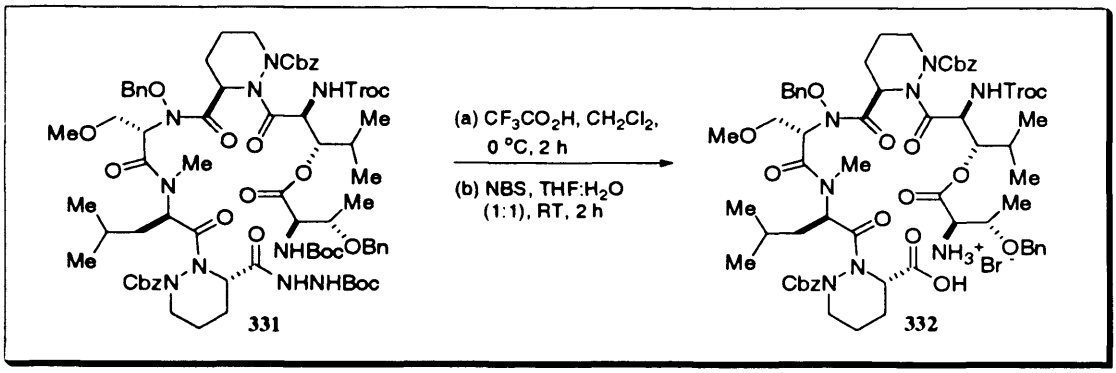

To a 0 °C solution of **331** (4.96 g, 3.2 mmol) in anhydrous CH_2Cl_2 (49 mL) under N_2, was added TFA (49 mL, 637.95 mmol) and the reaction mixture stirred at 0 °C for 2 hours. The reaction mixture was then concentrated *in vacuo* and the residue co-evaporated with toluene (4 x 15 mL) to remove excess TFA. To this residue was added H_2O/THF [1:1] (40 mL) at room temperature, and NBS (1.14 g, 6.4 mmol) was subsequently added in 3 portions over 5 mins with stirring. After stirring at RT for 1.5 hours the reaction mixture was diluted with EtOAc (150 mL) and washed with brine (2 x 50 mL). The organic extract was then dried ($MgSO_4$), filtered, and concentrated *in vacuo* to afford an off-white foam of sufficient purity for the next step.

Synthesis of Troc-protected cyclodepsipeptide 333

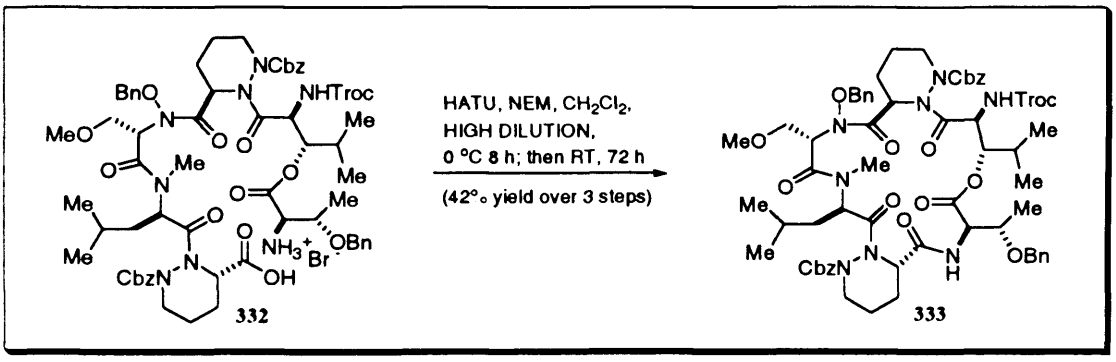

To a 0 °C solution of HATU (12.13 g, 31.9 mmol) in anhydrous CH_2Cl_2 (3.71 L) under N_2 was added dropwise over a 7-hour period, a mixture of **332** (4.28 g, 3.2 mmol) and *N*-ethylmorpholine (5.5 mL, 43.1 mmol) in anhydrous CH_2Cl_2 (3.71 L). When the addition was

complete the reactants were vigorously (using a mechanical stirrer) stirred for 72 hours. The reaction mixture was then concentrated *in vacuo*, diluted with EtOAc (200 mL), and washed with 1 N aq. HCl (2 x 30 mL), 10 % aq. $NaHCO_3$ (2 x 30 mL) and brine (30 mL). The organic extract was then dried ($MgSO_4$), filtered, concentrated *in vacuo* and purified by SiO_2 flash chromatography using hexanes/EtOAc (2:1 to 1:1) to afford the desired cyclodepsipeptide as a white foam (2.04 g). The product appeared as two inseparable spots on TLC, which were taken on to the next stage without separation.

Synthesis of Cbz-protected cyclodepsipeptide 334

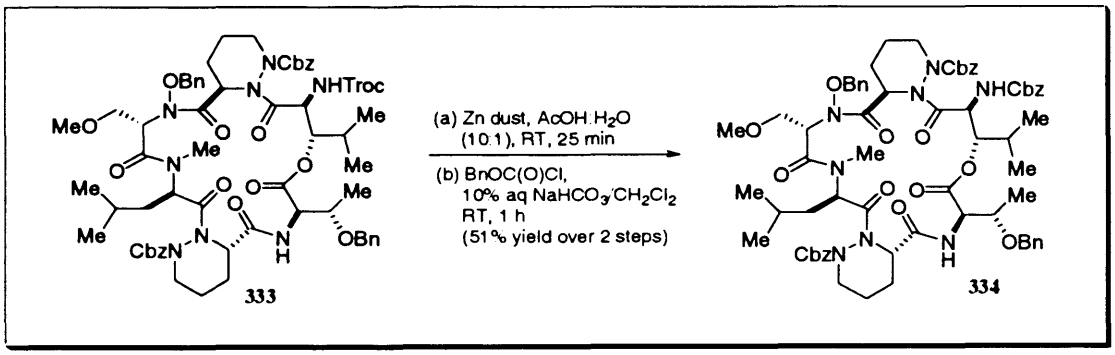

To a RT solution of **333** (2.04 g, 1.53 mmol) in $AcOH:H_2O$ [10:1] (40 mL) was added Zn dust (2 g, 30.5 mmol) in one portion and the reactants stirred for 1 hour. The reaction mixture was then diluted with THF (100 mL) and filtered through Celite, washing with copious amounts of THF. The filtrate was then concentrated *in vacuo*, and the residue co-evaporated with toluene to remove excess acetic acid. To this crude product was added simultaneously at RT, 10 % aq. $NaHCO_3$ (8 mL) and a solution of benzyl chloroformate (0.65 mL, 4.58 mmol) in anhydrous CH_2Cl_2 (8 mL) and the reaction mixture left to stir for 2 hours. The reaction mixture was diluted with EtOAc (100 mL), washed with brine and organic layer separated, dried ($MgSO_4$), filtered and concentrated *in vacuo*. TLC analysis at this stage () indicated two major products. The product (top spot – golden brown – 1:1 hexanes/EtOAc) was then separated and purified by SiO_2 flash chromatography using hexanes/EtOAc (5:1 to 3:1 to 1:1) to afford the Cbz-protected cyclodepsipeptide as a white foam (0.98 g, 51% over 2 steps). **IR (neat)** 3351 (br w), 3065 (w), 3032 (w), 2957 (m), 2934 (m), 2874 (w), 1728 (s), 1674 (s), 1499 (m), 1456 (m), 1385 (m), 1348 (w), 1242 (m), 1196 (w), 1178(w), 1157 (w), 1124 (w), 1082 (w), 1047 (w), 1028 (w), 735 (m), 698 (m); **^{1}H NMR (500 MHz, $CDCl_3$, 298 K)** δ 7.35–7.17 (br m, 25*H*, arom), 5.45–4.84 (br m, ~ 13*H*), 4.70–4.42 (br m, ~ 4*H*), 4.28– 4.01 (br m ~ 5*H*), 3.75–3.43 (br m, 2*H*), 3.27 (s, 3*H*, $OC\underline{H}_3$), 2.82

(br m, ~ 2*H*), 2.08-1.42 (br m, ~ 11*H*), 1.29-1.07 (br m, ~ 6*H*), 0.98-0.74 (br m, ~ 13*H*); **^{13}C NMR (125 MHz, $CDCl_3$, 298 K)** δ 173.7, 171.0, 170.2, 170.0, 169.7, 168.7, 168.0, 158.7, 158.1, 157.5, 155.3, 154.3, 137.1, 136.0, 135.5, 135.1, 134.7, 134.2, 127.7-129.4 – broad peaks, 79.7, 78.3, 75.0, 70.7, 70.5, 68.4-69.5 – broad peaks, 67.0, 58.9 ($O\underline{C}H_3$), 56.8, 54.4, 53.7, 52.4, 50.6, 46.2, 45.7, 43.3-44.3 – broad peaks, 41.0, 37.0, 31.8, 31.4, 29.6, 29.3, 28.6, 24.3, 24.0, 23.0, 22.9, 22.6, 22.2, 19.9, 19.7, 19.0, 18.6, 18.3, 16.7, 15.3, 15.0, 14.0; **FAB HRMS** Calcd. for $C_{69}H_{84}N_8O_{16}$ $(M+Na)^+$: *m/e* 1303.59027; Found: *m/e* 1303.59382.

Synthesis of cyclodepsipeptide hydrochloride salt 303

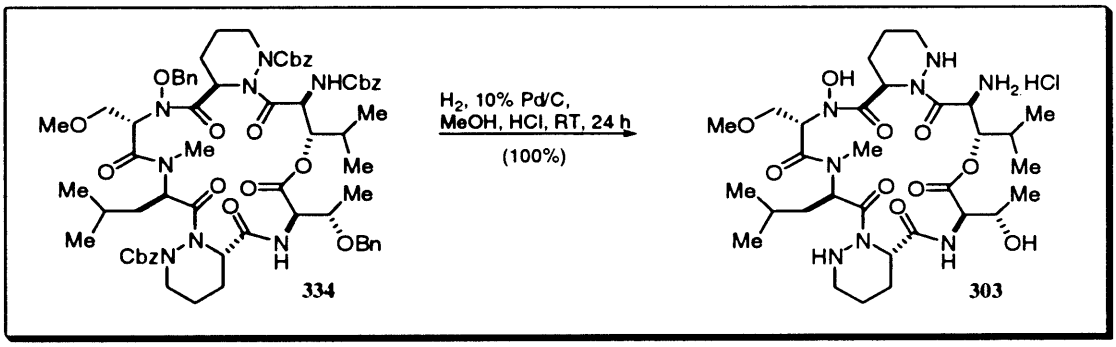

0.01 M MeOH.HCl was made by adding 0.17 mL of acetyl chloride to anhydrous MeOH (240 mL) under N_2 at RT and allowing the mixture to stir for 30 mins. To **334** (0.83 g, 0.65 mmol) dissolved in this anhydrous 0.01 M MeOH.HCl solution (65 mL, 0.65 mmol) under N_2, was added 10% Pd/C (0.6 g - Aldrich) and the reaction vessel purged with H_2. It was thereafter stirred vigorously for 24 hours at atmospheric pressure. The reaction mixture was then diluted with MeOH (50 mL) and filtered through Celite, washing the flask and residue with copious amounts of MeOH. The filtrate was then concentrated *in vacuo* to provide **303** as a white solid (0.47 g), which was sufficiently pure to be used directly for the next step. **IR (KBr)** 3279 (br s), 2936 (s), 2873 (s), 1733 (s), 1636 (s), 1445 (br s), 1394 (s), 1248 (s), 1157 (s), 1124 (s), 998 (m), 923 (m), 863 (w), 420 (br m); **^{1}H NMR (500 MHz, CD_3OD, 298 K)** δ 6.05 (br m, 1*H*), 5.47 (apparent br dd, *J* = 8.7 Hz, 1*H*), 5.29 (br m, 1*H*), 5.19 (br m 1*H*), 5.09-5.03 (br m, 1*H*), 4.70-4.67 (br m, 1*H*), 4.49-4.44 (br m, 2*H*), 4.02 (br m, 1*H*), 3.87 (apparent t, *J* = 9.1 10.5 Hz, 1*H*), 3.76-3.68 (br m, 1*H*), 3.64-3.55 (br m, 1*H*), 3.35 (s, 3*H*, $O\underline{C}H_3$), 3.16-2.94 (br m, 3*H*), 2.80 (br m, 1*H*), 2.71-2.67 (br m, 2*H*), 2.39-2.08 (br m, 4*H*), 1.94 (br m, 2*H*), 1.66 (br m, 4*H*), 1.52-1.47 (br m, 2*H*), 1.39-1.27 (br m, 1*H*), 1.23 (d, *J* = 6.7 Hz, 1*H*), 1.17 (d, *J* = 6.1 Hz, 2*H*), 1.12 (d, *J* = 6.1 Hz, 2*H*), 1.07 (d, *J* = 6.6 Hz, 1*H*), 1.04 (d, *J* = 6.4 Hz, 2*H*), 1.01 (d, *J* = 6.6 Hz, 1*H*), 0.94 (br d, *J* = 6.5 Hz, 8*H*); **^{13}C NMR**

(125 MHz, $CDCl_3$, 298 K) δ 175.0, 173.6, 173.1, 170.1, 169.9, 168.6, 80.7, 77.9, 70.1, 69.5, 68.1, 67.9, 59.9, 59.2, 56.8, 53.2, 51.3, 47.0, 43.3, 42.4, 37.9, 30.8-31.3 (br), 30.2, , 28.1, 26.1, 24.6, 23.0, 20.7-21.3, 19.1; **FAB HRMS** Calcd. for $C_{31}H_{54}N_8O_{10}$ $(M+Na)^+$: *m/e* 721.38551; Found: *m/e* 721.38597.

Swern oxidation to aldehyde 72

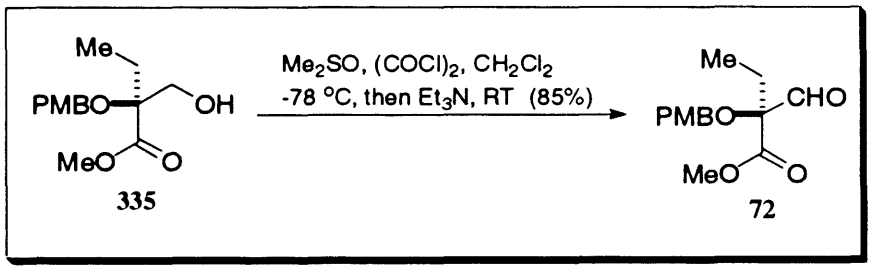

To a stirred solution of anhydrous DMSO (2.41 mL, 33.58 mmol) and anhydrous CH_2Cl_2 (20 mL) at –78 °C, under N_2, was added over a 2-minute period, $(COCl)_2$ (1.48 mL, 16.8 mmol) and the reaction mixture stirred at –78 °C for 10 mins. A solution of **335** [IV-LL-181](1.5 g, 5.6 mmol) in anhydrous CH_2Cl_2 (10 mL) was then added dropwise at –78 °C, followed by Et_3N (12 mL, 83.96 mmol) and the reaction mixture stirred at –78 °C for 10 mins, before being allowed to reach ambient temperature. The reaction mixture was then quenched *via* the addition of brine (30 mL) and the product extracted with CH_2Cl_2 (3 x 50 mL). The combined organic extracts were then dried ($MgSO_4$), filtered and concentrated *in vacuo* to provide a crude yellow oil. This crude oil was then purified by SiO_2 flash chromatography using hexanes/EtOAc (5:1) to afford the desired aldehyde as a pale yellow oil (1.33 g, 85%).

The ^1H NMR spectrum of 72 matched that obtained by Dr J. Cai[158(a),(b)]

Unification of 72 and 89 (Julia coupling) to provide 96

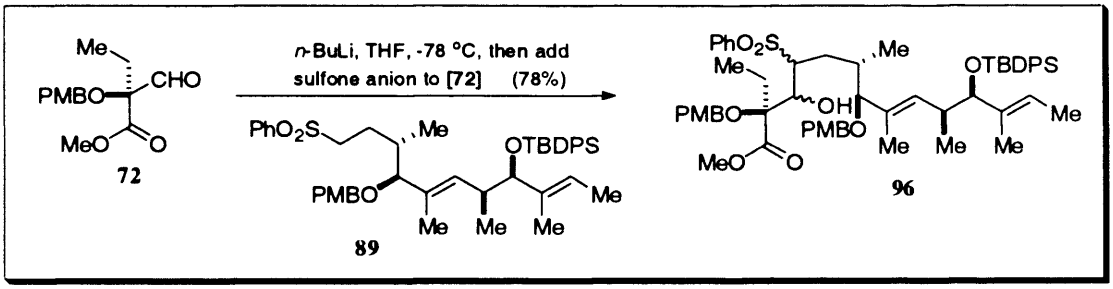

To a stirred solution of **89** [IV-LL-156] (3.39 g, 4.59 mmol) in anhydrous THF (12 mL) at –78 °C under N_2 was added *n*-BuLi (2 mL, 5.05 mmol) dropwise over 5 mins, and the reaction mixture stirred at –78 °C for 30 mins. The resulting lime-coloured solution was then cannulated at –78 °C into a pre-cooled (-78 °C) solution of **72** (1.22 g, 4.59 mmol) in anhydrous THF (12 mL) over a 2-minute period, and the resulting solution allowed to warm to RT. The mixture was then quenched by the addition of brine (50 mL) and the product was extracted with EtOAc (3 x 70 mL). The combined organic extracts were then dried over $MgSO_4$, filtered and concentrated *in vacuo*. The resulting crude oil was then purified by SiO_2 flash chromatography using hexanes/EtOAc (5:1 to 2:1) to afford the desired product as a viscous clear oil (3.59 g, 78%). **FAB HRMS** Calcd for $C_{59}H_{75}O_{10}SSi$ $(M+Na)^+$: *m/e* 1027.48259. Found: *m/e* 1027.48762.

The ^1H NMR spectrum of **72** matched that obtained by Dr J. Cai[158(a),(b)]

Swern Oxidation of 96

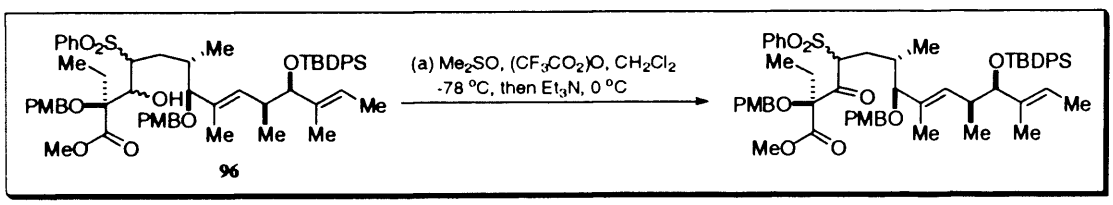

To a stirred –78 °C solution of dry DMSO (1 mL, 14.96 mmol) in dry CH_2Cl_2 (30 mL), under N_2 was added $(CF_3CO)_2O$ (1 mL, 7.34 mmol) dropwise over 1 min. After stirring at –78 °C for 20 mins, a solution of **96** (2.46 g, 2.45 mmol) in dry CH_2Cl_2 (15 mL) was added over 5 mins

followed by Et_3N (6.8 mL, 48.96 mmol), and the reactants stirred at –78 °C for 5 mins before being allowed to warm to RT. The reaction was then quenched with brine (50 mL) and extracted with CH_2Cl_2 (3 x 70 mL). The combined organic extracts were dried ($MgSO_4$), filtered, and concentrated *in vacuo* to give a yellow oil that was taken directly forward to the next step. **FAB HRMS** Calcd for $C_{59}H_{74}O_{10}SSi$ $(M+Na)^+$: *m/e* 1025.46694. Found: *m/e* 1025.46423.

The ^1H NMR spectrum matched with that obtained by Dr Linos Lazarides[192]

Desulfonylation to provide 97

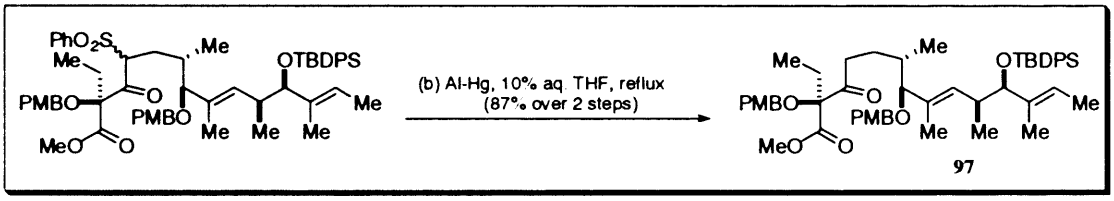

A 2% solution of $HgCl_2$ (2 g) in H_2O (100 mL) was made up in a 150 mL conical flask alongside two further flasks, which contained MeOH (80 mL) and Et_2O (80 mL) respectively. Aluminium foil was then cut into strips and the Al/Hg amalgam was made by dipping the foil into the $HgCl_2$ solution for 10 seconds, and then briefly immersing it in the MeOH and Et2O solutions for 2-3 secs. The Al/Hg amalgam foil was then continuously added into a solution of the above ketone (2.45 mmol) in THF:H_2O [10:1] (330 mL) at reflux until all the starting material had been consumed. This required close monitoring by TLC. When the reaction had gone to completion the reaction mixture was cooled to RT and filtered through a pad of Celite, and the residue washed with EtOAc. The filtrate was then concentrated *in vacuo* and the resulting material diluted with H_2O (50 mL) and extracted with ether (4 x 50 mL). The combined ethereal layers were then dried over $MgSO_4$, filtered and concentrated *in vacuo* to provide a crude residue which was purified by SiO_2 flash chromatography using hexanes/EtOAc (10:1) to afford the desired product as a viscous clear oil (1.84 g, 87% over 2 steps). **FAB HRMS** Calcd for $C_{53}H_{70}O_8Si$ $(M+Na)^+$: *m/e* 885.47374. Found: *m/e* 885.47503.

The ^1H NMR spectrum of **97** matched with that obtained by Dr Linos Lazarides[192]

DDQ deprotection of 97

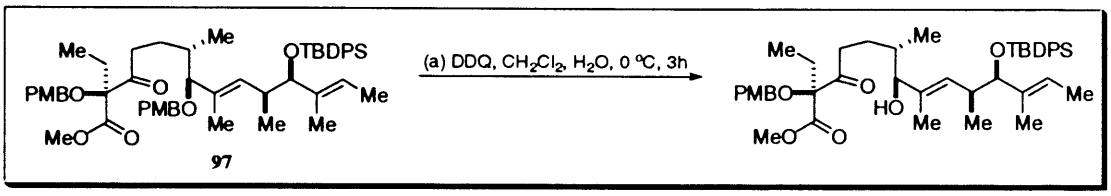

To a 0 °C solution of **97** (1.84 g, 2.13 mmol) in CH_2Cl_2 (45 mL) and H_2O (3 mL) was added, in one portion, DDQ (0.58 g, 2.56 mmol) and the reactants stirred at 0 °C for 3 hours. The reaction mixture was diluted with CH_2Cl_2 (50 mL) and filtered through Celite, and the residue washed with CH_2Cl_2 (100 mL). The filtrate was then washed with sat. aq. $NaHCO_3$ (50 mL) and brine (30 mL) and the organic layer was dried over $MgSO_4$, filtered and concentrated *in vacuo*. The resulting deep yellow oil was then taken onto the next step in the sequence without any further purification.

Acid catalysed cyclisation to 98

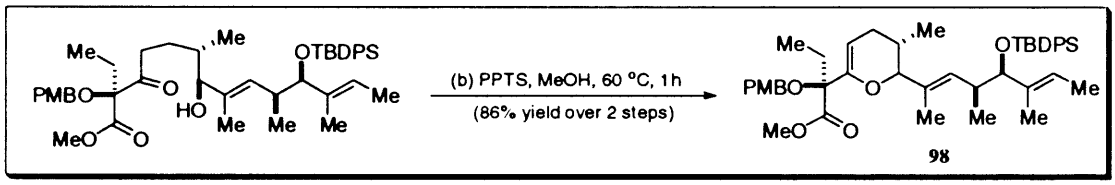

To a RT solution of the above ketone (2.13 mmol) in anhydrous methanol (30 mL) under N_2 was added PPTS (0.15 g) and the reaction mixture heated at 60 °C. After 1 hour the reactants were cooled to RT, diluted with EtOAc (50 mL) and the organic layer washed with H_2O (2 x 10 mL). The organic phase was separated, dried over $MgSO_4$, filtered and concentrated *in vacuo*. The residual oil was then purified by SiO_2 flash chromatography using hexanes/EtOAc (25:1) to afford the **98** as a clear oil (1.33 g, 86% over 2 steps).

The ^1H NMR spectrum matched with that obtained by Dr Linos Lazarides[192]

TBDPS deprotection of 98

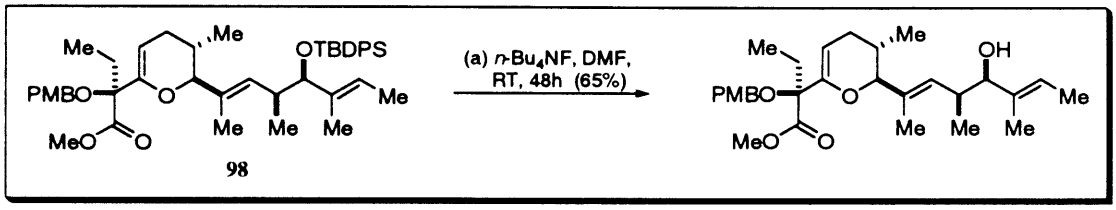

To a 100 mL round bottomed flask containing 1 M TBAF in THF (20 mL) under nitrogen was added anhydrous DMF, and the mixture concentrated *in vacuo* to remove the THF. The resulting solution (13 mL) was then added to **98** (1.3 g, 1.8 mmol) under N_2, and the reactants were stirred at RT for 48 hours. Et_2O (60 mL) was then added, and the organic layer was washed with brine (2 x 15 mL), dried over $MgSO_4$, filtered, concentrated *in vacuo* and purified by SiO_2 flash chromatography using hexanes/EtOAc (10:1 to 5:1) to give the desired allylic alcohol as a clear oil (0.58 g, 65%). **IR (neat)** 3457 (br m), 2954 (s), 2925 (s), 2871 (s) 1742 (s), 1670 (m), 1613 (m), 1514 (s), 1456 (m), 1380 (m), 1345 (w), 1302 (m), 1248 (s), 1176 (w), 1131 (s), 1082.0 (s), 1037 (s) 1013 (s), 823 (m); **^{1}H NMR (500 MHz, $CDCl_3$, 298 K)** δ 7.27 (d, J = 8.6 Hz, 2*H*, arom), 6.82 (d, J = 8.6 Hz, 2*H*, arom), 5.41 (apparent q, J = 6.6 Hz, 1*H*, $H_3CC=C\underline{H}CH_3$), 5.13 (d, J = 9.5 Hz, 1*H*, $H_3CC=C\underline{H}CHCH_3$), 4.94 (apparent d, J = 3.4 Hz, 1*H*, quart-$CC=C\underline{H}CH_2CHCH_3$), 4.52 (d, J = 10.8 Hz, 1*H*, $OC\underline{H}_2PhOMe$), 4.28 (d, J = 10.8 Hz, 1*H*, $OC\underline{H}_2PhOMe$), 3.78 (s, 3*H*, $OC\underline{H}_3$), 3.72 (d, J = 7.3 Hz, 1*H*, $H_3CCHC\underline{H}OH$), 3.70 (s, 3*H*, $CO_2C\underline{H}_3$), 3.61 (d, J = 9.3 Hz, 1*H*, $H_3CCC\underline{H}O$), 2.58 (m, 1*H*, $H_3CC\underline{H}CHOH$), 2.10 (m, 1*H*, PMB*O*-$C(CH_2CH_3)C=CHC\underline{H}_2CHCH_3$), 1.98 (m, 2*H* $PMBOCC\underline{H}_2CH_3$), 1.72 (2 x m overlapping, 2*H*, PMB*O*-$C(CH_2CH_3)C=CHC\underline{H}_2CHCH_3$ and $PMBOC(CH_2CH_3)C=CHCH_2C\underline{H}CH_3$), 1.56-1.49 (overlapping peaks, 11*H*, – 3 x CH_3 + others), 0.97 (d, J = 6.7 Hz, 3*H*, $\underline{H}_3CCHCHOH$), 0.84 (t, J = 7.4 Hz, 3*H*, $PMBOCCH_2C\underline{H}_3$), 0.74 (d, J = 6.3 Hz, 3*H*, $PMBOC(CH_2CH_3)C=CHCH_2CHC\underline{H}_3$); **^{13}C NMR (125 MHz, $CDCl_3$, 298 K)** δ 172.3 ($\underline{C}O$), 158.9 (arom), 150.6 ($PMBOC(CH_2CH_3)\underline{C}=CHCH_2$), 137.1, 132.3 ($H_3CC=\underline{C}HCHCH_3$), 132.2, 131.0, 129.0 (arom), 121.4 ($H_3CC\underline{C}HCH_3$), 113.5 (arom), 98.2 (quart-$CC=\underline{C}HCH_2CHCH_3$), 87.5 ($H_3CC\underline{C}HO$), 84.0 ($PMBO\underline{C}CH_2CH_3$), 81.7 ($H_3CCH\underline{C}HOH$), 66.2 ($O\underline{C}H_2PhOCH_3$), 55.2 ($O\underline{C}H_3$), 51.9 ($CO_2\underline{C}H_3$), 36.1 ($H_3C\underline{C}HCHOH$), 29.1 (PMB*O*-$C(CH_2CH_3)C=CH\underline{C}H_2CHCH_3$), 28.6 ($PMBOC(CH_2CH_3)C=CHCH_2\underline{C}HCH_3$), 25.8 ($PMBOC\underline{C}H_2CH_3$), 17.4 ($PMBOC(CH_2CH_3)C=CHCH_2CH\underline{C}H_3$), 16.5 ($H_3\underline{C}CHCHOH$), 12.9 11.7, 11.1, 7.7 ($PMBOCCH_2\underline{C}H_3$); **FAB HRMS** Calcd. for $C_{29}H_{42}O_6$ $(M+Na)^+$: *m/e* 509.28789; Found: *m/e* 509.28660.

Formation of Acid 99

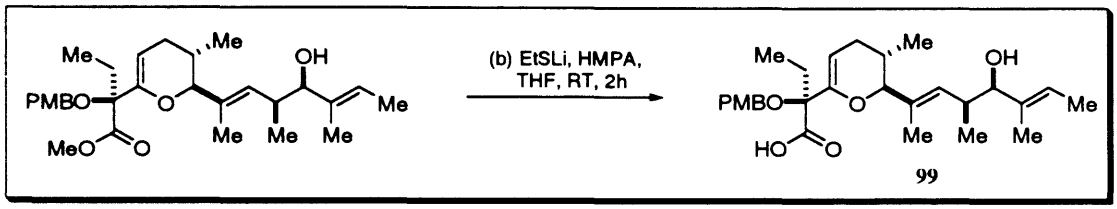

To a 0 °C solution of EtSH (0.35 mL, 5.04 mmol) in anhydrous THF (5 mL) under N_2 was added dropwise *n*-BuLi (1.9 mL, 4.64 mmol) and the resulting cloudy solution stirred at 0 °C for 30 mins. A solution of the above allylic alcohol (0.49 g, 1 mmol) in HMPA (10 mL) was then added dropwise over 5 mins *via* a cannula, and the resulting green coloured solution was allowed to reach ambient temperature over 1.5 h. EtOAc (20 mL) was then added, and the mixture acidified to pH2 with 2M aq. $NaHSO_4$ (aq). Following extraction with EtOAc (3 x 50 mL) and washing with H_2O (30 mL), drying ($MgSO_4$), filtration, and concentration *in vacuo* a pale yellow oil was afforded that was taken on directly to the next reaction in the sequence. **99** was difficult to purify and was generally taken on crude.

Formation of the BOP Ester

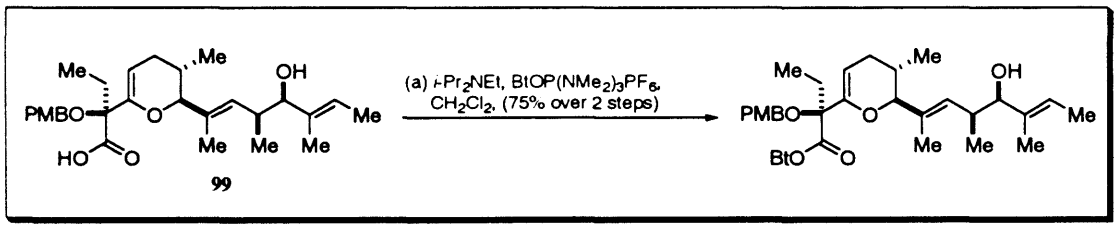

To a RT solution of **99** (0.48 g, 1 mmol) in dry CH_2Cl_2 (11 mL) under N_2 was added ^{i}PrNEt (0.75 mL) followed by the BOP reagent (0.89 g, 2.02 mmol). The reactants were stirred at RT for 10-15 mins and then diluted with EtOAc (50 mL) and washed with H_2O (2 x 20mL). The organic extract was then dried over $MgSO_4$, filtered and concentrated *in vacuo* and the residue purified by SiO_2 flash chromatography using hexanes/EtOAc (5:1 to 2:1). The desired ester was furnished as a pale yellow oil (0.45 g, 75% over 2 steps). **IR (neat)** 3424 (br m), 2954 (s), 2925 (s), 2872 (s) 1816 (m), 1671 (w), 1613 (w), 1514 (s), 1456 (m), 1380 (m), 1302 (m), 1248 (s), 1037 (s) 1010 (m), 822 (m), 743 (m); **^{1}H NMR (500 MHz, $CDCl_3$, 298 K)** δ 8.04 (d, J = 8.4 Hz, 1*H*, arom), 7.50 (m, 1*H*, arom), 7.40-7.33 (m, 4*H*, arom), 6.86 (d, J = 8.7 Hz, 2*H*, arom), 5.43 (q, J

= 6.7 Hz, 1*H*, $H_3CC=C\underline{H}CH_3$), 5.37 (d, *J* = 10.7 Hz, 1*H*, $H_3CC=C\underline{H}CHCH_3$), 5.26 (dd, *J* = 5.4, 2.2 Hz, 1*H*, quart-$CC=C\underline{H}CH_2CHCH_3$), 4.68 (d, *J* = 10.5 Hz, 1*H*, $OC\underline{H}_2PhOMe$), 4.53 (d, *J* = 10.5 Hz, 1*H*, $OC\underline{H}_2PhOMe$), 3.85 (d, *J* = 6.7 Hz, 1*H*, $H_3CCHC\underline{H}OH$), 3.83 (d, *J* = 9.6 Hz, 1*H*, $H_3CCC\underline{H}O$), 3.78 (s, 3*H*, $OC\underline{H}_3$), 2.65 (m, 1*H*, $H_3CC\underline{H}CHOH$), 2.28-2.21 (m, 3*H*, $PMBOCC\underline{H}_2CH_3$ and PMBO-$C(CH_2CH_3)C=CHC\underline{H}_2CHCH_3$), 1.95-1.83 (m, 2*H* PMBO-$C(CH_2CH_3)C=CHC\underline{H}_2CHCH_3$ and PMBO-$C(CH_2CH_3)C=CHCH_2C\underline{H}CH_3$), 1.66 (apparent d, J = 1.3 Hz, 3*H*, $\underline{H}_3CC=CHCHCH_3$), 1.55 (s, 3*H*, $\underline{H}_3CC=CHCH_3$), 1.51 (d, *J* = 6.7 Hz, 3*H*, $H_3CC=CHC\underline{H}_3$), 1.08 (t, *J* = 7.3 Hz, 3*H*, $PMBOCCH_2C\underline{H}_3$), 0.98 (d, *J* = 6.7 Hz, 3*H*, $H_3CC=CHCHC\underline{H}_3$), 0.83 (d, *J* = 6.5 Hz, 3H, PMBO-$C(CH_2CH_3)C=CHCH_2CHC\underline{H}_3$); **^{13}C NMR (125 MHz, $CDCl_3$, 298 K)** δ 168.3, 159.2, 149.1, 143.4, 136.9, 133.5 ($H_3CC=\underline{C}HCHCH_3$), 131.9, 130.0 (arom), 129.3 (arom), 128.7 (arom), 128.6 (arom), 124.7, 121.0 ($H_3CC=\underline{C}HCH_3$), 120.5 (arom), 113.7 (arom), 108.4, 100.4 (quart-$CC=\underline{C}HCH_2CHCH_3$), 88.3 ($H_3CC\underline{C}HO$), 84.1, 81.0 ($H_3CCH\underline{C}HOH$), 66.9, 55.3 ($O\underline{C}H_3$), 35.9, 29.4, 29.1, 26.4, 17.4, 15.8, 12.9, 12.1, 11.6, 7.7; **FAB HRMS** Calcd. for $C_{34}H_{43}N_3O_6$ $(M+Na)^+$: *m/e* 612.30494; Found: *m/e* 612.30501.

Swern oxidation to ketone

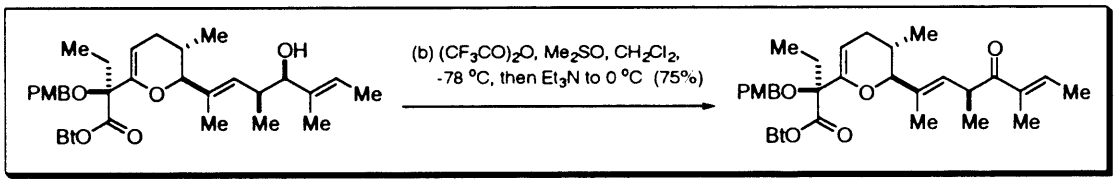

To a stirred –78 °C solution of DMSO (0.3 mL, 4.38 mmol) in dry CH_2Cl_2 (15 mL) under N_2 was added TFAA (0.3 mL, 2.19 mmol) and the reactants allowed to stir at –78 °C for 20 mins. A solution of the BOP-ester (0.43 g, 0.73 mmol) in dry CH_2Cl_2 (5 mL) was then added over 2 mins. After stirring at –78 °C for 5 mins, Et_3N (2 mL, 14.60 mmol) was added and the mixture stirred at –78 °C for further 5 mins before being allowed to warm to RT. CH_2Cl_2 (100 mL) was then added, and the organic layer washed with brine (2 x 30 mL). The organic extract was dried over $MgSO_4$, filtered, and concentrated *in vacuo*. Purification of the crude residue by SiO_2 flash chromatography using hexanes/EtOAc (10:1 to 5:1) gave a clear oil (0.32 g, 75%). **IR (neat)** 3444 (br s), 2929 (m), 2875 (w), 2838 (w), 1816 (m), 1664 (s), 1615 (m), 1514 (m), 1453 (w), 1381 (w), 1302 (w), 1248 (m), 1038 (s), 822 (w), 743 (m), 649 (w); **^{1}H NMR (500 MHz, $CDCl_3$, 298 K)** δ 8.02 (apparent doublet, *J* = 7.5 Hz, 1*H*, arom), 7.42-7.28 (br m, 3*H*, arom), 6.85 (apparent d, 1*H*, arom), 6.78 (q, 1*H*, $H_3CC=C\underline{H}CH_3$), 5.69 (d, *J* = 9.4 Hz, 1*H*, $H_3CCC\underline{H}CHCH_3$), 5.27 (dd, *J* = 5.8, 2.2 Hz, 1*H*, quart-$CC=C\underline{H}CH_2CHCH_3$), 4.67 (d, *J* = 10.5 Hz, 1*H*, $OC\underline{H}_2PhOMe$),

4.50 (d, *J* = 10.5 Hz, 1*H*, *O*C<u>H</u>$_2$Ph*O*Me), 4.16 (m, 1*H*, H$_3$CC<u>H</u>C=O), 3.92 (d, *J* = 9.7 Hz, 1*H*, H$_3$CCC<u>H</u>OC), 3.78 (s, 3*H*, *O*C<u>H</u>$_3$), 2.25 (q, *J* = 7.4 Hz, 2*H*, PMB*O*CC<u>H</u>$_2$CH$_3$), 2.24 (m, 1*H*, PMB*O*C(CH$_2$CH$_3$)C=CHC<u>H</u>$_2$), 1.95 (m, 1*H*, PMB*O*-C(CH$_2$CH$_3$)C=CHCH$_2$C<u>H</u>CH$_3$), 1.90 (m, 1*H*, PMB*O*C(CH$_2$CH$_3$)C=CHC<u>H</u>$_2$), 1.79 (dq, *J* = 1.1 Hz, H$_3$CC=CHC<u>H</u>$_3$), 1.78 (s, 3*H*, <u>H</u>$_3$CC=CHCH$_3$), 1.72 (d, *J* = 1.4 Hz, 3*H*, <u>H</u>$_3$CC=CHCHCH$_3$), 1.15 (d, *J* = 6.9 Hz, 3*H*, H$_3$CC=CHCHC<u>H</u>$_3$), 1.09 (t, *J* = 7.4 Hz, 3H, PMB*O*CCH$_2$C<u>H</u>$_3$), 0.84 (d, *J* = 6.4 Hz, 3*H*, quart-CC=CHCH$_2$CHC<u>H</u>$_3$); **^{13}C NMR (125 MHz, CDCl$_3$, 298 K)** δ 203.0 (<u>C</u>O), 168.2 (<u>C</u>OO), 149.1 (PMB*O*C(CH$_2$CH$_3$)<u>C</u>=CHCH$_2$), 137.7 (H$_3$CC=<u>C</u>HCH$_3$), 137.4 (H$_3$C<u>C</u>=CHCH$_3$), 133.0 (H$_3$C<u>C</u>=CHCHCH$_3$), 131.5 (H$_3$CC=<u>C</u>HCHCH$_3$), 130.0 (arom), 129.3 (arom), 129.3 (arom), 128.8 (arom), 128.6 (arom), 124.7 (arom), 120.3 (arom), 113.8 (arom), 113.8 (arom), 108.4 (arom), 100.6 (PMB*O*C(CH$_2$CH$_3$)C=<u>C</u>HCH$_2$), 88.1 (H$_3$CC<u>C</u>HOC), 84.0 (PMB*O*<u>C</u>CH$_2$CH$_3$), 66.7 (*O*<u>C</u>H$_2$Ph*O*Me), 55.3 (*O*<u>C</u>H$_3$), 38.9 (H$_3$C<u>C</u>HCO), 29.3 (PMB*O*C(CH$_2$CH$_3$)C=CH<u>C</u>H$_2$), 29.0 (PMB*O*-C(C<u>H</u>$_2$CH$_3$)C=CCH$_2$<u>C</u>HCH$_3$), 26.4 (PMB*O*C<u>C</u>H$_2$CH$_3$), 18.5 (H$_3$<u>C</u>CHCO), 17.3 (PMB*O*C(C<u>H</u>$_2$CH$_3$)C=CCH$_2$CH<u>C</u>H$_3$), 14.8 (H$_3$CC=CH<u>C</u>H$_3$), 11.4 (H$_3$<u>C</u>C=CHCH$_3$), 11.2 (H$_3$<u>C</u>C=CHCHCH$_3$), 7.8 (PMB*O*CCH$_2$<u>C</u>H$_3$); **FAB HRMS** Calcd for C$_{34}$H$_{41}$N$_3$O$_6$ (M+H)$^+$: *m/e* 588.30735. Found: *m/e* 588.30795.

DDQ deprotection to provide 68

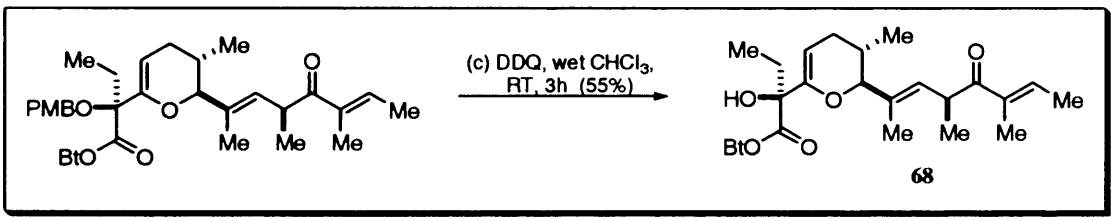

To a RT solution of the above ketone (0.32 g, 0.55 mmol) in wet CDCl$_3$ (25 mL + 2-3 drops of H$_2$O from pipette) was added DDQ (0.32 g, 1.41 mmol) and the reaction mixture stirred for 2.5 hours. The mixture was then diluted with EtOAc (100 mL) and quickly washed with saturated aqueous NaHCO$_3$ (3 x 20 mL) and brine (20 mL). The organic extract was then dried over MgSO$_4$, filtered, and concentrated *in vacuo*. The crude residue was then purified by SiO$_2$ flash chromatography using hexanes/EtOAc (8:1 to 4:1) to afford **68** as a clear oil (0.14 g, 55%).

68 was used in the next step <u>immediately</u> after purification.

Endgame coupling to 336 and A83586C/citropeptin hybrid

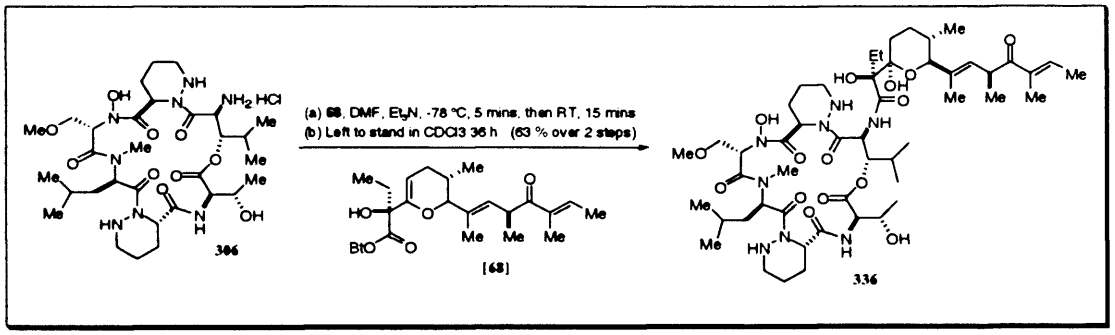

* Stock Solution was made using 1mL of Et_3N in 14 mL of anhydrous DMF

To a 20 mL pear shaped round bottom flask containing **68** (130 mg, 0.28 mmol) under N_2, was added **303** (200 mg, 0.28 mmol) and the vessel cooled to –78 °C. A stock solution (1.16 mL) of Et_3N (0.0776 mL, 0.56 mmol) in DMF was added and the reaction mixture stirred for 5 minutes, after which the vessel was allowed to reach ambient temperature, monitoring closely by TLC. After stirring at room temperature for 10-15 mins the reaction mixture was diluted with E_2O (70 mL) and washed with 0.5 N HCl (20 mL), saturated aqueous $NaHCO_3$ (20 mL) and brine (20 mL). The organic layer was separated and dried over $MgSO_4$, filtered and concentrated in vacuo to provide a crude residue. This residue was then loaded onto 3 separate thick preparative TLC plates and multi eluted (x 3) with 20:1 CH_2Cl_2:MeOH. The relevant material was scraped off with a spatula, crushed into fine pieces and purified by SiO_2 flash chromatography using hexanes/EtOAc (1:0 to 0:1) to afford a white solid (180 mg, 63%). $[\alpha]_D$ + 71º (*c* 0.1, CH_2Cl_2); **IR (KBr)** 3418 (br s), 3281 (br s), 2934 (s), 2872 (m), 1732 (s), 1634 (s), 1495 (s), 1456 (s), 1441 (s), 1393 (s), 1258 (m), 1215 (m), 1124 (m), 1069 (m), 1001 (m), 910 (m), 733 (m), 648 (w); **^{1}H NMR (500 MHz, $CDCl_3$, 298 K)** δ 9.96 (s, 1*H*, *N*O*H*), 8.20 (d, *J* = 10.7 Hz, 1*H*, 27-*N*H), 6.73 (apparent q, *J* = 6.9 4.5 Hz, 1*H*, H-44), 6.25 (br s, 1*H*, 34-*O*H), 6.17 (d, *J* = 8.5 Hz, 1*H*, 2-*N*H), 5.59 (dd, *J* = 7.5 1.4 Hz, 1*H*, H-40), 5.38 (dd, *J* = 8.5 2.2 Hz, 1*H*, H-28), 5.29 (apparent dd, *J* = 6.4 1.3 Hz, 1*H*, H-18), 5.16 (dd, *J* = 5.8 2.0 Hz, 1*H*, H-6), 4.88 (t, *J* = 10.7 Hz, 1*H*, H-27), 4.75 (apparent q, J = 5.5 Hz, 1*H*, H-3), 4.50 (distorted t, *J* = 8.5 Hz, 1*H*, H-2), 4.41-4.34 (br s, 1*H*, 3-*O*H), 4.39 (br m, 1*H*, 25-*N*H), 4.04 (m, 1*H*, H-41), 3.91-3.88 (br m, 1*H*, 9-*N*H), 3.85 (dd, *J* = 10.0 2.2 Hz, 1*H*, H_{eq}-19), 3.70 (dd, *J* = 10.1 3.6 Hz, 1*H*, H_{ax}-19), 3.33 (s, 3*H*, H-20[*O*CH_3]), 3.30 (br m, 1*H*, H_{eq}-9), 3.13 (br m, 1*H*, H_{eq}-25), 3.01 (s, 3*H*, H-16[*N*CH_3]), 2.94-2.90 (br m, 1*H*, H_{ax}-25), 2.91 (br s, 1*H*, 33-*O*H), 2.55 (br m, 1*H*, H_{ax}-9), 2.55 (br m, 1*H*, H_{eq}-7), 2.21 (br m, 1*H*, H_{eq}-23), 1.99 (q, 2*H*, *J* = 7.5 Hz, H-46), 1.82 (d, *J* = 6.3 Hz, 3*H*, H-45), 1.74 (m, 1*H*, H-29), 1.74 (t, *J* = 1.2 Hz, 3*H*, H-51), 1.69 (br m, 1*H*, H_{ax}-7), 1.72-1.51 (br m, 2*H*, H-24), 1.62-1.55 (br m, 2*H*, H-8), 1.55 (d, *J* = 1.4 Hz, 3*H*, H-49),

1.09 (d, *J* = 7.0 Hz, 3*H*, H-50), 1.02 (d, *J* = 6.5 Hz, 3*H*, H-4), 0.92 (d, *J* = 6.4 Hz, 3*H*, H-14), 0.92 (d, *J* = 6.4 Hz, 3*H*, H-15), 0.81 (t, *J* = 7.5 Hz, 3*H*, H-47), 0.79 (d, *J* = 6.9 Hz, 3*H*, H-31), 0.68 (d, *J* = 6.9 Hz, 3*H*, H-30); **^{13}C NMR (125 MHz, $CDCl_3$, 298 K)** δ 203.0 (C-42), 175.3 (C-32), 173.6 (C-21), 172.3 (C-10), 171.3 (C-17), 170.8 (C-26), 170.3 (C-1), 169.5 (C-5), 137.5 (C-43), 136.8 (C-44), 132.8 (C-39), 129.4 (C-40), 99.6 (C-34), 82.2 (C-38), 80.1 (C-33), 78.5 (C-28), 68.4 (C-19), 64.8 (C-3), 59.1 (C-20), 56.3 (C-2), 54.7 (C-27), 54.4 (C-18), 52.3 (C-6), 51.5 (C-22), 50.2 (C-11), 47.9 (C-9), 45.7 (C-25), 38.2 (C-41), 36.6 (C-12), 32.6 (C-37), 29.2 (C-16), 29.2 (C-29), 28.3 (C-35), 27.3 (C-36), 25.9 (C-46), 24.7 (C-13), 24.4 (C-7), 24.1 (C-23), 22.7 (C-14), 22.7 (C-15), 21.4 (C-8), 21.1 (C-24), 19.5 (C-50), 19.4 (C-30), 18.9 (C-4), 17.6 (C-48), 14.9 (C-31), 14.7 (C-45), 12.0 (C-49), 11.4 (C-51), 8.2 (C-47). **FAB HRMS** Calcd for $C_{51}H_{84}N_8O_{15}$ $(M+Na)^+$: *m/e* 1072.24735. Found: *m/e* 1072.24372.

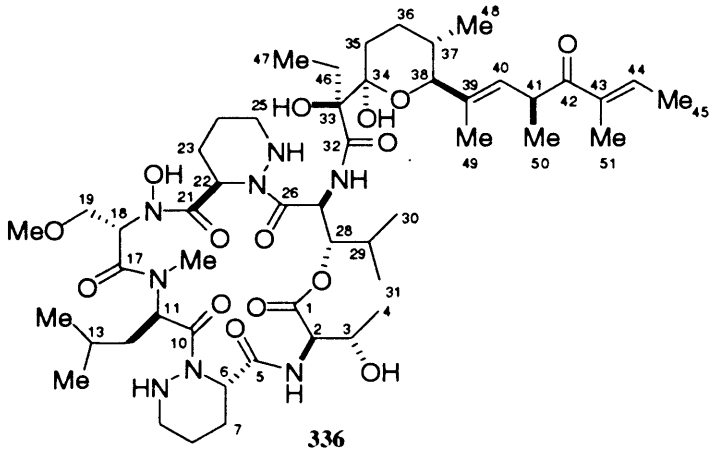

336

Synthesis of dipeptide 346

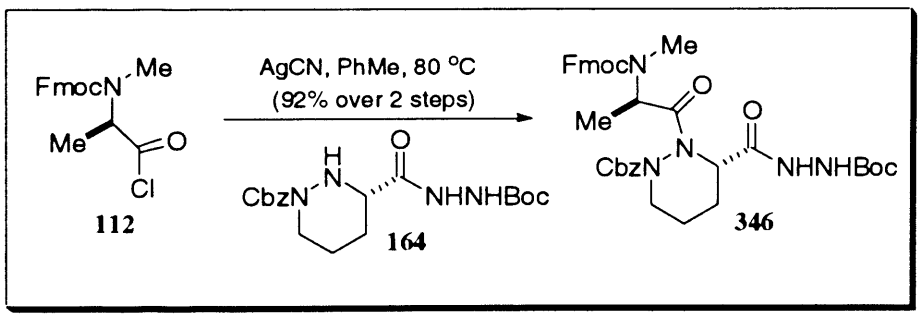

To the acid derivative of **112** (29.84 g, 91.71 mmol) in anhydrous CH_2Cl_2 (280 mL) at room temperature and under N_2, was added in a single portion, $(COCl)_2$ (280 mL, 3209.98 mmol)

and the resulting yellow solution stirred for 2 hours. The reaction mixture was then concentrated *in vacuo* and co-evaporated with C_6H_6 (3 x 50 mL) to remove the excess $(COCl)_2$ and put on a high vacuum pump for 15 mins. To the resulting golden foam was added a solution of **164** (34.72 g, 91.71 mmol) in anhydrous C_6H_6 (300 mL) and the vessel covered in aluminium foil and a condenser attached, while maintaining the nitrogen atmosphere. AgCN (18.43 g, 137.57 mmol) was then added and the reaction was heated at 80 °C for 30-40 mins. The reaction mixture was then filtered through Celite, washing the flask and residue with copious amounts of CH_2Cl_2, and the filtrate concentrated *in vacuo*. The resulting thick oil was then purified by SiO_2 flash chromatography using hexanes/EtOAc (5:1 to 2:1 to 1:1) to afford a white foam (57.86 g, 92% over 2 steps).); **$[\alpha]_D^{12}$** +20.9 ° (*c* 0.45, CH_2Cl_2); **IR (neat)** 3287 (br w), 2936 (w), 1699 (s), 1452 (m), 1404 (m), 1366 (m), 1312 (m), 1248 (m), 1159 (m), 1121 (w), 1045 (w), 1015 (w), 910 (w), 758 (m), 739 (m), 698 (w); **^{1}H NMR (500 MHz, Tol, 373 K)** δ 8.99 (br s, 1*H*, *NH*), 7.53 (d, *J* = 7.5 Hz, 2*H*, arom), 7.43 (br d, *J* = 7.2 Hz, 2*H*, arom), 7.23 (br d, *J* = 7.4 Hz, 2*H*, arom), 7.18 (apparent br t, J = 7.1 7.4 Hz, 2*H*, arom), 5.97 (br s, 1*H*, *NH*), 5.04 (s, 2*H*, NCO_2CH_2Ph), 4.93 (apparent br s, 2*H*, $NCOCHCH_3$ and $CHCONHNH$), 4.42 (br s, 1*H*, $NCO_2CH_2(C_{13}H_9)$), 4.34 (m, 1*H*, $NCO_2CH_2(C_{13}H_9)$), 4.04 (t, *J* = 6.2, 1*H*, $NCO_2CH_2(C_{13}H_9)$), 3.90 (br s, 1*H*, pip-CH_2), 2.80 (s, 3*H*, NCH_3), 2.72 (br s, 1*H*, pip-CH_2), 2.02 (apparent br s, 1*H*, pip-CH_2), 1.63 (br s, 1*H*, pip-CH_2), 1.47 (apparent br s, 1*H*, pip-CH_2), 1.35 (s, 11*H*, includes $NCO_2C(CH_3)_3$), 1.14 (br d, *J* = 6.1, 3*H*, $NCOCHCH_3$), 1.01 (br m, 1*H*, pip-CH_2); **^{13}C NMR (125 MHz, $CDCl_3$, 298 K)** δ 174.1 (CO), 169.2 (CO), 156.8 (CO), 156.3 (CO), 155.5 (CO), 145.0 (arom), 142.1 (arom), 136.5 (arom), 129.4 (arom), 128.9 (arom), 128.6 (arom), 127.9 (arom), 127.5 (arom), 125.8 (arom), 125.5 (arom), 120.3 (arom), 80.8 ($NCO_2C(CH_3)_3$), 69.5 (NCO_2CH_2Ph), 68.0 ($NCO_2CH_2(C_{13}H_9)$), 56.4 ($NCOCHCH_3$), 51.6 ($CHCONHNH$), 48.4 ($NCO_2CH_2(C_{13}H_9)$), 46.5 (pip-CH_2), 29.7 (NCH_3), 28.5 ($NCO_2C(CH_3)_3$), 24.1 (pip-CH_2), 20.1 (pip-CH_2), 15.3 ($NCOCHCH_3$); **FAB HRMS** Calcd. for $C_{37}H_{43}N_5O_8$ $(M+Na)^+$: *m/e* 708.30092; Found: *m/e* 708.30240.

Fmoc deprotection of 346 to 114

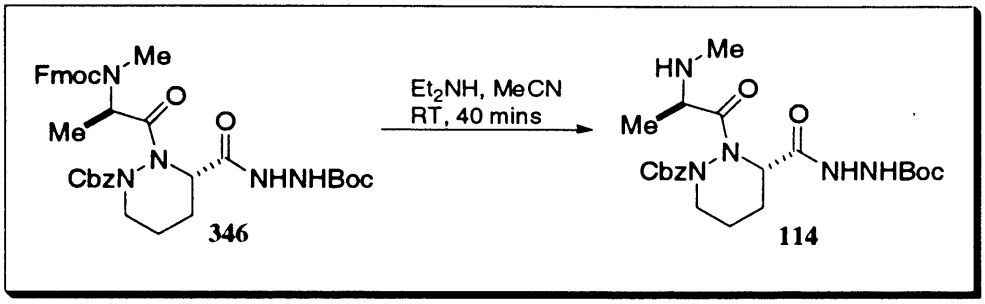

To a solution of **346** (4.17 g, 6.09 mmol) in anhydrous MeCN (8 mL) was added in a single portion, at room temperature and under N_2, diethylamine (6.4 mL. 60.81 mmol) and the reaction mixture stirred at room temperature for 30 mins. The reaction mixture was then diluted with EtOAc and concentrated *in vacuo* and put on a high vacuum pump for 30 mins. The resulting viscous crude oil was then of sufficient purity for the next step in the sequence and was subsequently taken on.

The [2 + 2] coupling of 114 and 304 to 347

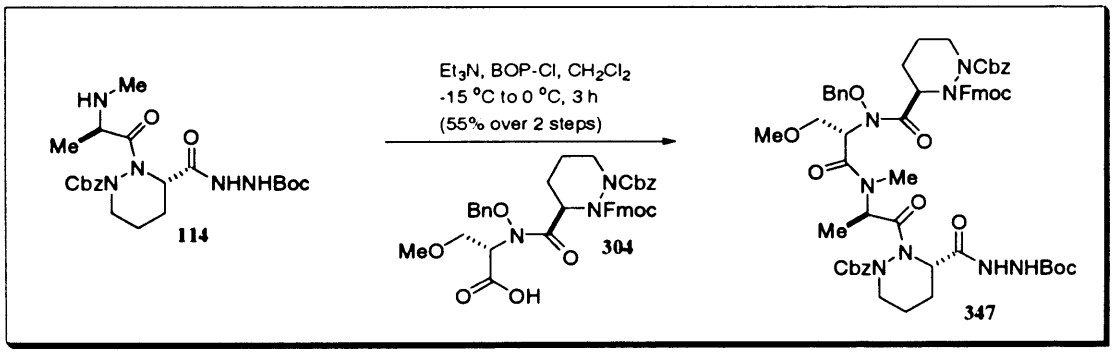

To a solution of **114** (6.09 mmol) and **304** (4.14 g, 5.97 mmol) in anhydrous CH_2Cl_2 (35 mL) at –20 °C and under N_2 was added dropwise, Et_3N (1.6 mL, 11.34 mmol) followed by BOP-Cl (1.8 g, 7.16 mmol) in a single portion. The reaction mixture was left to stir between –10 °C and 0 °C for 4 hours before being diluted with EtOAc (150 mL) and washed with 1 N HCl (2 x 20 mL), saturated aqueous $NaHCO_3$ (2 x 20 mL) and brine (20 mL). The organic extract was then dried ($MgSO_4$), filtered and concentrated in vacuo to provide a crude yellow oil that was purified by SiO_2 flash chromatography using hexanes/EtOAc (5:1 to 2:1 to 1:1) to afford a white foam (3.81 g, 55% over 2 steps). $[\alpha]_D^{12}$ -44.5 ° (*c* 0.638, CH_2Cl_2); **IR (neat)** 3304 (br w), 2934 (w), 2895 (w),

1705 (s), 1651 (m), 1452 (m), 1414 (m), 1366 (m), 1250 (s), 1196 (m), 1159 (m), 1123 (m), 1092 (m), 1047 (w), 980 (w), 743 (m), 698 (m), 546 (w); **^{1}H NMR (500 MHz, $CDCl_3$, 298 K)** δ 7.73 (br m, 2*H*, arom), 7.45-7.17 (br m, 21*H*, arom), 6.18 (br s, 1*H*, NH), 5.54 (br m, 1*H*), 4.50-5.38 (br m, 9*H*), 4.36-3.78 (br m, 6*H*), 3.73-3.48 (br m, 1*H*), 3.25 (br m, 3*H*, OCH_3), 3.11-2.69 (br m, 5*H*), 2.23-2.09 (br m, 2*H*), 1.91-1.65 (br m, 4*H*), 1.42 (broad based s, 15*H*); **FAB HRMS** Calcd. for $C_{61}H_{70}N_8O_{14}$ $(M+Na)^+$: *m/e* 1161.49089; Found: *m/e* 1161.491967.

Fmoc Deprotection of 347 to 308

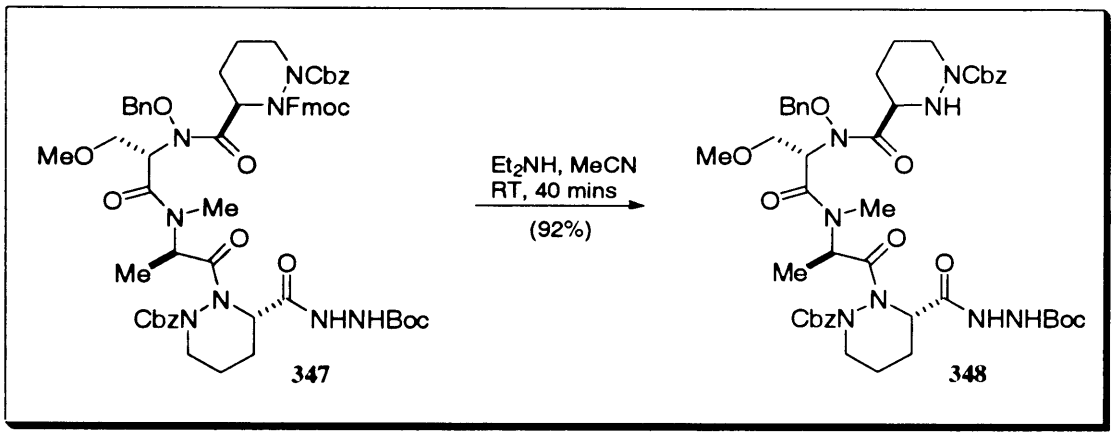

347 **348**

To a solution of **347** (10.5 g, 9.22 mmol) in anhydrous MeCN (25mL) was added in a single portion, at room temperature and under N_2, diethylamine (19 mL. 184.33 mmol) and the reaction mixture stirred at room temperature for 30 mins. The reaction mixture was then diluted with EtOAc, concentrated *in vacuo* and coevaporated with CH_2Cl_2 to remove excess diethylamine. The resulting crude oil was then purified by SiO_2 flash chromatography using hexanes/EtOAc (5:1 to 2:1 to 1:1) to afford **348** as a white foam (7.78 g, 92%). **IR (neat)** 3290 (br w), 3033 (w), 2936 (w), 2896 (w), 1697 (s), 1647 (m), 1497 (w), 1455 (m), 1405 (m), 1365 (m), 1252 (s), 1159 (m), 1122 (m), 1081 (w), 1031 (w), 1015 (w), 984 (w), 913 (w), 755 (m), 733 (m), 700 (m); **^{1}H NMR (500 MHz, $CDCl_3$, 298 K)** δ 7.38-7.24 (br m, 15*H*, arom), 5.51 (br m, 1*H*), 5.30-4.98 (br m, ~ 6*H*), 4.98-4.62 (br m, 3*H*), 4.36-4.12 (br m, 2*H*), 4.12-3.75 (br m, 3*H*), 3.72-3.56 (br m, 1*H*), 3.34-2.72 (br m, ~ 9*H*), 2.22-1.71 (br m, ~ 5*H*), 1.41 (br m, 18*H*); **^{13}C NMR (125 MHz, $CDCl_3$, 298 K)** δ 175.1 (CO), 167.9 (CO), 155.8 (CO), 154.7 (CO), 136.7 (arom), 136.4 (arom), 130.2 (arom), 129.5 (arom), 128.6 (arom), 128.4 (arom), 128.0 (arom), 127.8 (arom), 81.2, 78.9, 68.6, 68.3, 68.0, 67.4, 67.4, 58.8, 58.6, 56.8, 56.6, 52.1, 45.2, 29.6, 28.1, 27.5, 27.2, 23.2, 19.9; **FAB HRMS** Calcd. for $C_{46}H_{60}N_8O_{12}$ $(M+H)^+$: *m/e* 917.44087; Found: *m/e* 917.4396148.

The [4+2] Coupling of 348 and 101 to 351

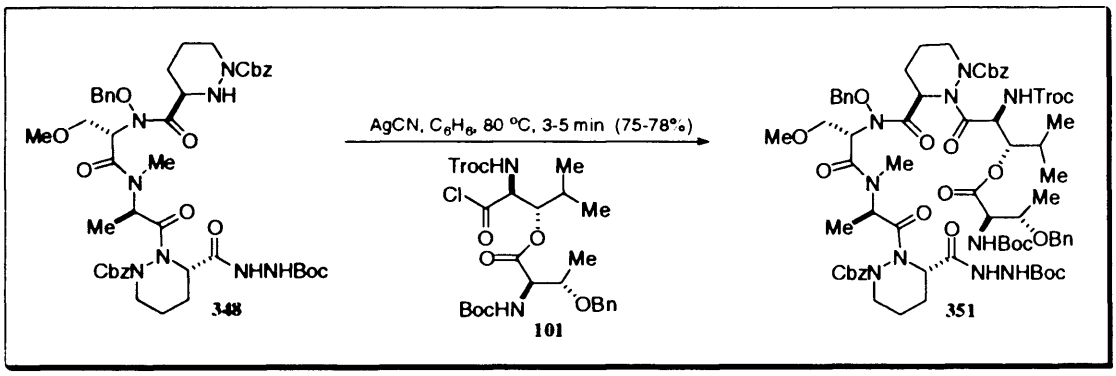

To a solution of the acid dipeptide precursor to **101** (3.53 g, 5.76 mmol) in anhydrous C_6H_6 (10 mL), at room temperature and under N_2, was added in one portion $(COCl)_2$ (10 mL, 115.08 mmol) and the mixture stirred for 2.5 hours. The reaction mixture was then concentrated in vacuo and excess $(COCl)_2$ removed *via* co-evaporation with C_6H_6 (3 x 10 mL) and the resulting yellow oil put on a high vacuum pump to provide **101** as a golden foam. To this golden foam of was added, at room temperature and under N_2, a solution of **348** (5.03 g, 5.49 mmol) in C_6H_6 (35 mL). The reaction vessel was then covered in aluminium foil and AgCN (1.18 g, 8.78 mmol) added, fitting the vessel with a reflux condenser and maintaining a nitrogen atmosphere. The reaction mixture was immersed into a pre-heated oil bath then at 80 °C for 3-5 mins, before being cooled, diluted with EtOAc (100 mL) and filtered through Celite, washing the flask and residue with copious amounts of EtOAc. The filtrate was then concentrated *in vacuo* and the resulting product purified by SiO_2 flash chromatography using hexanes/EtOAc (5:1 to 2:1 to 1:1) to afford the desired amine as a white foam (6.62 g, 76%). $[\alpha]_D^{12}$ –48.9 ° (*c* 0.184, CH_2Cl_2); **IR (neat)** 3306 (br w), 2976 (m), 2934 (m), 1717 (s), 1674 (s), 1499 (m), 1456 (m), 1393 (m), 1367 (m), 1308 (w), 1248 (s), 1196 (w), 1161 (s), 1123 (m), 1094 (w), 1045 (w), 1030 (w), 991 (w), 914 (w), 856 (w), 822 (w), 733 (m), 698 (m), 571 (w), 419 (w); **^{1}H NMR (500 MHz, $CDCl_3$, 298 K)** δ 7.33-7.13 (br m, 20*H*, arom), 5.75 (br m, 1*H*), 5.30-4.09 (br m, ~ 19*H*), 3.65-2.49 (br m, 9*H*), 2.20-1.63 (br m, ~ 6*H*), 1.52-1.28 (br m, 20*H*), 1.23-1.14 (br m, 6*H*), 1.03 (d, *J* = 6.7 Hz, 1*H*), 1.00-0.55 (br m, ~ 9*H*); **^{13}C NMR (125 MHz, $CDCl_3$, 298 K)** δ 170.1 (CO), 155.7 (CO), 137.7 (arom), 129.7 (arom), 128.6 (arom), 128.3 (arom), 128.2 (arom), 127.6 (arom), 127.5 (arom), 127.3 (arom), 126.3, 95.2, 79.8, 78.9, 74.8, 74.4, 74.2, 71.2, 70.4, 68.4, 68.1, 62.1, 58.7, 58.2, 45.6, 31.2, 28.2, 28.1, 25.3, 19.8, 19.1, 19.0, 17.2, 16.5, 16.2, 15.9, 14.1; **FAB HRMS** Calcd. for $C_{71}H_{93}N_{10}O_{20}Cl_3$ $(M+Na)^+$: *m/e* 1533.55306; Found: *m/e* 1533.55185.

Linear hexadepsipeptide deprotection for linear cyclisation precursor 352

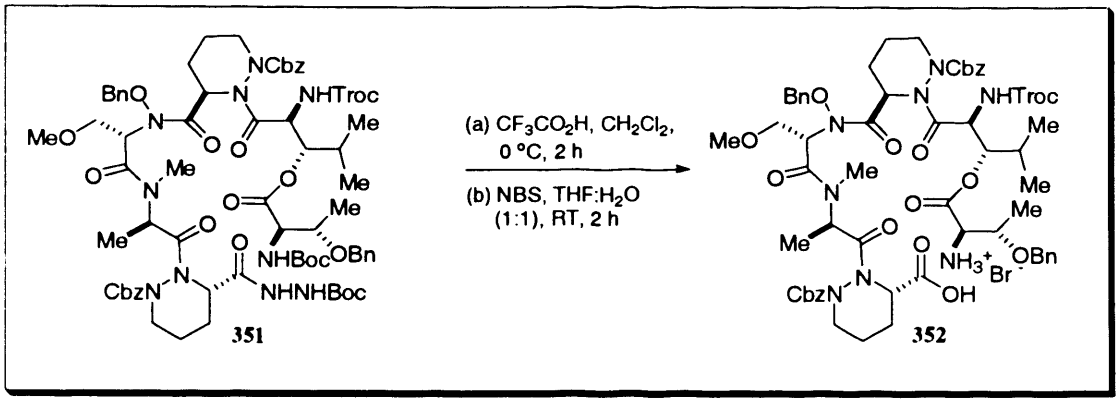

To a solution of **351** (3.85 g, 2.54 mmol) in anhydrous CH_2Cl_2 (38 mL), at 0 °C and under N_2, was added TFA (38 mL, 508.9 mmol) and the reaction mixture stirred at 0 °C for 2 hours. The reaction mixture was then concentrated *in vacuo* and co-evaporated with toluene (4 x 10 mL) to remove excess TFA. To this residue was added H_2O/THF [1:1] (64 mL) at room temperature and NBS (0.91 g, 5.09 mmol) in 3 portions over 5 mins with stirring. After stirring for 1.5 hours the reaction mixture was diluted with EtOAc (150 mL) and washed with brine (2 x 50 mL). The organic extract was then dried ($MgSO_4$), filtered and concentrated *in vacuo* to afford an off-white foam of sufficient purity for the next step.

HATU cyclisation of 352 to 353

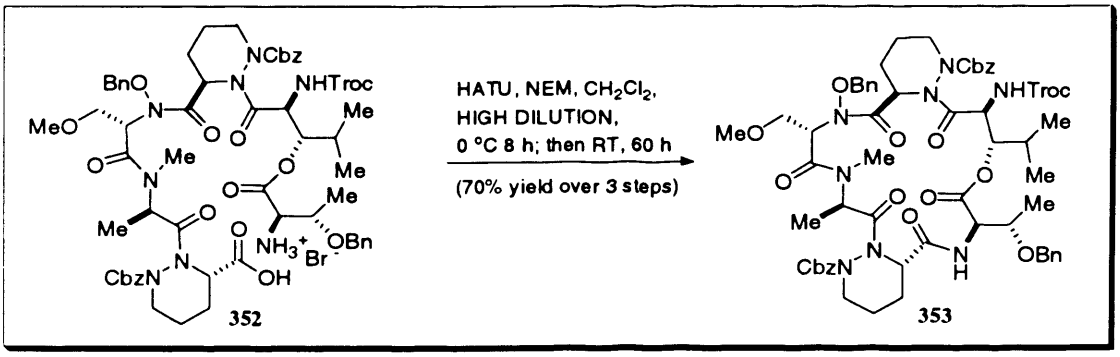

To a solution of HATU (9.68 g, 25.45 mmol) in anhydrous CH_2Cl_2 (2960 mL), at 0 °C and under N_2 was added dropwise over a 3 hour period, a mixture of **352** (2.54 mmol) and *N*-ethylmorpholine (4.4 mL, 34.35 mmol) in anhydrous CH_2Cl_2 (2960 mL). When the addition was

complete the reaction mixture was vigorously stirred for 72 hours. The reaction mixture was then concentrated *in vacuo*, diluted with EtOAc (200 mL) and washed with 1 N HCl (2 x 30 mL), 10 % aq. $NaHCO_3$ (2 x 30 mL) and brine (30 mL). The organic extract was then dried ($MgSO_4$), filtered, concentrated *in vacuo* and purified by SiO_2 flash chromatography using hexanes/EtOAc (2:1 to 1:1) to afford the desired cyclodepsipeptide as a white foam (2.28 g). The product appeared as two inseparable spots, which were taken on to a later stage to achieve a sufficient separation. Obtained FAB HRMS data for verification - **FAB HRMS** Calcd. for $C_{61}H_{73}N_8O_{16}Cl_3$ $(M+Na)^+$: *m/e* 1301.41076; Found: *m/e* 1301.40540.

Synthesis of Cbz-protected cyclodepsipeptide 354

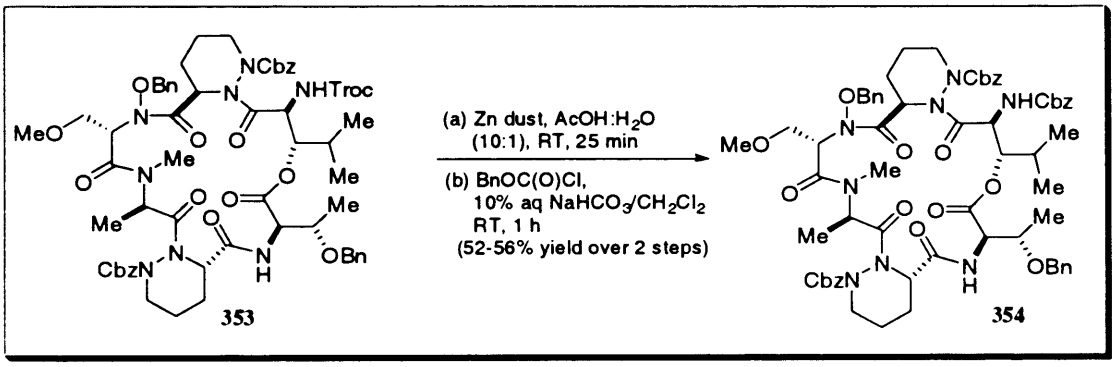

To a solution of **353** (3.21 g, 2.51 mmol) in AcOH:H_2O [10:1] (70 mL) was added in one portion at room temperature, Zn dust (3.28 g, 50.13 mmol) and the mixture stirred for 1 hour. The reaction mixture was then diluted with THF and filtered through Celite, washing with copious amounts of THF. The filtrate was then concentrated *in vacuo*, and the resulting residue co-evaporated with toluene (3 x 10 mL) to remove the excess acetic acid. To this crude product, was added simultaneously at room temperature, 10 % aq. $NaHCO_3$ (13 mL) and a solution of benzyl chloroformate (1.1 mL, 7.52 mmol) in anhydrous CH_2Cl_2 (13 mL) and the reaction mixture left to stir for 2 hours. The reaction mixture was diluted with EtOAc (150 mL), washed with brine (50 mL) and organic layer separated, dried ($MgSO_4$), filtered and concentrated *in vacuo*. The product was then purified by SiO_2 flash chromatography using hexanes/EtOAc (2:1 to 1:1) to afford the Cbz-protected cyclodepsipeptide as a white foam (1.68 g, 54% over 2 steps). $[\alpha]_D^{12}$ - 33.0 ° (*c* 0.218, MeOH); **IR (neat)** 3408 (br s), 3306 (br m), 3034 (w), 2937 (m), 2878 (m), 2829 (w), 1651 (s), 1531 (m), 1499 (m), 1456 (s), 1394 (s), 1352 (s), 1250 (s), 1198 (s), 1180 (m), 1124 (m), 1086 (m), 1047 (m), 1028 (m), 984 (m), 912 (m), 843 (s), 735 (m), 698 (m), 559 (m); **^{1}H NMR (500 MHz, $CDCl_3$, 298 K)** δ 7.35-7.20 (br m, 25*H*, arom), 5.41-4.84 (br m, ~ 11*H*), 4.65-4.29 (br

m, ~ 5*H*), 4.20-3.80 (br m, ~ 3*H*), 3.59 (br m, 1*H*), 3.50-3.31 (br m, 1*H*) 3.26-3.09 (br m, 3*H*), 3.03-2.90 (br m, 1*H*), 2.90-2.40 (br m, ~ 1*H*), 2.34-1.80 (br m, ~ 5*H*), 1.70-1.11 (br m, ~ 10*H*), 1.04-0.57 (br m, ~ 8*H*); **FAB HRMS** Calcd. for $C_{66}H_{78}N_8O_{16}$ $(M+Na)^+$: *m/e* 1261.54332; Found: *m/e* 1261.54528.

Synthesis of cyclodepsipeptide hydrochloride salt 339

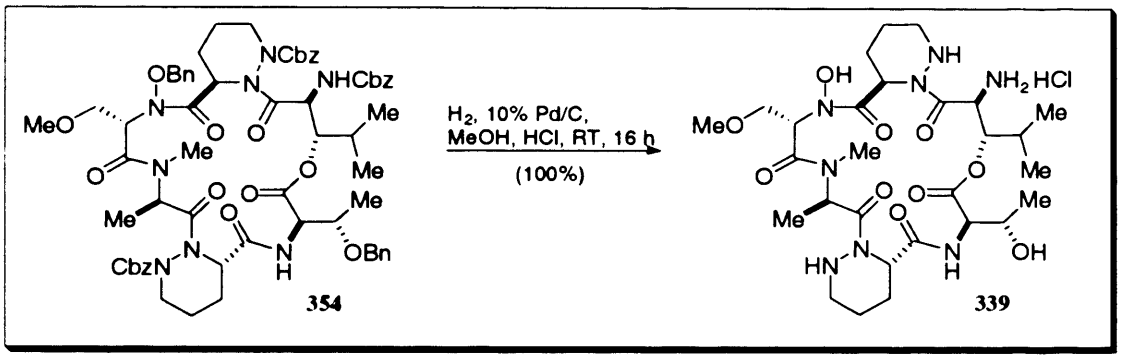

0.01 M MeOH.HCl was made by adding 0.17 mL of acetyl chloride to anhydrous MeOH (240 mL) under N_2 at RT. To a solution of **354** (1.33 g, 1.07 mmol) in this anhydrous 0.01 M MeOH.HCl solution (107 mL, 1.07 mmol), was added at room temperature and under N_2, Pd/C (0.9 g) and the reaction vessel purged with H_2 and stirred vigorously for 24 hours. The reaction mixture was then diluted with MeOH and filtered through Celite, washing the flask and residue with copious amounts of MeOH. The filtrate was then concentrated in vacuo to provide quantitatively **303** as a white solid (0.87 g). $[\alpha]_D^{12}$ –6.3 ° (*c* 0.43, MeOH); M.p. = 123-125 °C; **IR (KBr)** 3270 (br s), 2963 (br s), 1746 (s), 1647 (s), 1531 (m), 1454 (m), 1396 (m), 1249 (m), 1195 (m), 1051 (s), 923 (w), 846 (s), 732 (s), 668 (w), 558 (s), 496 (m), 476 (m); **^{1}H NMR (500 MHz, CD_3OD, 298 K)** δ 5.54-5.17 (br m), 4.63-4.35 (br m), 4.09 (apparent triplet, *J* = 9.9, 10.14 Hz), 3.97-3.83 (br m), 3.81-3.52 (br m), 3.45-3.34 (br m), 3.26-3.01 (br m), 2.87-2.68 (br m), 2.55-1.98 (br m), 1.86-1.48 (br m), 1.44-0.91 (br m), 0.81 (d, *J* = 6.6 Hz); **FAB HRMS** Calcd. for $C_{28}H_{48}N_8O_{10}$ $(M+H)^+$: *m/e* 657.35715; Found: *m/e* 657.35722.

Synthesis of *Syn*-aldol 363

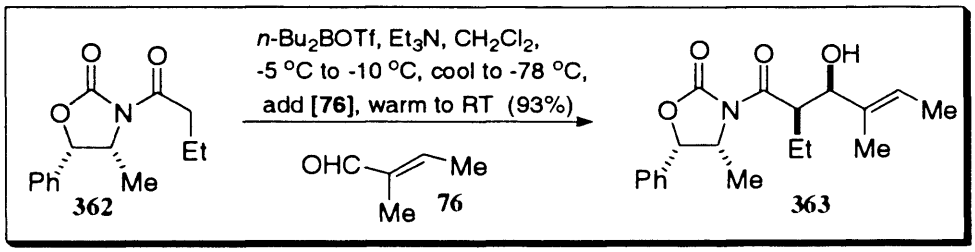

To a stirred solution of **362** (50.20 g, 0.2 mol) in anhydrous CH_2Cl_2 (700 mL) was added dropwise *via* a pressure equalised dropping funnel at –15 °C *n*-Bu_2BOTf (227.5 mL, 0.23 mol) followed by dropwise addition of Et_3N (35.5 mL, 0.26 mol) and the reaction mixture allowed to stir between –15 and –5 °C for 30 mins. A solution of tiglic aldehyde **76** (21.5 mL, 0.22 mol) in anhydrous CH_2Cl_2 (200 mL) was then added dropwise at –78 °C and the mixture stirred at this temperature for 1-hour before being allowed to reach –10 °C. The reaction mixture was then poured into a separating funnel containing Et_2O (600 mL) layered on top of sat. aq. NaH_2PO_4 (400 mL) and the organic layer separated. The aqueous layer was extracted further with Et_2O (2 x 400 mL) and the combined ethereal layers were then concentrated *in vacuo* and diluted with MeOH(700 mL) followed by a solution of 30% aq H_2O_2 and pH 7 phosphate buffer (400 mL) dropwise at 0 °C. After stirring this mixture for 1 hour the excess peroxides were quenched *via* the addition of solid ferrous sulphate (checked with starch paper – turns cream when peroxides not present/brown when they are) and the mixture concentrated *in vacuo* to remove MeOH. Once a comparable volume of MeOH has been removed the remaining solution was extracted with Et_2O (3 x 500 mL), washed with brine (500 mL) and the combined ethereal layers dried over $MgSO_4$, filtered and concentrated *in vacuo* to yield a crude brown oil. This crude material was purified by SiO_2 flash chromatography using hexanes/EtOAc (20:1 to 10:1 to 5:1 to 2:1) to afford a yellow oil (62 g, 93%).

NOTE: Phosphate Buffer pH 7 is made by combining 0.1 M solutions of Na_2HPO_4 (58 mL) and NaH_2PO_4 (42 mL), scaling up to the required quantity.

- 0.1 M solution of Na_2HPO_4 = 1.42 g in 100 mL.
- 0.1 M solution of NaH_2PO_4 = 1.2 g in 100 mL.

Synthesis of Weinreb amide 364

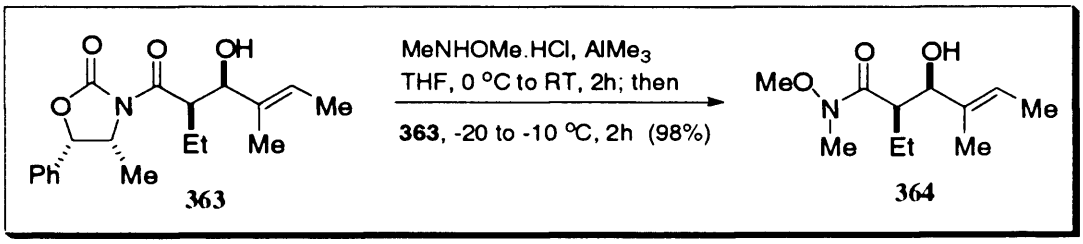

A stirred solution of *N,O*-dimethylhydroxylamine hydrochloride (40 g, 0.41 mol) in anhydrous THF (450 mL) at 0 °C was cautiously treated with $AlMe_3$ (178 mL, 0.41 mol) and the resulting reaction mixture stirred for 30 mins, before being allowed to reach ambient temperature for 1.5 hours. The reaction mixture was cooled to –20 °C and a solution of **363** (44.9 g, 0.14 mol), in anhydrous THF (200 mL), was slowly cannulated into the reaction mixture and the resulting mixture stirred between –20 °C and –10 °C for 2 hours. The reaction mixture was then cautiously poured into a pre-cooled mixture of CH_2Cl_2 (600 mL) and 1 N HCl (400 mL) and the resulting mixture stirred at 0 °C for 1 hour and at room temperature for 15 hours. The organic layer was separated and the aqueous layer extracted further with CH_2Cl_2 (2 x 300 mL). The combined organic layers were then dried over $MgSO_4$, filtered and concentrated *in vacuo* to furnish a crude yellow oil. Following purification by SiO_2 flash chromatography using hexanes/EtOAc (7:1 to 5:1 to 2:1) **364** was isolated as a white crystalline solid (28.84 g, 98%). %). $[\alpha]_D^{12}$ –8.9 ° (*c* 0.508, CH_2Cl_2); **IR (Neat)** 3418 (s), 2936 (s), 2873 (s), 1749 (m), 1636 (s), 1385 (s), 1300 (s), 1178 (s), 1121 (s) 999 (s), 941 (m), 895 (m), 839 (s), 800 (m), 725 (m), 629 (s), 606 (s), 552 (s), 486 (s), 442 (s); **^{1}H NMR (500 MHz, $CDCl_3$, 298 K)** δ 5.52 (m, 1*H*, $H_3CC=C\underline{H}CH_3$), 4.09 (apparent d, *J* = 4.5 Hz, 1*H*, *N*COCHEtC*H*), 3.62 (s, 3*H*, *N*OC$\underline{H}_3$), 3.38 (br s, 1*H*, O*H*), 3.11 (s, 3*H*, *N*C$\underline{H}_3$), 2.97 (br m, 1*H*, *N*COC*H*Et), 1.58 (m, 2*H*, NCOCH[C$\underline{H}_2$CH$_3$]-Et), 1.53 (d – overlaps with singlet, *J* = 6.9 Hz, 3*H*, $H_3CC=CHC\underline{H}_3$), 1.52 (s, 3*H*, $\underline{H}_3CC=CHCH_3$), 0.79 (t, 3*H*, *J* = 7.5 Hz, NCOCH[CH$_2$C$\underline{H}_3$]-Et); **^{13}C NMR (125 MHz, $CDCl_3$, 298 K)** δ 176.9 (*C*O), 134.2 ($H_3C\underline{C}=CHCH_3$), 120.3 ($H_3CC=\underline{C}HCH_3$), 76.2 (*N*COCHEt*C*H), 61.3 (*N*O*C*H3), 44.7 (*N*CO*C*HEt), 31.8 (*N*CH_3), 19.3 (NCOCH[*C*H$_2$CH$_3$]-Et), 12.8 ($H_3\underline{C}C=CHCH_3$), 12.7 ($H_3CC=CH\underline{C}H_3$), 12.1 (NCOCH[CH$_2$*C*H$_3$]-Et); **FAB HRMS** Calcd. for $C_{11}H_{21}NO_3$ (M+Na)$^+$: *m/e* 238.14191; Found: *m/e* 238.14203.

TBS Protection of Weinreb amide 365

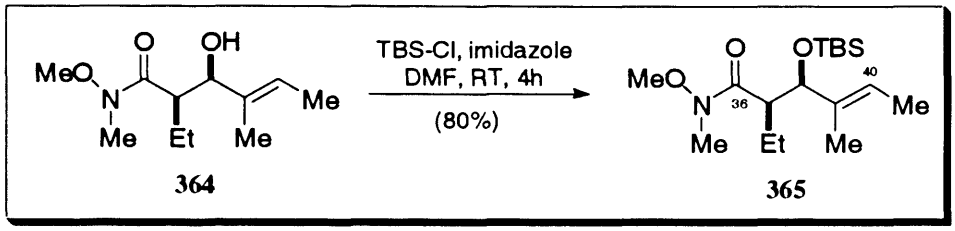

To a stirred solution of **364** (22 g, 0.1 mol) in anhydrous DMF (200 mL) was added at room temperature TBS-Cl (16.94 g, 0.11 mol) followed by imidazole (7.65 g, 0.11 mol) and the reaction mixture allowed to stir at room temperature for 4 hours. The mixture was then diluted with Et_2O (250 mL) and washed with sat. aq. $NaHCO_3$ (200 mL) and the organic layer separated, extracting the aqueous layer further with Et_2O (2 x 300 mL). The combined ethereal layers were then dried over $MgSO_4$, filtered and concentrated *in vacuo* to provide a crude yellow oil, which was purified by SiO_2 flash chromatography using hexanes/EtOAc (10:1 to 7:1 to 2:1) to afford **365** as a pale yellow oil (26.94 g, 80%). $[\alpha]_D^{12}$ +26.8 ° (*c* 1.116, CH_2Cl_2); **IR (neat)** 3501 (br w), 2856 (s), 1666 (s), 1651 (s), 1464 (s), 1447 (w), 1410 (m), 1379 (m), 1342 (w), 1300 (m), 1258 (s), 1177 (m), 1099 (w), 1067 (s), 1001 (s), 939 (m), 881 (s), 837 (s), 816 (w), 775 (s), 729 (w), 667 (m), 604 (w), 557 (m), 515 (w), 475 (w), 438 (w); **^{1}H NMR (500 MHz, $CDCl_3$, 298 K)** δ 5.25 (m, 1*H*, H_3CC=C$\underline{H}$CH_3), 4.02 (d, *J* = 9.4 Hz, 1*H*, *N*COCHEtC$\underline{H}$), 3.56 (s, 3*H*, *N*OC$\underline{H}_3$), 3.02 (s, 3*H*, *N*C$\underline{H}_3$), 2.99 (br m, 1*H*, *N*COC$\underline{H}$Et), 1.76 (m, 1*H*, NCOCH[C$\underline{H}_2$CH$_3$]-Et), 1.57 (m, 1*H*, NCOCH[C$\underline{H}_2$CH$_3$]-Et), 1.51 (s, 3*H*, $\underline{H}_3$CC=CHCH_3), 1.45 (d, *J* = 6.7 Hz, 3*H*, H_3CC=CHC$\underline{H}_3$), 0.81 (s, 9*H*, *O*Si(CH$_3$)$_2$C(C$\underline{H}_3$)$_3$), 0.80 (t, 3*H*, *J* = 7.5 Hz, NCOCH[CH$_2$C$\underline{H}_3$]-Et), – 0.03 (s, 3*H*, *O*Si(C$\underline{H}_3$)$_2$C(C$\underline{H}_3$)$_3$), – 0.11 (s, 3*H*, *O*Si(C$\underline{H}_3$)$_2$C(C$\underline{H}_3$)$_3$); **^{13}C NMR (125 MHz, $CDCl_3$, 298 K)** δ 175.7 (C$\underline{O}$), 136.7 (H_3C$\underline{C}$=CHCH$_3$), 121.0 (H_3CC=$\underline{C}$HCH$_3$), 80.0 (*N*COCHEt$\underline{C}$H), 61.3 (*N*O$\underline{C}$H$_3$), 48.2 (*N*COC$\underline{H}$Et), 32.1 (*N*C$\underline{H}_3$), 25.8 (*O*Si(CH$_3$)$_2$C(C$\underline{H}_3$)$_3$), 22.4 (NCOCH[C$\underline{H}_2$CH$_3$]-Et), 18.1 (*O*Si(CH$_3$)$_2$C(CH$_3$)$_3$), 12.8 (H_3CC=CHCH_3), 12.2 (NCOCH[CH$_2$C$\underline{H}_3$]-Et), 10.9 (H_3C$\underline{C}$=CHCH$_3$), – 5.0 (*O*Si(C$\underline{H}_3$)$_2$C(CH$_3$)$_3$), – 5.2 (*O*Si(C$\underline{H}_3$)$_2$C(CH$_3$)$_3$); **FAB HRMS** Calcd. for $C_{17}H_{35}NO_3Si$ (M+Na)$^+$: *m/e* 352.22838; Found: *m/e* 352.22762.

Reduction of Weinreb amide 366

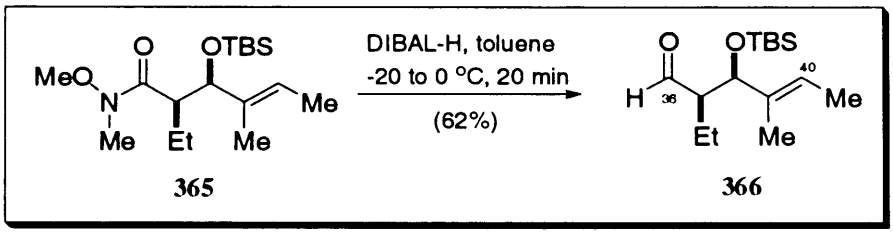

365 366

To a stirred solution of **365** (19.5 g, 59.17 mmol) in anhydrous toluene (200 mL) at –20 °C was added dropwise DIBAL-H (47 mL, 71.0 mmol) and the mixture stirred at –20 °C for 2 mins before being warmed to 0 °C. The reaction was quenched with MeOH at 0 °C and poured into a cooled (~ 2 °C) mixture of Et_2O (400 mL) and Rochelles salt solution (300 mL) with vigorous stirring for 1 hour. The organic layer was extracted and the aqueous layer extracted further with EtOAc (2 x 200 mL) and the combined organic layers washed with brine (200 mL), dried ($MgSO_4$), filtered and concentrated *in vacuo* to provide a crude yellow oil. Following purification by SiO_2 flash chromatography using hexanes/EtOAc (20:1 to 10:1) **366** was afforded as a clear oil (9.92 g, 62%). **$[\alpha]_D^{12}$** +14.4 ° (*c* 0.63, CH_2Cl_2); **IR (neat)** 2930 (s), 2858 (s), 2710 (w), 1724 (s), 1670 (w), 1472 (s), 1464 (s), 1387 (m), 1362 (m), 1335 (w), 1313 (w), 1252 (s), 1219 (w), 1061 (s), 1005 (m), 939 (m), 837 (s), 816 (w), 775 (s), 671 (m), 608 (w), 573 (w), 548 (w); **^{1}H NMR (500 MHz, $CDCl_3$, 298 K)** δ 9.48 (d, *J* = 3.6 Hz, 1*H*, C<u>H</u>O), 5.38 (q, *J* = 6.7 Hz, 1*H*, H_3CC=C<u>H</u>CH_3), 4.16 (d, *J* = 7.4 Hz, 1*H*, COHCHEtC<u>H</u>), 2.28 (m, 1*H*, CHOC<u>H</u>Et), 1.59 (apparent quint, *J* = 7.3 Hz, 2*H*, COHCH[C<u>H</u>$_2$$CH_3$]-Et), 1.52 (d, *J* = 6.9 Hz, 3*H*, H_3CC=CHC<u>H</u>$_3$), 1.50 (s, 3*H*, <u>H</u>$_3$$CC$=$CHCH_3$), 0.83 (s overlap with t, 12*H*, *O*Si(CH_3)$_2$C(C<u>H</u>$_3$)$_3$ and COHCH[CH_2C<u>H</u>$_3$]-Et), – 0.02 (s, 3*H*, *O*Si(C<u>H</u>$_3$)$_2$C(C<u>H</u>$_3$)$_3$), – 0.08 (s, 3*H*, *O*Si(C<u>H</u>$_3$)$_2$C(C<u>H</u>$_3$)$_3$); **^{13}C NMR (125 MHz, $CDCl_3$, 298 K)** δ 204.4 (<u>C</u>OH), 136.0 (H_3C<u>C</u>=$CHCH_3$), 121.9 (H_3CC=<u>C</u>HCH_3), 77.8 (COHCHEt<u>C</u>H), 58.4 (COH<u>C</u>HEt), 25.7 (*O*Si(CH_3)$_2$C(<u>C</u>H$_3$)$_3$), 18.5 (*O*Si(CH_3)$_2$<u>C</u>(CH$_3$)$_3$), 18.1 (COHCH[<u>C</u>H$_2$$CH_3$]-Et), 12.8 ($H_3CC$=CH<u>C</u>H$_3$), 11.8 ($H_3$<u>C</u>$C$=$CHCH_3$), 11.4 (COHCH[$CH_2$<u>C</u>H$_3$]-Et), – 4.7 (*O*Si(<u>C</u>H$_3$)$_2$C(CH$_3$)$_3$), – 5.4 (*O*Si(<u>C</u>H$_3$)$_2$C(CH$_3$)$_3$); **FAB HRMS** Calcd. for $C_{15}H_{30}O_2Si$ $(M+H)^+$: *m/e* 271.20932; Found: *m/e* 271.20978.

Wittig olefination to α,β-Unsaturated ester 368

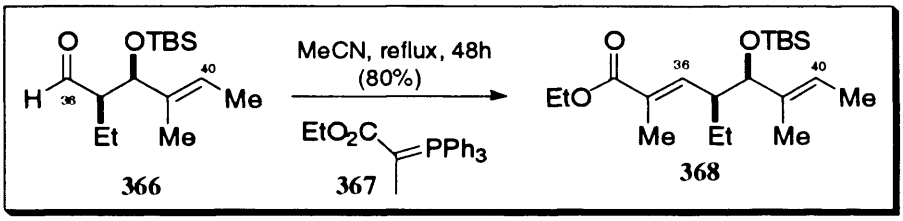

To a stirred solution of **366** (8.5 g, 31.43 mmol) in anhydrous MeCN (150 mL) was added at room temperature 1-carbethoxyethylidene triphenylphosphorane **367** (22.78 g, 62.85 mmol) and the reaction mixture heated at reflux for 48 hours. The mixture was then cooled to ambient temperature and diluted with EtOAc (300 mL) and washed with H_2O (200 mL). The organic layer was separated and the aqueous layer extracted further with EtOAc (2 x 100 mL), the combined organic layers were then dried ($MgSO_4$) filtered and concentrated *in vacuo* to provide a crude yellow oil. This was then purified by SiO_2 flash chromatography using hexanes/EtOAc (150:1 to 100:1 to 20:1) to afford **368** as a clear oil (8.91 g, 80%). **^{1}H NMR (500 MHz, $CDCl_3$, 298 K)** δ 6.38 (d, *J* = 9.6 Hz, 1*H*, H_3CC=C<u>H</u>CHEtCH), 5.30 (q, *J* = 6.3 Hz, 1*H*, H_3CC=C<u>H</u>CH_3), 4.14 (m, 2*H*, $CH_3C\underline{H}_2OC$=O), 3.79 (d, *J* = 7.5 Hz, 1*H*, H_3CC=CHCHEtC<u>H</u>), 2.44 (m, 1*H*, H_3CC=CHC<u>H</u>EtCH), 1.79 (s, 3*H*, $EtO_2CC(C\underline{H}_3)$=CH), 1.79 (m, 1*H*, CH_3C=CHCH[C<u>H</u>$_2CH_3$]-Et), 1.50 (d, *J* = 6.7 Hz, 3*H*, H_3CC=CHC<u>H</u>$_3$), 1.45 (s, 3*H*, <u>H</u>$_3CC$=CHC<u>H</u>$_3$), 1.25 (t, *J* = 7.1 Hz, 3*H*, C<u>H</u>$_3CH_2OC$=O), 1.19 (m, 1*H*, CH_3C=CHCH[C<u>H</u>$_2CH_3$]-Et), 0.88 (s, 9*H*, *O*Si$(CH_3)_2C(C\underline{H}_3)_3$), 0.76 (t, *J* = 7.5 Hz, 3*H*, CH_3C=CHCH[$CH_2C\underline{H}_3$]-Et), – 0.01 (s, 3*H*, *O*Si$(C\underline{H}_3)_2C(CH_3)_3$), – 0.08 (s, 3*H*, *O*Si$(C\underline{H}_3)_2C(CH_3)_3$); **^{13}C NMR (125 MHz, $CDCl_3$, 298 K)** δ 168.2 (<u>C</u>O), 143.8 (H_3CC=<u>C</u>HCHEtCH), 136.8 ($EtO_2C\underline{C}(CH_3)$=CH)), 127.7 ($H_3C\underline{C}$=$CHCH_3$), 121.0 ($H_3CC$=<u>C</u>H$CH_3$), 81.0 ($H_3CC$=CHCHEt<u>C</u>H), 60.2 ($CH_3\underline{C}H_2OC$=O), 45.4 (H_3CC=CH<u>C</u>HEtCH), 25.8 (*O*Si$(CH_3)_2C(\underline{C}H_3)_3$), 23.6 ($CH_3C$=CHCH[<u>C</u>$H_2CH_3$]-Et), 18.2 (*O*Si$(CH_3)_2\underline{C}(CH_3)_3$), 14.2 (<u>C</u>$H_3CH_2OC$=O), 12.8 ($H_3CC$=CH<u>C</u>$H_3$), 12.8 ($EtO_2CC(C\underline{H}_3)$=CH), 11.6 ($CH_3C$=CHCH[$CH_2\underline{C}H_3$]-Et), 11.4 (<u>H</u>$_3CC$=C<u>H</u>$CH_3$), – 4.7 (*O*Si$(\underline{C}H_3)_2C(CH_3)_3$), – 5.2 (*O*Si$(\underline{C}H_3)_2C(CH_3)_3$); **FAB HRMS** Calcd. for $C_{20}H_{38}O_3Si$ $(M+H)^+$: *m/e* 355.26683; Found: *m/e* 355.26599.

Reduction of ester 368 to alcohol 369

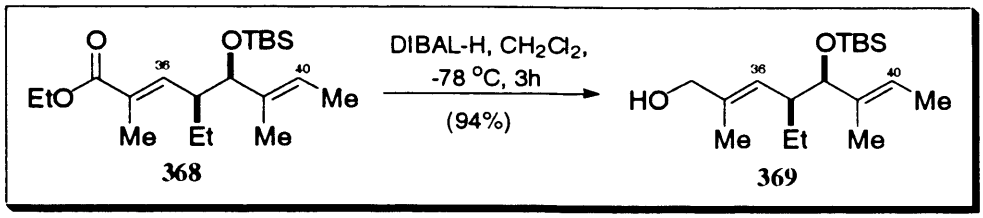

To a stirred solution of **368** (8 g, 22.56 mmol) in anhydrous CH_2Cl_2 (100 mL) was added dropwise at –78 °C DIBAL-H (31.6 mL, 47.38 mmol) and the mixture allowed to stir at –78 °C for 2 hours. The reaction mixture was quenched *via* the **cautious** addition of MeOH and the mixture poured into Et_2O (250 mL) layered on top of saturated Rochelles salt solution (100 mL) and the biphasic mixture stirred at room temperature for 1 hour. The organic layer was separated and the aqueous layer extracted further with EtOAc (2 x 100 mL) and combined organic layers dried ($MgSO_4$), filtered and concentrated *in vacuo* to provide a yellow oil that was purified by SiO_2 flash chromatography using hexanes/EtOAc (15:1 to 2:1) to afford **369** as a clear oil (6.63 g, 94%). $[\alpha]_D^{12}$ +51.3 ° (*c* 0.462, CH_2Cl_2); **IR (neat)** 3300 (br s), 2856 (br s), 2710 (w), 2646 (w), 1670 (m), 1462 (s), 1379 (s), 1360 (s), 1335 (w), 1300 (m), 1250 (s), 1219 (m), 1188 (w), 1005 (s), 982 (w), 939 (w), 903 (m), 835 (m), 773 (s), 667 (m), 615 (w), 573 (m), 519 (w); **^{1}H NMR (500 MHz, $CDCl_3$, 298 K)** δ 5.23 (q, *J* = 6.7 Hz, 1*H*, $H_3CC=C\underline{H}CH_3$), 4.95 (d, *J* = 9.2 Hz, 1*H*, $H_3CC=C\underline{H}CHEtCH$), 3.92 (s, 2*H*, $HOC\underline{H}_2C(CH_3)=CH$), 3.68 (d, *J* = 8.0 Hz, 1*H*, $H_3CC=CHCHEtC\underline{H}$), 2.30 (m, 1*H*, $H_3CC=CHC\underline{H}EtCH$), 1.75 (m, 1*H*, $CH_3C=CHCH[C\underline{H}_2CH_3]$-Et), 1.61 (s, 3*H*, $\underline{H}_3CC=CHCHEtCH$), 1.50 (d, *J* = 6.0 Hz, 3*H*, $H_3CC=CHC\underline{H}_3$), 1.45 (s, 3*H*, $\underline{H}_3CC=CHCH_3$), 1.41 (br s, 1*H*, *O*H), 1.06 (m, 1*H*, $CH_3C=CHCH[C\underline{H}_2CH_3]$-Et), 0.85 (s, 9*H*, $OSi(CH_3)_2C(C\underline{H}_3)_3$), 0.76 (t, *J* = 7.5 Hz, 3*H*, $CH_3C=CHCH[CH_2C\underline{H}_3]$-Et), – 0.02 (s, 3*H*, $OSi(C\underline{H}_3)_2C(C\underline{H}_3)_3$), – 0.09 (s, 3*H*, $OSi(C\underline{H}_3)_2C(C\underline{H}_3)_3$); **^{13}C NMR (125 MHz, $CDCl_3$, 298 K)** δ 137.5 ($H_3C\underline{C}=CHCH_3$), 135.1 ($HOCH_2\underline{C}(CH_3)=CH$), 128.1 ($H_3CC=\underline{C}HCHEtCH$), 120.5 ($H_3CC=\underline{C}HCH_3$), 81.8 ($H_3CC=CHCHEt\underline{C}H$), 69.2 ($HO\underline{C}H_2C(CH_3)=CH$), 43.9 ($H_3CC=CH\underline{C}HEtCH$), 25.9 ($OSi(CH_3)_2C(\underline{C}H_3)_3$), 24.1 ($CH_3C=CHCH[\underline{C}H_2CH_3]$-Et), 18.2 ($OSi(CH_3)_2\underline{C}(CH_3)_3$), 14.2 ($H_3\underline{C}C=CHCHEtCH$), 12.8 ($H_3CC=CH\underline{C}H_3$), 11.5 ($CH_3C=CHCH[CH_2\underline{C}H_3]$-Et), 11.2 ($H_3\underline{C}C=CHCH_3$); **FAB HRMS** Calcd. for $C_{18}H_{36}O_2Si$ $(M+Na)^+$: *m/e* 335.23821; Found: *m/e* 335.23789.

Oxidation of allylic alcohol 369 to α,β-Unsaturated aldehyde 370

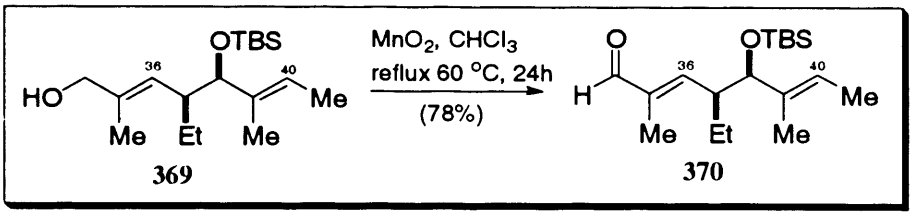

To a stirred solution of **369** (6.21g, 19.87 mmol) in $CHCl_3$ (100 mL) was added at room temperature and in a single portion MnO_2 [on activated carbon] (17.27 g, 198.68 mmol) and the mixture heated at reflux (60 °C) for 24 hours. The reaction mixture was then filtered through Celite and the resulting filtrate concentrated *in vacuo* and purified by SiO_2 flash chromatography using hexanes/EtOAc (100:1 to 70:1) to afford **370** as a clear oil with a distinctive odour (4.81 g, 78%). **$[\alpha]_D^{12}$** +68.8 ° (*c* 1.228, CH_2Cl_2); **IR (neat)** 2959 (s), 2930 (s), 2858 (s), 1690 (s), 1643 (w), 1472 (m), 1462 (m), 1421 (w), 1389 (m), 1360 (w), 1288 (w), 1252 (s), 1119 (s), 1070 (s), 1005 (w), 874 (m), 837 (s), 777 (s), 669 (w), 573 (w); **^{1}H NMR (500 MHz, $CDCl_3$, 298 K)** δ 9.31 (s, 1H, COH), 6.07 (d, *J* = 9.5 Hz, $COHC(CH_3)=CH$), 5.29 (q, *J* = 6.7 Hz, 1*H*, $H_3CC=CHCH_3$), 3.82 (d, *J* = 8.0 Hz, 1*H*, $H_3CC=CHCHEtCH$), 2.65 (m, 1*H*, $H_3CC=CHCHEtCH$), 1.86 (m, 1*H*, $CH_3C=CHCH[CH_2CH_3]$-Et), 1.69 (s, 3*H*, $H_3CC=CHCHEtCH$), 1.48 (d, *J* = 5.9 Hz, 3*H*, $H_3CC=CHCH_3$), 1.43 (s, 3*H*, $H_3CC=CHCH_3$), 1.24 (m, 1*H*, $CH_3C=CHCH[CH_2CH_3]$-Et), 0.85 (s, 9*H*, $OSi(CH_3)_2C(CH_3)_3$), 0.77 (t, *J* = 7.5 Hz, 3*H*, $CH_3C=CHCH[CH_2CH_3]$-Et), – 0.01 (s, 3*H*, $OSi(CH_3)_2C(CH_3)_3$), – 0.08 (s, 3*H*, $OSi(CH_3)_2C(CH_3)_3$); **^{13}C NMR (125 MHz, $CDCl_3$, 298 K)** δ 195.4 (COH,), 156.1 ($COHC(CH_3)=CH$), 139.5 ($COHC(CH_3)CH$), 136.8 ($H_3CC=CHCH_3$), 121.5 ($H_3CC=CHCH_3$), 80.9 ($H_3CC=CHCHEtCH$), 45.7 ($H_3CC=CHCHEtCH$), 25.8 ($OSi(CH_3)_2C(CH_3)_3$), 23.9 ($CH_3C=CHCH[CH_2CH_3]$-Et), 18.1 ($OSi(CH_3)_2C(CH_3)_3$), 12.7 ($H_3CC=CHCH_3$), 11.5 ($CH_3C=CHCH[CH_2CH_3]$-Et), 11.1 ($H_3CC=CHCH_3$), 9.6 ($H_3CC=CHCHEtCH$), – 4.7 ($OSi(CH_3)_2C(CH_3)_3$), – 5.2 ($OSi(CH_3)_2C(CH_3)_3$).

(*R,R*)-Diisopropyl tartrate (*E*)-crotylboronate 371

A 500 mL 3-necked round bottom flask equipped with a magnetic stirrer bar and containing potassium *tert*-butoxide (20 g, 0.18 mol) was sealed and connected to a high vacuum oil pump and heated at 80 °C for 15 hours. The vessel was then cooled to ambient temperature and connected with a thermometer, to read the internal temperature, and flushed with N_2. Anhydrous THF (100 mL) was then added and the suspension cooled to –78 °C and trans-2-

butene (18 mL, 0.18 mol) was condensed into a graduated measuring cylinder and transferred *via* cannula into the vessel at –78 °C. To this mixture was added dropwise at –78 °C *n*-BuLi (71.3 mL, 0.18 mol), ensuring that the internal temperature does not rise above –65 °C during addition, and the reaction mixture allowed to reach –50 °C after complete addition. The solution is maintained at –50 °C for exactly 15 mins and then immediately recooled to -78°C and triisopropylborate (41 mL, 0.18 mol) was added dropwise at a rate at which the internal temperature did not exceed –65 °C and resulting mixture stirred for 10 minutes. After this time the reaction mixture was rapidly poured into a separating funnel containing 1 N HCl (300 mL) saturated with NaCl and ensuring that the pH is 1 the mixture was extracted with a solution of (*R,R*)-diisopropyl tartrate (37.5 mL, 0.18 mol) in Et_2O (80 ml). The organic layer was separated and the aqueous layer extracted further with Et_2O (3 x 100 mL) and combined ethereal layers dried over $MgSO_4$, under N_2, for at least 2 hours at room temperature. The suspension was then filtered and concentrated in vacuo to yield a thick clear oil following treatment under a high vacuum oil pump until the product is of constant weight (51.5 g). The provided material was of sufficient purity to progress to the next step.

Crotylboration of 370 to 372

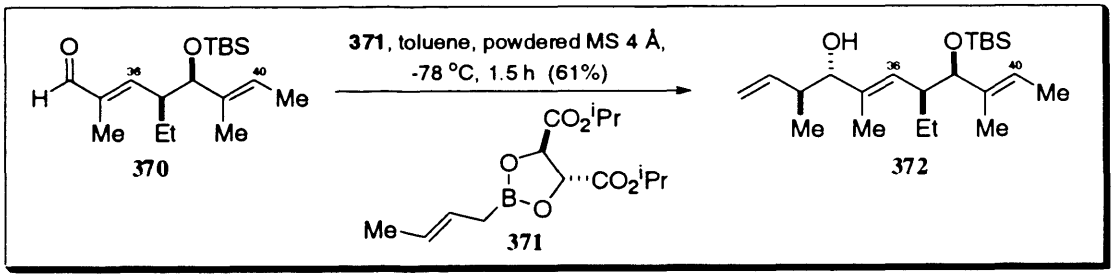

To a stirred solution of **371** (26 mL, 26.08 mmol) in anhydrous toluene (80 mL) at room temperature was added activated 4 Å powdered molecular sieves (2 g) and the suspension stirred for 10 mins and then cooled to –78 °C. A solution of **370** (4.5 g, 14.49 mmol) in anhydrous toluene (20 mL) was then added *via* cannulation over 10 mins and the mixture allowed to stir at –78 °C for 1.5 hours. The reaction mixture was quenched *via* the **cautious** addition of pre-cooled 2M NaOH and Et_2O (50 mL) and the biphasic mixture allowed to reach ambient temperature over 45 mins. The resulting mixture was then filtered through Celite and the organic phase separated, extracting the aqueous layer further with Et_2O (2 x 100 mL) and combined ethereal layers dried ($MgSO_4$), filtered and concentrated *in vacuo* to yield a crude oil. Following purification by SiO_2 flash chromatography using hexanes/EtOAc (150:1 to 100:1 to 50:1) **372** was afforded as a clear

oil (3.24 g, 61% - 2:1 ratio in favour of desired *anti*-product [1.93:1]). $[\alpha]_D^{12}$ +44.7 ° (*c* 0.246, CH_2Cl_2); **IR (neat)** 3477 (br w), 3078 (w), 2959 (s), 2929 (s), 2857 (s), 1638 (w), 1472 (m), 1462 (m), 1379 (m), 1361 (m), 1251 (s), 1080 (s), 1053 (s), 1005 (s), 906 (m), 872 (s), 836 (s), 774 (s), 668 (w), 573 (w); **^{1}H NMR (500 MHz, $CDCl_3$, 298 K)** δ 5.73 (m, 1*H*, H_2C=C<u>H</u>CHCH$_3$), 5.25 (q, *J* = 6.7 Hz, 1*H*, H_3CC=C<u>H</u>CH$_3$), 5.10 (d, *J* = 17.1 Hz, 1*H*, <u>H</u>$_2$C=CHCCH$_3$-*trans*), 5.08 (d, *J* = 9.5 Hz, 1*H*, <u>H</u>$_2$C=CHCCH$_3$-*cis*), 4.97 (d, *J* = 10.4 Hz, 1*H*, H_3CC=C<u>H</u>CHEt), 3.71 (d, *J* = 8.1 Hz, 1*H*, H_3CC=CHCHEtC<u>H</u>), 3.61 (d, *J* = 8.1 Hz, 1*H*, H_3CCHC<u>H</u>OH), 2.32 (m, 2*H*, H_3CC=CHC<u>H</u>Et and H_3CC<u>H</u>CHOH), 1.76 (m, 1*H*, CH_3C=CHCH[C<u>H</u>$_2$CH$_3$]-Et), 1.57 (s, 3*H*, <u>H</u>$_3$CC=CHCHEt), 1.51 (d, *J* = 6.7 Hz, 3*H*, H_3CC=CHC<u>H</u>$_3$), 1.49 (br s, 1*H*, O<u>H</u>), 1.47 (s, 3*H*, <u>H</u>$_3$CC=CHCH$_3$), 1.09 (m, 1*H*, CH_3C=CHCH[C<u>H</u>$_2$CH$_3$]-Et), 0.89 (d, *J* = 6.8 Hz, 3*H*, <u>H</u>$_3$CCHCHOH), 0.85 (s, 9*H*, *O*Si(CH$_3$)$_2$C(C<u>H</u>$_3$)$_3$), 0.77 (t, *J* = 7.5 Hz, 3*H*, CH_3C=CHCH[CH$_2$C<u>H</u>$_3$]-Et), – 0.01 (s, 3*H*, *O*Si(C<u>H</u>$_3$)$_2$C(CH$_3$)$_3$), – 0.08 (s, 3*H*, *O*Si(C<u>H</u>$_3$)$_2$C(C<u>H</u>$_3$)$_3$); **^{13}C NMR (125 MHz, $CDCl_3$, 298 K)** δ 141.1 (H_2C=<u>C</u>HCCH$_3$), 137.5 (H_3CC=CHCHEt), 135.5 (H_3CC=CHCH$_3$), 130.1 (H_3CC=<u>C</u>HCHEt), 120.6 (H_3CC=<u>C</u>HCH$_3$), 115.8 (H_2C=CHCCH$_3$), 81.8 (H_3CC=CHCHEt<u>C</u>H), 81.3 (H_3CCHC<u>H</u>OH), 43.9 (H_3CC=CH<u>C</u>HEt), 41.4 (H_3C<u>C</u>HCHOH), 25.8 (*O*Si(CH$_3$)$_2$C(<u>C</u>H$_3$)$_3$), 24.1 (CH_3C=CHCH[<u>C</u>H$_2$CH$_3$]-Et), 18.2 (*O*Si(CH$_3$)$_2$<u>C</u>(CH$_3$)$_3$), 16.5 (H_3<u>C</u>CHCHOH), 12.8 (H_3CC=CH<u>C</u>H$_3$), 12.1 (H_3<u>C</u>C=CHCHEt), 11.5 (CH_3C=CHCH[CH$_2$<u>C</u>H$_3$]-Et), 11.2 (H_3<u>C</u>C=CHCH$_3$), – 4.7 (*O*Si(<u>C</u>H$_3$)$_2$C(CH$_3$)$_3$), – 5.2 (*O*Si(<u>C</u>H$_3$)$_2$C(CH$_3$)$_3$).

O-PMB protection of 372 to 373

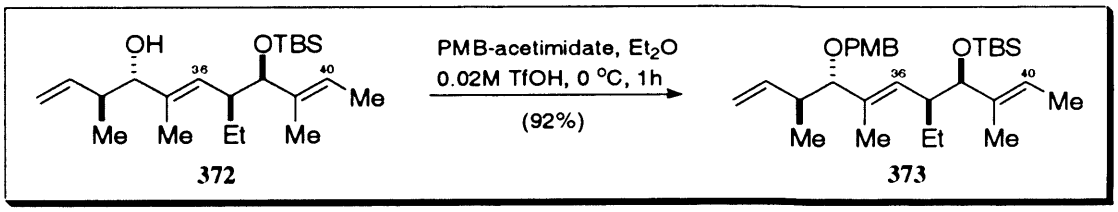

To a stirred solution of **372** (3.16 g, 8.62 mmol) in anhydrous Et_2O (50 mL) was added at 0 °C PMB-acetimidate (7.3 g, 25.86 mmol) followed by a 0.02 M solution of TfOH in Et_2O (2.2 mL, 0.04 mmol) and the reaction mixture stirred at 0 °C for 1 hour. The mixture was then diluted with Et_2O (50 mL) and washed with sat. aq. $NaHCO_3$ (30 mL), organic layer separated and the aqueous layer extracted further with Et_2O (2 x 50 mL). The combined ethereal layers were then dried ($MgSO_4$), filtered and concentrated *in vacuo* to provide a crude yellow oil that was purified by SiO_2 flash chromatography using hexanes/EtOAc (70:1 to 50:1 to 30:1) to afford **373** as a clear oil (3.86 g, 92%).

Hydroboration of 373 to alcohol 374

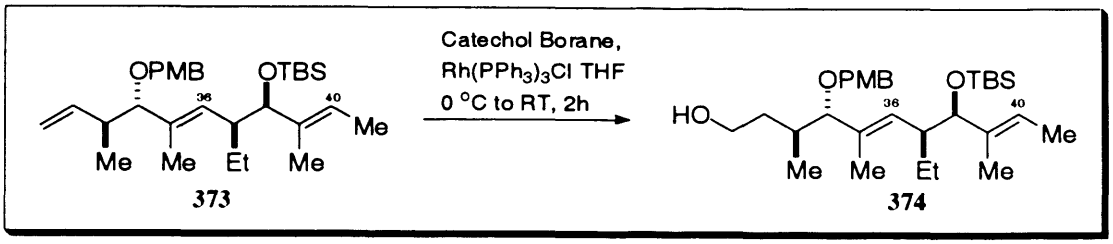

To a stirred solution of **373** (3.73 g, 7.66 mmol) in anhydrous THF (75 mL) at 0 °C was added in a single portion $Rh(PPh_3)_3Cl$ (0.14 g, 0.15 mmol) followed by the dropwise addition of catechol borane [1 M solution in THF] (19.2 mL, 19.16 mmol) and the mixture stirred at 0 °C for 30 mins before being allowed to reach ambient temperature for 3 hours. Following oxidative work up with EtOH/THF [1:1] (16 mL), 2 M NaOH (16 mL) and 30% H_2O_2 in H_2O (16 mL) at room temperature over 1 hour the mixture was diluted with Et_2O (70 mL) and the organic layer separated. The aqueous layer was further extracted with Et_2O (2 x 50 mL) and the combined ethereal layers were washed with 2M NaOH (50 mL), brine (50 mL) and dried over $MgSO_4$. After attempting purification by SiO_2 flash chromatography it became evident that the desired product **374** was difficult to completely separate from boronate derivative thus it was taken onto the next step. **^{1}H NMR (500 MHz, $CDCl_3$, 298 K)** δ 7.18 (d, *J* = 8.5 Hz, 2*H*, arom), 6.83 (d, *J* = 8.6 Hz, 2*H*, arom), 6.73 (m, 1*H*, *O*H), 5.30 (q, *J* = 6.6 Hz, 1*H*, $H_3CC=CHCH_3$), 4.93 (d, *J* = 10.5 Hz, 1*H*, $H_3CC=CHCHEt$), 4.24 (d, *J* = 11.0 Hz, 1*H*, OCH_2Ph-*O*Me), 3.95 (d, *J* = 11.0 Hz, 1*H*, OCH_2Ph-*O*Me), 3.76 (s, 3*H*, $PhOCH_3$), 3.74 (d, *J* = 9.1 Hz, 1*H*, $H_3CC=CHCHEtCH$), 3.63 (m, 1*H*, $HOCH_2CH_2$), 3.54 (m, 1*H*, $HOCH_2CH_2$), 3.22 (d, *J* = 9.4 Hz, 1*H*, $H_3CCHCHOPMB$), 2.48 (m, 1*H*, $H_3CC=CHCHEtCH$), 1.86 (m, 1*H*, $CH_3C=CHCH[CH_2CH_3]$-Et), 1.77 (m, 1*H*, $H_3CCHCHOPMB$), 1.71 (m, 1*H*, $HOCH_2CH_2$), 1.57 (s, 3*H*, $H_3CC=CHCHEt$), 1.53 (s, 3*H*, $H_3CC=CHCH_3$), 1.47 (m, 1*H*, $HOCH_2CH_2$), 1.41 (d, *J* = 6.7 Hz, 3*H*, $H_3CC=CHCH_3$), 1.10 (m, 1*H*, $CH_3C=CHCH[CH_2CH_3]$-Et), 0.87 (s, 9*H*, $OSi(CH_3)_2C(CH_3)_3$), 0.82 (t, *J* = 7.5 Hz, 3*H*, $CH_3C=CHCH[CH_2CH_3]$-Et), 0.76 (d, *J* = 6.8 Hz, 3*H*, $HOCH_2CH_2CHCH_3$), 0.02 (s, 3*H*, $OSi(CH_3)_2C(CH_3)_3$), – 0.06 (s, 3*H*, $OSi(CH_3)_2C(CH_3)_3$); **^{13}C NMR (125 MHz, $CDCl_3$, 298 K)** δ 159.2 (arom), 138.2 ($H_3CC=CHCHEt$), 133.5 ($H_3CC=CHCH_3$), 132.9 ($H_3CC=CHCHEt$), 130.2 (arom), 129.9 (arom), 121.3 ($H_3CC=CHCH_3$), 113.8 (arom), 91.1 ($H_3CCHCHOPMB$), 82.5 ($H_3CC=CHCHEtCH$), 69.3 (OCH_2Ph-*O*Me), 61.6 ($HOCH_2CH_2$), 55.2 ($PhOCH_3$), 44.3 ($H_3CC=CHCHEtCH$), 38.0 ($HOCH_2CH_2$), 33.3 ($H_3CCHCHOPMB$), 25.9 ($OSi(CH_3)_2C(CH_3)_3$), 24.9 ($CH_3C=CHCH[CH_2CH_3]$-Et), 18.2 ($OSi(CH_3)_2C(CH_3)_3$), 18.1 ($HOCH_2CH_2CHCH_3$), 13.0 ($H_3CC=CHCH_3$), 11.6 ($CH_3C=CHCH[CH_2CH_3]$-Et), 11.1 ($H_3CC=CHCHEt$), 10.8 ($H_3CC=CHCH_3$), – 4.6

($OSi(\underline{C}H_3)_2C(CH_3)_3$), – 5.1 ($OSi(\underline{C}H_3)_2C(CH_3)_3$); **FAB HRMS** Calcd. for $C_{30}H_{52}O_4Si$ $(M+Na)^+$: *m/e* 527.35324; Found: *m/e* 527.35435.

Synthesis of sulfide 375

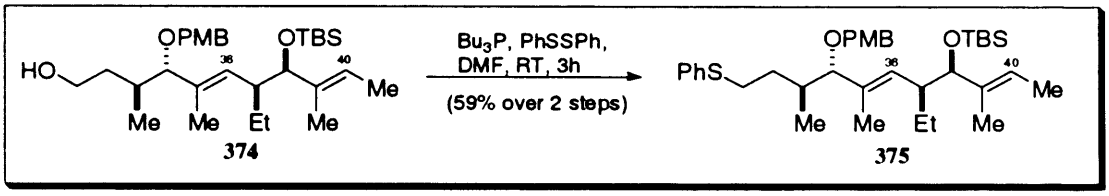

To a stirred solution of **374** (3.87 g, 7.66 mmol) in anhydrous DMF (60 mL) was added in single portions and at room temperature diphenyl disulfide (3.35 g, 15.33 mmol) followed by Bu_3P (4.4 mL, 17.64 mmol) and the reaction mixture stirred at room temperature for 3 hours. The mixture was then diluted with Et_2O (80 mL) and washed with H_2O (100 mL), separating the organic layer and extracting the aqueous layer further with Et_2O (2 x 100 mL). The combined ethereal layers were then dried ($MgSO_4$), filtered and concentrated *in vacuo* to provide a crude yellow oil that was purified by SiO_2 flash chromatography using hexanes/EtOAc (50:1 to 30:1 to 15:1) to afford **375** as a clear oil (2.7 g, 59% over 2 steps). $[\alpha]_D^{12}$ +10.6 ° (*c* 0.47, CH_2Cl_2); **IR (neat)** 2956 (s), 2929 (s), 2856 (s), 2359 (s), 1612 (m), 1585 (w), 1513 (s), 1460 (m), 1382 (w), 1300 (w), 1249 (s), 1175 (w), 1053 (s), 874 (m), 836 (s), 774 (m), 738 (m), 691 (w); **^{1}H NMR (500 MHz, $CDCl_3$, 298 K)** δ 7.33-7.10 (m, *7H*, arom), 6.82 (d, *J* = 8.6 Hz, *2H*, arom), 5.31 (q, *J* = 6.7 Hz, *1H*, $H_3CC=C\underline{H}CH_3$), 4.90 (d, *J* = 10.5 Hz, *1H*, $H_3CC=C\underline{H}CHEt$), 4.22 (d, *J* = 11.3 Hz, *1H*, $OC\underline{H}_2Ph$-*O*Me), 3.93 (d, *J* = 11.3 Hz, *1H*, $OC\underline{H}_2Ph$-*O*Me), 3.77 (s, *3H*, $PhOC\underline{H}_3$), 3.74 (d, *J* = 9.0 Hz, *1H*, $H_3CC=CHCHEtC\underline{H}$), 3.17 (d, *J* = 9.6 Hz, *1H*, $H_3CCHC\underline{H}OPMB$), 2.86 (apparent t, *J* = 7.6 and 8.5 Hz, *2H*, $PhSC\underline{H}_2$), 2.48 (m, *1H*, $H_3CC=CHC\underline{H}EtCH$), 2.02 (m, *1H*, $PhSCH_2C\underline{H}_2$), 1.88 (m, *1H*, $CH_3C=CHCH[C\underline{H}_2CH_3]$-Et), 1.79 (m, *1H*, $H_3CC\underline{H}CHOPMB$), 1.55 (s, *3H*, $\underline{H}_3CC=CHCHEt$), 1.54 (s, *3H*, $\underline{H}_3CC=CHCH_3$), 1.46 (d, *J* = 6.6 Hz, *3H*, $H_3CC=CHC\underline{H}_3$), 1.45 (m, 1H, $PhSC\underline{H}_2$), 1.10 (m, *1H*, $CH_3C=CHCH[C\underline{H}_2CH_3]$-Et), 0.88 (s, *9H*, $OSi(CH_3)_2C(C\underline{H}_3)_3$), 0.83 (t, *J* = 7.4 Hz, *3H*, $CH_3C=CHCH[CH_2C\underline{H}_3]$-Et), 0.75 (d, *J* = 6.9 Hz, *3H*, $PhSCH_2CH_2CHC\underline{H}_3$), 0.04 (s, *3H*, $OSi(C\underline{H}_3)_2C(C\underline{H}_3)_3$), – 0.04 (s, *3H*, $OSi(C\underline{H}_3)_2C(C\underline{H}_3)_3$); **^{13}C NMR (125 MHz, $CDCl_3$, 298 K)** δ 158.9 (arom), 138.2 ($H_3C\underline{C}=CHCHEt$), 137.1 (arom), 133.7 ($H_3C\underline{C}=CHCH_3$), 132.3 ($H_3CC=\underline{C}HCHEt$), 131.0 (arom), 129.5 (arom), 128.7 (arom), 125.4 (arom), 128.7 (arom), 121.2 ($H_3CC=\underline{C}HCH_3$), 113.6 (arom), 89.9 ($H_3CCH\underline{C}HOPMB$), 82.5 ($H_3CC=CHCHEt\underline{C}H$), 69.0 ($O\underline{C}H_2Ph$-*O*Me), 55.2 ($PhO\underline{C}H_3$), 44.3 ($H_3CC=CH\underline{C}HEtCH$), 34.6 ($PhSCH_2CH_2\underline{C}H$), 33.2 ($PhSCH_2\underline{C}H_2$), 31.0 ($PhS\underline{C}H_2$), 25.9 ($OSi(CH_3)_2C(\underline{C}H_3)_3$), 24.9 ($CH_3C=CHCH[\underline{C}H_2CH_3]$-Et), 18.2

($OSi(CH_3)_2\underline{C}(CH_3)_3$), 16.2 ($PhSCH_2CH_2CH\underline{C}H_3$), 13.1 ($H_3CC=CH\underline{C}H_3$), 11.6 ($CH_3C=CHCH[CH_2\underline{C}H_3]$-Et), 11.2 ($H_3\underline{C}C=CHCHEt$ or $H_3\underline{C}C=CHCH_3$), 10.8 ($H_3\underline{C}C=CHCHEt$ or $H_3\underline{C}C=CHCH_3$), – 4.6 ($OSi(\underline{C}H_3)_2C(CH_3)_3$), – 5.1 ($OSi(\underline{C}H_3)_2C(CH_3)_3$); **FAB HRMS** Calcd. for $C_{36}H_{56}O_3SSi$ $(M+Na)^+$: *m/e* 619.36169; Found: *m/e* 619.35996.

Preparation of diphenyl-*tert*-butyl silyl triflate

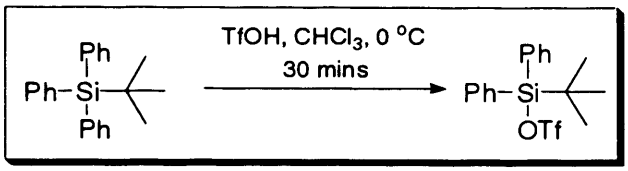

To a stirred solution of triphenyl-*tert*-butyl silane (42.25 g, 0.13 mol) in anhydrous $CHCl_3$ (65 mL) was added dropwise at 0 °C triflic acid (11.6 mL, 0.13 mol) and the reaction mixture allowed to stir at 0 °C for 30 mins. The resulting solution was taken on and used for the next step.

TBDPS Protection of Weinreb amide 377

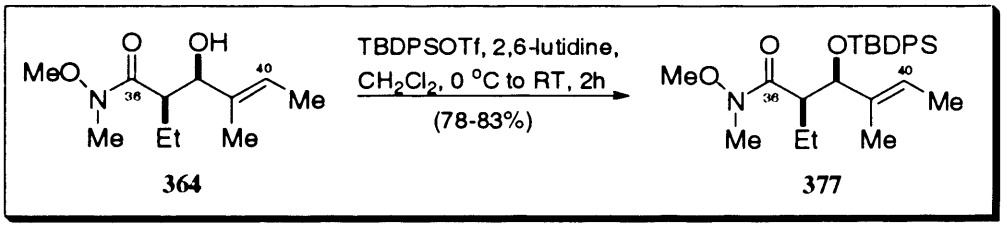

To a stirred solution of **364** (23.08 g, 0.11 mol) in anhydrous CH_2Cl_2 (300 mL) was added dropwise at 0 °C, 2,6-lutidine (25 mL, 0.21 mol) followed by the dropwise addition of TBDPS-OTf (65 mL, 0.13 mol) and the reaction mixture allowed to reach ambient temperature over 1.5 hours. The mixture was then poured into a separating funnel containing Et_2O (600 mL) layered on top of pre-cooled sat. aq. $NaHCO_3$ (500 mL) and the organic layer separated. The aqueous layer was extracted further with Et_2O (2 x 500 mL) and the combined ethereal layers dried ($MgSO_4$), filtered and concentrated *in vacuo* to provide a crude yellow oil. This was then purified by SiO_2 flash chromatography using hexanes/EtOAc (15:1 to 10:1 to 5:1) to afford **377** as a thick clear oil

(38.91 g, 80%). %). **$[\alpha]_D^{12}$** +34.1 ° (*c* 0.454, CH_2Cl_2); **IR (neat)** 3071 (w), 3047 (w), 2964 (s), 2932 (s), 2858 (m), 1663 (s), 1472 (m), 1462 (m), 1427 (m), 1379 (m), 1362 (w), 1177 (w), 1113 (s), 1067 (s), 999 (s), 868 (m), 824 (m), 812 (w), 741 (m), 700 (s), 689 (m), 610 (m), 503 (m), 488 (m); **^{1}H NMR (500 MHz, $CDCl_3$, 298 K)** δ 7.62 (d, *J* = 6.6 Hz, 2*H*, arom), 7.59 (d, *J* = 6.7 Hz, 2*H*, arom), 7.39-7.27 (m, 6*H*, arom), 5.00 (m, 1*H*, $H_3CC=C\underline{H}CH_3$), 4.26 (d, *J* = 9.2 Hz, 1*H*, *N*COCHEtC*H*), 3.59 (s, 3*H*, *NOCH*$_3$), 3.10 (br m, 1*H*, *N*COC*H*Et), 3.01 (s, 3*H*, *NCH*$_3$), 1.89 (m, 1*H*, NCOCH[$C\underline{H}_2CH_3$]-Et), 1.54 (m, 1*H*, NCOCH[$C\underline{H}_2CH_3$]-Et), 1.40 (s, 3*H*, $\underline{H}_3CC=CHCH_3$), 1.23 (d, *J* = 6.7 Hz, 3*H*, $H_3CC=CHC\underline{H}_3$), 1.05 (s, 9*H*, *O*SiPh$_2$C($C\underline{H}_3$)$_3$), 0.81 (t, 3*H*, *J* = 7.4 Hz, NCOCH[$CH_2C\underline{H}_3$]-Et); **^{13}C NMR (125 MHz, $CDCl_3$, 298 K)** δ 175.5 (*C*O), 136.2 (arom), 136.1 (arom), 135.5 ($H_3C\underline{C}=CHCH_3$), 134.1 (arom), 129.4 (arom), 129.3 (arom), 127.2 (arom), 127.1 (arom), 122.4 ($H_3CC=\underline{C}HCH_3$), 81.0 (*N*COCHEt*C*H), 61.3 (*NO*$\underline{C}H_3$), 48.8 (*N*CO*C*HEt), 32.1 (*NC*H$_3$), 27.2 (*O*SiPh$_2$*C*($\underline{C}H_3$)$_3$), 22.6 (NCOCH[$\underline{C}H_2CH_3$]-Et), 19.6 (*O*SiPh$_2$*C*(CH_3)$_3$), 12.7 ($H_3CC=CH\underline{C}H_3$), 12.4 (NCOCH[$CH_2\underline{C}H_3$]-Et), 11.4 ($H_3\underline{C}C=CHCH_3$); **FAB HRMS** Calcd. for $C_{27}H_{39}NO_3Si$ (M+Na)$^+$: *m/e* 476.25968; Found: *m/e* 476.26048.

Reduction of Weinreb amide 377 to TBDPS-aldehyde 378

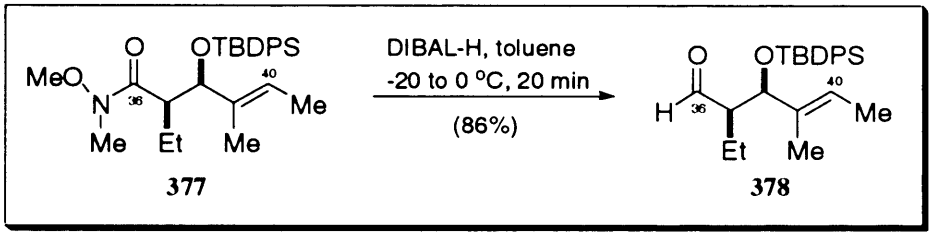

To a stirred solution of **377** (35 g, 77.15 mmol) in anhydrous toluene (400 mL) at –20 °C was added dropwise DIBAL-H (72 mL, 108 mmol) and the mixture stirred at –20 °C for 2 mins before being warmed to 0 °C. The reaction was quenched with MeOH at 0 °C and poured into a cooled (~ 2 °C) mixture of Et_2O (600 mL) and Rochelles salt solution (400 mL) with vigorous stirring for 1 hour. The organic layer was extracted and the aqueous layer extracted further with EtOAc (2 x 300 mL) and the combined organic layers washed with brine (300 mL), dried ($MgSO_4$), filtered and concentrated *in vacuo* to provide a crude yellow oil. Following purification by SiO_2 flash chromatography using hexanes/EtOAc (15:1 to 10:1) **378** was afforded as a clear oil (26.18 g, 86%). **$[\alpha]_D^{12}$** –8.2 ° (*c* 0.716, CH_2Cl_2); **IR (neat)** 3423 (br w), 3071 (w), 3049 (w), 2961 (s), 2932 (s), 2858 (s), 1722 (s), 1466 (m), 1427 (m), 1385 (m), 1362 (w), 1109 (s), 1053 (s), 1005 (w), 845 (m), 822 (m), 741 (m), 704 (s), 611 (m), 505 (s); **^{1}H NMR (500 MHz, $CDCl_3$, 298 K)** δ

9.57 (d, *J* = 3.3 Hz, 1*H*, C<u>H</u>O), 7.65 (d, *J* = 6.6 Hz, 2*H*, arom), 7.60 (d, *J* = 6.7 Hz, 2*H*, arom), 7.43-7.32 (m, 6*H*, arom), 5.12 (apparent q, *J* = 6.7, 6.2 Hz, 1*H*, H_3CC=C<u>H</u>CH_3), 4.25 (d, *J* = 7.3 Hz, 1*H*, COHCHEtC<u>H</u>), 2.35 (m, 1*H*, CHOC<u>H</u>Et), 1.49 (s overlap with br m, 5*H*, <u>H</u>$_3$CC=CHCH$_3$ and COHCH[C<u>H</u>$_2$CH$_3$]-Et respectively), 1.38 (d, *J* = 6.7 Hz, 3*H*, H_3CC=CHC<u>H</u>$_3$), 1.06 (s, 9*H*, *O*SiPh$_2$C(C<u>H</u>$_3$)$_3$), 0.74 (t, *J* = 7.5 Hz, 3*H*, COHCH[CH$_2$C<u>H</u>$_3$]-Et); **^{13}C NMR (125 MHz, CDCl$_3$, 298 K)** δ 204.1 (<u>C</u>OH), 136.1 (arom), 135.9 (arom), 134.8 (H_3C<u>C</u>=CHCH$_3$), 133.8 (arom), 133.5 (arom), 129.7 (arom), 129.6 (arom), 127.5 (arom), 127.3 (arom), 123.5 (H_3CC=<u>C</u>HCH$_3$), 79.2 (COHCHEt<u>C</u>H) 59.1 (CHO<u>C</u>HEt), 27.0 (*O*SiPh$_2$<u>C</u>(CH$_3$)$_3$), 19.4 (*O*SiPh$_2$<u>C</u>(CH$_3$)$_3$), 18.7 (COHCH[<u>C</u>H$_2$CH$_3$]-Et), 12.8 (H_3CC=CH<u>C</u>H$_3$), 11.8 (COHCH[CH$_2$<u>C</u>H$_3$]-Et), 11.7 (H_3<u>C</u>C=CHCH$_3$); **FAB HRMS** Calcd. for $C_{25}H_{34}O_2Si$ (M+Na)$^+$: *m/e* 417.22256; Found: *m/e* 417.22300.

Wittig olefination to the α,β-Unsaturated ester

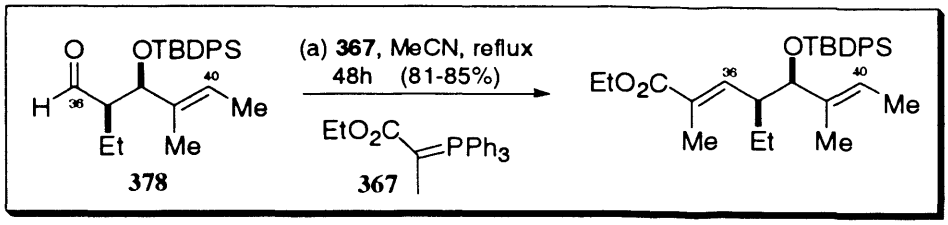

To a stirred solution of **378** (26.02 g, 65.94 mmol) in anhydrous MeCN (450 mL) was added at room temperature 1-carbethoxyethylidene triphenylphosphorane **367** (47.79 g, 131.87 mmol) and the reaction mixture heated at reflux for 48 hours. The mixture was then cooled to ambient temperature and diluted with EtOAc (500 mL) and washed with H_2O (300 mL). The organic layer was separated and the aqueous layer extracted further with EtOAc (2 x 200 mL), the combined organic layers were then dried ($MgSO_4$) filtered and concentrated *in vacuo* to provide a crude yellow oil. This was then purified by SiO_2 flash chromatography using hexanes/EtOAc (100:1 to 70:1 to 30:1) to afford the desired ester as a clear oil (25.57 g, 81%). **[α]$_D^{12}$** +12.8 ° (*c* 0.376, CH_2Cl_2); **IR (neat)** 2961 (s), 2932 (s), 2858 (s), 1709 (s), 1651 (w), 1472 (w), 1427 (m), 1391 (w), 1367 (w), 1269 (w), 1227 (m), 1113 (s), 1051 (s), 1007 (w), 843 (w), 822 (w), 739 (m), 700 (s), 613 (m), 503 (m), 486 (m); **^{1}H NMR (500 MHz, CDCl$_3$, 298 K)** δ 7.63 (d, *J* = 6.6 Hz, 2*H*, arom), 7.58 (d, *J* = 6.7 Hz, 2*H*, arom), 7.41-7.29 (m, 6*H*, arom), 6.27 (d, *J* = 9.7 Hz, 1*H*, H_3CC=C<u>H</u>CHEt), 5.00 (apparent q, *J* = 6.7, 6.2 Hz, 1*H*, H_3CC=C<u>H</u>CH$_3$), 4.12 (m, 2*H*, CH$_3$C<u>H</u>$_2$OC=O), 3.93 (d, *J* = 7.6 Hz, 1*H*, H_3CC=CHCHEtC<u>H</u>), 2.52 (m, 1*H*, H_3CC=CHC<u>H</u>EtCH), 1.82 (m, 1*H*, CH$_3$C=CHCH[C<u>H</u>$_2$CH$_3$]-Et), 1.78 (s, 3*H*, EtO$_2$CC(C<u>H</u>$_3$)=CH), 1.37 (s, 3*H*, <u>H</u>$_3$CC=CHCH$_3$), 1.28 (d, *J* = 6.7 Hz, 3*H*, H_3CC=CHC<u>H</u>$_3$), 1.23 (t, *J* = 7.1 Hz, 3*H*, C<u>H</u>$_3$CH$_2$O$_2$C), 1.05 (m, 1*H*, CH$_3$C=CHCH[C<u>H</u>$_2$CH$_3$]-Et), 1.04 (s, 9*H*, *O*SiPh$_2$C(C<u>H</u>$_3$)$_3$), 0.69 (t, *J* = 7.5 Hz, 3*H*,

CH_3C=CHCH[$CH_2C\underline{H}_3$]-Et); **^{13}C NMR (125 MHz, $CDCl_3$, 298 K)** δ 168.2 ($\underline{C}O$), 143.3 (H_3CC=$\underline{C}$HCHEt), 136.2 (arom), 136.1 (arom), 135.8 ($H_3C\underline{C}$=CHCHEt), 134.3 (arom), 134.0 (arom), 129.4 (arom), 129.4 (arom), 127.7 ($H_3C\underline{C}$=$CHCH_3$), 127.3 (arom), 127.1 (arom), 122.5 (H_3CC=$\underline{C}HCH_3$), 82.0 (H_3CC=CHCHEt$\underline{C}$H), 60.2 ($CH_3\underline{C}H_2O_2C$), 46.1 (H_3CC=CH$\underline{C}$HEtCH), 27.1 (*O*$SiPh_2C(\underline{C}H_3)_3$), 24.2 ($CH_3C$=CHCH[$\underline{C}H_2CH_3$]-Et), 19.5 (*O*$SiPh_2\underline{C}(CH_3)_3$), 14.2 ($\underline{C}H_3CH_2O_2C$), 12.9 ($EtO_2CC(\underline{C}H_3)$=CH), 12.7 ($H_3CC$=$CH\underline{C}H_3$), 11.6 ($H_3\underline{C}C$=$CHCH_3$), 11.6 ($CH_3C$=CHCH[$CH_2\underline{C}H_3$]-Et); **FAB HRMS** Calcd. for $C_{30}H_{42}O_3Si$ $(M+Na)^+$: *m/e* 501.28008; Found: *m/e* 501.27914.

Reduction to allylic alcohol 379

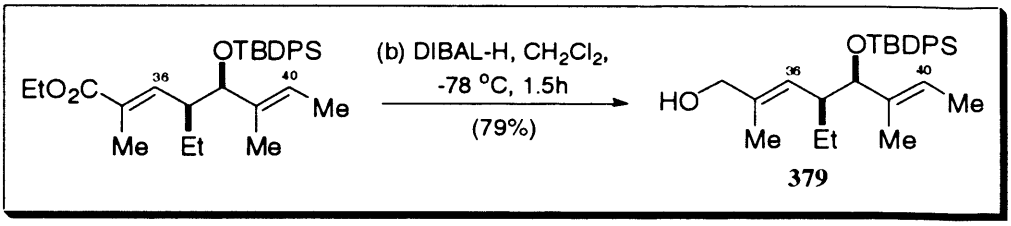

To a stirred solution of the α,β-unsaturated ester (24.16 g, 50.47 mmol) in anhydrous CH_2Cl_2 (300 mL) was added dropwise at –78 °C DIBAL-H (70.6 mL, 105.98 mmol) and the mixture allowed to stir at –78 °C for 2 hours. The reaction mixture was quenched *via* the **cautious** addition of MeOH and the mixture poured into Et_2O (400 mL) layered on top of saturated Rochelles salt solution (300 mL) and the biphasic mixture stirred at room temperature for 1 hour. The organic layer was separated and the aqueous layer extracted further with EtOAc (2 x 200 mL) and combined organic layers dried ($MgSO_4$), filtered and concentrated *in vacuo* to provide a yellow oil that was purified by SiO_2 flash chromatography using hexanes/EtOAc (20:1 to 10:1 to 2:1) to afford **379** as a clear oil (17.41 g, 79%). **IR (neat)** 3331 (br s), 3071 (w), 2959 (s), 2930 (s), 2856 (s), 1589 (w), 1472 (m), 1427 (s), 1391 (m), 1377 (m), 1362 (w), 1302 (w), 1192 (w), 1111 (s), 1049 (s), 1007 (s), 939 (w), 905 (w), 847 (m), 822 (m), 773 (w), 739 (m), 700 (s), 611 (m), 503 (m), 488 (m); **^{1}H NMR (500 MHz, $CDCl_3$, 298 K)** δ 7.65 (d, *J* = 6.5 Hz, 2*H*, arom), 7.59 (d, *J* = 6.7 Hz, 2*H*, arom), 7.42-7.29 (m, 6*H*, arom), 5.01 (apparent q, *J* = 6.7, 6.2 Hz, 1*H*, H_3CC=C$\underline{H}CH_3$), 4.85 (d, *J* = 9.3 Hz, 1*H*, H_3CC=C$\underline{H}$CHEtCH), 3.87 (d, *J* = 7.4 Hz, 1*H*, CHEtC$\underline{H}$), 3.85 (s, 2*H*, $HOC\underline{H}_2C(CH_3)$=CH), 2.37 (m, 1*H*, H_3CC=CHC$\underline{H}$EtCH), 1.80 (m, 1*H*, CH_3C=CHCH[$C\underline{H}_2CH_3$]-Et), 1.60 (s, 3*H*, $\underline{H}_3CC$=CHCHEtCH), 1.40 (s, 3*H*, $\underline{H}_3CC$=$CHCH_3$), 1.32 (d, *J* = 6.0 Hz, 3*H*, H_3CC=CHC$\underline{H}_3$), 1.04 (s, 9*H*, *O*$Si(CH_3)_2C(C\underline{H}_3)_3$), 0.99 (br m, 1*H*, CH_3C=CHCH[$C\underline{H}_2CH_3$]-Et), 0.70 (t, *J* = 7.4 Hz, 3*H*, CH_3C=CHCH[$CH_2C\underline{H}_3$]-Et); **^{13}C NMR (125 MHz, $CDCl_3$, 298 K)** δ 136.4, 136.2 (arom), 136.1 (arom), 135.1, 134.6, 134.3, 129.3 (arom),

129.3 (arom), 127.8 (H_3CC=$\underline{C}$HCHEtCH), 127.2 (arom), 127.1 (arom), 121.8 (H_3CC=$\underline{C}$HCH_3), 82.5 (CHEt$\underline{C}$H), 69.1 (HO$\underline{C}H_2C(CH_3)$=CH), 44.5 (H_3CC=CH$\underline{C}$HEtCH), 27.2 (*O*Si$Ph_2C(\underline{C}H_3)_3$), 24.2 ($CH_3C$=CHCH[$\underline{C}H_2CH_3$]-Et), 19.6 (*O*Si$Ph_2\underline{C}(CH_3)_3$), 14.2 ($H_3\underline{C}CC$=CHCHEtCH), 12.7 ($H_3CC$=CH$\underline{C}H_3$), 11.8 ($H_3\underline{C}CC$=CH$CH_3$), 11.7 ($CH_3C$=CHCH[$CH_2\underline{C}H_3$]-Et); **FAB HRMS** Calcd. for $C_{28}H_{40}O_2Si$ $(M+Na)^+$: *m/e* 459.26951; Found: *m/e* 459.26991.

Oxidation of 379 to α,β-Unsaturated aldehyde 380

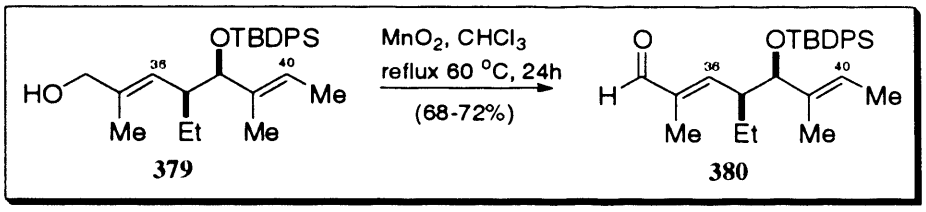

To a stirred solution of **379** (17 g, 38.93 mmol) in $CHCl_3$ (220 mL) was added at room temperature and in a single portion MnO_2 [on activated carbon] (33.84 g, 389.28 mmol) and the mixture heated at reflux (60 °C) for 24 hours. The reaction mixture was then filtered through Celite and the resulting filtrate concentrated *in vacuo* and purified by SiO_2 flash chromatography using hexanes/EtOAc (150:1 to 100:1 to 70:1) to afford **380** as a clear oil (12.01 g, 71%). **IR (neat)** 3071 (w), 2961 (m), 2932 (m), 2858 (m), 1690 (s), 1643 (w), 1472 (w), 1462 (w), 1427 (m), 1379 (w), 1362 (w), 1302 (w), 1200 (w), 1113 (s), 1053 (m), 1026 (m), 854 (w), 822 (m), 741 (m), 702 (s), 613 (m), 503 (m), 486 (w); **^{1}H NMR (500 MHz, $CDCl_3$, 298 K)** δ 9.19 (s, 1H, CO$\underline{H}$), 7.65 (d, *J* = 6.6 Hz, 2*H*, arom), 7.58 (d, *J* = 6.7 Hz, 2*H*, arom), 7.43-7.30 (m, 6*H*, arom), 5.95 (d, *J* = 10.9 Hz, COHC(CH_3)=C$\underline{H}$), 5.08 (apparent q, *J* = 6.7, 6.2 Hz, 1*H*, H_3CC=C$\underline{H}CH_3$), 3.99 (d, *J* = 7.4 Hz, 1*H*, H_3CC=CHCHEtC$\underline{H}$), 2.72 (m, 1*H*, H_3CC=CHC$\underline{H}$EtCH), 1.89 (m, 1*H*, CH_3C=CHCH[C$\underline{H}_2CH_3$]-Et), 1.69 (s, 3*H*, $\underline{H}_3CC$=CHCHEtCH), 1.41 (s, 3*H*, $\underline{H}_3CC$=CHCH_3), 1.33 (d, *J* = 5.9 Hz, 3*H*, H_3CC=CHC$\underline{H}_3$), 1.13 (m, 1*H*, CH_3C=CHCH[C$\underline{H}_2CH_3$]-Et), 1.05 (s, 9*H*, *O*Si$(CH_3)_2C(C\underline{H}_3)_3$), 0.70 (t, *J* = 7.5 Hz, 3*H*, CH_3C=CHCH[$CH_2C\underline{H}_3$]-Et); **^{13}C NMR (125 MHz, $CDCl_3$, 298 K)** δ 195.5 ($\underline{C}$OH,), 156.0 (COHC(CH_3)=$\underline{C}$H), 139.4 (COH$\underline{C}$(CH_3)=CH), 136.1 (arom), 136.0 (arom), 135.7, 134.1, 133.8, 129.5 (arom), 129.5 (arom), 127.4 (arom), 127.2 (arom), 122.8 (H_3CC=$\underline{C}$HCH_3), 81.6 (H_3CC=CHCHEt$\underline{C}$H), 46.2 (H_3CC=CH$\underline{C}$HEtCH), 27.1 (*O*Si$Ph_2C(\underline{C}H_3)_3$), 24.0 ($CH_3C$=CHCH[$\underline{C}H_2CH_3$]-Et), 19.5 (*O*Si$Ph_2\underline{C}(CH_3)_3$), 12.7 ($H_3CC$=CH$\underline{C}H_3$), 11.7 ($H_3\underline{C}CC$=C$HCH_3$), 11.6 ($CH_3C$=CHCH[$CH_2\underline{C}H_3$]-Et), 9.6 ($H_3\underline{C}CC$=CHCHEtCH); **FAB HRMS** Calcd. for $C_{28}H_{38}O_2Si$ $(M+Na)^+$: *m/e* 457.25386; Found: *m/e* 457.25250.

Crotylboration of 380 to 381

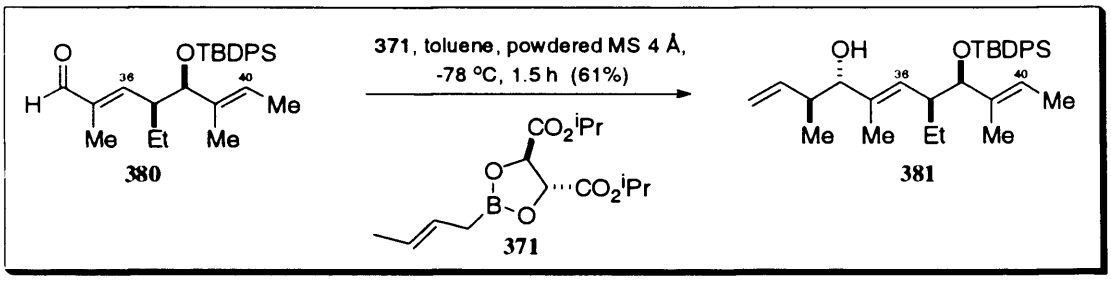

To a stirred solution of **371** (15.68 g, 52.59 mmol) in anhydrous toluene (150 mL) at room temperature was added activated 4 Å powdered molecular sieves (2 g) and the suspension stirred for 10 mins and then cooled to –78 °C. A solution of **380** (11.43 g, 26.29 mmol) in anhydrous toluene (90 mL) was then added *via* cannulation over 10 mins and the mixture allowed to stir at –78 °C for 1.5 hours. The reaction mixture was quenched *via* the **cautious** addition of pre-cooled 2M NaOH (40 mL) and Et_2O (100 mL) and the biphasic mixture allowed to reach ambient temperature over 45 mins. The resulting mixture was then filtered through Celite and the organic phase separated, extracting the aqueous layer further with Et_2O (2 x 150 mL) and combined ethereal layers dried ($MgSO_4$), filtered and concentrated *in vacuo* to yield a crude oil. Following purification by SiO_2 flash chromatography using hexanes/EtOAc (100:1 to 70:1 to 50:1) **381** was afforded as a clear oil (7.65 g, 61% - ratio 2.08:1 in favour of the desired *anti*-product). **IR (neat)** 3477 (br m), 3071 (w), 2961 (s), 2930 (s), 2858 (s), 1638 (w), 1456 (m), 1427 (m), 1383 (m), 1188 (w), 1109 (s), 1049 (s), 1005 (s), 910 (w), 858 (w), 822 (w), 739 (m), 704 (s), 611 (m), 505 (s), 486 (m); **^{1}H NMR (500 MHz, $CDCl_3$, 298 K)** δ 7.66 (d, *J* = 6.5 Hz, 2*H*, arom), 7.60 (d, *J* = 6.7 Hz, 2*H*, arom), 7.41-7.29 (m, 6*H*, arom), 5.71 (m, 1*H*, H_2C=C<u>H</u>CHCH_3), 5.09 (d, *J* = 18.5 Hz, 1*H*, <u>H</u>$_2$C=CHCHCH_3-*trans*), 5.06 (d, *J* = 10.3 Hz, 1*H*, <u>H</u>$_2$C=CHCHCH_3-*cis*), 4.99 (q, *J* = 6.8, 6.1 Hz, 1*H*, H_3CC=C<u>H</u>CH_3), 4.85 (d, *J* = 10.5 Hz, 1*H*, H_3CC=C<u>H</u>CHEt), 3.87 (d, *J* = 7.7 Hz, 1*H*, H_3CC=CHCHEtC<u>H</u>), 3.52 (d, *J* = 5.4 Hz, 1*H*, H_3CCHC<u>H</u>OH), 2.43 (m, 1*H*, H_3CC=CHC<u>H</u>Et), 2.29 (m, 1*H*, H_3CC<u>H</u>CHOH), 1.81 (m, 1*H*, CH_3C=CHCH[C<u>H</u>$_2$CH$_3$]-Et), 1.57 (s, 3*H*, <u>H</u>$_3$CC=CHCHEt), 1.41 (s, 3*H*, <u>H</u>$_3$CC=CHCH$_3$), 1.36 (d, *J* = 3.0 Hz, 1*H*, O<u>H</u>), 1.31 (d, *J* = 5.8 Hz, 3*H*, H_3CC=CHC<u>H</u>$_3$), 1.04 (s, 9*H*, *O*Si(CH$_3$)$_2$C(C<u>H</u>$_3$)$_3$), 1.00 (m, 1*H*, CH_3C=CHCH[C<u>H</u>$_2$CH$_3$]-Et), 0.86 (d, *J* = 6.8 Hz, 3*H*, <u>H</u>$_3$CCHCHOH), 0.71 (t, *J* = 7.5 Hz, 3*H*, CH_3C=CHCH[CH$_2$C<u>H</u>$_3$]-Et); **^{13}C NMR (125 MHz, $CDCl_3$, 298 K)** δ 141.1 (H_2C=<u>C</u>HCCH$_3$), 136.5 (H_3C<u>C</u>=CHCHEt), 136.2 (arom), 136.1 (arom), 135.6 (H_3C<u>C</u>=CHCH$_3$), 134.6 (arom), 134.3 (arom), 129.8 (H_3CC=<u>C</u>HCHEt), 129.3 (arom), 129.3 (arom), 127.2 (arom), 127.0 (arom), 121.9 (H_3CC=<u>C</u>HCH$_3$), 115.7 (H_2<u>C</u>=CHCCH$_3$), 82.6 (H_3CC=CHCHEt<u>C</u>H), 81.3 (H_3CCH<u>C</u>HOH), 44.5 (H_3CC=CH<u>C</u>HEt), 41.4 (H_3C<u>C</u>HCHOH),

27.2 ($\underline{O}Si(CH_3)_2C(\underline{C}H_3)_3$), 24.4 ($CH_3C{=}CHCH[\underline{C}H_2CH_3]$-Et), 19.6 ($\underline{O}Si(CH_3)_2\underline{C}(CH_3)_3$), 16.6 ($H_3\underline{C}CHCHOH$), 12.6 ($H_3CC{=}CH\underline{C}H_3$), 12.1 ($H_3\underline{C}C{=}CHCHEt$), 11.7 ($CH_3C{=}CHCH[CH_2\underline{C}H_3]$-Et), 11.7 ($H_3\underline{C}C{=}CHCH_3$); **FAB HRMS** Calcd. for $C_{32}H_{46}O_2Si$ $(M+H)^+$: *m/e* 491.33451; Found: *m/e* 491.33251.

Chapter 7: REFERENCES

1) www.cancerresearchuk.org
2) F. Sarabia, S. Chammaa, S.A. Ruiz, L.M. Ortiz and F.J.L. Herrera. Chemistry and Biology of cyclic depsipeptides of medicinal and biological interest. *Current Medicinal Chemistry*. **2004**, *11*, 1309-1332.
3) D.G. Johnson, R. Schneider-Broussard. Role of E2F in cell cycle control and cancer. *Frontiers in Bioscience*. **1998**, *3*, 447-458.
4) H. Maehr, L. Chao-min, N.J. Palleroni, J. Smallheer, L. Torado, T.H. Williams and J.F. Blount. Microbial Products VIII. Azinothricin, a novel hexadepsipeptide antibiotic. *The Journal of Antibiotics*. **1986**, *39*, 17-24.
5) C.H. Hassall, R.B. Mortow, Y. Ogihara and D.A.S. Phillips. Amino-acids and peptides. XII. The molecular structures of the monamycins, cyclodepsipeptide antibiotics. *The Journal of the Chemical Society*. **1971**, 526-532.
6) G. Germain, P. Main and M.M. Woolfson. Application of phase relationships to complex structures: The optimum use of phase relationships. *Acta Crystallographica*. **1971**, *A27*, 368-376.
7) J.C. Sheehan, D. Mania, S. Nakamura, J.A. Stock and K. Maeda. The structure of telomycin. *Journal of the American Chemical Society*. **1968**, *90*, 462-470.
8) J.C. Sheehan, K. Maeda, A.K. Sen and J.A. Stock. The isolation, characterisation and synthesis of *(2S,3S)*-3-hydroxyleucine, a new amino acid from the antibiotic telomycin. *Journal of the American Chemical Society*. **1962**, *84*, 1303-1305.
9) T.A. Smitka, J.B. Deeter, A.H. Hunt, F.P. Mertz, R.M. Ellis, L.D. Boeck and R.C. Yao. A83586C, A new depsipeptide antibiotic. *The Journal of Antibiotics*. **1988**, 726-733.
10) Y. Hayakawa, M. Nakagawa, Y. Toda and H. Seto. A new depsipeptide antibiotic, Citropeptin. *Agricultural and Biological Chemistry*. **1990**, *54*, 1007-1011.
11) M. Nakagawa, Y. Hayakawa, K. Furihata and H. Seto. Structural studies on New Depsipeptide Antibiotics Variapeptin and Citropeptin. *The Journal of Antibiotics*. **1990**, *43*, 477-484.
12) Y. Sakai, T. Yoshida, T. Tsujita, K. Ochiai, T. Agatsuma, Y. Saitoh, F. Tanaka, T. Akiyama, S. Akinaga and T. Mizukami. I.GE3, a Novel Hexadepsipeptide antitumour antibiotic produced by streptomyces sp. *The Journal of Antibiotics*. **1997**, *50*, 659-664.

13) T.Agatsuma, Y. Sakai, T. Mizukami and Y. Saitoh. . II .GE3, a Novel Hexadepsipeptide antitumour antibiotic produced by streptomyces sp. *The Journal of Antibiotics*. **1997**, 704-708.

14) O.D. Hensens, R.P. Borris, L.R. Koupal, C.G Caldwell, S.A. Currie, A.A. Haidri, C.F. Homnick, S.S Honeycutt and others. L-156,602, A C5a antagonist with a novel cyclic hexadepsipeptide structure from streptomyces. sp. MA6348. *The Journal of Antibiotics*. **1990**, *44*, 249-254.

15) M. Nakagawa, Y. Hayakawa, K. Adachi and H. Seto. A new depsipeptide antibiotic, Variapeptin. *Agricultural and Biological Chemistry*. **1990**, *54*, 791-794.

16) K.Sugawara, Y. Nishiyama and H. Yamamoto. Antitumour antibiotic BU-3983T. *Jpn. Kokai 218394 ('91)*, Sept. 25, **1991** (Patent).

17) Y. Nishiyama, K.Sugawara, K. Tomita, H. Yamamoto, H. Kamei and T. Oki. Verucopeptin, a new antitumour antibiotic active against B16 melanoma. I. *The Journal of Antibiotics*. **1993**, *46*, 921-927.

18) K. Sugawara, S. Toda, T. Moriyama, M. Konishi and T. Oki. Verucopeptin, a new antitumour antibiotic active against B16 melanoma. II. *The Journal of Antibiotics*. **1993**, *46*, 928-935.

19) J.D. Westley. Polyether antibiotics. Volume I. Marcel Dekker, New York and Basel. **1982**.

20) U. Grafe, R.Schlegel, M. Ritzau, W Ihn, K. Dornberger, C. Stengel, W.F. Fleck, W.Gutsche and A. Hartl. Aurantimycins, New depsipeptide antibiotics from *streptomyces aurantiacus* IMET 43917 production, isolation, structure elucidation and biological activity. *The Journal of Antibiotics*. **1995**, *48*, 119-125.

21) K. Umezawa, K. Nakazawa, T. Uemura, Y.Ikeda, S. Kondo, H. Naganawa N. Kinoshita, H. Hashizume, M. Hamada, T. Takeuchi and S. Ohba. *Tetrahedron Letters*. **1998**, *39*, 1389.

22) K. Umezawa, K. Nakazawa, Y.Ikeda, H. Naganawa and S. Kondo. *The Journal of Organic Chemistry*. **1999**, *64*, 3034.

23) K. Umezawa, K. Nakazawa, Y. Uchihata and M. Otsuka. Screening for inducers of apoptosis in apoptosis-resistant human carcinoma cells. In *Advances in Enzyme Regulation;* ed. G. Weber, Elsevier Science, Oxford, UK. **1999**, *39*, 145-156.

24) K. Umezawa, Y. Ikeda, O. Kawase, H. Naganawa and S. Kondo. Biosynthesis of Polyoxypeptin A: novel amino acid 3-hydroxy-3-methylproline derived from Isoleucine. *The Journal of the Chemical Society. Perkin Transactions 1.* **2001**, 1550-1553.

25) Y. Uchihata, N. Ando, Y. Ikeda, S. Kondo, M. Hamada and K. Umezawa. Isolation of a novel cyclic hexadepsipeptide pipalamycin from *streptomyces* as an apoptosis-inducing agent. *Journal of Antibiotics*. **2002**, *55*, 1-5.

26) M. Ueno, M. Amemiya, T. Someno, T. Masuda, H. Inuma, H. Naganawa, M. Hamada, M. Ishizyka and T. Takeuchi. IC101, extra-cellular matrix antagonist produced by *streptomyces* sp. MJ.202-72F3. *Journal of Antibiotics*. **1993**, *46*, 1658-1665.

27) S.P. Chellappan, S. Hiebert, M. Mudryj, J.M. Horowitz and J. R. Nevins. The E2F transcription factor is a cellular target for the RB protein. *Cell*. **1991**, *65*, 1053-1061.

28) D.M. Parkin. Global cancer statistics in the year 2000. *The Lancet Oncology*. **2001**, *9*, 533-543.

29) G. Brooks and N.B. La Thangue. The cell cycle and drug discovery: the promise and the hope. *Drug Discovery Today*. **1999**, *4*, 455-464.

30) K.A. Heichman and J.M. Roberts. Rules to replicate by. *Cell*. **1994**, *79*, 557-562.

31) J. Fuxe. $p16^{INK4A}$ and $p15^{INK4B}$ in senescence, immortalisation and cancer. Gene transfer by adenovirus vectors. *ISBN 91-7349-081-4 PhD Thesis*. Reproprint AB. **2001**.

32) L.H. Hartwell and T.A. Weinert. Checkpoints: controls that ensure the order of cell cycle events. *Science*. **1989**, *246*, 629-634.

33) P. Nurse. Ordering S phase and M phase in the cell cycle. *Cell*. **1994**, *79*, 547-550.

34) L.H. Hartwell, J. Culotti, J.R. Pringle and B.J. Reid. Genetic control of the cell division cycle in yeast. *Science*. **1974**, *183*, 46-51.

35) A. Zetterberg, O. Larsson and K.G. Wiman. What is the restriction point? *Current opinion in cell biology*. **1995**, *7*, 835-842.

36) P. Nurse. Checkpoint pathways come of age. *Cell*. **1997**, *91*, 865-867.

37) A.W. Murray. Cyclin dependent kinases: regulators of the cell cycle and more. *Chemistry and Biology*. **1994**, *1*, 191-195.

38) J. Pines. Cyclins and cyclin-dependent kinases: take your partners. *Trends in Biochemical Sciences*. **1993**, *18*, 195-197.

39) T. Evans, E.T. Rosenthal, J. Youngblom, D. Distel and T. Hunt. Cyclin: a protein specified by maternal mRNA in sea urchin eggs that is destroyed at each cleavage division. *Cell.* **1983**, *33*, 389-396.

40) R.W. King, R.J. Deshaies, J.M. Peters and M.W. Kirschner. How proteolysis drives the cell cycle. *Science.* **1996**, *274*, 1652-1659.

41) J. Pines. Cyclins and cyclin-dependent kinases: a biochemical view. *Biochemical Journal.* **1995**, *308*, 697-711.

42) C.J. Sherr. Cancer cell cycles. *Science.* **1996**, *274*, 1672-1677.

43) G.F. Draetta. Mammalian G1 cyclins. *Current opinion in cell biology.* **1994**, *6*, 842-846.

44) C.J. Sherr. Mammalian G1 cyclins. *Cell.* **1993**, *73*, 1059-1065.

45) H. Matsushime, M.E. Ewen, D.K. Strom, J.Y. Kato, S.K. Hanks, M.F. Roussel and C.J. Sherr. Identification and properties of an atypical catalytic subunit (p34PSK-J3/cdk4) for mammalian D type G1 cyclins. *Cell.* **1992**, *71*, 323-324.

46) C.J. Sherr. G1 Phase progreesion: cycling on cue. *Cell.* **1994**, *79*, 551-555.

47) J.R. Nevins. E2F: A link between the tumour suppressor protein and viral oncoproteins. *Science.* **1992**, *258*, 424-429.

48) E.Neuman, E.K. Flemington, W.R. Sellers and W.G. Kaelin Jr. Transcription of the E2F-1 gene is rendered cell cycle dependent by E2F DNA-binding sites within its promoter. *Molecular and Cellular Biology.* **1994**, *14*, 6607-6615.

49) J.E. Darnell Jr. Transcription factors as targets for cancer therapy. *Nature Reviews.* **2002**, *2*, 740-749.

50) I. Kovedsi, R. Reichel and J.R. Nevins. Identification of a cellular transcription factor involved in E1A transactivation. *Cell.* **1986**, *45*, 219-228.

51) J.E. Slansky and P.J. Farnham. Introduction to the E2F family: protein structure and gene regulation. *Current Topics in Microbiology and Immunology.* **1996**, *208*, 1-30.

52) L. Yamasaki. Growth regulation by the E2F and DP transcription factor families. *Results and Problems in Cell Differentiation.* **1998**, *22*, 199-227.

53) J. DeGregori. The genetics of the E2F family of transcription factors: shared functions and unique roles. *Biochimica et Biophysica Acta (BBA)-Reviews on Cancer.* **2002**, *1602*, 131-150.

54) N. Dyson. The regulation of E2F by pRb-family proteins. *Genes and Development.* **1998**, *12*, 2245-2262.

55) E. Ormondroyd, S. De La Luna, N.B. La Thangue. A new member of the DP family, DP-3, with distinct protein products suggests a regulatory role for alternative splicing in the cell cycle transcription factor DRTF1/E2F. *Oncogene.* **1995**, *11*, 1437-1446.

56) A.R. Black and J. Azizkhan-Clifford. Regulation of E2F: a family of transcription factors involved in proliferation control. *Gene.* **1999**, *237*, 281-302.

57) H.E. Huber, G. Edwards, P.J. Goodhart, D.R Patrick, P.S. Huang, M. Ivey-Hoyle, S.F. Barnett, A. Oliff and D.C. Heimbrook. Transcription factor E2F binds DNA as a heterodimer. *Proceedings of the National Academy of Sciences of the United States of America.* **1993**, *90*, 3525-3529.

58) W.D. Cress and J.R. Nevins. A role for a bent DNA structure in E2F-mediated transcription activation. *Molecular and Cellular Biology.* **1996**, *16*, 2119-2127.

59) C. Sardet, M. Vidal, D. Cobrinik, Y. Geng, C. Onufryk, A. Chen and R.A. Weinberg. E2F-4 and E2F-5, two members of the E2F family, are expressed in the early phases of the cell cycle. *Proceedings of the National Academy of Sciences of the United States of America.* **1995**, *92*, 2403-2407.

60) S. Gaubatz, J.G. Wood and D.M. Livingston. Unusual proliferation arrest and transcriptional control properties of a newly discovered E2F family member, E2F-6. *Proceedings of the National Academy of Sciences of the United States of America.* **1998**, *95*, 9190-9195.

61) R.L. Beijersbergen, R.M Kerkhoven, L. Zhu, L. Carlee, P.M. Voorhoeve and R.Bernards. E2F-4, a new member of the E2F gene family, has oncogenic activity and associates with p107 *in vivo*. *Genes and Development.* **1994**, *8*, 2680-2690.

62) L.C. Wu, L.R. Zukerberg, C. Ngwu, E. Harlow and J.A. Lees. In *vivo* association of E2F and DP family proteins. *Molecular and Cellular Biology.* **1995**, *15*, 2536-2546.

63) S. Bagchi, R. Weinmann and R. Raychaudhuri. The retinoblastoma protein copurifies with E2F-1, an E1A-regulated inhibitor of the transcription factor E2F. *Cell.* **1991**, *65*, 1063-1072.

64) X. Grana, J. Garriga and X. Mayol. Role of the retinoblastoma protein family, pRb, p107 and p130 in the negative control of cell growth. *Oncogene.* **1998**, *17*, 3365-3383.

65) X. Mayol and X. Grana. The p130 pocket protein: keeping order at cell cycle exit/re-entrance transitions. *Frontiers in Bioscience.* **1998**, *3*, 11-24.

66) L. Lania, B. Majello and G. Napolitano. Transcriptional control by cell-cycle regulators: a review. *Journal of Cellular Physiology*. **1999**, *179*, 134-141.

67) L. Yamasaki. Balancing proliferation and apoptosis in vivo: the Goldilocks theory of E2F/DP action. *Biochimica et Biophysica Acta (BBA)-Minireview*. **1999**, *1423*, M9-M15.

68) M. Morkel, J. Wenkel, A.J. Bannister, T Kouzarides and C. Hagemeier. An E2F-like repressor of transcription. *Nature*. **1997**, *390*, 567-568.

69) P. Cartwright, H. Muller, C. Wagener, K. Holm and K. Helin. A novel member of the E2F family in an inhibitor of E2F-dependent transcription. *Oncogene*. **1998**, *17*, 611-623.

70) K. Helin, C.L. Wu, A.R Fattaey, J.A Lees, D.B. Dynlacht, C. Ngwu and E. Harlow. Heterodimerisation of the transcription factors E2F-1 and DP-1 leads to cooperative transactivation. *Genes and Development*. **1993**, *7*, 1850-1861.

71) W. Krek, D.M. Livingston and S. Shirodkar. Binding to DNA and the retinoblastoma gene product promoted by complex formation of different E2F family members. *Science*. **1993**, *262*, 1557-1560.

72) S.F. Dowdy, P.W. Hinds, K. Louie, S.I. Reed, A. Arnold and R.A. Weinberg. Physical interaction of the retinoblastoma protein with human D cyclins. *Cell*. **1993**, *73*, 499-511.

73) M.E. Ewen, H.K. Sluss, C.J. Sherr, H. Matsushime, J. Kato and D.M. Livingston. Functional interactions of the retinoblastoma protein with mammalian D-type cyclins. *Cell*. **1993**, *73*, 487-497.

74) A.S. Lundberg and R.A Weinberg. Functional inactivation of the retinoblastoma protein requires sequential modification by at least two distinct cyclin-cdk complexes. *Molecular and Cellular Biology*. **1998**, *18*, 753-761.

75) J. Kato, H. Matsushime, S.W. Hiebert, M.E. Ewen and C.J. Sherr. Direct binding of cyclin D to the retinoblastoma gene product (pRb) and pRb phosphorylation by the cyclin D-dependent kinase CDK4. *Genes and Development*. **1993**, *7*, 331-342.

76) R.L. Beijersbergen, L. Carlee, R.M. Kerkhoven and R. Bernards. Regulation of the retinoblastoma protein-related p107 by G1 cyclin complexes. *Genes and Development*. **1995**, *9*, 1340-1353.

77) M. Peter. The regulation of cyclin-dependent kinase inhibitors (CKIs). *Progress in Cell Cycle Research*. **1997**, *3*, 99-108.

78) J.W Harper, G.R. Adami, N. Wei, K. Keyomarsi and S.J. Elledge. The p21 Cdk-interacting protein Cip1 is a potent inhibitor of G1 cyclin-dependent kinases. *Cell*. **1993**, *75*, 805-816.

79) K. Polyak, M.H. Lee, H. Erdjument-Bromage, A. Koff, J.M. Roberts, P. Tempst and J. Massague. Cloning of $p27^{Kip1}$, a cyclin-dependent kinase inhibitor and a potential mediator of extracellular antimitogenic signals. *Cell.* **1994**, *78*, 59-66.

80) S. Matsuoka, M.C. Edwards, C. Bai, S. Parker, P. Zhang, A. Baldini, J.W. Harper and S.J. Elledge. p57KIP2, a structurally distinct member of the p21CIP1 Cdk-inhibitor family, is a candidate tumour suppressor gene. *Genes and Development.* **1995**, *9*, 650-662.

81) M. Serrano, G.J. Hannon and D. Beach. A new regulatory motif in cell-cycle control causing specific inhibition of cyclinD/CDK4. *Nature.* **1993**, *366*, 704-707.

82) G.J. Hannon and D. Beach. $p15^{INK4B}$ is a potential effector of TGF-beta induced cell cycle arrest. *Nature.* **1994**, *371*, 257-261.

83) K.L. Guan, C.W. Jenkins, Y. Li, M.A. Nichols, X. Wu, C.L. O'Keefe, A.G. Matera and Y. Xiong. Growth suppression by p18, a $p16^{INK4/MTS1-}$ and $p14^{INK4B/MTS2-}$ related CDK6 inhibitor, correlates with wild-type pRb function. *Genes and Development.* **1994**, *8*, 2939-2952.

84) F.K. Chan, J. Zhang, L. Cheng, D.N. Shapiro and A. Winoto. Identification of human and mouse p19, a novel CDK4 and CDK6 inhibitor with homology to $p16^{INK4}$. *Molecular and Cellular Biology.* **1995**, *15*, 2682-2688.

85) M. Hall, S. Bates and G. Peters. Evidence for different modes of action of cyclin-dependent kinase inhibitors: p15 and p16 bind to kinases, p21 and p27 bind to cyclins. *Oncogene.* **1995**, *11*, 1581-1588.

86) W.S. el-Deiry, T. Tokino, V.E. Velculescu, D.B. Levy, R. Parsons, J.M. Trent, D. Lin, W.E. Mercer, K.W. Kinzler and B. Vogelstein. WAF1, a potential mediator of p53 tumour suppression. *Cell.* **1993**, *75*, 817-825.

87) A. Noda, Y. Ning, S.F. Venable, O.M. Pereira-Smith and J.R. Smith. Cloning of senescent cell-derived inhibitors of DNA synthesis using an expression screen. *Experimental Cell Research.* **1994**, *211*, 90-98.

88) Y. Gu, C.W. Turck and D.O. Morgan. Inhibition of CDK2 activity in vivo by an associated 20K regulatory subunit. *Nature.* **1993**, *366*, 707-710.

89) Y. Xiong, G.J. Hannon, H. Zhang, D. Casso, R. Kobayashi and D. Beach. p21 is a universal inhibitor of cyclin kinases. *Nature.* **1993**, *366*, 701-704.

90) Y. Xiong, H. Zhang and D. Beach. D type cyclins associate with multiple protein kinases and the DNA replication and repair factor PCNA. *Cell.* **1992**, *71*, 505-514.

91) R. Li, S. Waga, G.J. Hannon D. Beach and B. Stillman. Differential effects of the p21 CDK inhibitor on PCNA-dependent DNA replication and repair. *Nature*. **1994**, *371*, 534-537.

92) S.W. Blain, E. Montalvo and J. Massague. Differential interaction of the cyclin-dependent kinase (Cdk)inhibitor $p27^{Kip1}$ with cyclin A-Cdk2 and cyclin D2-Cdk4. *Journal of Biological chemistry*. **1997**, *272*, 25863-25872.

93) M. Cheng, P. Olivier, J.A. Diehl, M. Fero, M.F. Roussel, J.M. Roberts and C.J. Sherr. The p21(Cip1) and p27 (Kip1) CDK 'inhibitors' are essential activators of cyclin D-dependent kinases in murine fibroblasts *The EMBO Journal*. **1999**, *18*, 1571-1583.

94) C.J. Sherr and J.M. Roberts. CDK inhibitors: positive and negative regulators of G1-phase progression. *Genes and Development*. **1999**, *13*, 1501-1512.

95) A. Montagnoli, F. Fiore, E. Eytan, A.C. Carrano, G.F. Draetta, A. Hershko and M. Pagano. Ubiquitination of p27 is regulated by Cdk-dependent phosphorylation and trimeric complex formation. *Genes and Development*. **1999**, *13*, 1181-1189.

96) H. Hirai, M.F. Roussel, J.Y. Kato, R.A. Ashmun and C.J. Sherr. Novel INK4 proteins, p19 and p18, are specific inhibitors of the cyclin D-dependent kinases CDK4 and CDK6. **1995**, *15*, 2672-2681.

97) D.E. Quelle, R.A. Ashmun, G.J. Hannon, P.A. Rehberger, D. Trono, K.H. Richter, C.Walker, D. Beach, C.J. Sherr and M. Serrano. Cloning and characterisation of murine p16INK4a and p15INK4b genes. *Oncogene*. **1995**, *11*, 635-645.

98) F. Zindy, D.E. Quelle, M.F, Roussel and C.J. Sherr. Expression of the p16INK4a tumour suppressor versus other INK4 family members during mouse development and ageing. *Oncogene*. **1997**, *15*, 203-211.

99) A.J. Brenner, M.R. Stampfer and C.M. Aldaz. Increased p16 expression with first senescence arrest in human mammary epithelial cells and extended growth capacity with p16 inactivation. *Oncogene*. **1998**, *17*, 199-205.

100) Y. Xiong, H. Zhang and D. Beach. Subunit rearrangement of the cyclin-dependent kinases is associated with cellular transformation. *Genes and Development*. **1993**, *7*, 1572-1583.

101) D. Duro, O. Bernard, V. Della Valle, R. Berger and C.J. Larsen. A new type of p16INK4/MTS1 gene transcript expressed in B-cell malignancies. *Oncogene*. **1995**, *11*, 21-29.

102) S.M. Ivanchuck, S. Mondal, P.B. Dirks and J.T. Rutka. The INK4A/ARF Locus: Role in cell cycle control and apoptosis and implications for glioma growth. *Journal of Neuro-Oncology.* **2001**, *51*, 219-229.

103) D.E. Quelle, F, Zindy, R.A. Ashmun and C.J. Sherr. Alternative reading frames for the INK4a tumour suppressor gene encode two unrelated proteins capable of inducing cell cycle arrest. *Cell.* **1995**, *83*, 993-1000.

104) J. Pomerantz, N. Schreiber-Agus, N.J. Liegeois, A. Silverman, L. Alland, L. Chin, J. Potes, K. Chen, I. Orlow, H.W. Lee, C. Cordon-Cardo and R.A. DePinho. The Ink4a tumour suppressor gene product, p19Arf, interacts with MDM2 and neutralises MDM2's inhibition of p53. *Cell.* **1998**, *92*, 713-723.

105) H.X. An, D. Niederacher, F. Picard, C. van Roeyen, H.G. Bender and M.W. Beckman. Frequent allele loss on 9p21-22 defines a smallest common region in the vicinity of the CDKN2 gene in sporadic breast cancer. *Genes Chromosomes Cancer.* **1996**, *17*, 14-20.

106) W. Arap, E. Knudsen, D.A Sewell, D. Sidransky, J.Y. Wang, H.J. Huang and W.K. Cavanee. Functional analysis of wild-type and malignant glioma derived CDKN2Abeta alleles: evidence for an RB-independent growth suppressive pathway. *Oncogene.* **1997**, *15*, 2013-2020.

107) T. Kamijo, F. Zindy, M.F. Roussel, D.E. Quelle, J.R Downing, R.A. Ashmun, G. Grosveld and C.J. Sherr. Tumour suppression at the mouse INK4a locus mediated by the alternative reading frame product p19ARF. *Cell.* **1997**, *91*, 649-659.

108) L. Zhu, S. van den Heuvel, K. Helin, A. Fattaey, M. Ewen, D. Livingston, N. Dyson and E. Harlow. Inhibition of cell proliferation by p107, a relative of the retinoblastoma protein. *Genes and Development.* **1993**, *7*, 1111-1125.

109) J. DeGregori, G. Leone, K. Ohtani, A. Miron and J.R. Nevins. E2F-1 accumulation bypasses a G1 arrest resulting from the inhibition of G1 cyclin-dependent kinase activity. *Genes and Development.* **1995**, *9*, 2873-2887.

110) J. Lukas, B.O. Petersen, K. Holm, J. Bartek and K. Helin. Deregulated expression of E2F family members induces S-Phase entry and overcomes $p16^{INK4a}$-mediated growth suppression. *Molecular and Cellular Biology.* **1996**, *16*, 1047-1057.

111) J. DeGregori, G. Leone, A. Miron, L. Jakoi and J.R. Nevins. Distinct roles for E2F proteins in cell growth control and apoptosis. *Proceedings of the National Academy of Sciences of the United States of America.* **1997**, *94*, 7245-7250.

112) B. Shan, and W.H. Lee. Deregulated expression of E2F1 induces S-Phase entry and leads to apoptosis. *Molecular and Cellular Biology.* **1994**, *14*, 8166-8173.

113) T.F. Kowalik, J. DeGregori, J.K. Schwarz and J.R. Nevins. E2F1 overexpression in quiescent fibroblasts leads to an induction of cellular DNA synthesis and apoptosis. *Journal of Virology.* **1995**, *69*, 2491-2500.

114) S.W. Hiebert, G. Packham, D.K. Strom, R. Haffner, M. Oren, G. Zambetti and J.L. Cleveland. E2F-1:DP-1 induces p53 and overrides survival factors to trigger apoptosis. *Molecular and Cellular Biology.* **1995**, *15*, 6864-6874.

115) T.F. Kowalik, J. DeGregori, G. Leone, L. Jakoi and J.R. Nevins. E2F1-specific induction of apoptosis and p53 accumulation, which is blocked by Mdm2. *Cell Growth and Differentiation.* **1998**, *9*, 113-118.

116) L.J. Ko and C. Prives. p53: puzzle and paradigm. *Genes and Development.* **1996**, *10*, 1054-1072.

117) T. Crook, N.J. Marston, E.A. Sara and K.H. Vousden. Transcriptional activation by p53 correlates with suppression of growth but not transformation. *Cell.* **1994**, *79*, 817-827.

118) E. White. Life, death, and the pursuit of apoptosis. *Genes and Development.* **1996**, *10*, 1-15.

119) D.P. Lane. p53, guardian of the genome. *Nature.* **1992**, *258*, 15-16.

120) N.C. Reich and A.J. Levine. Growth regulation of a cellular tumour antigen, p53, in non-transformed cells. *Nature.* **1984**, *308*, 199-201.

121) P.B. Dirks, J.T. Rutka, S.L. Hubbard, S. Mondal and P.A. Hamel. The E2F-family proteins induce distinct cell cycle regulatory factors in p16-arrested, U343 astrocytoma cells. *Oncogene.* **1998**, *17*, 867-876.

122) K. Martin, D. Trouche, C. Hagemeier, T.S. Sorensen, N.B. La Thangue and T. Kouzarides. Stimulation of E2F1/DP1 transcriptional activity by MDM2 oncoprotein. *Nature.* **1995**, *375*, 691-694.

123) Y. Haupt, R. Maya, A. Kazaz and M. Oren. Mdm2 promotes the rapid degradation of p53. *Nature.* **1997**, *387*, 296-299.

124) Z.X. Xiao, J. Chen, A.J. Levine, N. Modjtahedi, J. Xing, W.R. Sellers and D.M. Livingston. Interaction between the retinoblastoma protein and the oncoprotein Mdm2. *Nature*. **1995**, *375*, 694-698.

125) D.A. Haas-Kogan, S.C. Kogan, D. Levi, P. Dazin, A. T'Ang, Y.K. Fung and M.A. Israel. Inhibition of apoptosis by the retinoblastoma gene product. *The EMBO Journal*. **1995**, *14*, 461-472.

126) K.F. Macleod, Y.W. Hu and T. Jacks. Loss of Rb activates both p-53-dependent and independent cell death pathways in the developing mouse nervous system. *The EMBO Journal*. **1996**, *15*, 6178-6188.

127) E. Zacksenhaus, Z. Jiang, D. Chung, J.D. Marth, R.A. Phillips and B.L. Gallie. pRb controls proliferation, differentiation and death of skeletal muscle cells and other lineages during embryogenesis. *Genes and Development*. **1996**, *10*, 3051-3064.

128) G.W. Demers, S.A. Foster, C.L. Halbert and D.A. Galloway. Growth arrest by induction of p53 in DNA damaged keratinocytes is bypassed by human papillomavirus 16 E7. *Proceedings of the National Academy of Sciences of the United States of America*. **1994**, *91*, 4382-4386.

129) S.W. Lowe and H.E. Ruley. Stabilisation of the p53 tumour suppressor is induced by adenovirus-5 E1A and accompanies apoptosis. *Genes and Development*. **1993**, *7*, 535-545.

130) K.Y. Tsai, Y. Hu, K.F. Macleod, D. Crowley, L. Yamasaki and T. Jacks. Mutation of E2F1 suppresses apoptosis and inappropriate S-phase entry and extends survival of RB-deficient mouse embryos. *Molecular Cell*. **1998**, *2*, 293-304.

131) H. Hermeking, C. Lengauer, K. Polyak, T.C. He, L. Zhang, S. Thiagalingam, K.W. Kinzler and B. Vogelstein. 14-3-3σ is a p53-regulated inhibitor of G2/M progression. *Molecular Cell*. **1997**, *1*, 3-11.

132) C.J. Sherr. Tumour surveillance via the ARF-p53 pathway. *Genes and Development*. **1998**, *12*, 2984-2991.

133) T. Kamijo, J.D. Weber, G. Zambetti, F. Zindy, M.F. Roussell and C.J. Sherr. Functional and physical interactions of the ARF tumour suppressor with p53 and Mdm2. *Proceedings of the National Academy of Sciences of the United States of America*. **1998**, *95*, 8292-8297.

134) M. Serrano, H.W. Lee, L. Chin, C. Cordon-Cardo, D. Beach and R.A. DePinho. Role of the INK4a locus in tumour suppression and cell mortality. *Cell*. **1996**, *85*, 27-37.

135) M.G. Paggi, A. Baldi, F. Bonetto and A. Giordano. Retinoblastoma protein family in cell cycle and cancer. *Journal of Cellular Biochemistry.* **1996**, *62*, 418-430.

136) M. Hall and G. Peters. Genetic alterations of cyclins, cyclin-dependent kinases and cdk inhibitors in human cancer. *Advances in Cancer Research.* **1996**, *68*, 67-108.

137) E. Harlow. A research shortcut from a common cold virus to human cancer. *Cancer.* **1996**, *78*, 558-565.

138) M. Hollstein, D. Sidransky, B. Vogelstein and C.C. Harris. p53 mutations in human cancers. *Science.* **1991**, *253*, 49-53.

139) S.J. Field, F.Y. Tsai and F. Kuo. E2F1 functions in mice to promote apoptosis and suppress proliferation. *Cell.* **1996**, *85*, 549-561.

140) L. Yamasaki, T. Jacks, R. Bronson, E. Goillot, E. Harlow and N.J. Dyson. Tumour induction and tissue atrophy in mice lacking E2F1. *Cell.* **1996**, *85*, 537-548.

141) R.A. Weinberg. E2F and cell proliferation: a world turned upside down. *Cell.* **1996**, *85*, 457-459.

142) M. Saito, K. Helin, M.B. Valentine, B.B. Griffith, C.L. Willman, E. Harlow and A.T. Look. Amplification of the E2F1 transcription factor gene in the HEL erythroleukaemia cell line. *Genomics.* **1995**, 25, 130-138.

143) T. Yoshitaka, N. Matsubara, M. Ikeda, M. Tanino, H. Hanafusa, N. Tanaka and K. Shimuzu. Mutations of E2F4 trinucleotiderepeats in colorectal cancer with microsattelite instability. *Biochemical and Biophysical Research Communications.* **1996**, *227*, 553-557.

144) T.L. Sladek. E2F transcription factor action, regulation and possible role in human cancer. *Cell Proliferation.* **1997**, *30*, 97-105.

145) P.L. Durette, F. Baker, P.L. Barker, J. Boger, S.S. Bondy, M.L. Hammond, T.J. Lanza, A.A. Pessolano and C.G. Caldwell. Total synthesis of L-156,602, a novel cyclic hexadepsipeptide antibiotic. *Tetrahedron Letters.* **1990**, *31*, 1237-1240.

146) C.G. Caldwell, K.M. Rupprecht, S.S. Bondy and A.A. Davis. Synthesis of the lipophilic side chain of the cyclic hexadepsipeptide antibiotic L-156,602. *Journal of Organic Chemistry.* **1990**, *55*, 2355-2361.

147) H. Wissman, H.J. Kleiner. New peptide synthesis. *Angewandte Chemie International Addition.* **1980**, *19*, 133-134.

148) D. Seebach, R. Naef and G. Calderari. α-Alkylation of α-heterosubstituted carboxylic acids without racemisation. *Tetrahedron.* **1984**, *40*, 1313-1324.

149) D. Seebach and D. Wasmuth. Herstellung von erythro-2-hydroxybernsteinsäure-Derivaten aus Äpfelsäureester. *Helvetica Chimica Acta.* **1980**, *63*, 197-200.

150) O. Dangles, F. Guibe, G. Balavoine, S. Lavielle and A. Marquet. Selective cleavage of the allyl and (allyloxy)carbonyl groups through palladium-catalyzed hydrostannolysis with tributyltin hydride. Application to the selective protection-deprotection of amino acid derivatives and in peptide synthesis. *Journal of Organic Chemistry.* **1987**, *52*, 4984-4993.

151) C.H. Hassall, W.H. Johnson and C.J. Theobald. Amino-acids and peptides. Part 21. Synthesis of a congener of the cyclohexadepsipeptide antibiotic, Monamycin. *Journal of the Chemical Society, Perkin Transactions 1.* **1979**, 1451-1454.

152) L.A. Carpino, B.J. Cohen, K.E. Stephens Jr, S.Y. Sadat-Aalaee, J.H.Tien and D.C. Langridge. (Fluoren-9-ylmethoxy)carbonyl (Fmoc) amino acid chlorides. Synthesis, characterization, and application to the rapid synthesis of short peptide segments. *Journal of Organic Chemistry.* **1986**, *51*, 3732-3734.

153) C.G. Caldwell and S.S. Bondy. A convenient synthesis of enantiomerically pure (2*S*,3*S*)- or (2*R*,3*R*)-3-hydroxyleucine. *Synthesis.* **1990**, 34-36.

154) G. Frater. Über die Stereospezifität der α-Alkylierung von β-Hydroxycarbonsäureestern. Vorläufige Mitteilung. *Helvetica Chimica Acta.* **1979**, *62*, 2825-2828.

155) D.S. Matteson, K.M. Sadhu and M.L. Peterson. 99% Chirally selective synthesis via pinanediol boronic esters: insect pheromones, diols and an amino alcohol. *Journal of the American Chemical Society.* **1986**, *108*, 810-819.

156) B. Castro, J.R. Dormoy, G. Evin and C. Selve. Reactifs de couplage peptidique IV (1)- L'hexafluorophosphate de benzotrizolyl N-oxytrisdimethylamino phosphonium (BOP). *Tetrahedron Letters.* **1975**, *14*, 1219-1222.

157) H. Wissman, and H.-J. Kleiner. New Peptide Synthesis. *Angewandte Chemie International Edition.* **1980**, *19*, 133-194.

158) (a) K.J. Hale and J. Cai. Asymmetric total synthesis of antitumour antibiotic A83586C. *Chemical Communications.* **1997**, *23*, 2319-2320.
(b) K.J. Hale, J. Cai and V.M. Delisser. Asymmetric synthesis of the C(1)-C(47) backbone of antitumour antibiotic A83586C. *Tetrahedron Letters.* **1996**, *37*, 9345-9348. (c) K.J. Hale and J. Cai. Synthetic studies on the

azinothricin family of antitumour antibiotics. 5. Asymmetric synthesis of two activated esters for the northern sector of A83586C. *Tetrahedron Letters*. **1996**, *37*, 4233-4236. (d) K.J. Hale, J. Cai, S. Manaviazar and S.A. Peak. Synthetic studies on the azinothricin family of antibiotics. 4. Enantioselective synthesis of the northern half of antitumour antibiotics A83586C and citropeptin. *Tetrahedron Letters*. **1995**, *36*, 6965-6968.

(e) K.J. Hale, V.M. Delisser, L.-K. Yeh, S.A. Peak, S. Manaviazar and G.S. Bhatia. Synthetic studies on the azinothricin family of antibiotics. 3. Enantioselective synthesis of a haxadepsipeptide precursor for antitumour antibiotic A83586C. *Tetrahedron Letters*. **1994**, *35*, 7685-7688. (f) K.J. Hale, G.S. Bhatia S.A. Peak and S. Manaviazar. Synthetic studies on the azinothricin family of antibiotics. 2. Asymmetric synthesis of the C(28)-C(47) subunit of A83586C. *Tetrahedron Letters*. **1993**, *34*, 5343-5346.

159) (a) D.A. Evans, J. Bartroli and T.L. Shih. Enantioselective aldol condensations. 2. Erythro-selective chiral aldol condensations via boron enolates. *Journal of the American Chemical Society*. **1981**, *103*, 2127-2129.

(b) R. Baker and J.L. Castro. Total synthesis of (+)-macbecin I. *Journal of the Chemical Society, Perkin Transactions. 1*. **1990**, 47-65.

160) B.M. Trost and D.P. Curran. Chemoselective oxidation of sulfides to sulfones with potassium hydrogen persulfate. *Tetrahedron Letters*. **1981**, *22*, 1287-1290.

161) H.A. Vaccaro, D.A. Levy, A. Sawabe, T. Jaetsch and S. Masamune. Towards the synthesis of Calyculin. A synthetic intermediate corresponding to the C(26)-C(37) fragment. *Tetrahedron Letters*. **1992**, *33*, 1937-1940.

162) T. Suzuki, H. Saimoto, H. Tomioka, K. Oshima and H. Nozaki. Regio- and stereoselective ring-opening of epoxy alcohols with organoaluminium compounds leading to 1,2-diols. *Tetrahedron Letters*. **1982**, *23*, 3597-3600.

163) S. Takano, M. Akiyama, S. Sato and K. Ogasawara. *Chemistry Letters*. **1983**, 1593-1596.

164) A.B. Smith III, K.J. Hale and J.P. McCauley Jr. An efficient new method for the desulfonylation of β-keto phenylsulfones. *Tetrahedron Letters*. **1989**, *30*, 5579-5582.

165) J.K. Stille. The palladium catalysed cross coupling reactions of organotin reagents with organic electrophiles [New synthetic methods (58)]. *Angewandte Chemie International Edition*. **1986**, *25*, 508-524.

166) J.E. McMurry and W.J. Scott. A method for the regiospecific synthesis of enol triflates by enolate trapping. *Tetrahedron Letters*. **1982**, *24*, 979-982.

167) K.B. Sharpless, W. Amberg, Y.L. Bennani, G.A. Crispino, J. Hartung, K.-S. Jeong, H.-L. Kwong, K. Morikawa, Z.-W. Wang, D. Xu and X.-L. Zhang. The osmium-catalysed asymmetric dihydroxylation: a new ligand class and a process improvement. *Journal of Organic Chemistry*. **1992**, *57*, 2768-2771.

168) (a) E.J. Corey and M. Chaykovsky. A new synthesis of ketones. *Journal of the American Chemical Society*. **1964**, *86*, 1639-1640.

(b) E.J. Corey and M. Chaykovsky. Methylsulfinyl carbanion (CH_3-SO_2-CH_2^-). Formation and applications to organic synthesis. *Journal of the American Chemical Society*. **1965**, *87*, 1345-1353.

169) K. Horita, T. Yoshioka, T, Tanaka, Y. Oikawa and O. Yonemitsu. On the selectivity of deprotection of benzyl, mpm (4-methoxybenzyl) and dmpm (3,4-dimethoxybenzyl) protecting groups for hydroxyl function. *Tetrahedron*. **1986**, *42*, 3021-3028.

170) (a) K.J. Hale, V.M. Delisser and S. Manaviazar. Azinothricin synthetic studies 1. Efficient asymmetric synthesis of (3*R*)- and (3*S*)- piperazic acids. *Tetrahedron Letters*. **1992**, *33*, 7613-7616.

(b) K.J. Hale, J. Cai V.M. Delisser, S. Manaviazar, A. Peak, G.S. Bhatia, T.C. Collins and N. Jogiya. Enantioselective synthesis of (3R)- and (3S)-piperazic acid. The comparative unimportance of DMPU mediated retrohydrazination. *Tetrahedron*. **1996**, *52*, 1047-1068.

(c) K.J. Hale, N. Jogiya, and S. Manaviazar. Monamycin synthetic studies. Part. 1. An enantiospecific total synthesis of (3*S*,5*S*)-5-hydroxypiperazic acid from D-mannitol. *Tetrahedron Letters*. **1998**, *39*, 7163-7166.

171) K.J. Hale, S. Manaviazar and V.M. Delisser. A practical new asymmetric synthesis of (2*S*,3*S*)- and (2*R*,3*R*)-3-hydroxyleucine. *Tetrahedron*. **1994**, *50*, 9181-9188.

172) (a) D.A. Evans, T.C. Britton, R.L. Dorow and J.F. Dellaria. Stereoselective amination of chiral enolates. A new approach to the asymmetric synthesis of α-hydrazino and α-amino acid derivatives. *Journal of the American Chemical Society*. **1986**, *108*, 6395-6397.

(b) D.A. Evans, T.C. Britton, R.L. Dorow and J.F. Dellaria. The asymmetric synthesis of α-hydrazino and α-amino acid derivatives via the stereoselective amination of chiral enolates with azodicarboxylate esters. *Tetrahedron*. **1988**, *44*, 5525-5540.

173) R.A. Boissannas, S.T. Guttmann and P.-A. Jaquenoud. Synthèse de la L-arginyl-L-prolyl-L-prolyl-glycyl-L-phénylalanyl-L-Séryl-L-prolyl-L-phénylalanyl-L-arginine, un nonapeptide présentant les propriétés de la bradykinine. *Helvetica Chimica Acta*. **1960**, *43*, 1349-1358.

174) H.T. Cheung and E.R. Blout. The hydrazide as a carboxylic protecting group in peptide synthesis. *Journal of Organic Chemistry*. **1965**, *30*, 315-316.

175) L.A. Carpino. 1-Hydroxy-7-azabenzotriazole: an efficient peptide coupling additive. *Journal of the American Chemical Society*. **1993**, *115*, 4397-4398.

176) K.J. Hale, J. Cai and G. Williams. Total synthesis of 4-*Epi*-A83586C. Epimerisation in a macrolactamisation mediated by BOP and DMAP. *Synletters*. **1998**, 149-152.

177) K.J. Hale and L. Lazarides. Synthesis of an L-proline modified mimetic of the A83586C antitumour cyclodepsipeptide. *Chemical Communications*. **2002**, *17*, 1832-1833.

178) M.R. Attwood, C.H. Hassall, A. Krohn, G. Lawton and S. Redshaw. The design and synthesis of the angeotensin converting enzyme inhibitor cilazapril and related bicyclic compounds. *Journal of the Chemical Society, Perkin Transactions. 1*. **1986**, 1011-1019.

179) L.A. Carpino and G.Y. Han. 9-Fluorenylmethoxycarbonyl amino-protecting group. *Journal of Organic Chemistry*. **1972**, *37*, 3404-3409.

180) (a) T.B. Windholz and D.B.R. Johnston. Trichloroethoxycarbonyl: a generally applicable protecting group. *Tetrahedron Letters*. **1967**, *8*, 2555-2557.

(b) F.R. Pfeiffer, S.R. Cohen and J.A. Weisbach. Glycerolipids. II. Use of the β,β,β-trichloroethoxycarbonyl protecting group in phosp-Hatidylethanolamine synthesis. *Journal of Organic Chemistry*. **1969**, *34*, 2795-2796.

181) K.J. Hale and L. Lazarides. Synthetic route to the GE3 cyclodepsipeptide. *Organic Letters*. **2002**, *4*, 1903-1906.

190) L. Lazarides. Synthetic studies on the A83586C/GE3 family of antitumour antibiotics. *Thesis*. **2004**, 82-84.

191) K.J. Hale, L. Lazarides and J. Cai. A synthetic strategy for the cyclodepsipeptide core of the antitumour antibiotic verucopeptin. *Organic Letters*. **2001**, *3*, 2927-2930.

192) L. Lazarides. Synthetic studies on the A83586C/GE3 family of antitumour antibiotics. *Thesis*. **2004**, 62-64.

193) T. Kolasa and A. Chimiak. *O*-Protected derivatives of *N*-hydroxy-amino acids. *Tetrahedron*. **1974**, *30*, 3591-3595.

194) G.C. Stelakatos, A. Paganou and L. Zervas. New methods in peptide synthesis. Part III. Protection of carboxyl group. *Journal of the Chemical Society*. **1966**, *C*, 1191-1199.

195) J.C. Sheehan and G.P. Hess. A new method of forming peptide bonds. *Journal of the American Chemical Society*. **1955**, *77*, 1067-1068.

196) R.D. Tung and D.H. Rich. Bis(2-oxo-3-oxazolidinyl)phosphinic Chloride (1) as a coupling reagent for *N*-alkyl amino acids. *Journal of the American Chemical Society*. **1985**, *107*, 4342-4343.

197) Y. Noguchi, H. Uchiro, T. Yamada and S. Kobayashi. Synthetic study of polyoxypeptin: stereoselective synthesis of (2*S*,3*R*)-3-hydroxy-3-methylproline. *Tetrahedron Letters*. **2001**, *42*, 5253-5256.

198) D.-G. Qin, H.-Y Zha and Z.-J. Yao. Enantioselective synthesis of (2*S*,3*R*)-3-hydroxy-3-methylproline, a novel amino acid found in polyoxypeptins. *Journal of Organic Chemistry*. **2002**, *67*, 1038-1040.

199) K. Makino, A. Kondoh and Y. Hamada. Synthetic studies on Polyoxypeptins: stereoselective synthesis of (2*S*,3*R*)-3-hydroxy-3-methylproline using SmI_2-mediated cyclisation. *Tetrahedron Letters*. **2002**, *43*, 4695-4698.

200) C.H. Hassall and K.L. Ramachandran. The synthesis of (3*S*,5*S*)-5-Hydroxyhexahydropyridazine-3-carboxylic acid. *Heterocycles*. **1977**, *7*, 119-122.

201) (a) T.M. Kamenecka and S.J. Danishefsky. Total synthesis of Himastatin: confirmation of the revised stereostructure. *Angewandte Chemie International Edition*. **1998**, *37*. 2995-2998.

(b) K.M. Depew, T.M. Kamenecka and S.J. Danishefsky. Enantioselective synthesis of protected forms of (3*R*,5*R*)-5- hydroxypiperazic acid useful for synthesis. *Tetrahedron Letters*. **2000**, *41*, 289-292.

202) Y. Noguchi, T. Yamada, H. Uchiro and S. Kobayashi. Synthetic study of polyoxypeptin: stereoselective synthesis of the acyl side-chain segment. *Tetrahedron Letters*. **2000**, *41*, 7499-7502.

203) M. Lorca and M. Kurosu. A practical synthesis of the lipophilic side chain of the polyoxypeptins. *Tetrahedron Letters*. **2001**, *42*, 2431-2434.

204) D.-G. Qin and Z.-J. Yao. An efficient enantioselective synthesis of the acyl side chain of polyoxypeptins. *Tetrahedron Letters*. **2003**, *44*, 571-574.

205) Y. Noguchi, T. Yamada, H. Uchiro and S. Kobayashi. Pd-catalysed hydrogenolysis of 4,5-epoxy-2-alkenoates: mode study of the acyl side chain of polyoxypeptin. *Tetrahedron Letters*. **2000**, *41*, 7493-7497.

206) V. Schurig, U. Leyrer and D. Wistuba. Simple access to highly enantiomerically enriched (S)-3-methyl-1-pentanol, (S)-3-methyl-1-pentene (2S,3S)-2-deuterio-3-methyl-1- pentanol and (2S,3S)-3-methyl-2-pentanol from natural (L)- isoleucine. *Journal of Organic Chemistry*. **1986**, *51*, 242-245.

207) T. Katsuki and B.K. Sharpless. The first practical method for asymmetric epoxidation. *Journal of the American Chemical Society*. **1980**, *102*, 5974-5976.

208) W.C. Still and C. Gennari. Direct synthesis of Z-unsaturated esters. A useful modification of the Horner-Emmons olefination. *Tetrahedron Letters*. **1983**, *24*, 4405-4408.

209) Y. Gao, R.M. Hanson, J.M. Klunder, S.Y. Ko, H. Masamune and B.K. Sharpless. Catalytic asymmetric epoxidation and kinetic resolution: modified procedures including in situ derivatization. *Journal of the American Chemical Society*. **1987**, *109*, 5765-5780.

210) U. Peters, W. Bankova and P. Welzel. Platelet activating factor synthetic studies. *Tetrahedron*. **1987**, *43*, 3803-3816.

211) C.A. Broka and J. Ehler. Enantioselective total synthesis of bengamides B and E. *Tetrahedron Letters*. **1991**, *32*, 5907-5910.

212) A. Blanchette, W. Choy, J.T. Davies, A.P. Essenfield, S. Masamune, W.R. Roush and T. Sakai. Horner-Wadsworth-Emmons reaction: use of lithium chloride and an amine for base sensitive compounds. *Tetrahedron Letters*. **1984**, *25*, 2183-2186.

213) V. Jäger and V. Wehner. 2-*O*-Benzylglyceraldehyde: A synthetic building block available in both enantiomeric forms and configurationally stable owing to rapid oligomerisation. *Angewandte Chemie International Edition*. **1989**, *4*, 469-470.

214) K.S. Lam, G.A. Hesler, J.M. Mattei, S.W. Mamber, S. Forenza and K. Tomita. Himastatin, a new antitumour antibiotic from streptomyces hygroscopius. I. Taxonomy of producing organism, fermentation and biological activity. *Journal of Antibiotics*. **1990**, *43*, 956-960.

215) U. Ravid, R.M. Silverstein and L.R. Smith. Synthesis of the enantiomers of 4-substituted γ-lactones with known absolute configuration. **1978**, *34*, 1449-1452.

216) P.-T. Ho and N. Davies. A practical synthesis of (R)-(-)- γ- hydroxymethyl- γ-butyrolactone from natural glutamic acid. *Synthesis*. **1983**, 462.

217) K. Tago, M. Arai and H. Kogen. A practical total synthesis of plaunotol *via* highly *Z*-selective Wittig olefination of α-acetal ketones. *Journal of the Chemical Society. Perkin* E.N. *Transactions 1*. **2000**, 2073-2078.

218) Jacobsen, I. Marko, W. Mungall, G. Schroder and B.K. Sharpless. Asymmetric dihydroxylation via ligand-accelerated catalysis. *Journal of the American Chemical Society*. **1988**, *110*, 1968-1970.

219) E.J. Corey and J.A. Katzenellenbogen. Stereospecific Synthesis of trisubstituted and tetrasubstituted olefins. Conjugate addition of dialkylcopper-lithium reagents to α,β-acetylinic esters. *Journal of the American Chemical Society*. **1969**, *91*, 1851-1852.

220) D.B. Dess and J.C. Martin. Readily accessible 12-I- 5 oxidant for the conversion of primary and secondary alcohols to aldehydes and ketones. *Journal of Organic Chemistry*. **1983**, *48*, 4155-4156.

221) M.J. Diem, D.F. Burow and J.L. Fry. Oxonium salt alkylation of structurally and optically labile alcohols. *Journal of Organic Chemistry*. **1977**, *42*, 1801-1802.

222) (a) M.D. Wittman, R.L. Halcomb and S.J. Danishefsky. On the conversion of biologically interesting amines to hydroxylamines. *Journal of Organic Chemistry*. **1990**, *55*, 1981-1983.

(b) A. Detomaso and R. Curci. Oxidation of natural targets by dioxiranes. Part 4: A novel approach to the synthesis of *N*-hydroxyamino acids using dioxiranes. *Tetrahedron Letters*. **2001**, *42*, 755-758.

223) (a) N. Baggett and P. Stribblehill. *Journal of the Chemical Society, Perkin Transactions*. **1977**, *1*, 1123-1126.
(b) C.L. Winn and J.M. Goodmann. Studies on the formation of tricyclic C_2-symmetric sulphide. *Tetrahedron Letters*. **2001**, *42*, 7091-7093.

224) R.W. Feenstra, E.H.M. Stokkingreef, R.J.F. Nivard and H.C.J. Ottenheijm. Interconversion or (*R*) and (*S*)-α-hydroxy esters: precursors of (*S*) and (*R*)-*O*-benzylhydroxylamino acid esters of high optical purity. *Tetrahedron*. **1988**, *44*, 5583-5595.

225) S.B. Balkrishna, W.E. Childers Jnr and H.W. Pinnick. Oxidation of α,β-unsaturated aldehydes. *Tetrahedron*. **1981**, *37*, 2091-2096.

226) Acid chloride **112** was synthesised using $(COCl)_2$ in CH_2Cl_2 on known Fmoc-*N*(Me)-D-Ala, which in turn was synthesised according to the method developed by R.M. Freidinger, J.S. Hinkle, and D.S. Perlow. Synthesis of 9-fluorenylmethyloxycarbonyl-protected N-alkyl amino acids by reduction of oxazolidinones. *Journal of Organic Chemistry* **1983**, *48*, 77-81.

227) J. Wang, Y. Okada, W. Li, T. Yokoi and J. Zhu. 2,2-Difluoro-1,3,2-oxazaborolidin-5-ones: novel approach for selective side-chain protection of serine and threonine. *Journal of the Chemical Society. Perkin Transactions 1*. **1997**, 621-624.

228) W.R. Roush, A.E. Walts and L.K. Hoong. Diastereo- and enantioselective aldehyde addition reactions of 2-allyl-1,3,2-dioxaborolane-4,5-dicarboxylic esters, a useful class of tartrate ester modified allylboronates. *Journal of the American Chemical Society*. **1985**, *107*, 8186-8190.

229) H.C. Brown and P.K. Jadhav. Asymmetric carbon-carbon bond formation via β-allyldiisopinocampheylborane. Simple synthesis of secondary homoallylic alcohols with excellent enantiomeric purities. *Journal of the American Chemical Society*. **1983**, *105*, 2092-2093.

230) H.C. Brown, K.S. Bhat and R.S. Randad. Chiral synthesis via organoboranes. 21. Allyl- and crotylboration of α-chiral aldehydes with diisopinocampheylboron as the chiral auxiliary. *Journal of Organic Chemistry*. **1989**, *54*, 1570-1576.

231) W.R. Roush, K. Ando, D.B. Powers, A.D. Palkowitz and R.L Halterman. Asymmetric synthesis using diisopropyl

232) G.F. Weber. The metastasis gene osteopontin: a candidate target for cancer therapy. *Biochimica et Biophysica Acta (BBA)- Reviews on Cancer*. **2001**, *1552*, 61-85.

233) P. Jung, M.V. Motwani and G.K. Schwartz. Flavopiridol increases sensitisation to gemcitabine in human gastrointestinal cancer cell lines and correlates with down- regulation of ribonucleotide reductase M2 subunit. *Clinical Cancer Research*. **2001**, *7*, 2527-2536.

234) Spectral data for all compounds here within are contained in Appendix 1.

235) W.C. Still, M. Kahn and A. Mitra. Rapid chromatographic technique for preparative separations with moderate resolution. *Journal of Organic Chemistry*. **1978**, *43*, 2923-2925.

Chapter 8: APPENDIX

NMR Spectra, FAM HRMS, IR SPECTRA

III-MW-159
in CDCl3 at 298 K

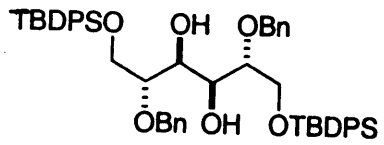

314

III-MW-159
Carbon 13
in CDCl3 at 298 K

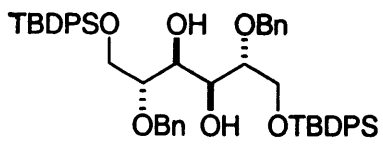

314

III-MW-159
DEPT in
CDCl3 at 298 K

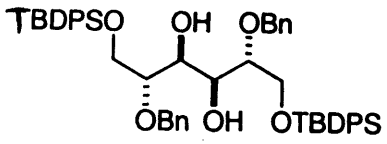

314

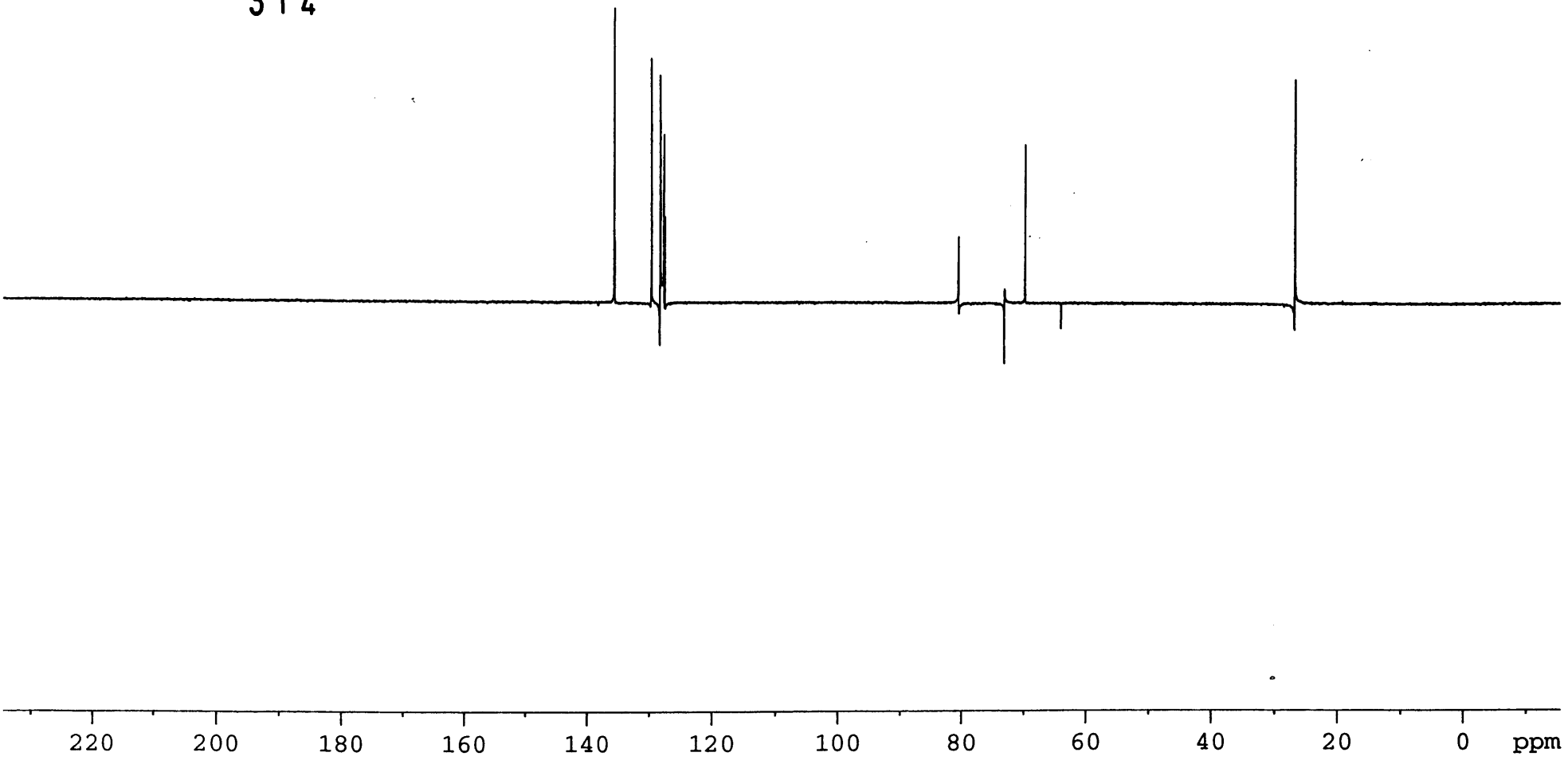

III-MW-159
COSY in
CDCl3 at 298 K

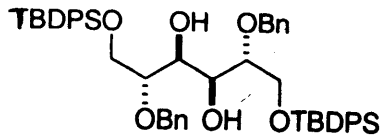

314

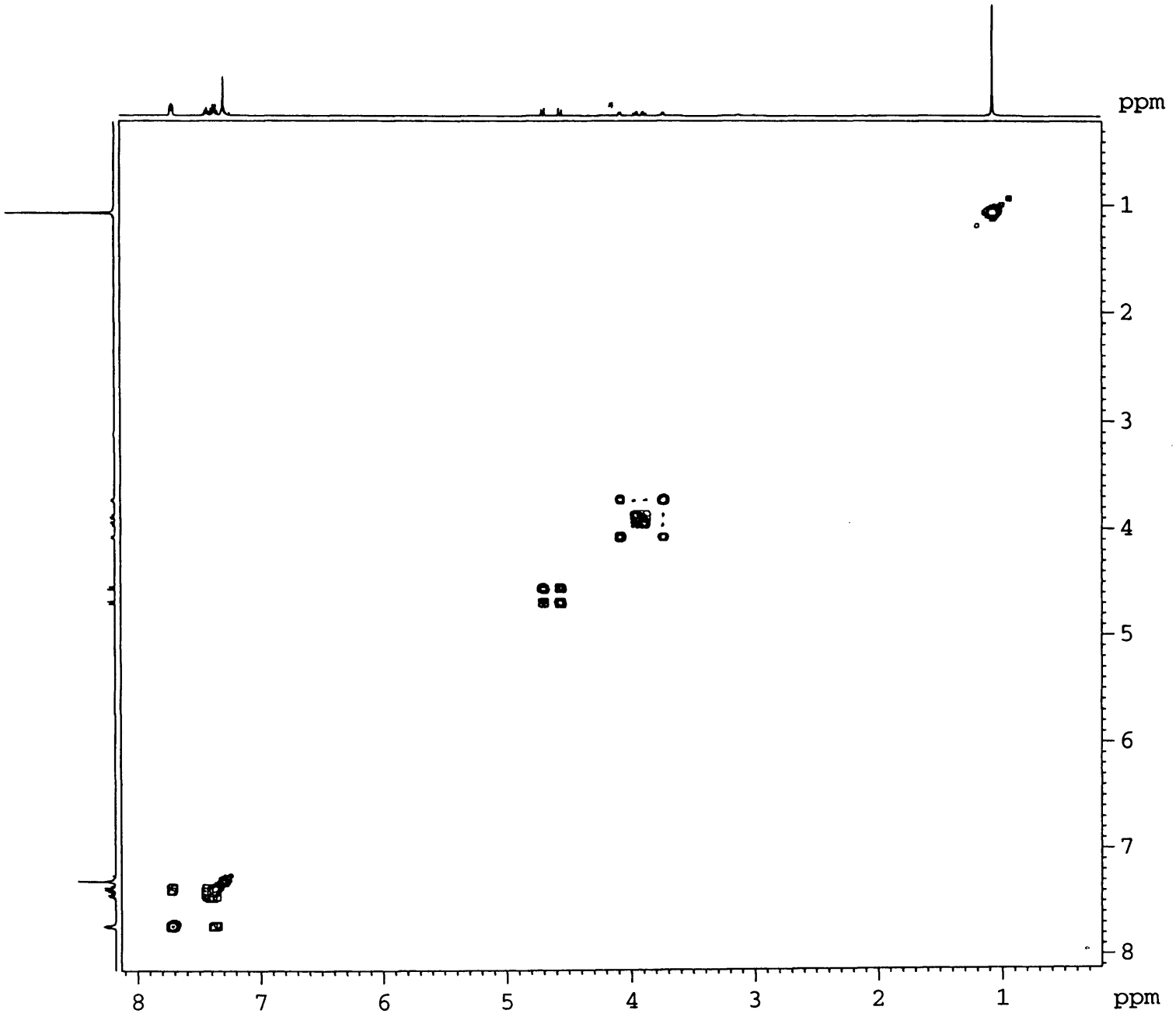

III-MW-159
HMQC in
CDCl3 at 298 K

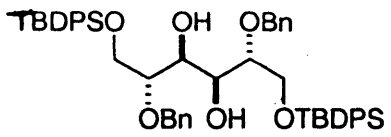

314

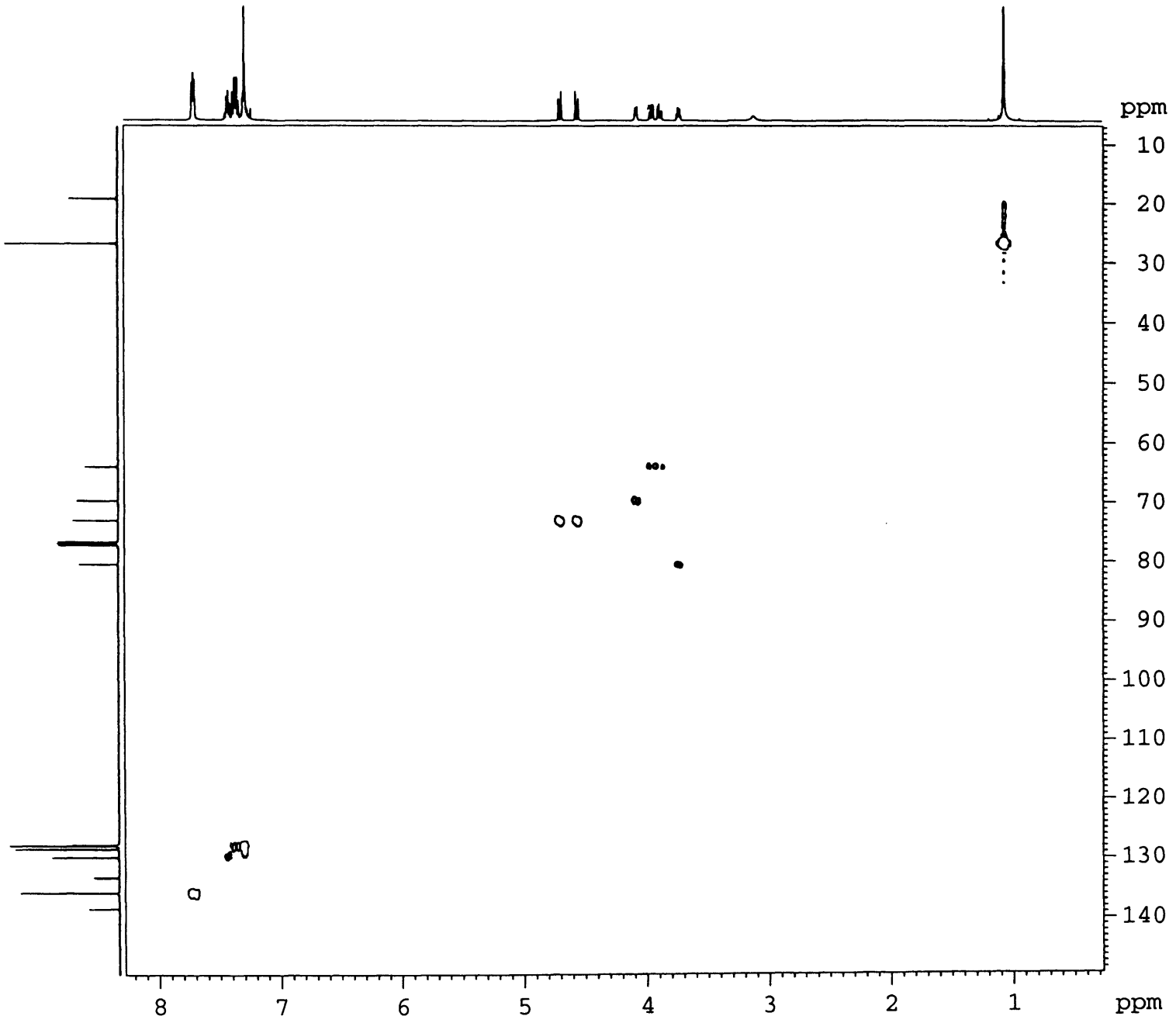

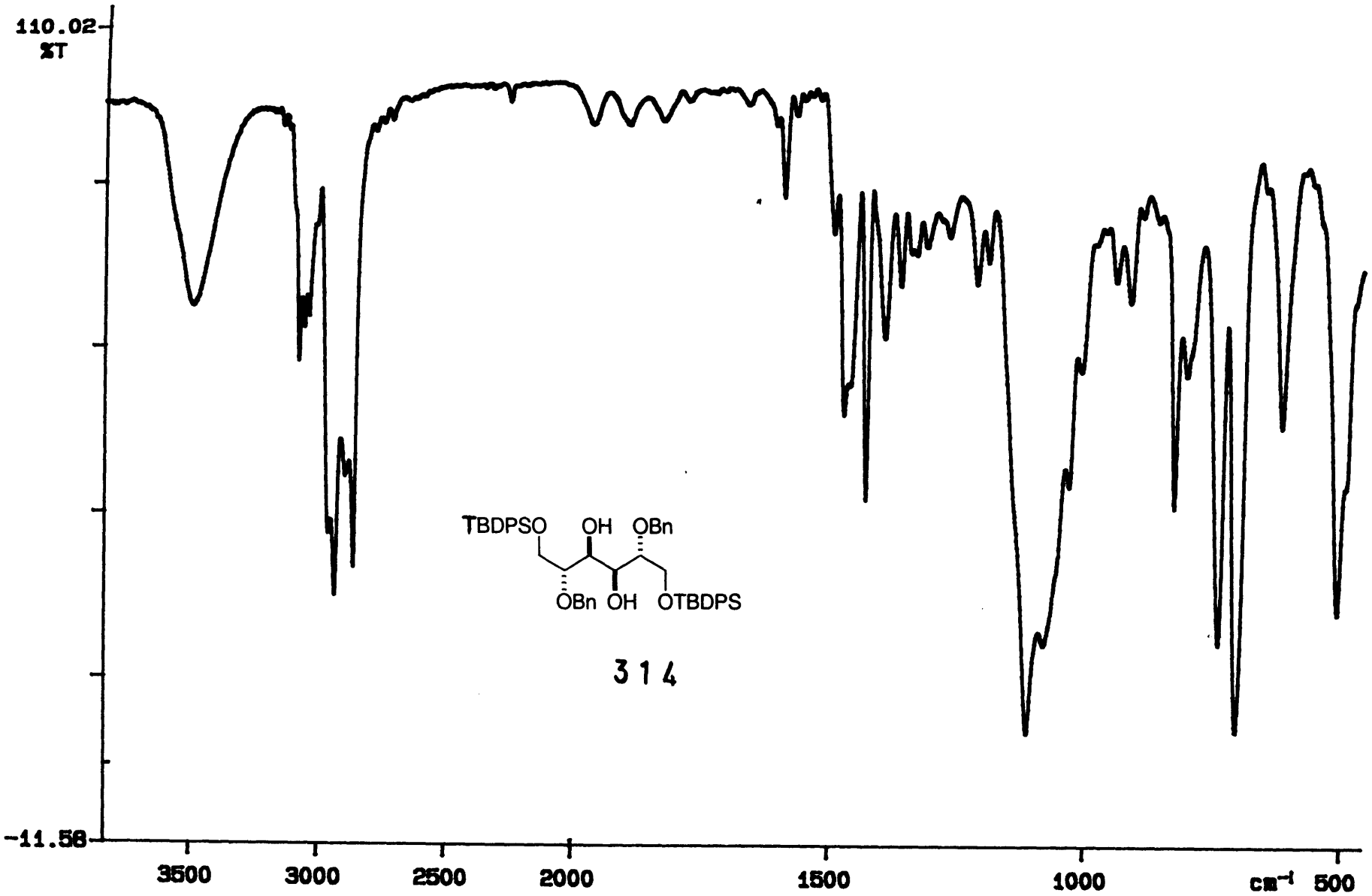
110.02
%T
-11.58
3500
3000
2500
2000
1500
1000
cm⁻¹
500
TBDPSO
OH
OBn
OBn
OH
OTBDPS

314

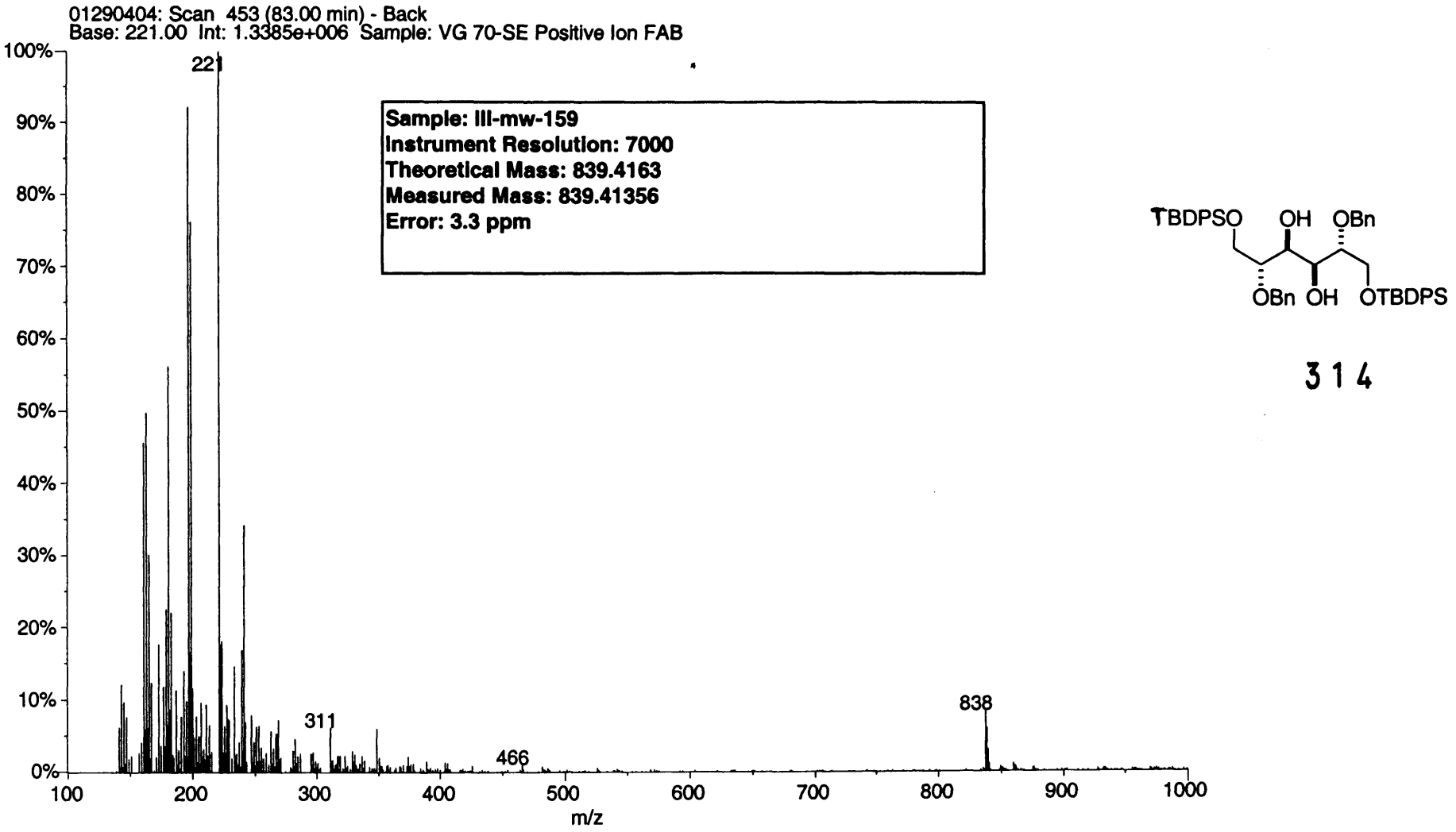
01290404: Scan 453 (83.00 min) - Back
Base: 221.00 Int: 1.3385e+006 Sample: VG 70-SE Positive Ion FAB
Sample: III-mw-159
Instrument Resolution: 7000
Theoretical Mass: 839.4163
Measured Mass: 839.41356
Error: 3.3 ppm
221
311
466
838
100%
90%
80%
70%
60%
50%
40%
30%
20%
10%
0%
100
200
300
400
500
600
700
800
900
1000
m/z

TBDPSO
OH
OBn
OBn
OH
OTBDPS

314

III-MW-166
in CDCl3 at 298 K

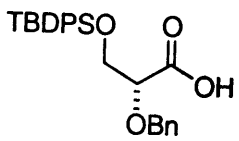

315

III-MW-166
Carbon 13
in CDCl3 at 298 K

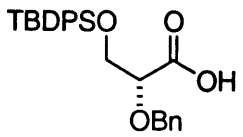

315

III-MW-166
DEPT in
CDCl3 at 298 K

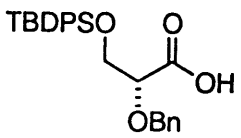

315

III-MW-166
COSY in
CDCl3 at 298 K

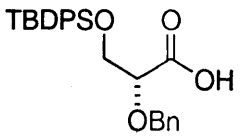

315

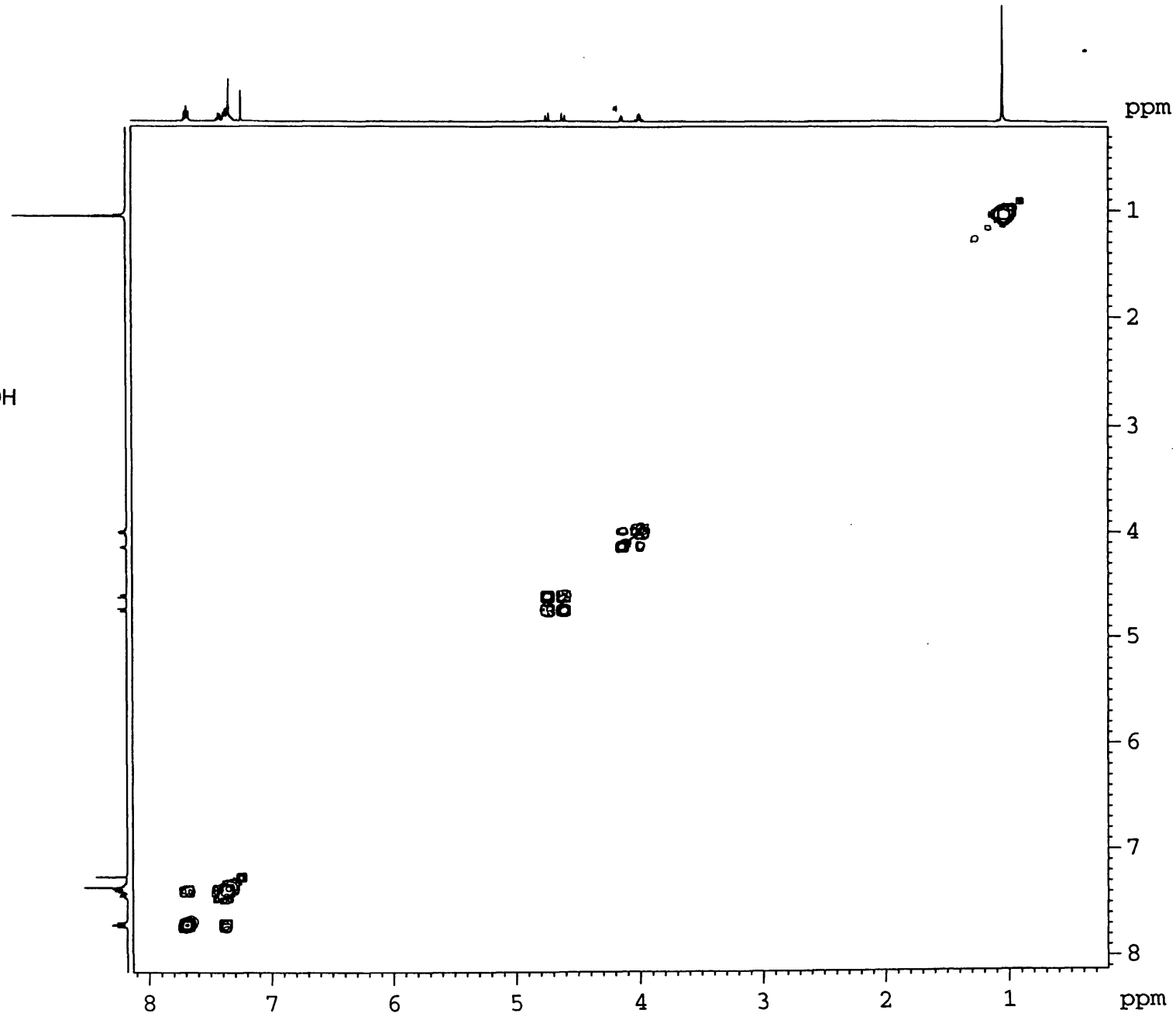

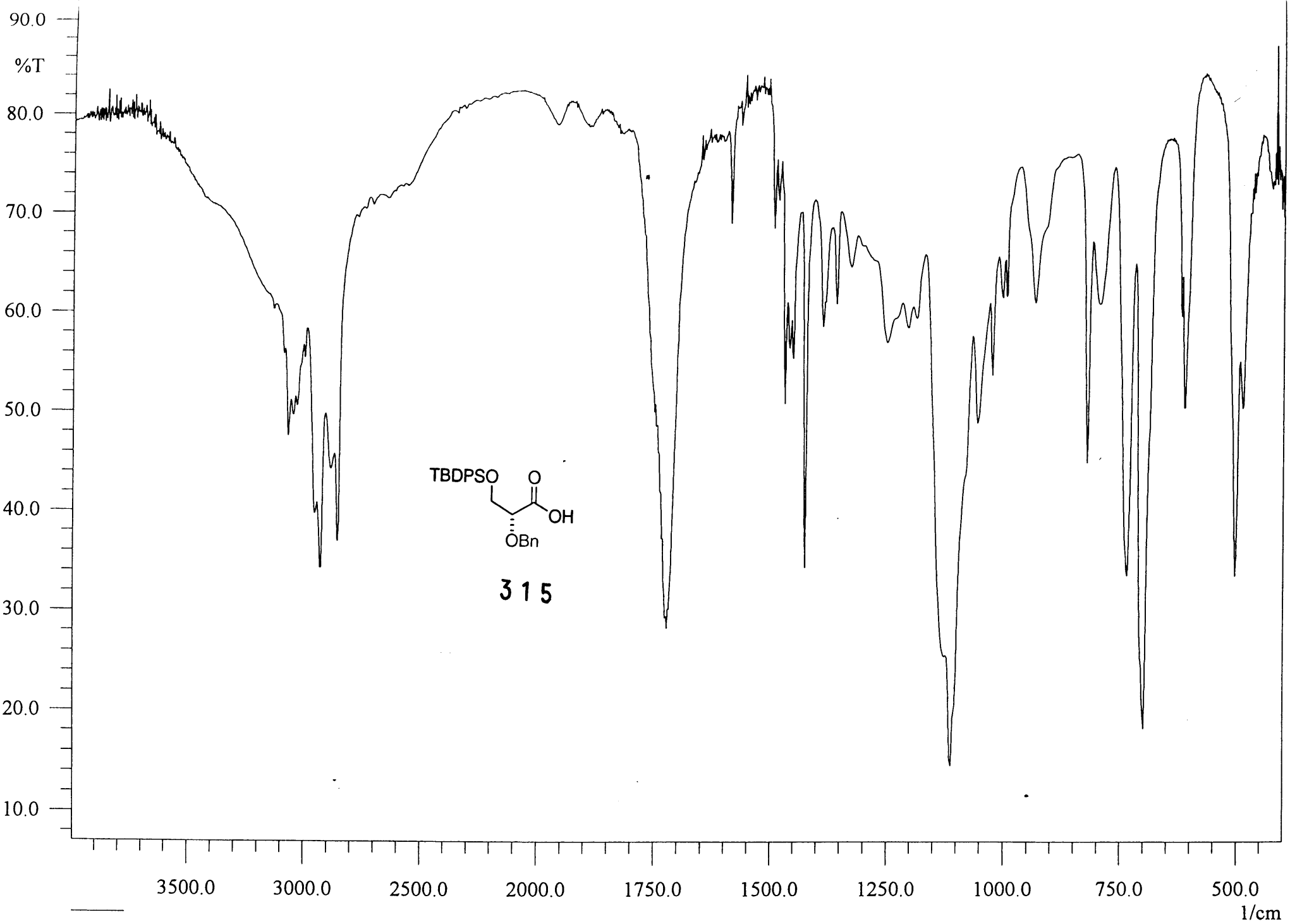
90.0
%T
80.0
70.0
60.0
50.0
40.0
30.0
20.0
10.0
TBDPSO
O
OH
OBn
315
3500.0
3000.0
2500.0
2000.0
1750.0
1500.0
1250.0
1000.0
750.0
500.0
1/cm

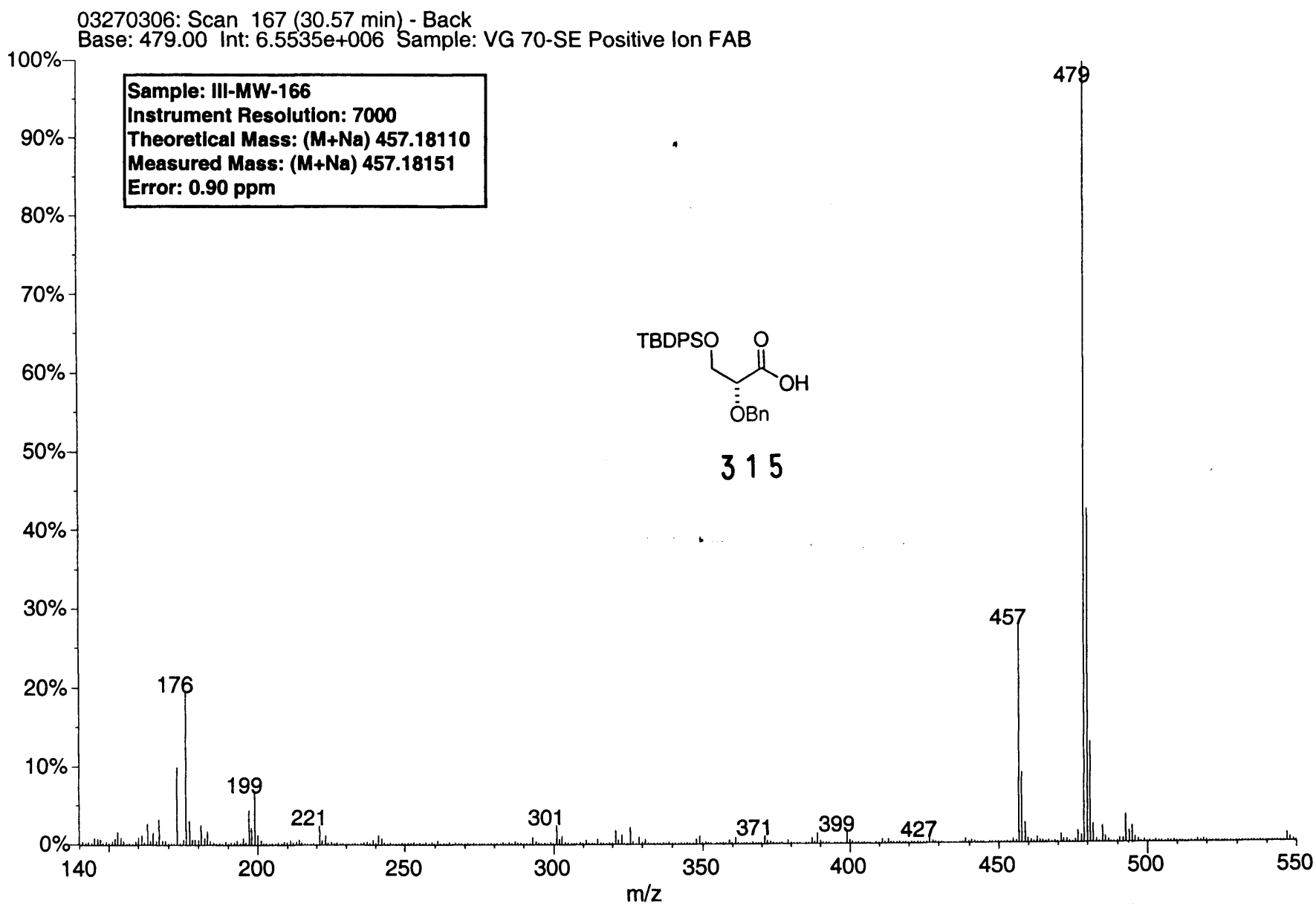
03270306: Scan 167 (30.57 min) - Back
Base: 479.00 Int: 6.5535e+006 Sample: VG 70-SE Positive Ion FAB
Sample: III-MW-166
Instrument Resolution: 7000
Theoretical Mass: (M+Na) 457.18110
Measured Mass: (M+Na) 457.18151
Error: 0.90 ppm
TBDPSO
O
OH
OBn
315
479
457
176
199
221
301
371
399
427
100%
90%
80%
70%
60%
50%
40%
30%
20%
10%
0%
140
200
250
300
350
400
450
500
550
m/z

III-MW-175
in CDCl3 at 298 K

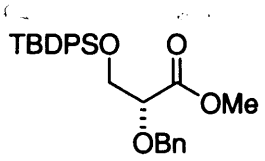

316

III-MW-175
Carbon 13
in CDCl3 at 298 K

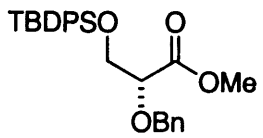

316

III-MW-175
DEPT in
CDCl3 at 298 K

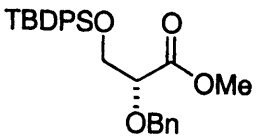

316

III-MW-175
COSY in
CDCl3 at 298 K

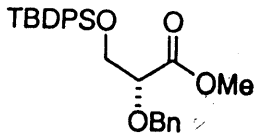

316

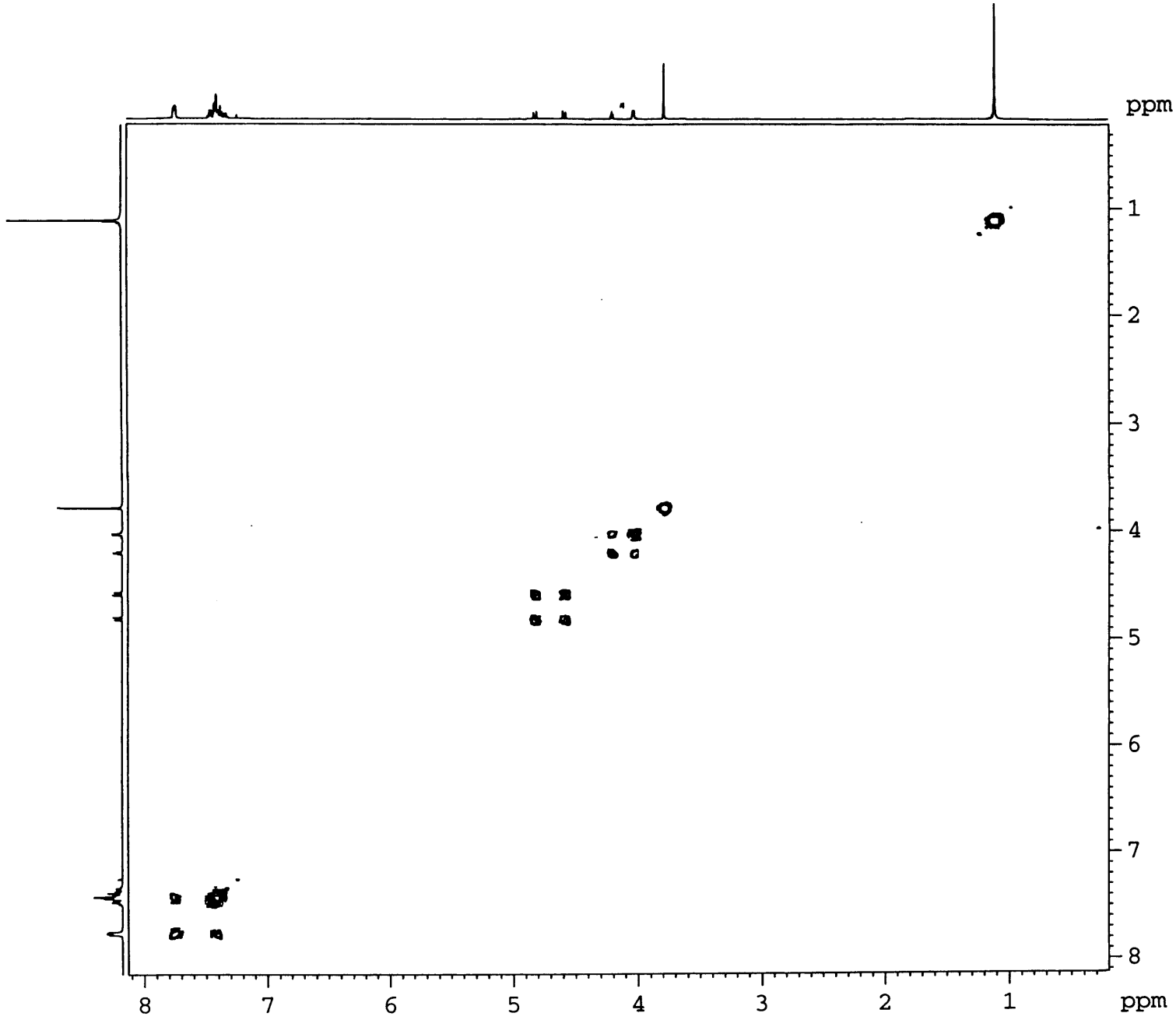

III-MW-175
HMQC in
CDCl3 at 298 K

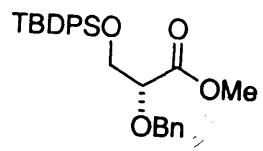

316

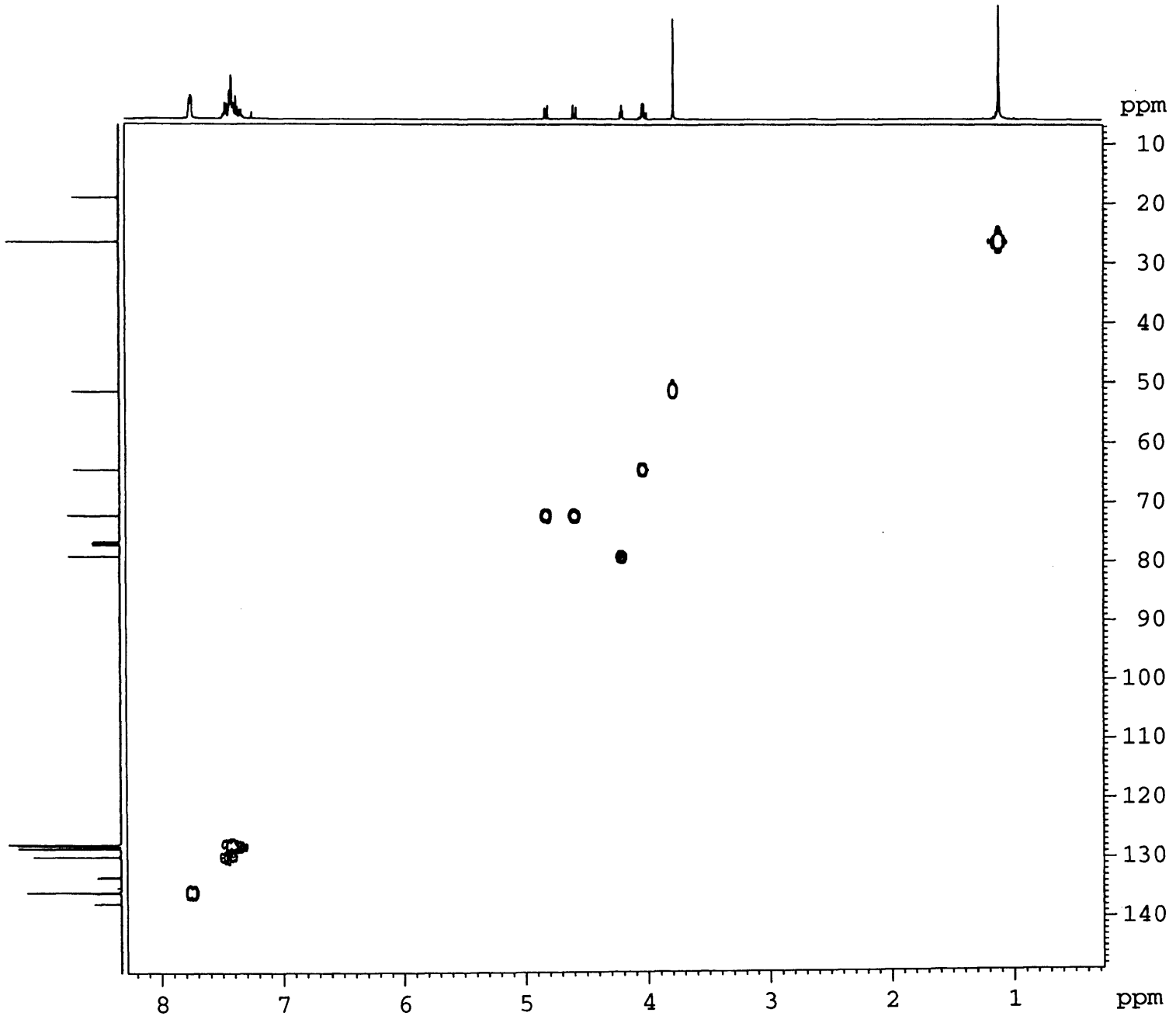

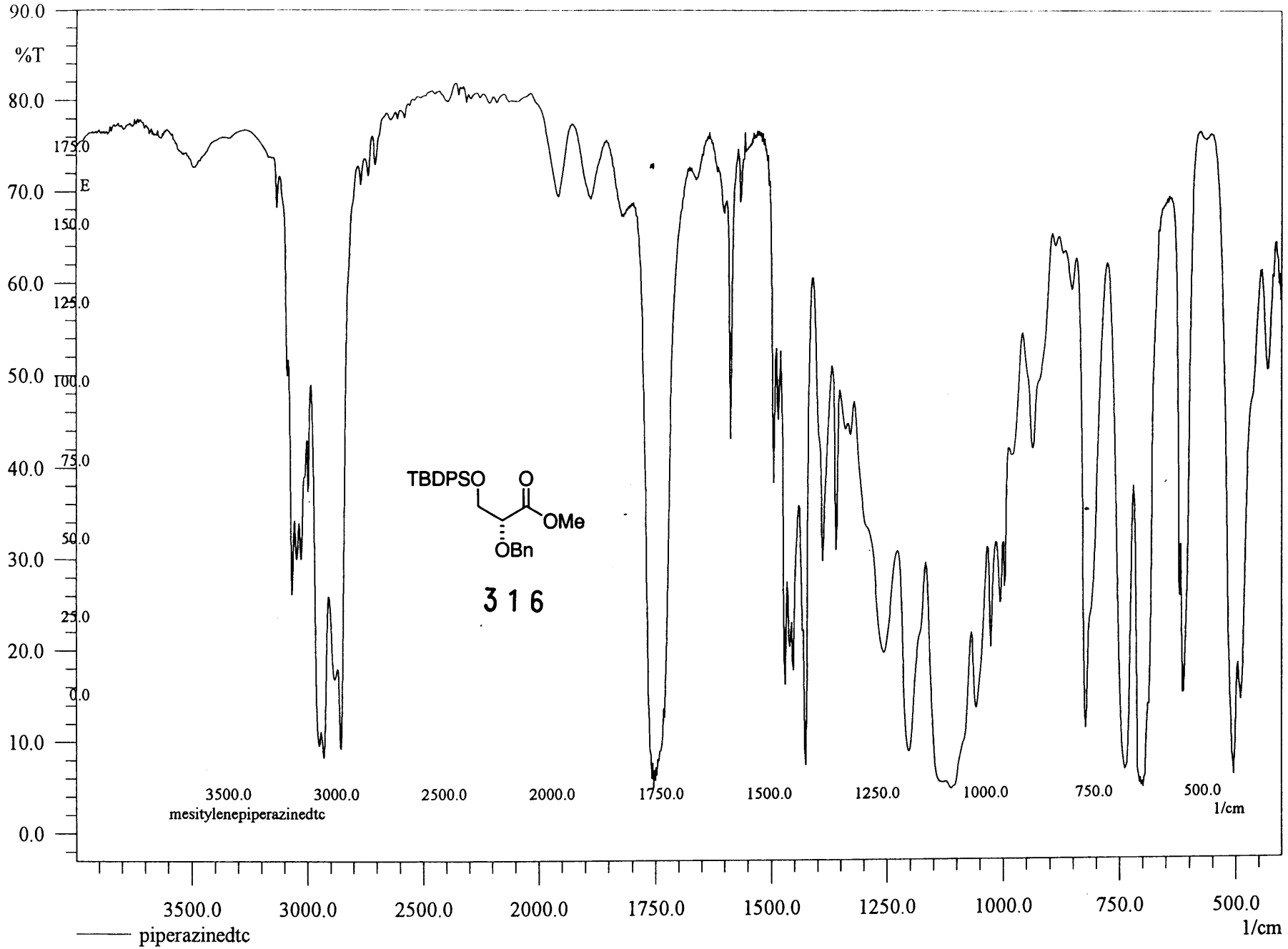
%T
90.0
80.0
70.0
60.0
50.0
40.0
30.0
20.0
10.0
0.0
E
175.0
150.0
125.0
100.0
75.0
50.0
25.0
0.0
TBDPSO
O
OMe
OBn
316
3500.0
3000.0
2500.0
2000.0
1750.0
1500.0
1250.0
1000.0
750.0
500.0
1/cm
mesitylenepiperazinedtc
piperazinedtc

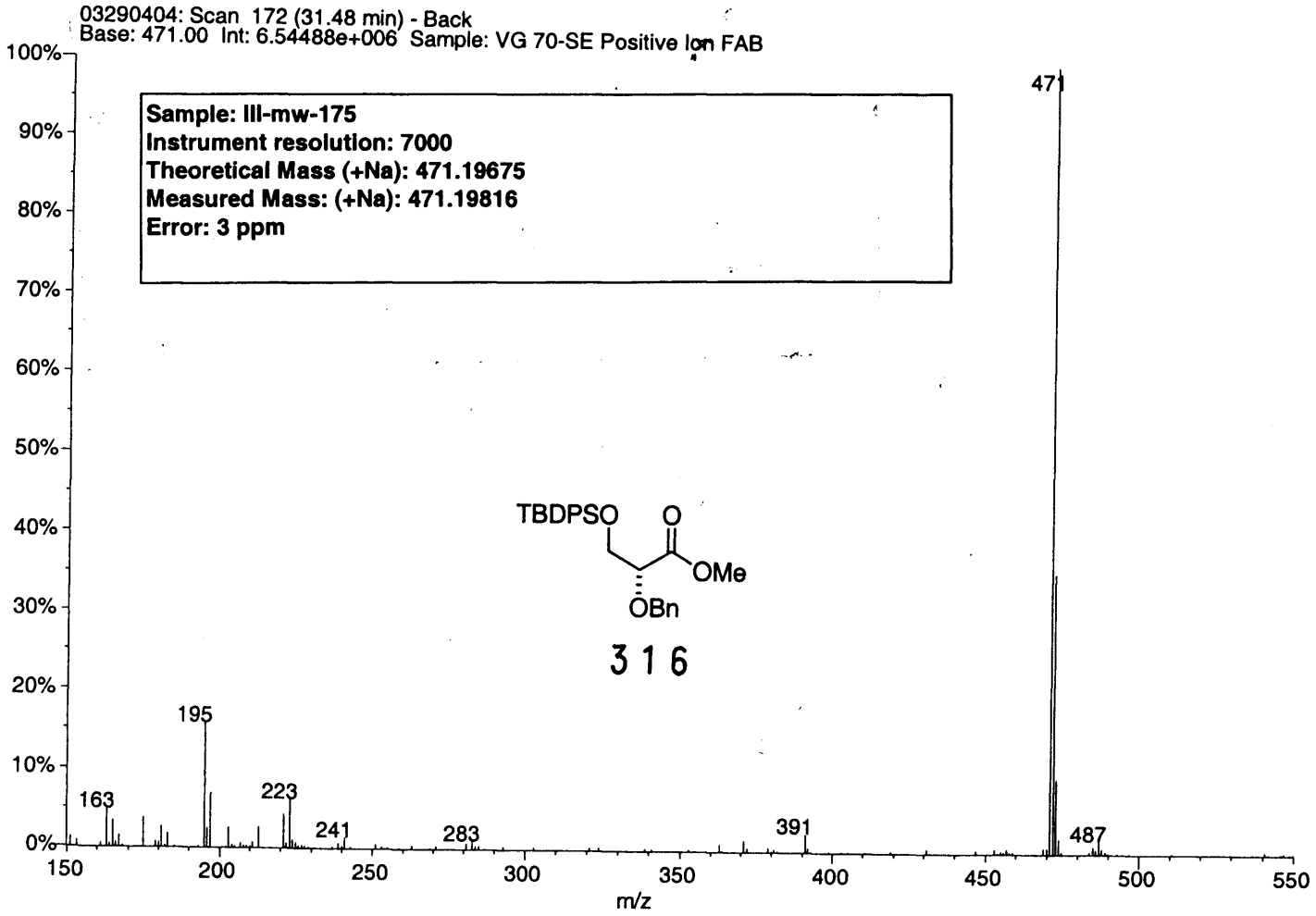
03290404: Scan 172 (31.48 min) - Back
Base: 471.00 Int: 6.54488e+006 Sample: VG 70-SE Positive Ion FAB
Sample: III-mw-175
Instrument resolution: 7000
Theoretical Mass (+Na): 471.19675
Measured Mass: (+Na): 471.19816
Error: 3 ppm
TBDPSO
O
OMe
OBn
316
471
195
163
223
241
283
391
487
100%
90%
80%
70%
60%
50%
40%
30%
20%
10%
0%
150
200
250
300
350
400
450
500
550
m/z

III-MW-184
in CDCl3 at 298 K

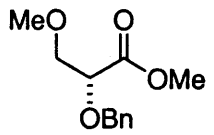

317

III-MW-184
Carbon 13 in
CDCl3 at 298 K

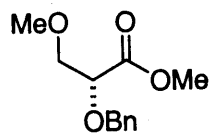

317

III-MW-184
DEPT in
CDCl3 at 298 K

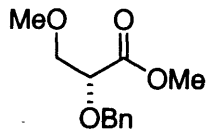

317

III-MW-184
COSY in
CDCl3 at 298 K

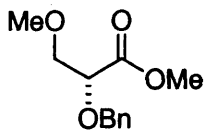

317

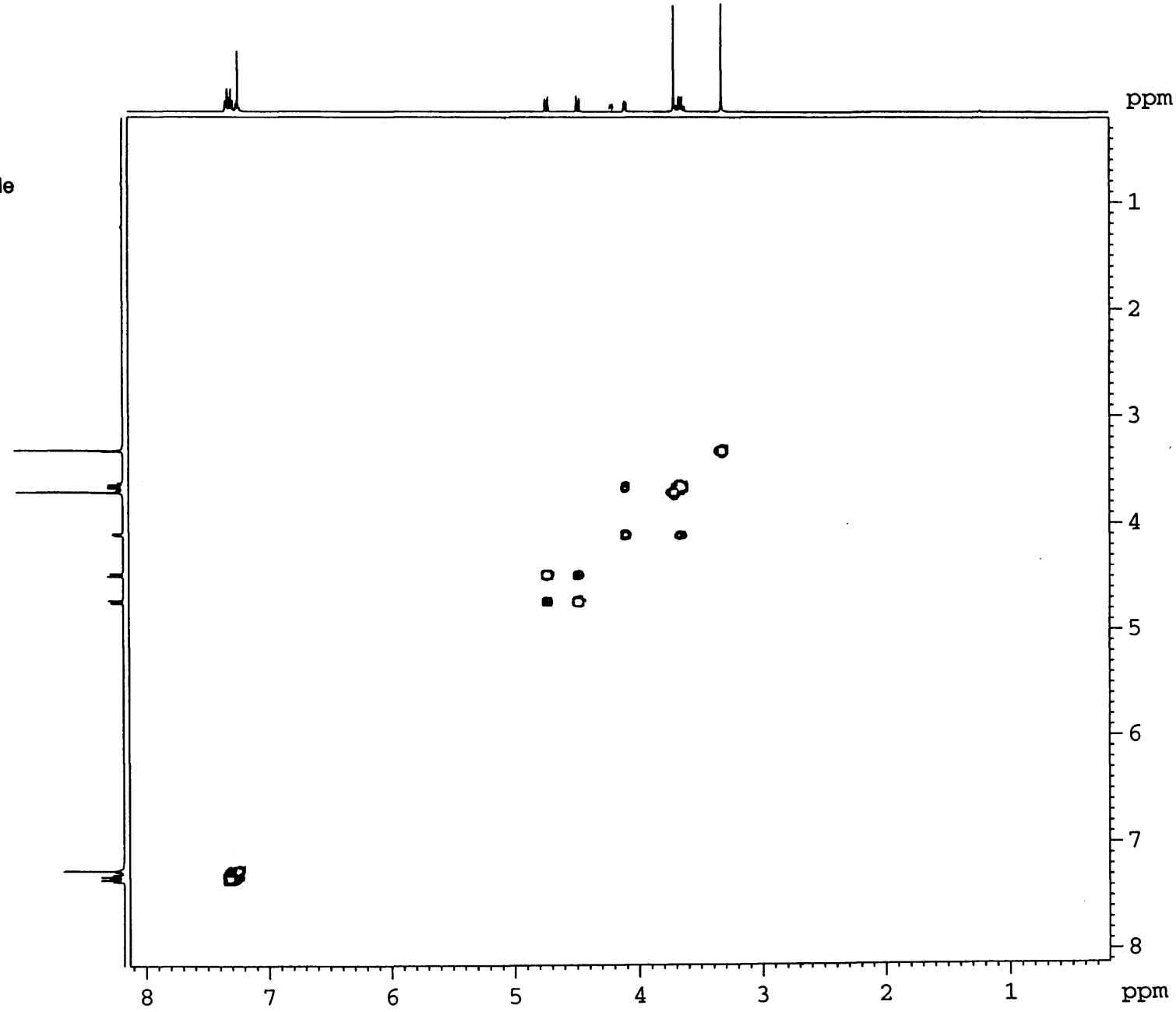

III-MW-184
HMQC in
CDCl3 at 298 K

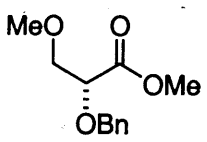

317

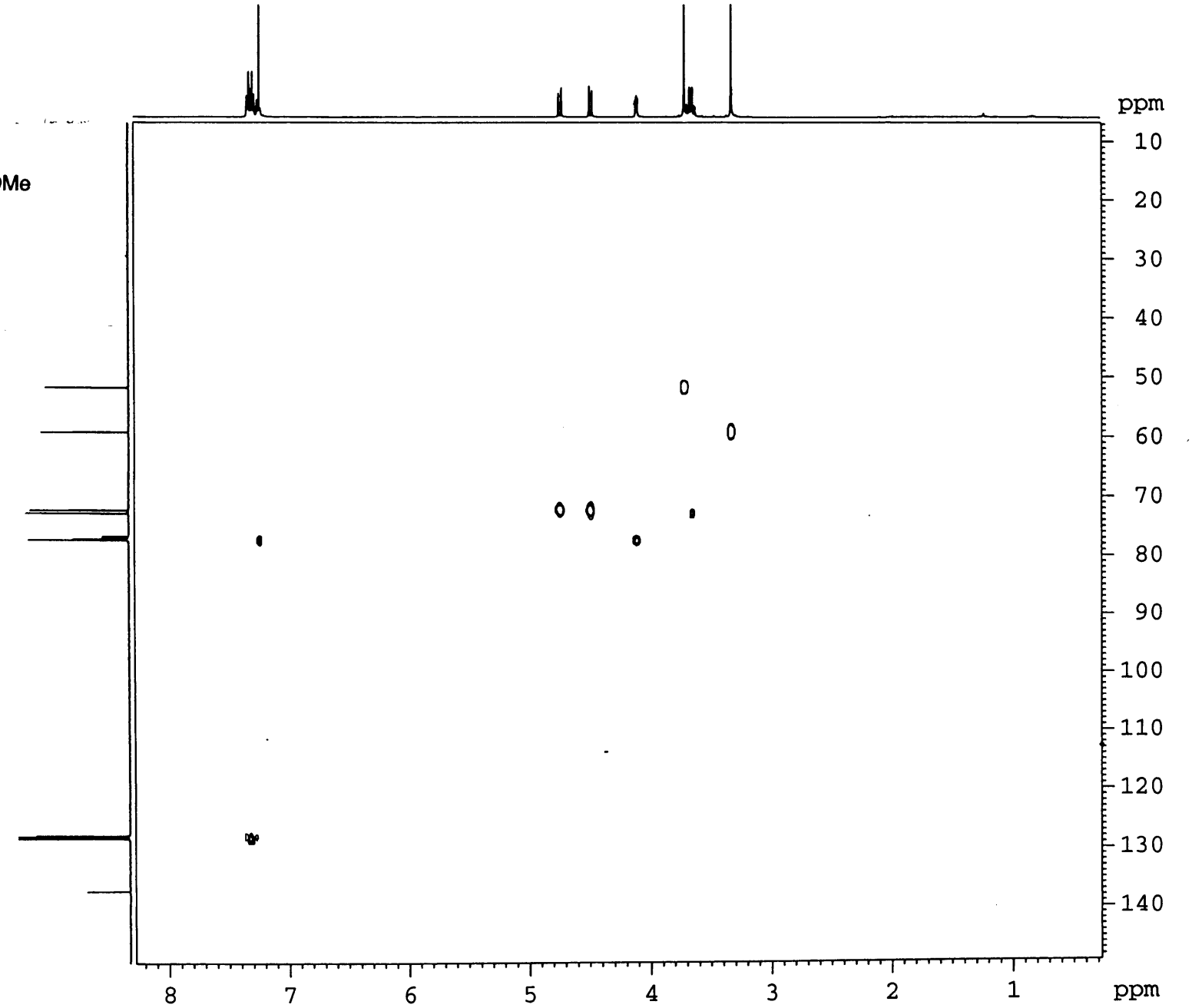

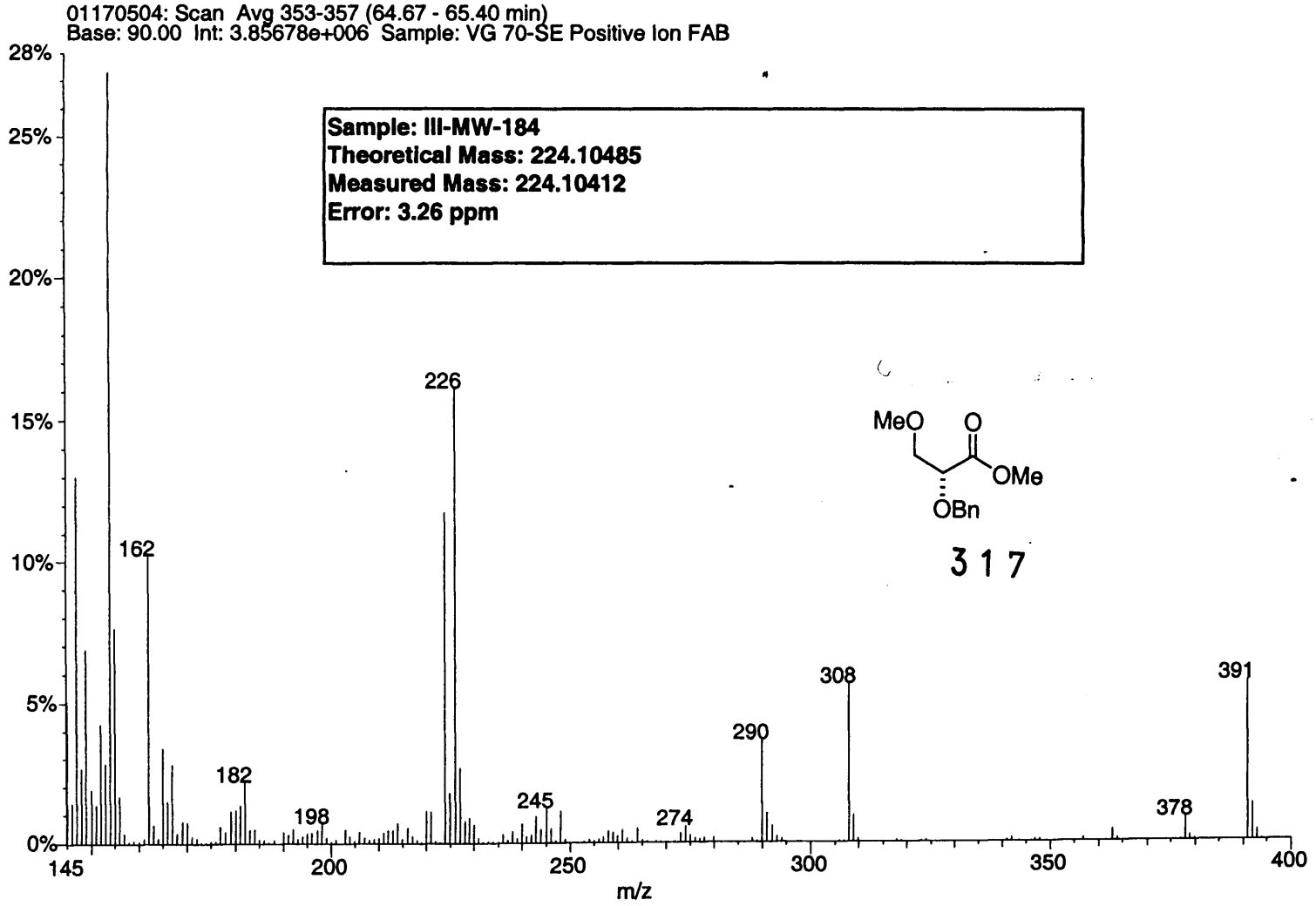
01170504: Scan Avg 353-357 (64.67 - 65.40 min)
Base: 90.00 Int: 3.85678e+006 Sample: VG 70-SE Positive Ion FAB
Sample: III-MW-184
Theoretical Mass: 224.10485
Measured Mass: 224.10412
Error: 3.26 ppm
MeO
O
OMe
OBn
317
28%
25%
20%
15%
10%
5%
0%
145
200
250
300
350
400
m/z
226
162
182
198
245
274
290
308
378
391

III-MW-23 in
CDCl3 at 298 K

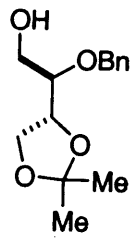

325

III-MW-23
Carbon 13 in
CDCl3 at 298 K

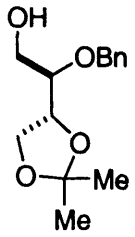

325

III-MW-23
COSY in
CDCl3 at 298 K

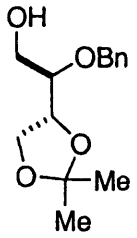

325

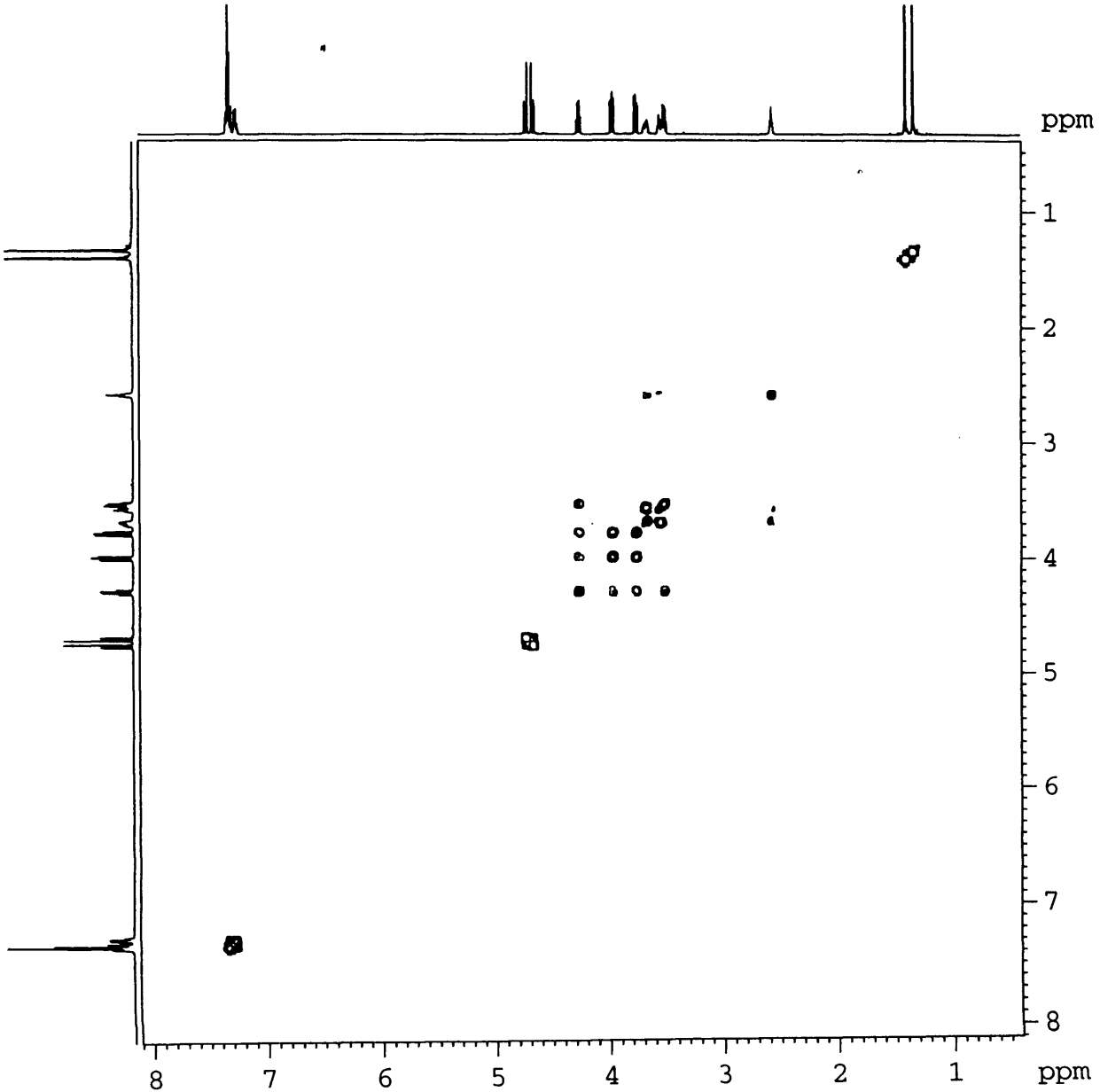

III-MW-23
HMQC in
CDCl3 at 298 K

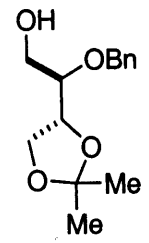

325

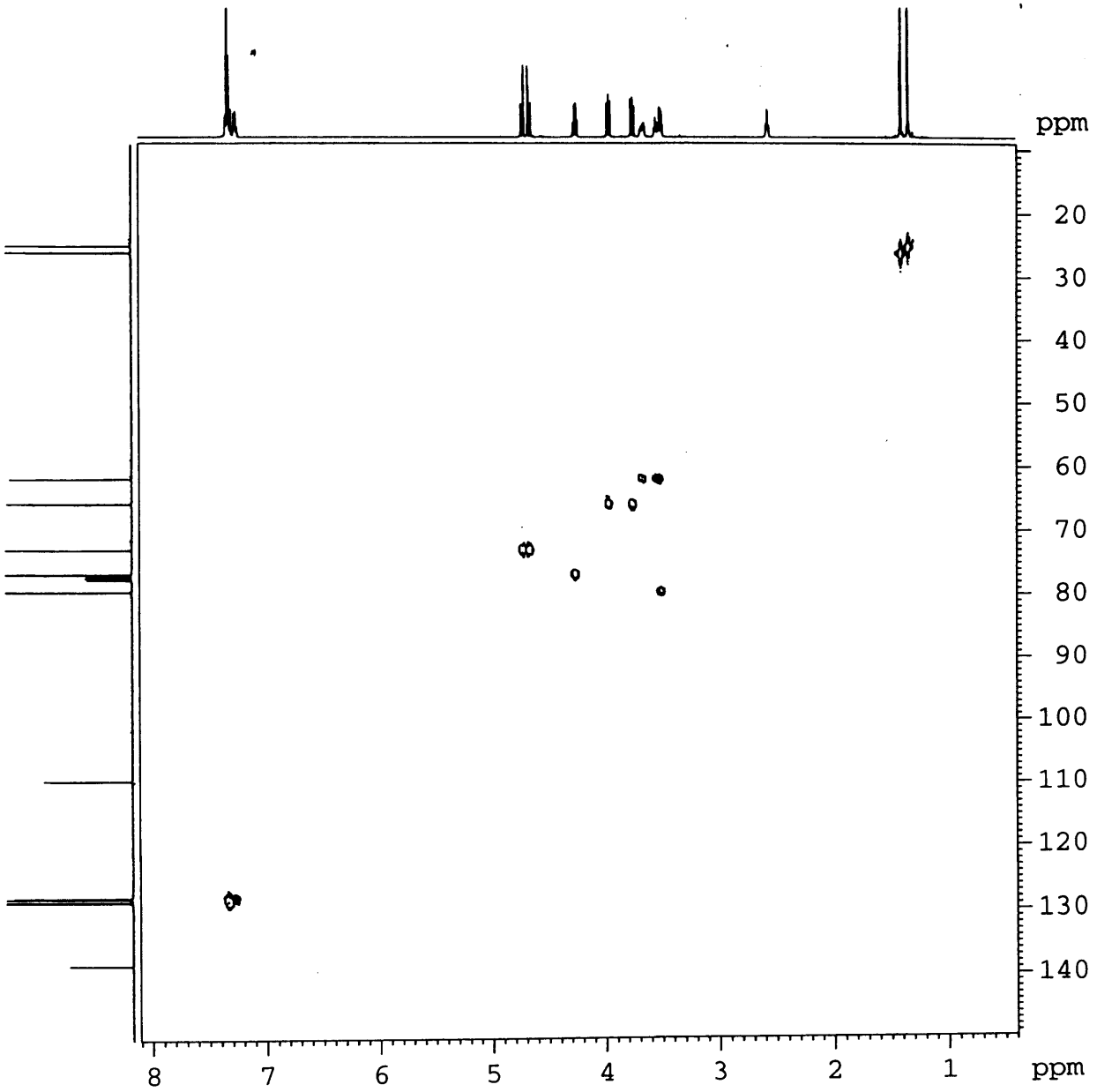

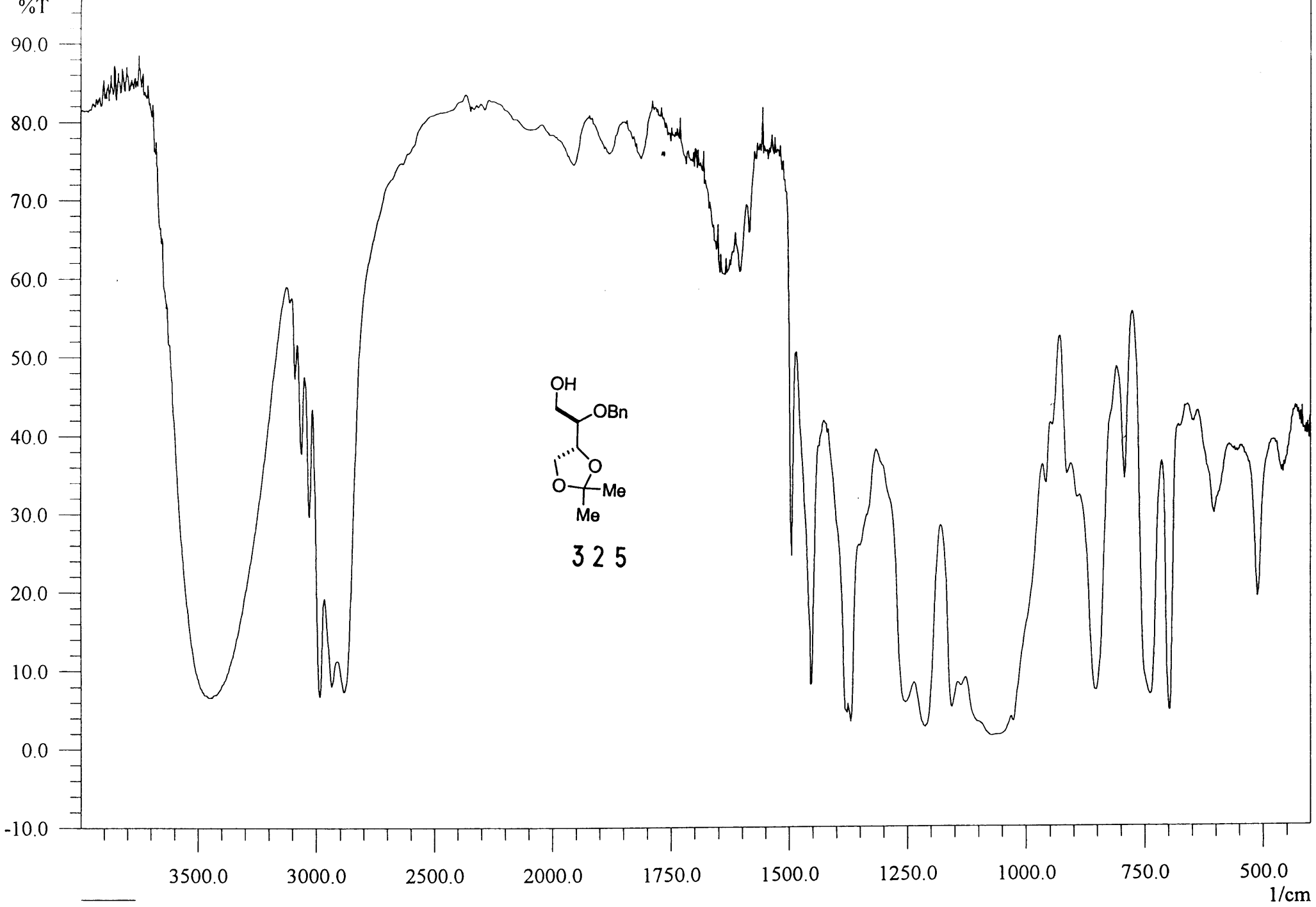
%T
90.0
80.0
70.0
60.0
50.0
40.0
30.0
20.0
10.0
0.0
-10.0
3500.0
3000.0
2500.0
2000.0
1750.0
1500.0
1250.0
1000.0
750.0
500.0
1/cm
OH
OBn
O
O
Me
Me
325

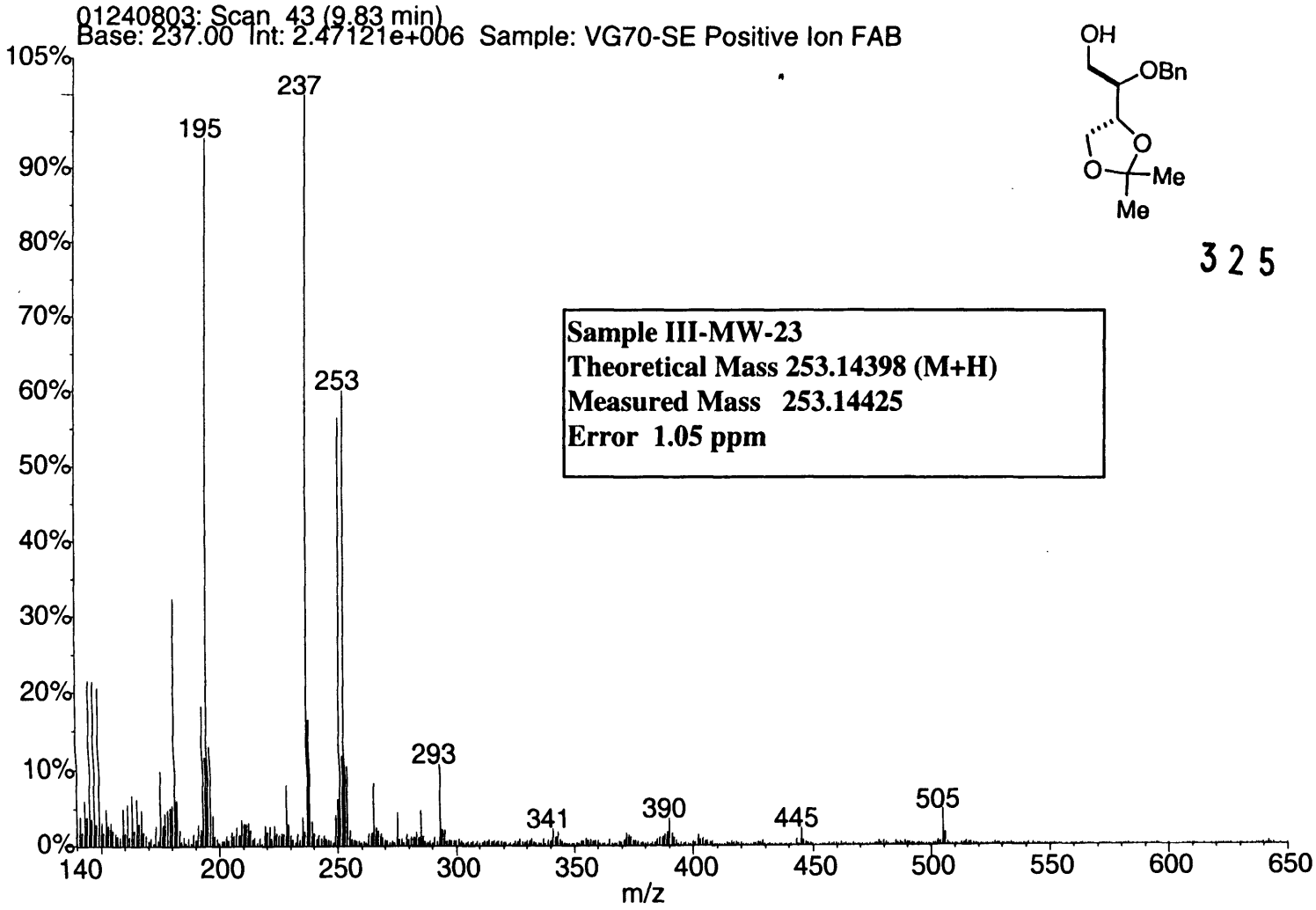
01240803: Scan 43 (9.83 min)
Base: 237.00 Int: 2.47121e+006 Sample: VG70-SE Positive Ion FAB
105%
90%
80%
70%
60%
50%
40%
30%
20%
10%
0%
237
195
253
293
341
390
445
505
140
200
250
300
350
400
450
500
550
600
650
m/z
OH
OBn
O
O
Me
Me
Sample III-MW-23
Theoretical Mass 253.14398 (M+H)
Measured Mass 253.14425
Error 1.05 ppm

325

III-MW-98 in
CDCl3 at 298 K

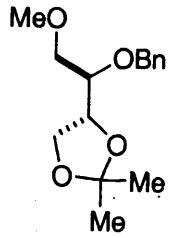

326

III-MW-98
Carbon 13 in
CDCl3 at 298 K

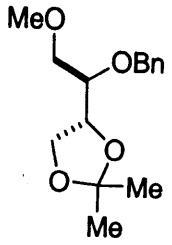

326

III-MW-98
DEPT in
CDCl3 at 298 K

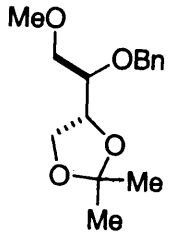

326

COSY in
CDCl3 at 298 K

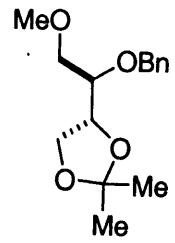

326

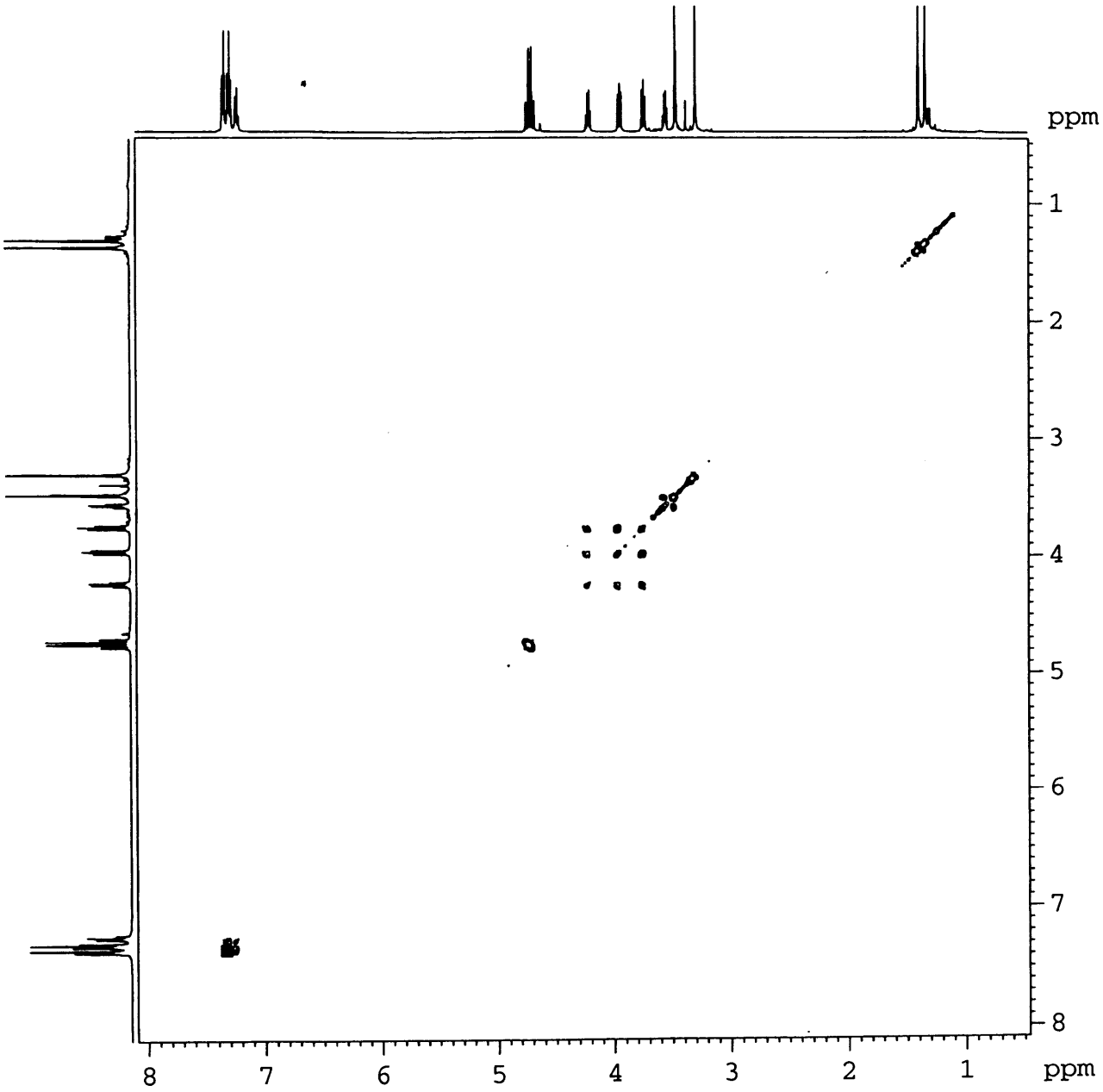

111-MW-98
HMQC in
CDCl3 at 298 K

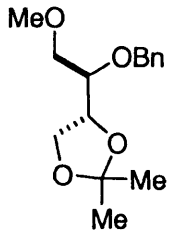

326

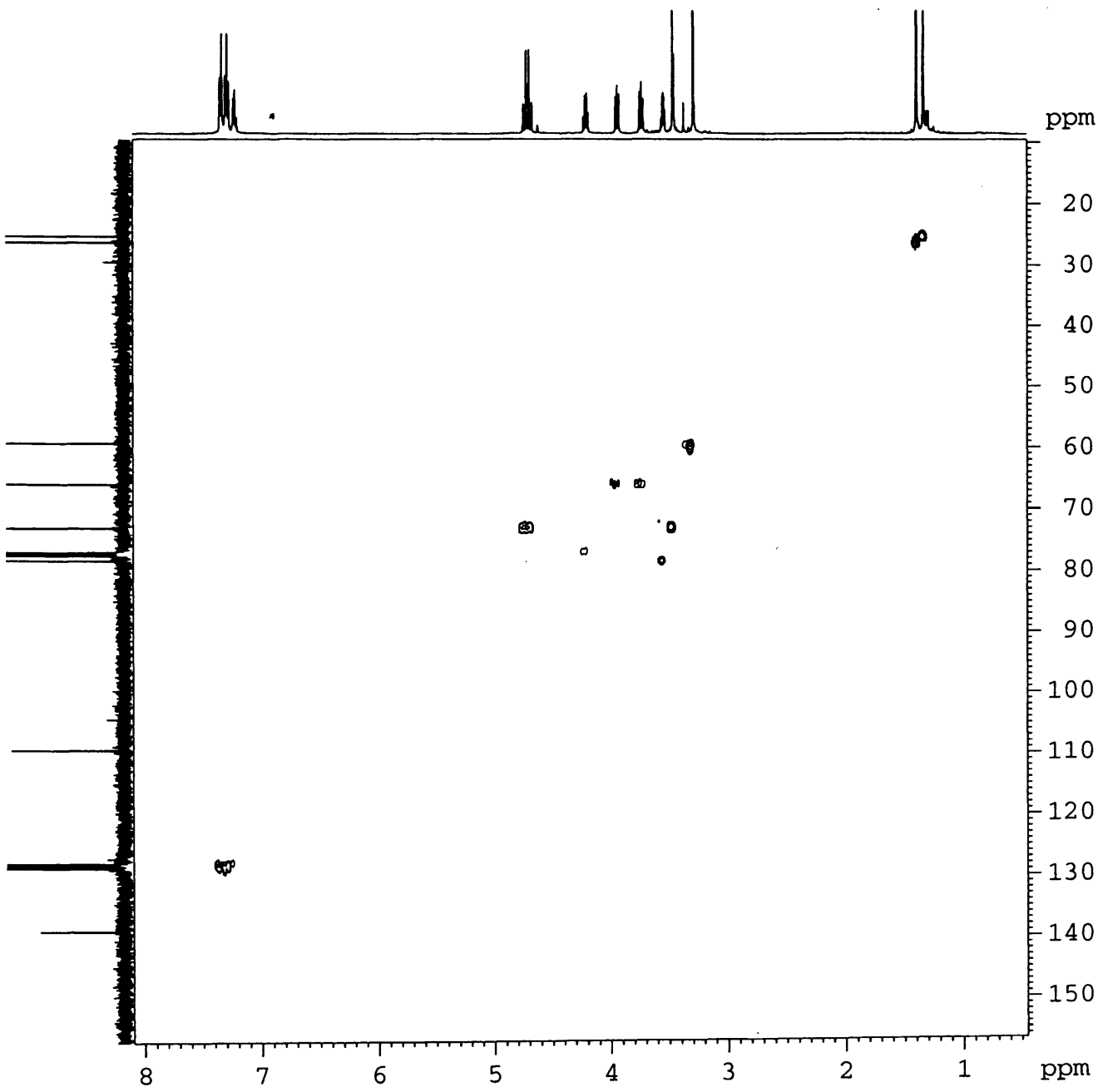

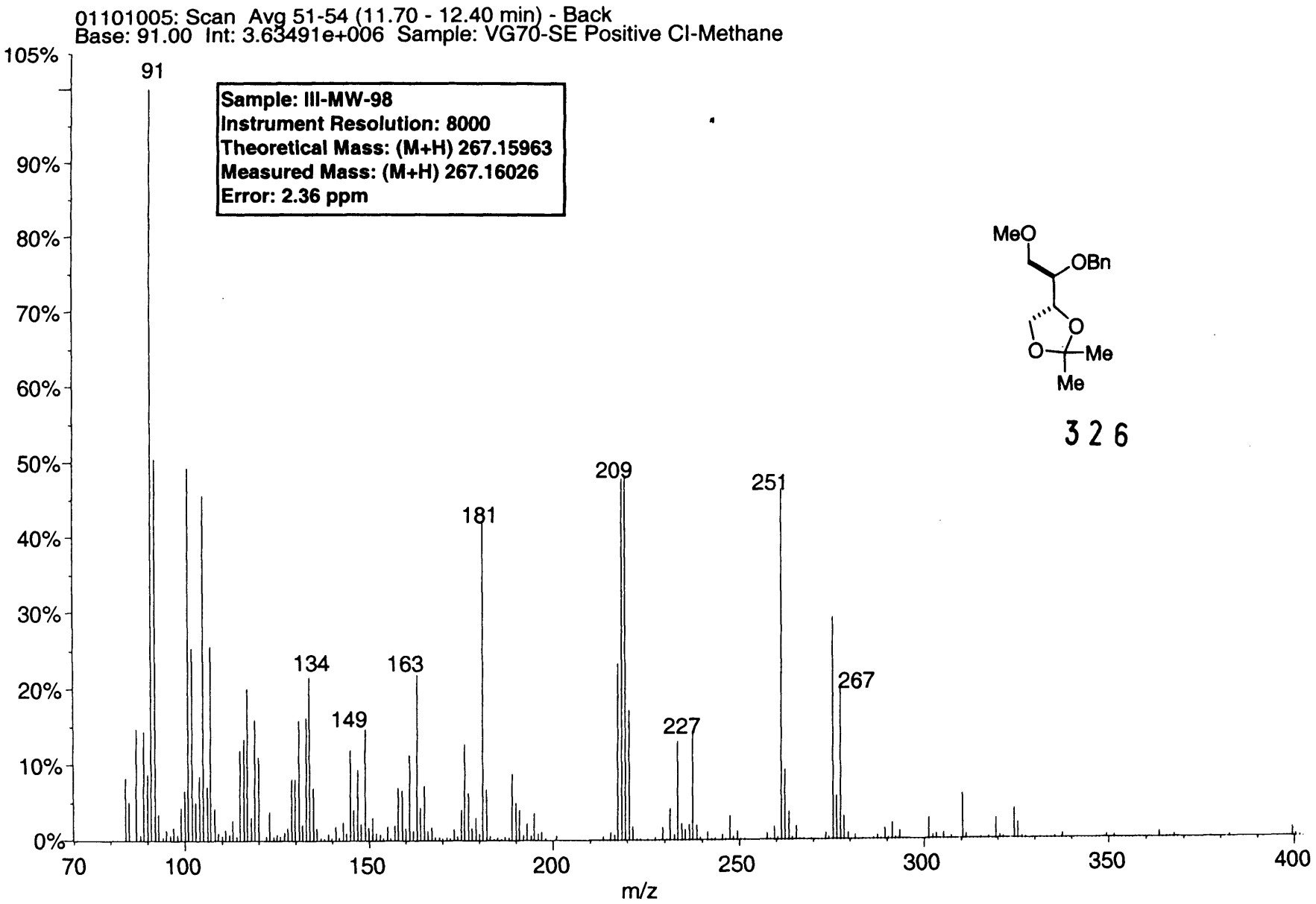
01101005: Scan Avg 51-54 (11.70 - 12.40 min) - Back
Base: 91.00 Int: 3.63491e+006 Sample: VG70-SE Positive CI-Methane
Sample: III-MW-98
Instrument Resolution: 8000
Theoretical Mass: (M+H) 267.15963
Measured Mass: (M+H) 267.16026
Error: 2.36 ppm
MeO
OBn
O
O
Me
Me
326
105%
90%
80%
70%
60%
50%
40%
30%
20%
10%
0%
91
209
251
181
134
163
149
227
267
70
100
150
200
250
300
350
400
m/z

III-MW-107 in
CDCl3 at 298 K

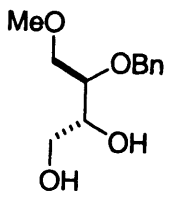

321

III-MW-107
Carbon 13 in
CDCl3 at 298 K

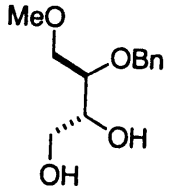

321

III-MW-107
DEPT in
CDCl3 at 298 K

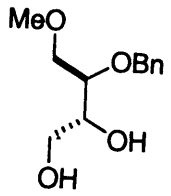

321

III-MW-107
COSY in
CDCl3 at 298 K

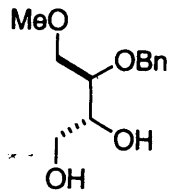

321

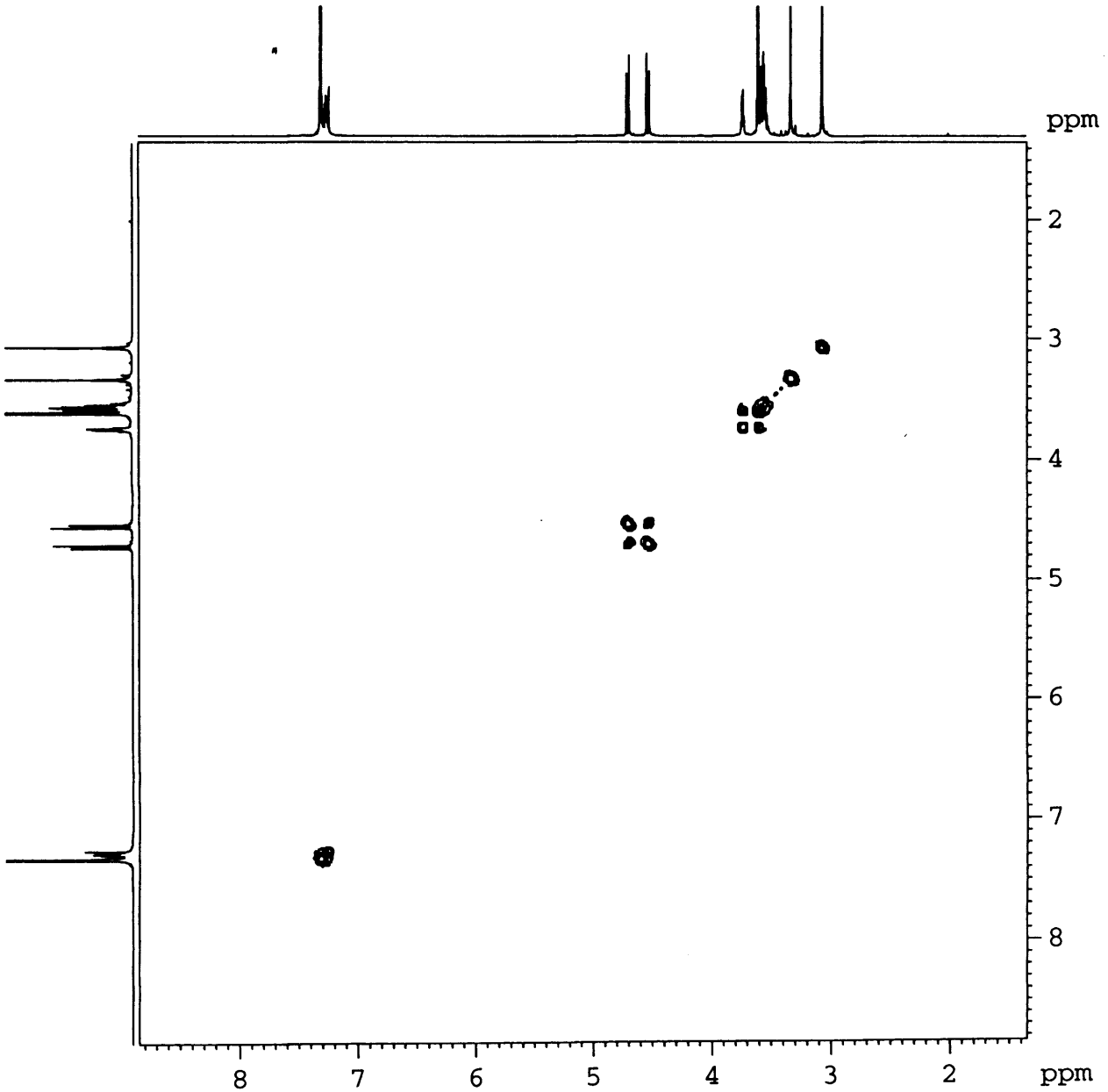

III-MW-107
HMQC in
CDCl3 at 298 K

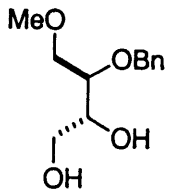

321

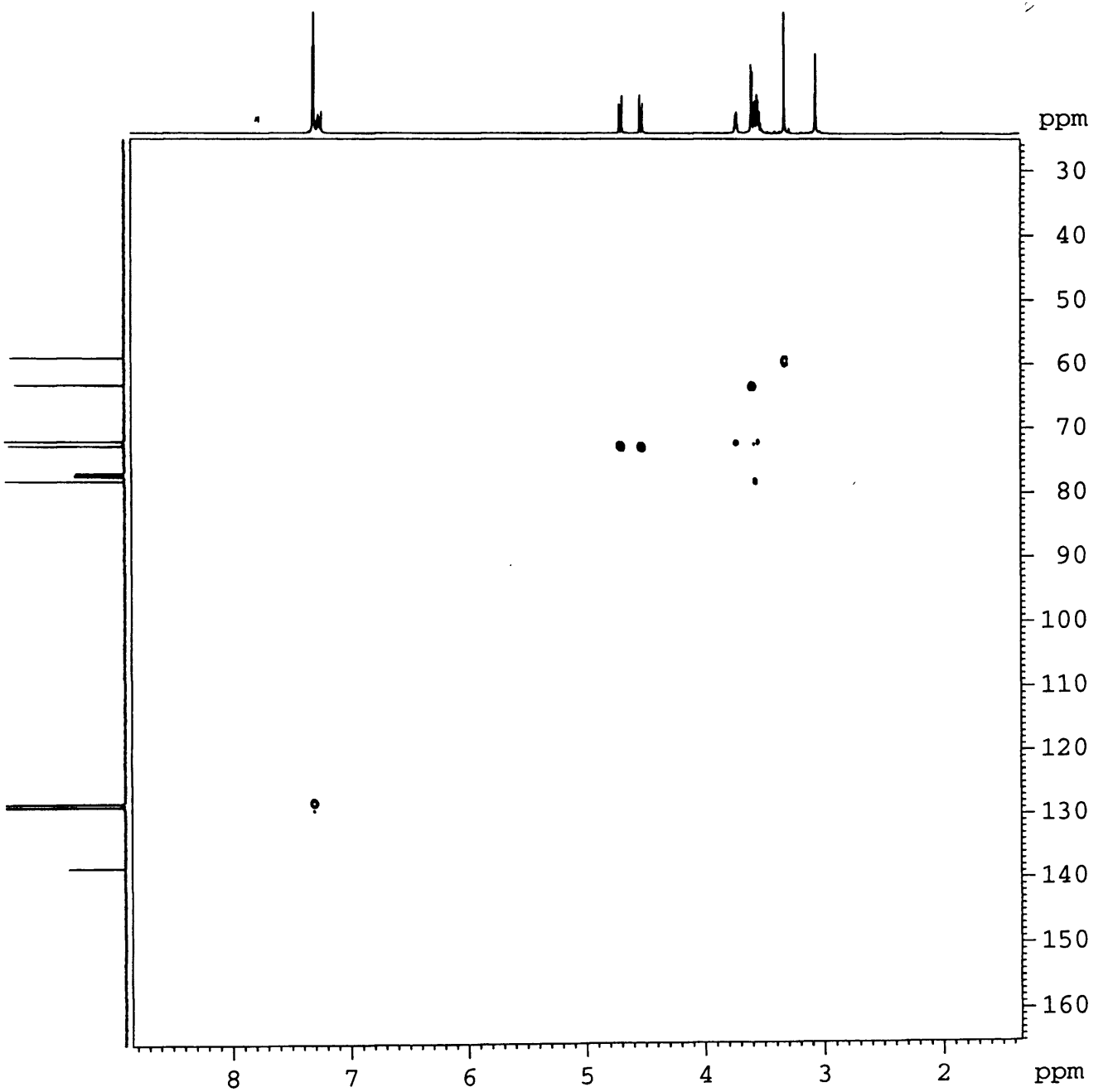

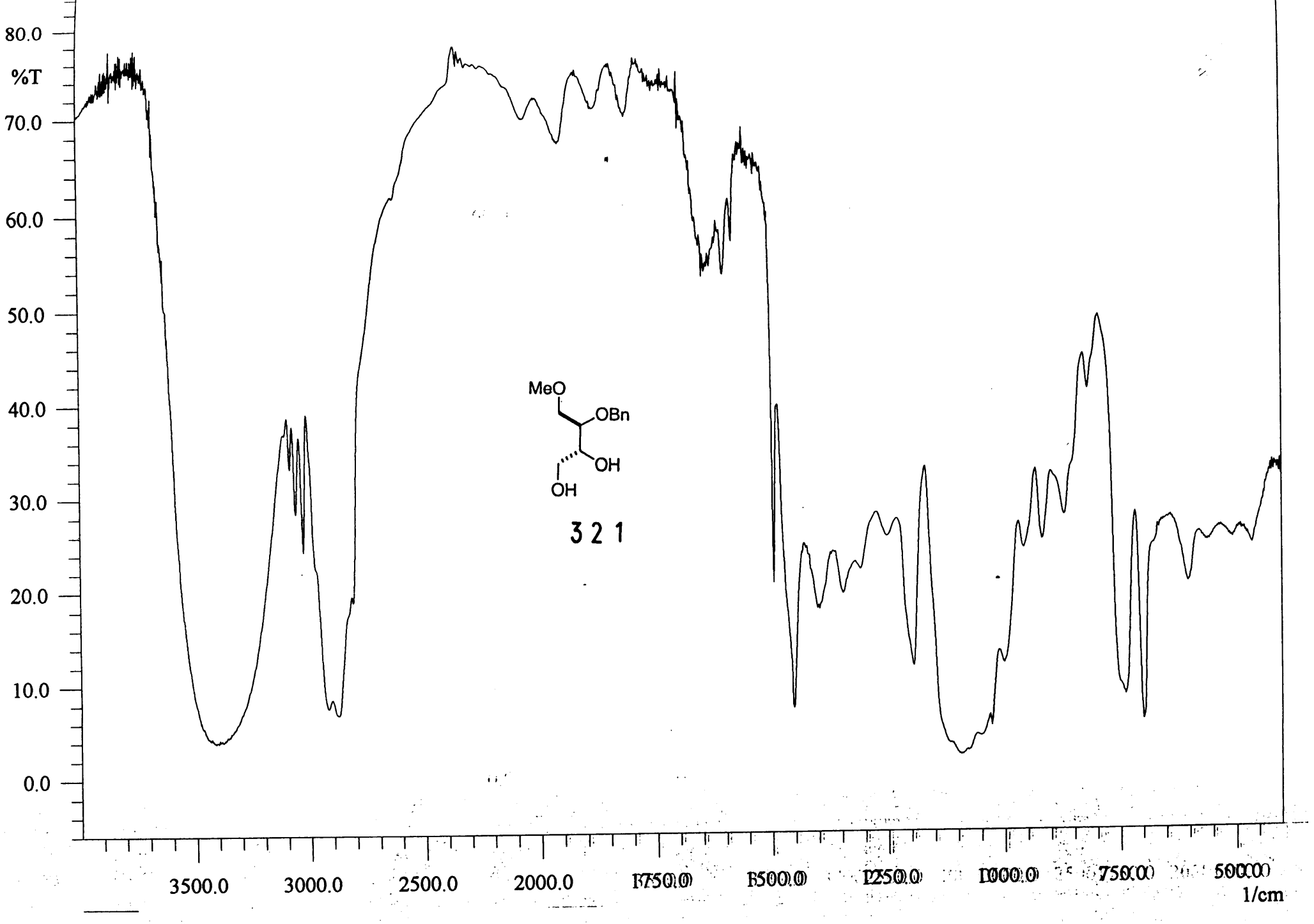
80.0
%T
70.0
60.0
50.0
40.0
30.0
20.0
10.0
0.0
3500.0
3000.0
2500.0
2000.0
1750.0
1500.0
1250.0
1000.0
750.00
500.00
1/cm
MeO
OBn
OH
OH
321

sg54381 #1626 RT: 56.28 AV: 1 SB: 1028 0.72-27.63 , 25.90-34.48 NL: 1.42E8
T: + c CI Full ms [97.50-800.50]

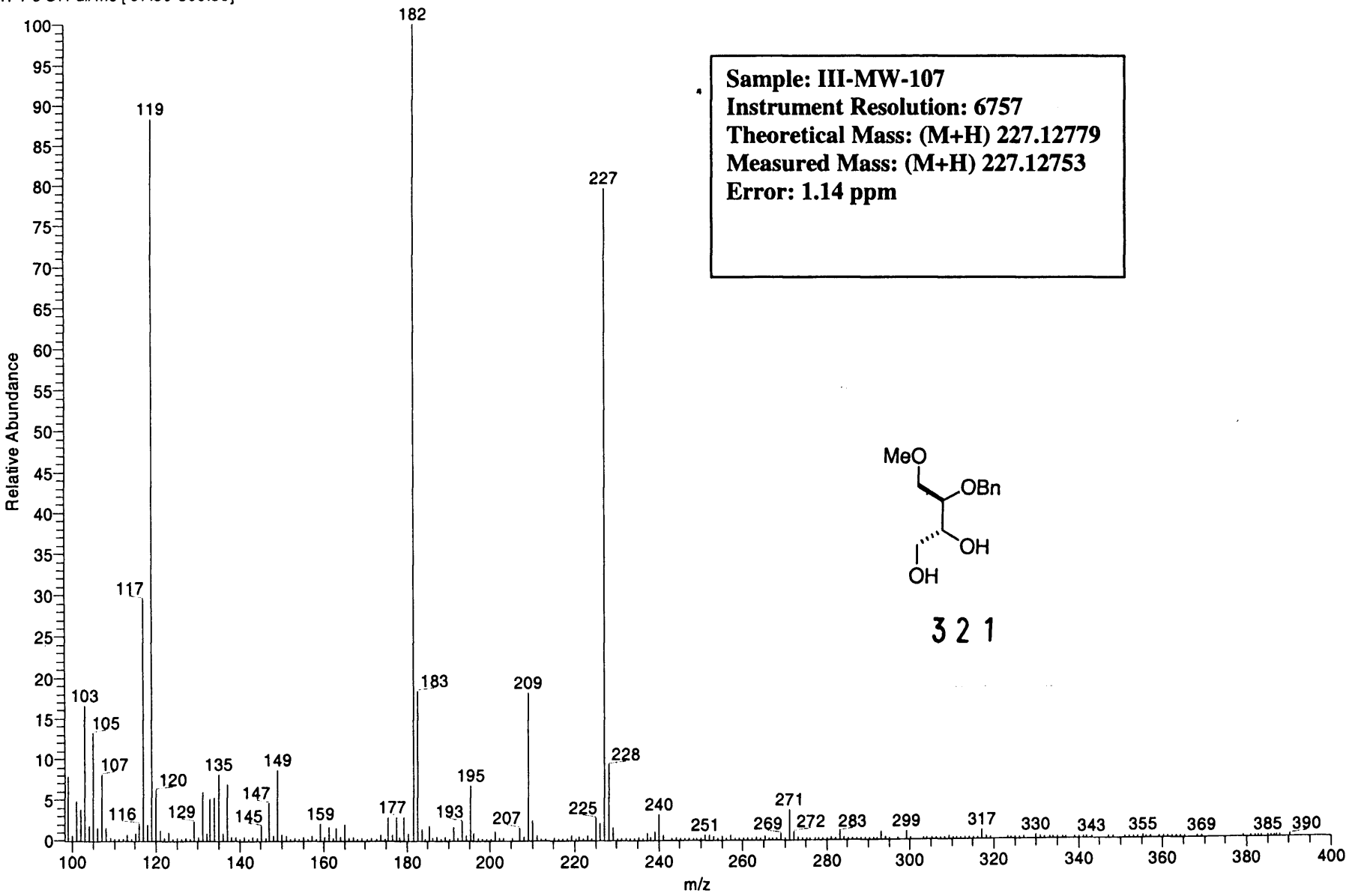

Sample: III-MW-107
Instrument Resolution: 6757
Theoretical Mass: (M+H) 227.12779
Measured Mass: (M+H) 227.12753
Error: 1.14 ppm

321

III-MW-116
in CDCl3
at 298 K

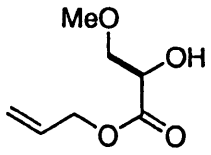

320

III-MW-116
DEPT in
CDCl3 at 298 K

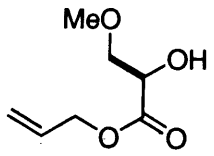

320

III-MW-116
COSY in
CDCl3 at 298 K

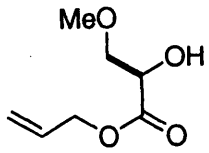

320

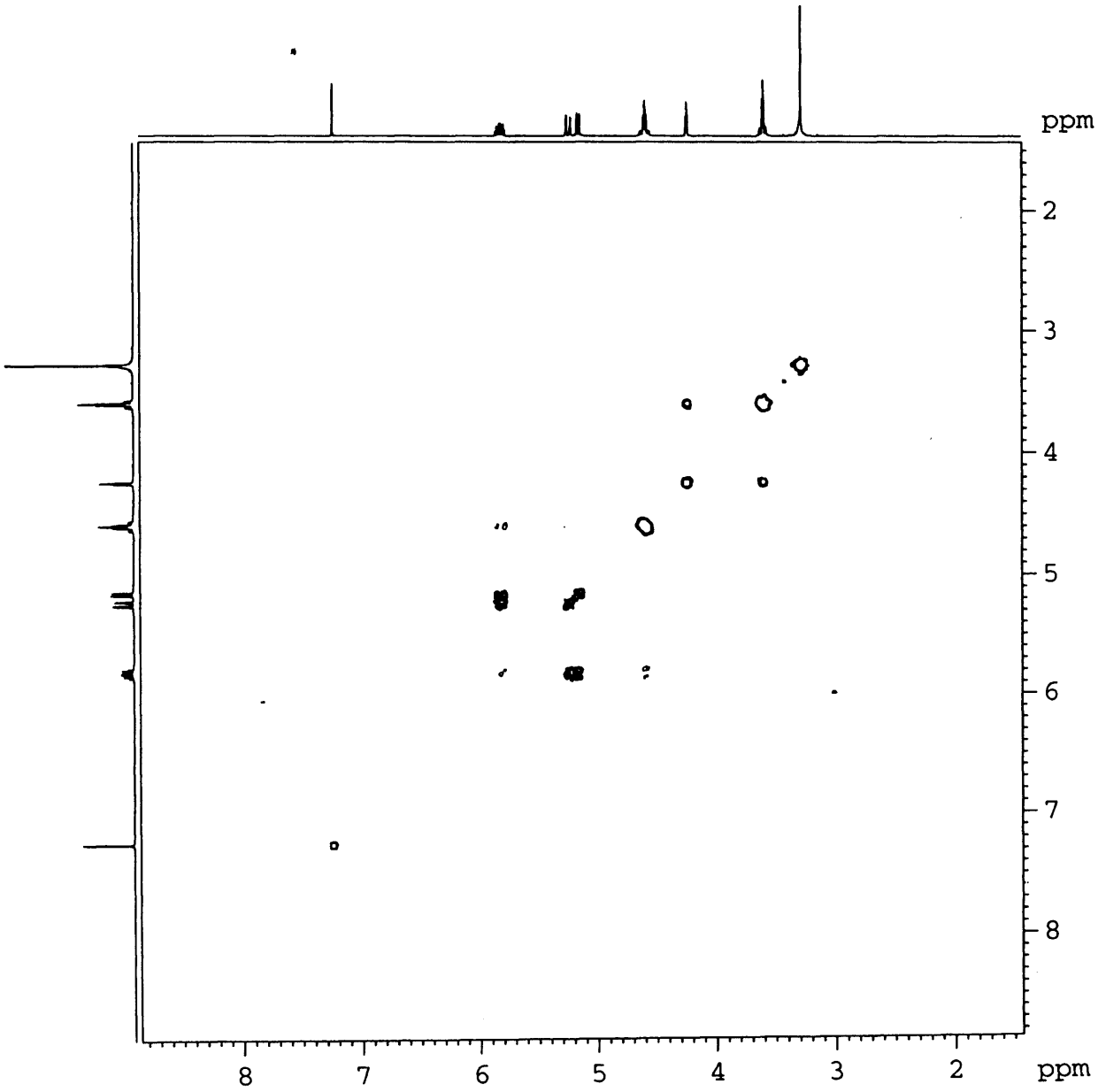

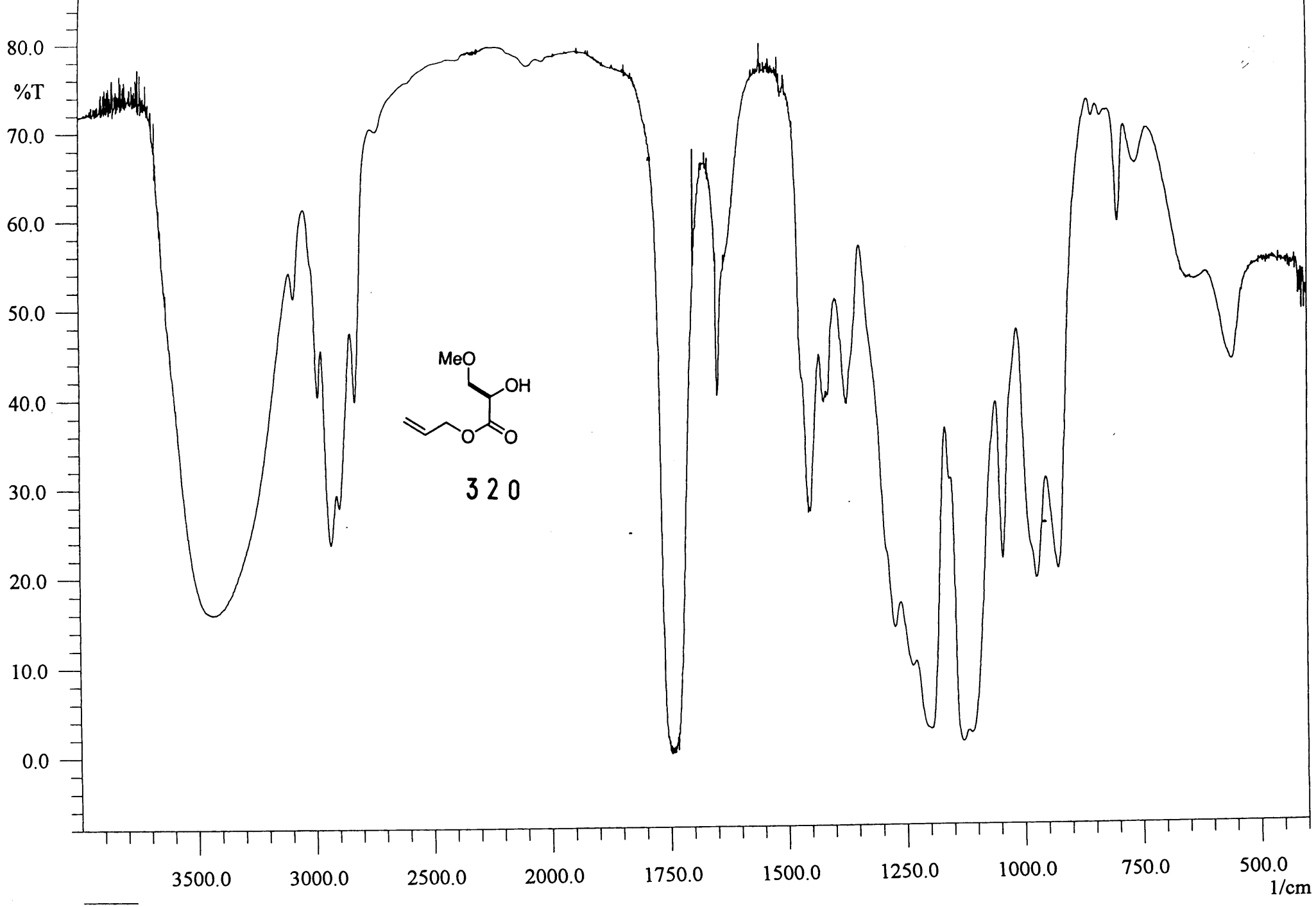
80.0
%T
70.0
60.0
50.0
40.0
30.0
20.0
10.0
0.0
MeO
OH
O
O
320
3500.0
3000.0
2500.0
2000.0
1750.0
1500.0
1250.0
1000.0
750.0
500.0
1/cm

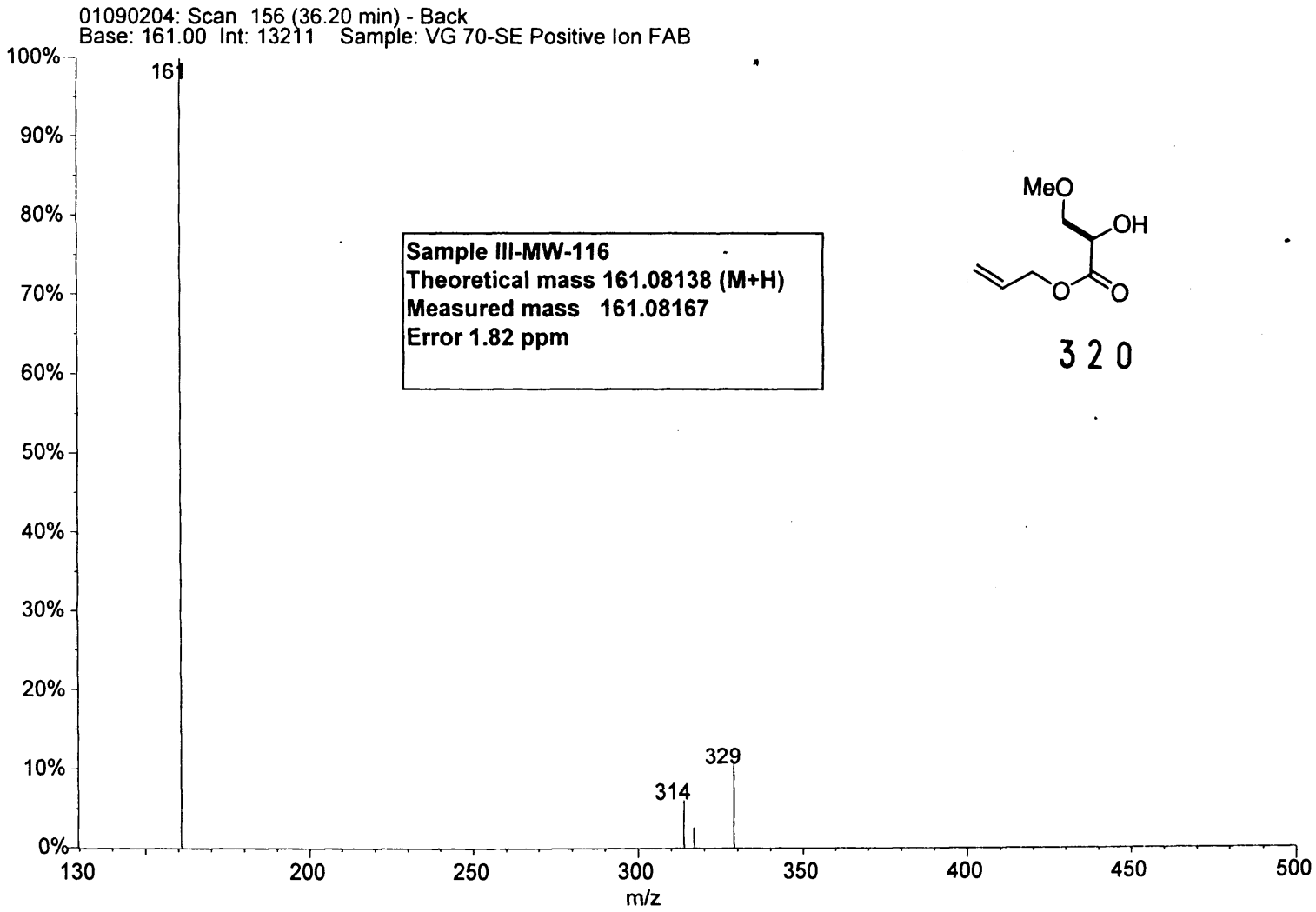
01090204: Scan 156 (36.20 min) - Back
Base: 161.00 Int: 13211 Sample: VG 70-SE Positive Ion FAB
100%
90%
80%
70%
60%
50%
40%
30%
20%
10%
0%
161
329
314
130
200
250
300
350
400
450
500
m/z
Sample III-MW-116
Theoretical mass 161.08138 (M+H)
Measured mass 161.08167
Error 1.82 ppm
MeO
OH
O
O
320

III-MW-51
in CDCl3
at 298 K

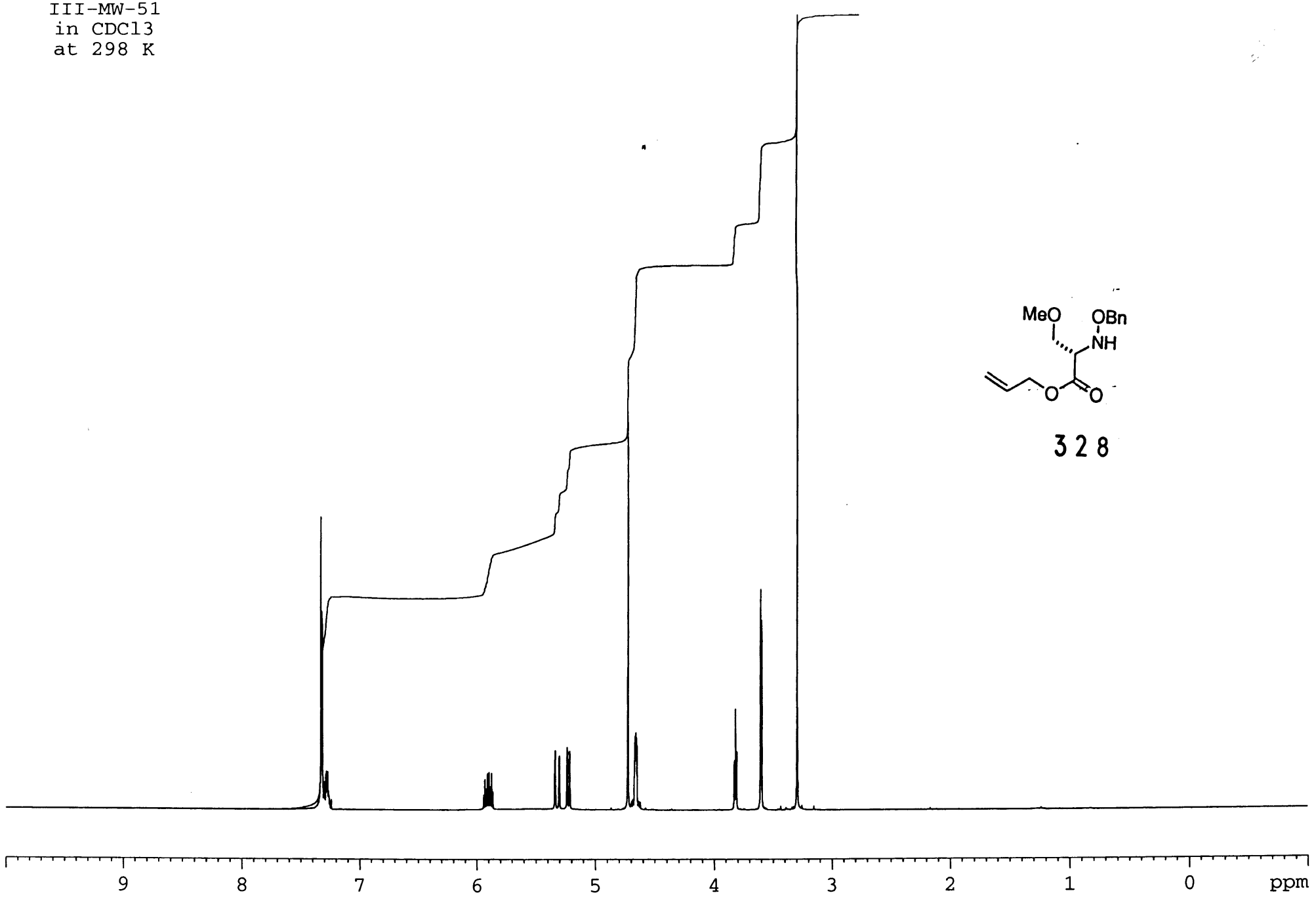

328

III-MW-51
Carbon 13 in
CDCl3 at 298 K

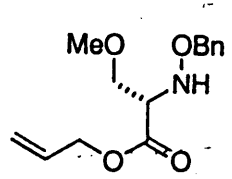

328

III-MW-51
COSY in
CDCl3 at 298 K

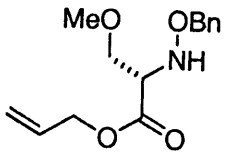

328

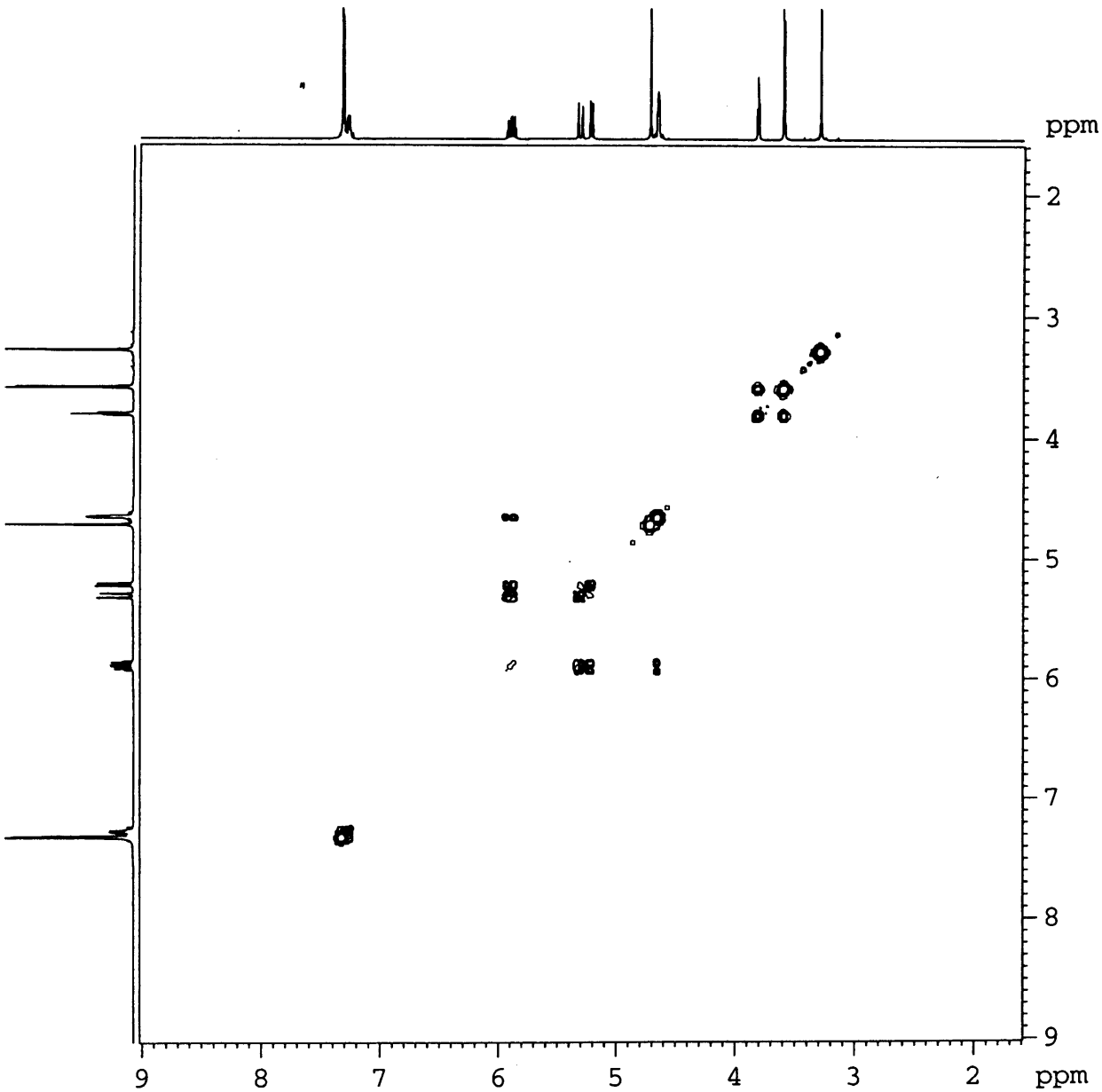

III-MW-51
HMQC in
CDCl3 at 298 K

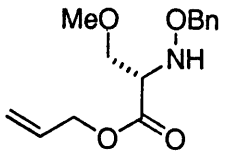

328

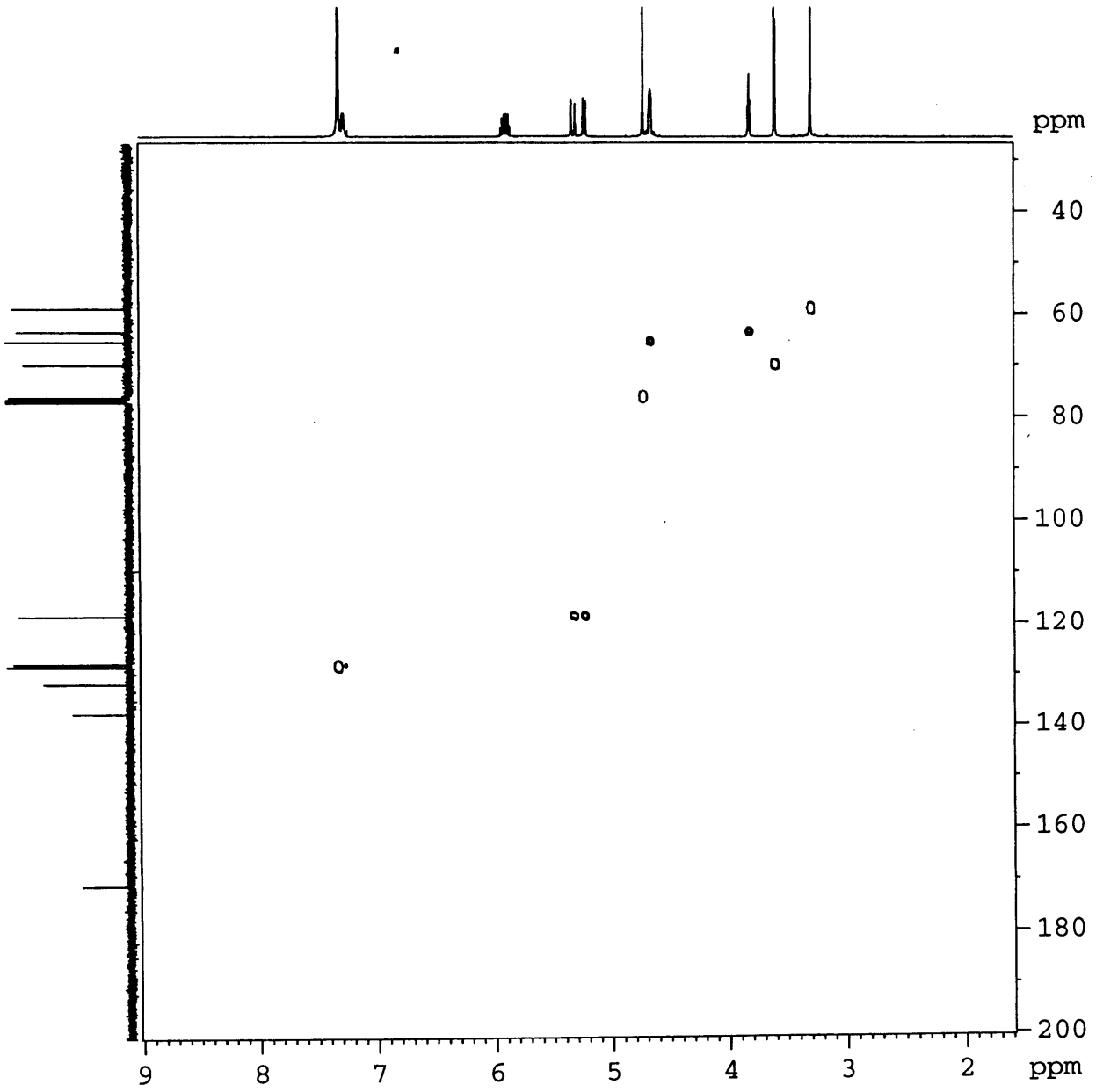

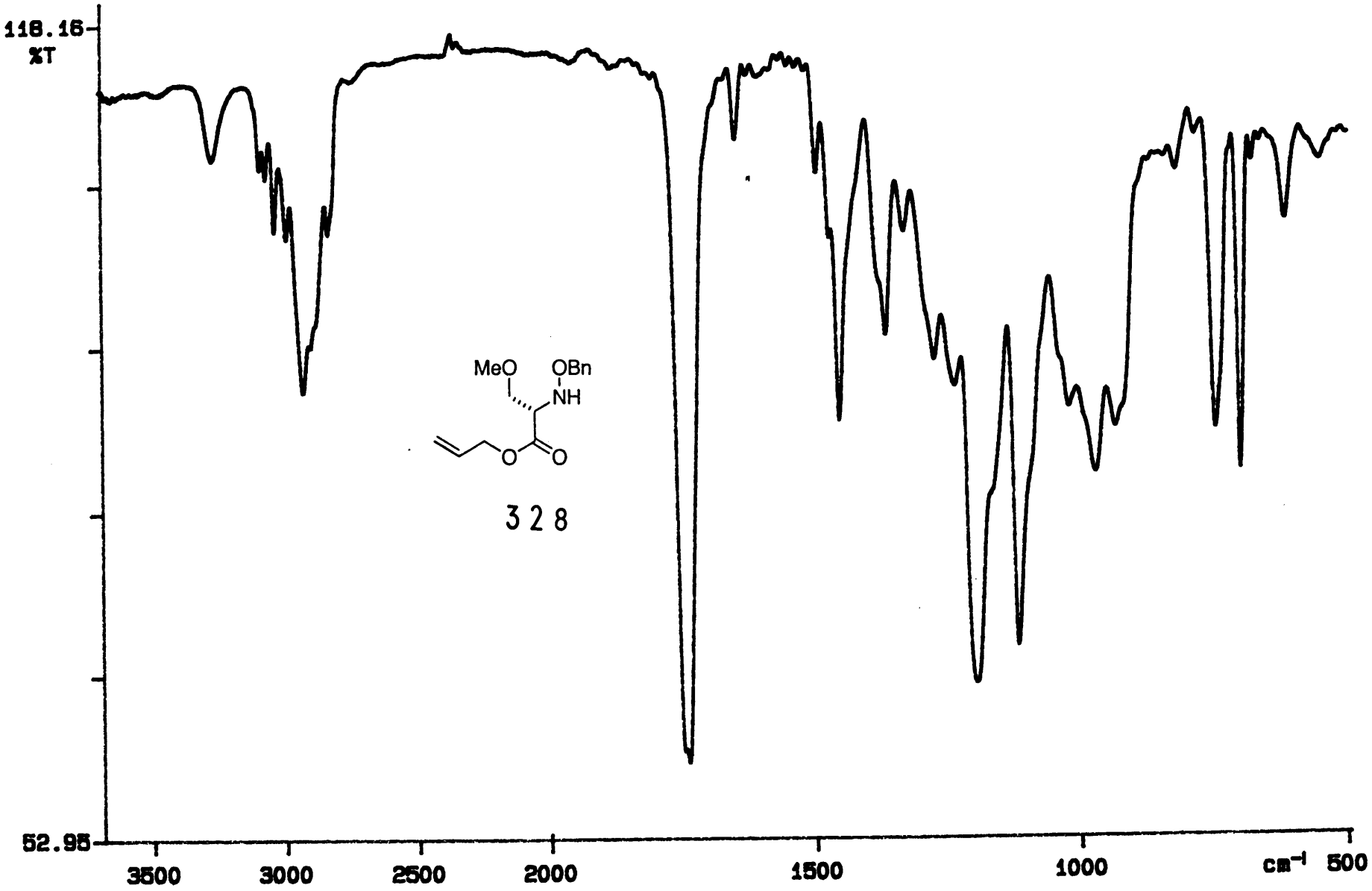
118.16
%T
52.95
3500
3000
2500
2000
1500
1000
cm⁻¹
500
MeO
OBn
NH
O
O
328

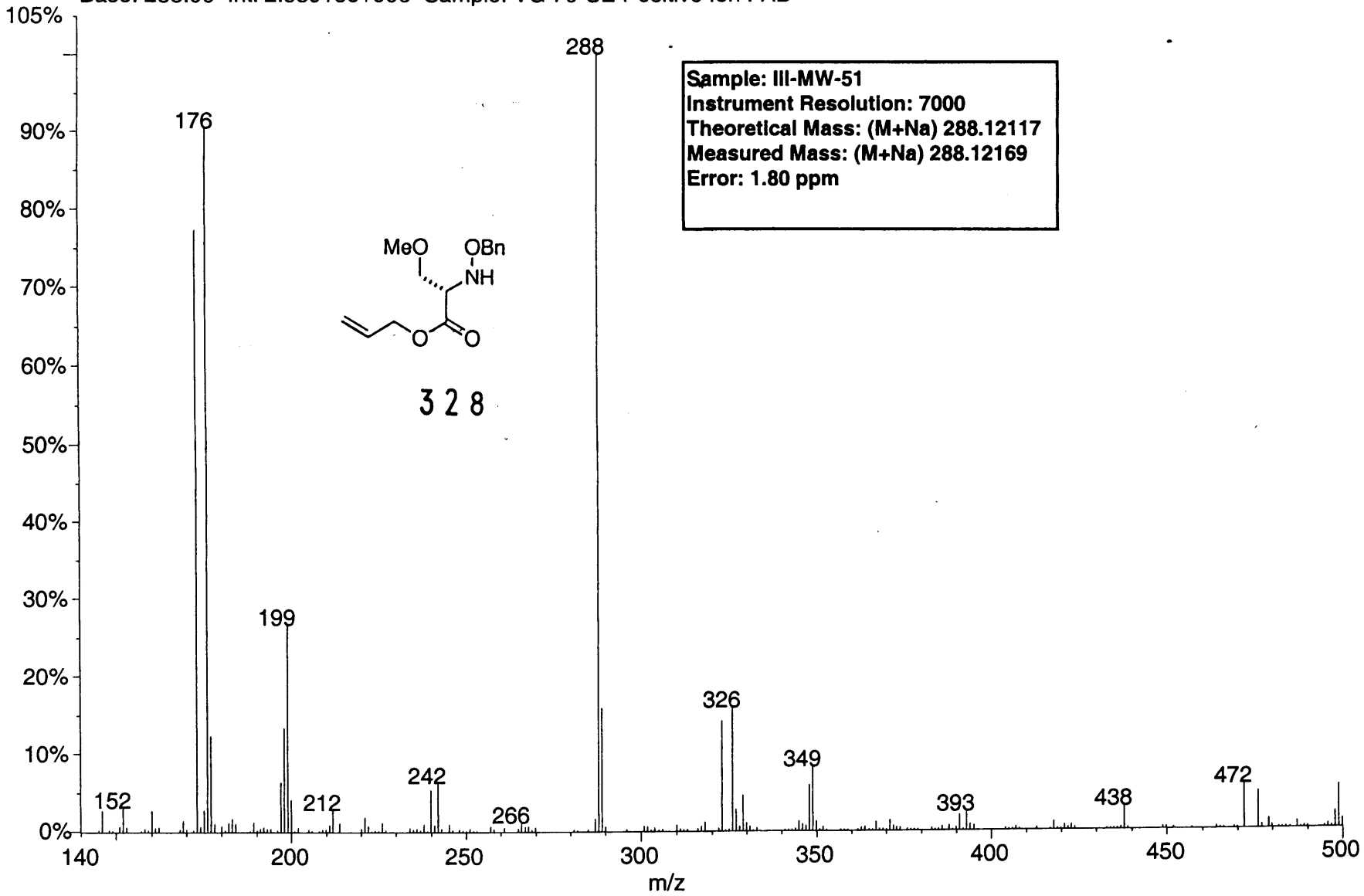
01270206: Scan 225 (41.20 min) - Back
Base: 288.00 Int: 2.53916e+006 Sample: VG 70-SE Positive Ion FAB
Sample: III-MW-51
Instrument Resolution: 7000
Theoretical Mass: (M+Na) 288.12117
Measured Mass: (M+Na) 288.12169
Error: 1.80 ppm
MeO
OBn
NH
O
O
328
105%
90%
80%
70%
60%
50%
40%
30%
20%
10%
0%
140
200
250
300
350
400
450
500
m/z
288
176
199
326
349
242
212
266
152
393
438
472

IV-MW-61 in
DMSO at 298 K

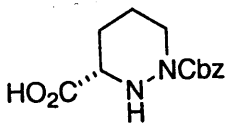

30

IV-MW-61 in
DMSO at 363 K

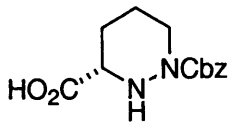

30

IV-MW-61
DEPT in
DMSO at 298 K

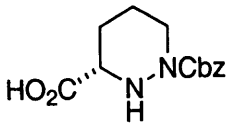

30

IV-MW-61
COSY in
DMSO at 298 K

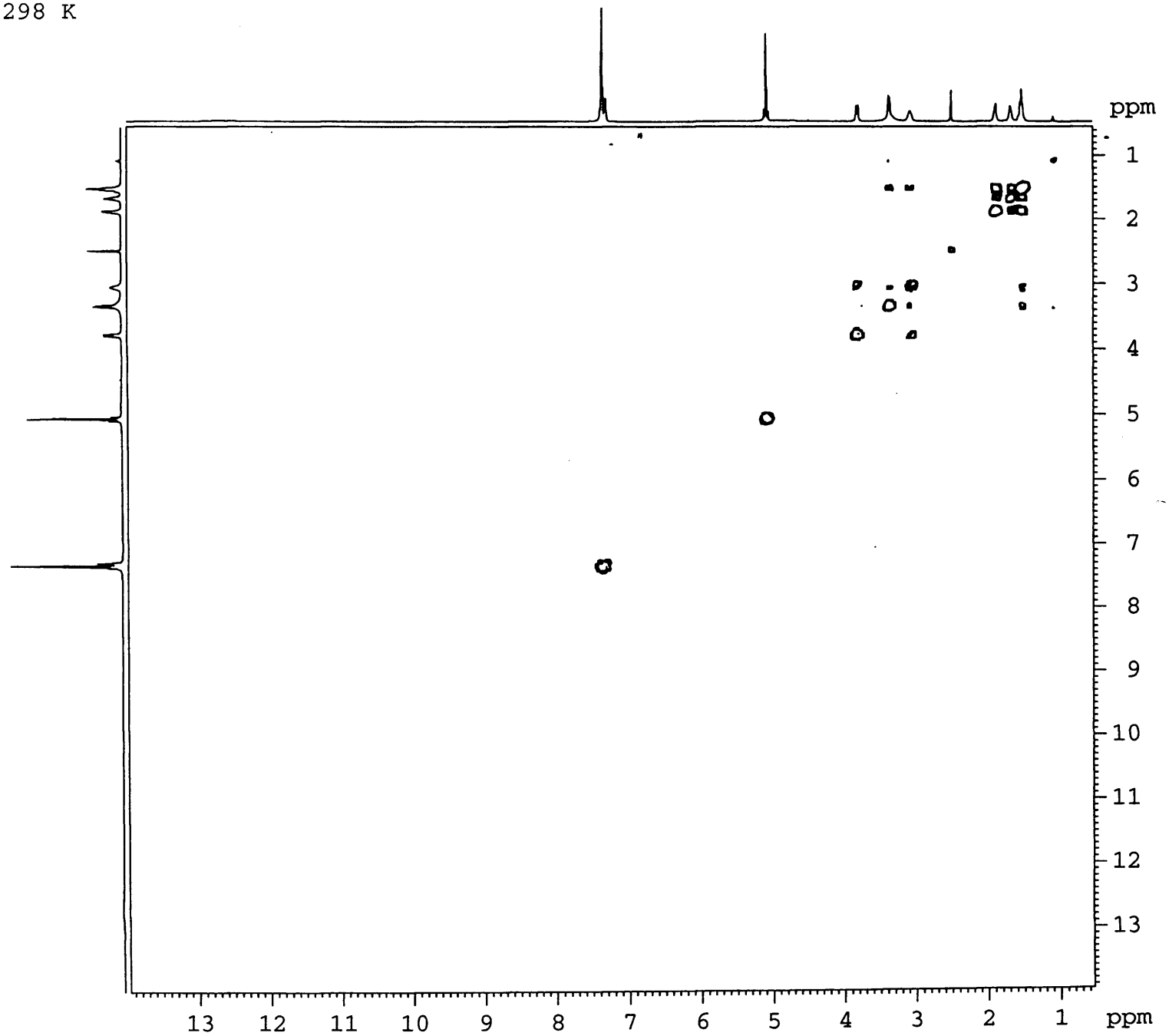

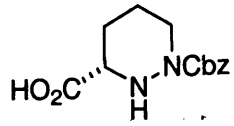

30

IV-MW-61
HMQC in
DMSO at 298 K

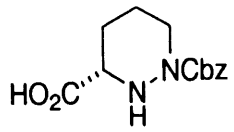

30

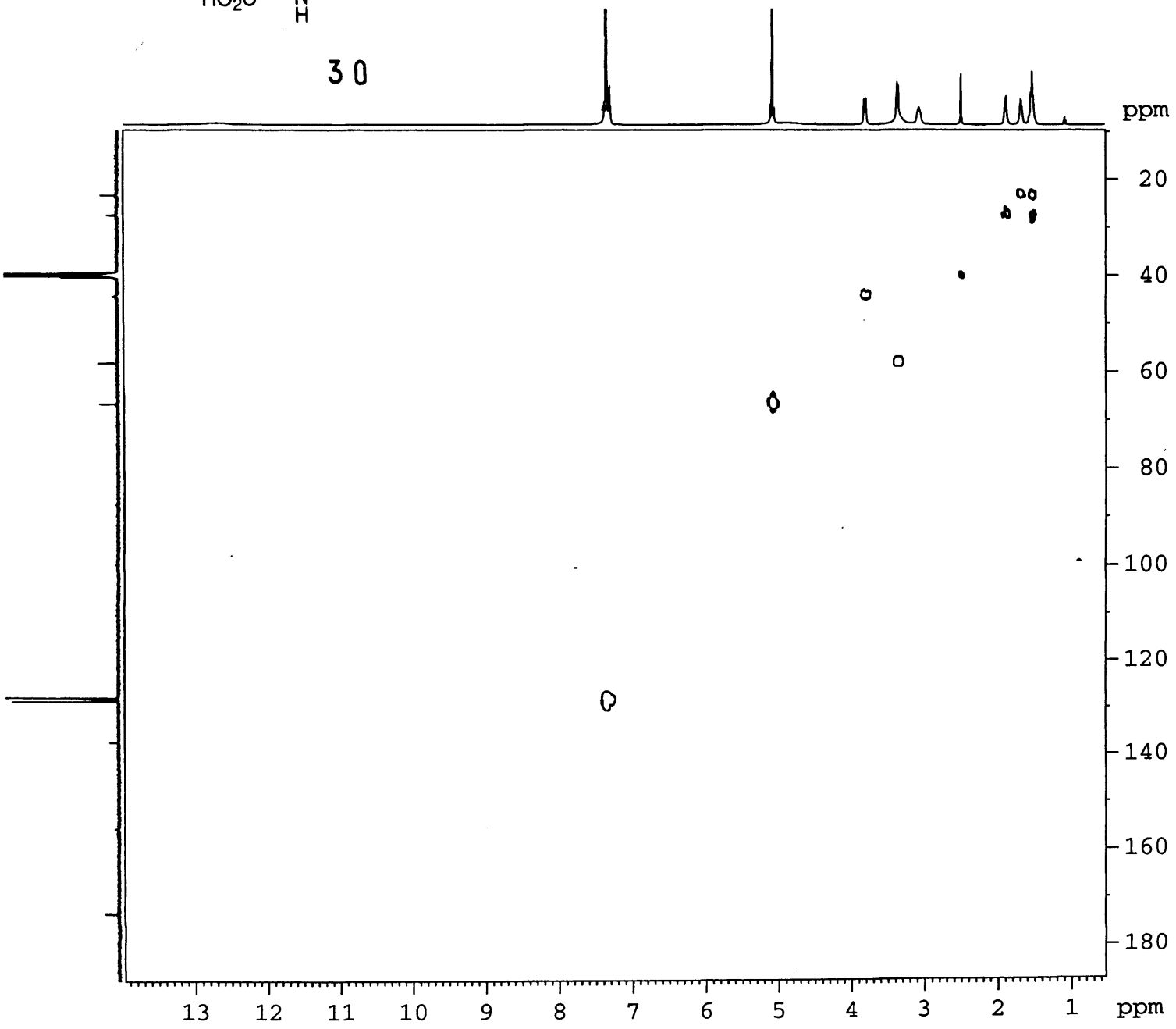

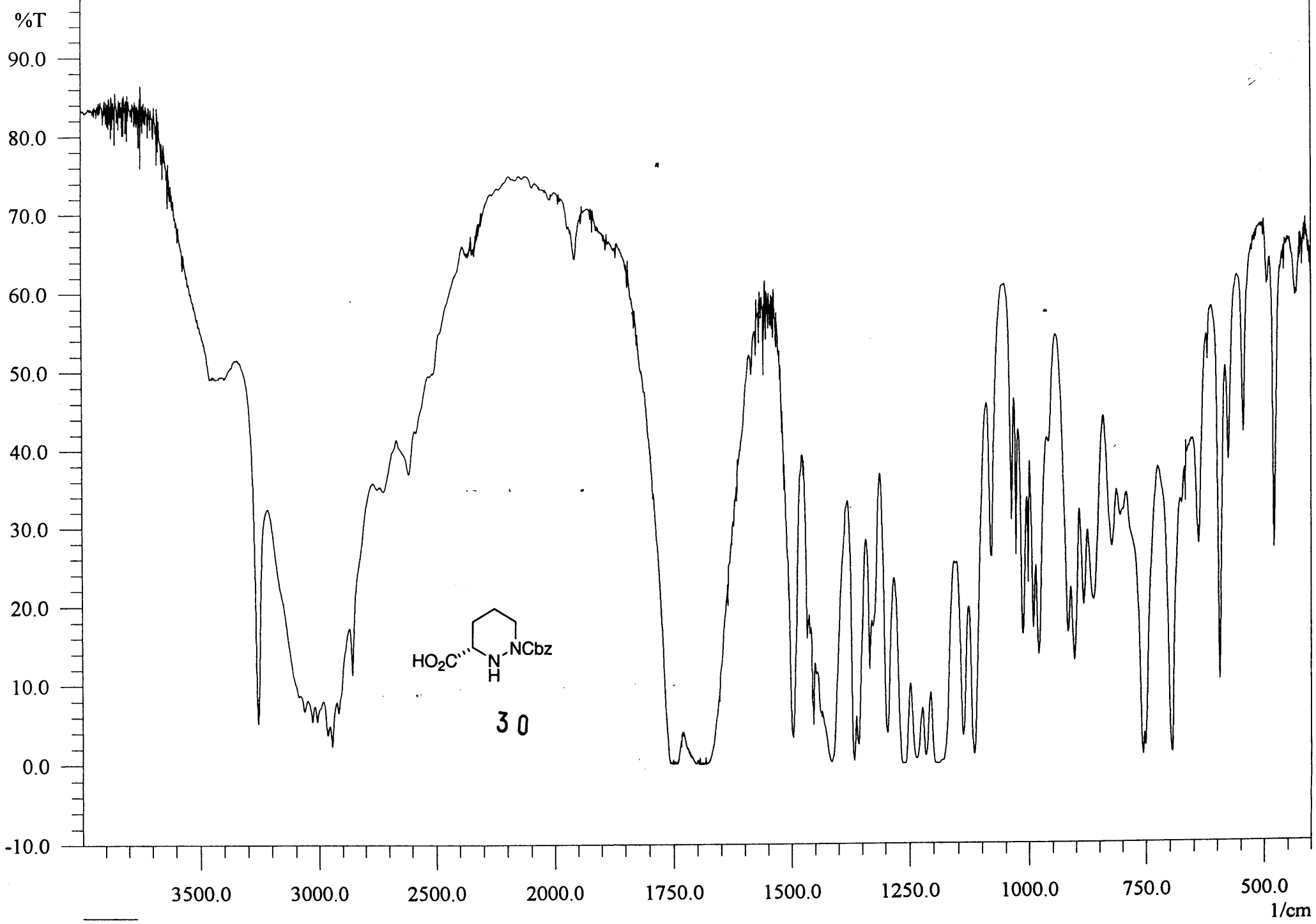
%T
90.0
80.0
70.0
60.0
50.0
40.0
30.0
20.0
10.0
0.0
-10.0
3500.0
3000.0
2500.0
2000.0
1750.0
1500.0
1250.0
1000.0
750.0
500.0
1/cm
HO2C
N
H
NCbz
30

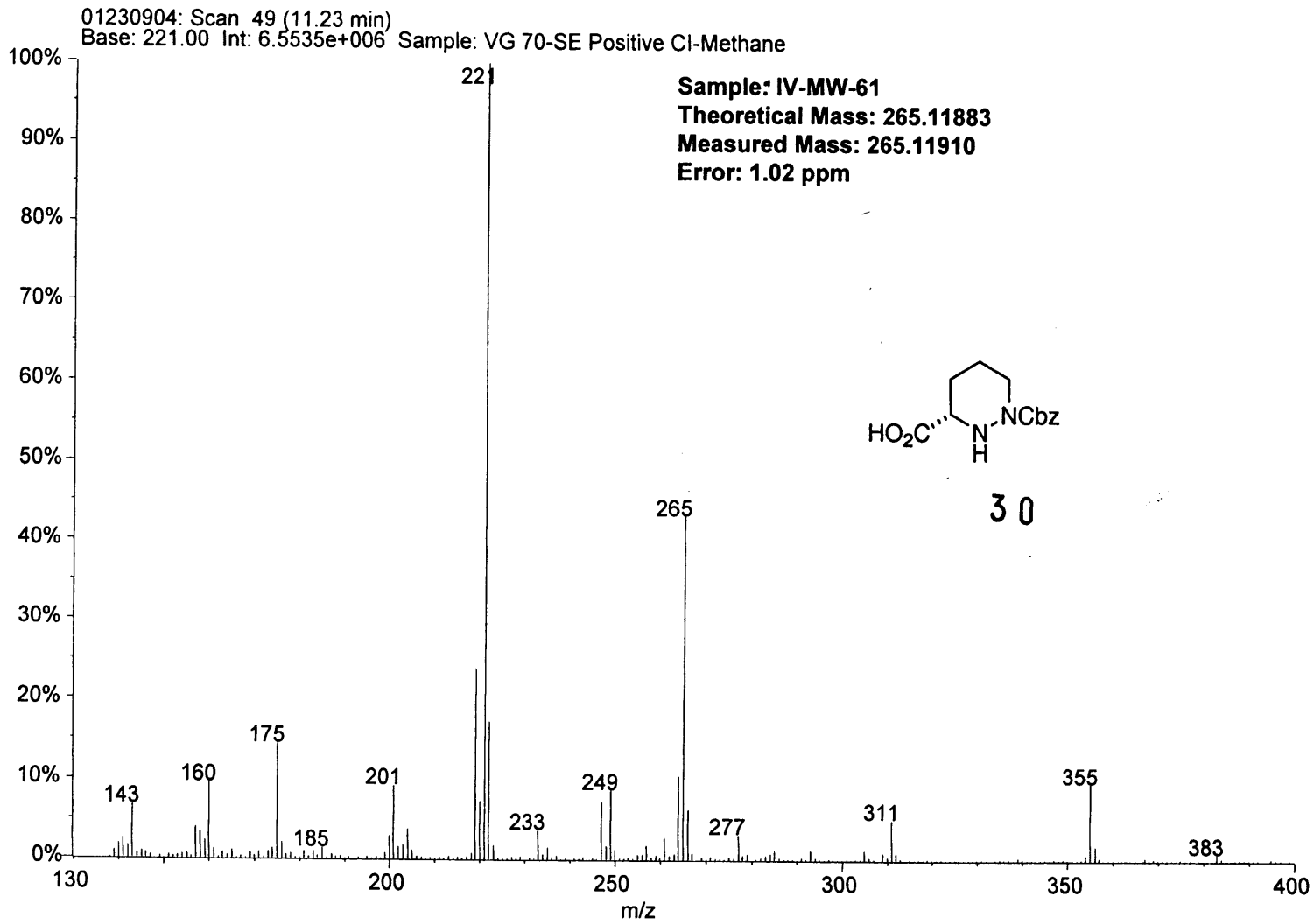
01230904: Scan 49 (11.23 min)
Base: 221.00 Int: 6.5535e+006 Sample: VG 70-SE Positive CI-Methane
Sample: IV-MW-61
Theoretical Mass: 265.11883
Measured Mass: 265.11910
Error: 1.02 ppm
HO2C
N
H
NCbz
30
100%
90%
80%
70%
60%
50%
40%
30%
20%
10%
0%
130
200
250
300
350
400
m/z
221
265
175
160
143
201
249
355
233
277
311
185
383

DMSO at 413 K

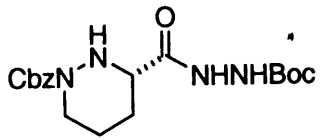

164

Carbon 13 in
DMSO at 413 K

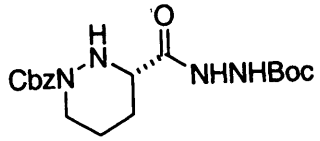

164

IV-MW-25
COSY in
DMSO at 413 K

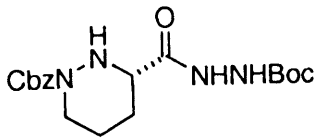

164

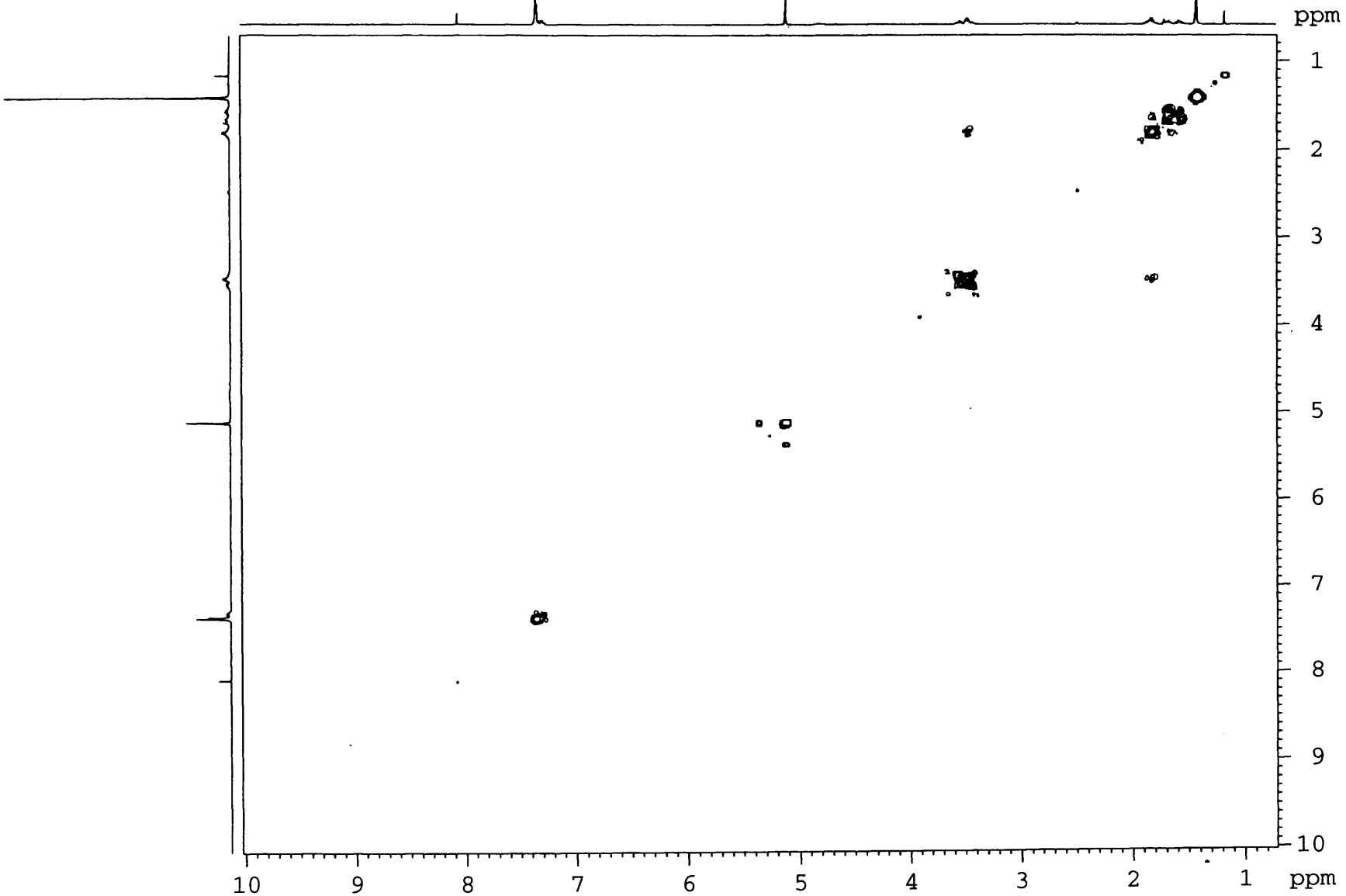

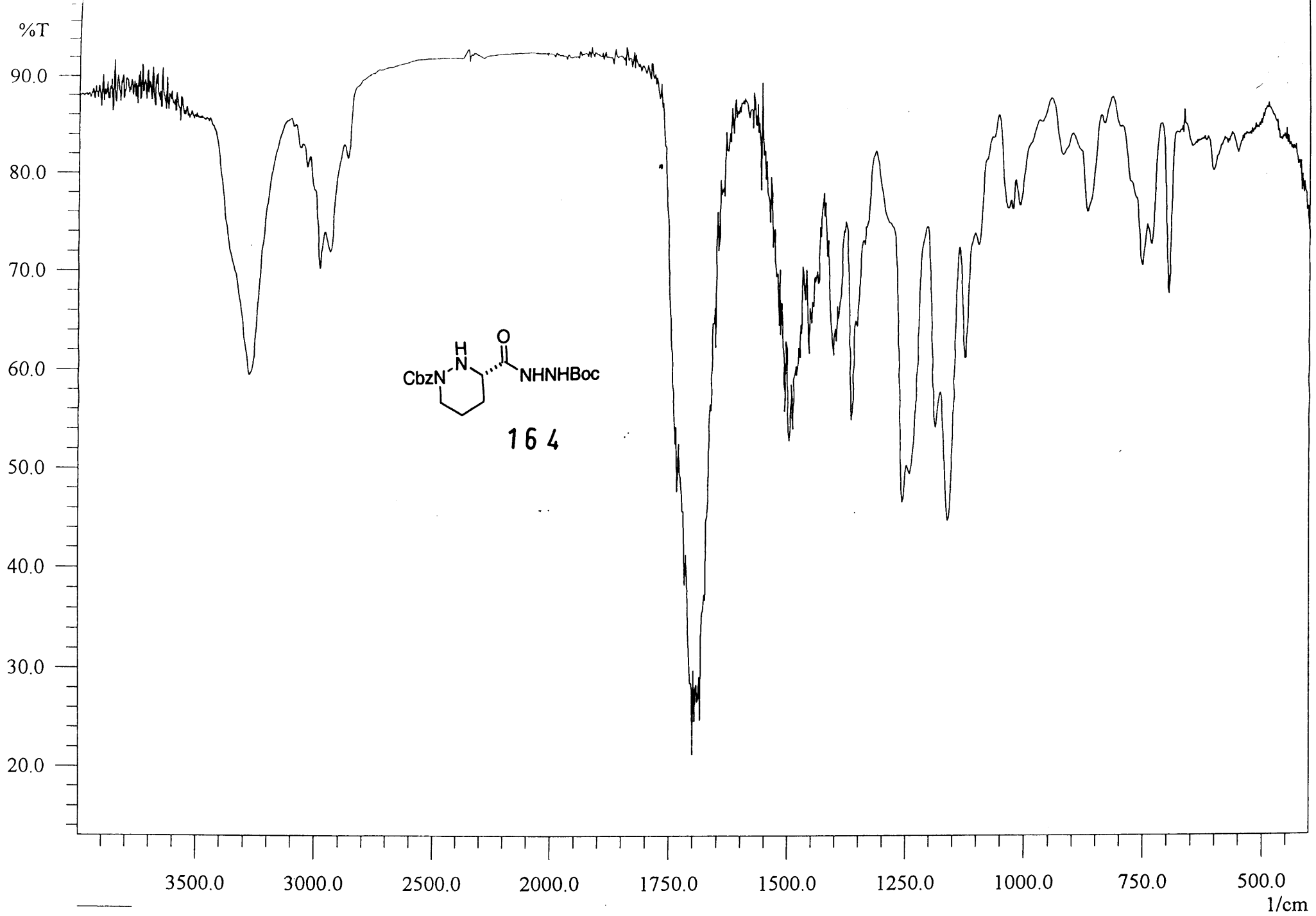
%T
90.0
80.0
70.0
60.0
50.0
40.0
30.0
20.0
CbzN
H
N
O
NHNHBoc
164
3500.0
3000.0
2500.0
2000.0
1750.0
1500.0
1250.0
1000.0
750.0
500.0
1/cm

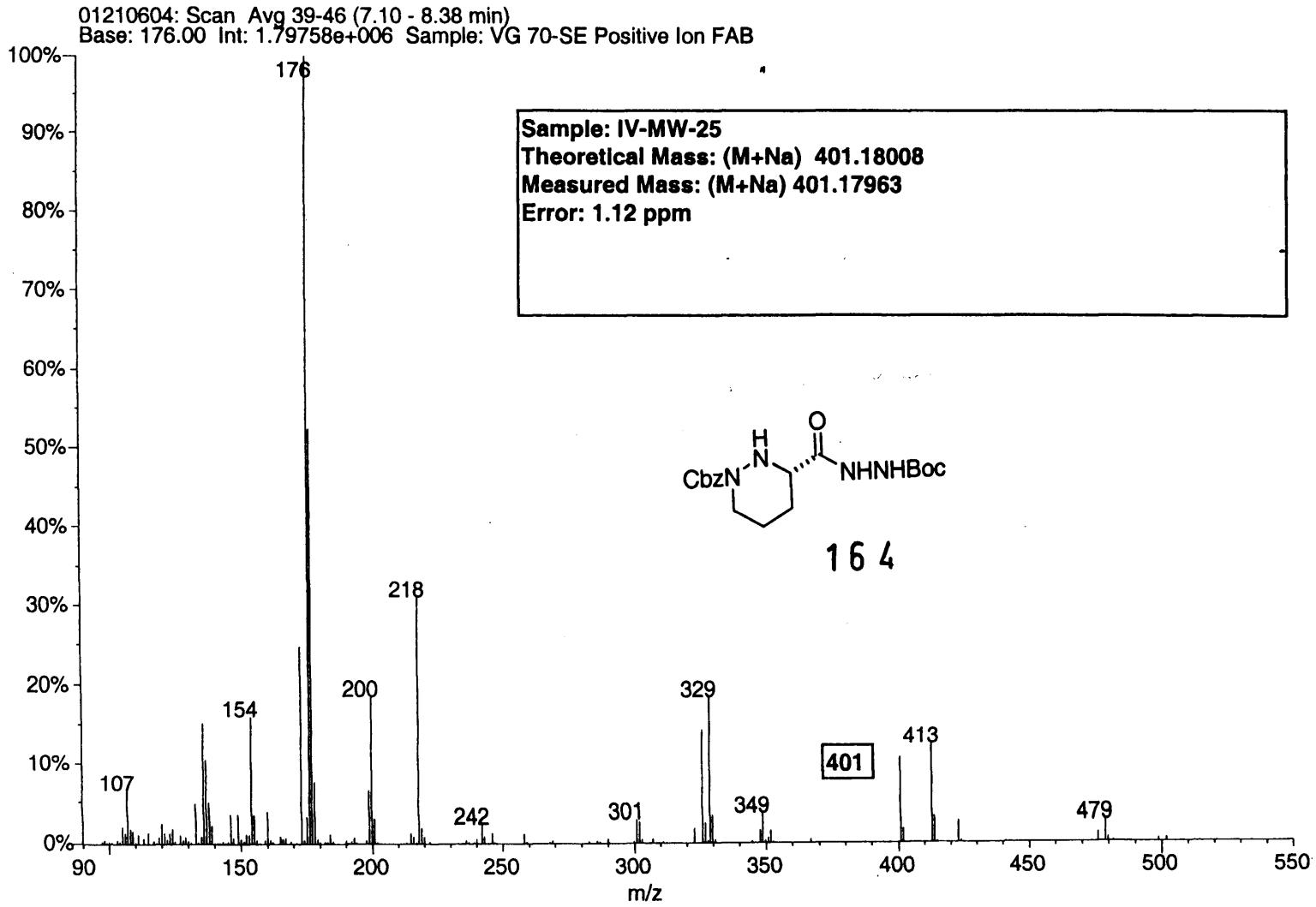
01210604: Scan Avg 39-46 (7.10 - 8.38 min)
Base: 176.00 Int: 1.79758e+006 Sample: VG 70-SE Positive Ion FAB
Sample: IV-MW-25
Theoretical Mass: (M+Na) 401.18008
Measured Mass: (M+Na) 401.17963
Error: 1.12 ppm
CbzN
H
N
O
NHNHBoc
164
176
218
200
329
154
413
401
107
242
301
349
479
100%
90%
80%
70%
60%
50%
40%
30%
20%
10%
0%
90
150
200
250
300
350
400
450
500
550
m/z

IV-MW-54 in
CDCl3 at 298 K

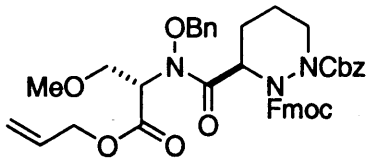

329

IV-MW-54 in
Toluene at 363 K

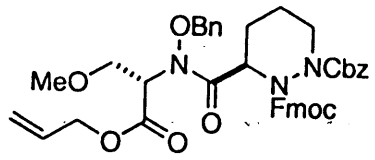

329

IV-MW-54
Carbon 13 in
CDCl3 at 298 K

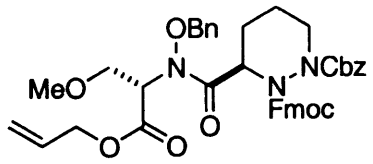

329

IV-MW-54
Carbon 13 in
Toluene at 363 K

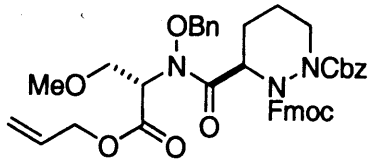

329

IV-MW-54
DEPT in
CDCl3 at 298 K

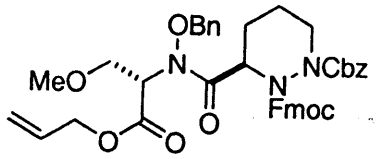

329

IV-MW-54
COSY in
CDCl3 at 298 K

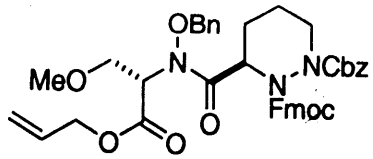

329

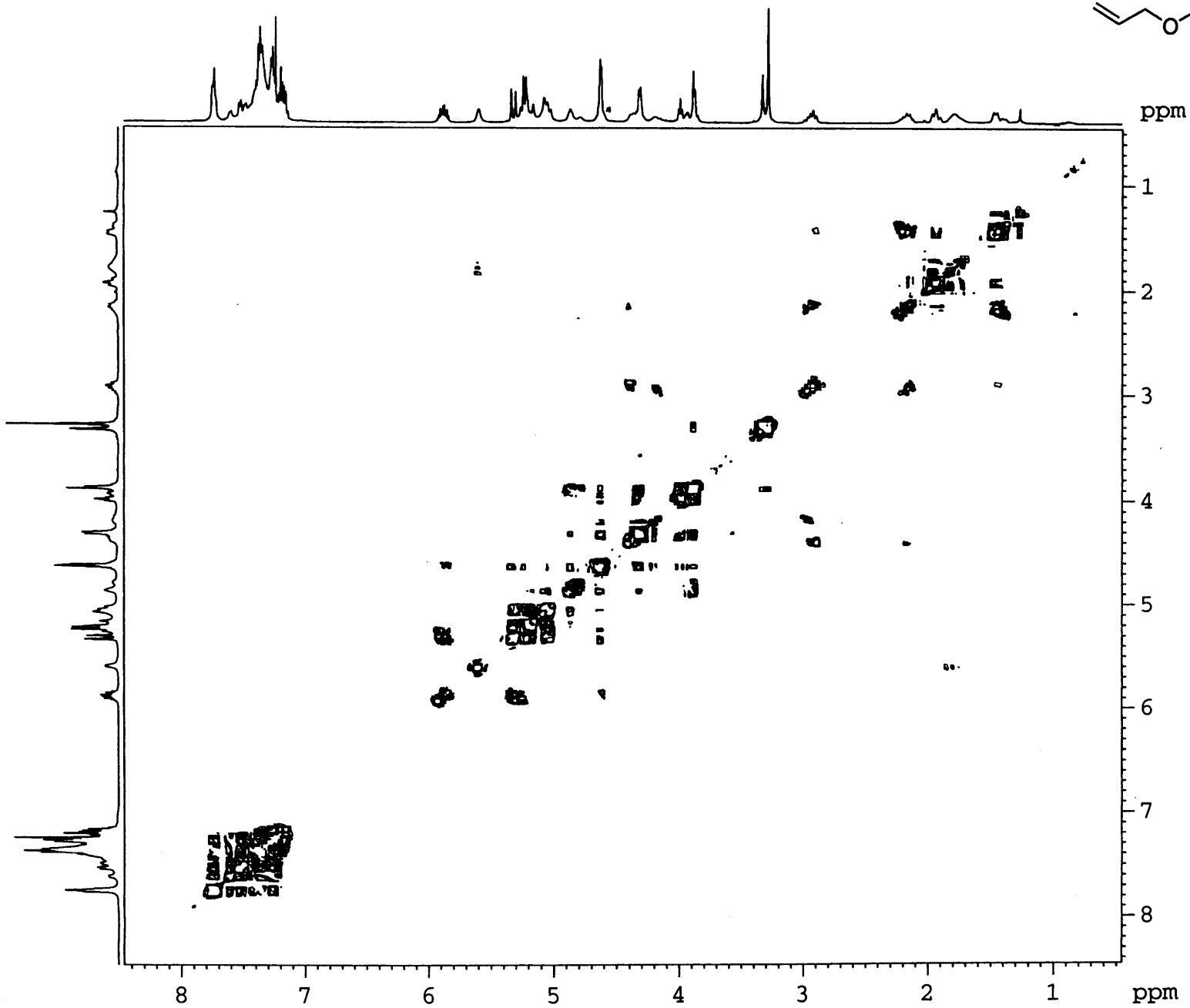

IV-MW-54
HMQC in
CDCl3 at 298 K

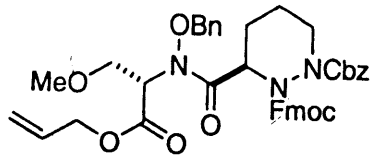

329

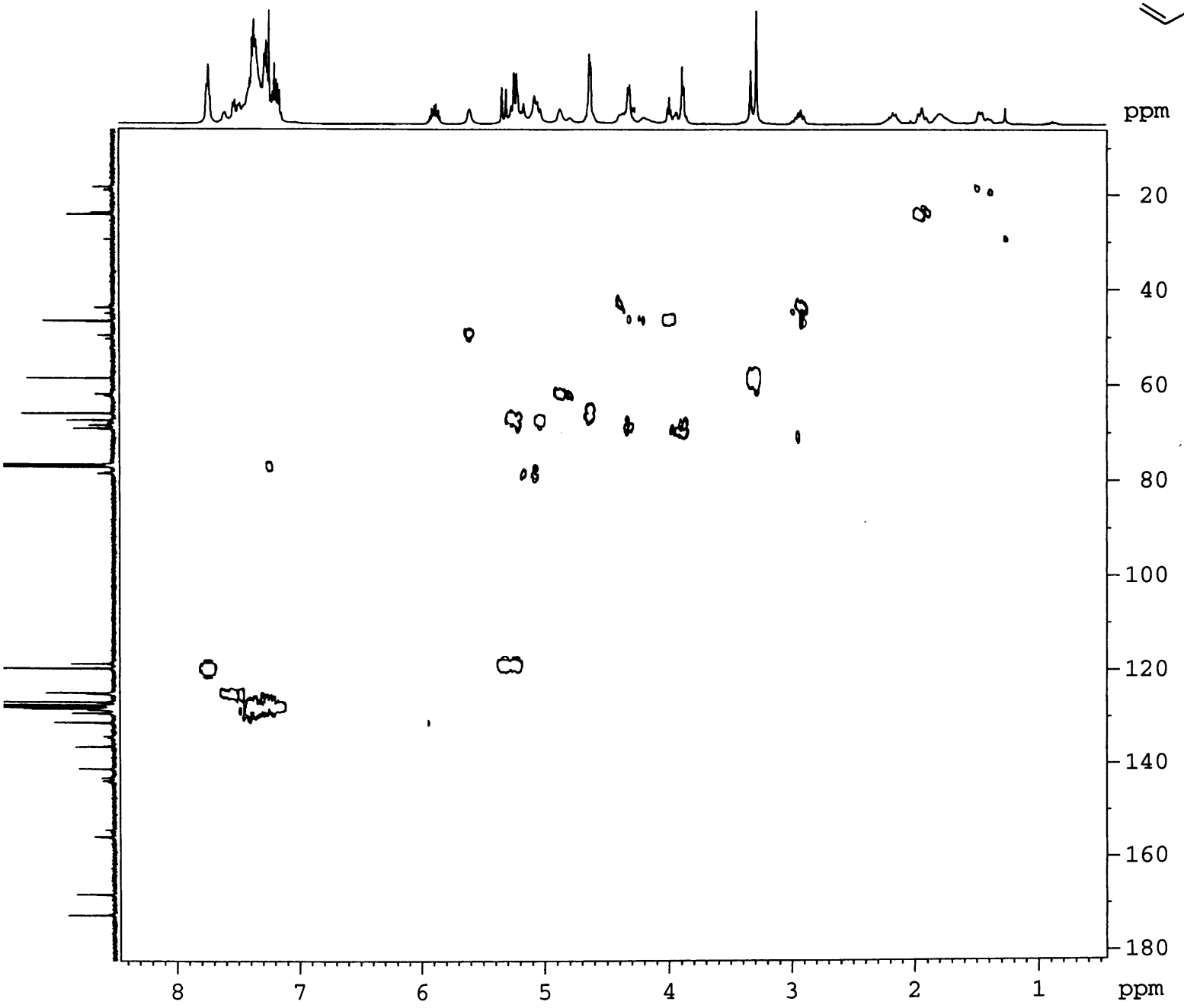

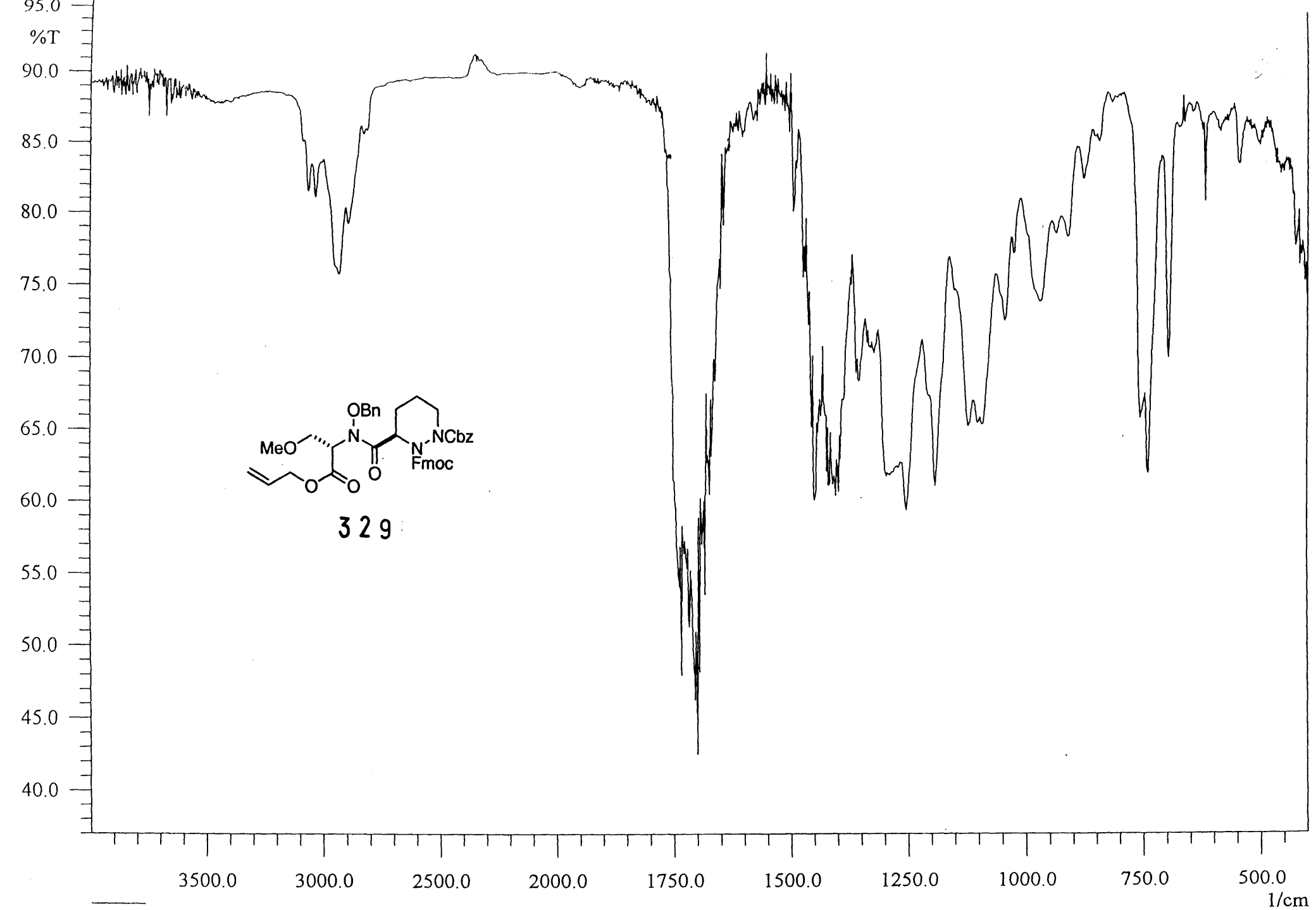
95.0
%T
90.0
85.0
80.0
75.0
70.0
65.0
60.0
55.0
50.0
45.0
40.0
OBn
N
MeO
O
N
NCbz
Fmoc
O
O
O
3500.0
3000.0
2500.0
2000.0
1750.0
1500.0
1250.0
1000.0
750.0
500.0
1/cm

329

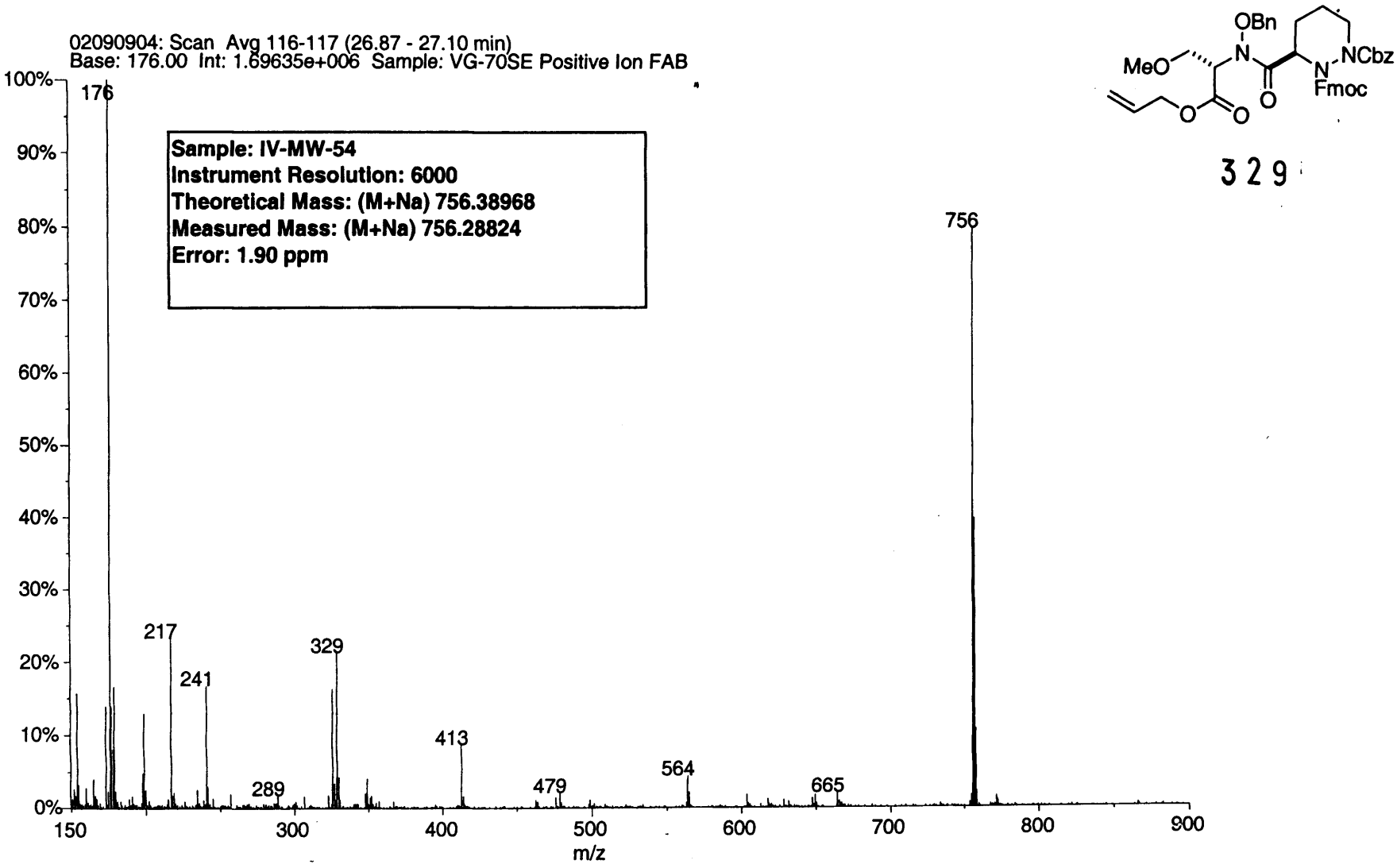
02090904: Scan Avg 116-117 (26.87 - 27.10 min)
Base: 176.00 Int: 1.69635e+006 Sample: VG-70SE Positive Ion FAB
Sample: IV-MW-54
Instrument Resolution: 6000
Theoretical Mass: (M+Na) 756.38968
Measured Mass: (M+Na) 756.28824
Error: 1.90 ppm
100%
90%
80%
70%
60%
50%
40%
30%
20%
10%
0%
176
217
241
289
329
413
479
564
665
756
150
300
400
500
600
700
800
900
m/z

OBn
MeO
N
NCbz
N
Fmoc
O
O
O

329

IV-MW-71 in
CDCl3 at 298 K

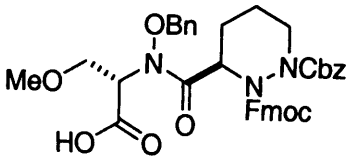

304

IV-MW-71
DEPT in
CDCl3 at 298 K

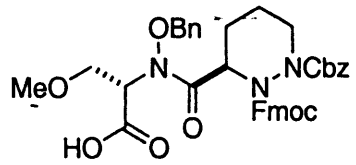

304

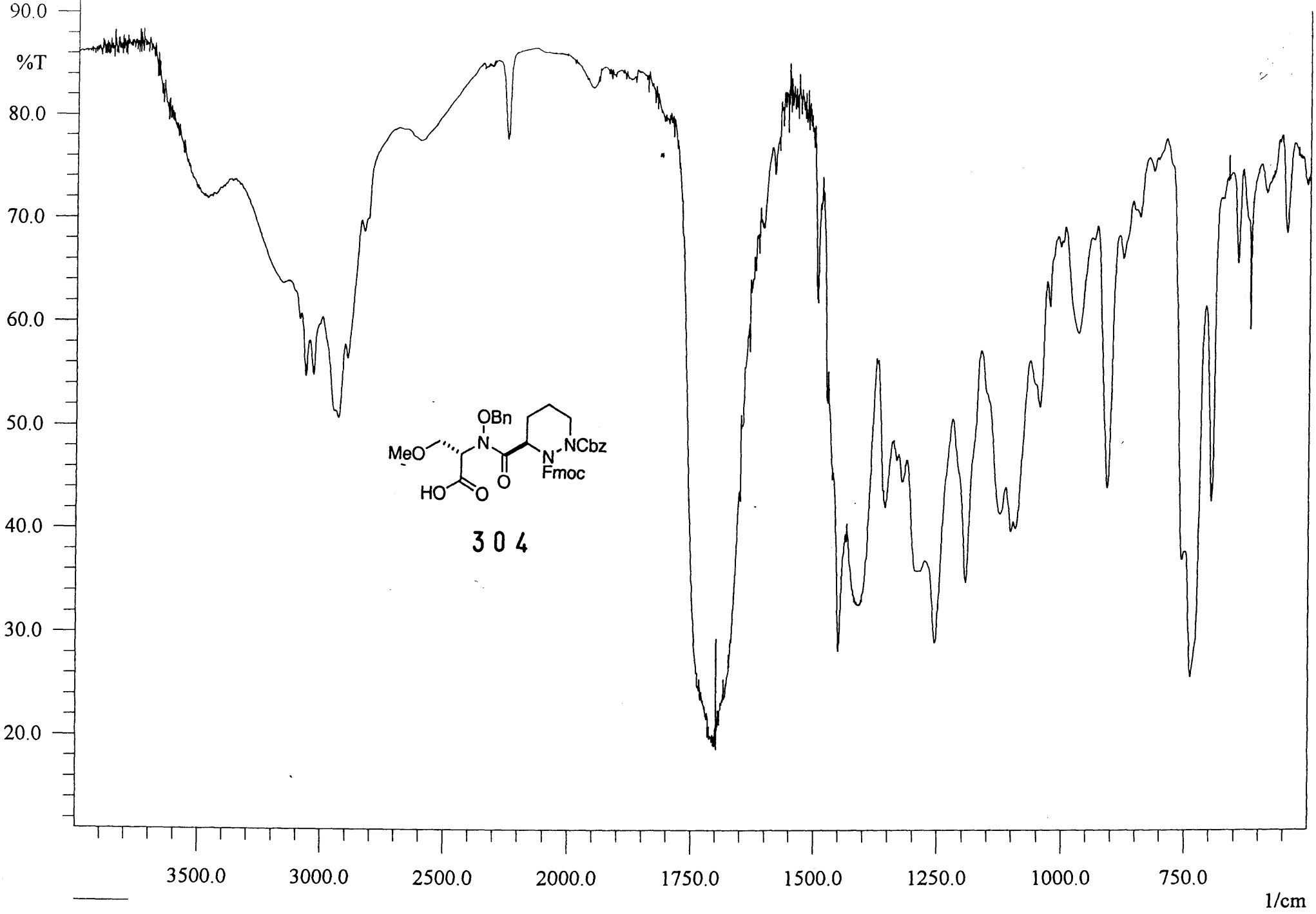
90.0
%T
80.0
70.0
60.0
50.0
40.0
30.0
20.0
OBn
N
MeO
O
HO
O
N
NCbz
Fmoc
3500.0
3000.0
2500.0
2000.0
1750.0
1500.0
1250.0
1000.0
750.0
1/cm

304

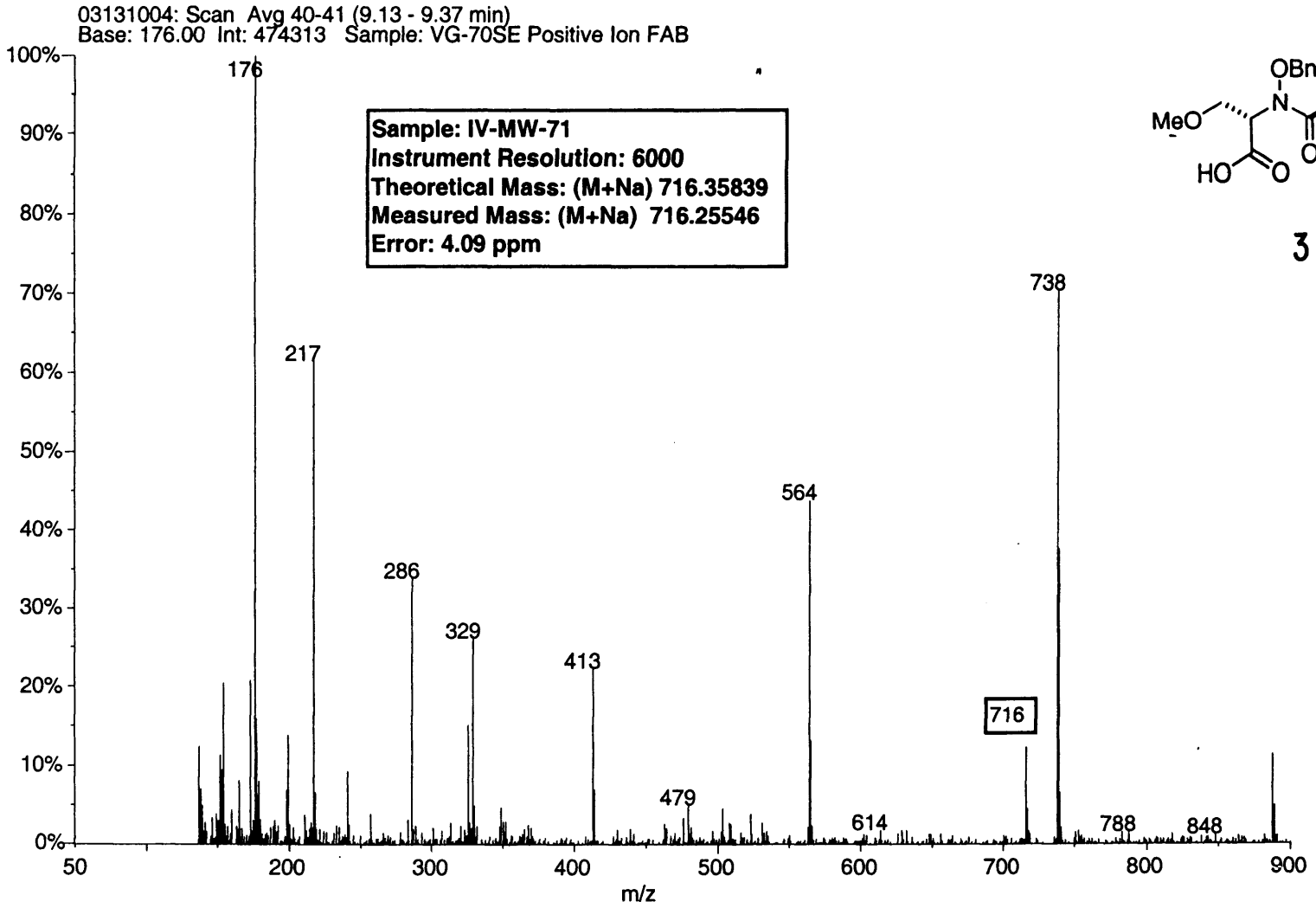
03131004: Scan Avg 40-41 (9.13 - 9.37 min)
Base: 176.00 Int: 474313 Sample: VG-70SE Positive Ion FAB
Sample: IV-MW-71
Instrument Resolution: 6000
Theoretical Mass: (M+Na) 716.35839
Measured Mass: (M+Na) 716.25546
Error: 4.09 ppm
176
217
286
329
413
479
564
614
716
738
788
848
100%
90%
80%
70%
60%
50%
40%
30%
20%
10%
0%
50
200
300
400
500
600
700
800
900
m/z

OBn
N
NCbz
MeO
N
Fmoc
O
HO
O

304

in CDCl3
at 298 K

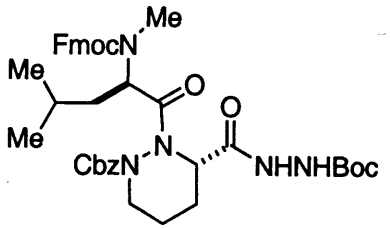

168

III-MW-146
carbon 13 in
CDCl3 at 298 K

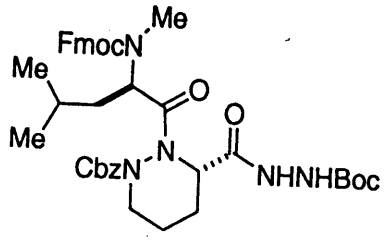

168

111-MW-146
DEPT in CDCl3
at 298 K

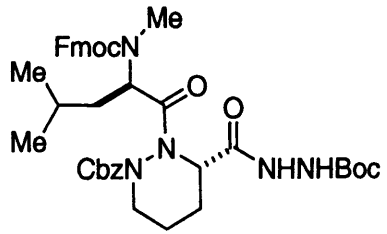

168

III-MW-146
COSY in CDCl3
at 298 K

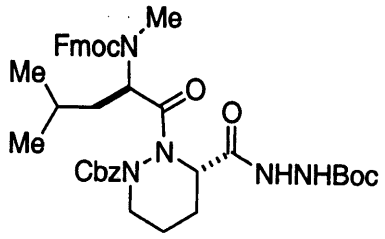

168

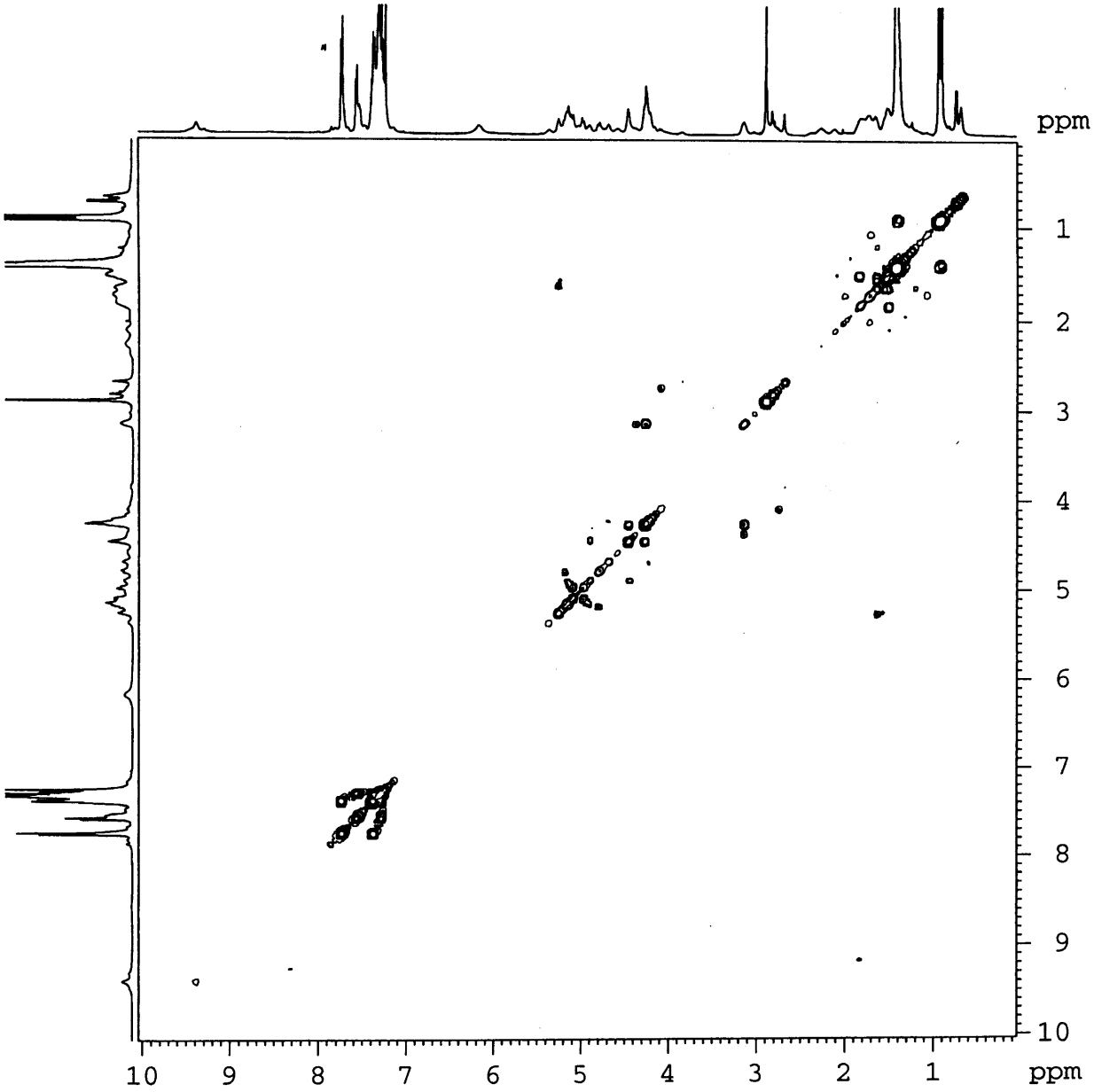

III-MW-146
HMQC in CDCl3
at 298 K

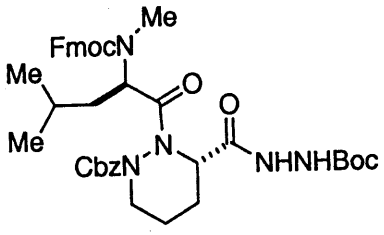

168

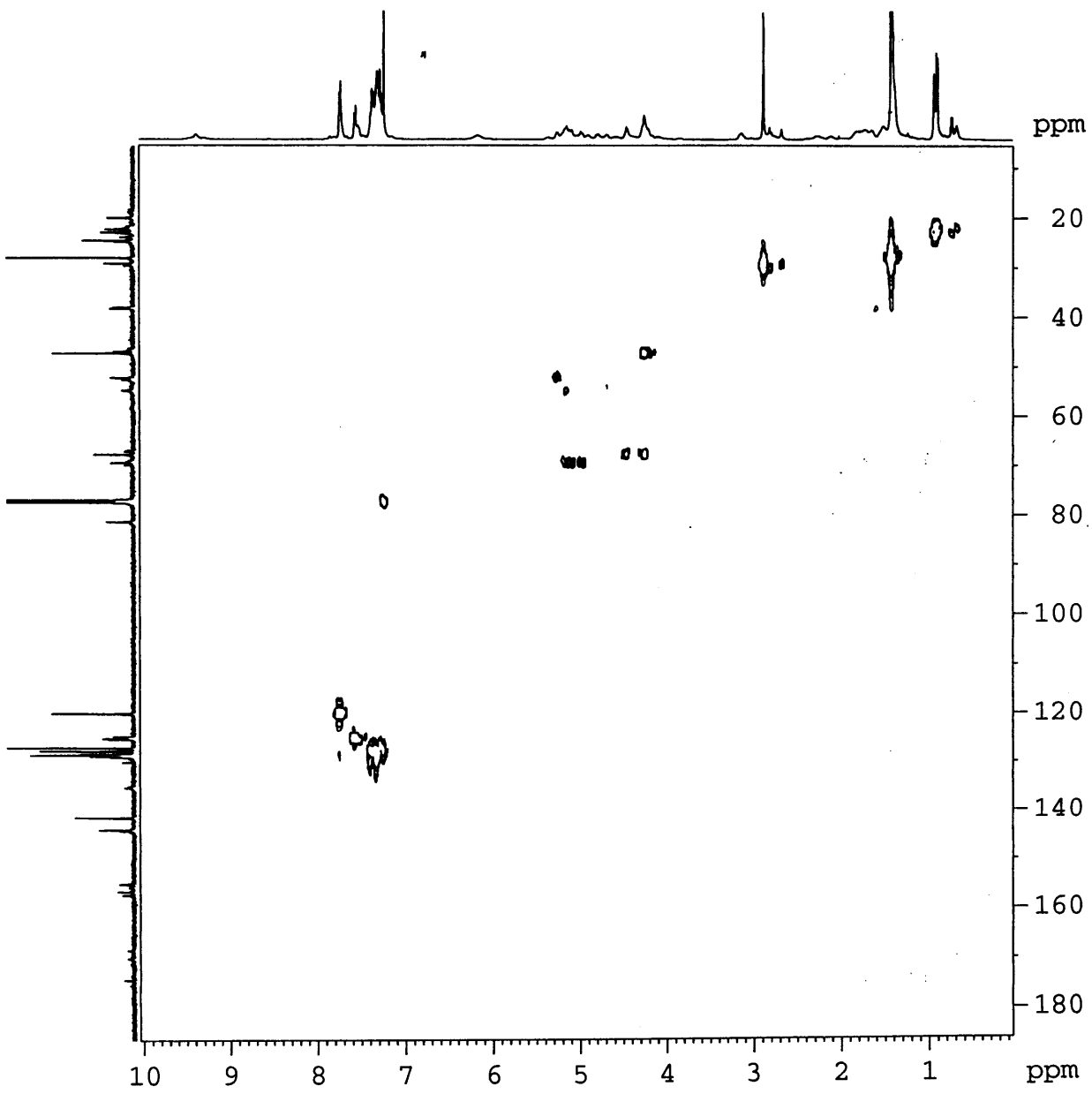

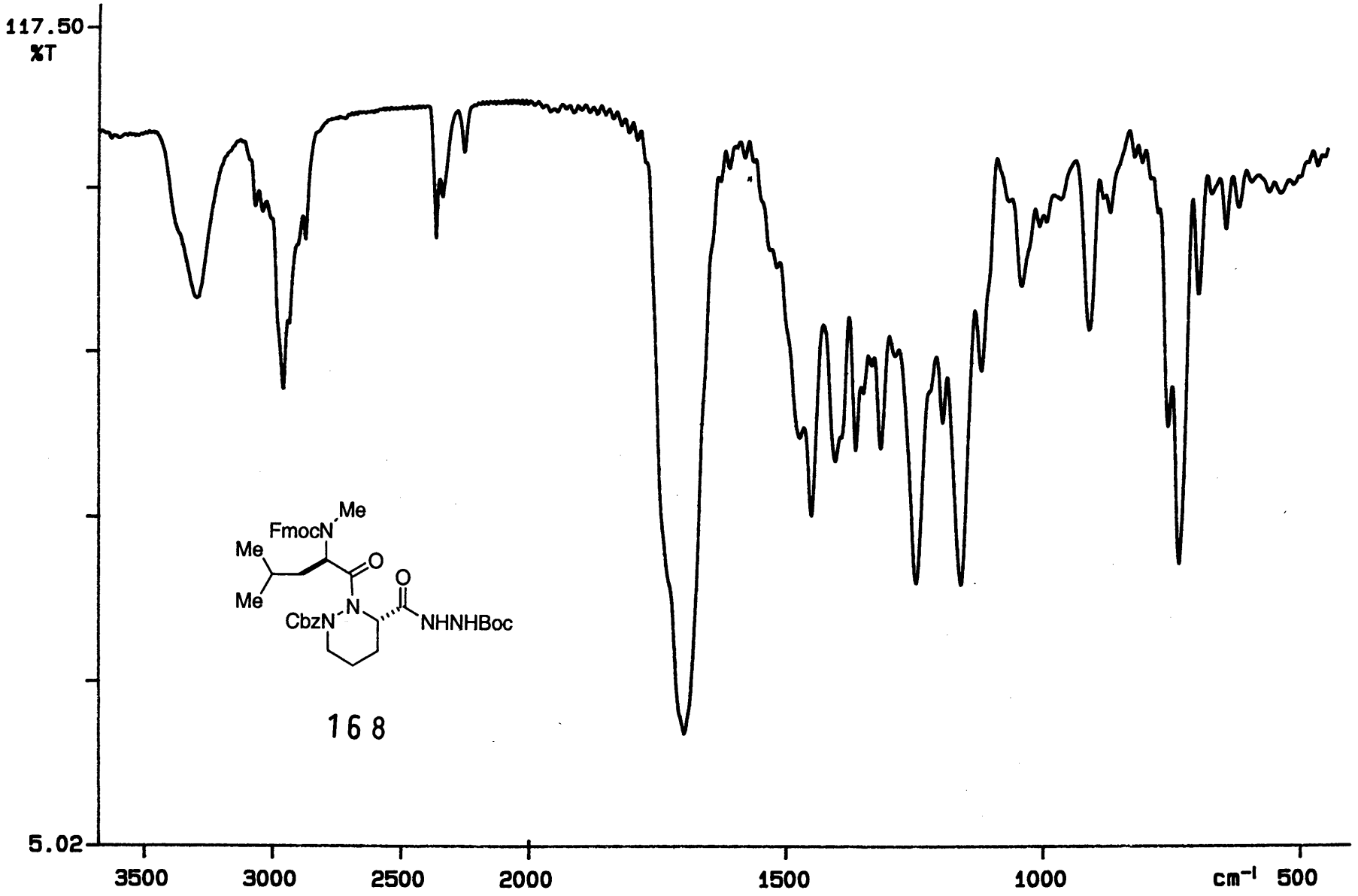
117.50
%T
5.02
3500
3000
2500
2000
1500
1000
cm-1
500
FmocN
Me
Me
Me
O
O
N
CbzN
NHNHBoc

168

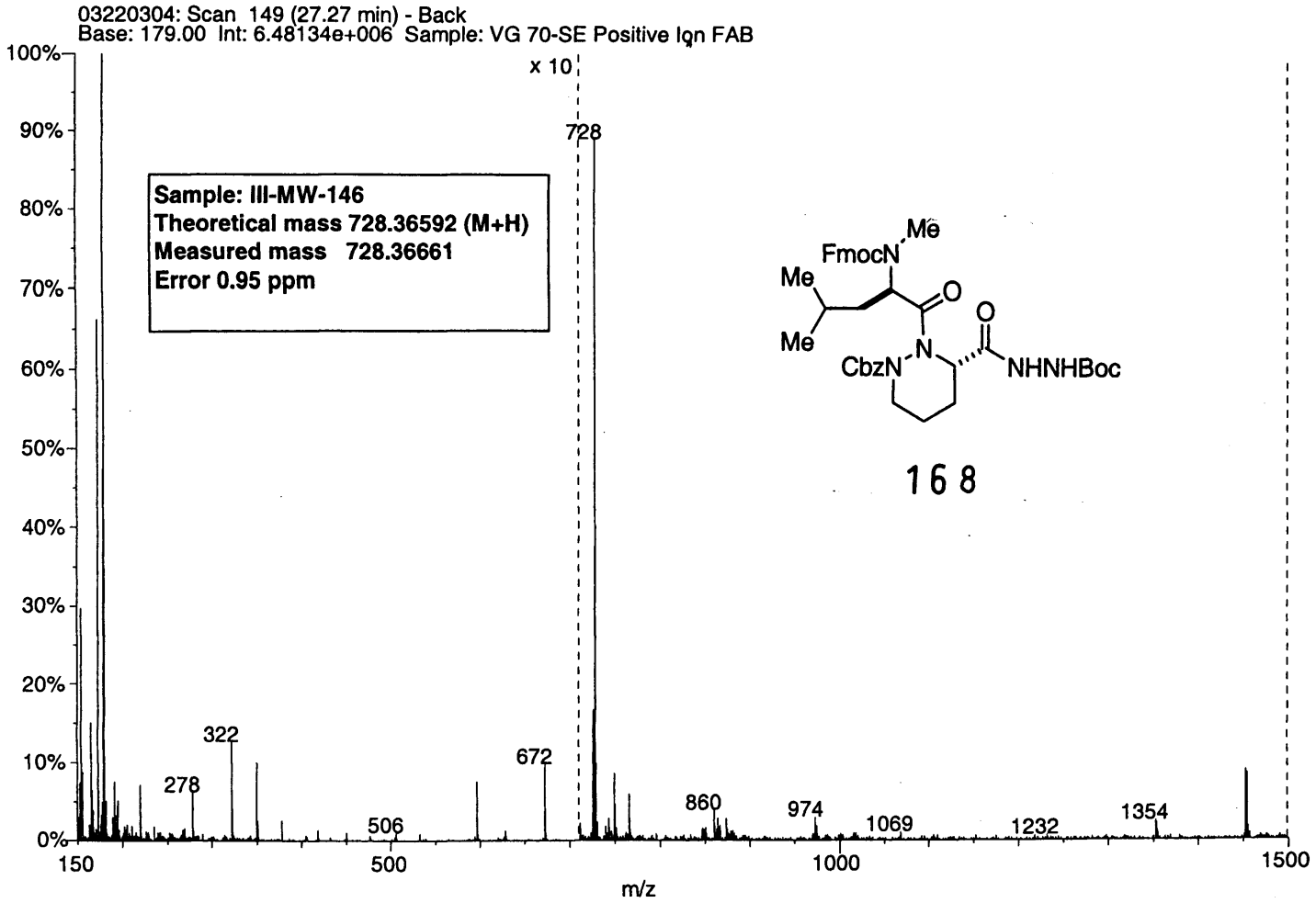
03220304: Scan 149 (27.27 min) - Back
Base: 179.00 Int: 6.48134e+006 Sample: VG 70-SE Positive Ion FAB
x 10
728
Sample: III-MW-146
Theoretical mass 728.36592 (M+H)
Measured mass 728.36661
Error 0.95 ppm
FmocN
Me
Me
Me
O
O
N
CbzN
NHNHBoc
322
278
672
506
860
974
1069
1232
1354
100%
90%
80%
70%
60%
50%
40%
30%
20%
10%
0%
150
500
1000
1500
m/z

168

III-MW-147
in CDCl3
at 298 K

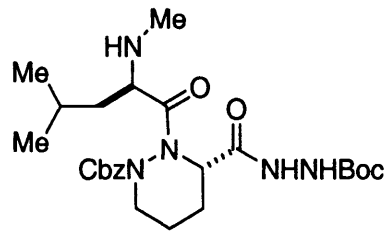

163

carbon 13 in
CDCl3 at 298 K

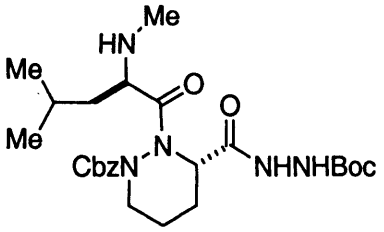

163

DEPT in CDCl3
at 298 K

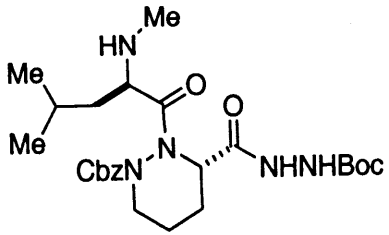

163

III-MW-147
COSY in
CDCl3 at 298 K

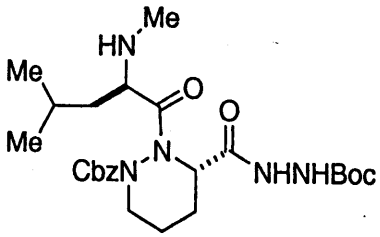

163

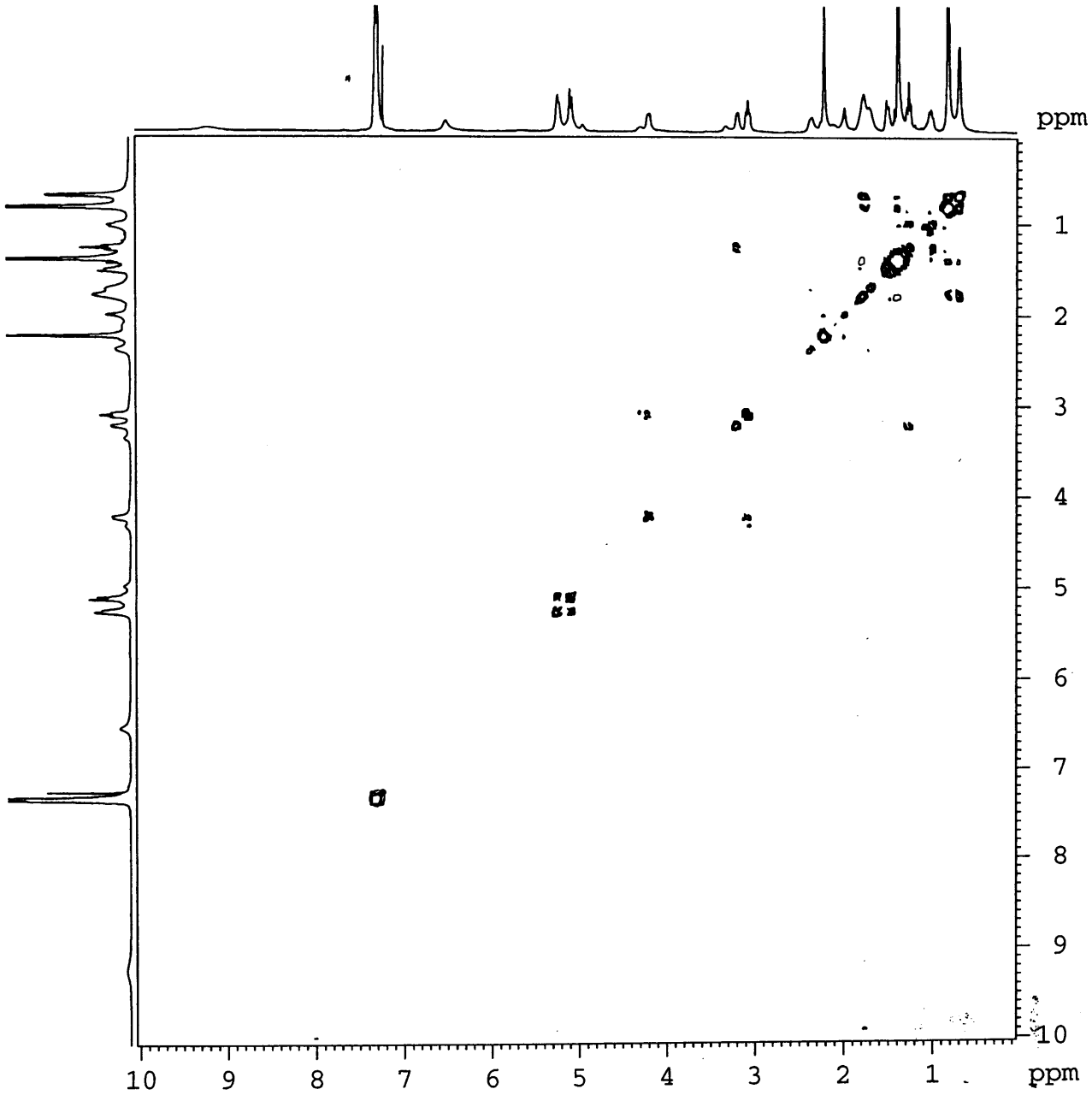

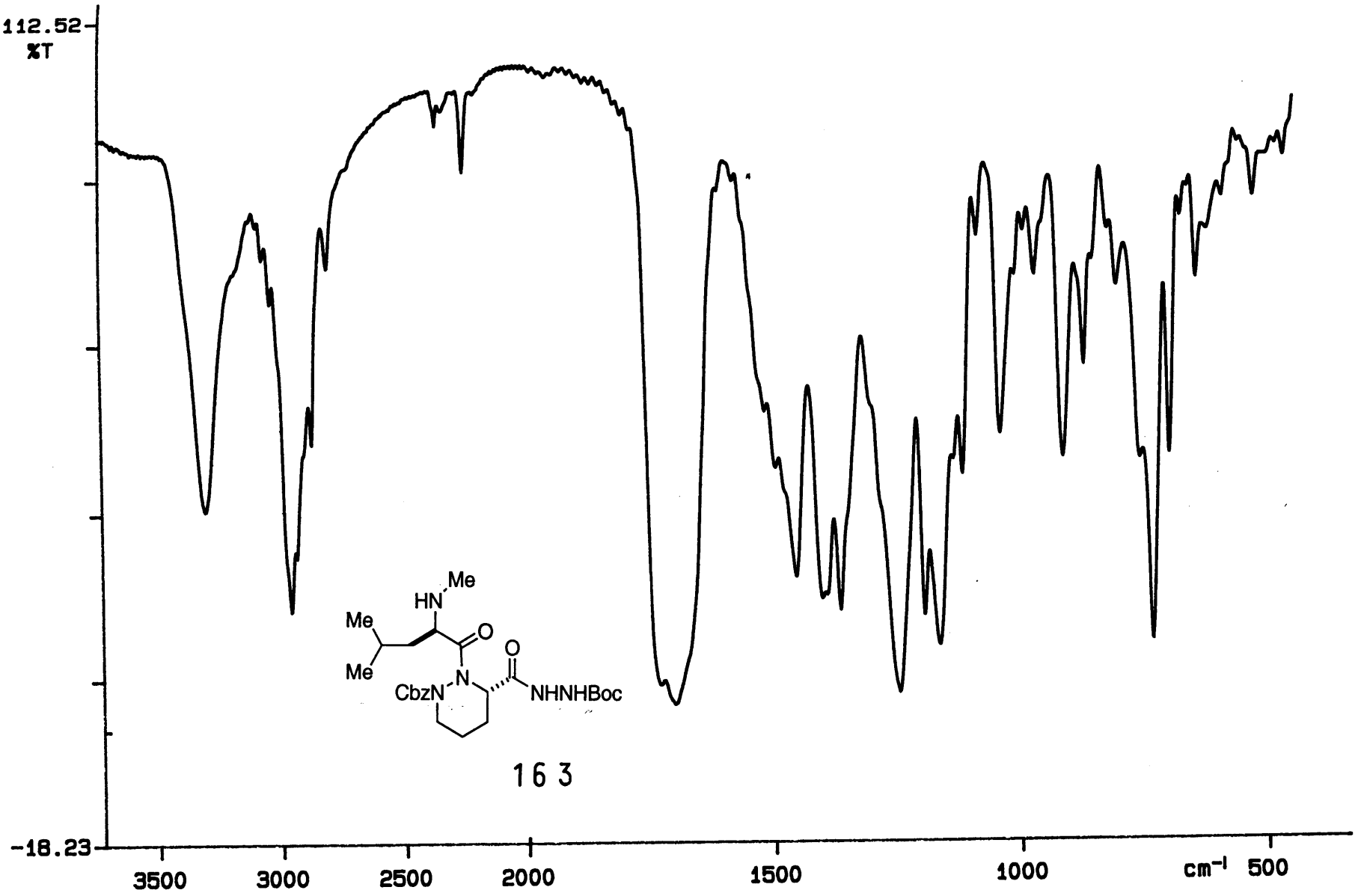
112.52
%T
-18.23
3500
3000
2500
2000
1500
1000
cm-1
500
Me
HN
Me
Me
O
O
N
CbzN
NHNHBoc

163

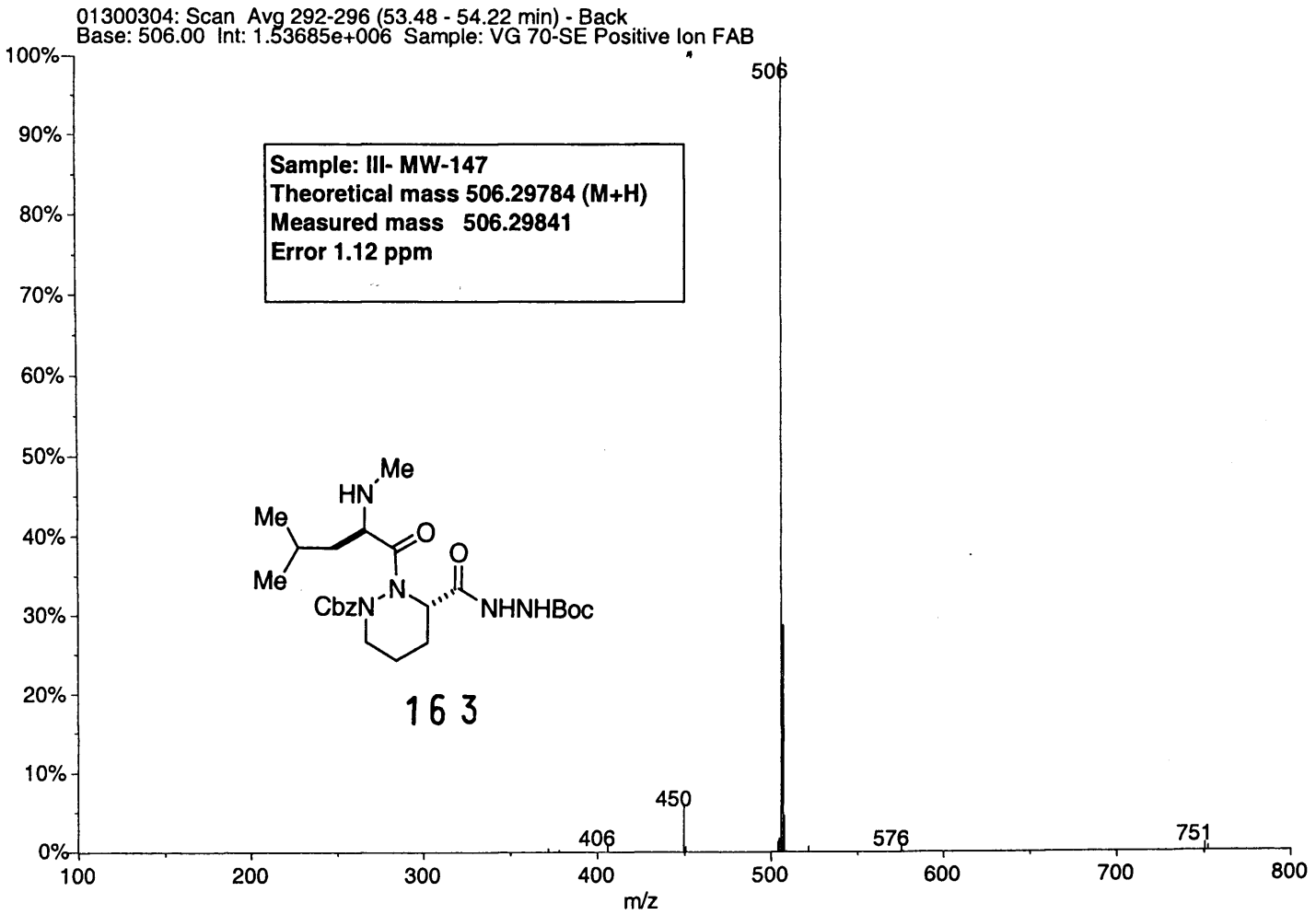
01300304: Scan Avg 292-296 (53.48 - 54.22 min) - Back
Base: 506.00 Int: 1.53685e+006 Sample: VG 70-SE Positive Ion FAB
Sample: III- MW-147
Theoretical mass 506.29784 (M+H)
Measured mass 506.29841
Error 1.12 ppm
Me
HN
Me
O
Me
O
N
CbzN
NHNHBoc
163
506
450
406
576
751
100%
90%
80%
70%
60%
50%
40%
30%
20%
10%
0%
100
200
300
400
500
600
700
800
m/z

III-MW-148
in CDCl3
at 298 K

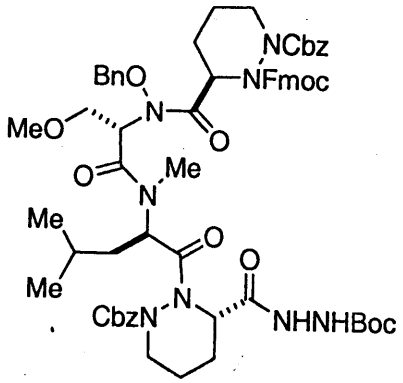

330

III-MW-148
carbon 13
in CDCl3 at 298 K

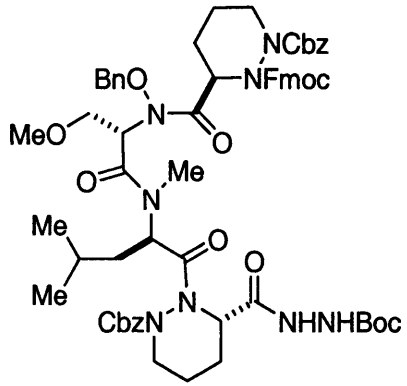

330

III-MW-148
DEPT in
CDCl3 at 298 K

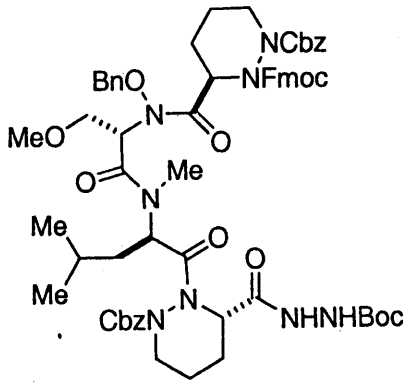

330

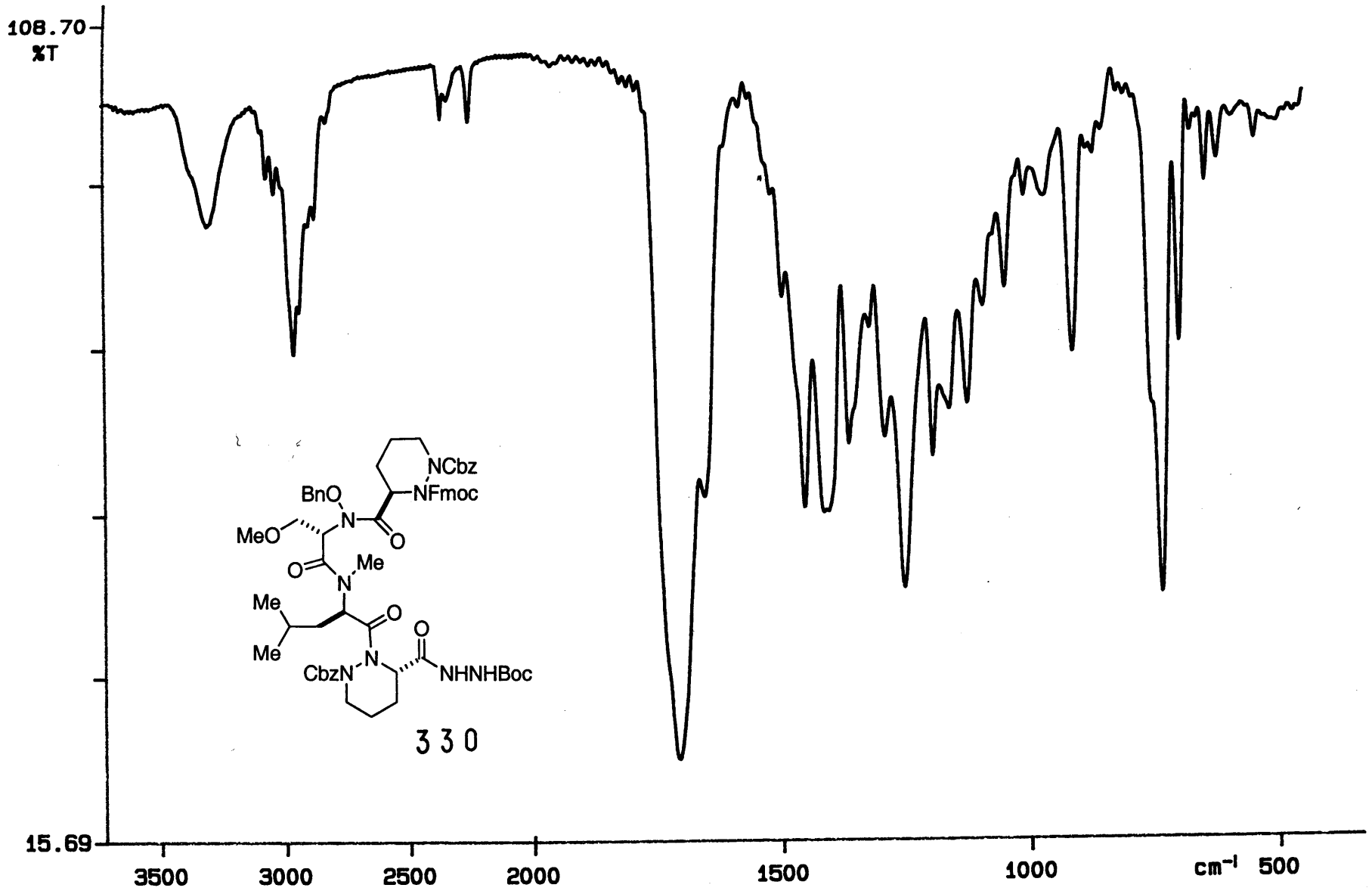
108.70
%T
15.69
3500
3000
2500
2000
1500
1000
cm-1
500
NCbz
NFmoc
BnO
MeO
N
O
Me
Me
Me
CbzN
NHNHBoc
330

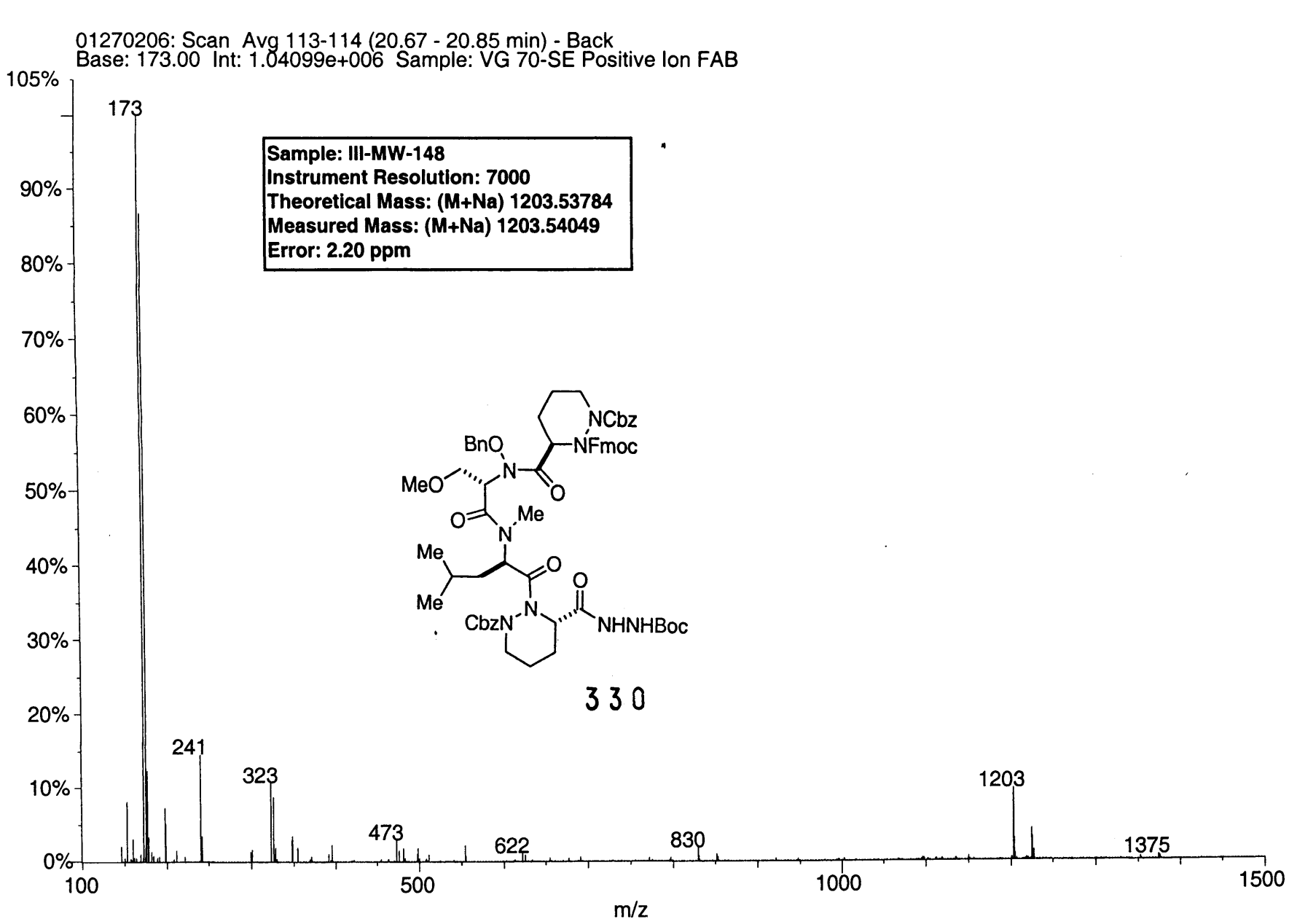
01270206: Scan Avg 113-114 (20.67 - 20.85 min) - Back
Base: 173.00 Int: 1.04099e+006 Sample: VG 70-SE Positive Ion FAB
Sample: III-MW-148
Instrument Resolution: 7000
Theoretical Mass: (M+Na) 1203.53784
Measured Mass: (M+Na) 1203.54049
Error: 2.20 ppm
NCbz
NFmoc
BnO
MeO
N
O
Me
Me
Me
CbzN
NHNHBoc
330
105%
90%
80%
70%
60%
50%
40%
30%
20%
10%
0%
173
241
323
473
622
830
1203
1375
100
500
1000
1500
m/z

III-MW-151
in CDCl3
at 298 K

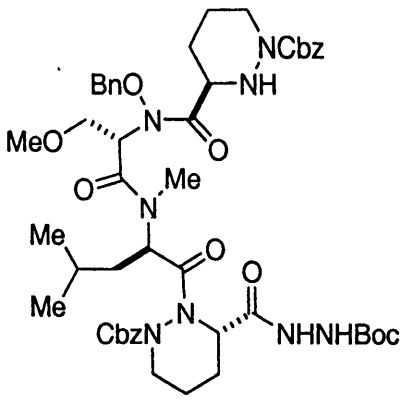

III-MW-151
Carbon 13
in CDCl3 at 298 K

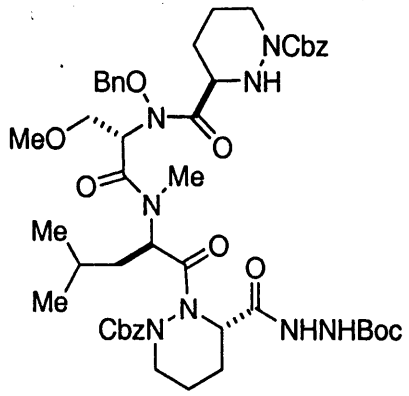

SPECIAL NOTE

THIS ITEM IS BOUND IN SUCH A MANNER AND WHILE EVERY EFFORT HAS BEEN MADE TO REPRODUCE THE CENTRES, FORCE WOULD RESULT IN DAMAGE

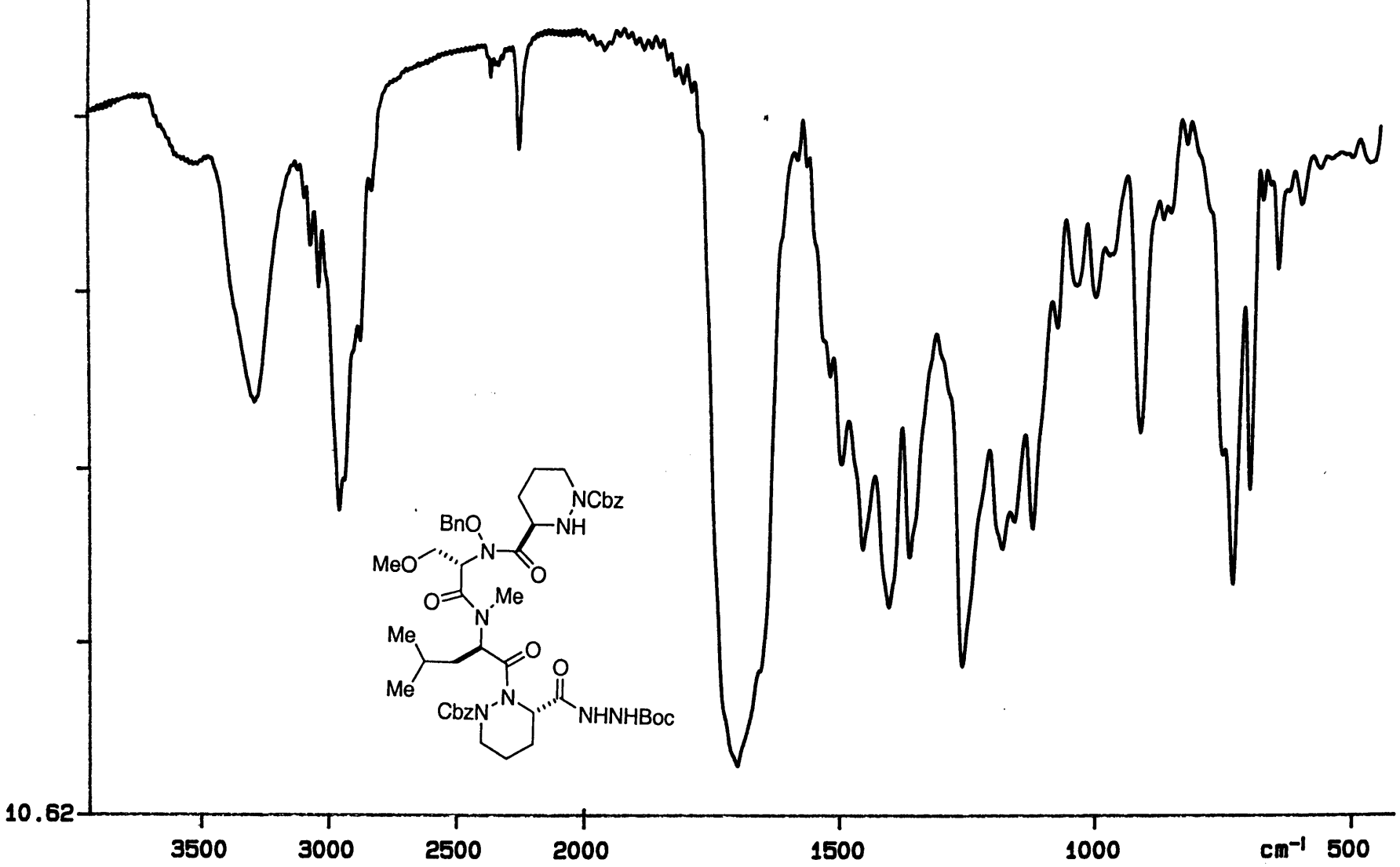
NCbz
NH
BnO
N
MeO
O
O
N
Me
Me
Me
O
O
N
CbzN
NHNHBoc
10.62
3500
3000
2500
2000
1500
1000
cm-1
500

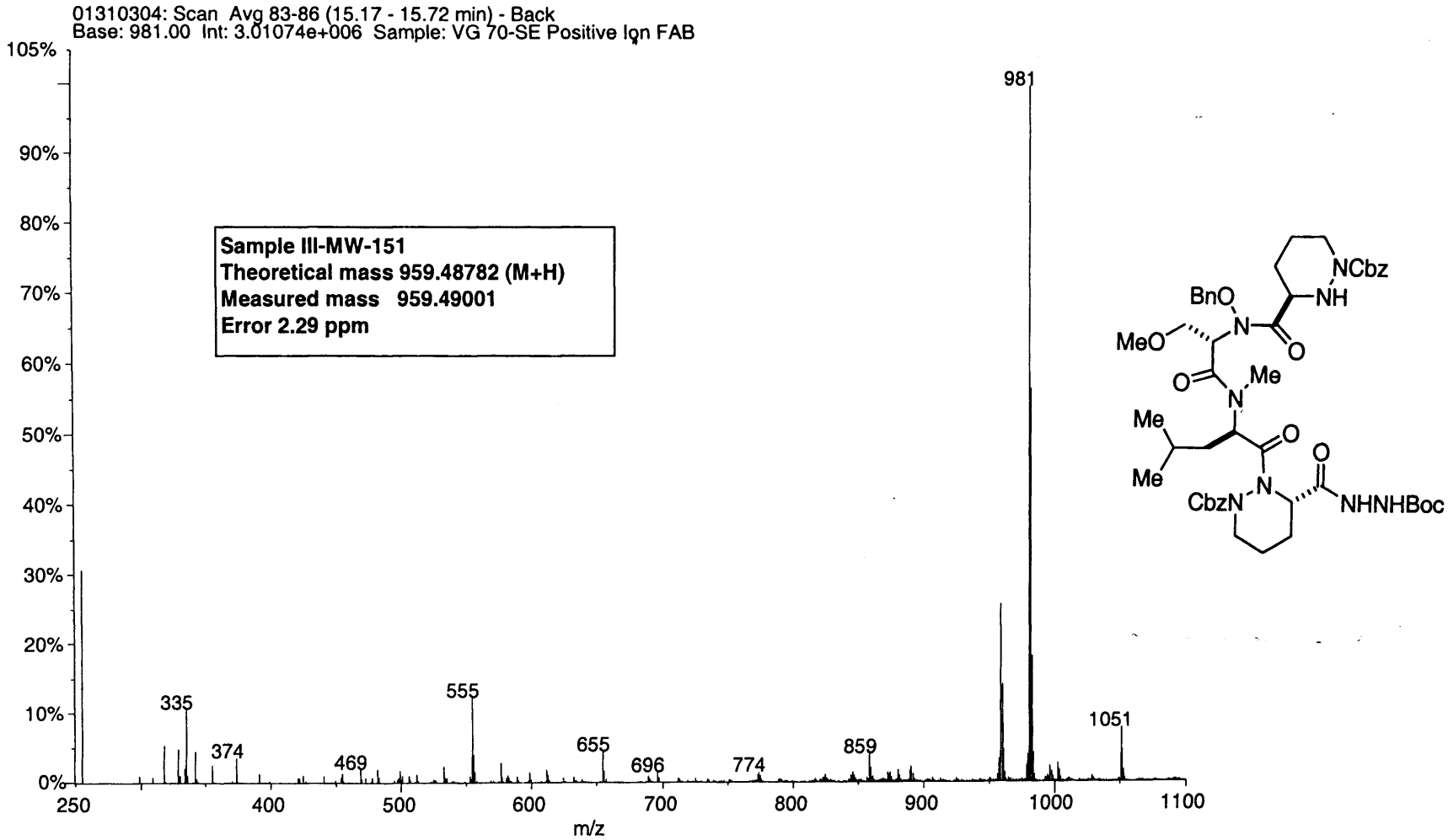
01310304: Scan Avg 83-86 (15.17 - 15.72 min) - Back
Base: 981.00 Int: 3.01074e+006 Sample: VG 70-SE Positive Ion FAB
Sample III-MW-151
Theoretical mass 959.48782 (M+H)
Measured mass 959.49001
Error 2.29 ppm
105%
90%
80%
70%
60%
50%
40%
30%
20%
10%
0%
250
400
500
600
700
800
900
1000
1100
m/z
981
335
374
469
555
655
696
774
859
1051
NCbz
NH
BnO
MeO
N
O
Me
Me
Me
CbzN
NHNHBoc

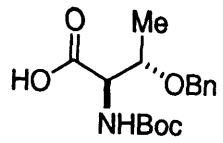

123

SPECIAL NOTE

THIS ITEM IS BOUND IN SUCH A MANNER AND WHILE EVERY EFFORT HAS BEEN MADE TO REPRODUCE THE CENTRES, FORCE WOULD RESULT IN DAMAGE

Carbon 13 1H
CDCl3 at 298 K

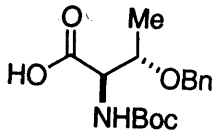

123

II-MW-151
DEPT in
CDCl3 at 298 K

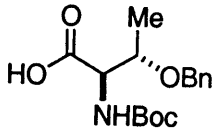

123

11-MW-151
DEPT in
CDCl3 at 298 K

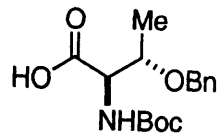

123

COSY in
CDCl3 at 298 K

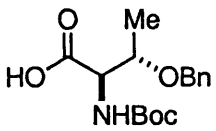

123

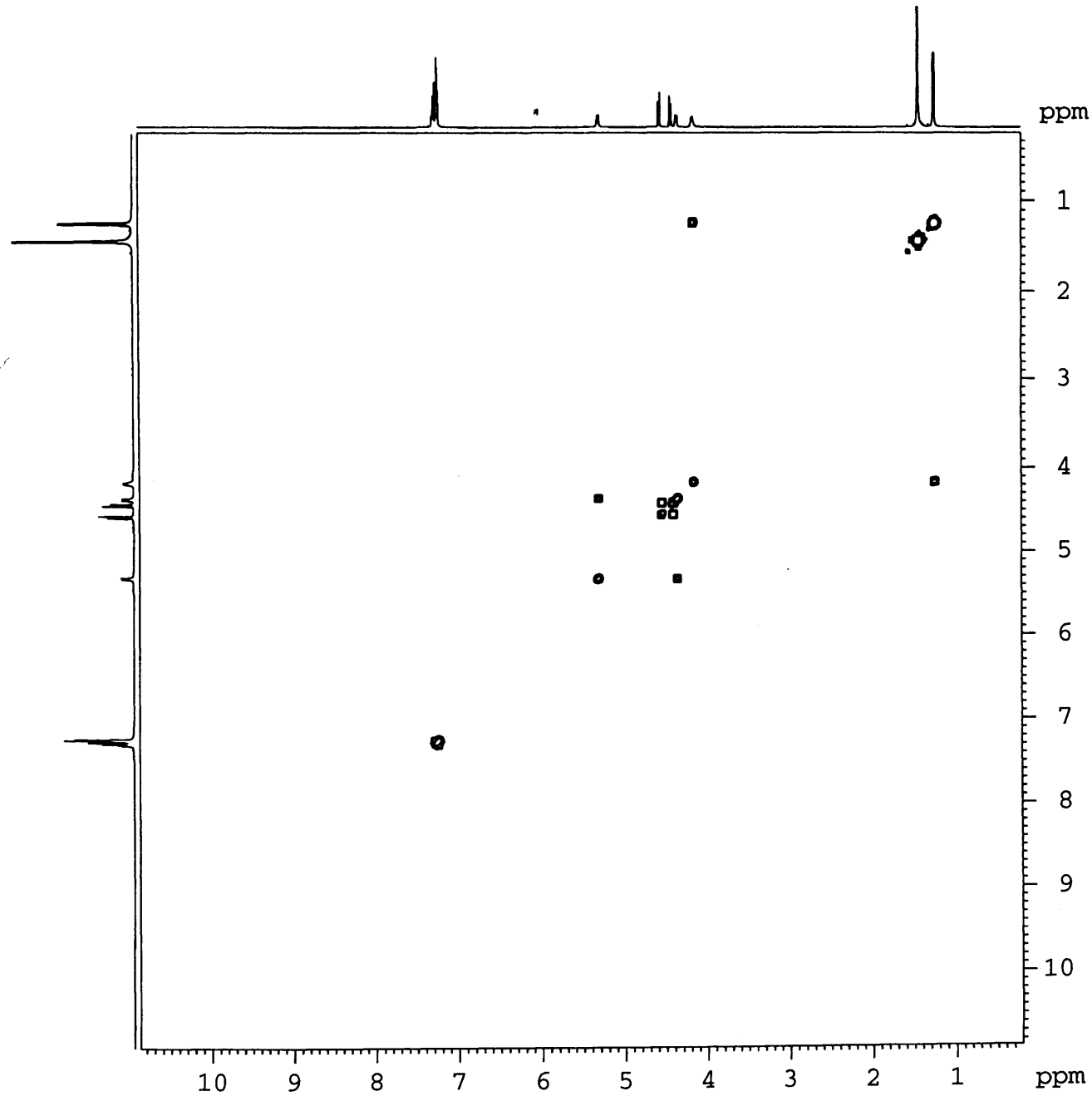

HMQC in
CDC13 at 298 K

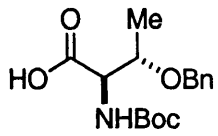

123

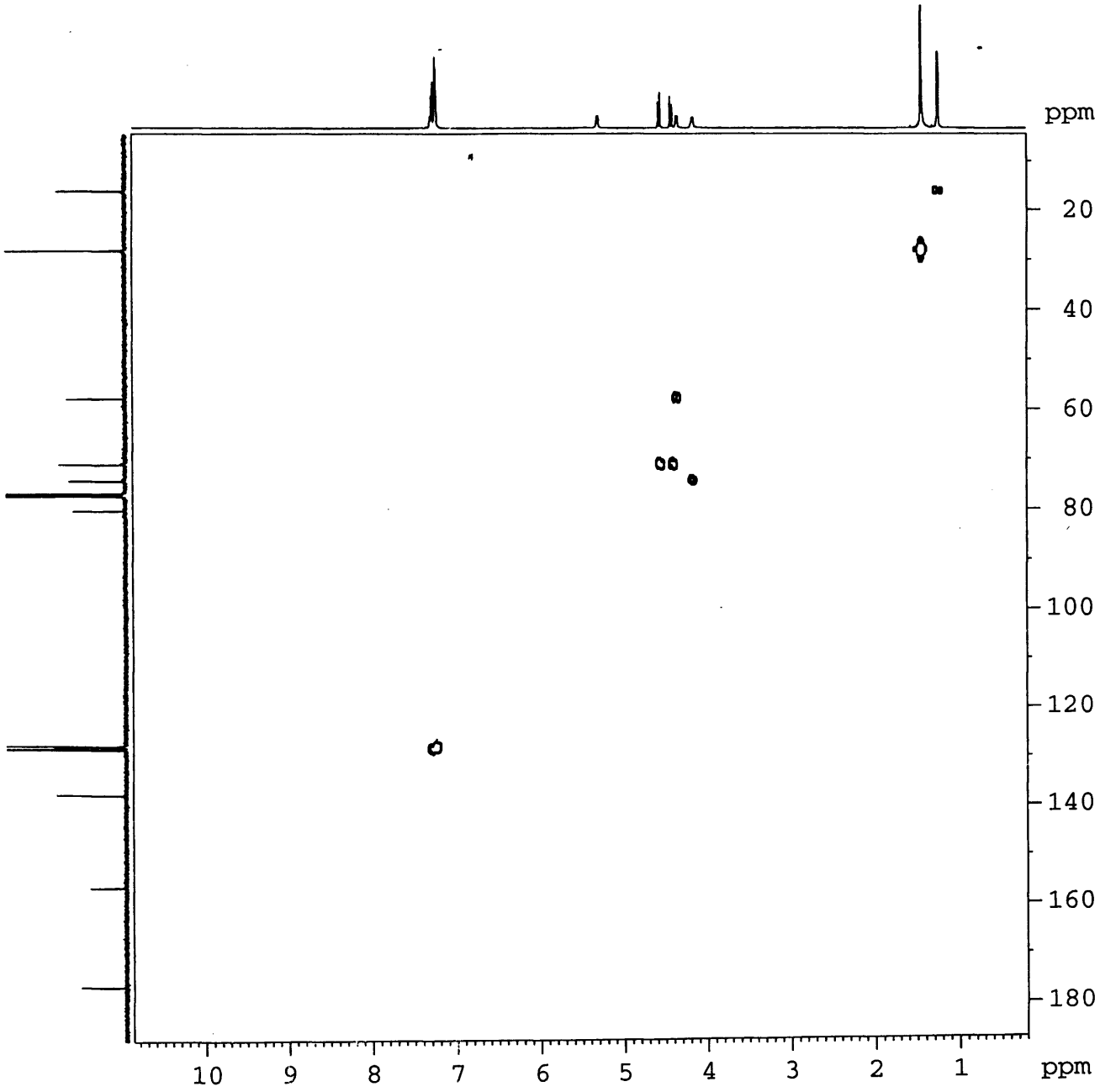

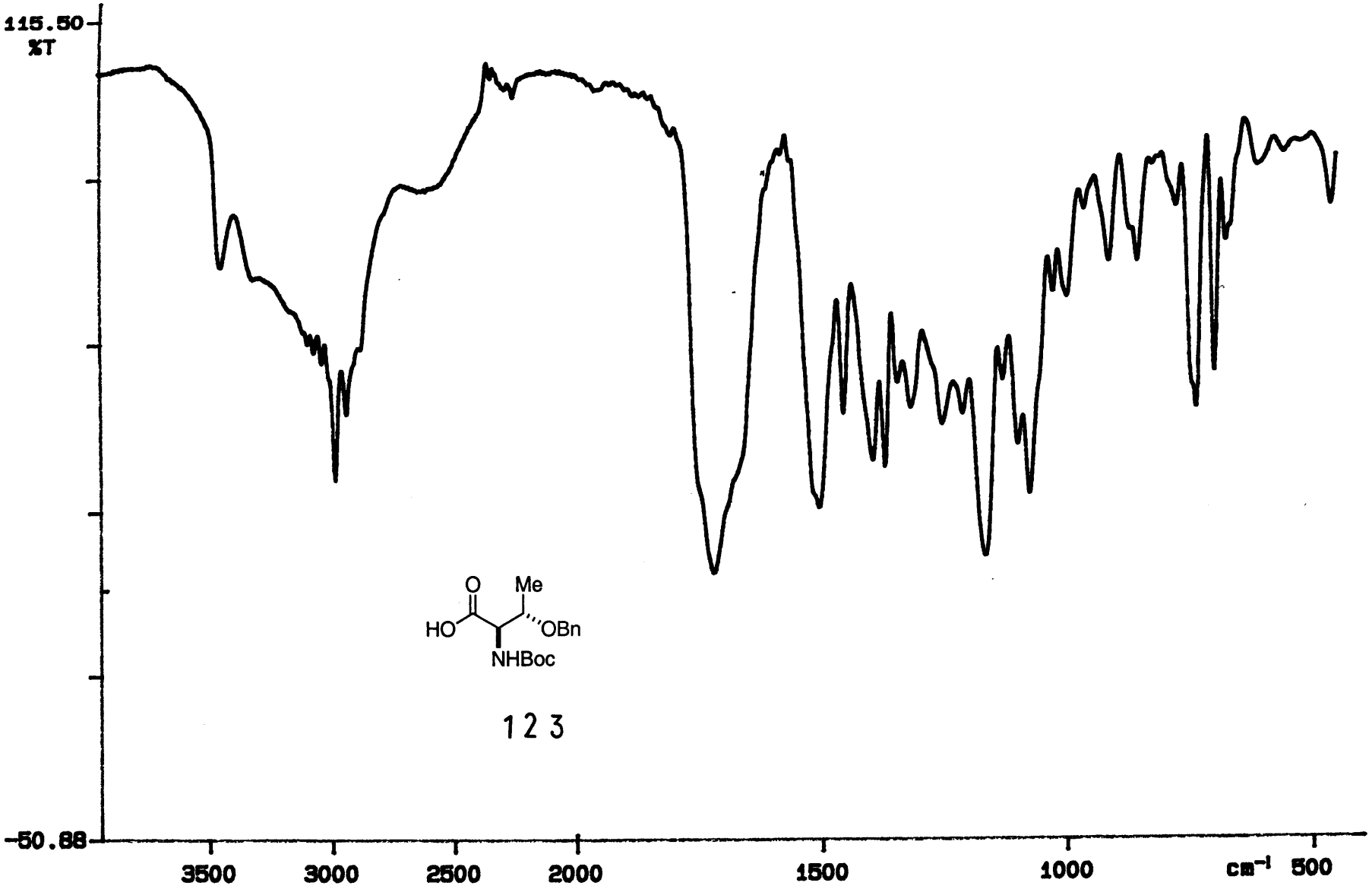
115.50
%T
-50.88
3500
3000
2500
2000
1500
1000
cm-1
500
O
Me
HO
OBn
NHBoc

1 2 3

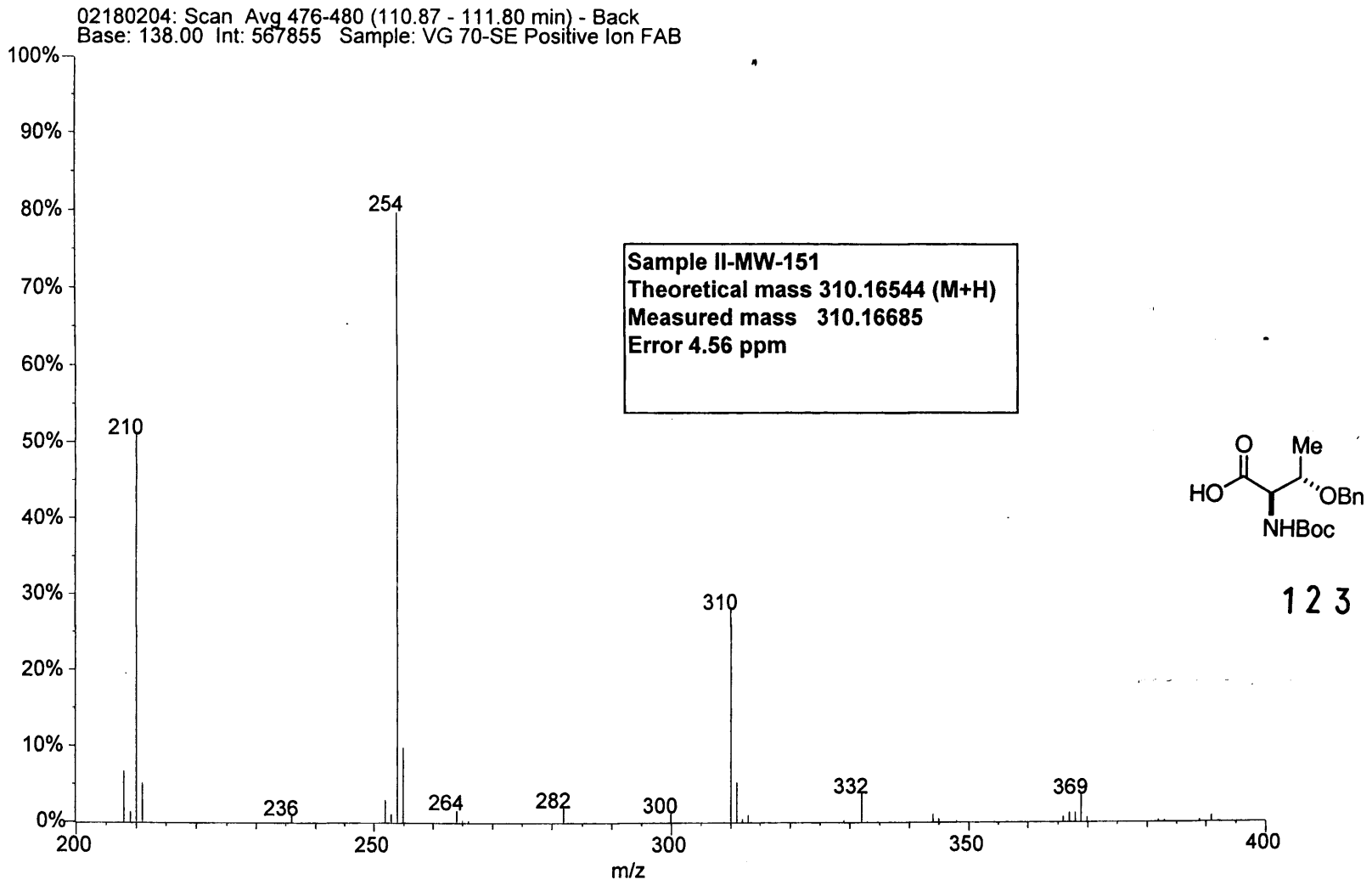
02180204: Scan Avg 476-480 (110.87 - 111.80 min) - Back
Base: 138.00 Int: 567855 Sample: VG 70-SE Positive Ion FAB
100%
90%
80%
70%
60%
50%
40%
30%
20%
10%
0%
254
210
310
236
264
282
300
332
369
200
250
300
350
400
m/z
Sample II-MW-151
Theoretical mass 310.16544 (M+H)
Measured mass 310.16685
Error 4.56 ppm
O
Me
HO
OBn
NHBoc

123

CDCl3 at 298 K

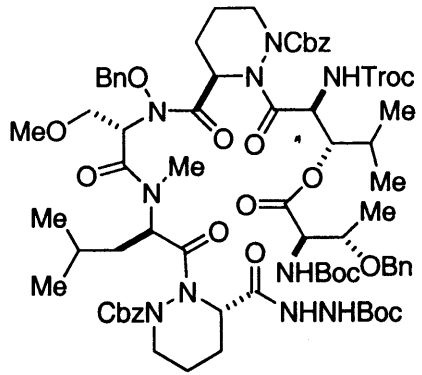

331

III-MW-157
Carbon 13 in
CDCl3 at 298 K

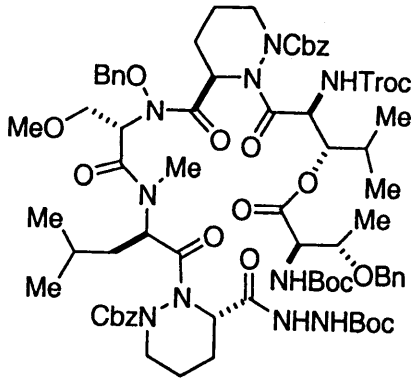

331

III-MW-157
DEPT in
CDCl3 at 298 K

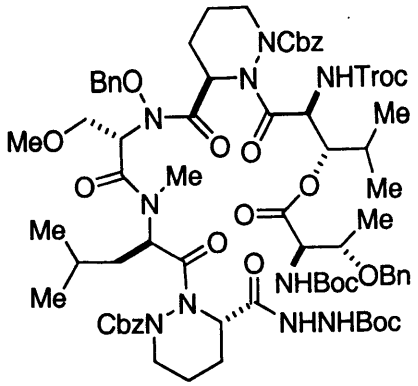

331

COSY in
CDCl3 at 298 K

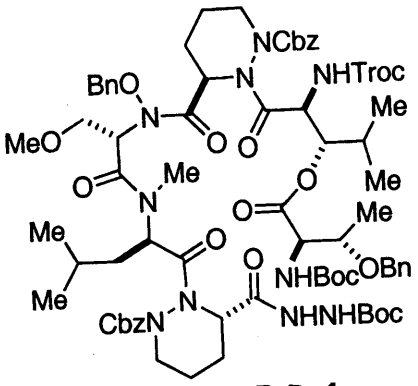

331

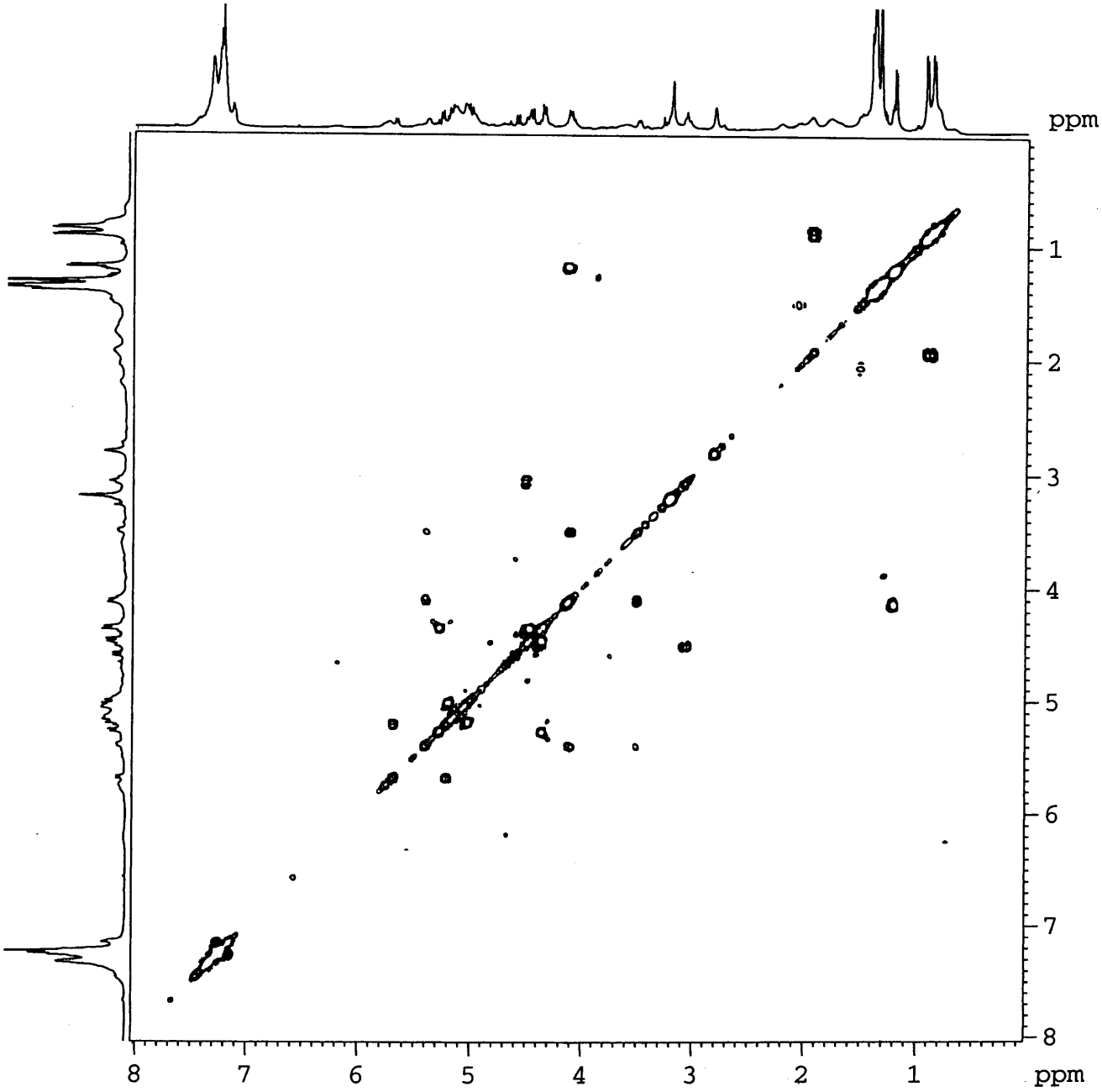

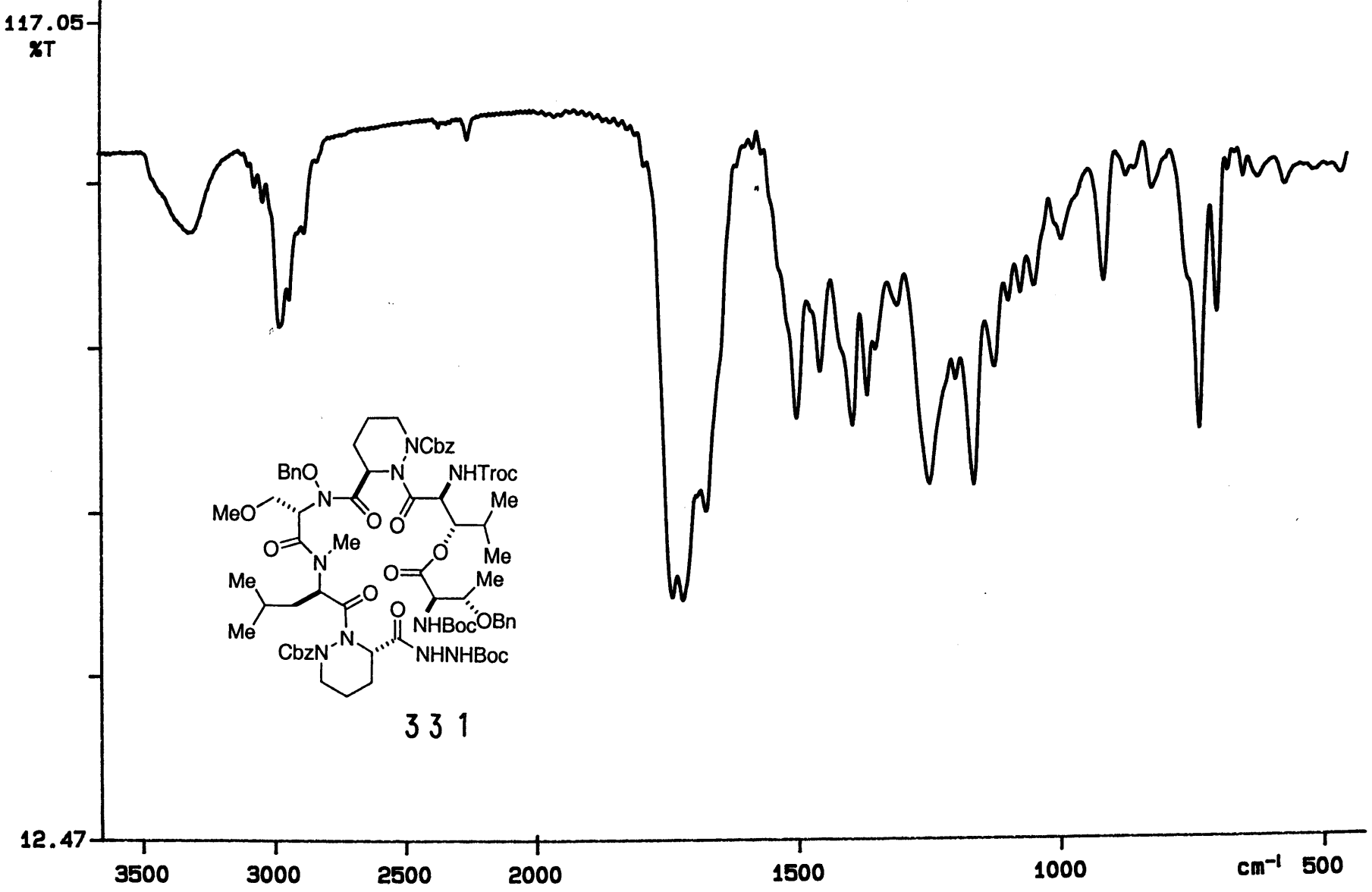
117.05
%T
12.47
3500
3000
2500
2000
1500
1000
cm-1
500
NCbz
BnO
N
NHTroc
MeO
Me
O
Me
N
O
Me
Me
Me
Me
NHBocOBn
CbzN
N
NHNHBoc

331

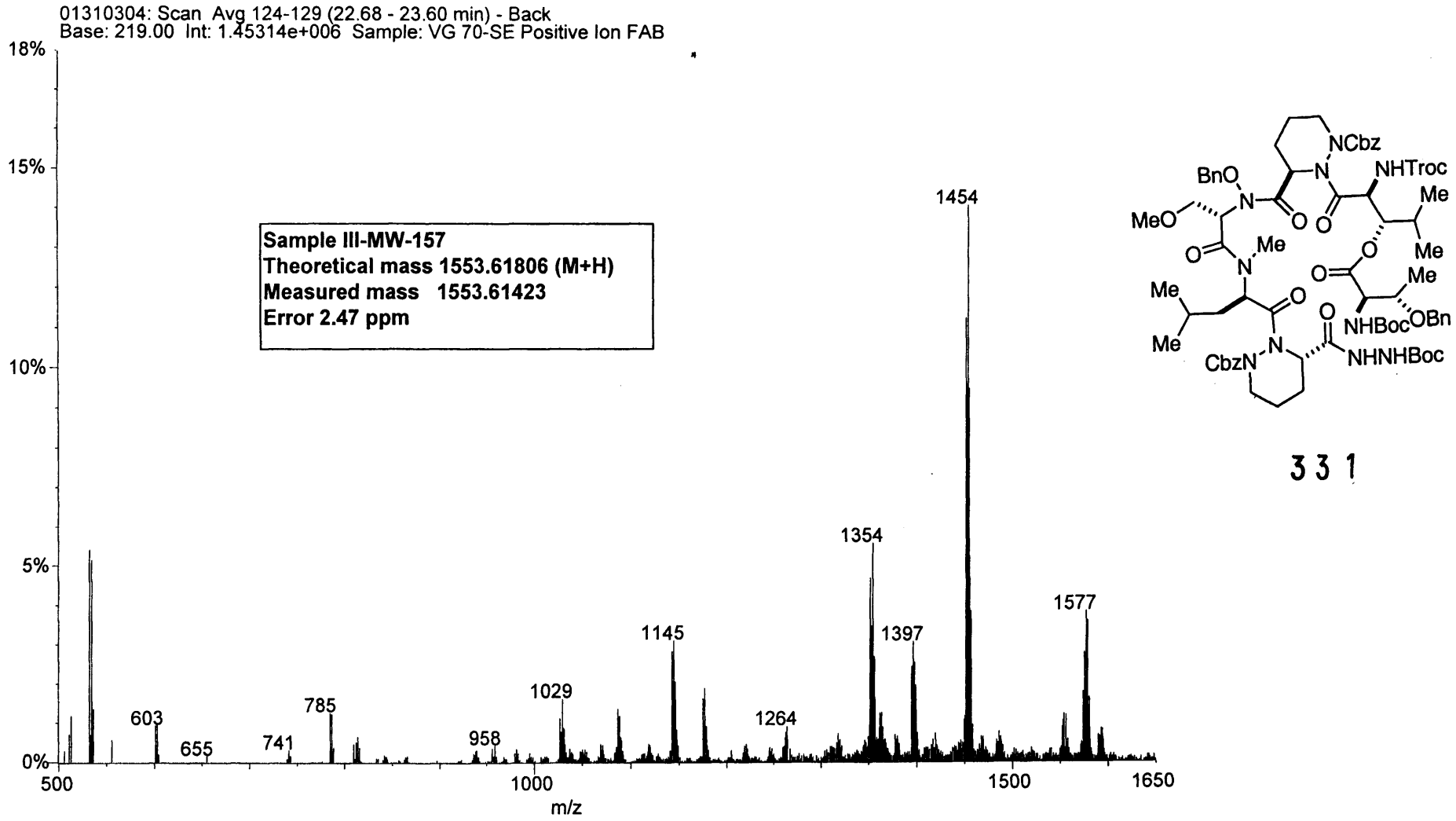
01310304: Scan Avg 124-129 (22.68 - 23.60 min) - Back
Base: 219.00 Int: 1.45314e+006 Sample: VG 70-SE Positive Ion FAB
Sample III-MW-157
Theoretical mass 1553.61806 (M+H)
Measured mass 1553.61423
Error 2.47 ppm
18%
15%
10%
5%
0%
500
1000
1500
1650
m/z
1454
1354
1577
1145
1397
1029
1264
785
603
655
741
958
NCbz
BnO
NHTroc
MeO
Me
Me
Me
Me
Me
NHBocOBn
NHNHBoc
CbzN

331

III-MW-171 in
CDCl3 at 298 K

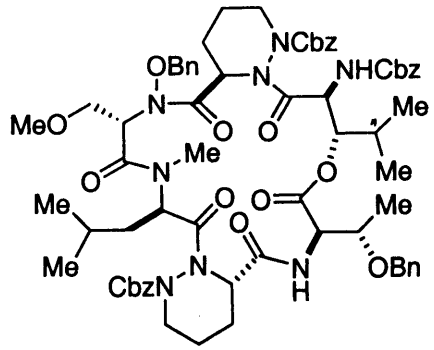

334

III-MW-171
Carbon 13 in
CDCl3 at 298 K

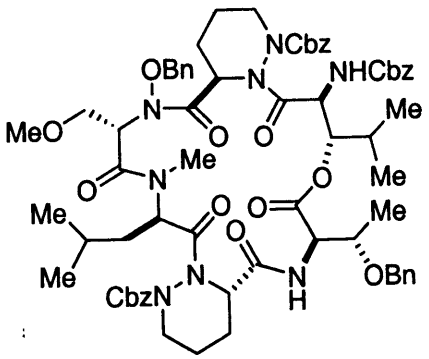

334

III-MW-171
DEPT in
CDCl3 at 298 K

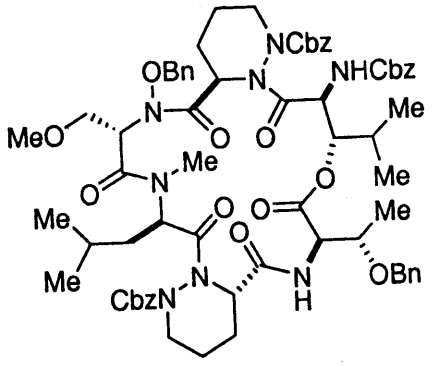

334

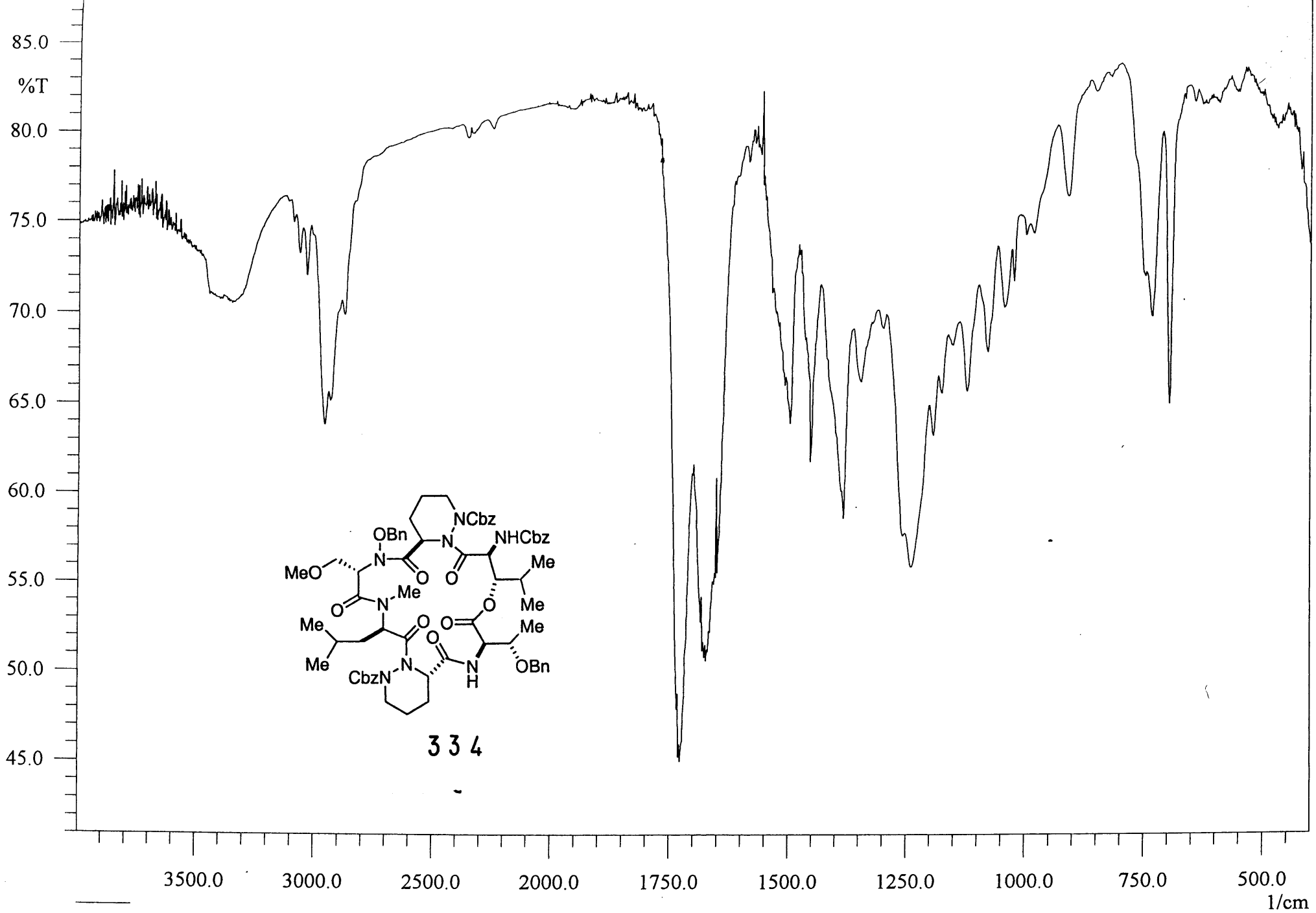
85.0
%T
80.0
75.0
70.0
65.0
60.0
55.0
50.0
45.0
3500.0
3000.0
2500.0
2000.0
1750.0
1500.0
1250.0
1000.0
750.0
500.0
1/cm
NCbz
OBn
NHCbz
MeO
Me
Me
Me
Me
Me
Me
Me
CbzN
N
H
OBn

334

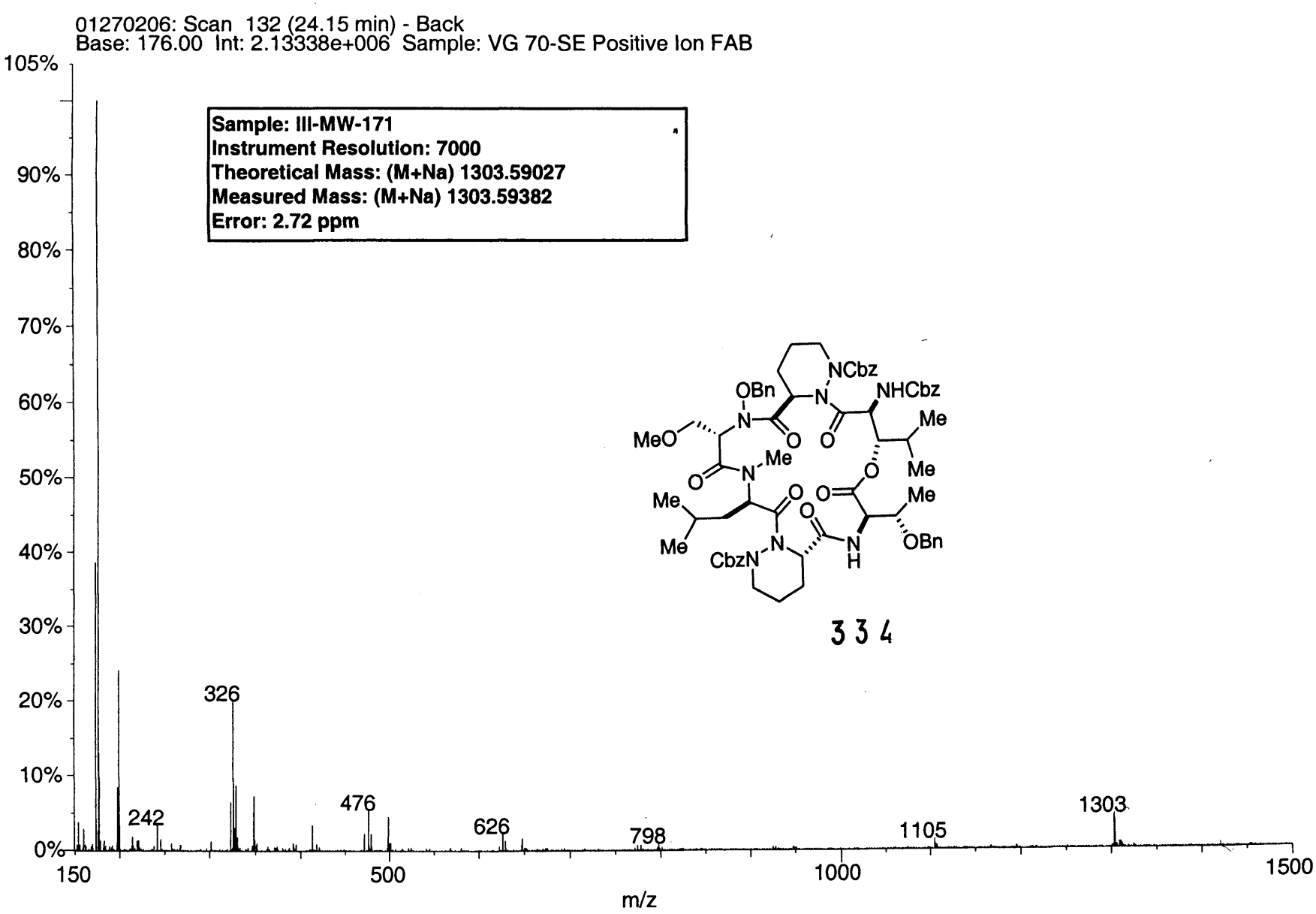
01270206: Scan 132 (24.15 min) - Back
Base: 176.00 Int: 2.13338e+006 Sample: VG 70-SE Positive Ion FAB
Sample: III-MW-171
Instrument Resolution: 7000
Theoretical Mass: (M+Na) 1303.59027
Measured Mass: (M+Na) 1303.59382
Error: 2.72 ppm
105%
90%
80%
70%
60%
50%
40%
30%
20%
10%
0%
326
242
476
626
798
1105
1303
150
500
1000
1500
m/z
NCbz
OBn
NHCbz
MeO
Me
CbzN
OBn
334

111-MW-174
in MeOH at
298 K

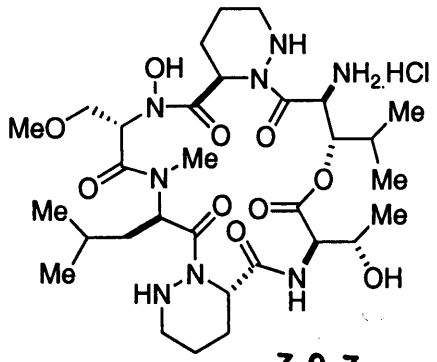

303

III-MW-174
Carbon 13 in
MeOH at 298 K

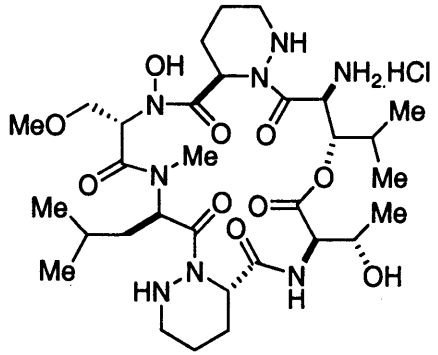

303

III-MW-174
DEPT in
MeOH at 298 K

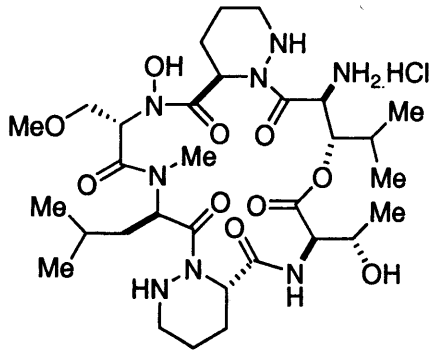

303

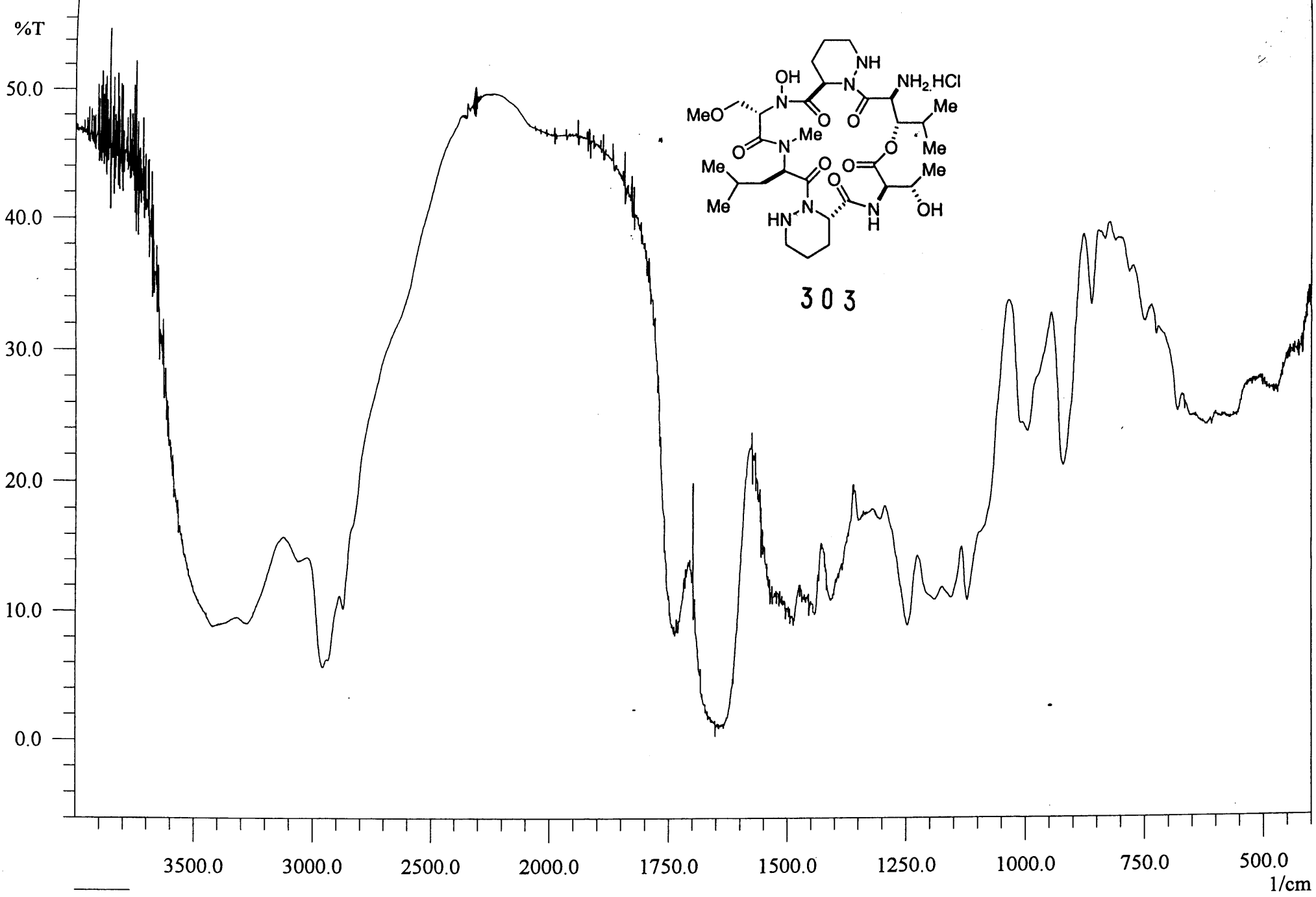
%T
50.0
40.0
30.0
20.0
10.0
0.0
3500.0
3000.0
2500.0
2000.0
1750.0
1500.0
1250.0
1000.0
750.0
500.0
1/cm
NH
OH
N
NH2.HCl
MeO
Me
O
N
Me
Me
Me
Me
Me
OH
HN
N
H
303

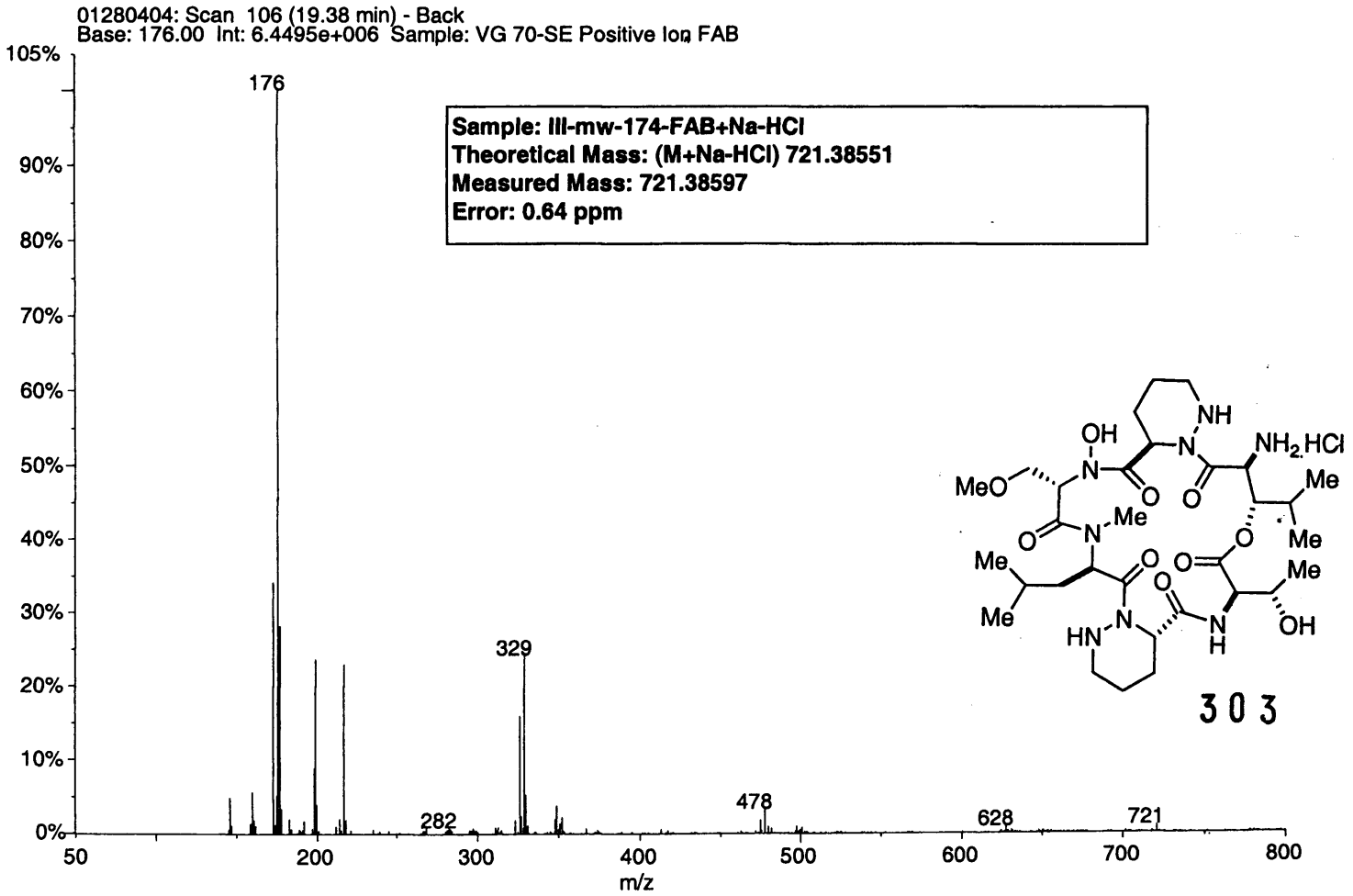
01280404: Scan 106 (19.38 min) - Back
Base: 176.00 Int: 6.4495e+006 Sample: VG 70-SE Positive Ion FAB
Sample: III-mw-174-FAB+Na-HCl
Theoretical Mass: (M+Na-HCl) 721.38551
Measured Mass: 721.38597
Error: 0.64 ppm
105%
90%
80%
70%
60%
50%
40%
30%
20%
10%
0%
176
329
282
478
628
721
50
200
300
400
500
600
700
800
m/z
MeO
OH
NH
NH2.HCl
Me
Me
Me
Me
Me
Me
OH
HN
N
H
303

IV-MW-26 in
CDCl3 at 298 K

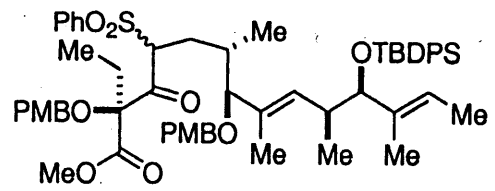

IV-MW-26
Carbon 13 in
CDCl3 at 298 K

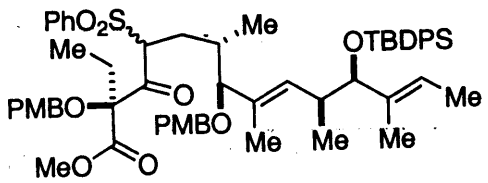

IV-MW-26
DEPT in CDCl3
at 298 K

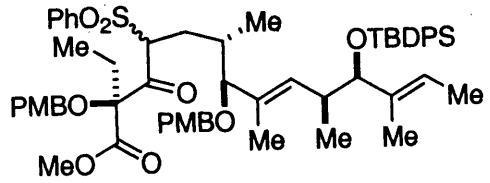

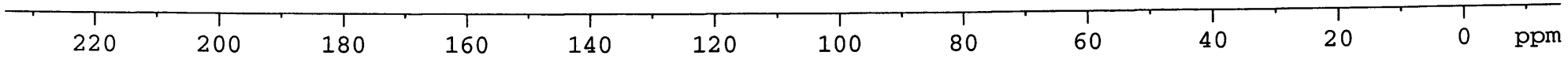

IV-MW-26
COSY in CDCl3
at 298 K

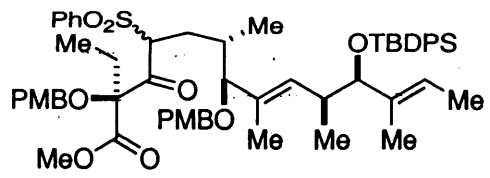

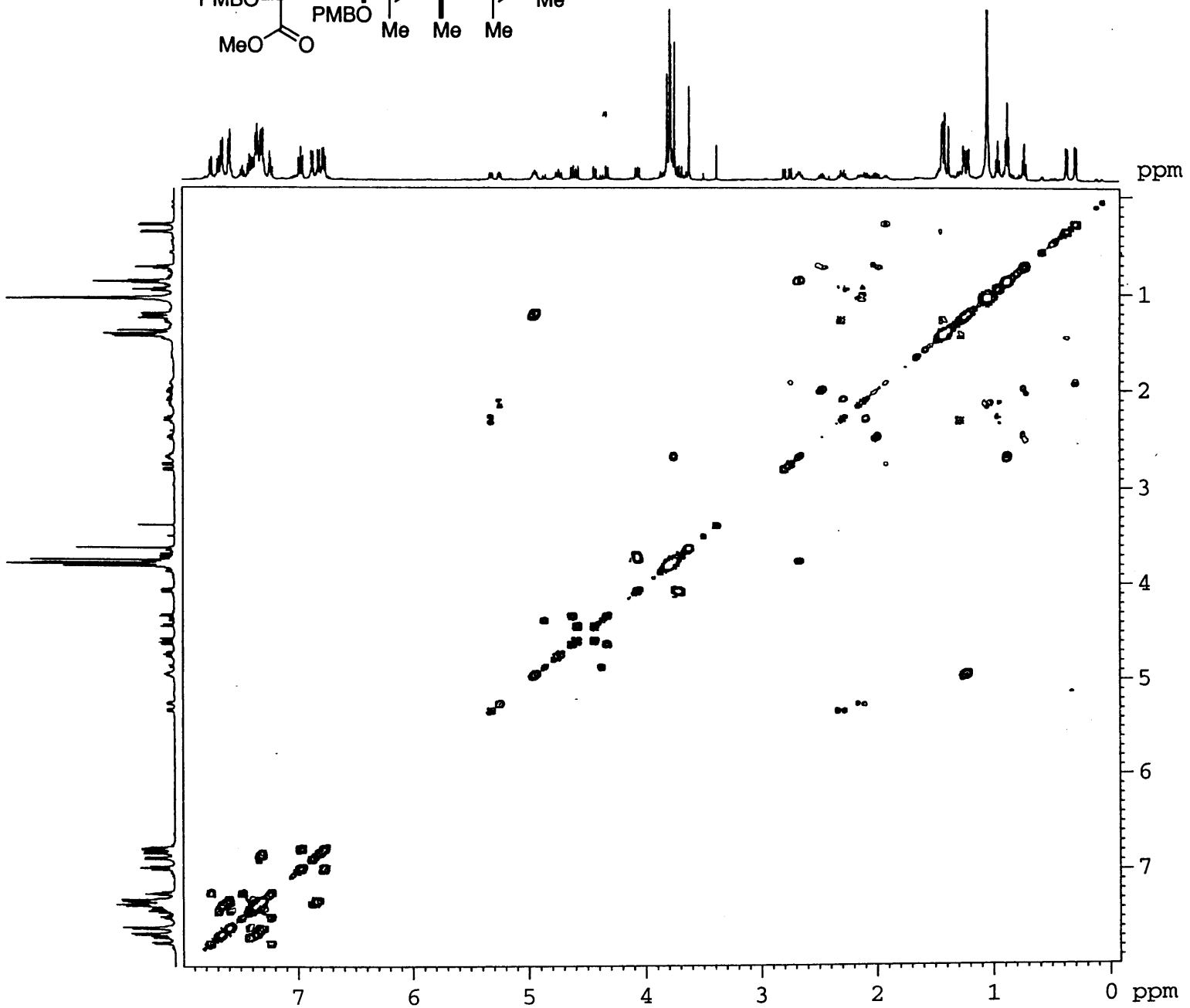

IV-MW-26
HMQC in CDCl3
at 298 K

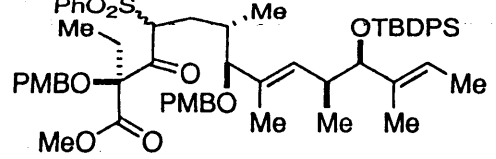

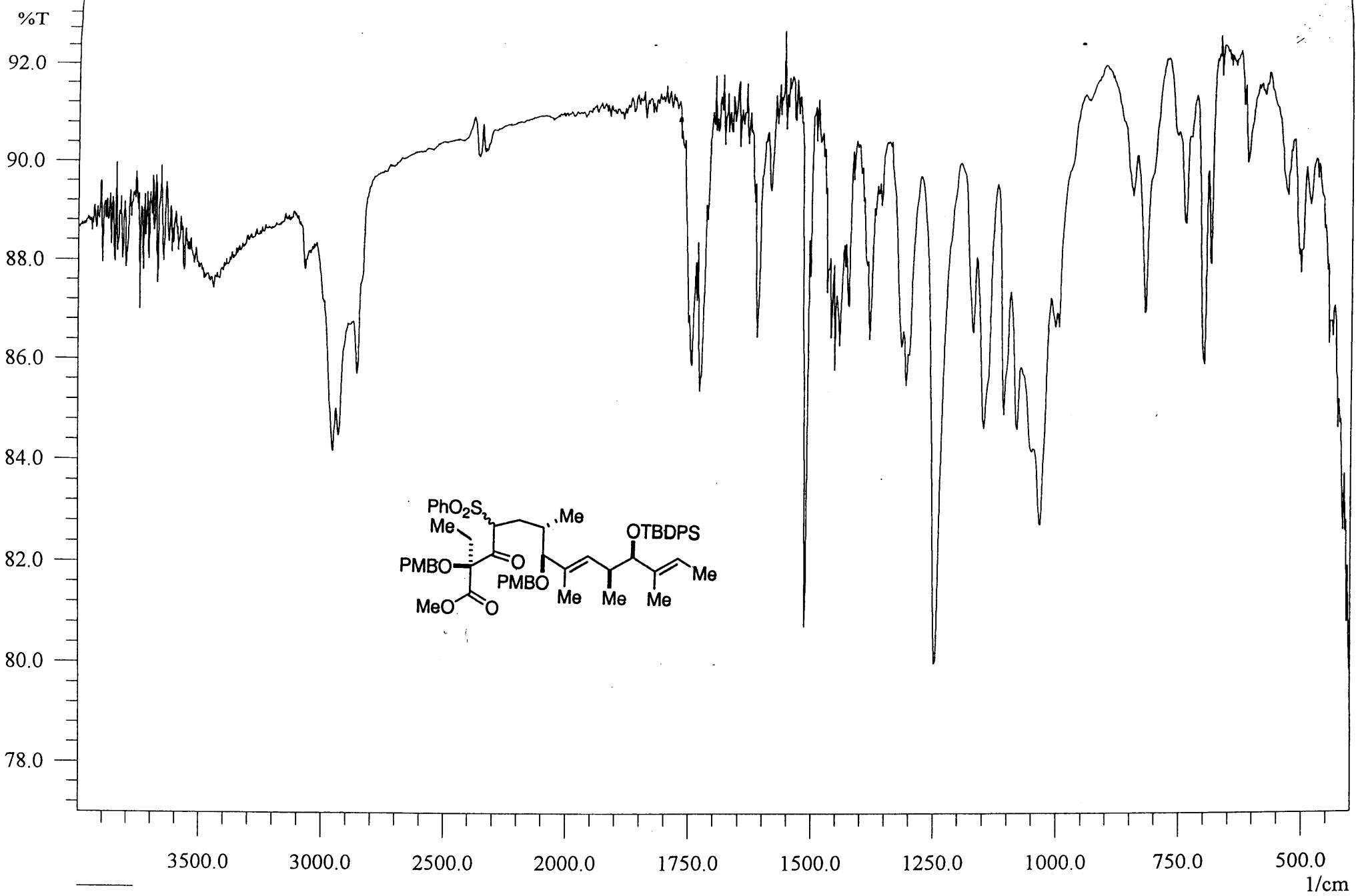
%T
92.0
90.0
88.0
86.0
84.0
82.0
80.0
78.0
3500.0
3000.0
2500.0
2000.0
1750.0
1500.0
1250.0
1000.0
750.0
500.0
1/cm
PhO2S
Me
Me
PMBO
O
MeO
O
PMBO
Me
Me
Me
OTBDPS
Me

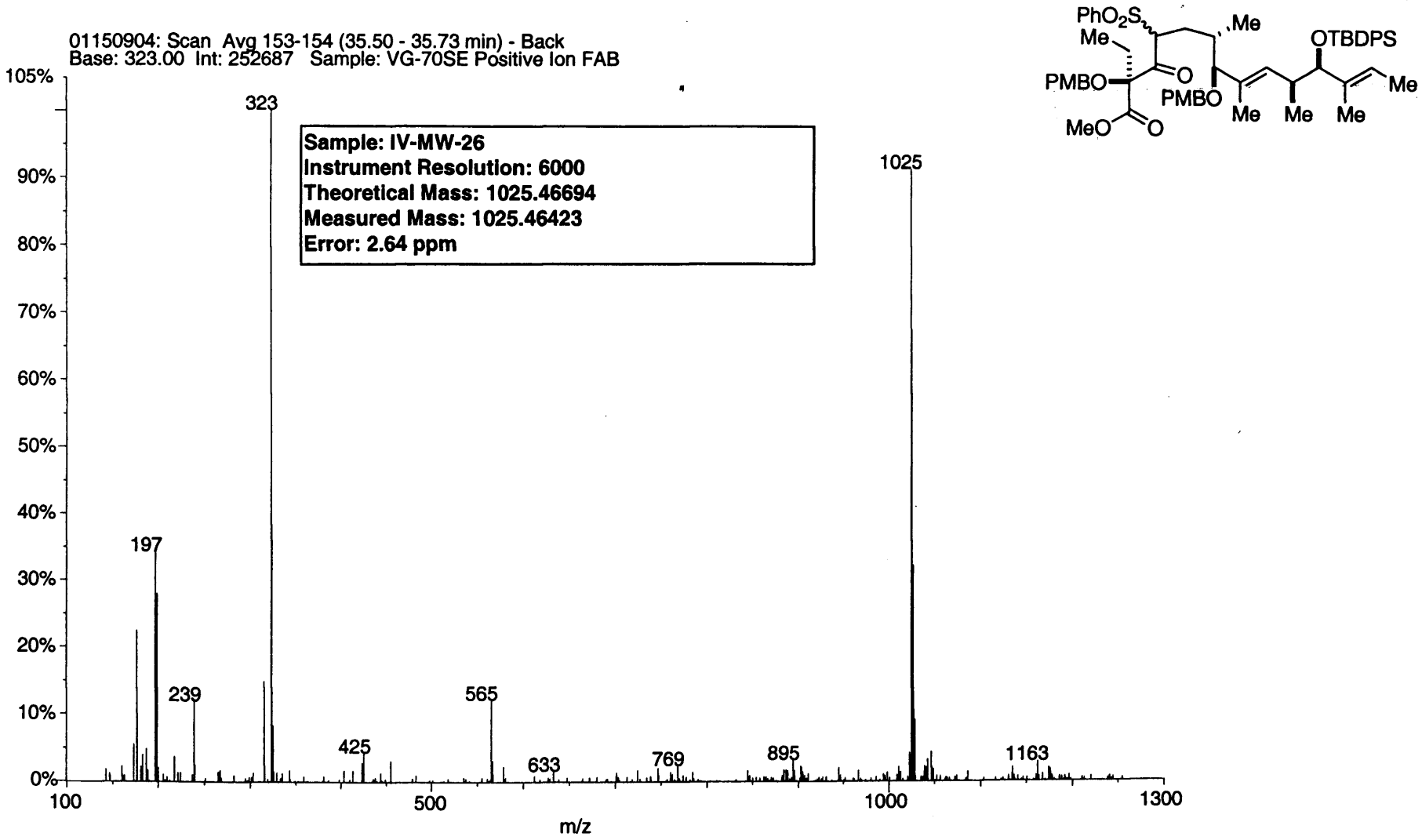
01150904: Scan Avg 153-154 (35.50 - 35.73 min) - Back
Base: 323.00 Int: 252687 Sample: VG-70SE Positive Ion FAB
Sample: IV-MW-26
Instrument Resolution: 6000
Theoretical Mass: 1025.46694
Measured Mass: 1025.46423
Error: 2.64 ppm
105%
90%
80%
70%
60%
50%
40%
30%
20%
10%
0%
323
1025
197
239
565
425
633
769
895
1163
100
500
1000
1300
m/z
PhO2S
Me
Me
OTBDPS
PMBO
O
PMBO
Me
Me
Me
Me
MeO
O

IV-MW-33 in
CDCl3 at 298 K

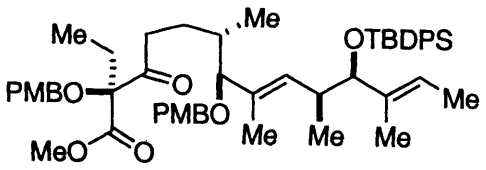

97

IV-MW-33
Carbon 13 in
CDCl3 at 298 K

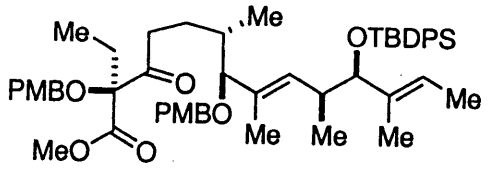

97

IV-MW-33
DEPT in CDCl3
at 298 K

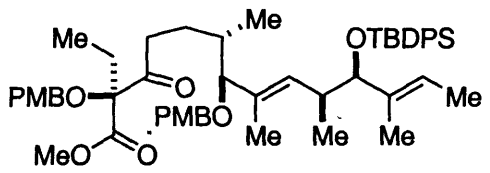

97

IV-MW-33
COSY in CDCl3
at 298 K

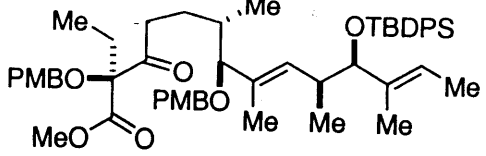

97

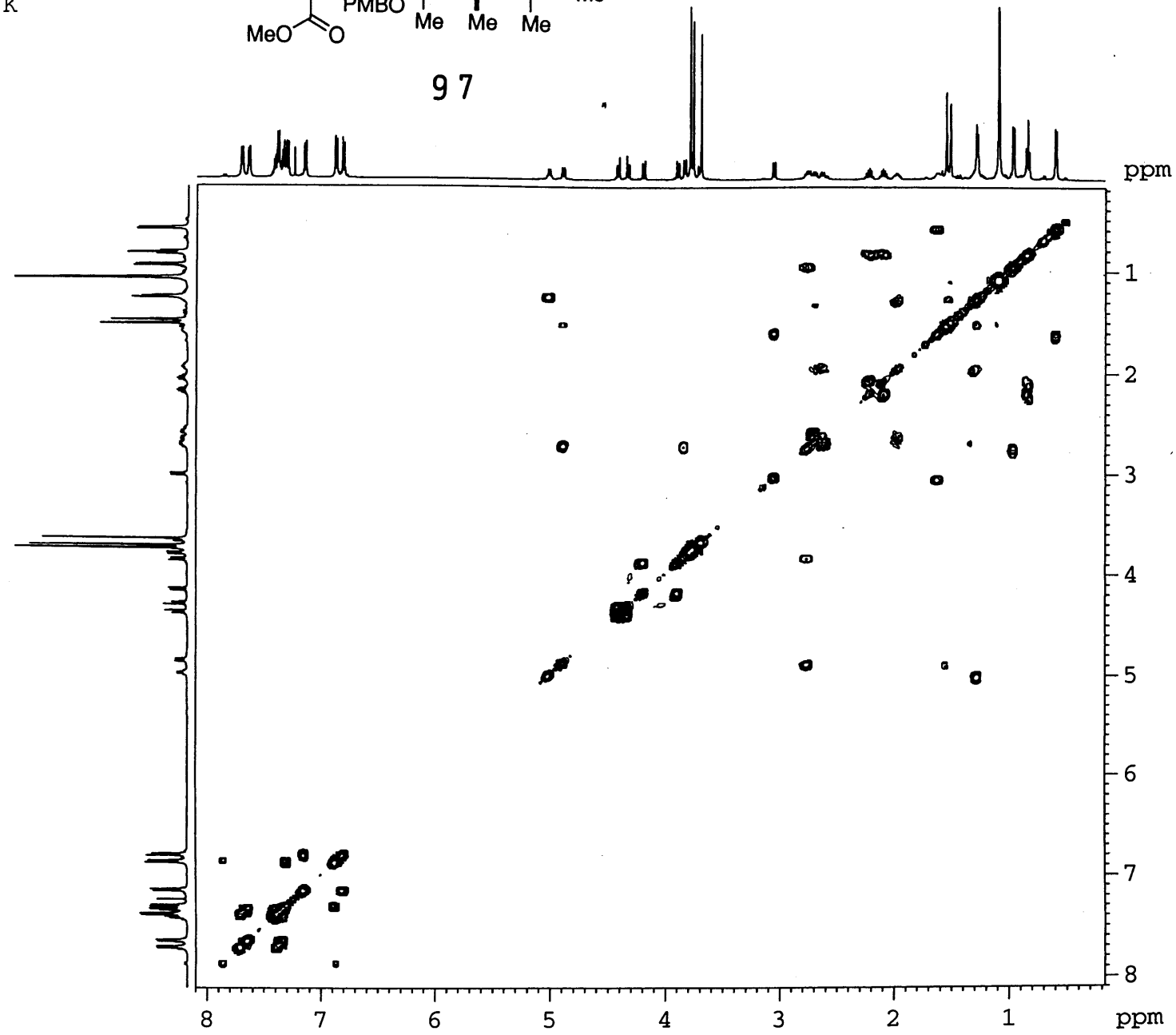

IV-MW-33
HMQC in CDCl3
at 298 K

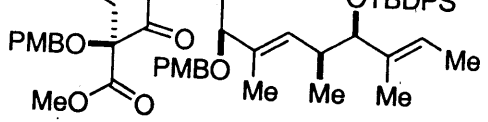

97

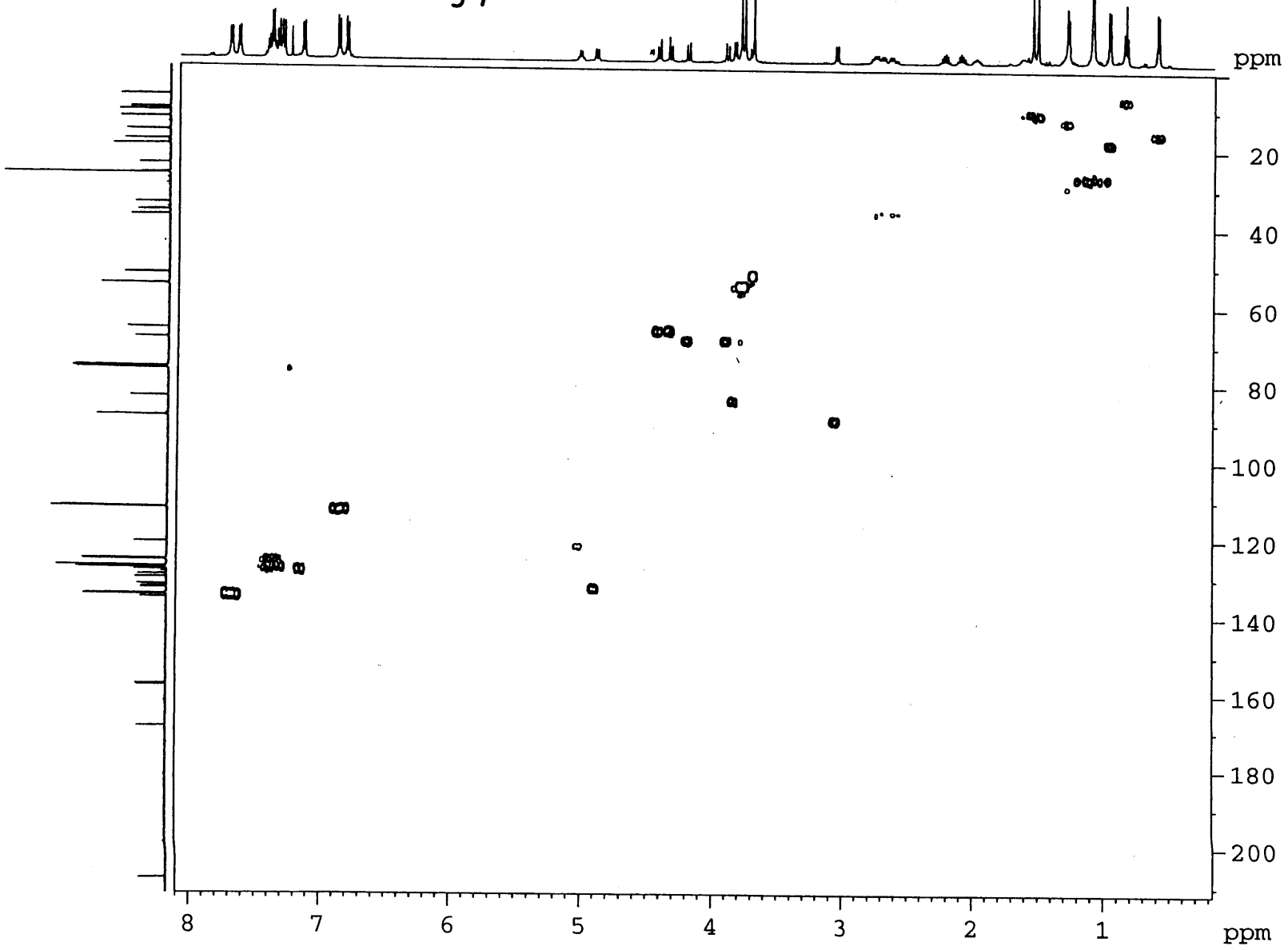

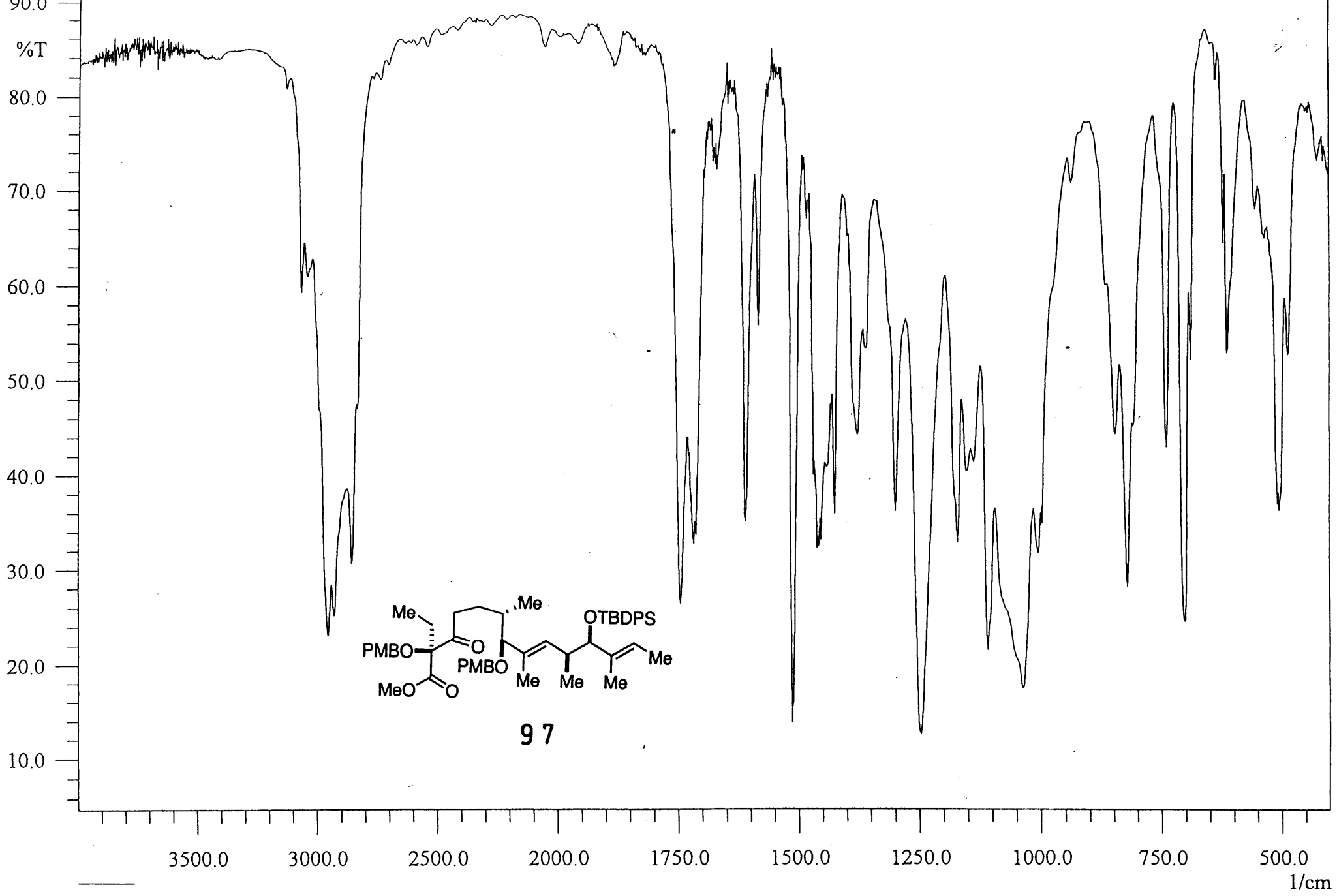
%T
90.0
80.0
70.0
60.0
50.0
40.0
30.0
20.0
10.0
3500.0
3000.0
2500.0
2000.0
1750.0
1500.0
1250.0
1000.0
750.0
500.0
1/cm
Me
Me
OTBDPS
PMBO
O
PMBO
Me
Me
Me
Me
MeO
O

97

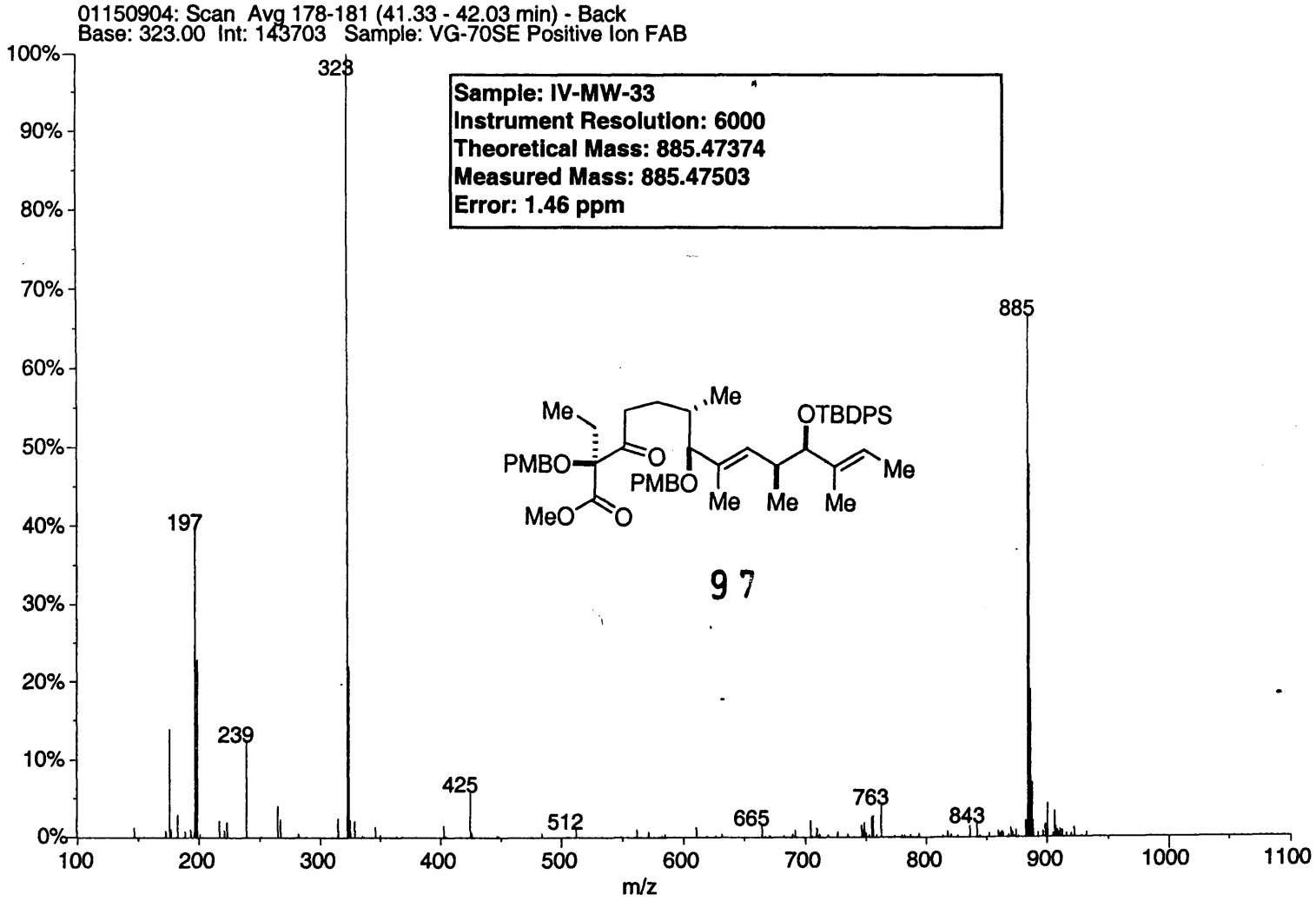
01150904: Scan Avg 178-181 (41.33 - 42.03 min) - Back
Base: 323.00 Int: 143703 Sample: VG-70SE Positive Ion FAB
Sample: IV-MW-33
Instrument Resolution: 6000
Theoretical Mass: 885.47374
Measured Mass: 885.47503
Error: 1.46 ppm
100%
90%
80%
70%
60%
50%
40%
30%
20%
10%
0%
323
885
197
239
425
512
665
763
843
Me
Me
OTBDPS
PMBO
O
PMBO
Me
Me
Me
Me
MeO
O
100
200
300
400
500
600
700
800
900
1000
1100
m/z

97

IV-MW-66 in
CDCl3 at 298 K

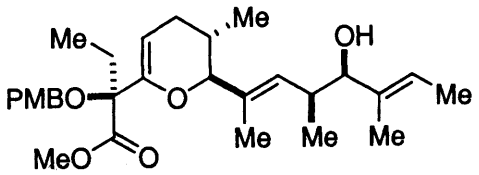

IV-MW-66
DEPT in
CDCl3 at 298 K

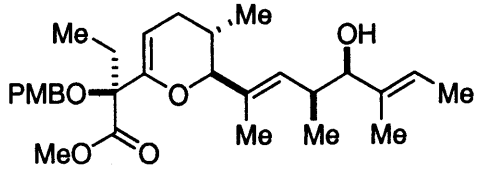

COSY 1H
CDCl3 at 298 K

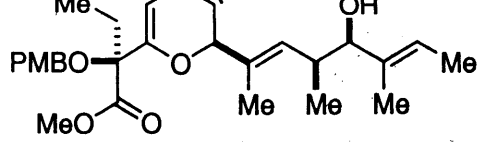

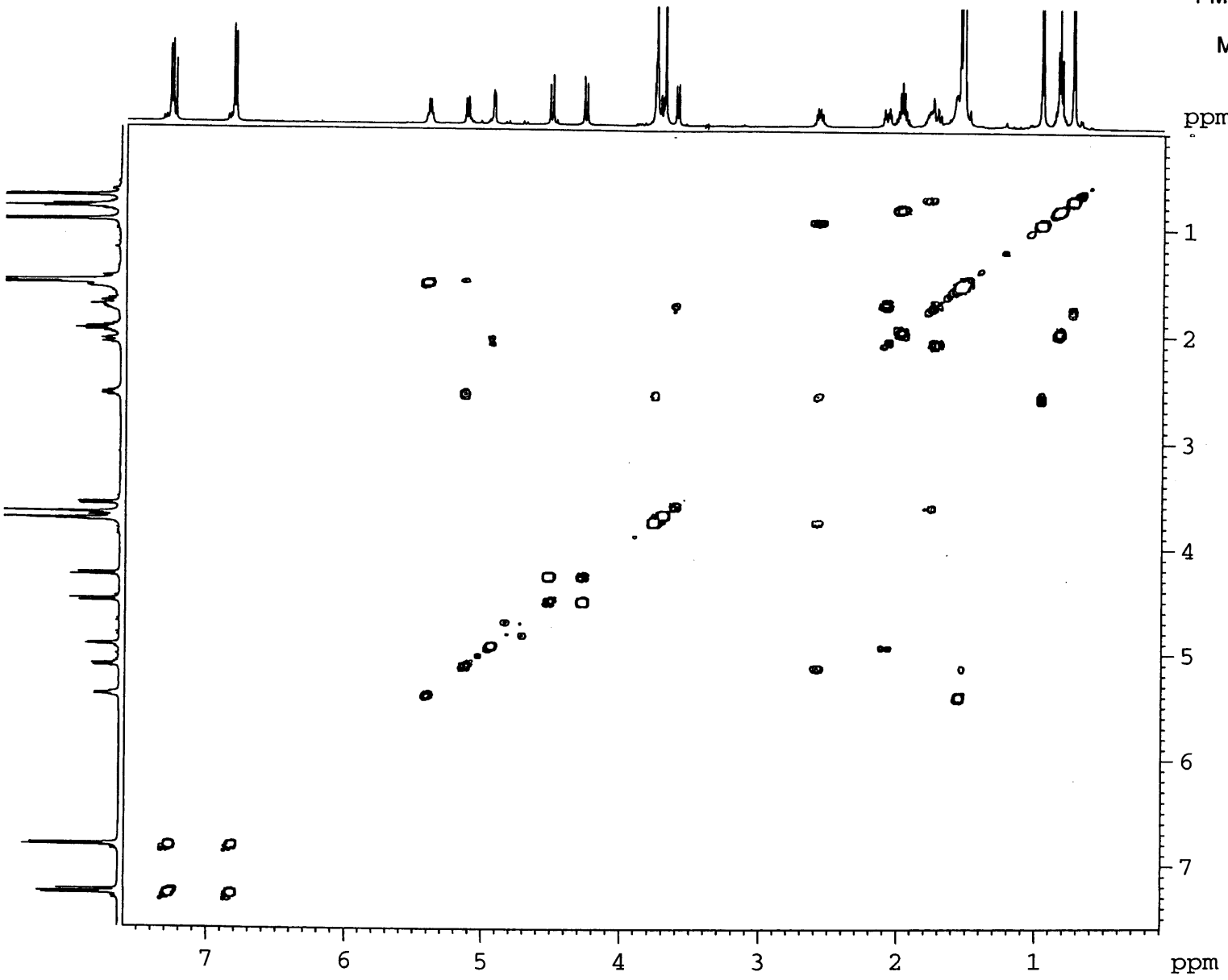

IV-MW-66
HMQC in
CDCl3 at 298 K

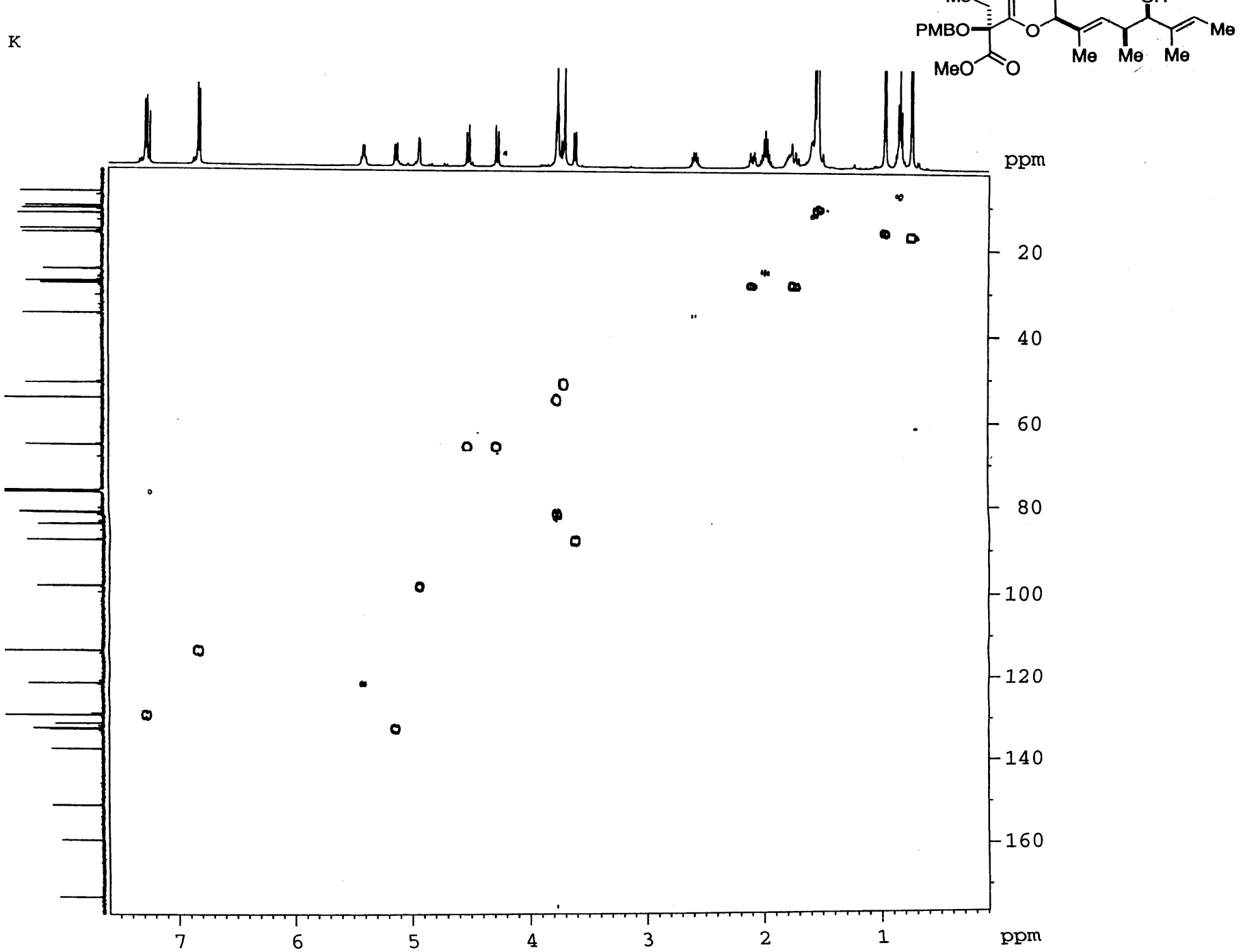

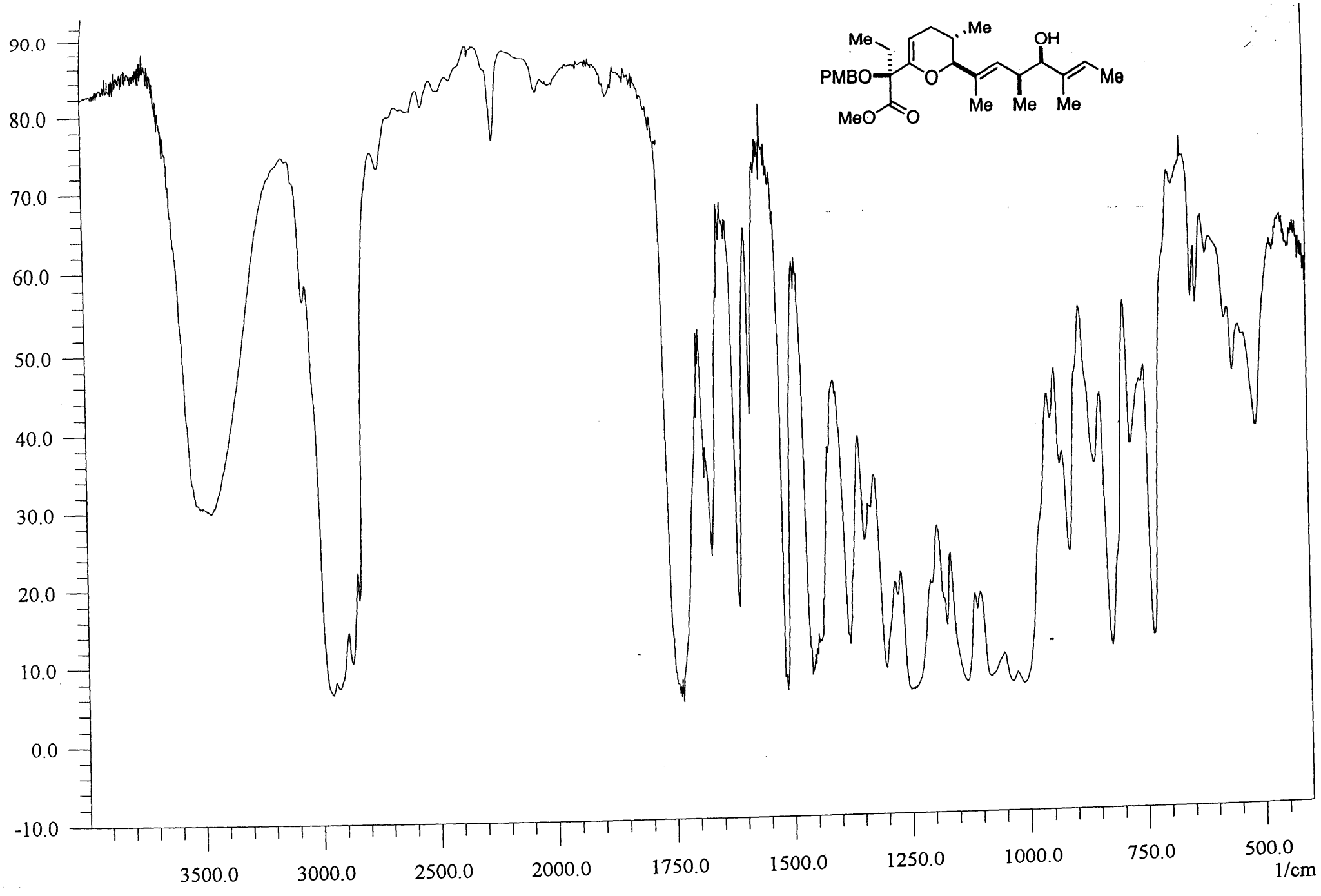
90.0
80.0
70.0
60.0
50.0
40.0
30.0
20.0
10.0
0.0
-10.0
3500.0
3000.0
2500.0
2000.0
1750.0
1500.0
1250.0
1000.0
750.0
500.0
1/cm
Me
Me
OH
PMBO
O
Me
Me
Me
Me
MeO
O

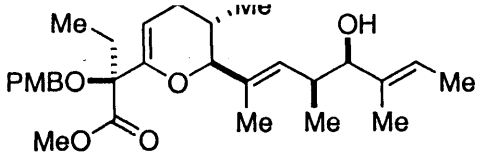

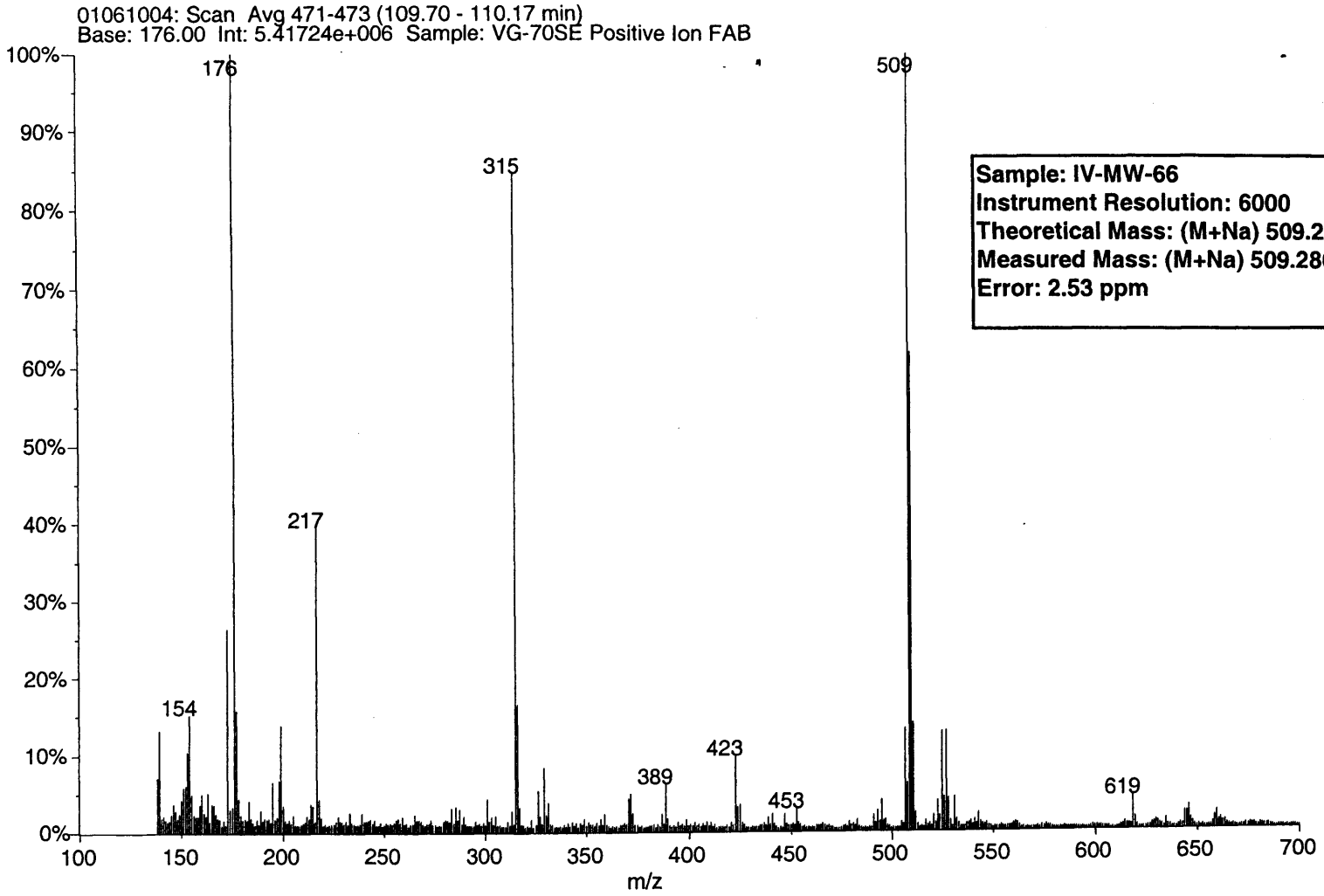

Sample: IV-MW-66
Instrument Resolution: 6000
Theoretical Mass: (M+Na) 509.28789
Measured Mass: (M+Na) 509.28660
Error: 2.53 ppm

IV-MW-172
in CDCl3
at 298 K

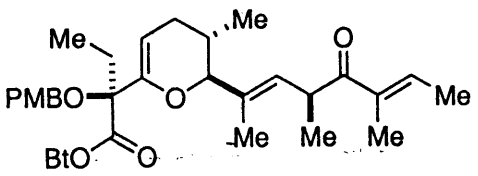

IV-MW-172
CARBON 13 in
CDC13 at 298 K

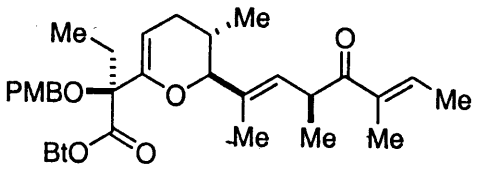

IV-MW-172
DEPT in CDCl3
at 298 K

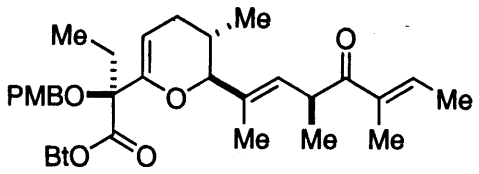

IV-MW-172
COSY in
CDCl3 at 298 K

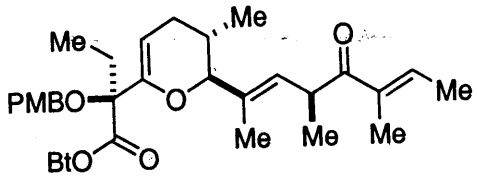

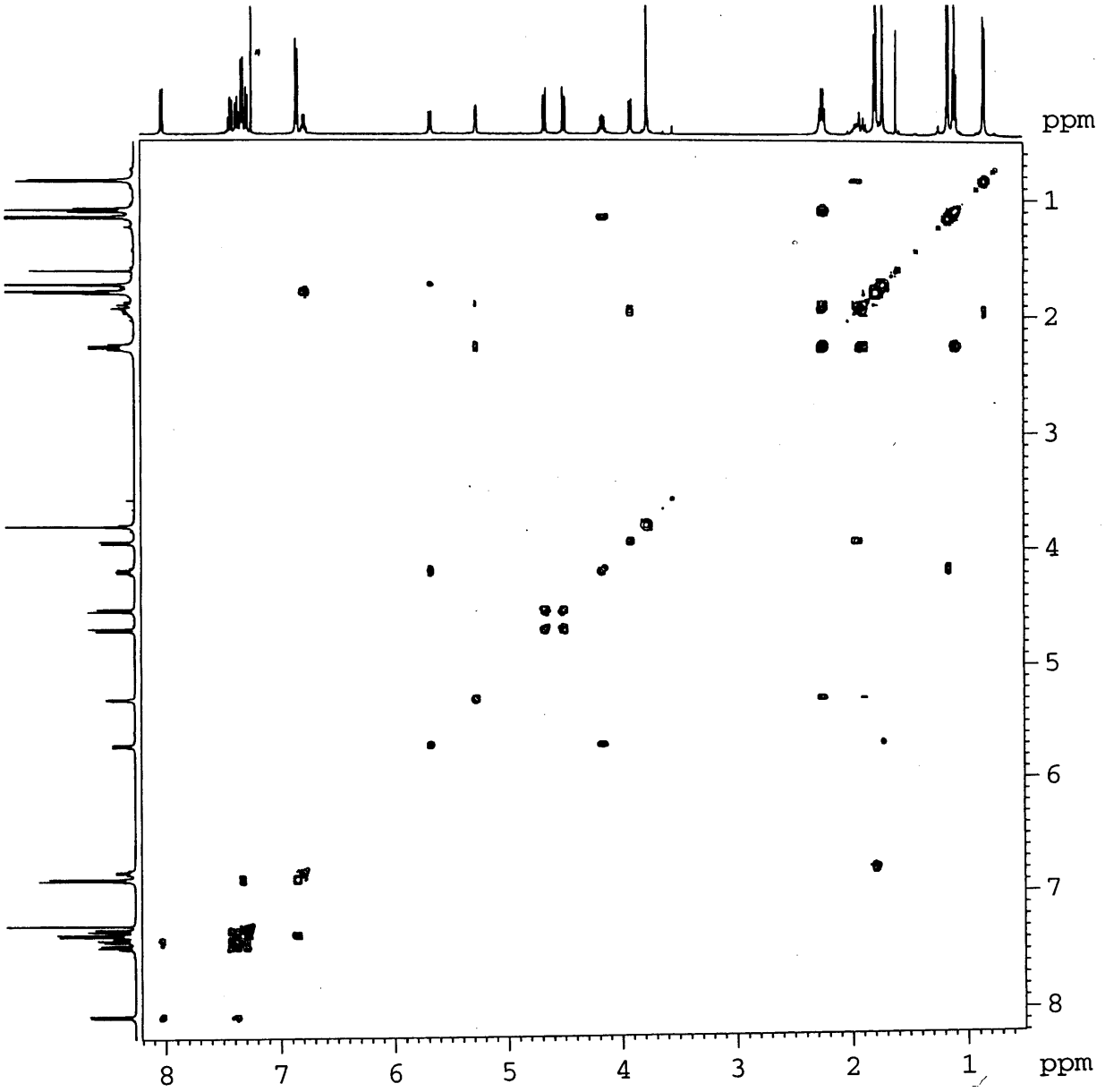

IV-MW-172
HMQC in
CDCl3 at 298 K

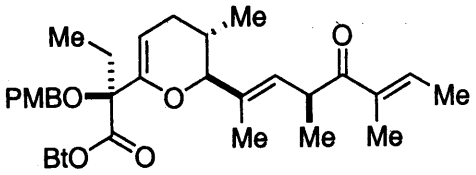

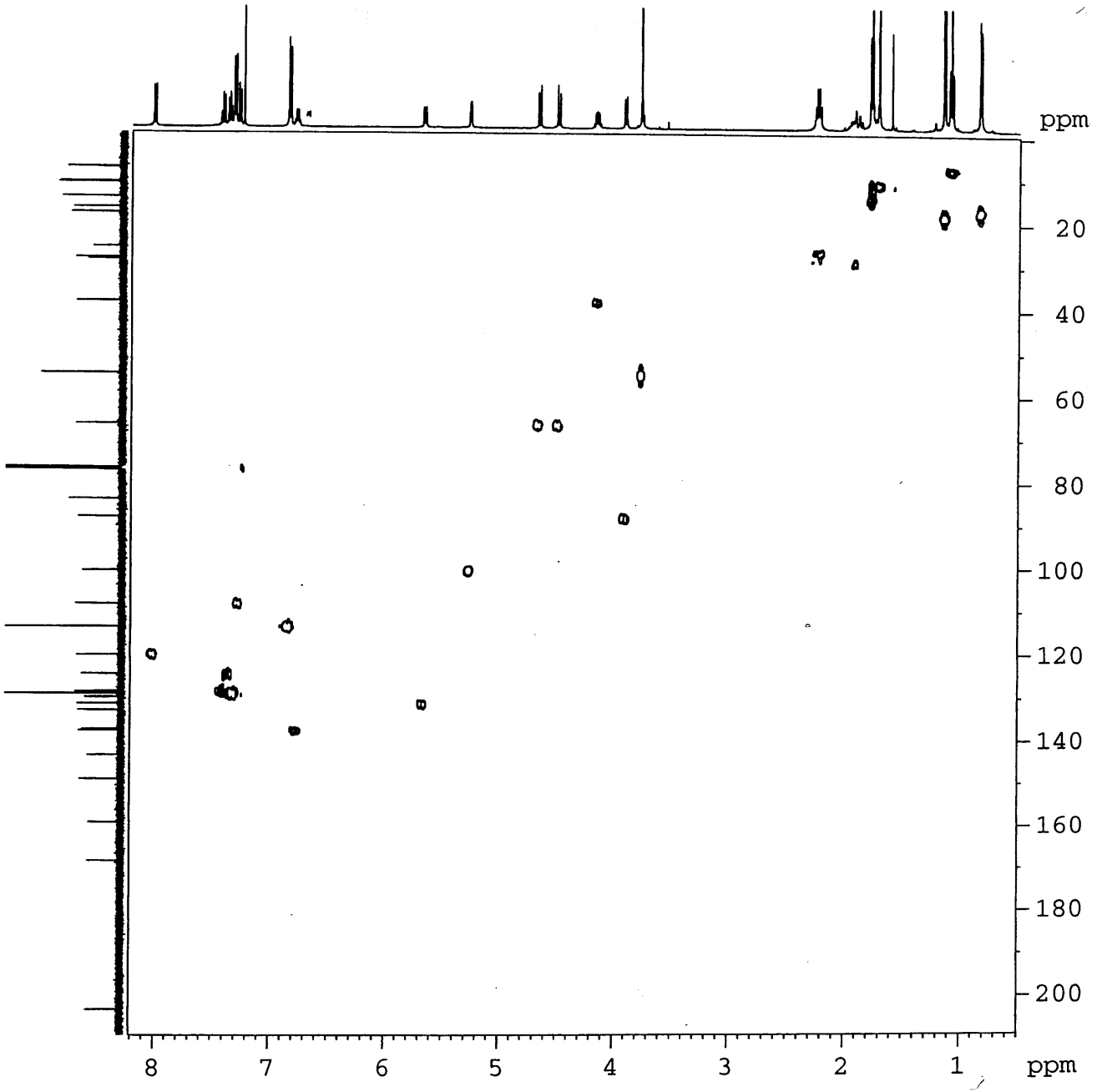

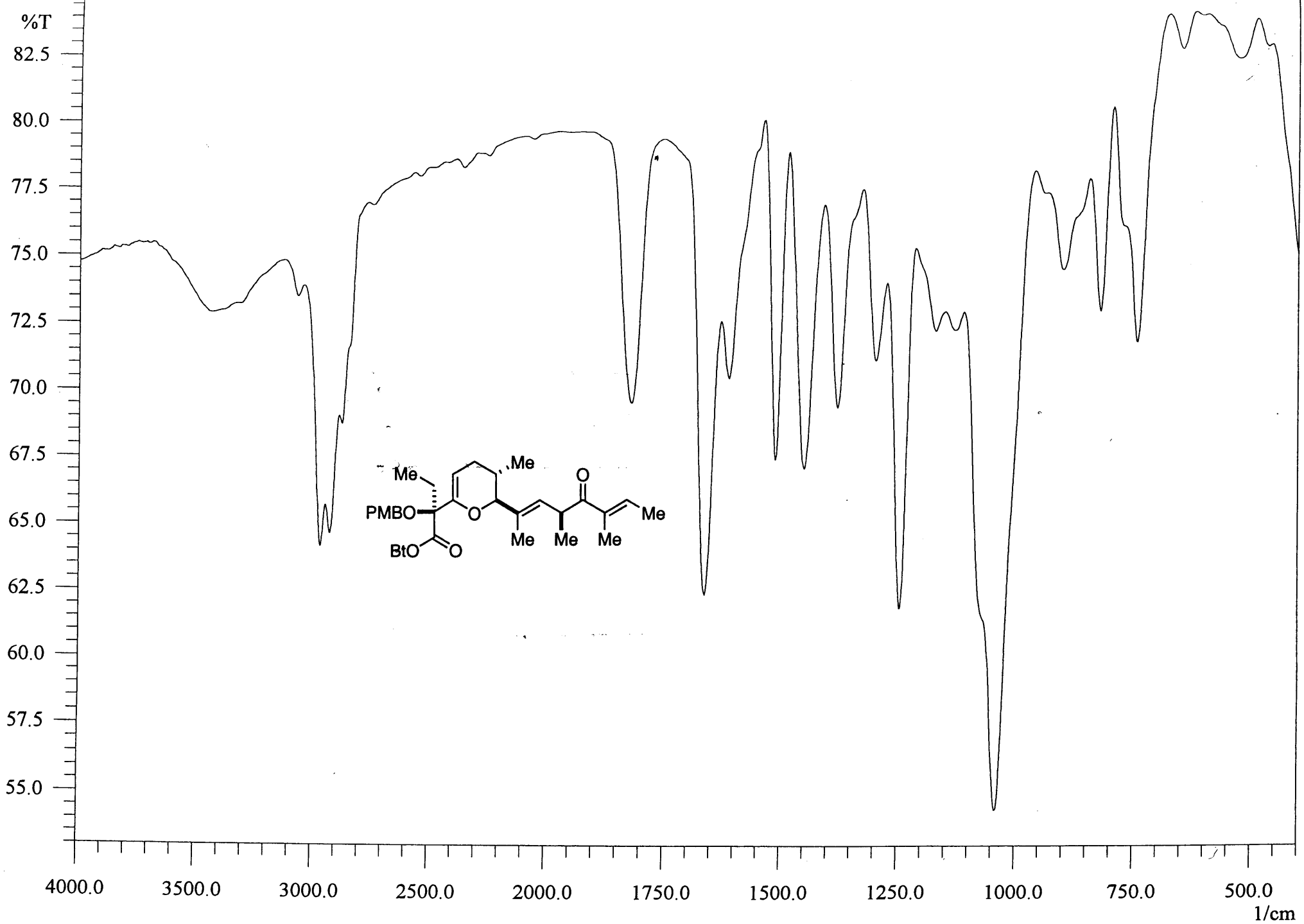
%T
82.5
80.0
77.5
75.0
72.5
70.0
67.5
65.0
62.5
60.0
57.5
55.0
4000.0
3500.0
3000.0
2500.0
2000.0
1750.0
1500.0
1250.0
1000.0
750.0
500.0
1/cm
Me
Me
PMBO
O
Me
BtO
O
Me
Me
Me
O

SPECIAL NOTE

THIS ITEM IS BOUND IN SUCH A MANNER AND WHILE EVERY EFFORT HAS BEEN MADE TO REPRODUCE THE CENTRES, FORCE WOULD RESULT IN DAMAGE

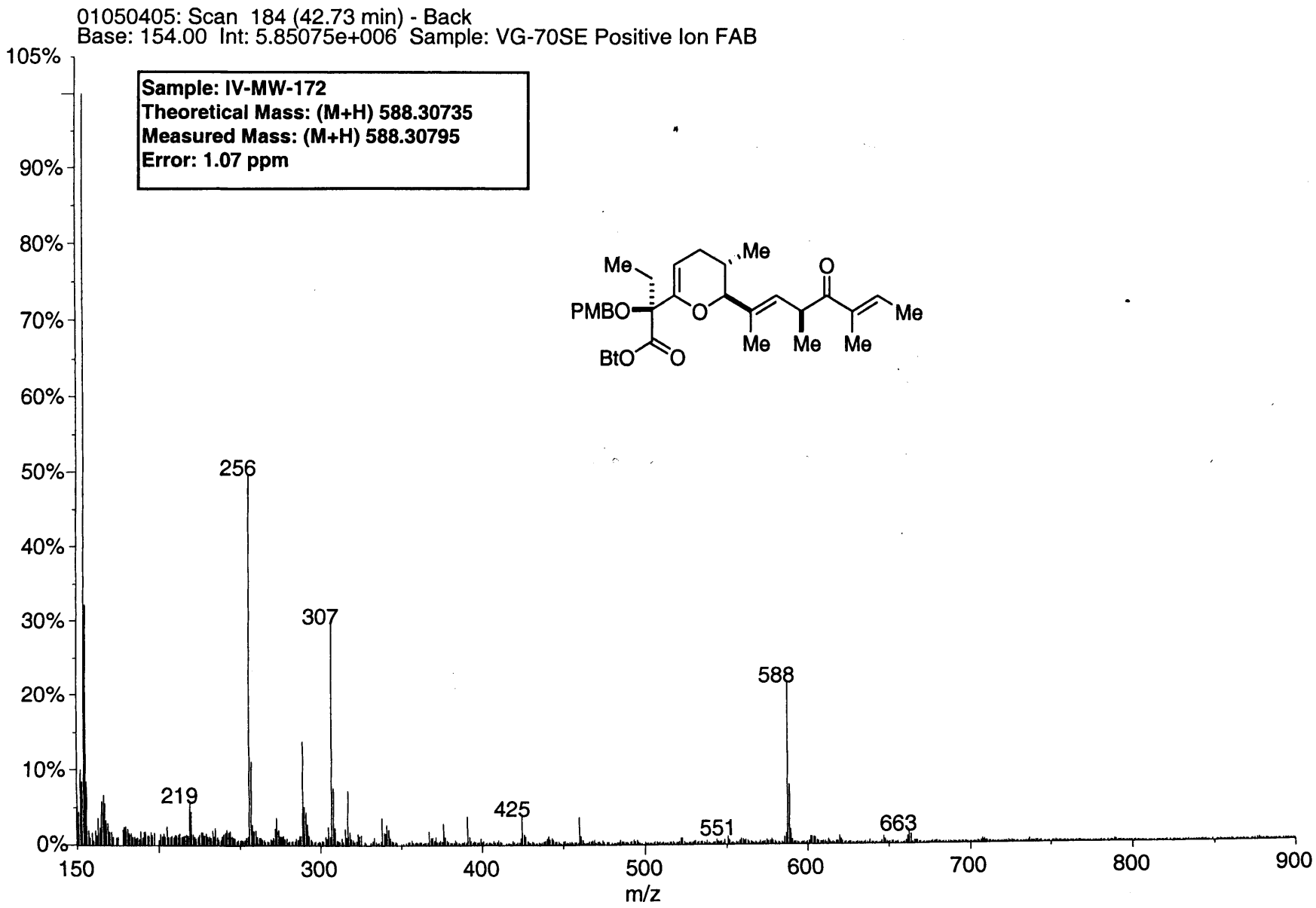
01050405: Scan 184 (42.73 min) - Back
Base: 154.00 Int: 5.85075e+006 Sample: VG-70SE Positive Ion FAB
Sample: IV-MW-172
Theoretical Mass: (M+H) 588.30735
Measured Mass: (M+H) 588.30795
Error: 1.07 ppm
Me
Me
O
PMBO
O
Me
Me
Me
Me
BtO
O
105%
90%
80%
70%
60%
50%
40%
30%
20%
10%
0%
256
307
588
219
425
551
663
150
300
400
500
600
700
800
900
m/z

IV-MW-6 in
CDCl3 at 298 K

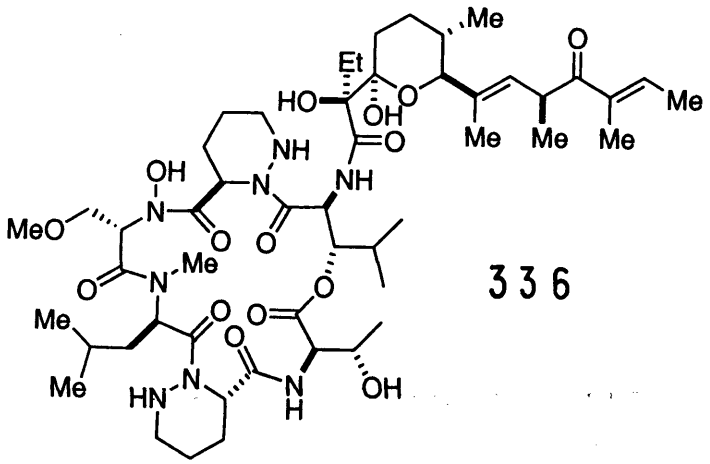

336

IV-MW-6
Carbon 13
in CDCl3 at 298 K

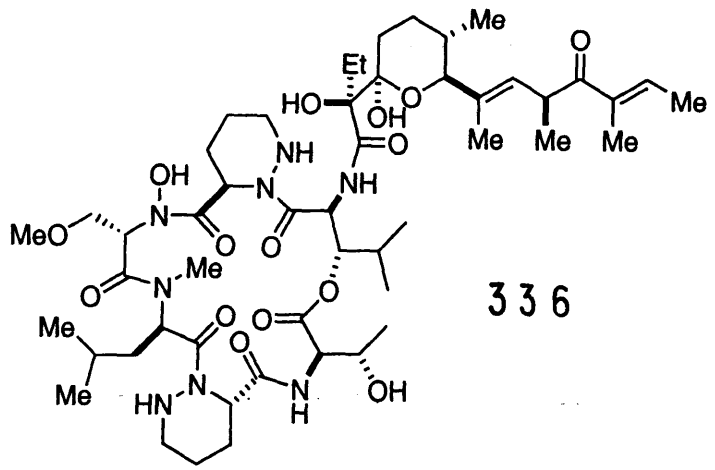

336

SPECIAL NOTE

THIS ITEM IS BOUND IN SUCH A MANNER AND WHILE EVERY EFFORT HAS BEEN MADE TO REPRODUCE THE CENTRES, FORCE WOULD RESULT IN DAMAGE

IV-MW-6
DEPT in
CDCl3 at 298 K

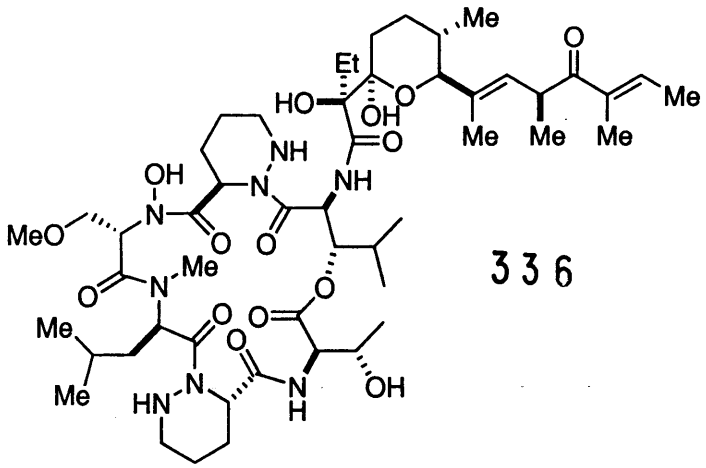

336

IV-MW-6
COSY in
CDCl3 at 298 K

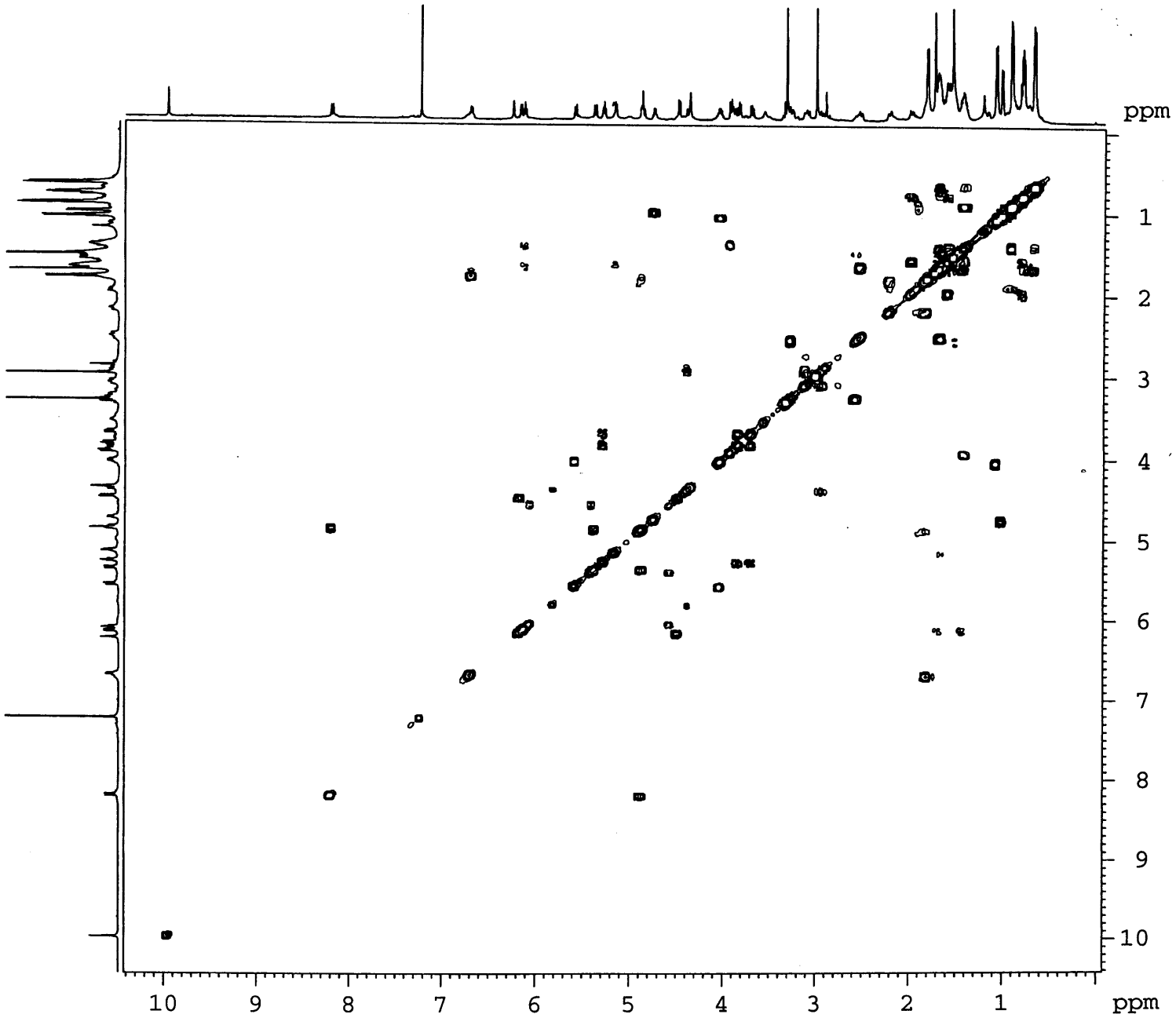

IV-MW-6
HMQC in
CDCl3 at 298 K

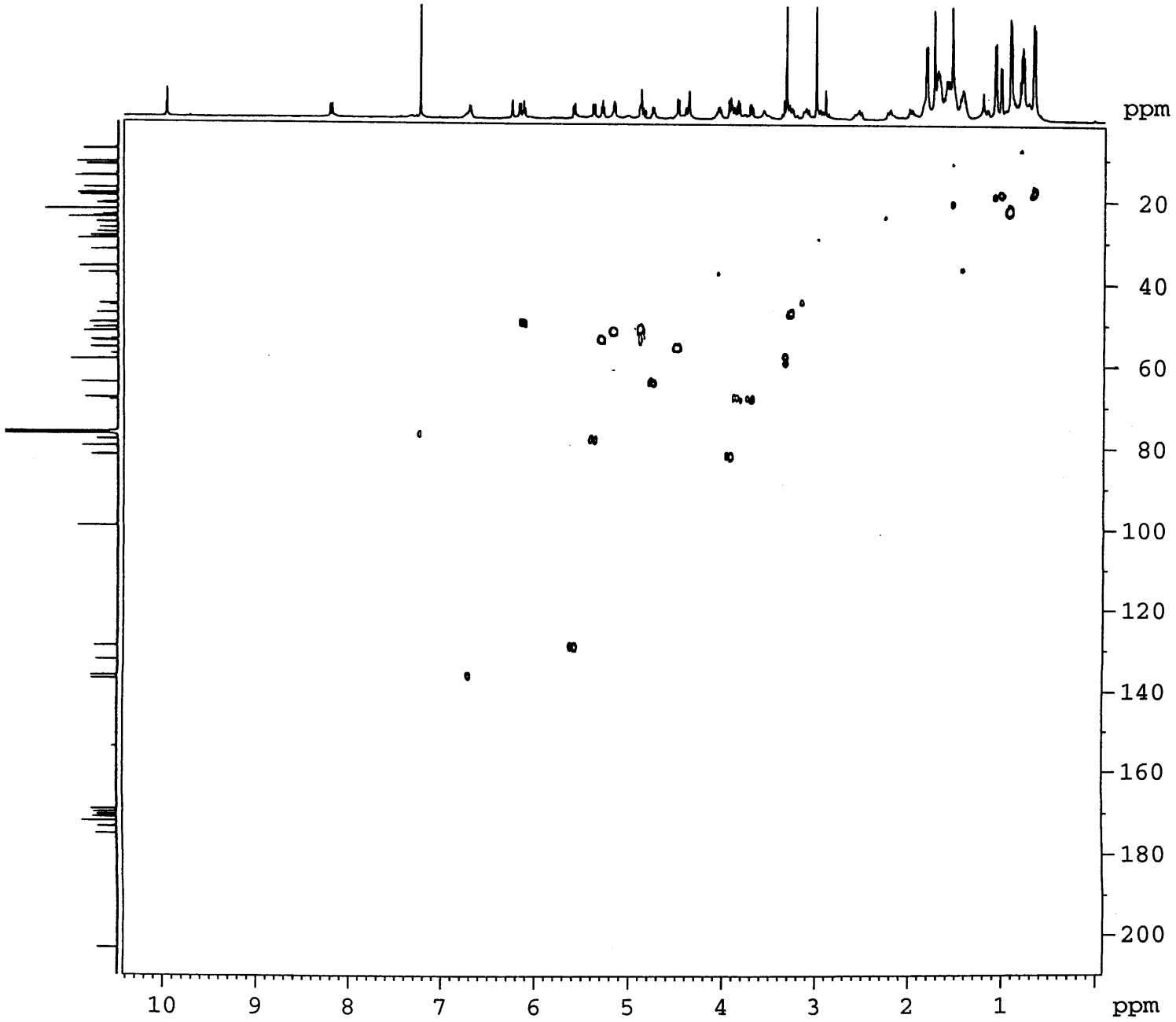

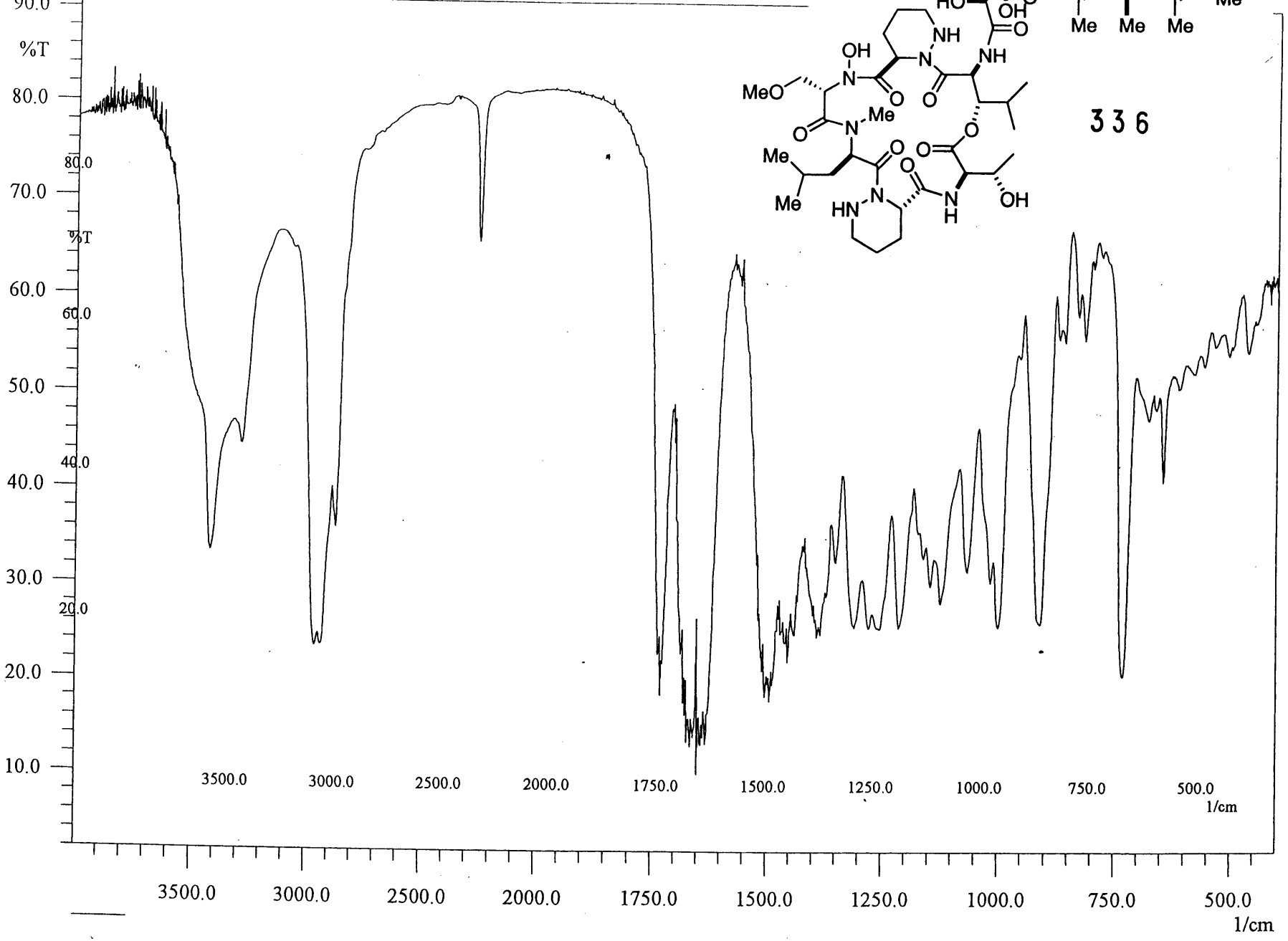
%T
90.0
80.0
70.0
60.0
50.0
40.0
30.0
20.0
10.0
3500.0
3000.0
2500.0
2000.0
1750.0
1500.0
1250.0
1000.0
750.0
500.0
1/cm
MeO
OH
NH
Me
HN
Me
Me
Me
Me
Me
336

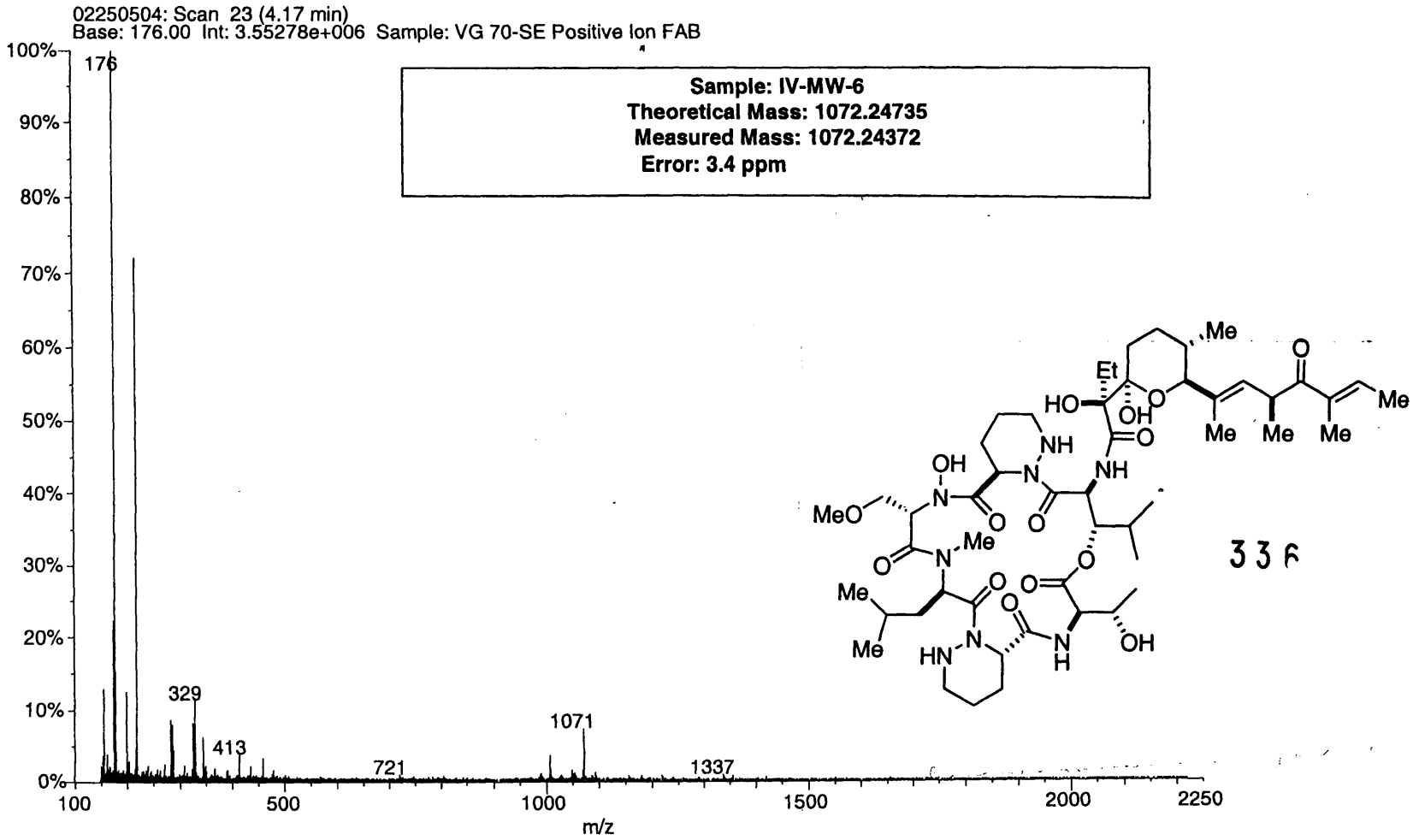
02250504: Scan 23 (4.17 min)
Base: 176.00 Int: 3.55278e+006 Sample: VG 70-SE Positive Ion FAB
Sample: IV-MW-6
Theoretical Mass: 1072.24735
Measured Mass: 1072.24372
Error: 3.4 ppm
100%
90%
80%
70%
60%
50%
40%
30%
20%
10%
0%
176
329
413
721
1071
1337
100
500
1000
1500
2000
2250
m/z
Me
Et
HO
OH
O
Me
Me
Me
Me
Me
NH
NH
OH
N
MeO
Me
Me
Me
HN
N
H
OH
336

IV-MW-27 in
Toluene at 373 K

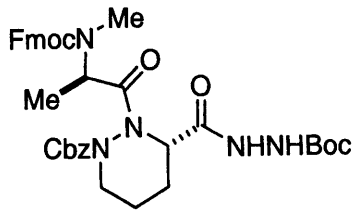

346

IV-MW-27
Carbon 13 in
Toluene at 373 K

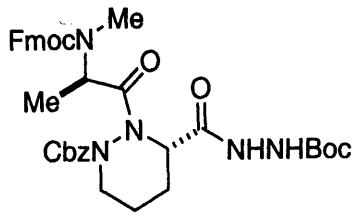

346

IV-MW-27
DEPT in Toluene
at 373 K

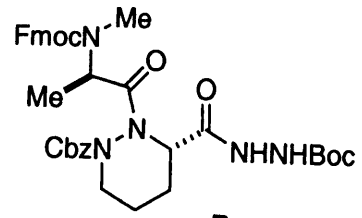

346

COSY 1H
Toluene at 373 K

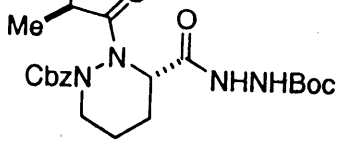

346

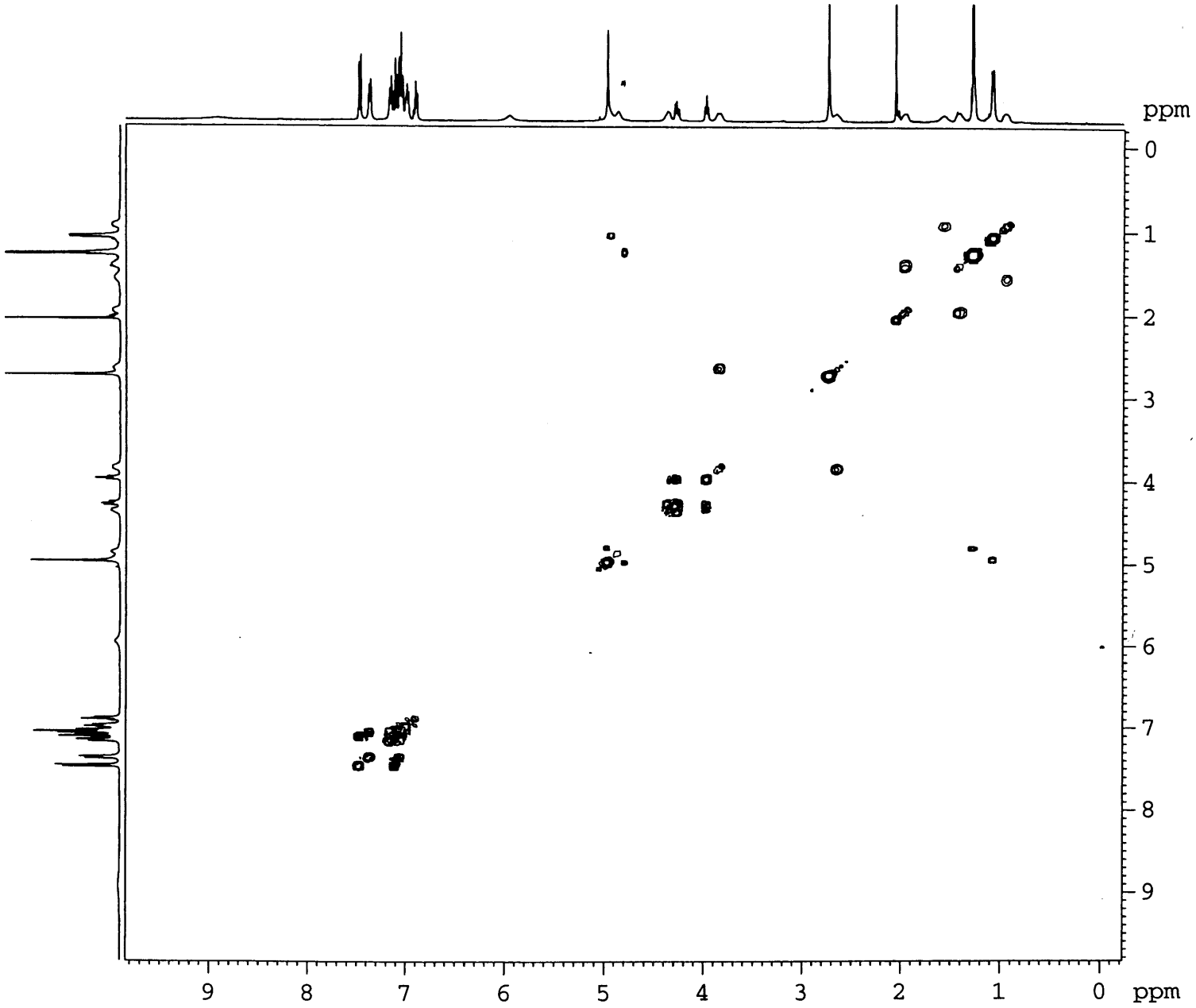

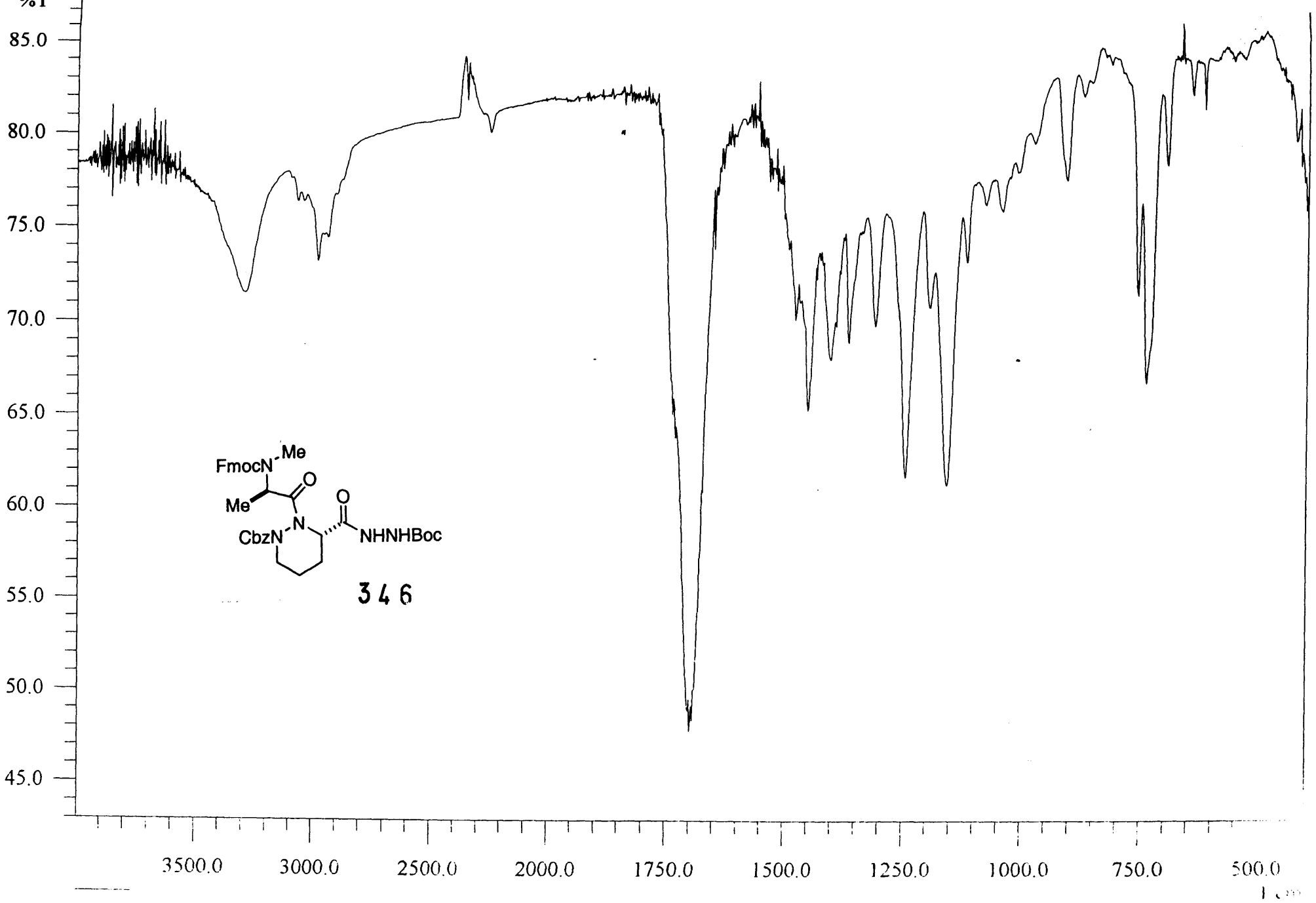
%T
85.0
80.0
75.0
70.0
65.0
60.0
55.0
50.0
45.0
FmocN
Me
Me
O
O
CbzN
N
NHNHBoc
346
3500.0
3000.0
2500.0
2000.0
1750.0
1500.0
1250.0
1000.0
750.0
500.0

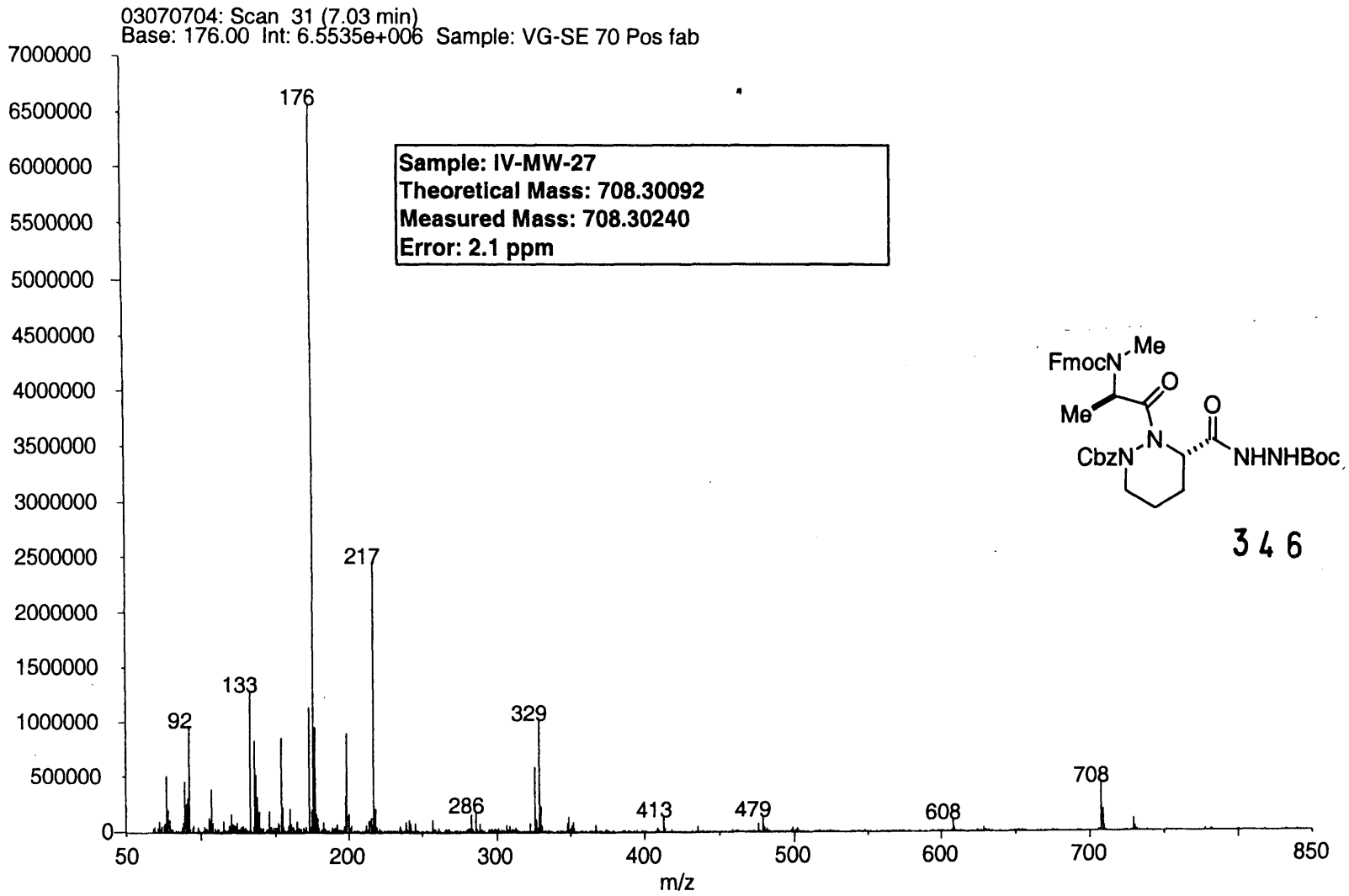
03070704: Scan 31 (7.03 min)
Base: 176.00 Int: 6.5535e+006 Sample: VG-SE 70 Pos fab
Sample: IV-MW-27
Theoretical Mass: 708.30092
Measured Mass: 708.30240
Error: 2.1 ppm
FmocN
Me
Me
O
O
N
CbzN
NHNHBoc
346
m/z

IV-MW-122 1H
CDCl3 at 298 K

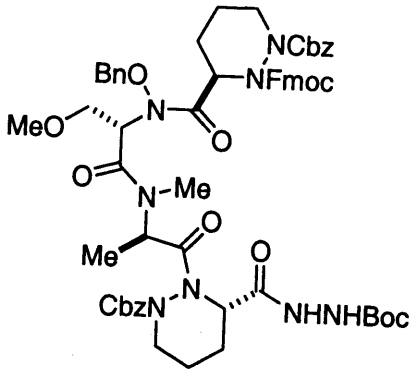

347

IV-MW-122
Carbon 13 in
CDCl3 at 298 K

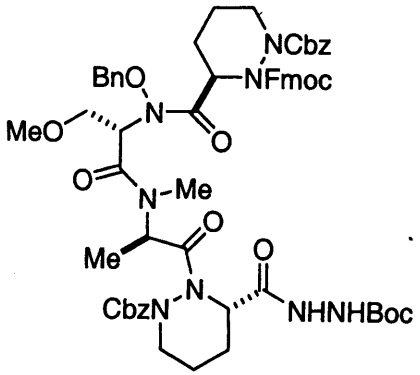

347

DEPT 1H
CDCl3 at 298 K

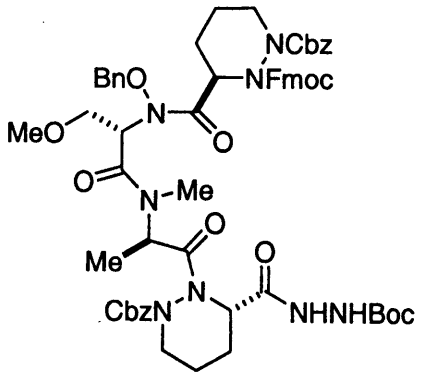

347

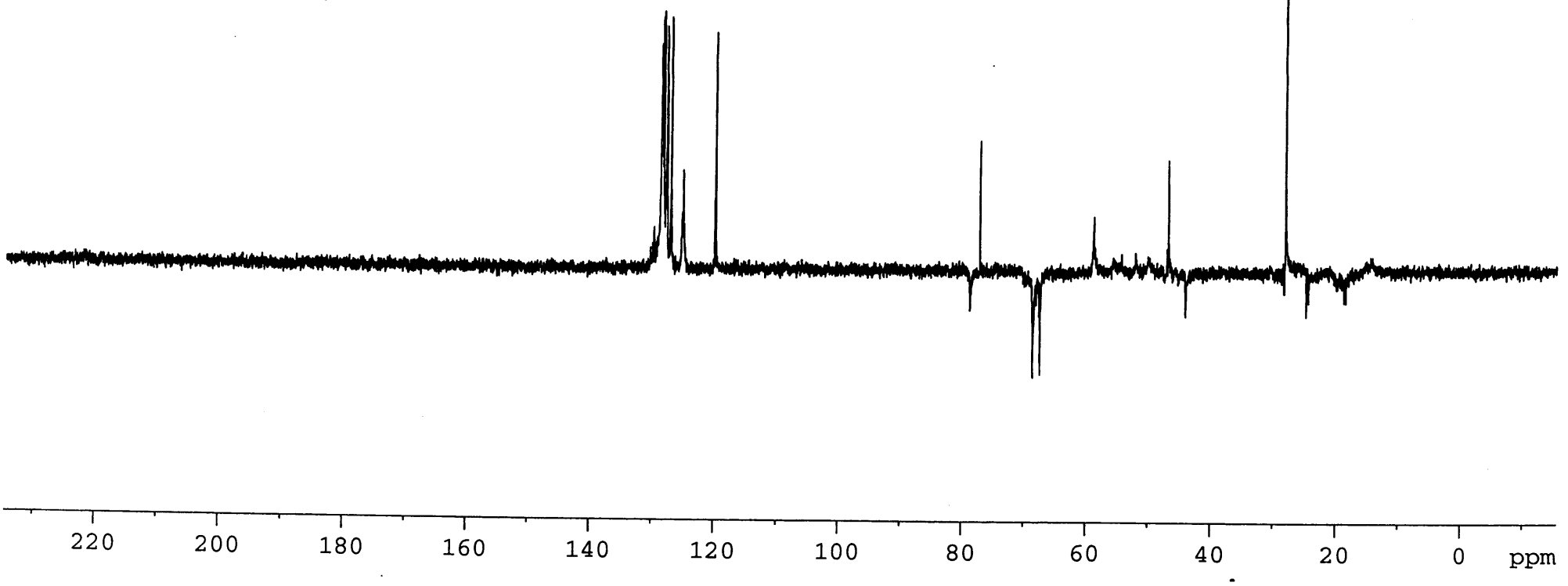

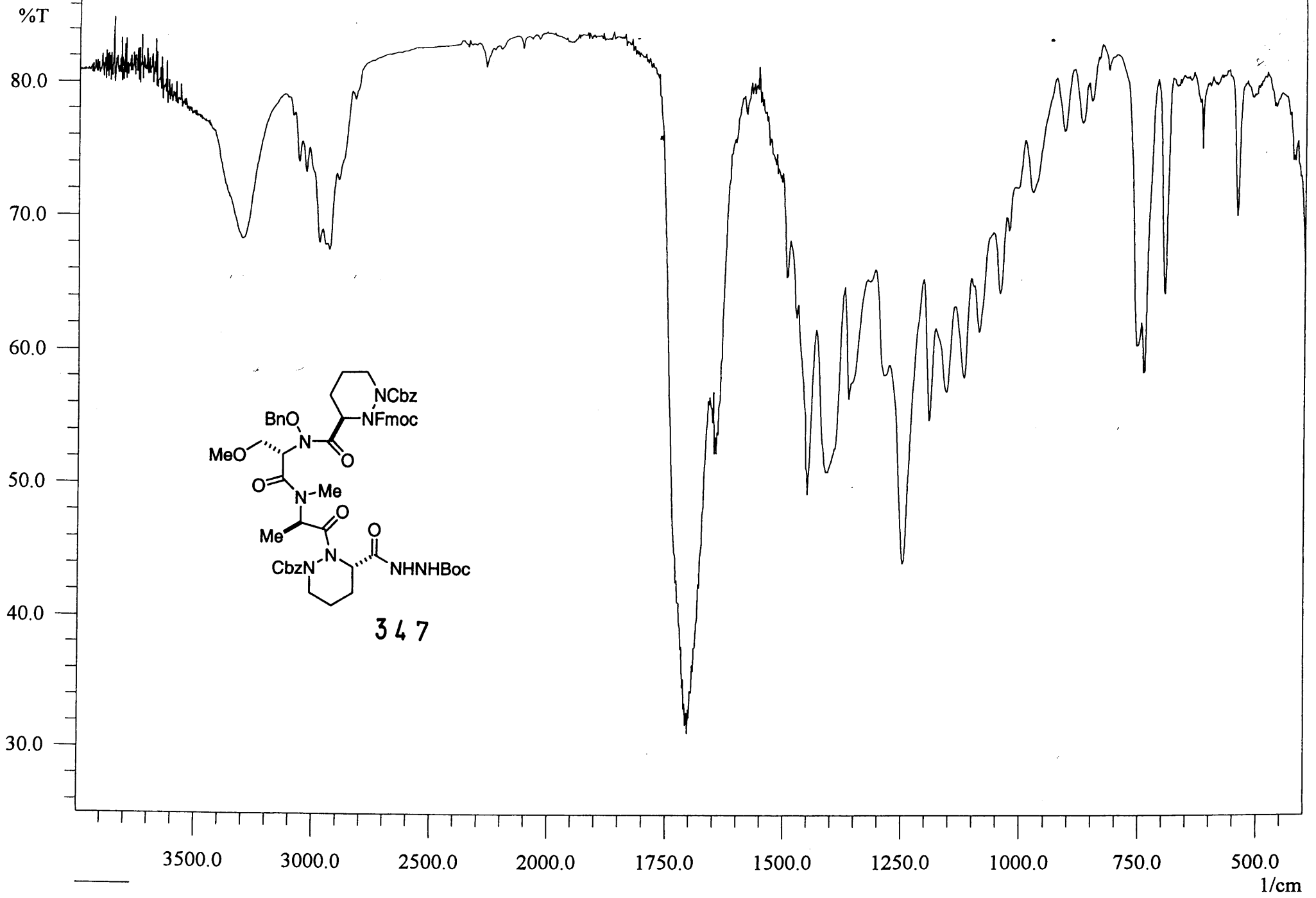
%T
80.0
70.0
60.0
50.0
40.0
30.0
3500.0
3000.0
2500.0
2000.0
1750.0
1500.0
1250.0
1000.0
750.0
500.0
1/cm
NCbz
NFmoc
BnO
N
MeO
O
N-Me
Me
CbzN
NHNHBoc
347

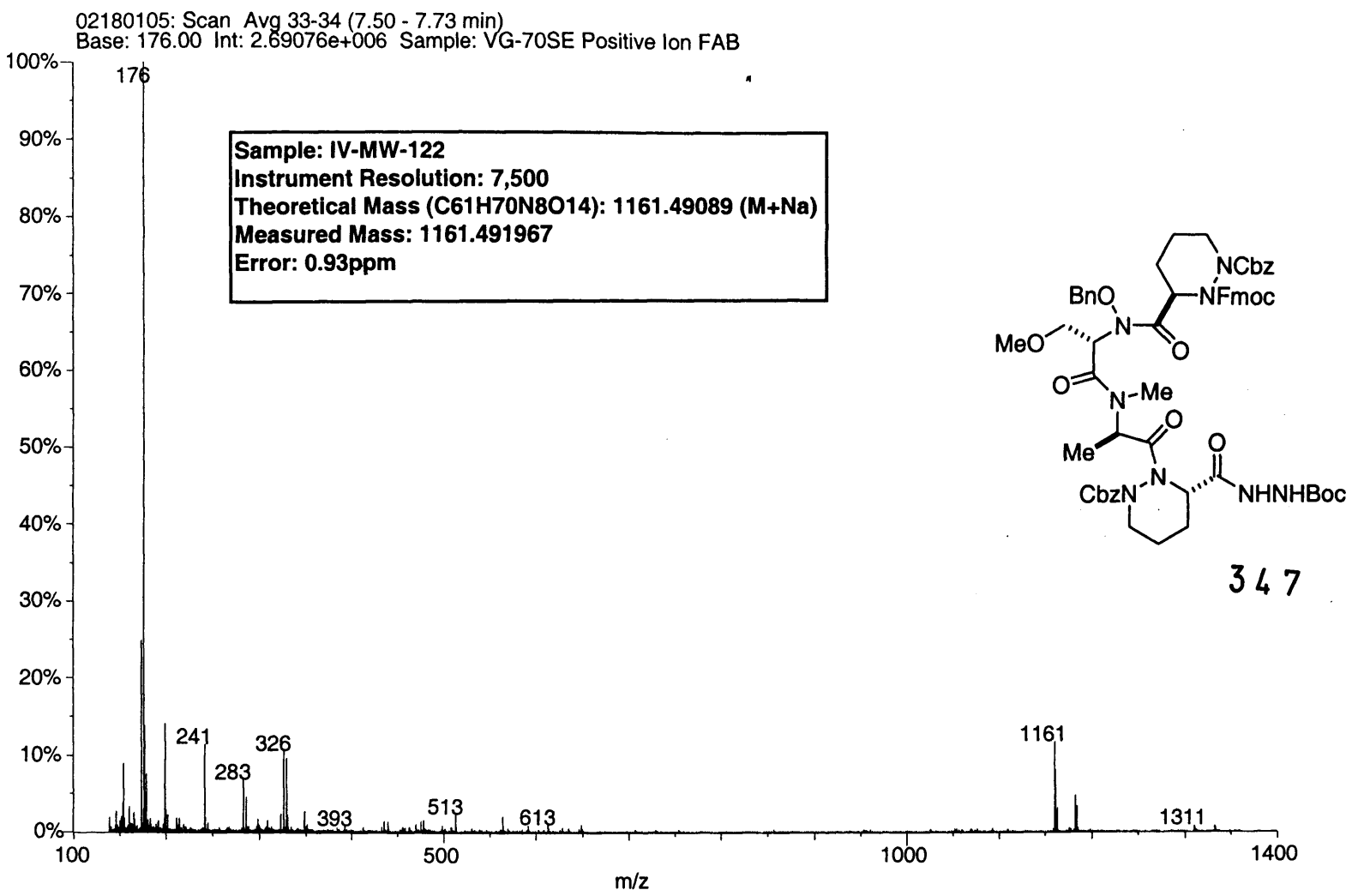
02180105: Scan Avg 33-34 (7.50 - 7.73 min)
Base: 176.00 Int: 2.69076e+006 Sample: VG-70SE Positive Ion FAB
Sample: IV-MW-122
Instrument Resolution: 7,500
Theoretical Mass (C61H70N8O14): 1161.49089 (M+Na)
Measured Mass: 1161.491967
Error: 0.93ppm
100%
90%
80%
70%
60%
50%
40%
30%
20%
10%
0%
176
241
283
326
393
513
613
1161
1311
100
500
1000
1400
m/z
NCbz
NFmoc
BnO
N
O
MeO
O
N-Me
O
Me
O
N
CbzN
N
NHNHBoc

347

CDCl3 at 298 K

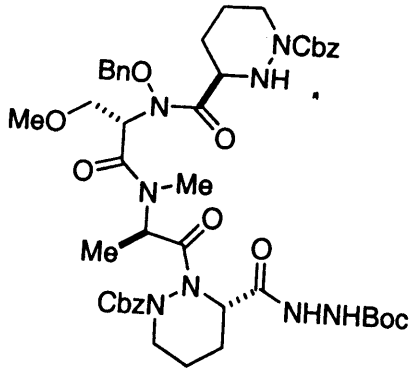

348

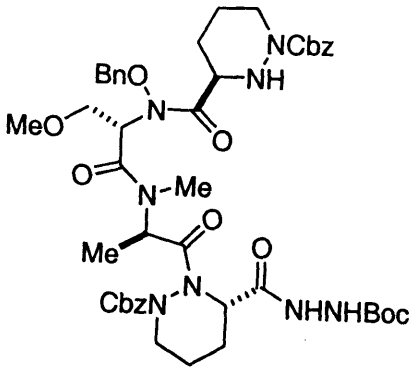
NCbz
NH
BnO
N
MeO
O
O
N-Me
O
Me
O
N
CbzN
NHNHBoc

348

220
200
180
160
140
120
100
80
60
4

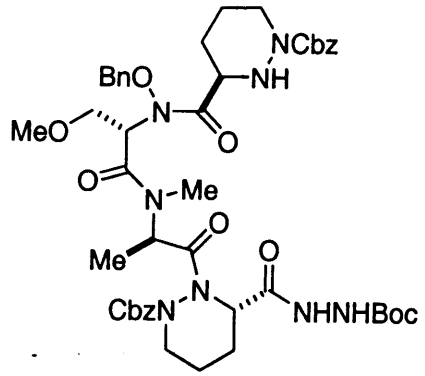
NCbz
NH
BnO
N
MeO
O
O
N-Me
O
Me
O
N
N
CbzN
NHNHBoc

348

220
200
180
160
140
120
100
80
60
40
20
0
ppm

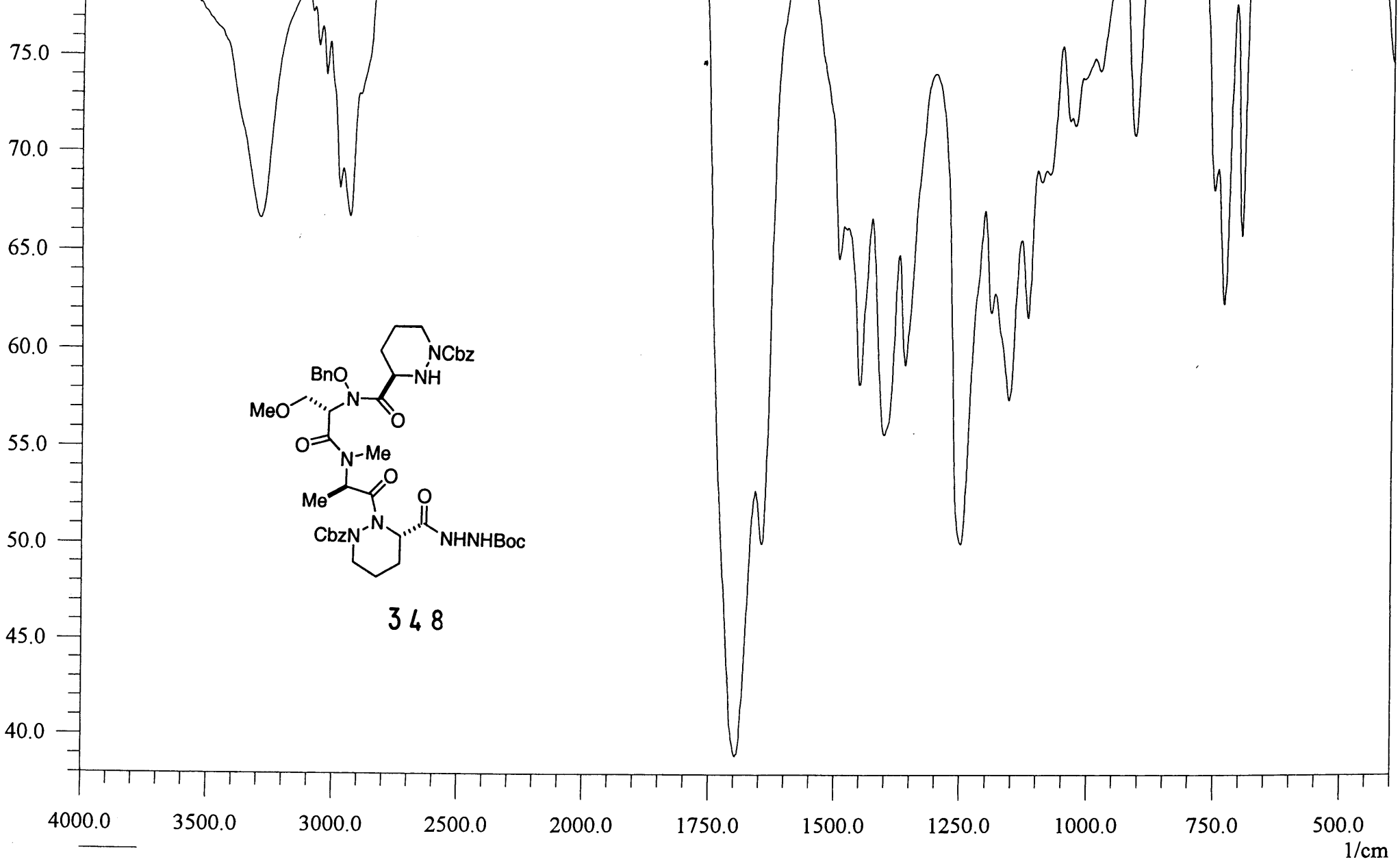
75.0
70.0
65.0
60.0
55.0
50.0
45.0
40.0
4000.0
3500.0
3000.0
2500.0
2000.0
1750.0
1500.0
1250.0
1000.0
750.0
500.0
1/cm
NCbz
NH
BnO
N
MeO
O
N-Me
Me
CbzN
NHNHBoc
348

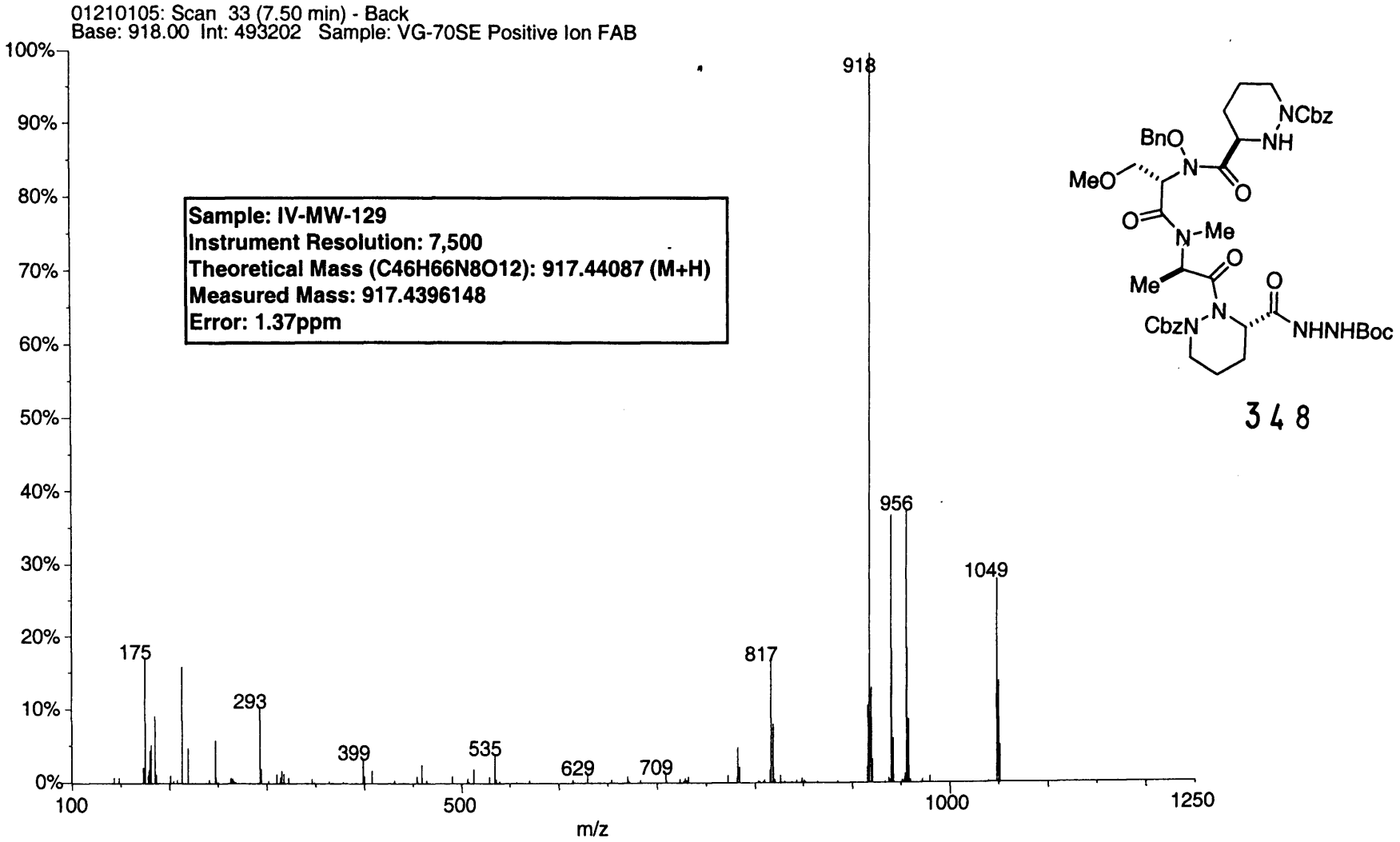
01210105: Scan 33 (7.50 min) - Back
Base: 918.00 Int: 493202 Sample: VG-70SE Positive Ion FAB
Sample: IV-MW-129
Instrument Resolution: 7,500
Theoretical Mass (C46H66N8O12): 917.44087 (M+H)
Measured Mass: 917.4396148
Error: 1.37ppm
100%
90%
80%
70%
60%
50%
40%
30%
20%
10%
0%
100
500
1000
1250
m/z
918
956
1049
817
175
293
399
535
629
709
NCbz
NH
BnO
N
MeO
O
N-Me
Me
CbzN
NHNHBoc

348

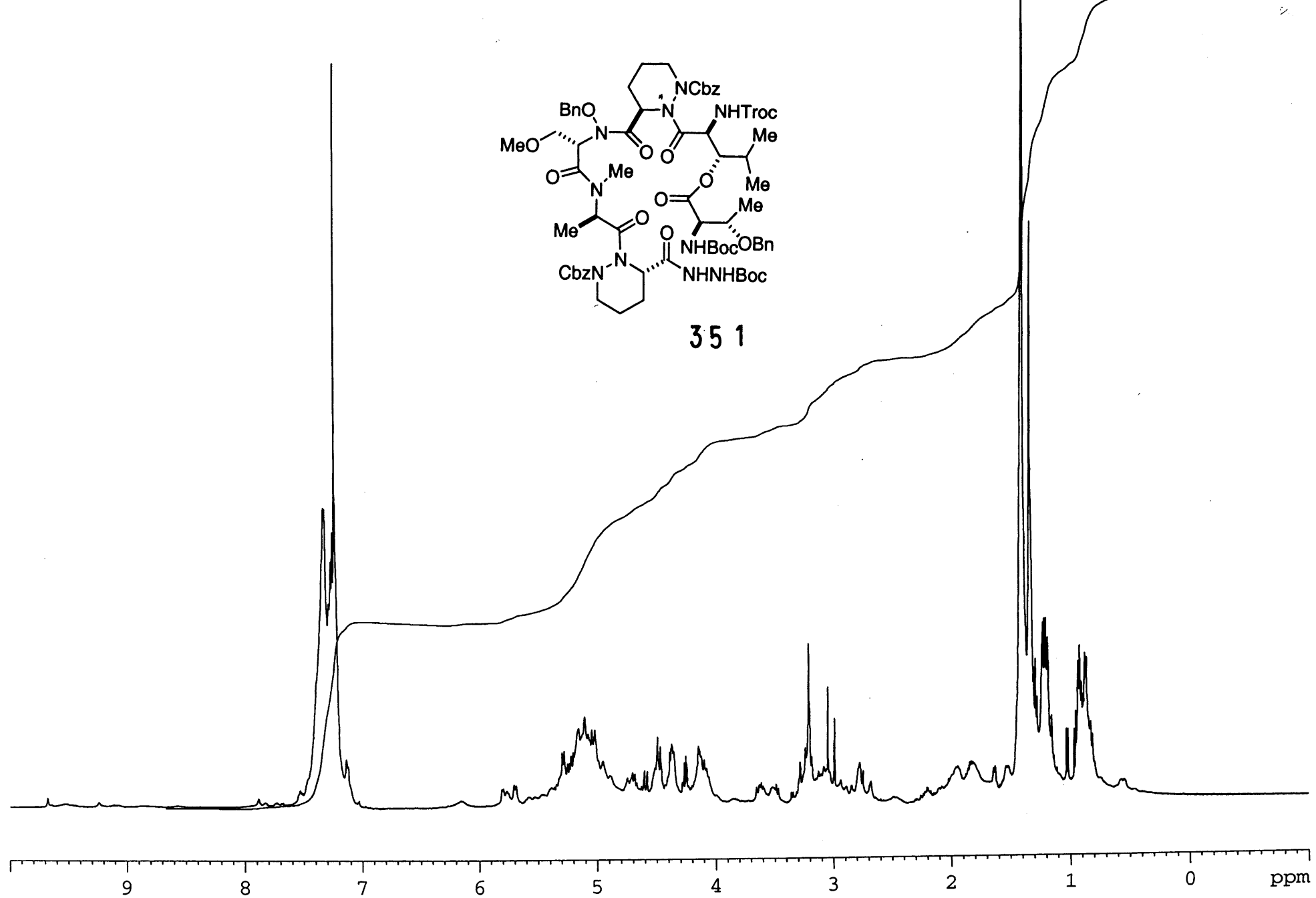
NCbz
BnO
N
NHTroc
MeO
Me
O
Me
Me
Me
NHBocOBn
CbzN
NHNHBoc
9
8
7
6
5
4
3
2
1
0
ppm

351

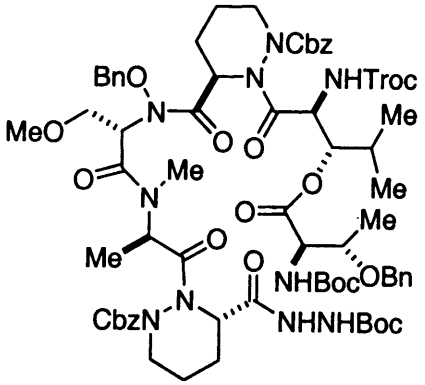
NCbz
BnO
N
NHTroc
Me
MeO
O
O
O
N
Me
O
Me
Me
O
Me
O
NHBoc
OBn
Me
N
CbzN
NHNHBoc

351

220
200
180
160
140
120
100
80
60
40
20
0
ppm

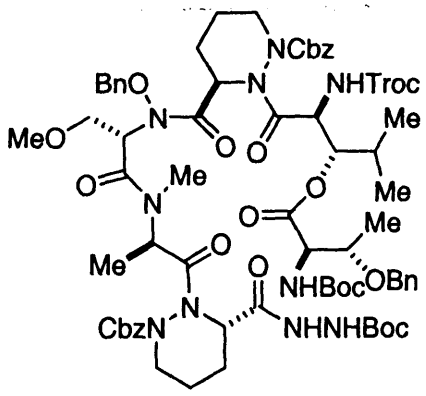
NCbz
BnO
N
NHTroc
Me
MeO
O
O
O
N
Me
O
Me
Me
O
Me
Me
O
NHBocOBn
CbzN
N
NHNHBoc

351

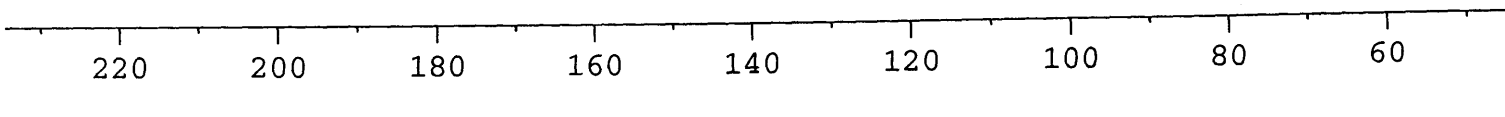
220
200
180
160
140
120
100
80
60

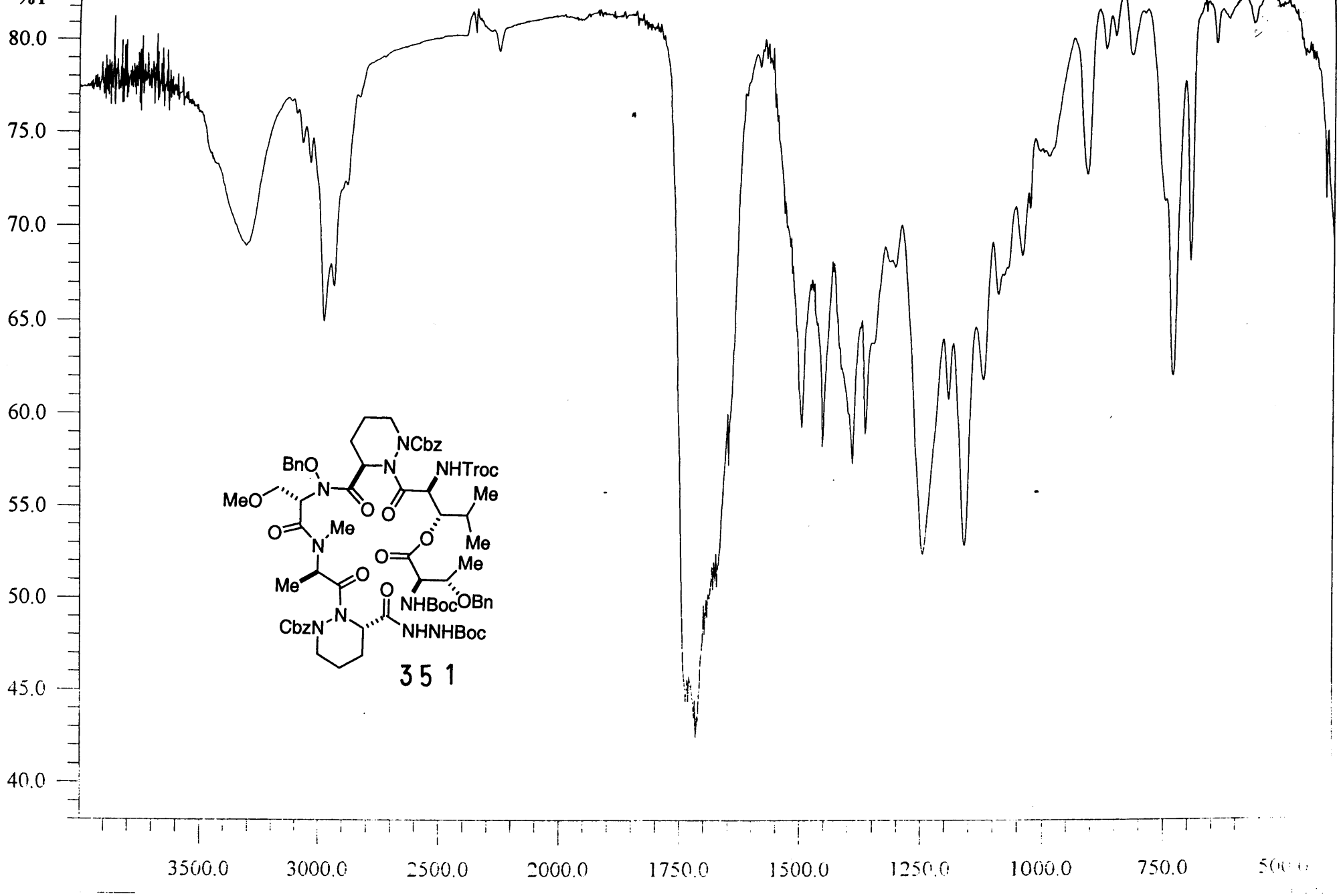
80.0
75.0
70.0
65.0
60.0
55.0
50.0
45.0
40.0
3500.0
3000.0
2500.0
2000.0
1750.0
1500.0
1250.0
1000.0
750.0
NCbz
BnO
NHTroc
MeO
Me
Me
Me
Me
Me
NHBocOBn
CbzN
NHNHBoc
351

01050405: Scan 99 (22.90 min) - Back
Base: 241.00 Int: 739801 Sample: VG-70SE Positive Ion FAB

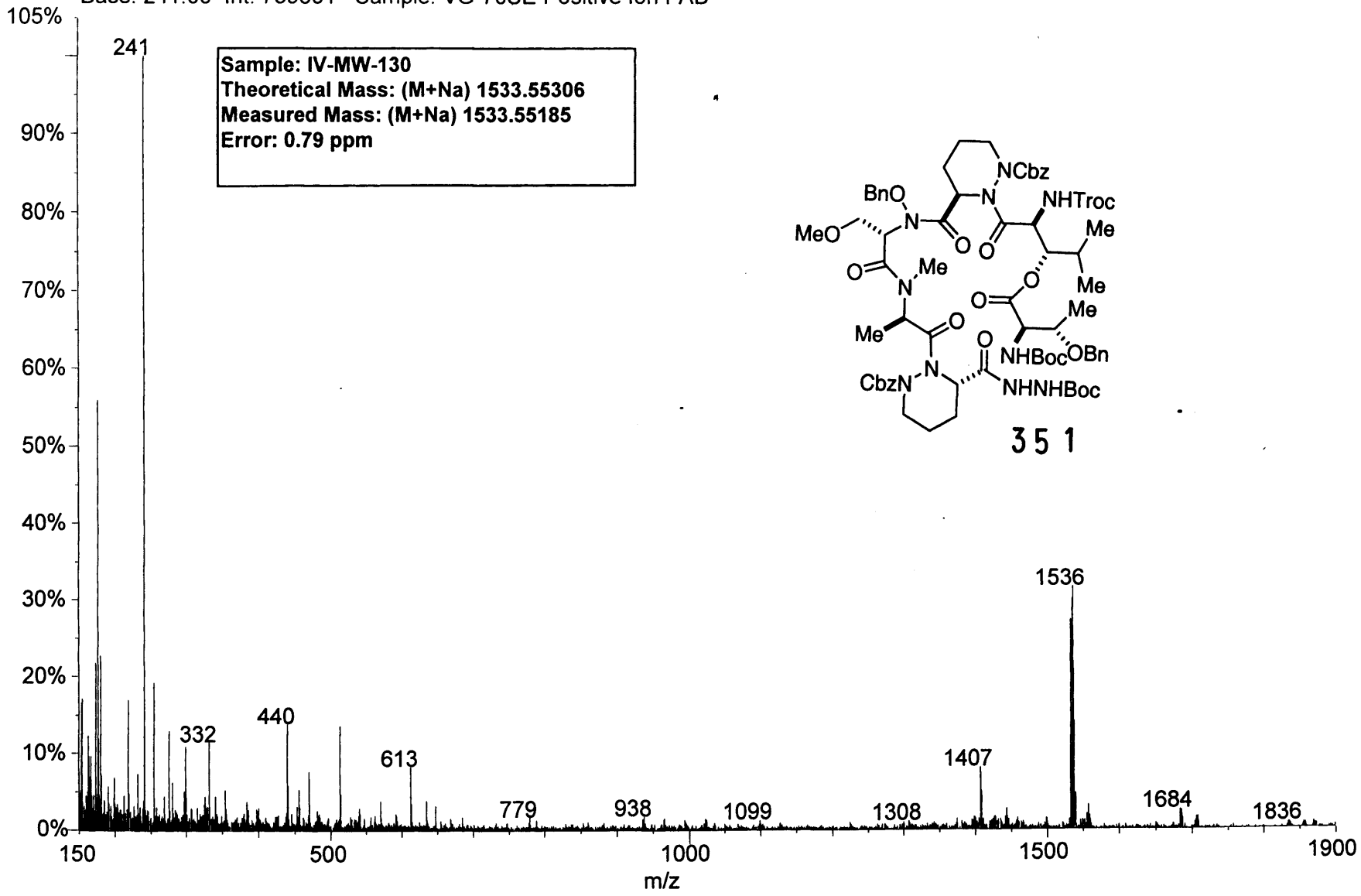

351

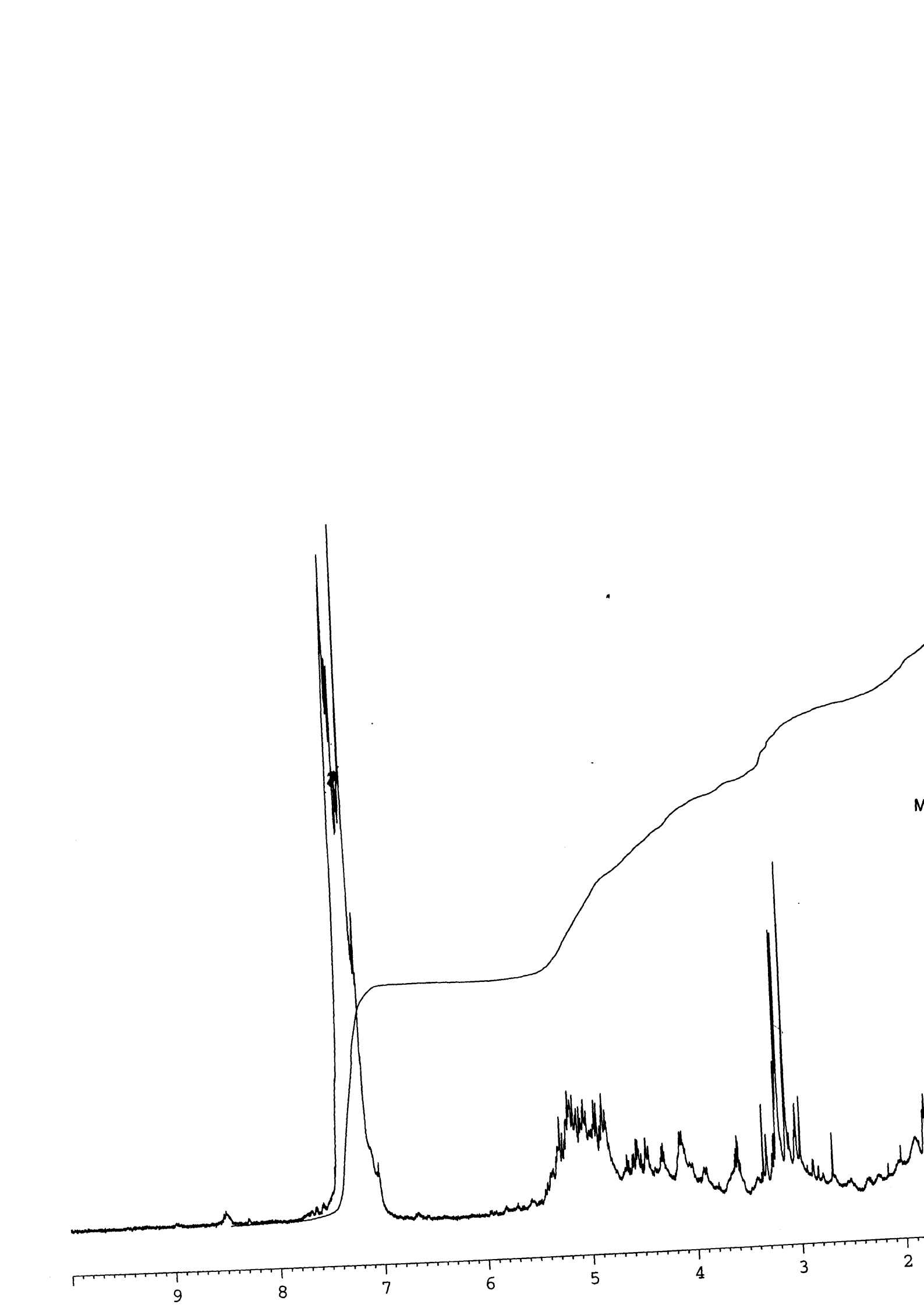
9
8
7
6
5
4
3
2

CDCl3 at 298 K

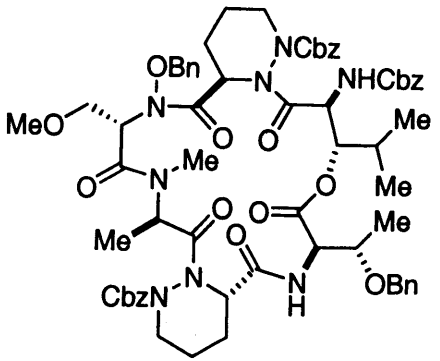

354

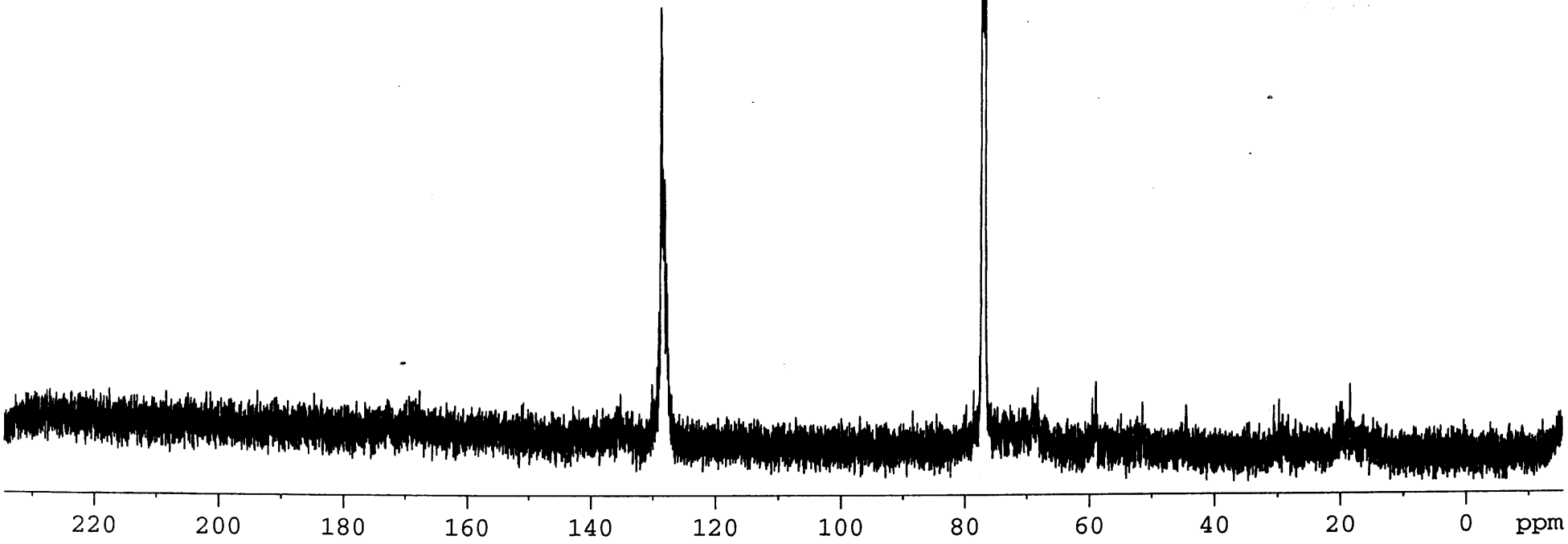

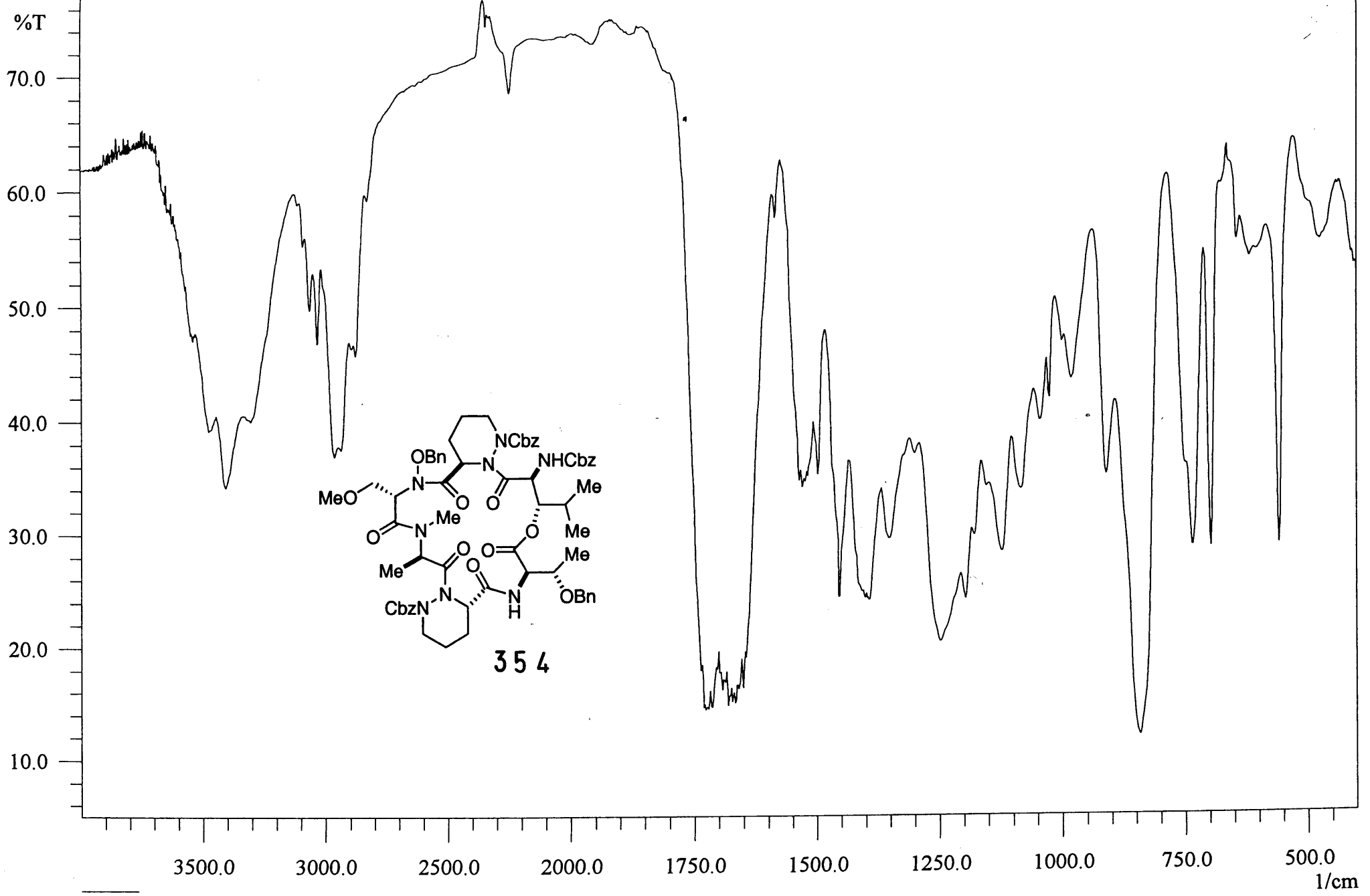
%T
70.0
60.0
50.0
40.0
30.0
20.0
10.0
3500.0
3000.0
2500.0
2000.0
1750.0
1500.0
1250.0
1000.0
750.0
500.0
1/cm
NCbz
OBn
NHCbz
MeO
Me
Me
Me
Me
Me
OBn
CbzN
H

354

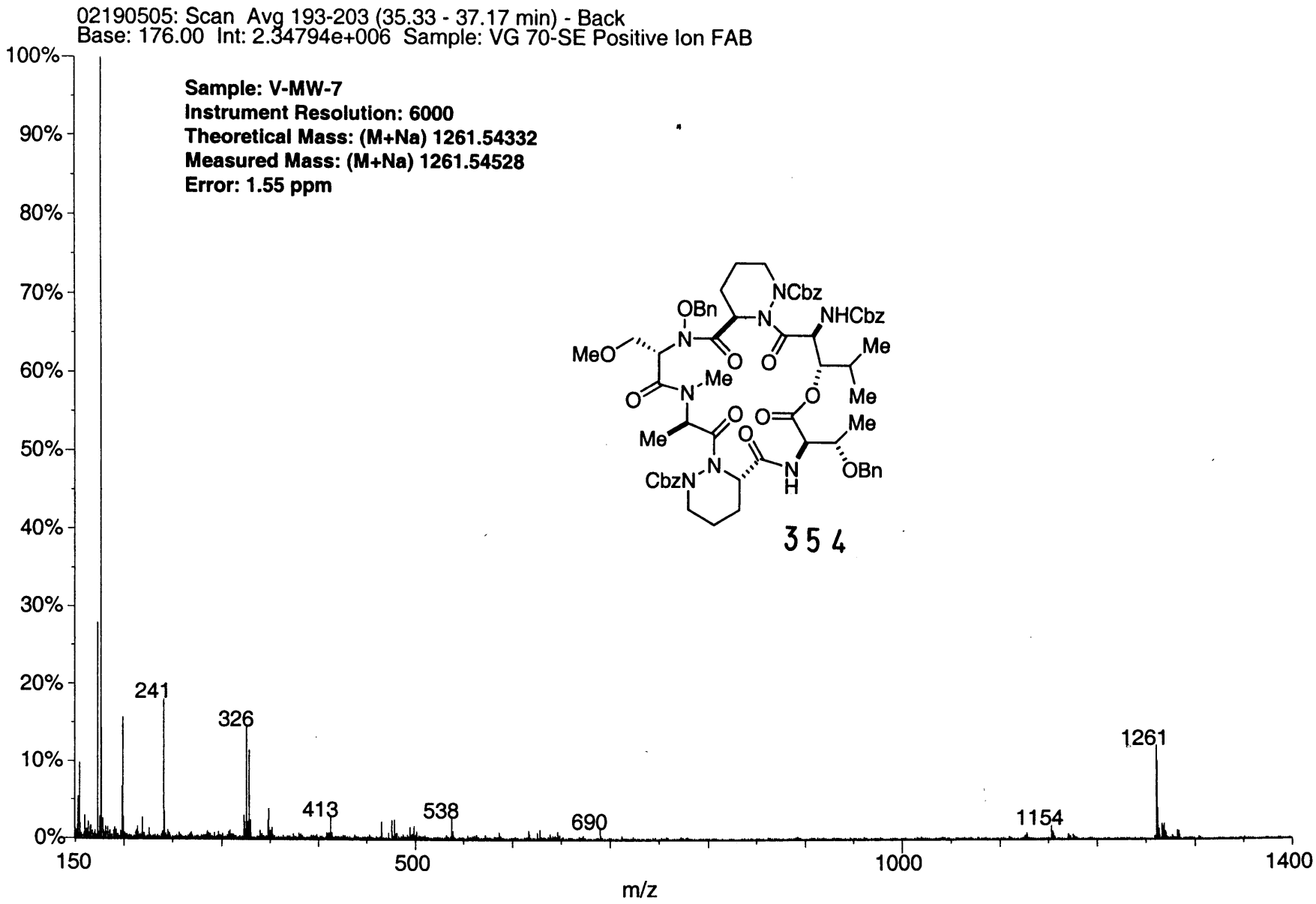
02190505: Scan Avg 193-203 (35.33 - 37.17 min) - Back
Base: 176.00 Int: 2.34794e+006 Sample: VG 70-SE Positive Ion FAB
Sample: V-MW-7
Instrument Resolution: 6000
Theoretical Mass: (M+Na) 1261.54332
Measured Mass: (M+Na) 1261.54528
Error: 1.55 ppm
100%
90%
80%
70%
60%
50%
40%
30%
20%
10%
0%
241
326
413
538
690
1154
1261
150
500
1000
1400
m/z
NCbz
OBn
NHCbz
MeO
Me
Me
Me
Me
Me
CbzN
OBn
H

354

MeOH at 298 K

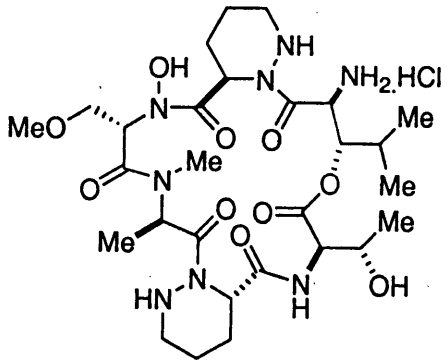

339

V-MW-9
Carbon 13 in
MeOH at 298 K

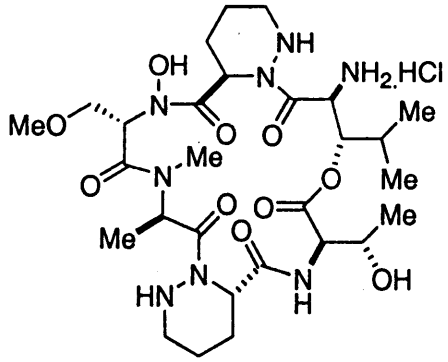

339

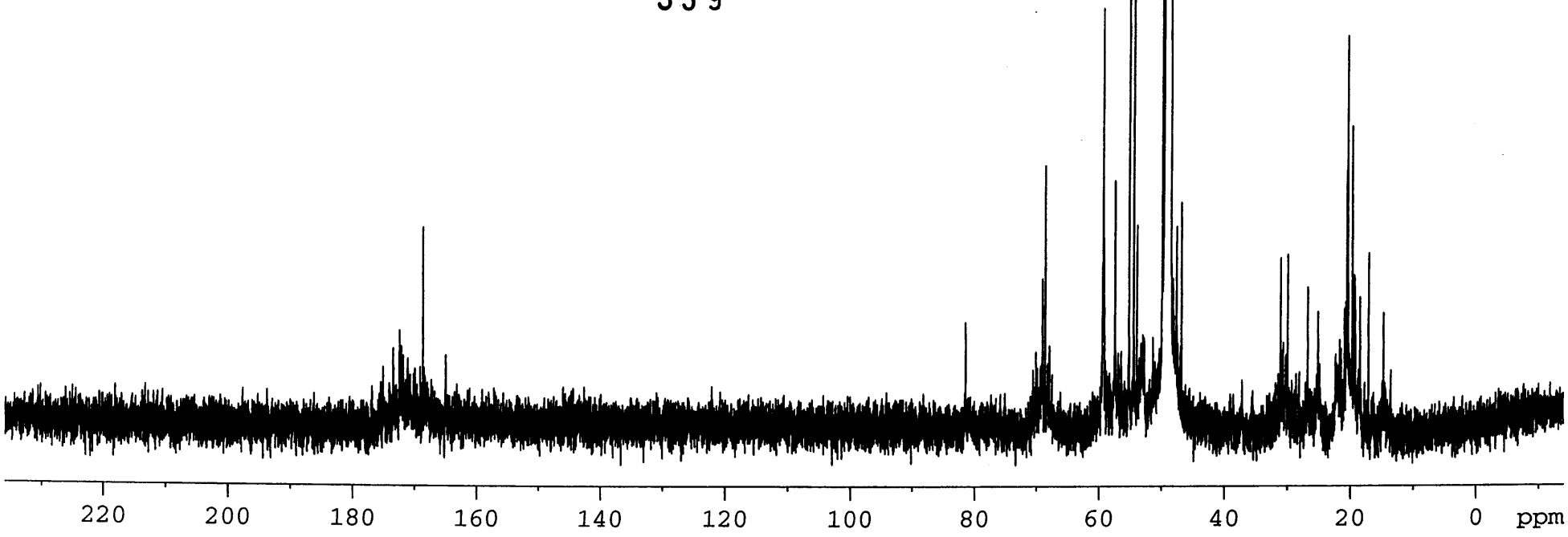

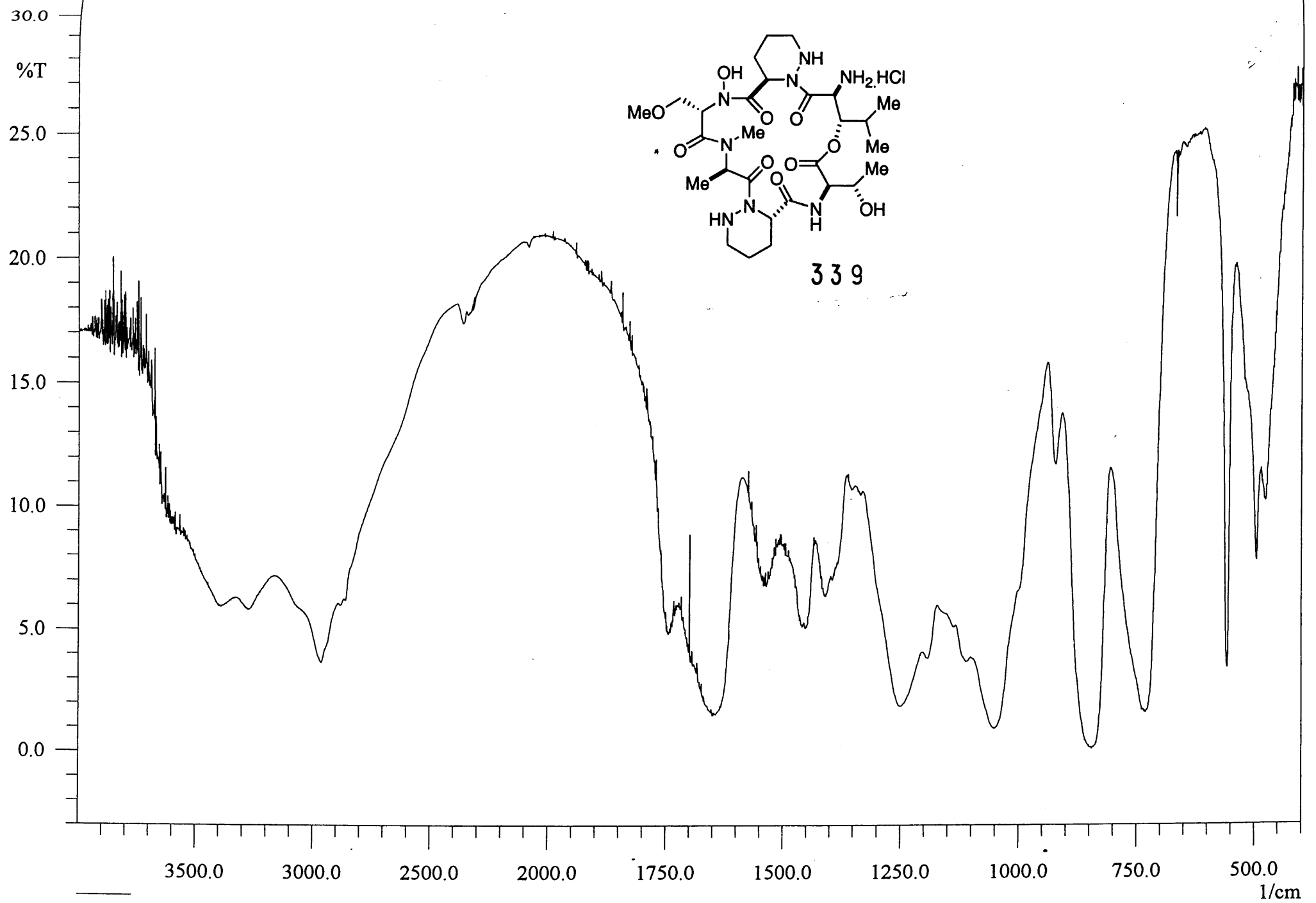
30.0
%T
25.0
20.0
15.0
10.0
5.0
0.0
3500.0
3000.0
2500.0
2000.0
1750.0
1500.0
1250.0
1000.0
750.0
500.0
1/cm
NH
OH
N
NH2.HCl
MeO
Me
O
N
Me
Me
Me
Me
Me
HN
N
N
H
OH

339

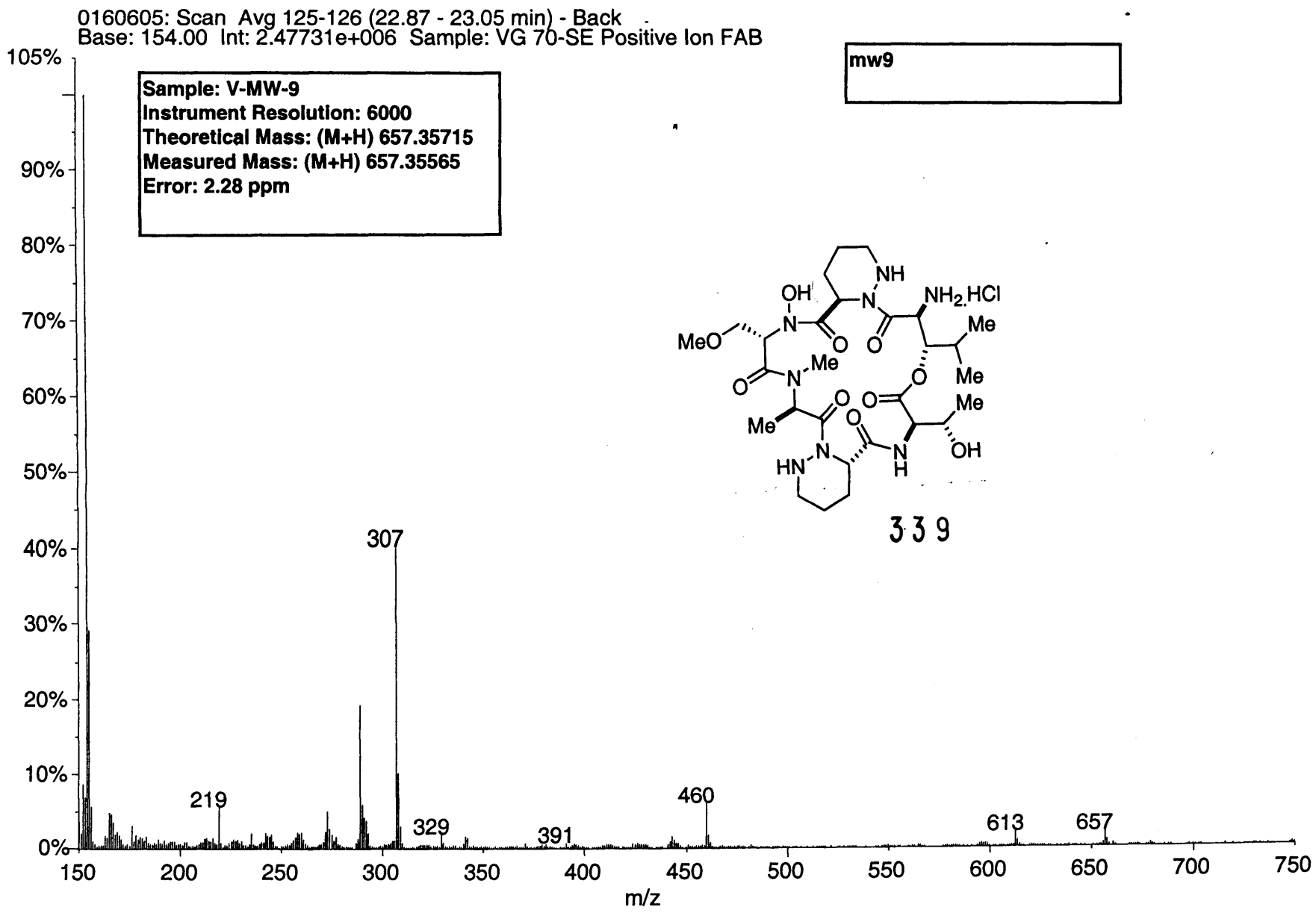
0160605: Scan Avg 125-126 (22.87 - 23.05 min) - Back
Base: 154.00 Int: 2.47731e+006 Sample: VG 70-SE Positive Ion FAB
mw9
Sample: V-MW-9
Instrument Resolution: 6000
Theoretical Mass: (M+H) 657.35715
Measured Mass: (M+H) 657.35565
Error: 2.28 ppm
105%
90%
80%
70%
60%
50%
40%
30%
20%
10%
0%
307
219
329
391
460
613
657
150
200
250
300
350
400
450
500
550
600
650
700
750
m/z
NH
OH
N
NH2.HCl
MeO
Me
O
N
Me
Me
Me
Me
HN
N
N
H
OH
339

CDC13 at 298 K

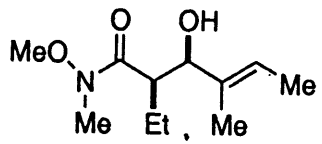

364

Carbon 13 in
CDCl3 at 298 K

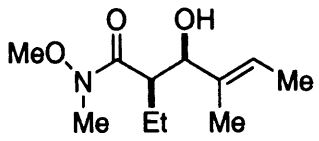

364

CDC13 at 298 K

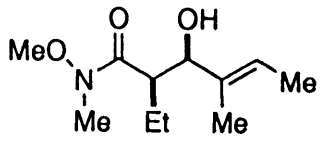

364

CDCl3 at 298 K

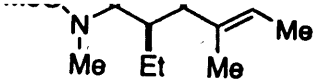

364

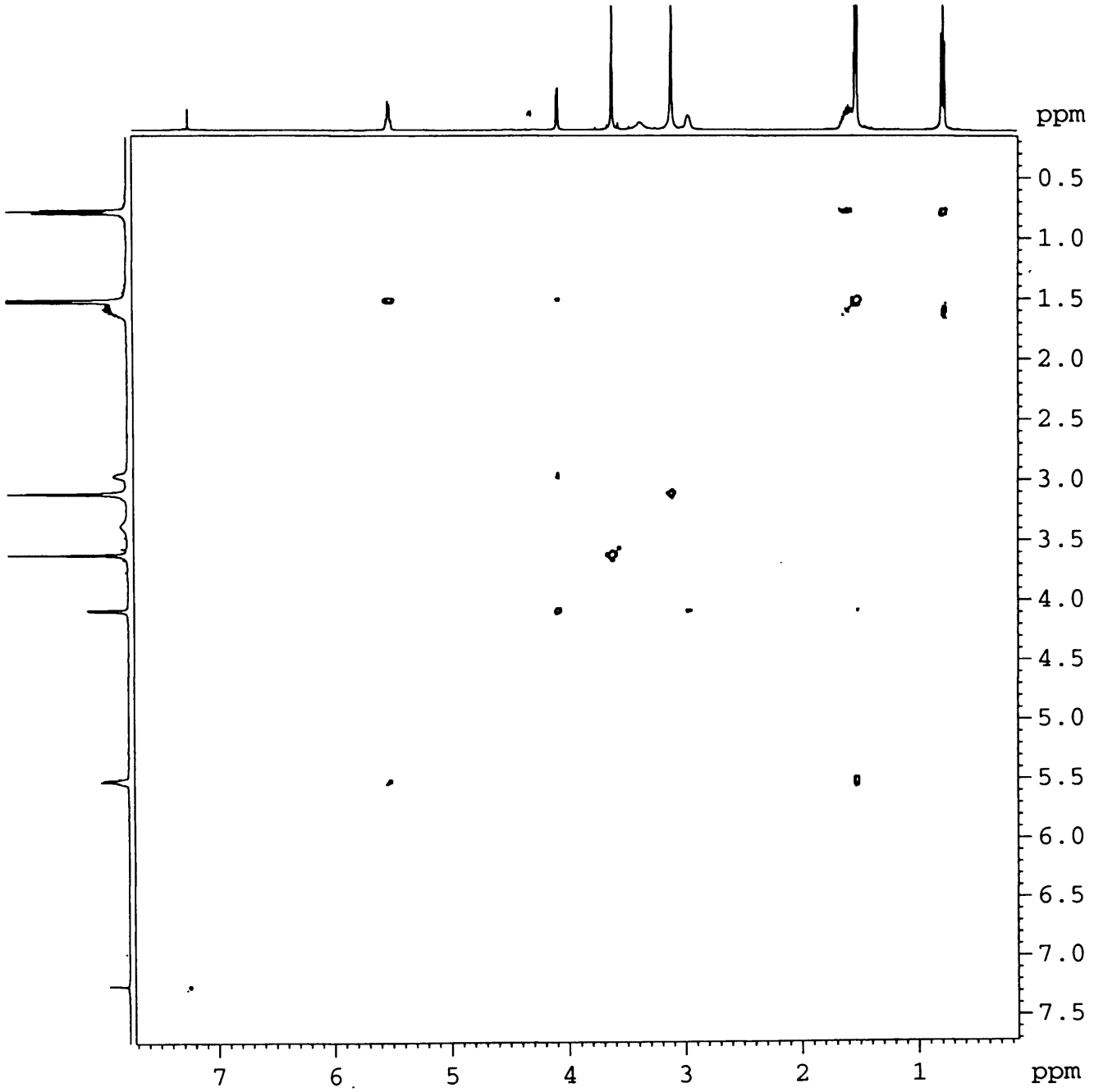

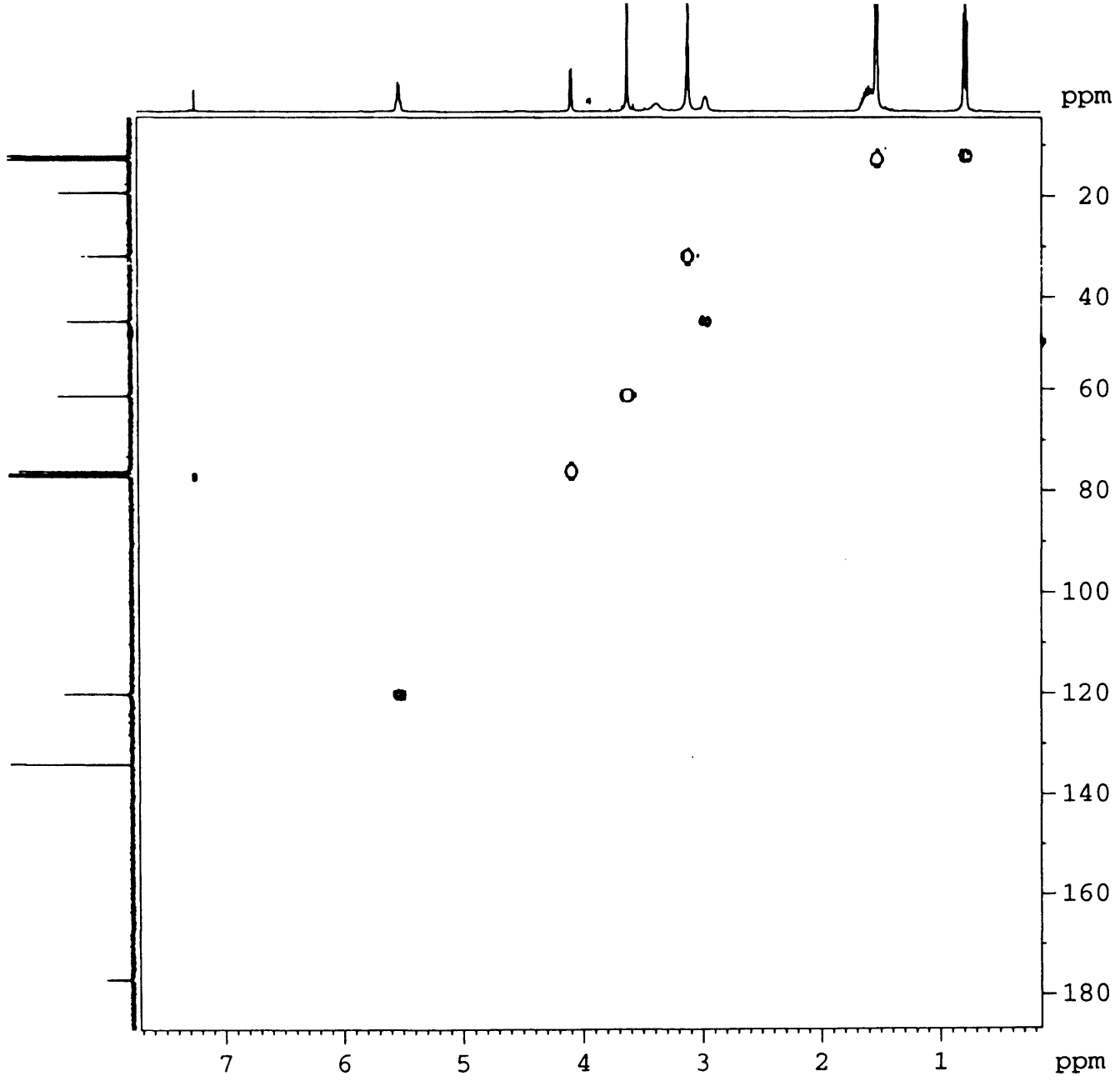

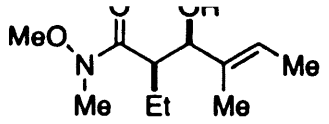

364

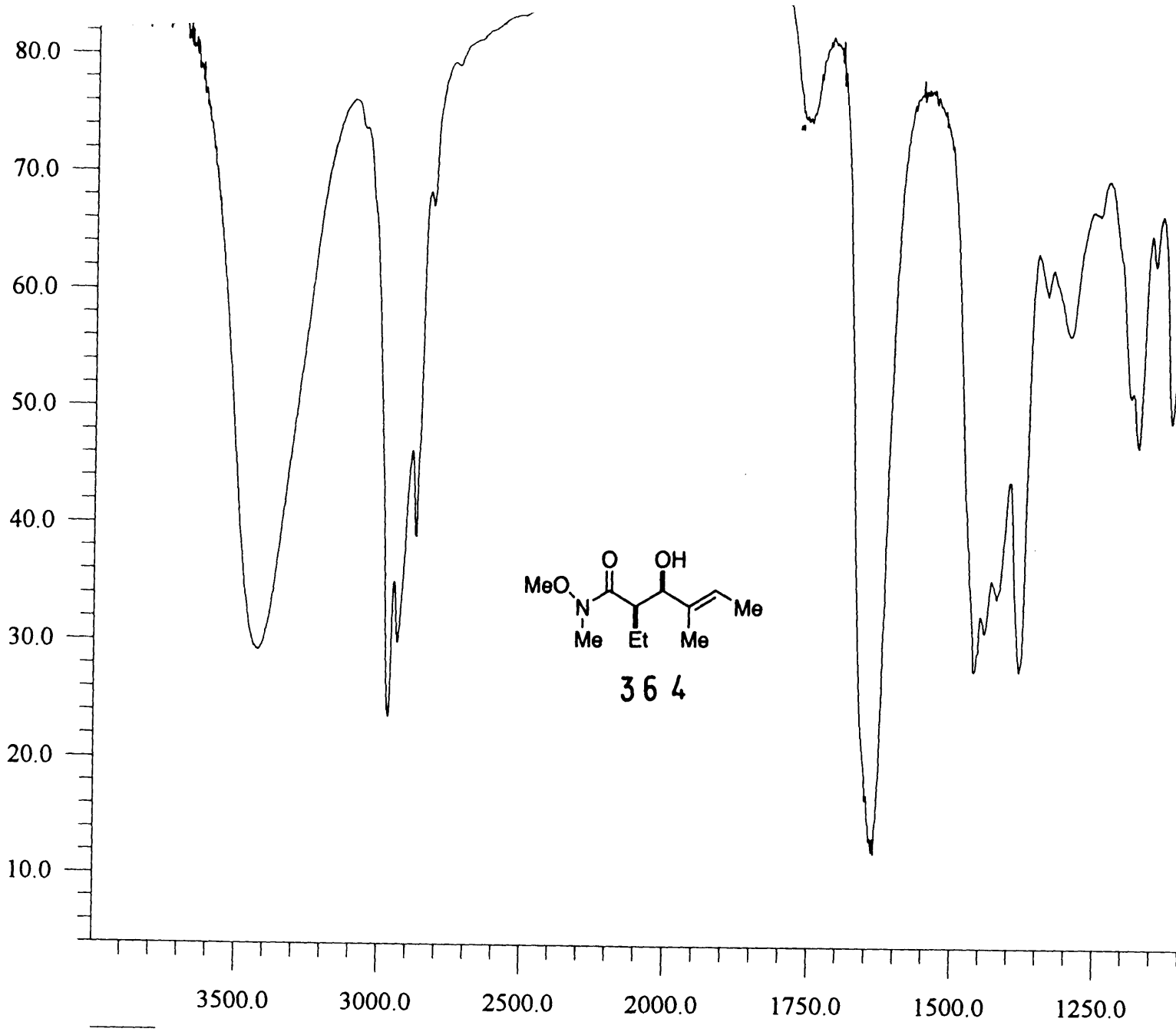
80.0
70.0
60.0
50.0
40.0
30.0
20.0
10.0
3500.0
3000.0
2500.0
2000.0
1750.0
1500.0
1250.0
O
OH
MeO
N
Me
Me
Et
Me
Me

364

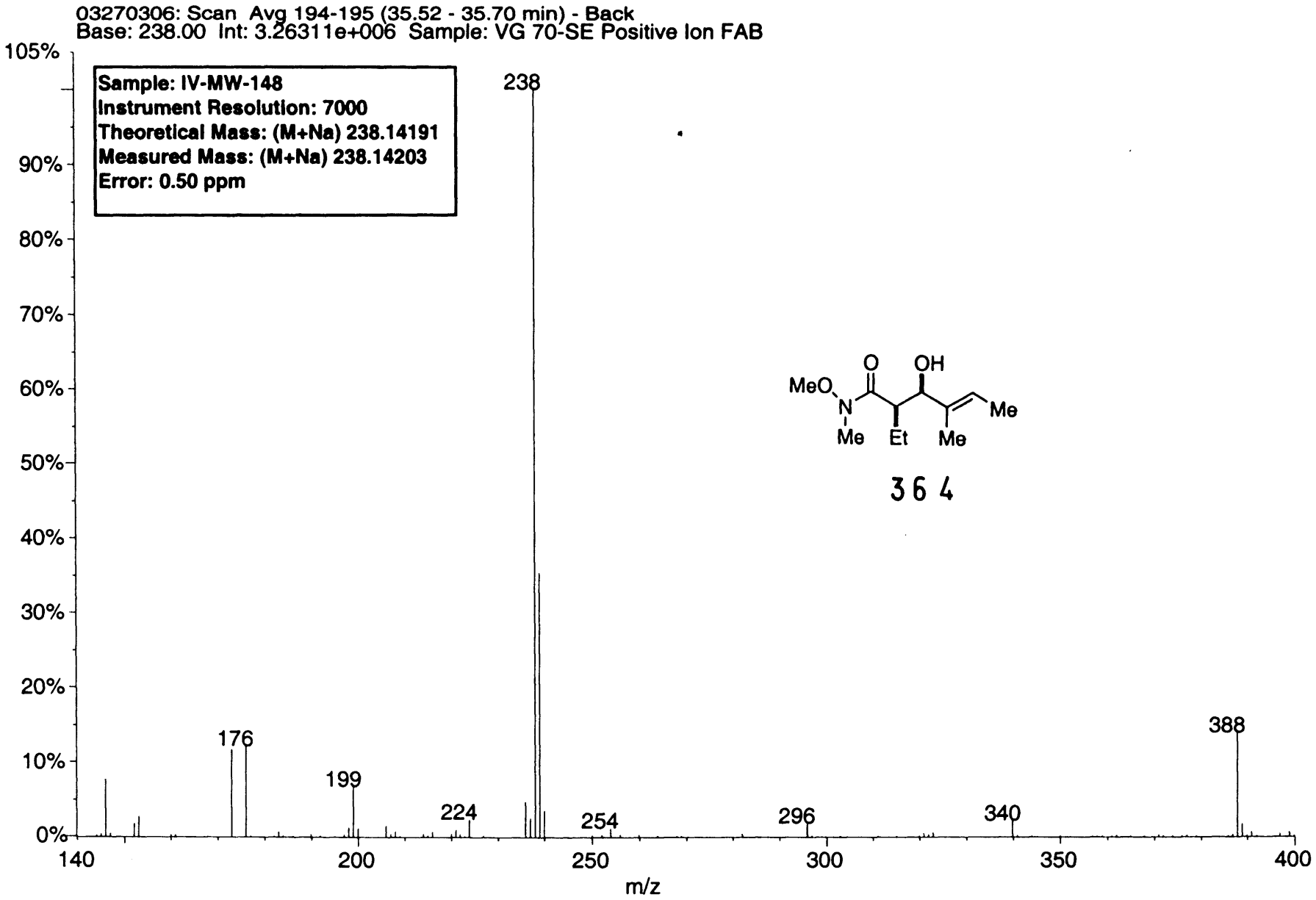
03270306: Scan Avg 194-195 (35.52 - 35.70 min) - Back
Base: 238.00 Int: 3.26311e+006 Sample: VG 70-SE Positive Ion FAB
Sample: IV-MW-148
Instrument Resolution: 7000
Theoretical Mass: (M+Na) 238.14191
Measured Mass: (M+Na) 238.14203
Error: 0.50 ppm
105%
90%
80%
70%
60%
50%
40%
30%
20%
10%
0%
238
176
199
224
254
296
340
388
140
200
250
300
350
400
m/z
MeO
N
Me
O
OH
Et
Me
Me
364

IV-MW-151 in
CDCl3 at 298 K

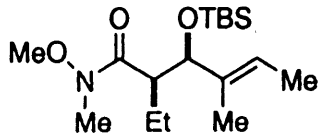

365

IV-MW-151
DEPT in
CDCl3 at 298 K

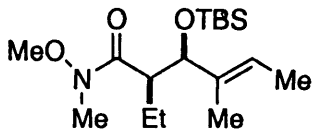

365

IV-MW-151
COSY in
CDCl3 at 298 K

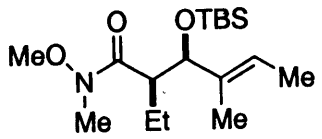

365

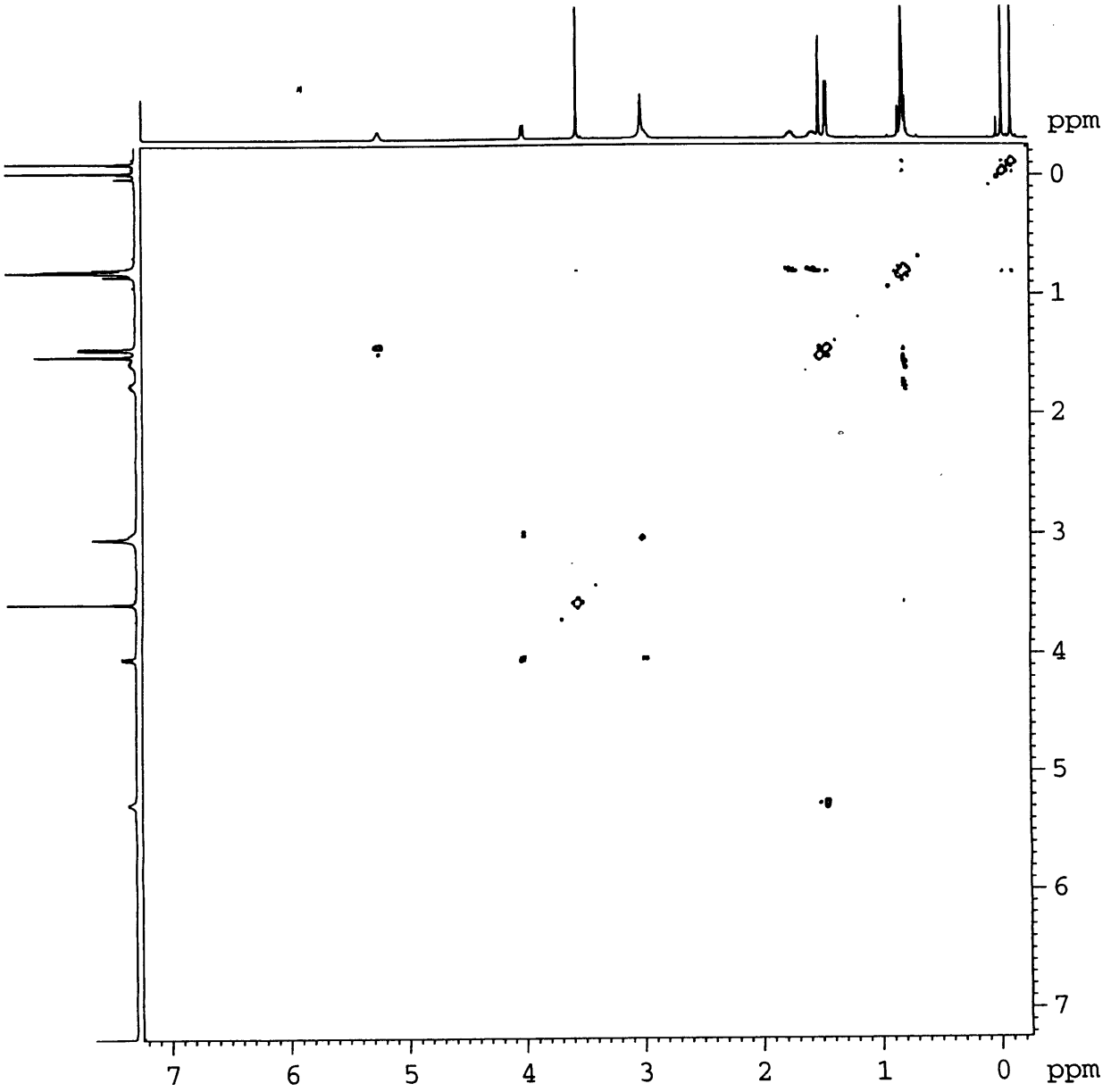

IV-MW-151
HMQC in
CDCl3 at 298 K

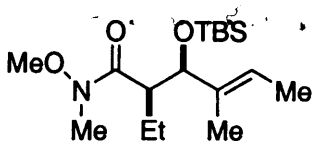

365

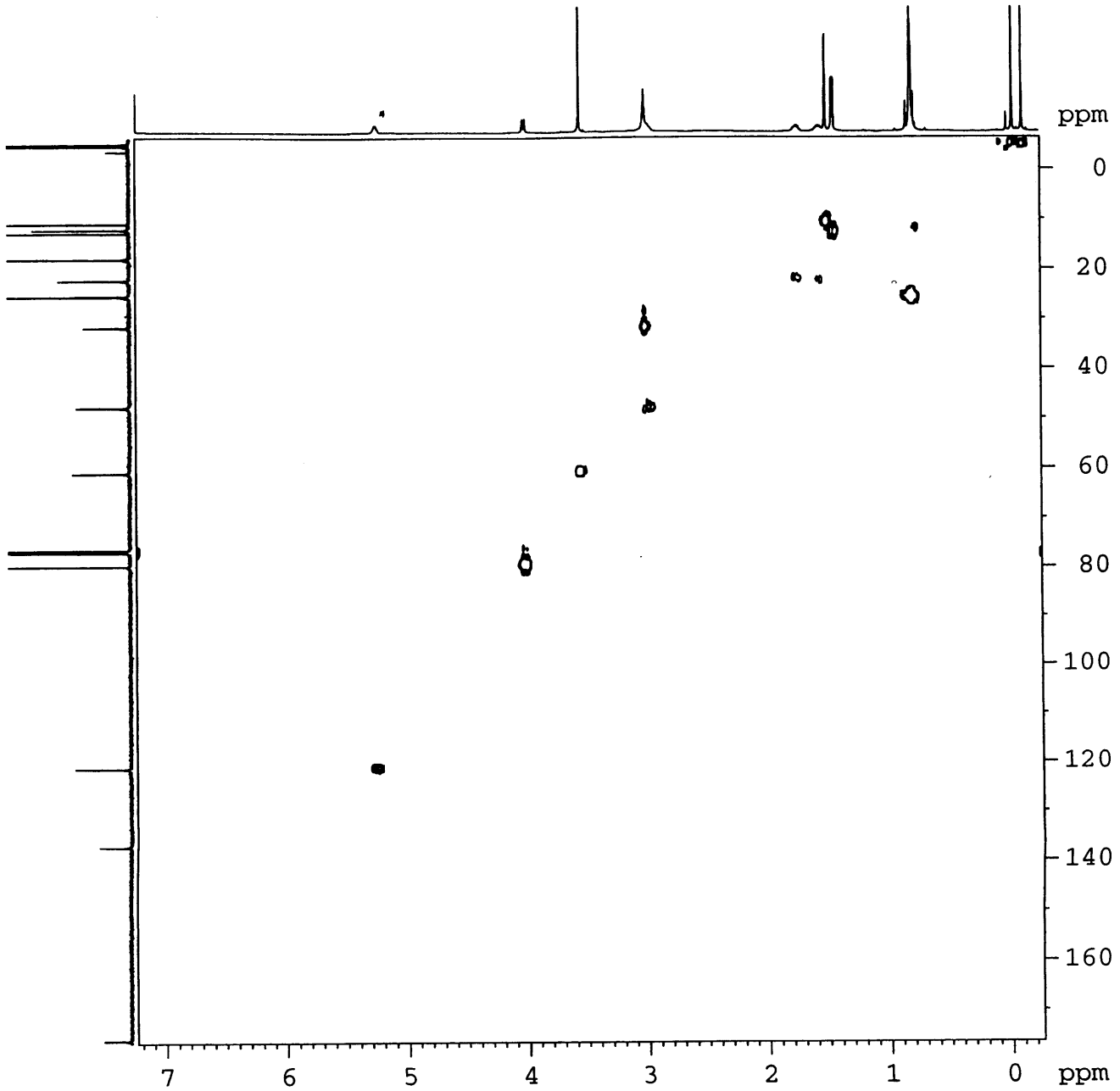

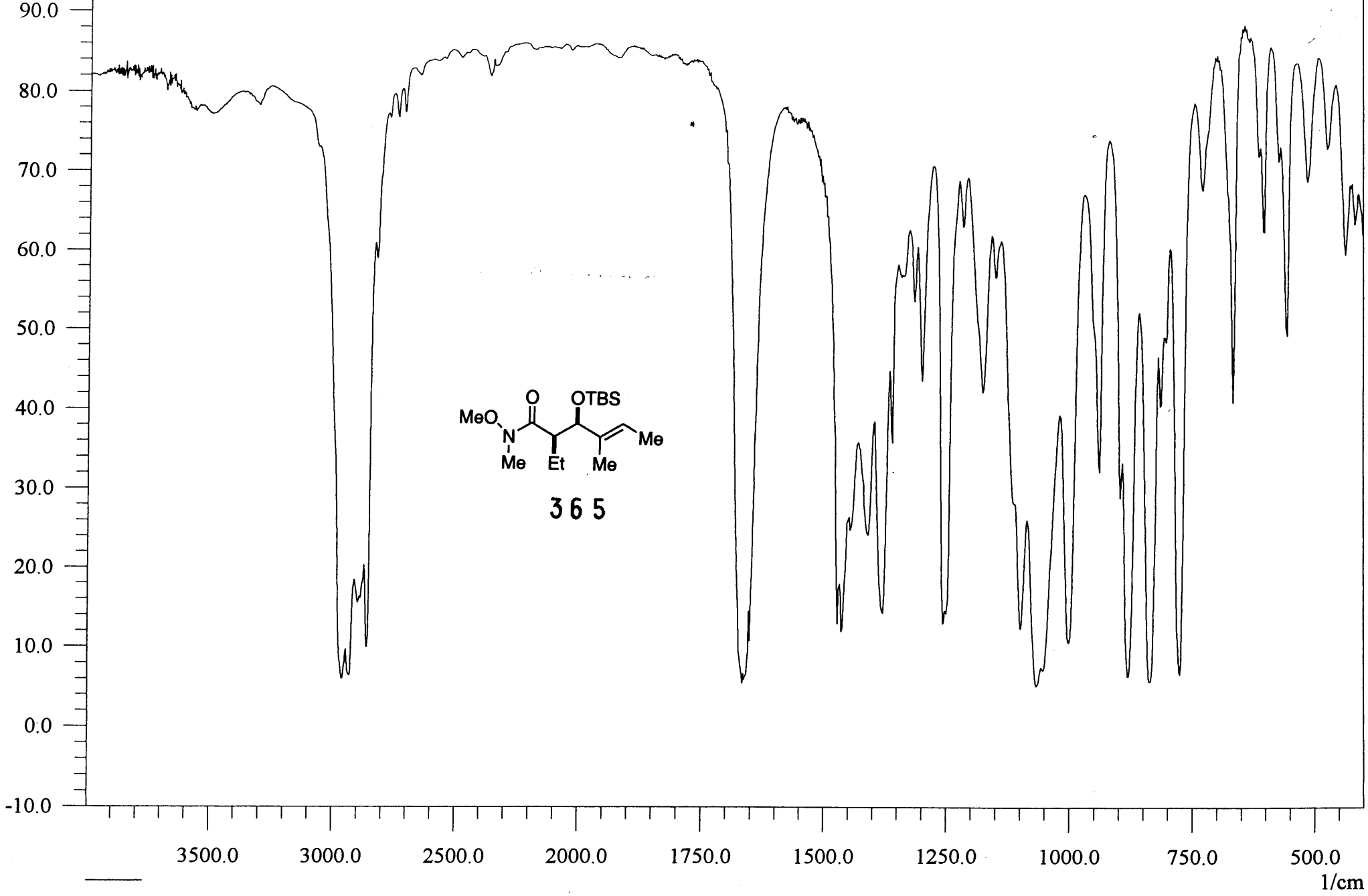
90.0
80.0
70.0
60.0
50.0
40.0
30.0
20.0
10.0
0.0
-10.0
3500.0
3000.0
2500.0
2000.0
1750.0
1500.0
1250.0
1000.0
750.0
500.0
1/cm
MeO
N
Me
O
OTBS
Et
Me
Me

365

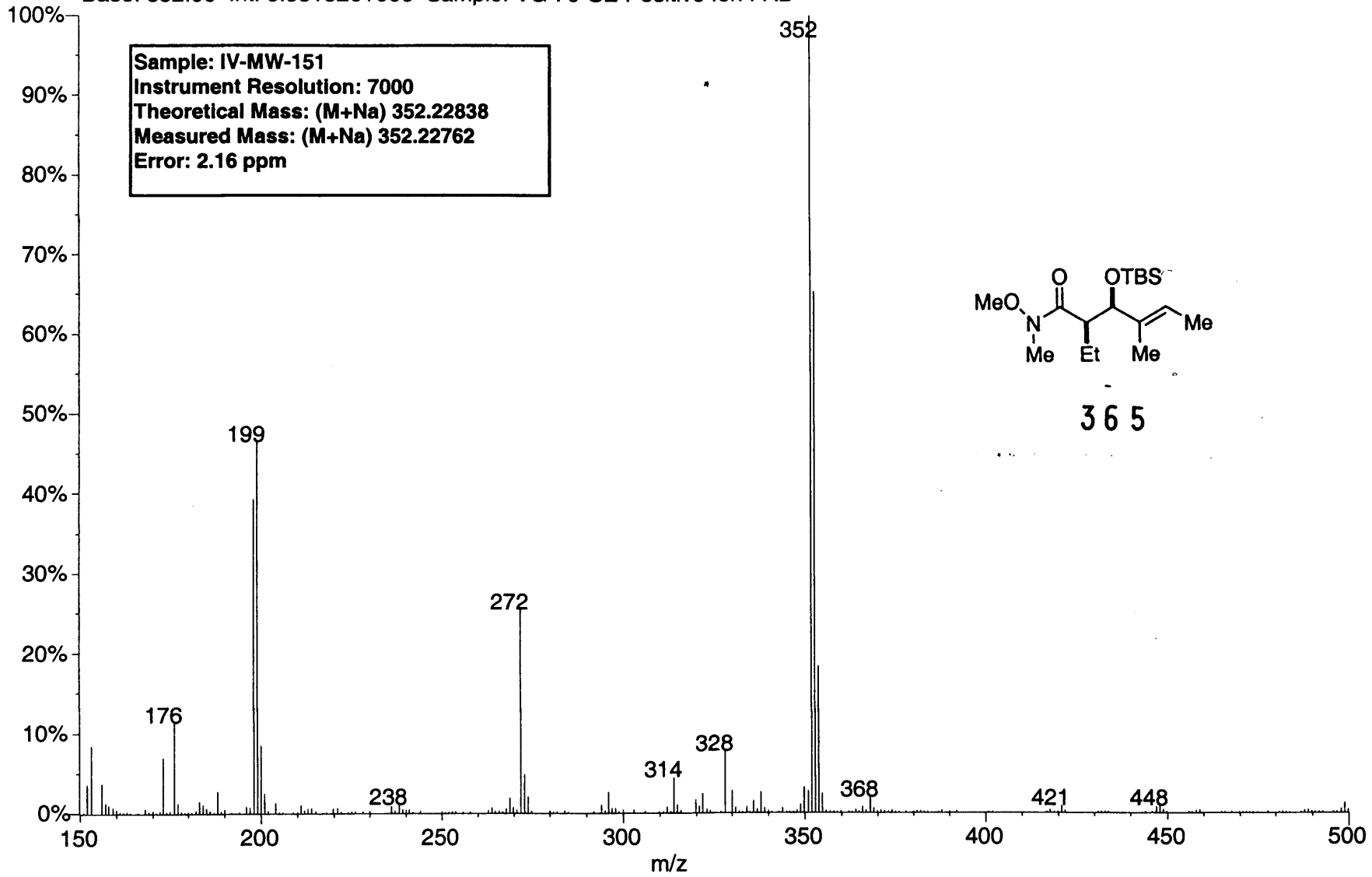
03270306: Scan 213 (39.00 min) - Back
Base: 352.00 Int: 6.53152e+006 Sample: VG 70-SE Positive Ion FAB
Sample: IV-MW-151
Instrument Resolution: 7000
Theoretical Mass: (M+Na) 352.22838
Measured Mass: (M+Na) 352.22762
Error: 2.16 ppm
352
199
272
176
328
314
238
368
421
448
100%
90%
80%
70%
60%
50%
40%
30%
20%
10%
0%
150
200
250
300
350
400
450
500
m/z
MeO
N
Me
O
OTBS
Et
Me
Me
365

CDCl3 at 298 K

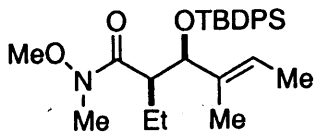

377

Carbon 13 in
CDCl3 at 298 K

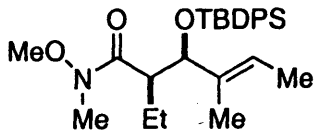

377

IV-MW-185
DEPT in
CDCl3 at 298 K

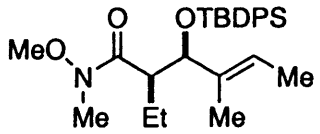

377

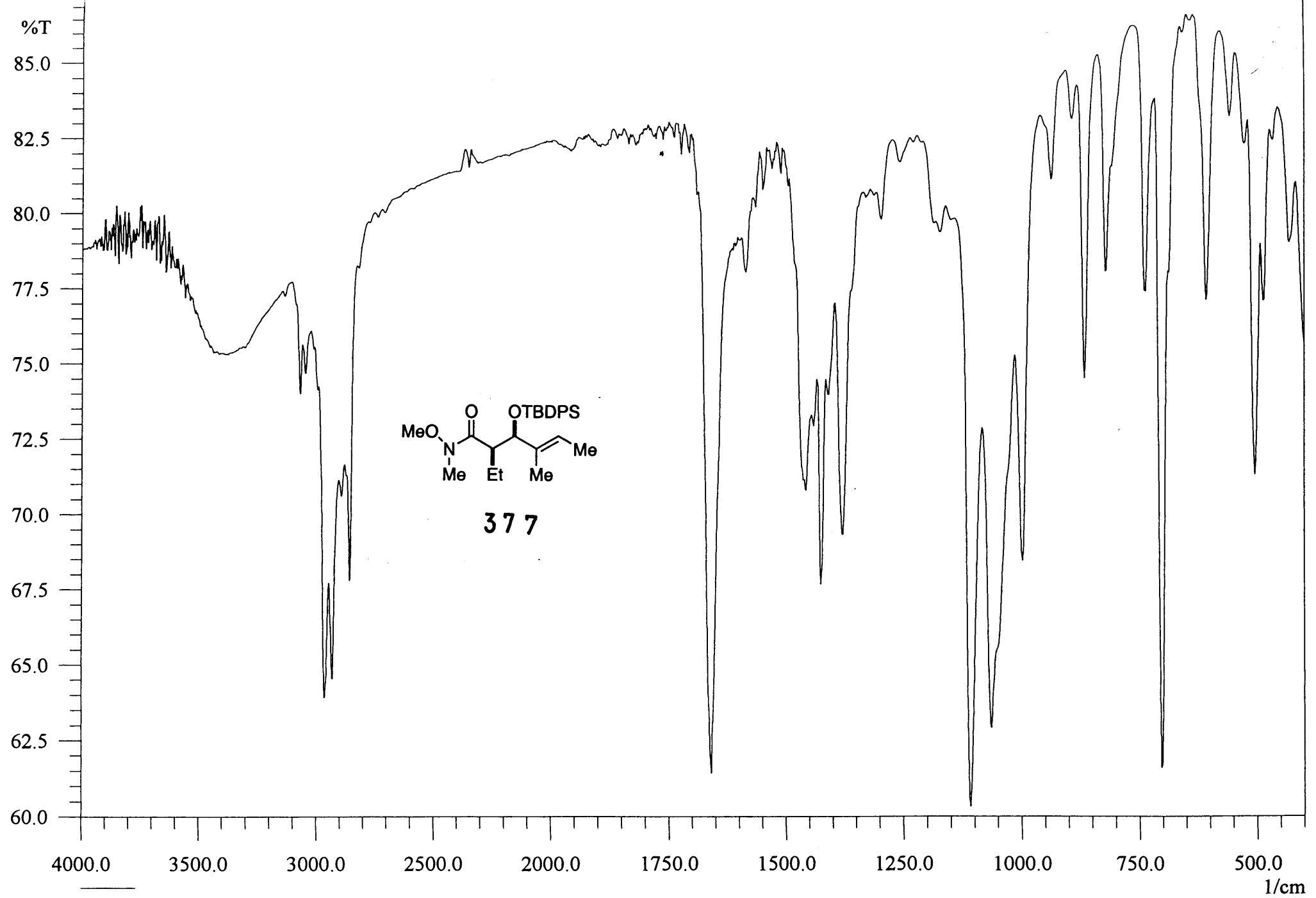
%T
85.0
82.5
80.0
77.5
75.0
72.5
70.0
67.5
65.0
62.5
60.0
4000.0
3500.0
3000.0
2500.0
2000.0
1750.0
1500.0
1250.0
1000.0
750.0
500.0
1/cm
MeO
N
Me
O
OTBDPS
Et
Me
Me

377

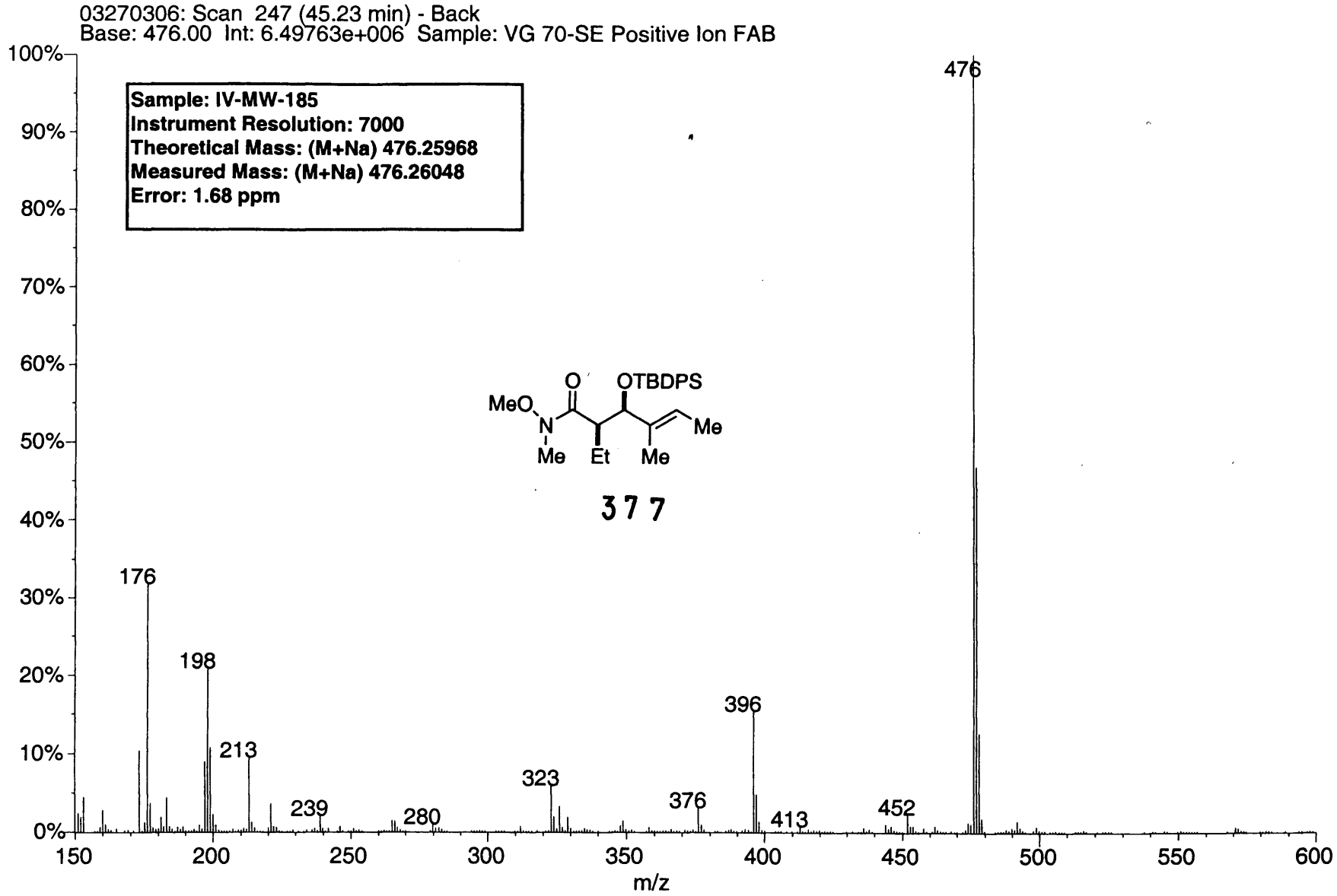
03270306: Scan 247 (45.23 min) - Back
Base: 476.00 Int: 6.49763e+006 Sample: VG 70-SE Positive Ion FAB
Sample: IV-MW-185
Instrument Resolution: 7000
Theoretical Mass: (M+Na) 476.25968
Measured Mass: (M+Na) 476.26048
Error: 1.68 ppm
MeO
N
Me
O
OTBDPS
Et
Me
Me
377
476
176
198
213
239
280
323
376
396
413
452
100%
90%
80%
70%
60%
50%
40%
30%
20%
10%
0%
150
200
250
300
350
400
450
500
550
600
m/z

CDCl3 at 298 K

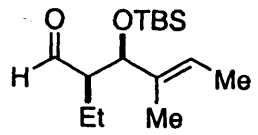

366

Carbon 13 in
CDCl3 at 298 K

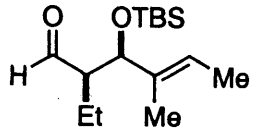

366

DEPT 135
CDCl3 at 298 K

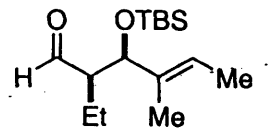

366

CDCl3 at 298 K

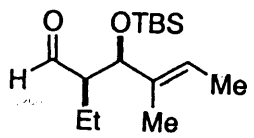

366

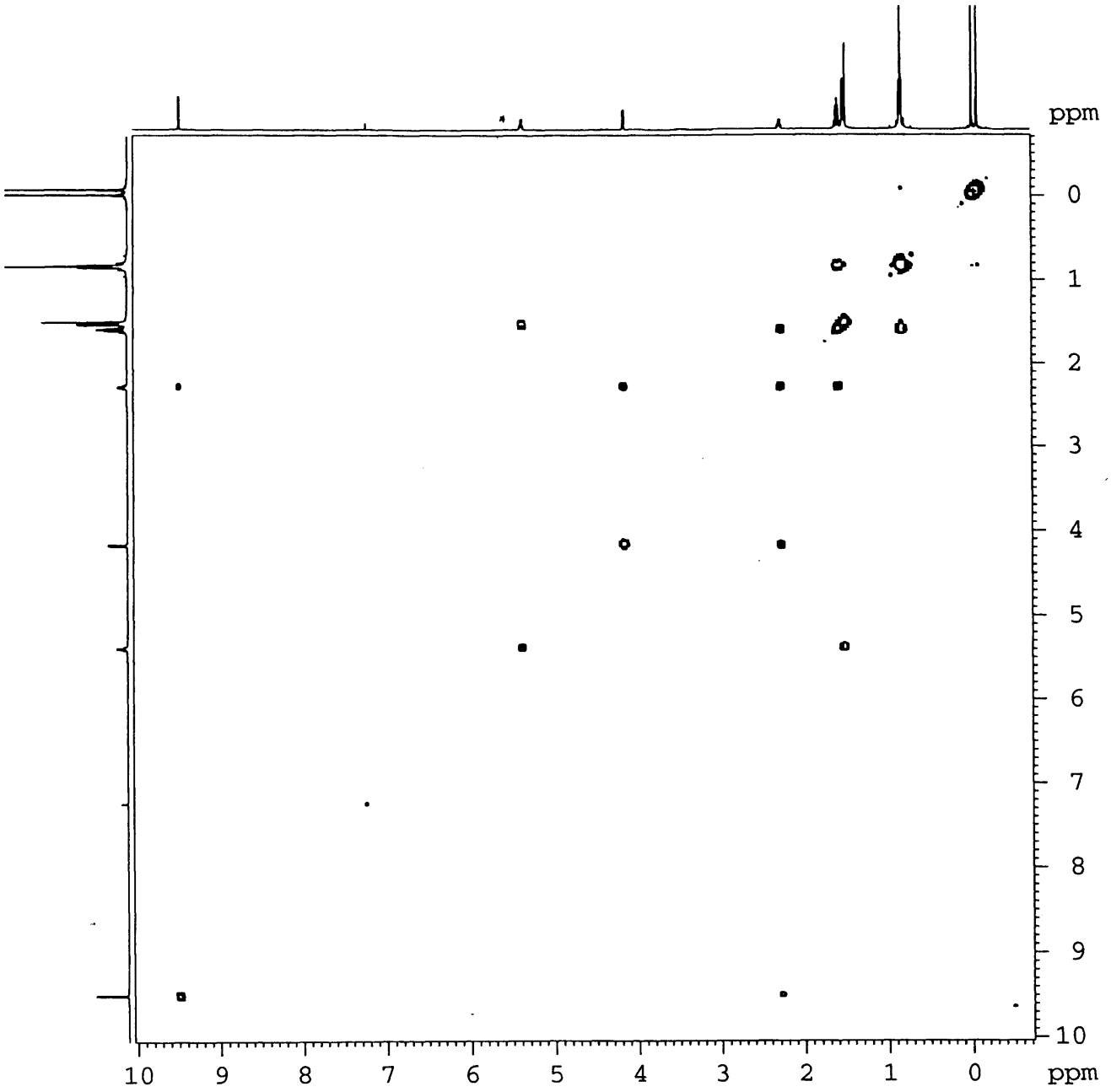

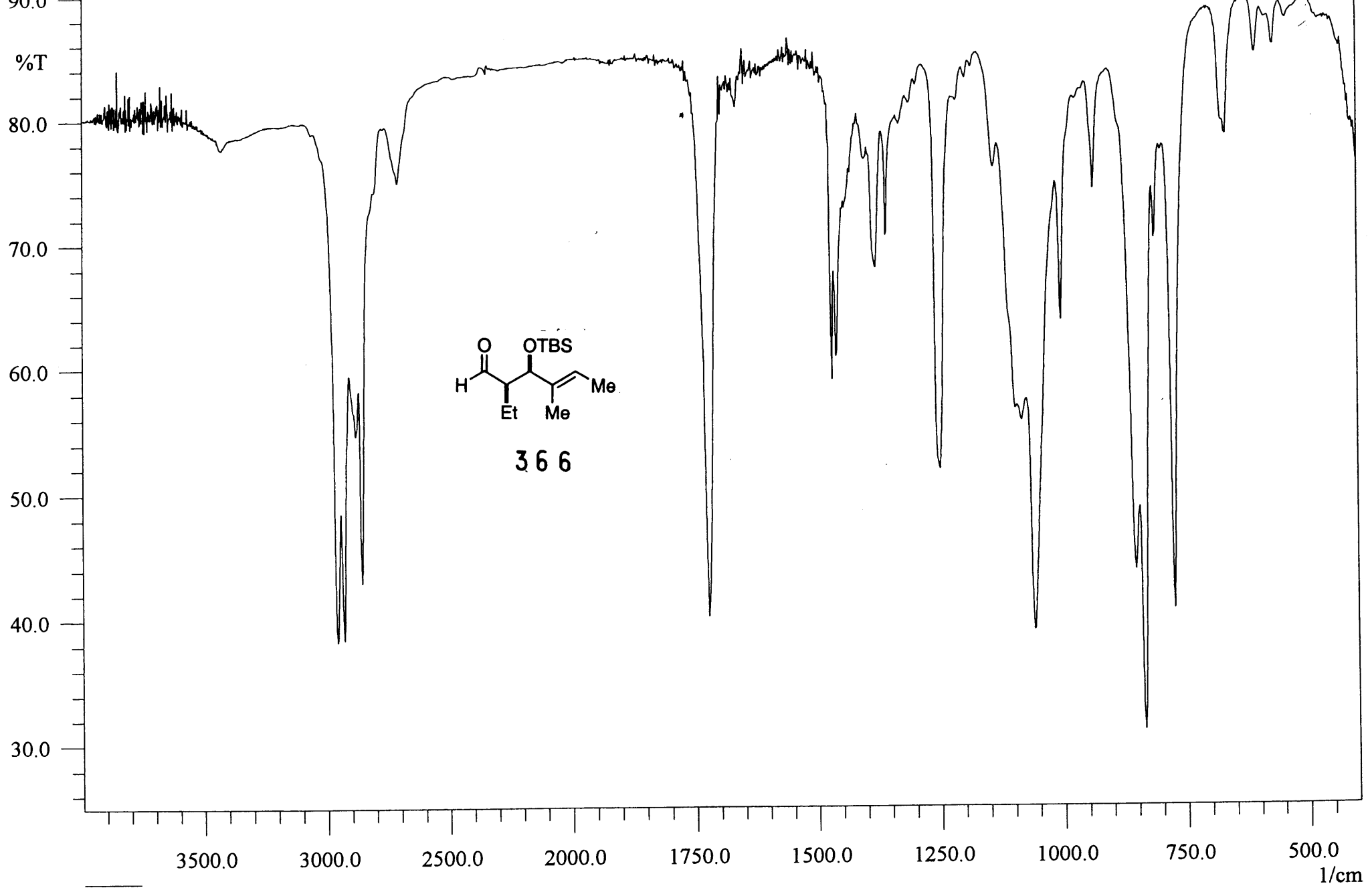
%T
90.0
80.0
70.0
60.0
50.0
40.0
30.0
O
OTBS
H
Me
Et
Me
366
3500.0
3000.0
2500.0
2000.0
1750.0
1500.0
1250.0
1000.0
750.0
500.0
1/cm

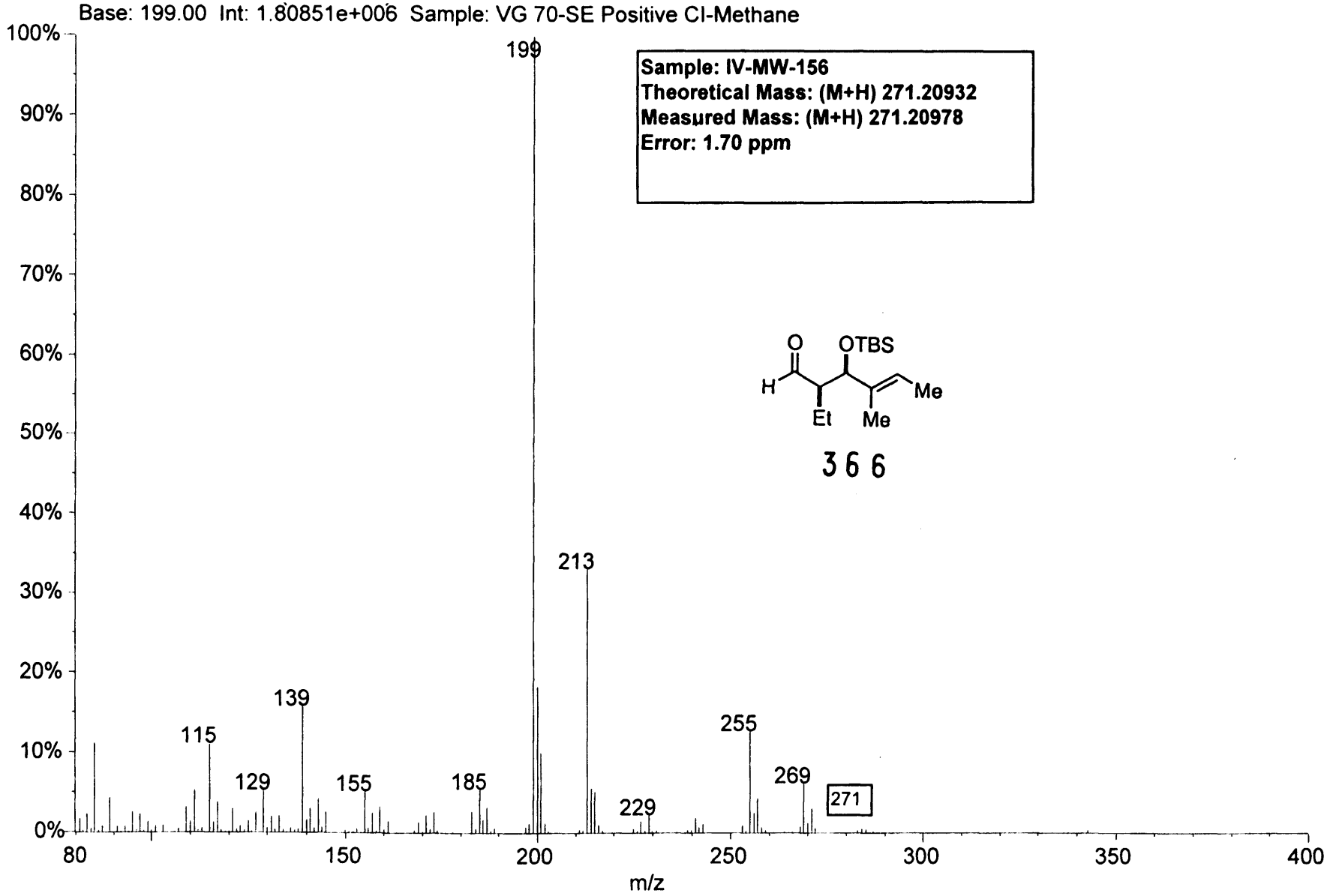
Base: 199.00 Int: 1.80851e+006 Sample: VG 70-SE Positive CI-Methane
Sample: IV-MW-156
Theoretical Mass: (M+H) 271.20932
Measured Mass: (M+H) 271.20978
Error: 1.70 ppm
O
OTBS
H
Me
Et
Me
366
100%
90%
80%
70%
60%
50%
40%
30%
20%
10%
0%
199
213
139
115
255
269
129
155
185
229
271
80
150
200
250
300
350
400
m/z

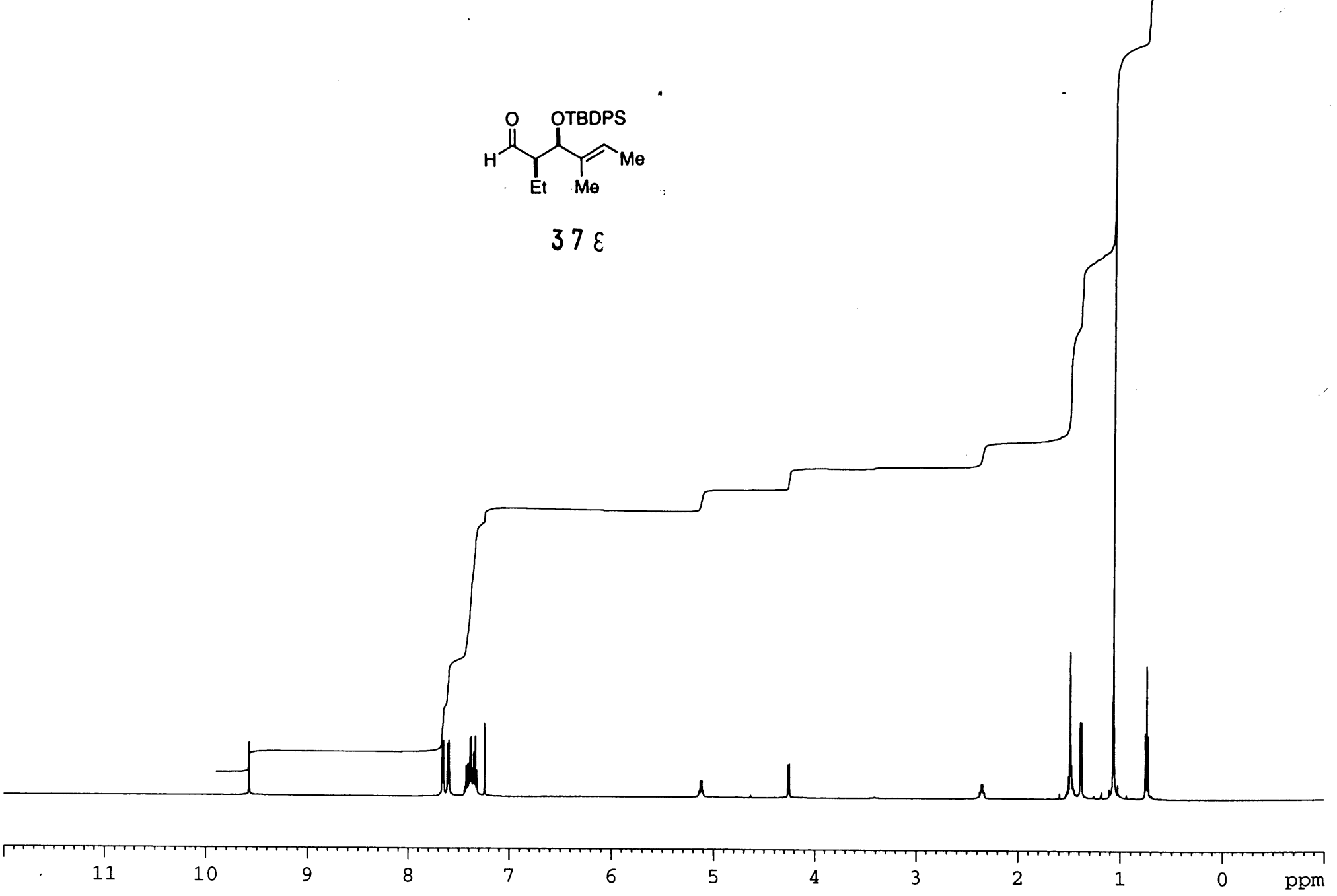

37 ε

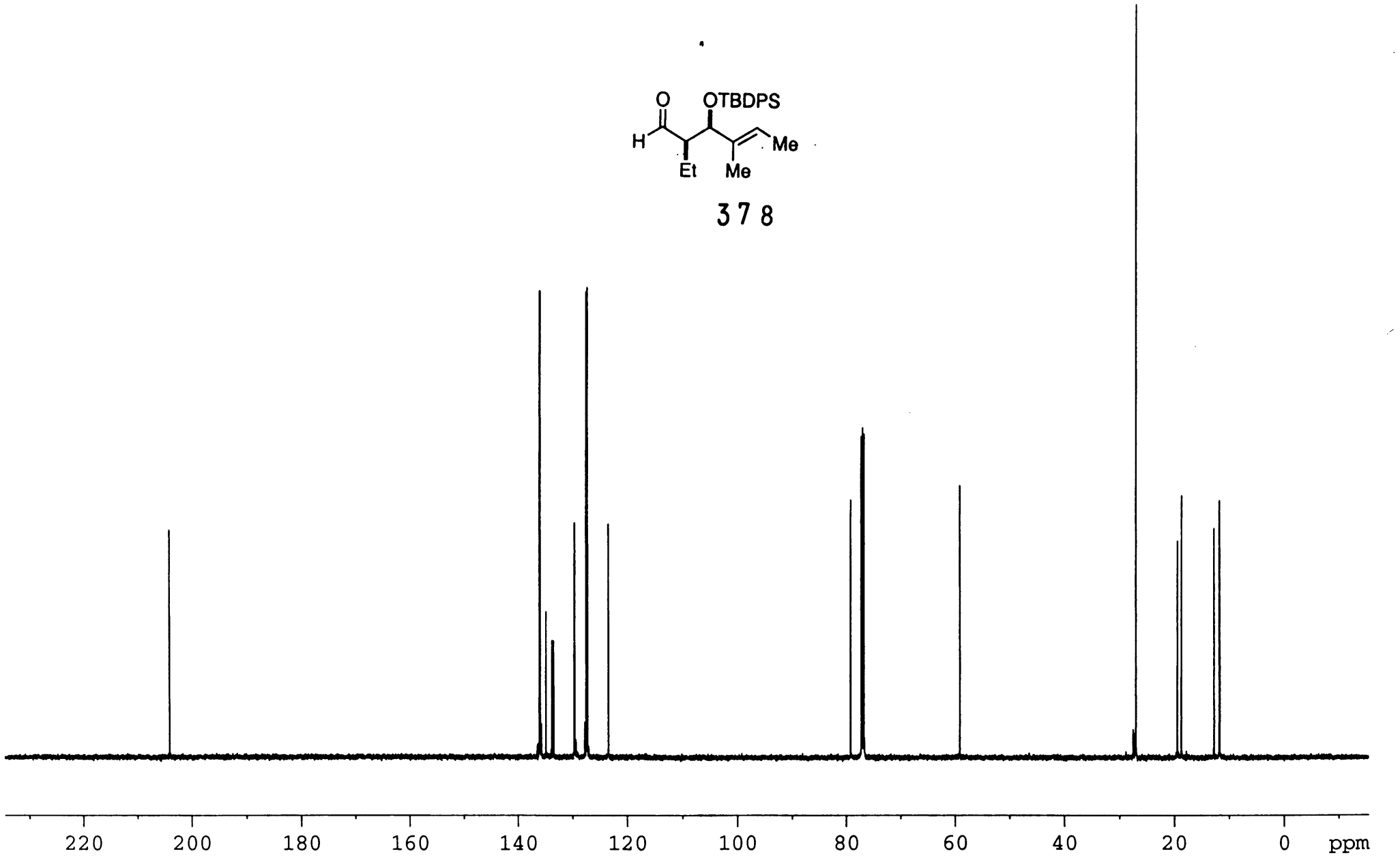

378

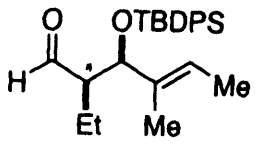

378

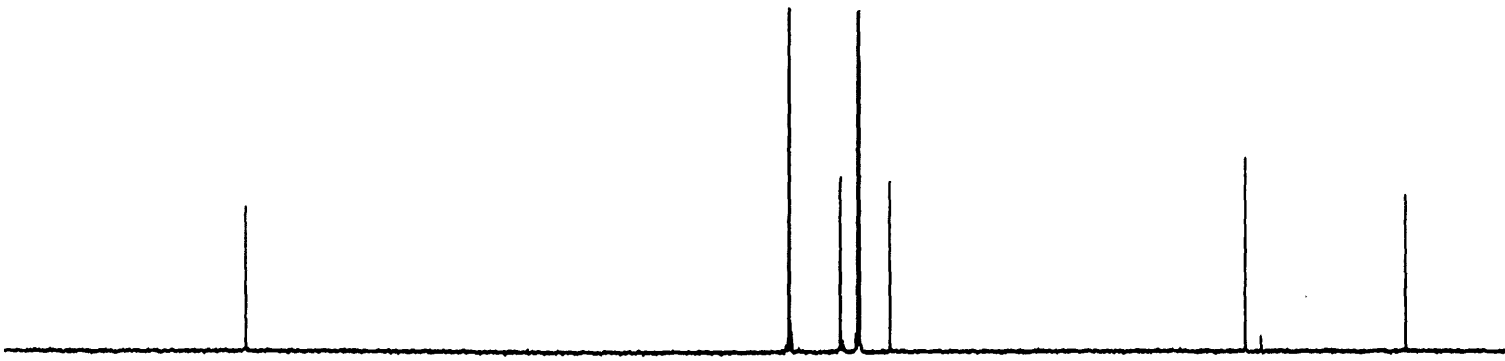

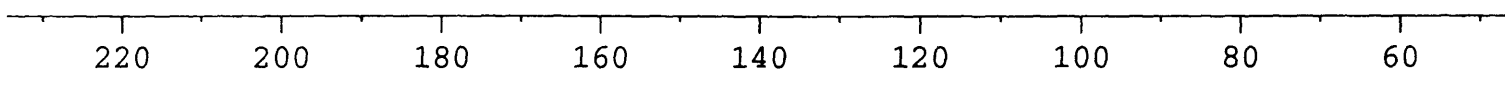

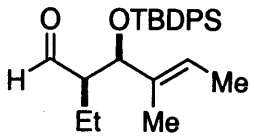

378

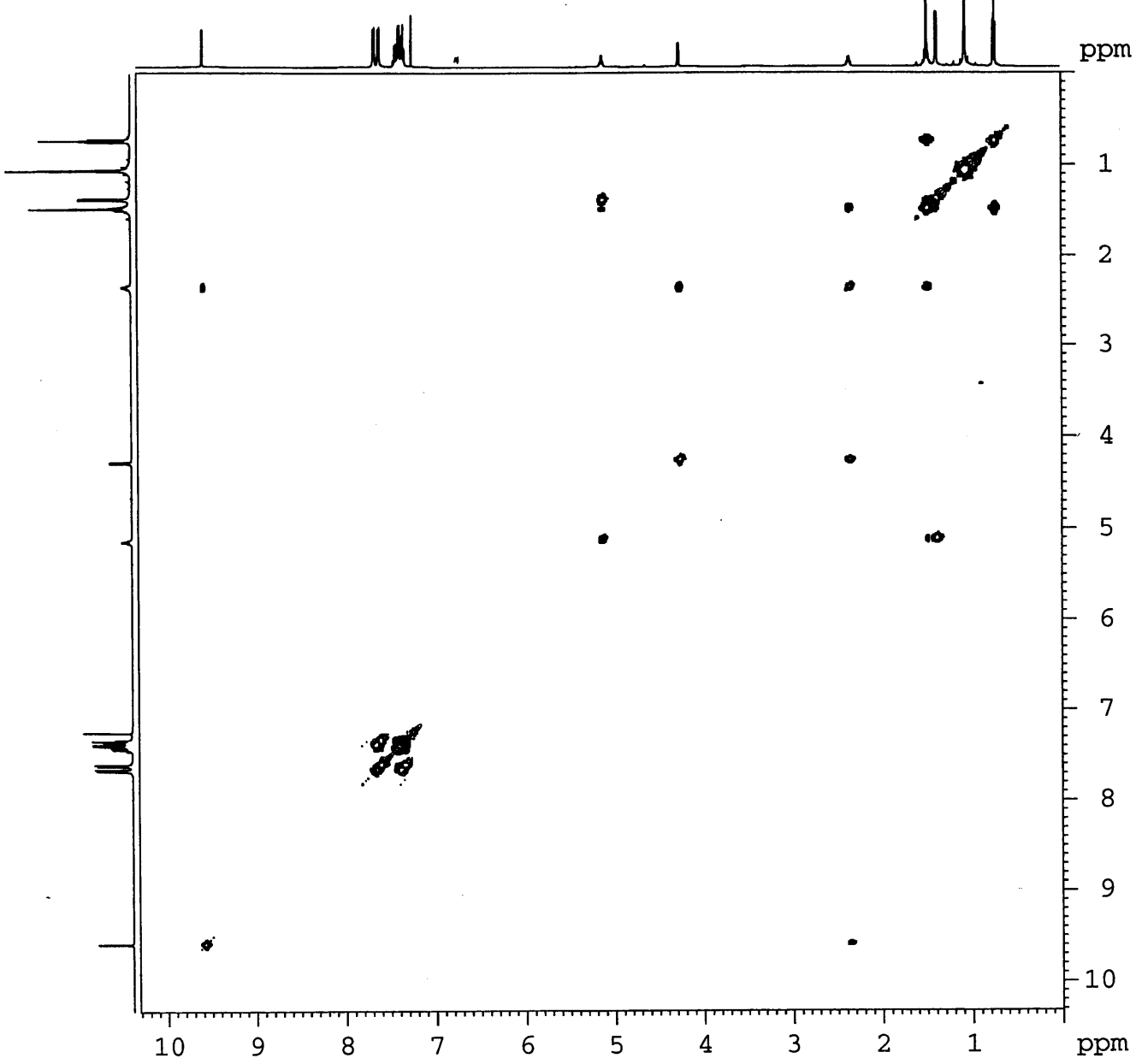

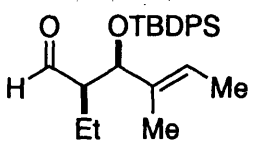

378

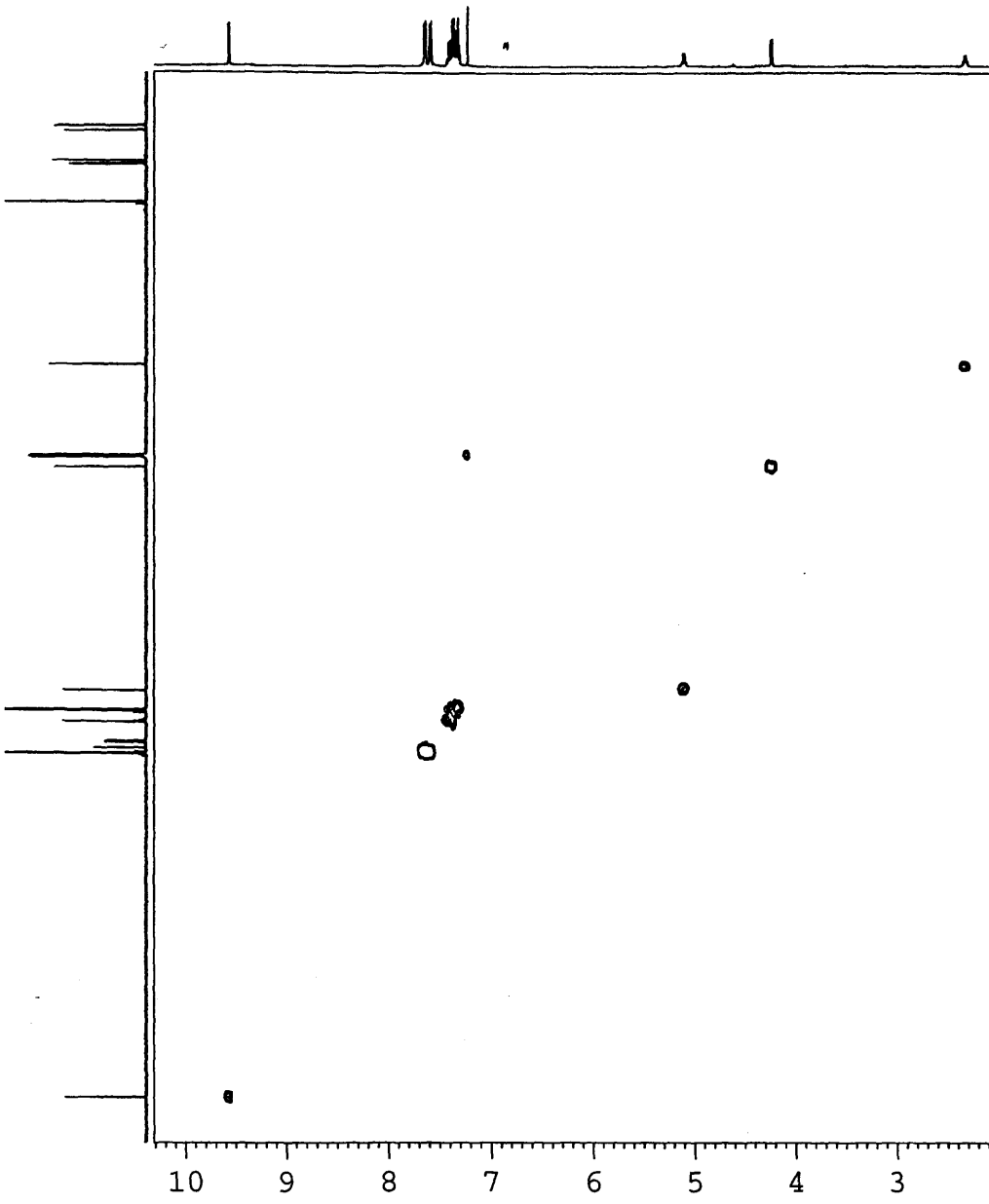

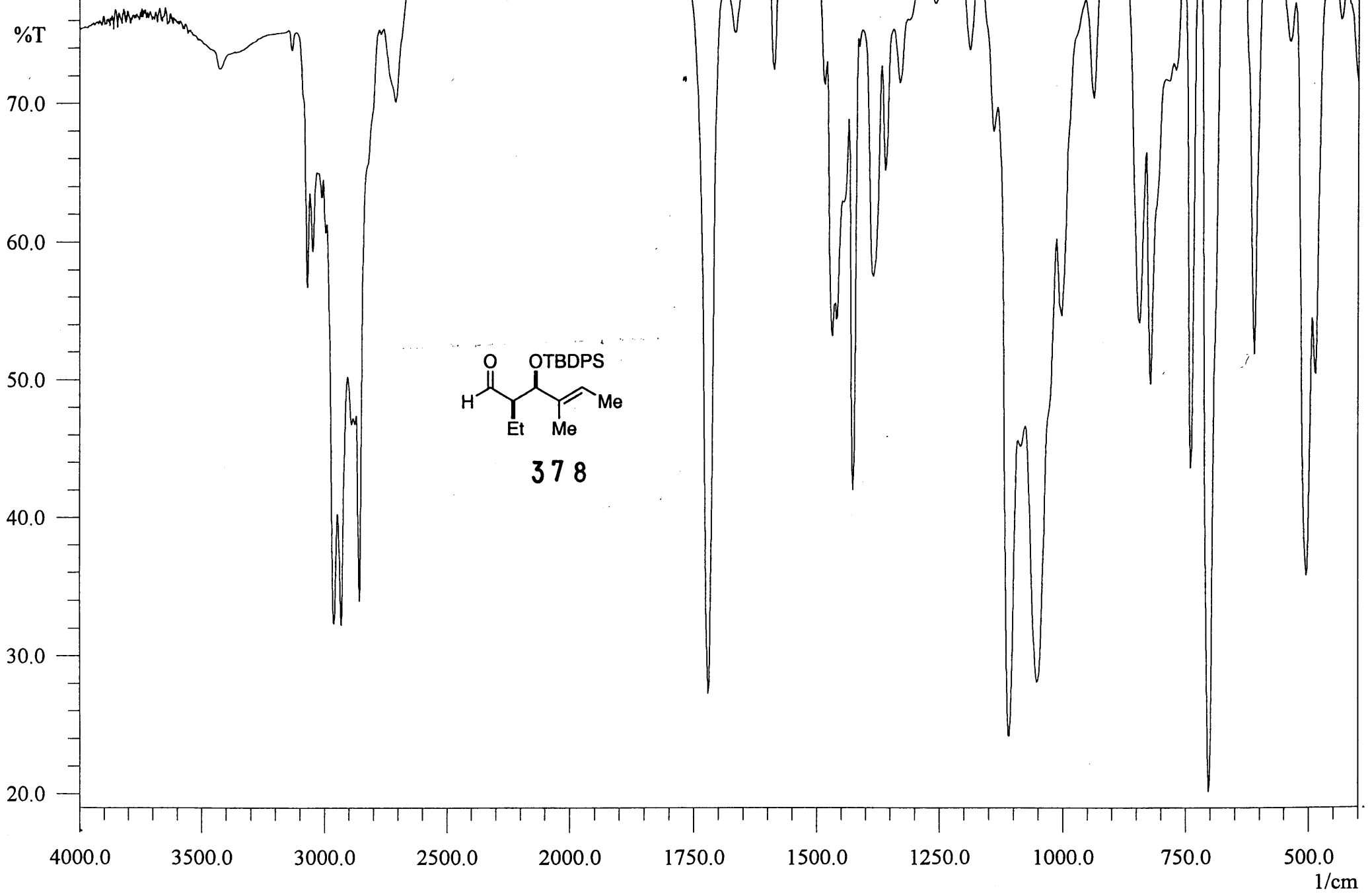
%T
70.0
60.0
50.0
40.0
30.0
20.0
O
OTBDPS
H
Me
Et
Me
378
4000.0
3500.0
3000.0
2500.0
2000.0
1750.0
1500.0
1250.0
1000.0
750.0
500.0
1/cm

Base: 417.00 Int: 1.8838e+006 Sample: VG 70-SE Positive Ion FAB

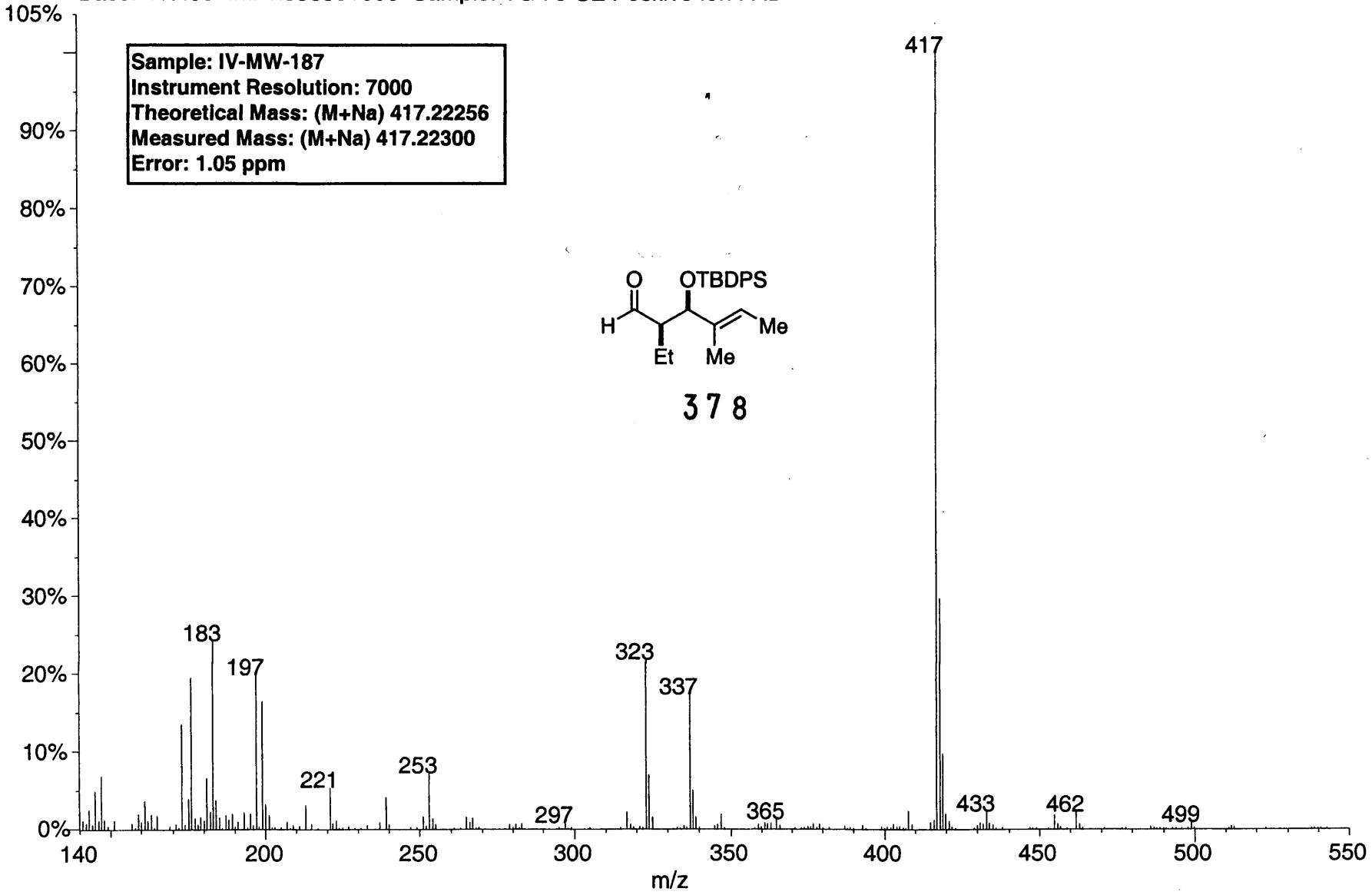

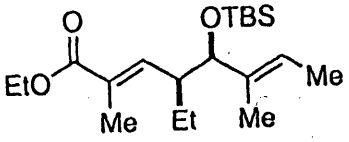

368

CDCl3 at 298 K

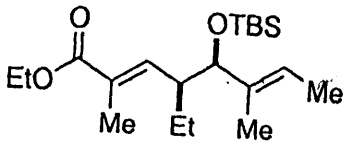

368

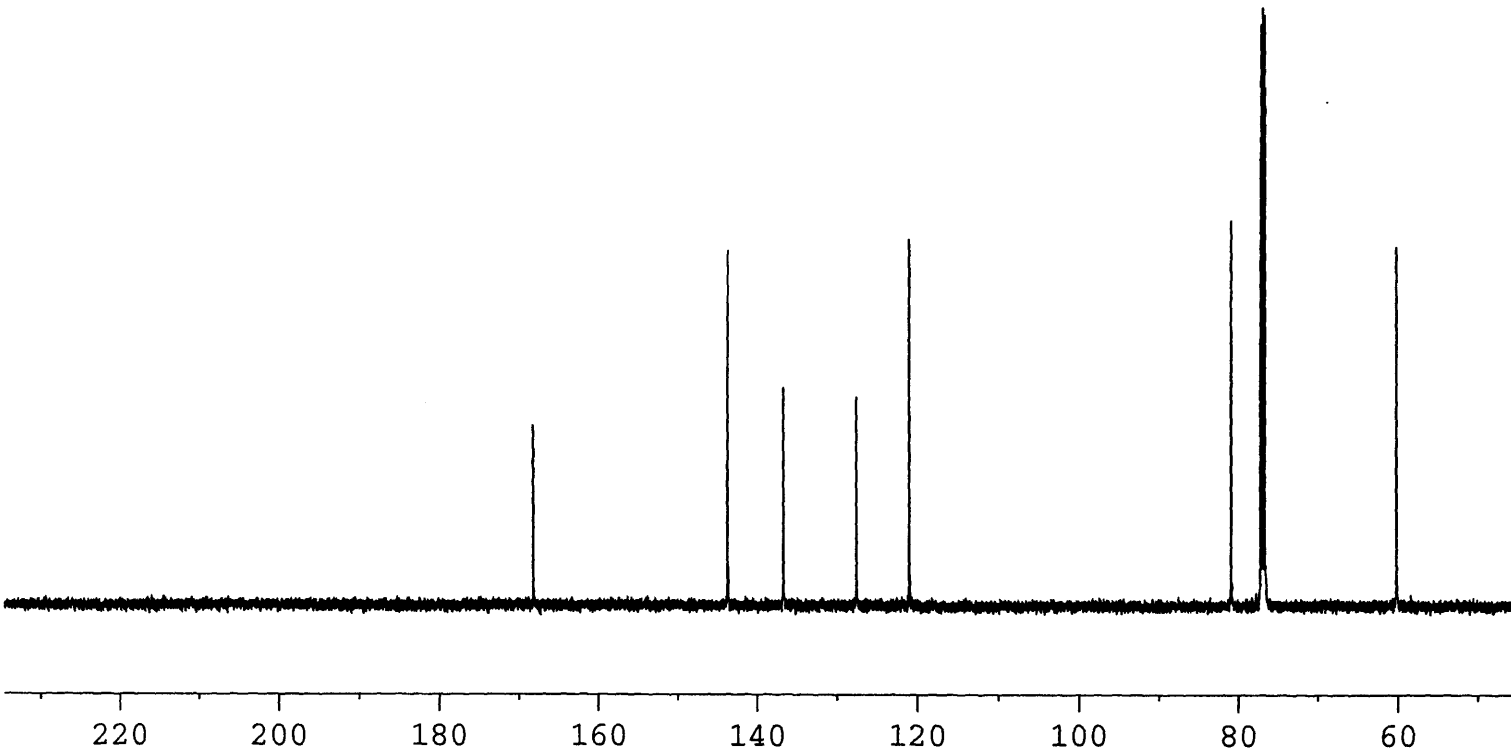

DEPT 1H
CDCl3 at 298 K

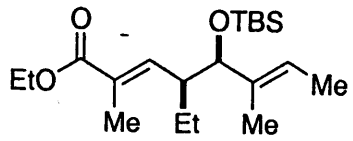

368

CDCl3 at 298 K

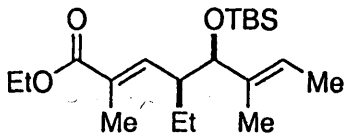

368

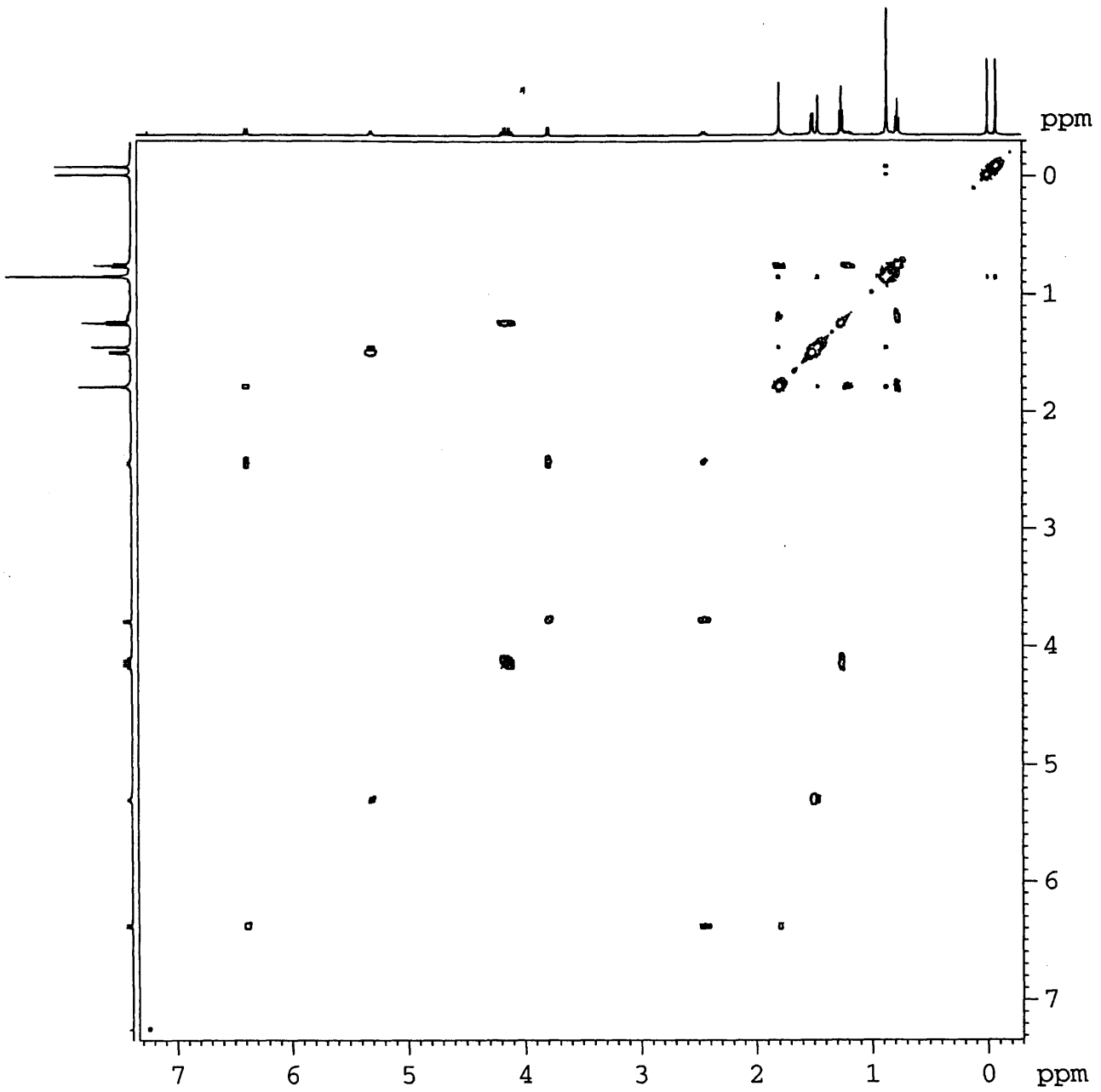

IV-MW-164
HMQC in
CDCl3 at 298 K

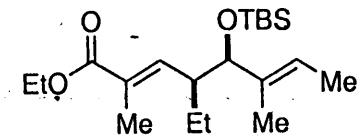

368

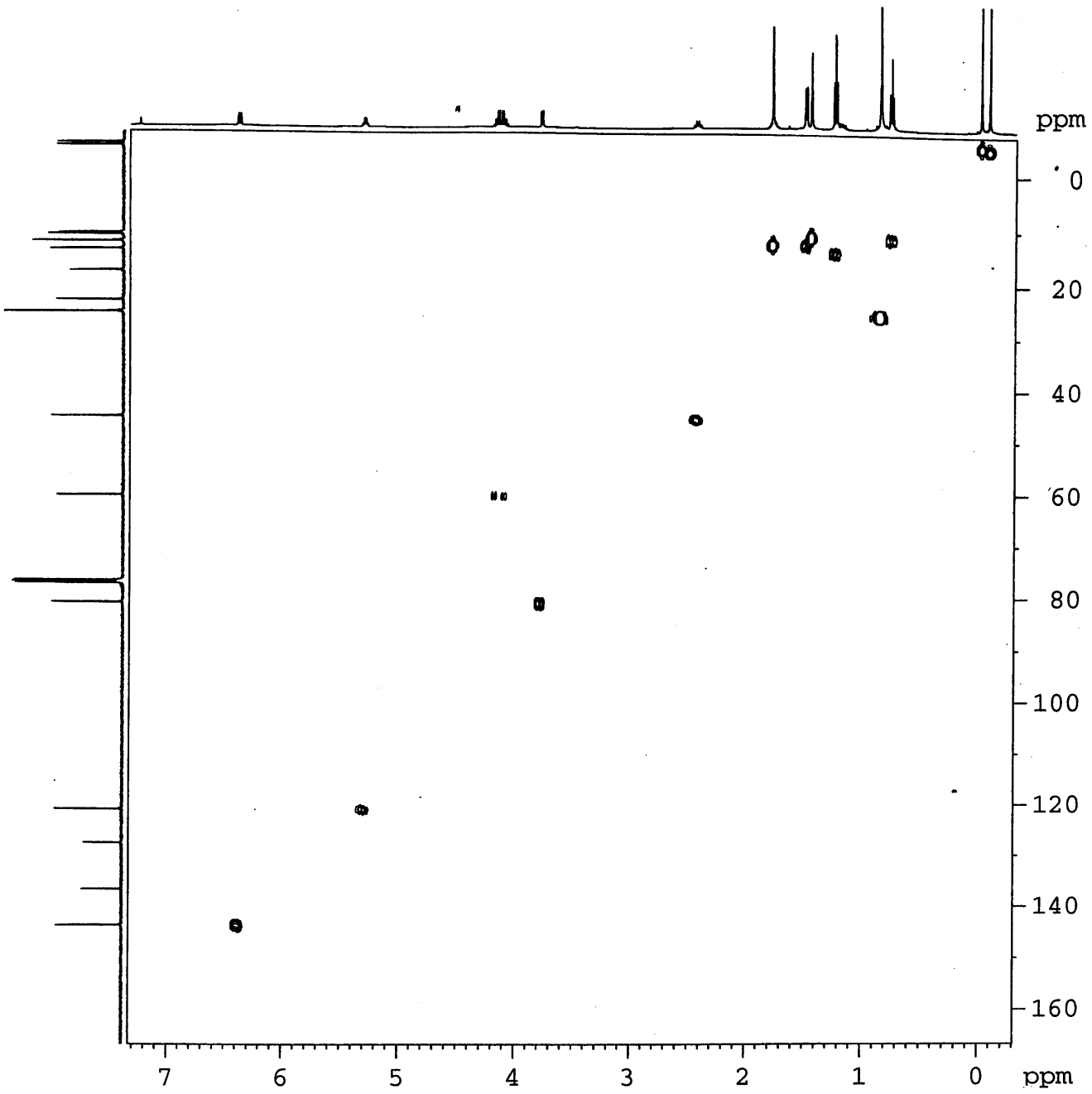

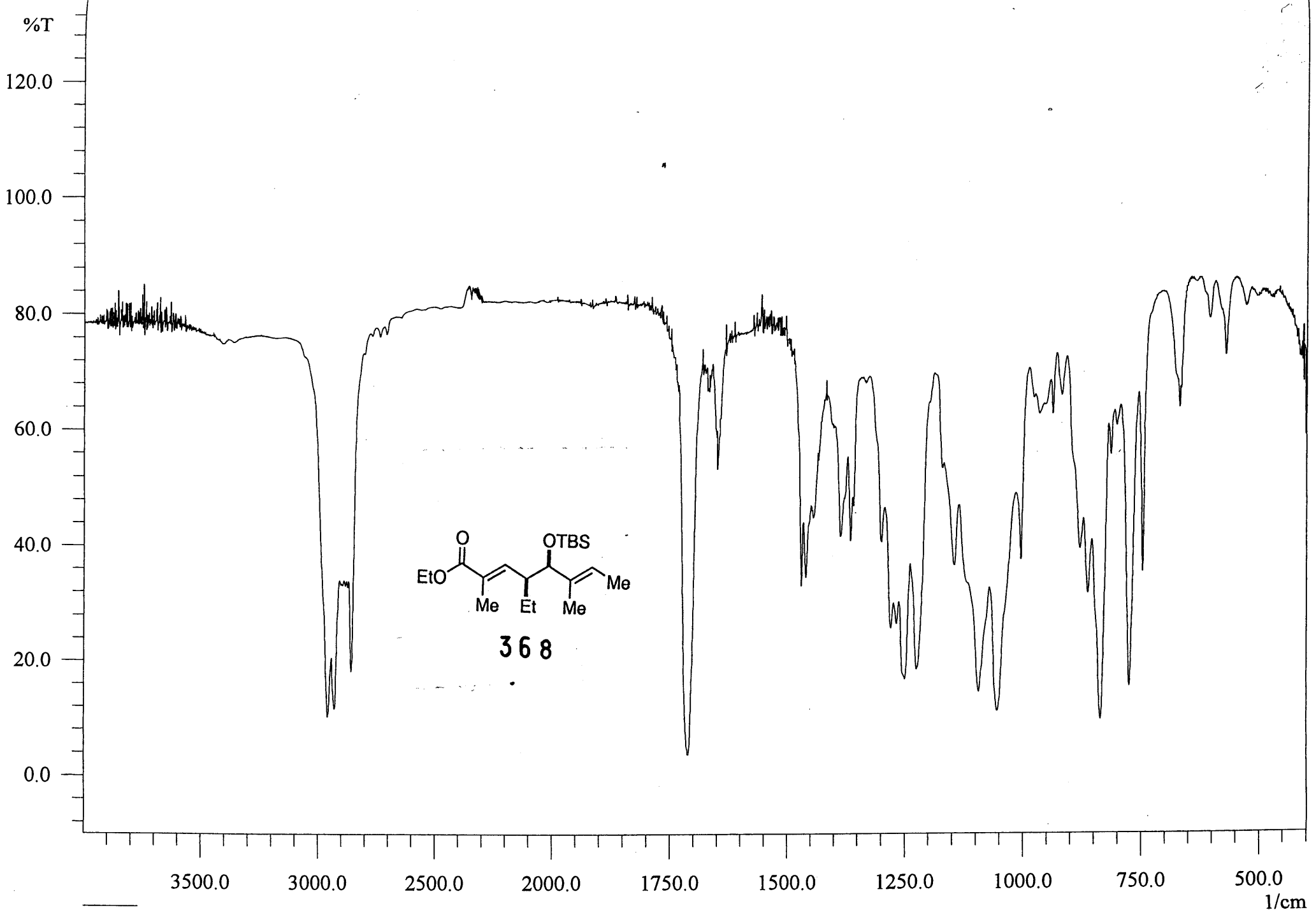
%T
120.0
100.0
80.0
60.0
40.0
20.0
0.0
3500.0
3000.0
2500.0
2000.0
1750.0
1500.0
1250.0
1000.0
750.0
500.0
1/cm
O
OTBS
EtO
Me
Me
Et
Me
368

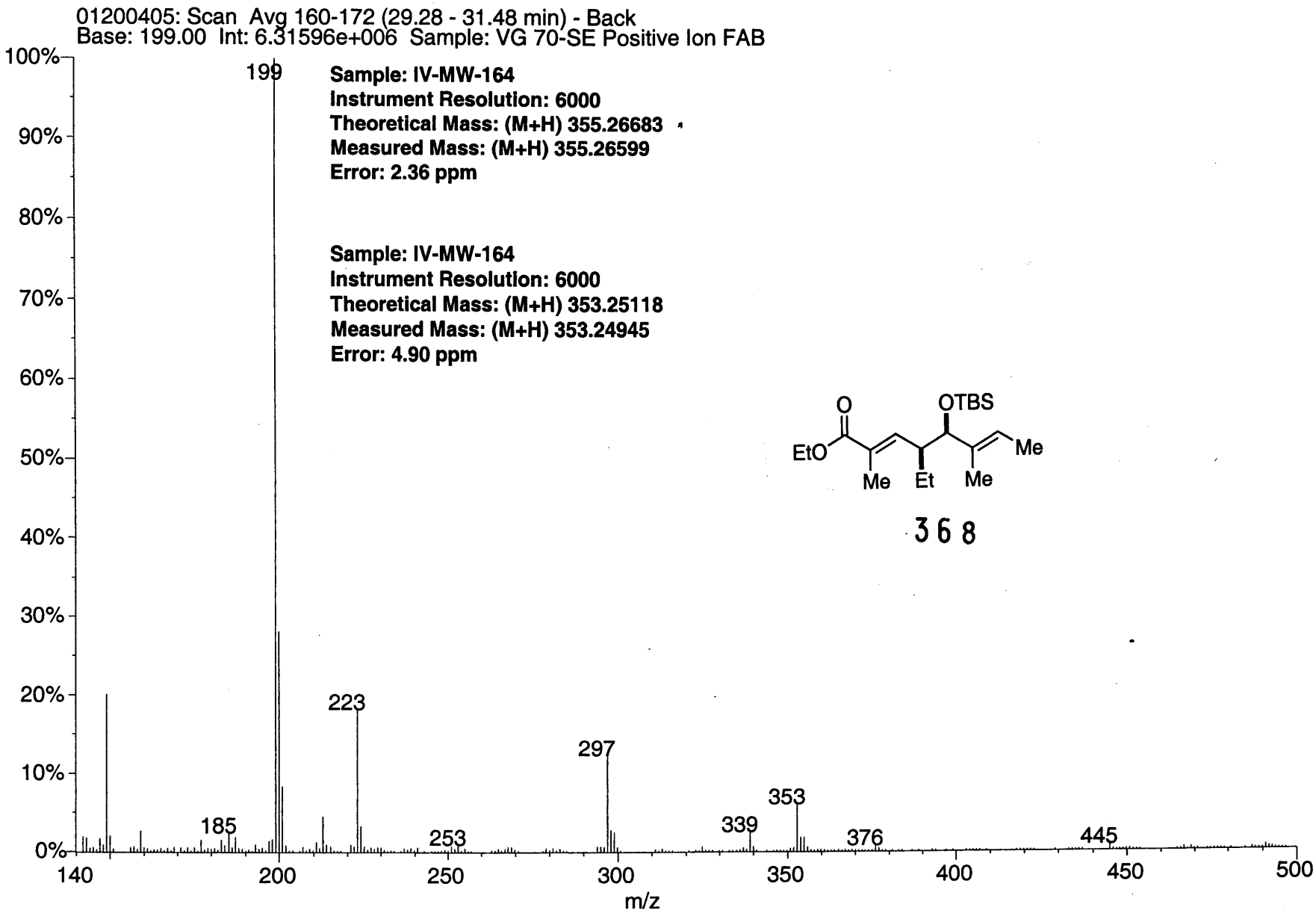
01200405: Scan Avg 160-172 (29.28 - 31.48 min) - Back
Base: 199.00 Int: 6.31596e+006 Sample: VG 70-SE Positive Ion FAB
Sample: IV-MW-164
Instrument Resolution: 6000
Theoretical Mass: (M+H) 355.26683
Measured Mass: (M+H) 355.26599
Error: 2.36 ppm
Sample: IV-MW-164
Instrument Resolution: 6000
Theoretical Mass: (M+H) 353.25118
Measured Mass: (M+H) 353.24945
Error: 4.90 ppm
O
OTBS
EtO
Me
Me
Et
Me
368
100%
90%
80%
70%
60%
50%
40%
30%
20%
10%
0%
199
223
297
353
185
253
339
376
445
140
200
250
300
350
400
450
500
m/z

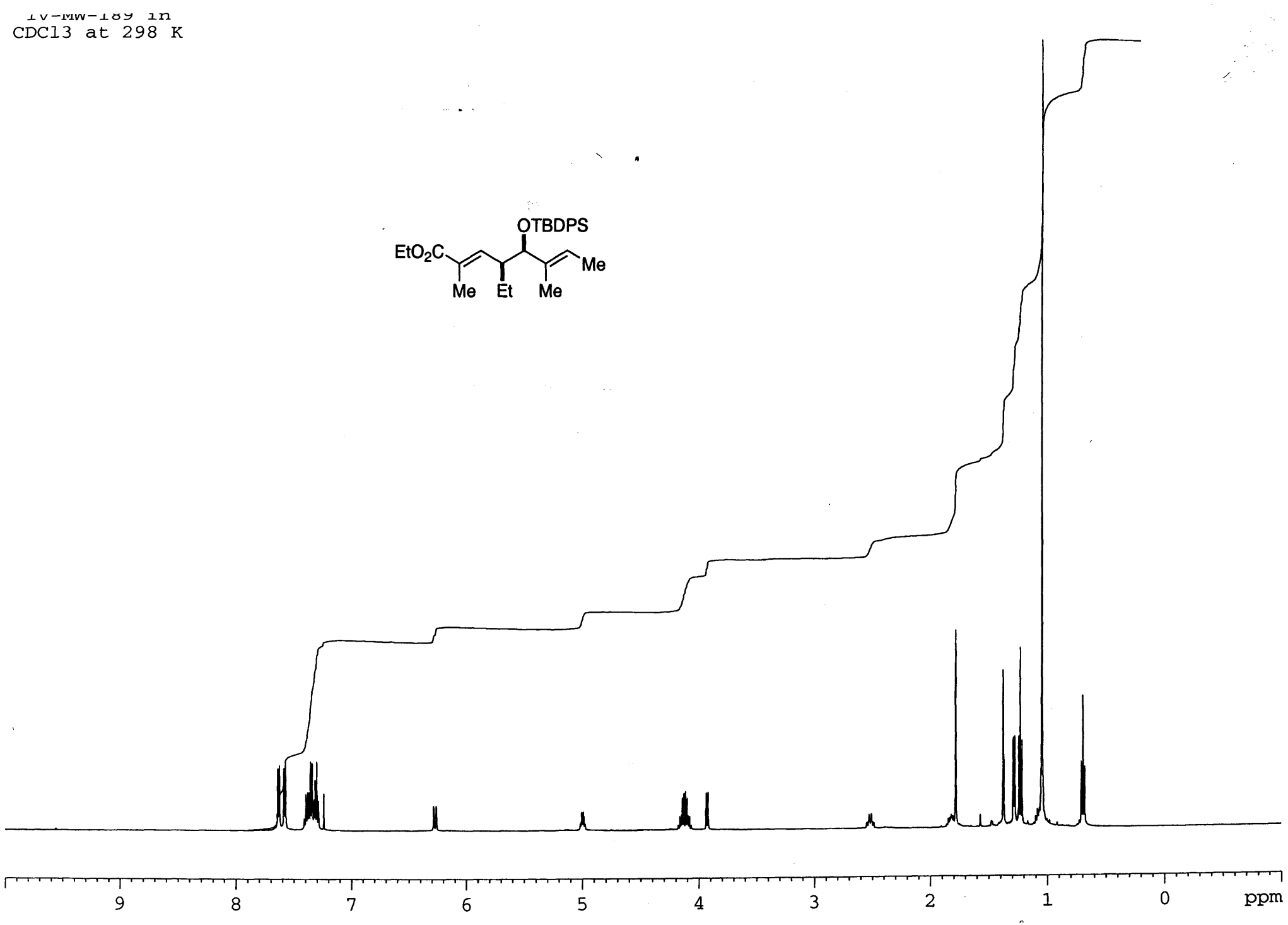
Iv-MW-189 1H
CDCl3 at 298 K
OTBDPS
EtO2C
Me
Me
Et
Me
9
8
7
6
5
4
3
2
1
0
ppm

IV-MW-189
Carbon 13 in
CDCl3 at 298 K

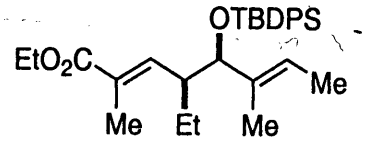

IV-MW-189
DEPT in
CDCl3 at 298 K

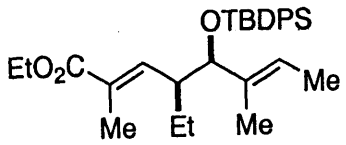

IV-MW-189
COSY in
CDCl3 at 298 K

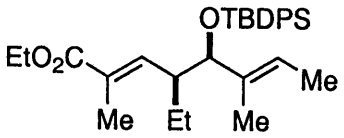

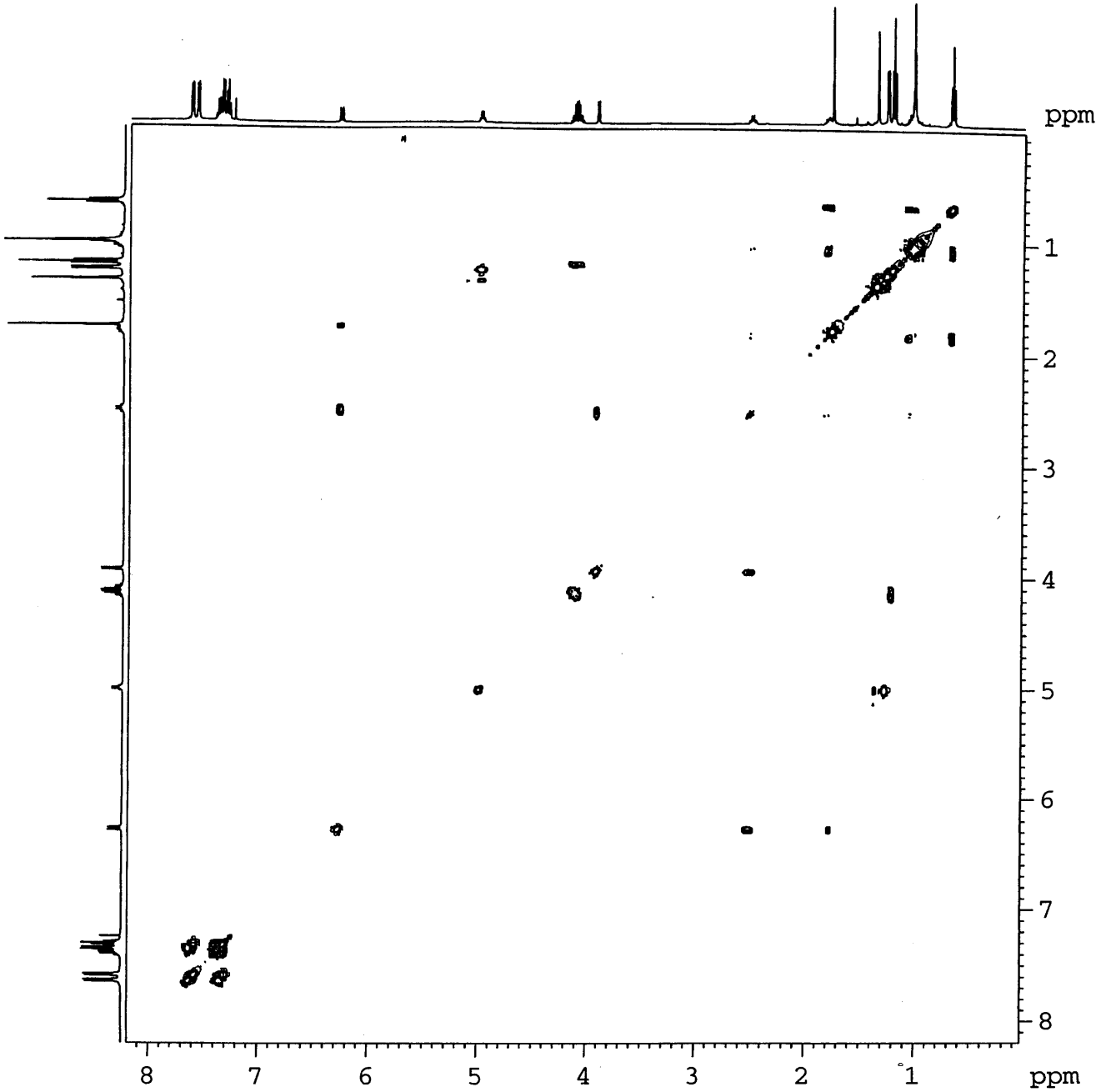

IV-MW-189
HMQC in
CDCl3 at 298 K

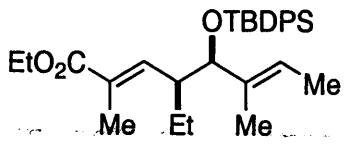

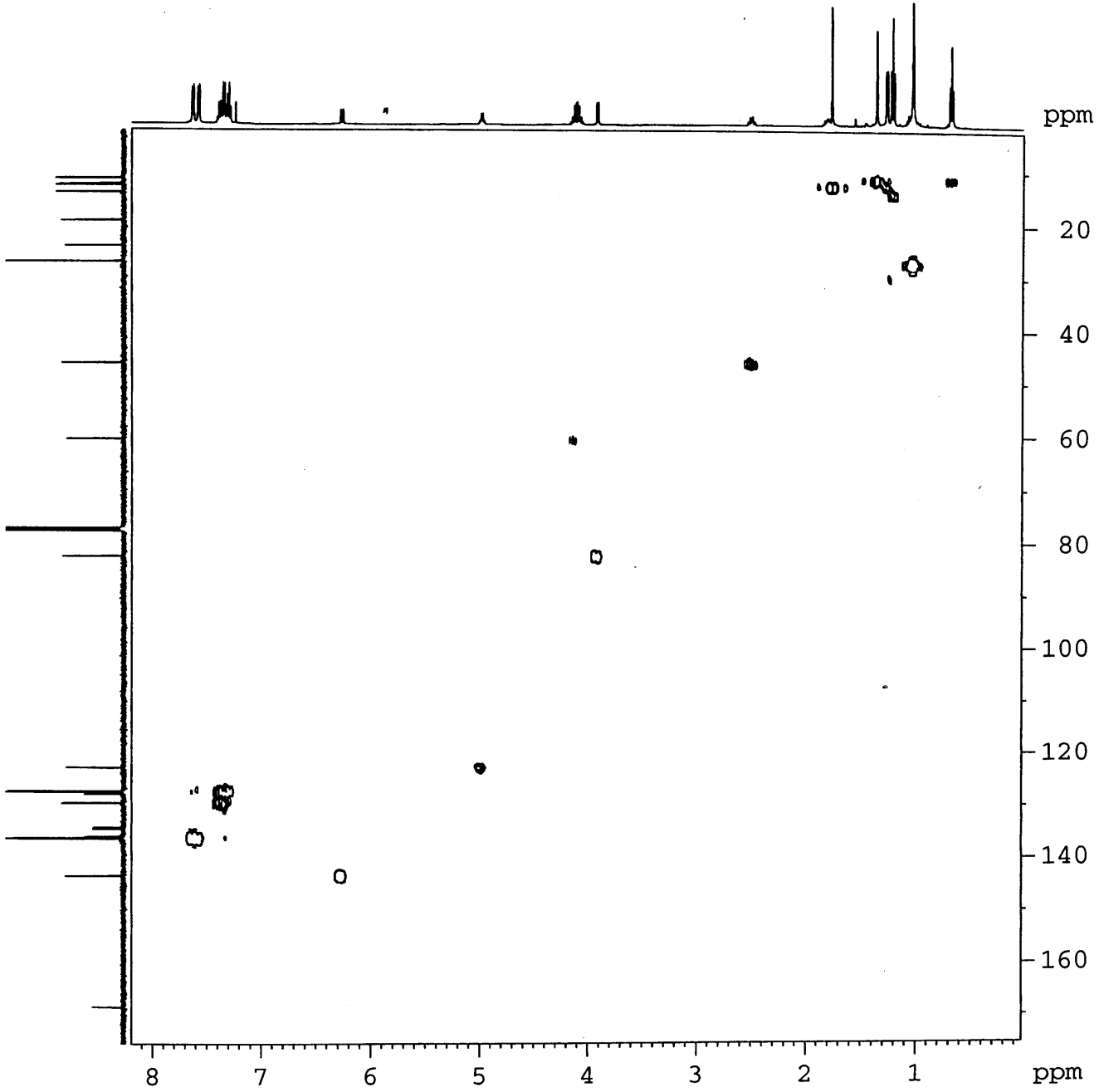

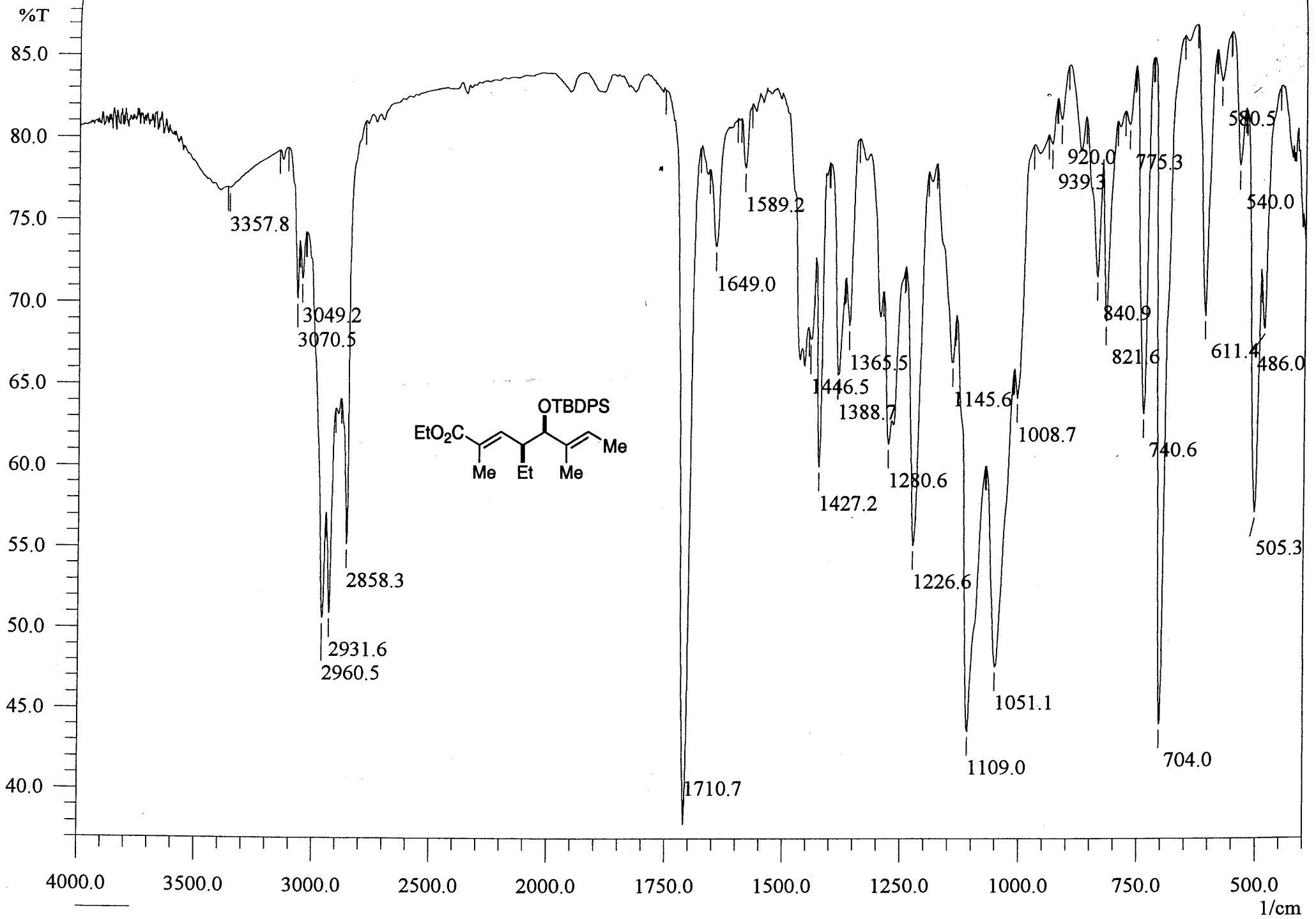
%T
85.0
80.0
75.0
70.0
65.0
60.0
55.0
50.0
45.0
40.0
3357.8
3049.2
3070.5
2858.3
2931.6
2960.5
1649.0
1589.2
1710.7
1446.5
1365.5
1388.7
1427.2
1280.6
1226.6
1145.6
1008.7
1109.0
1051.1
920.0
939.3
840.9
821.6
775.3
740.6
704.0
611.4
580.5
540.0
486.0
505.3
OTBDPS
EtO2C
Me
Me
Et
Me
4000.0
3500.0
3000.0
2500.0
2000.0
1750.0
1500.0
1250.0
1000.0
750.0
500.0
1/cm

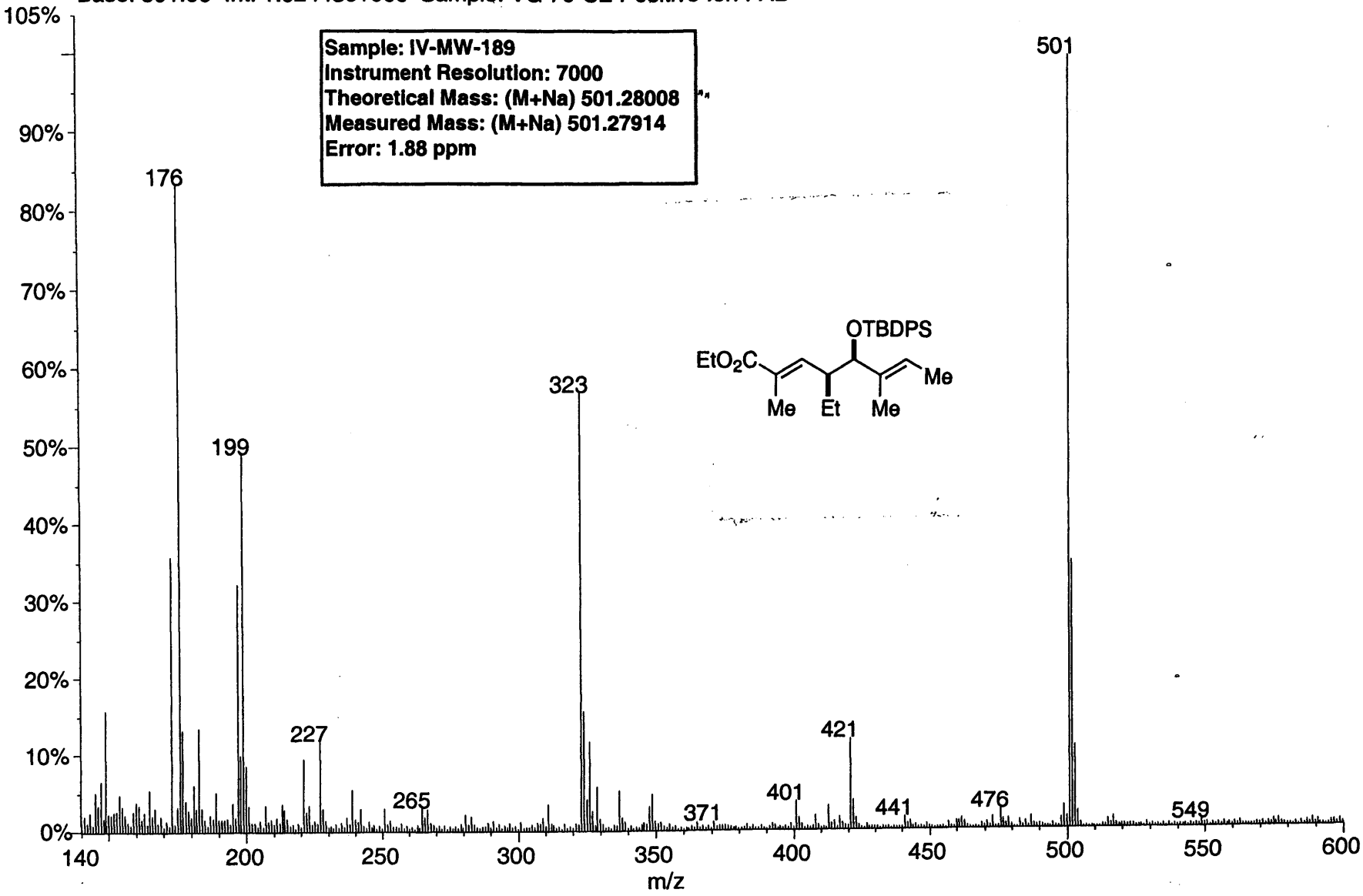
03270306: Scan 281 (51.47 min) - Back
Base: 501.00 Int: 1.62443e+006 Sample: VG 70-SE Positive Ion FAB
Sample: IV-MW-189
Instrument Resolution: 7000
Theoretical Mass: (M+Na) 501.28008
Measured Mass: (M+Na) 501.27914
Error: 1.88 ppm
OTBDPS
EtO2C
Me
Me
Et
Me
105%
90%
80%
70%
60%
50%
40%
30%
20%
10%
0%
140
200
250
300
350
400
450
500
550
600
m/z
176
199
227
265
323
371
401
421
441
476
501
549

IV-MW-178 in
CDCl3 at 298 K

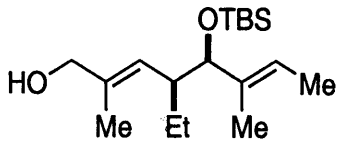

369

IV-MW-178
Carbon 13 in
CDCl3 at 298 K

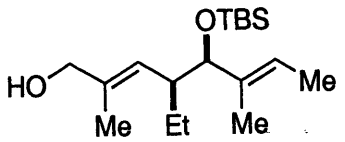

369

IV-MW-178
DEPT in
CDCl3 at 298 K

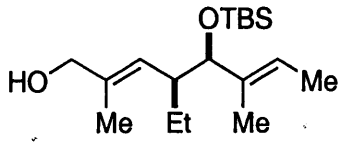

369

IV-MW-178
COSY in
CDCl3 at 298 K

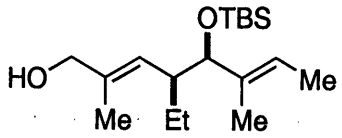

369

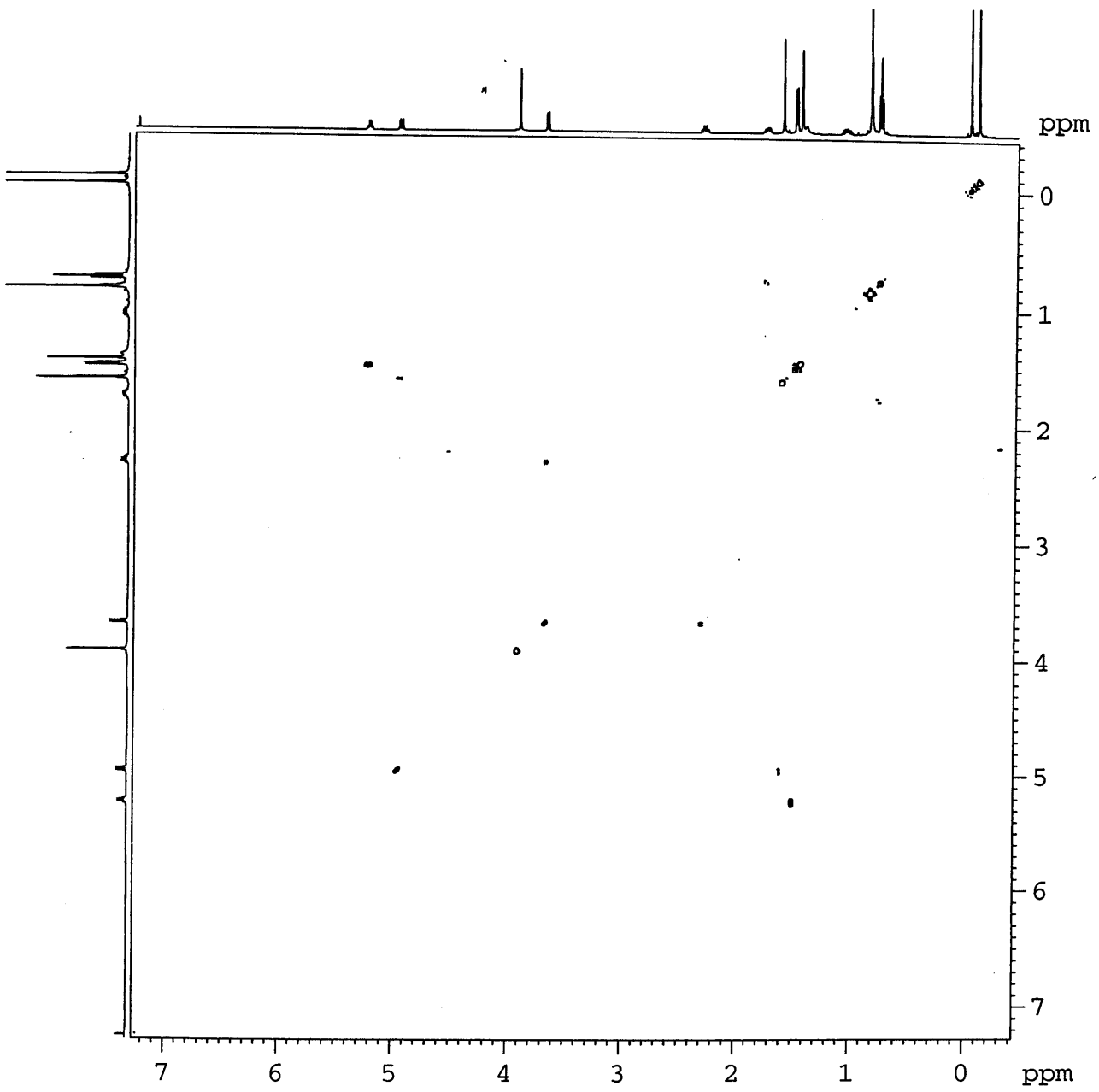

IV-MW-178
HMQC in
CDCl3 at 298 K

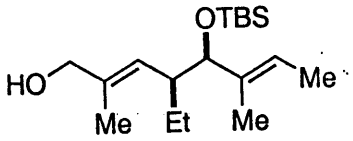

369

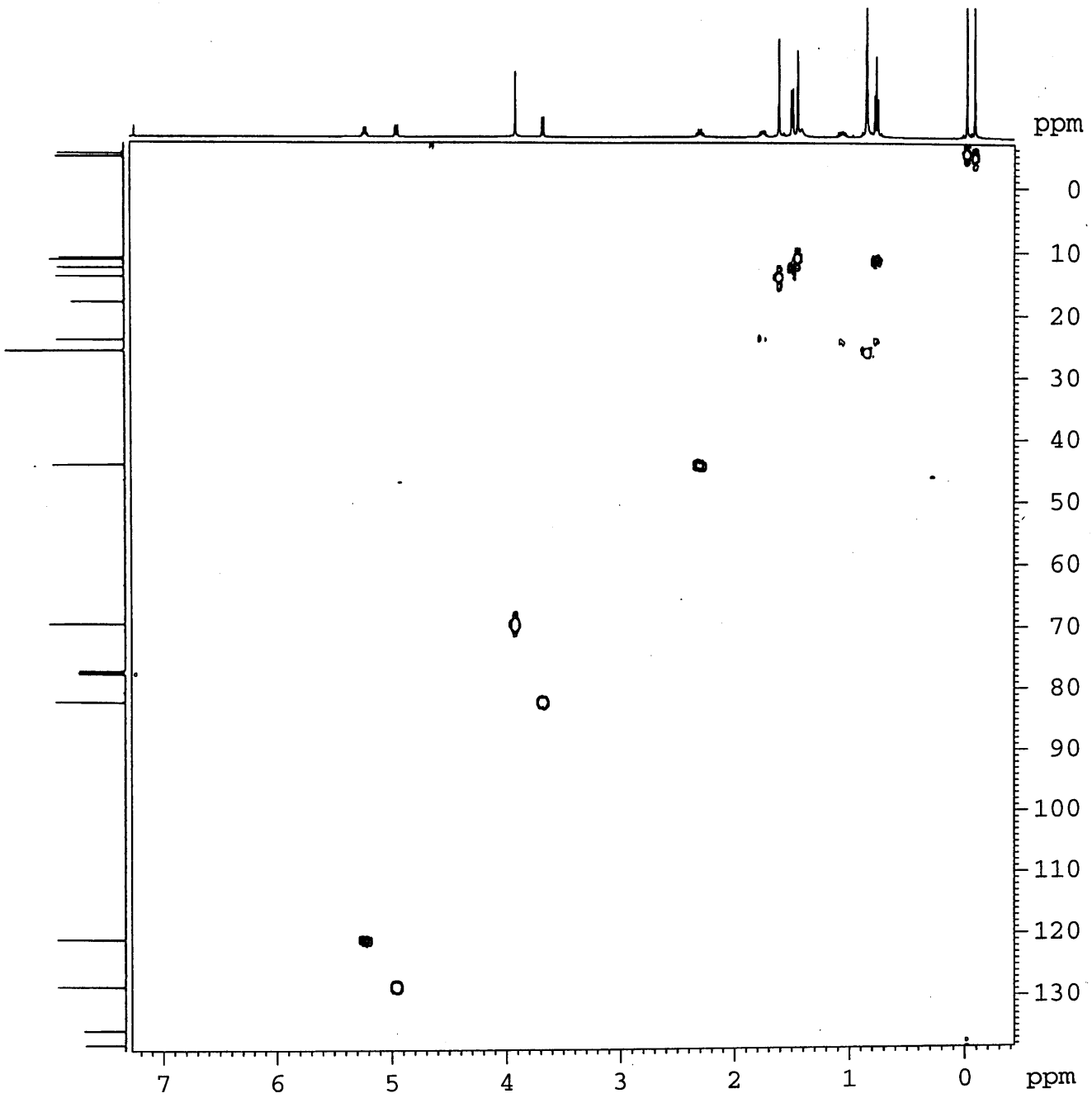

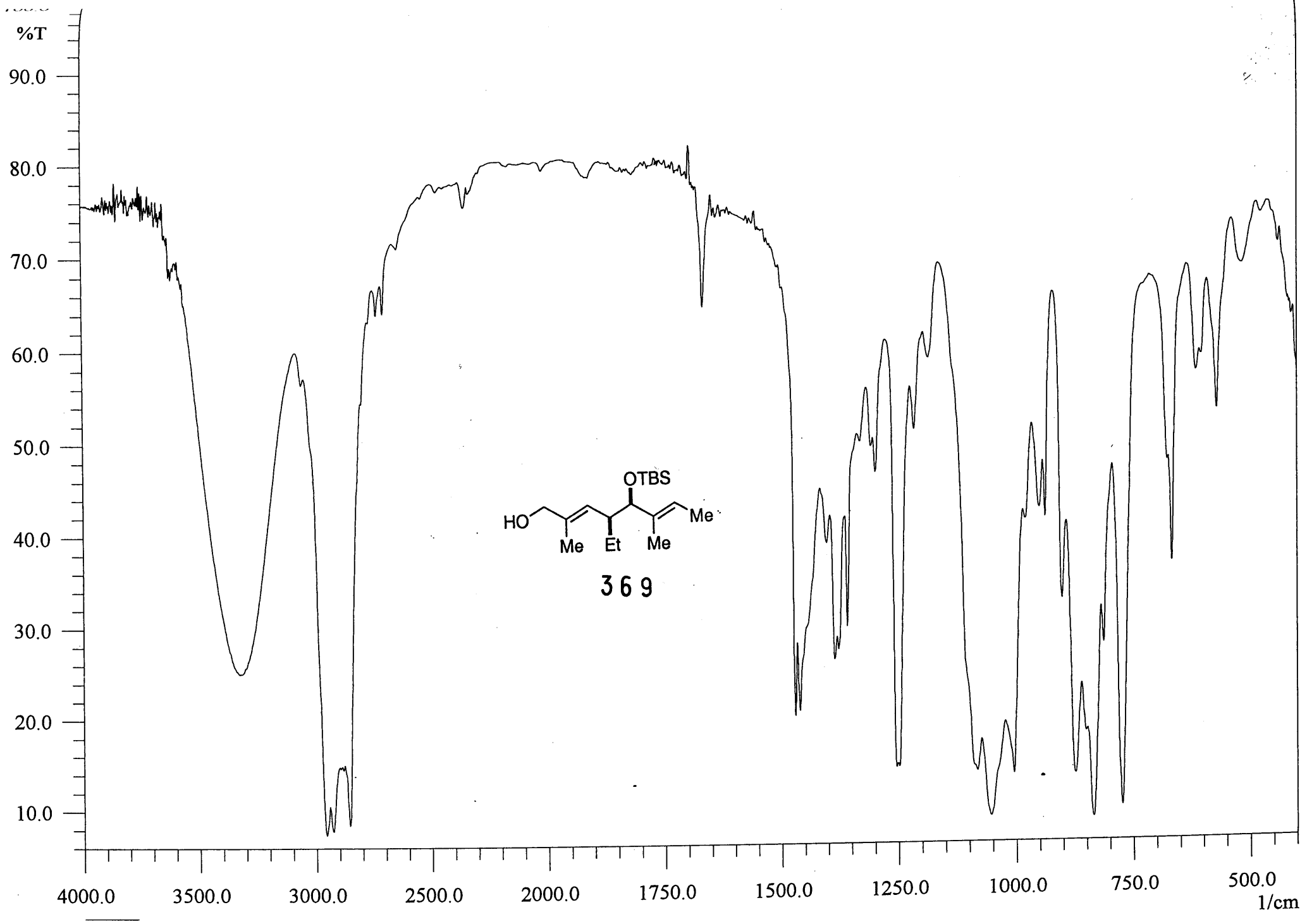
%T
90.0
80.0
70.0
60.0
50.0
40.0
30.0
20.0
10.0
4000.0
3500.0
3000.0
2500.0
2000.0
1750.0
1500.0
1250.0
1000.0
750.0
500.0
1/cm
OTBS
HO
Me
Et
Me
Me
369

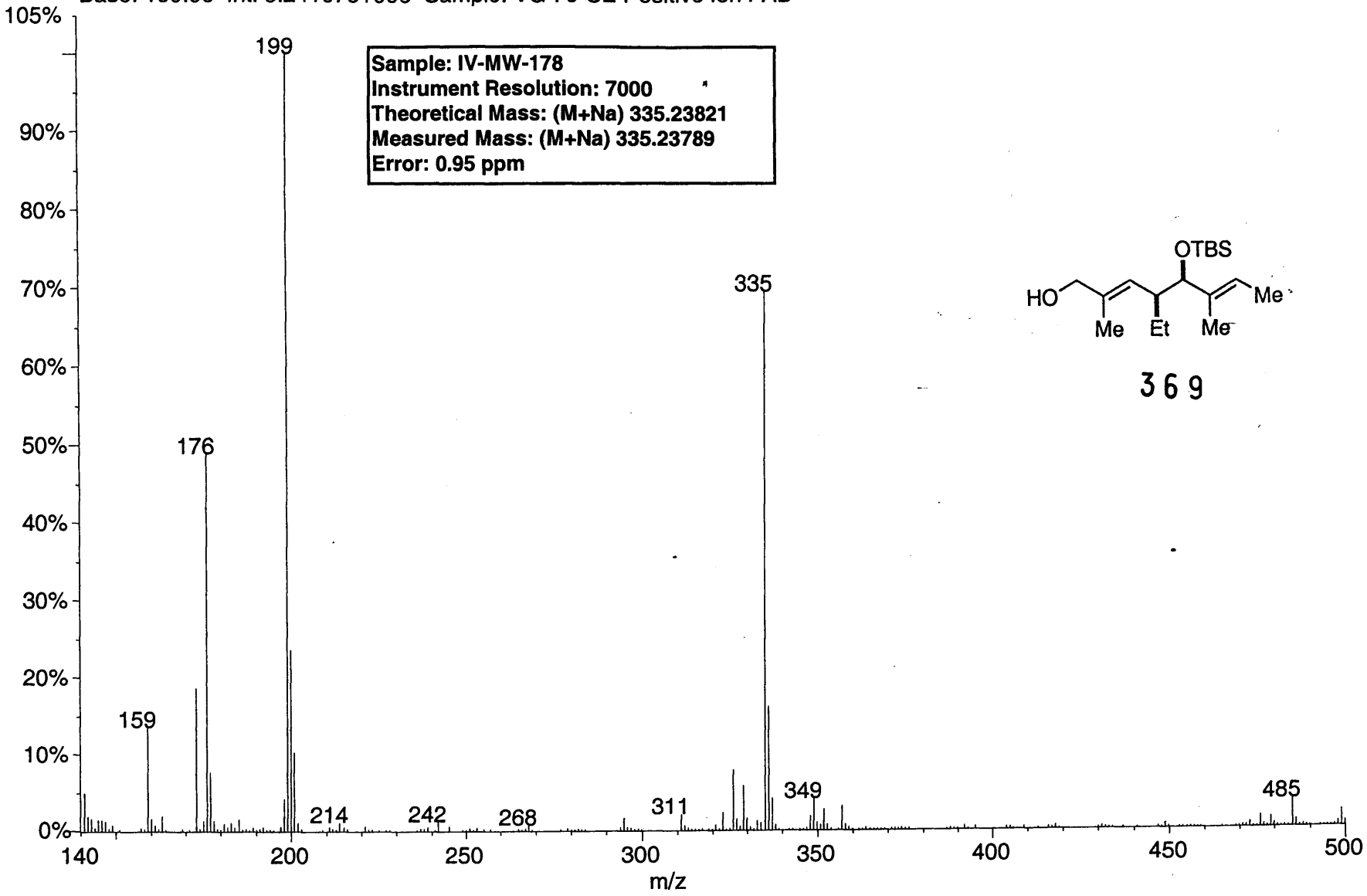
03270306: Scan 232 (42.48 min) - Back
Base: 199.00 Int: 6.24107e+006 Sample: VG 70-SE Positive Ion FAB
Sample: IV-MW-178
Instrument Resolution: 7000
Theoretical Mass: (M+Na) 335.23821
Measured Mass: (M+Na) 335.23789
Error: 0.95 ppm
105%
90%
80%
70%
60%
50%
40%
30%
20%
10%
0%
199
335
176
159
214
242
268
311
349
485
140
200
250
300
350
400
450
500
m/z
OTBS
HO
Me
Et
Me
Me
369

V-MW-1 in
CDCl3 at 298 K

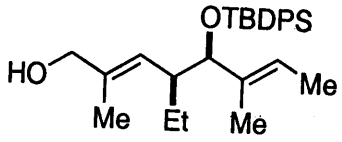

379

V-MW-1
Carbon 13 in
CDC13 at 298 K

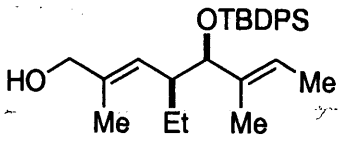

379

v-mw-1
DEPT in
CDCl3 at 298 K

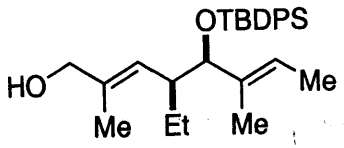

379

V-MW-1
COSY in
CDCl3 at 298 K

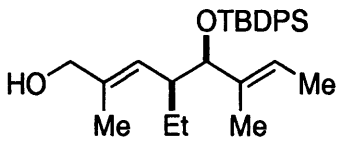

379

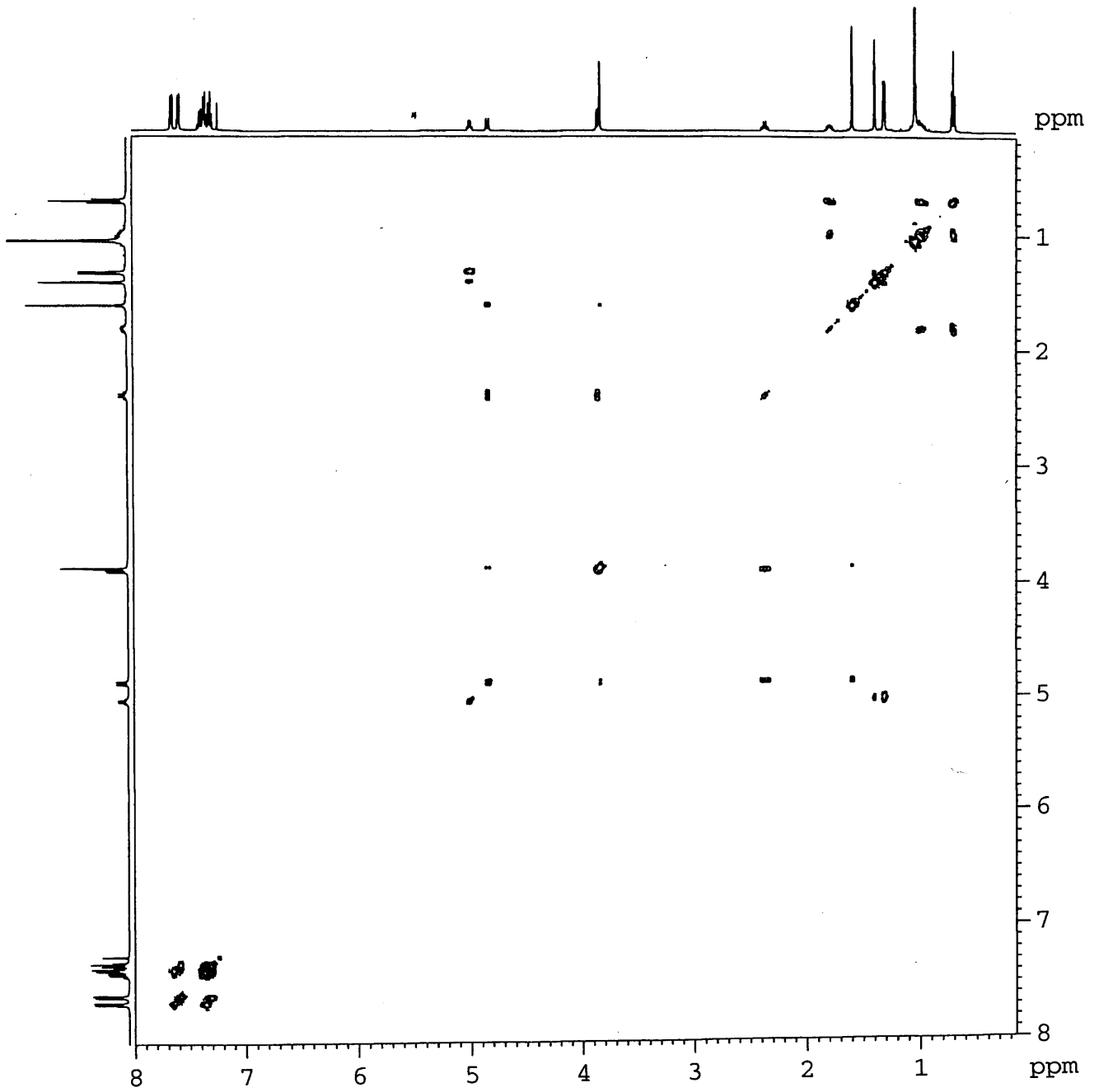

V-MW-1
HMQC in
CDCl3 at 298 K

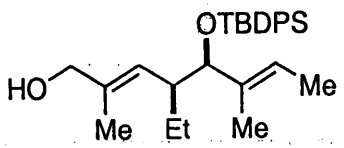

379

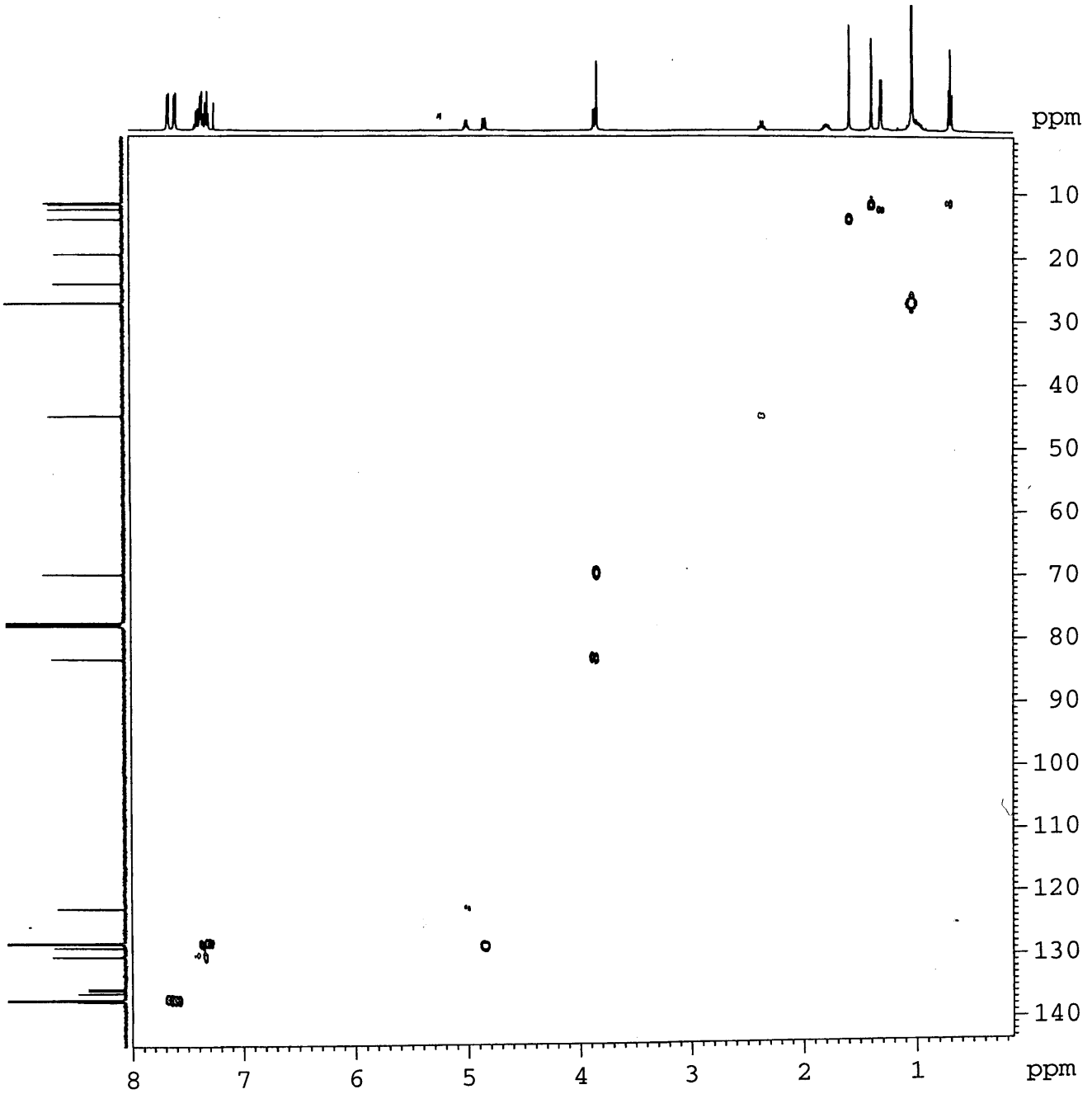

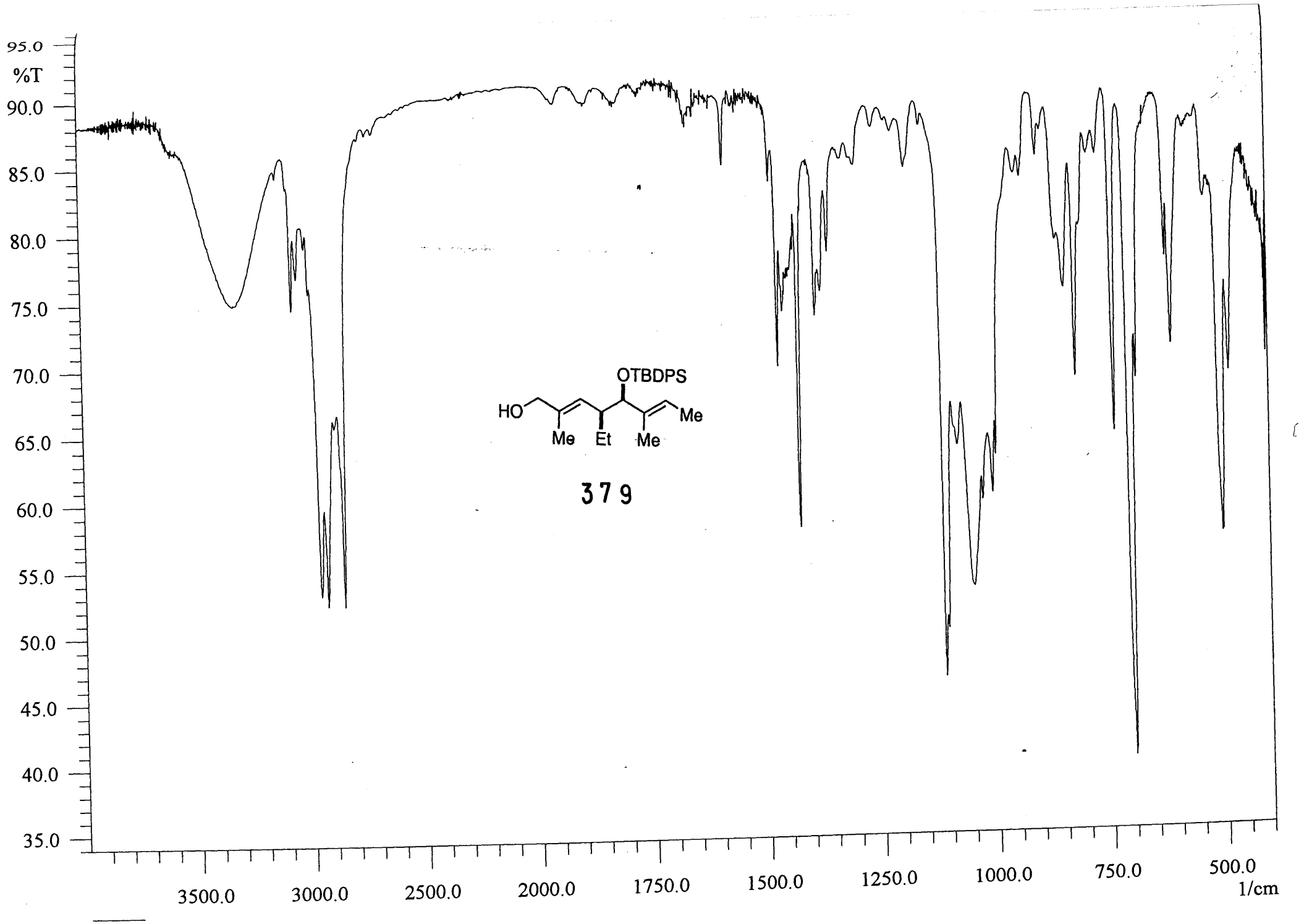
95.0
%T
90.0
85.0
80.0
75.0
70.0
65.0
60.0
55.0
50.0
45.0
40.0
35.0
3500.0
3000.0
2500.0
2000.0
1750.0
1500.0
1250.0
1000.0
750.0
500.0
1/cm
OTBDPS
HO
Me
Me
Et
Me
379

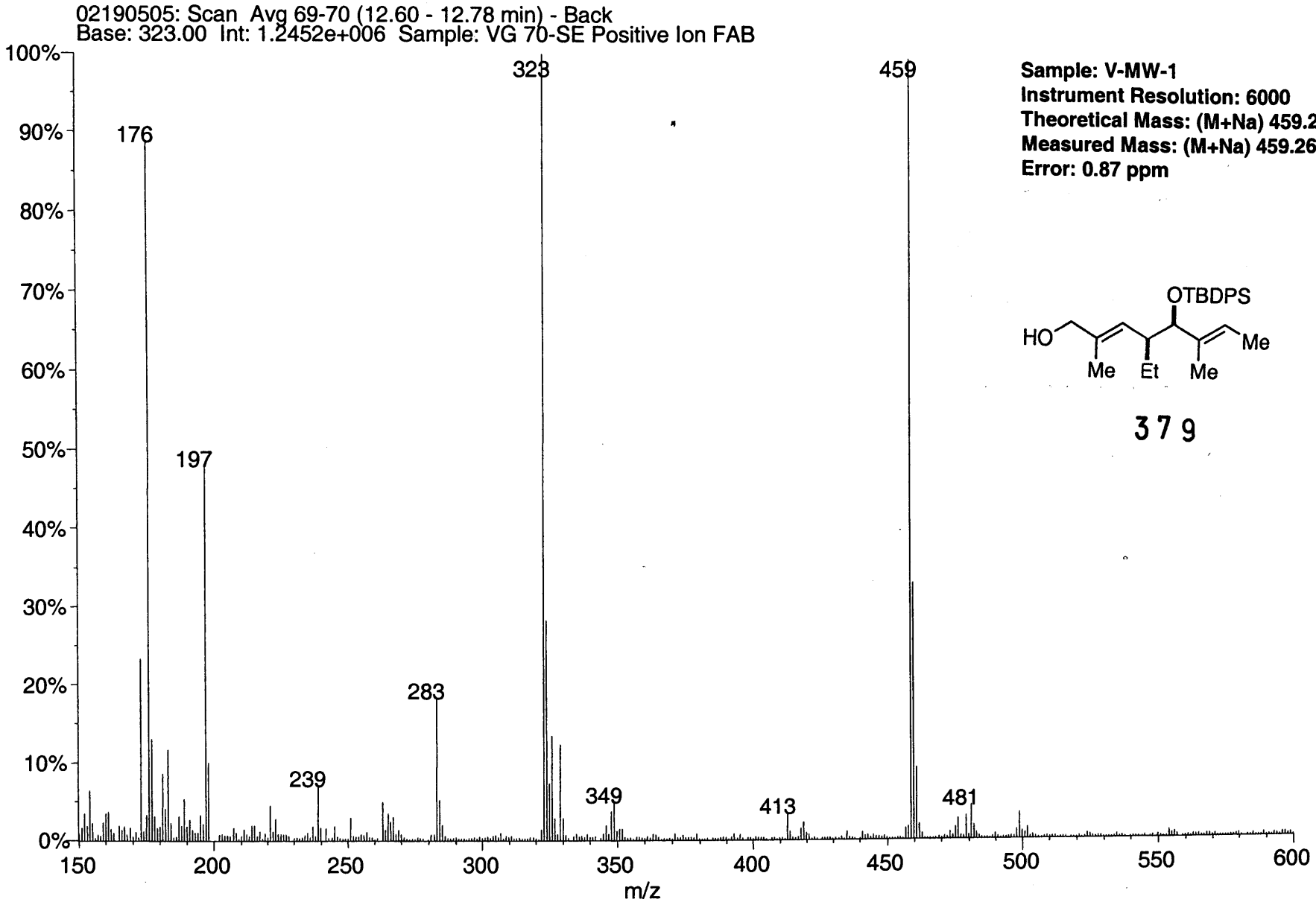
02190505: Scan Avg 69-70 (12.60 - 12.78 min) - Back
Base: 323.00 Int: 1.2452e+006 Sample: VG 70-SE Positive Ion FAB
100%
90%
80%
70%
60%
50%
40%
30%
20%
10%
0%
176
197
239
283
323
349
413
459
481
150
200
250
300
350
400
450
500
550
600
m/z
Sample: V-MW-1
Instrument Resolution: 6000
Theoretical Mass: (M+Na) 459.26951
Measured Mass: (M+Na) 459.26991
Error: 0.87 ppm
OTBDPS
HO
Me
Et
Me
Me

379

V-MW-30 in
CDCl3 at 298 K

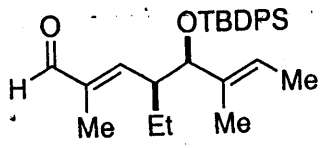

380

V-MW-30
Carbon 13 in
CDC13 at 298 K

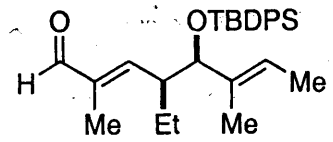

380

V-MW-30
DEPT in
CDCl3 at 298 K

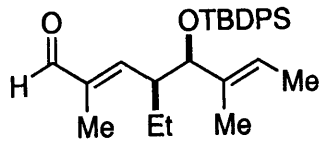

380

V-MW-30
COSY in
CDCl3 at 298 K

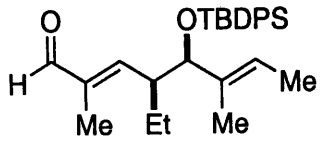

380

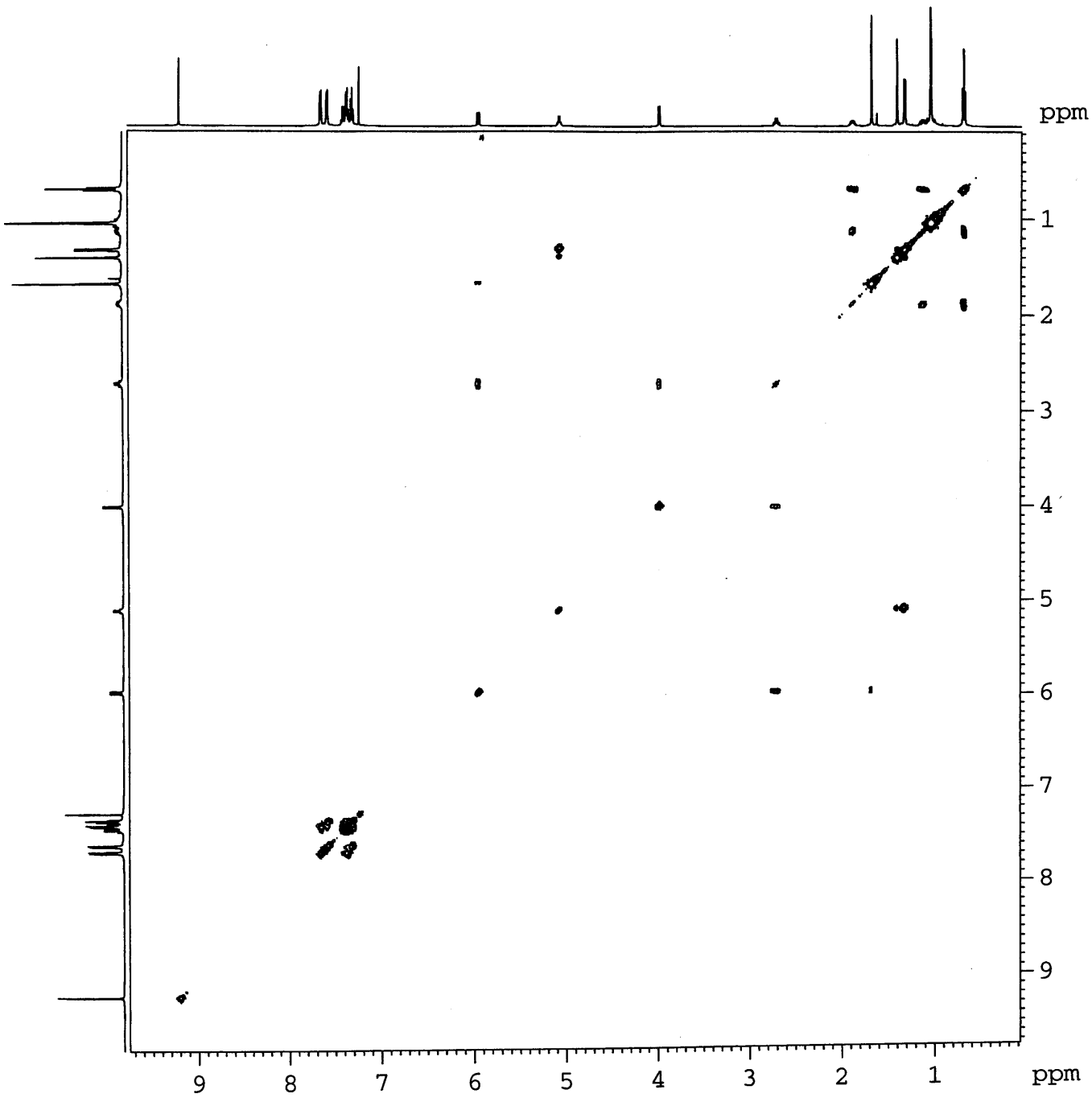

V-MW-30
HMQC in
CDCl3 at 298 K

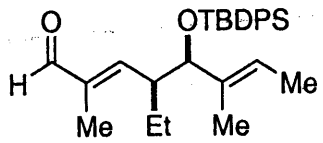

380

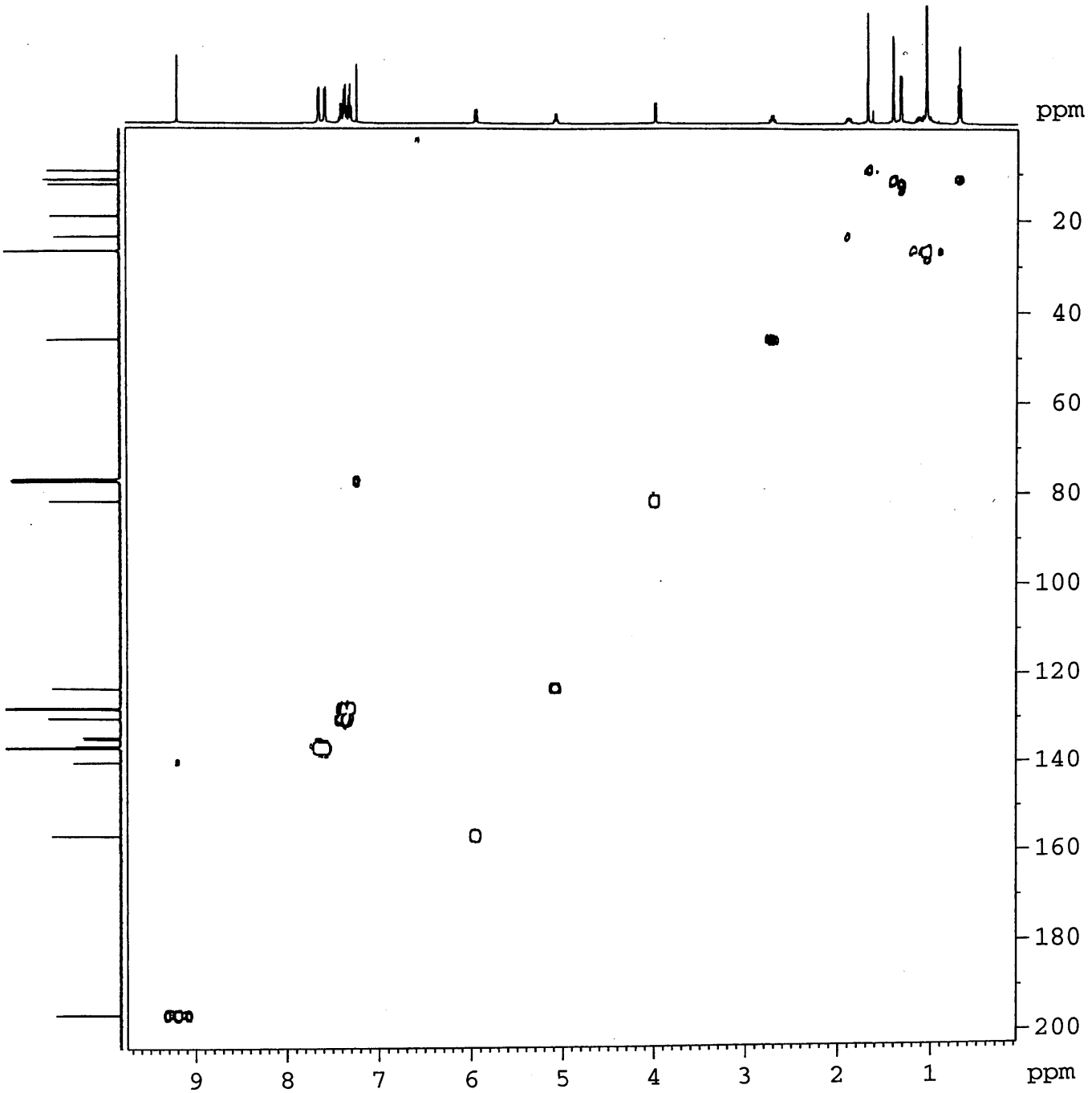

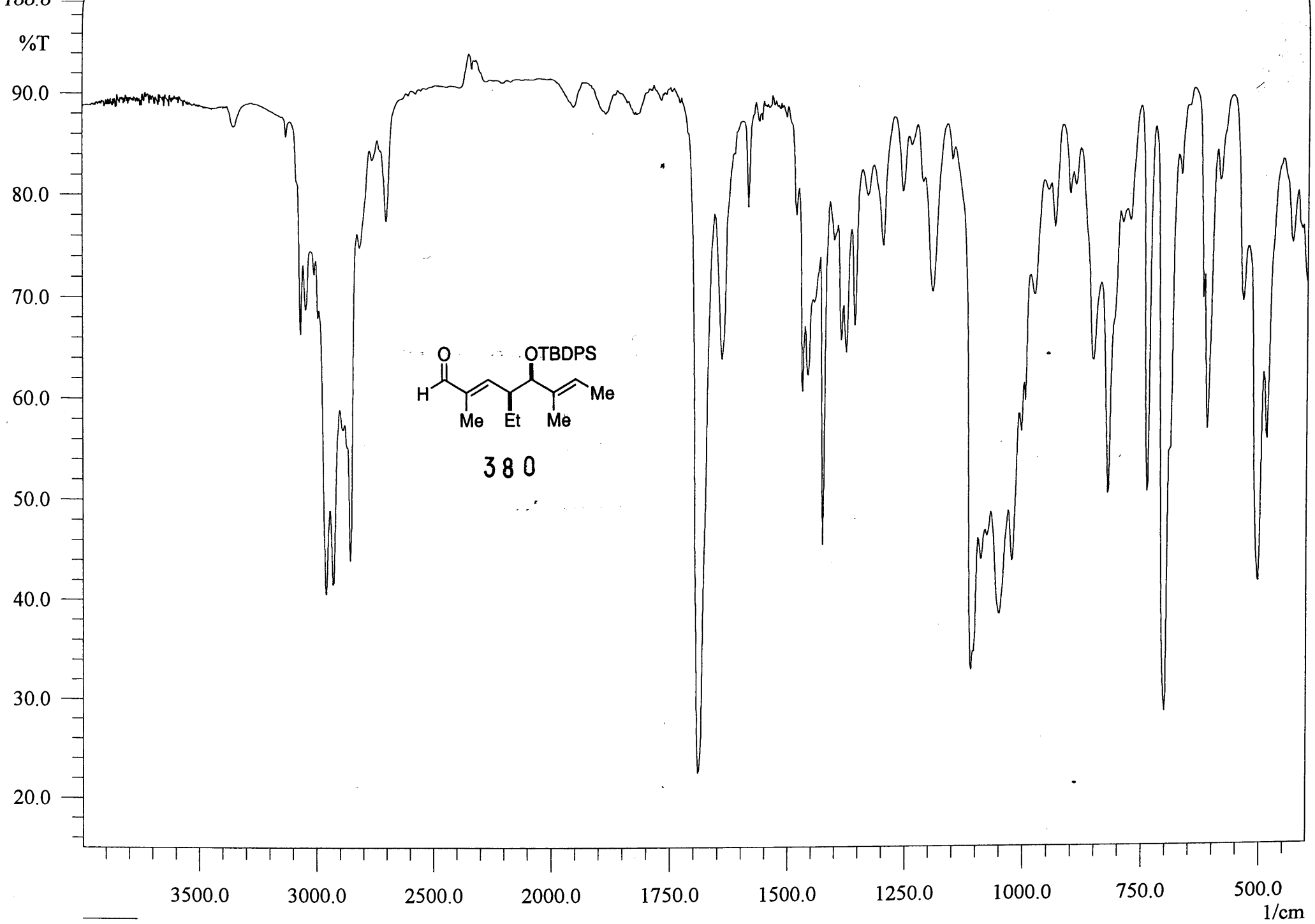
%T
90.0
80.0
70.0
60.0
50.0
40.0
30.0
20.0
O
H
OTBDPS
Me
Me
Et
Me
380
3500.0
3000.0
2500.0
2000.0
1750.0
1500.0
1250.0
1000.0
750.0
500.0
1/cm

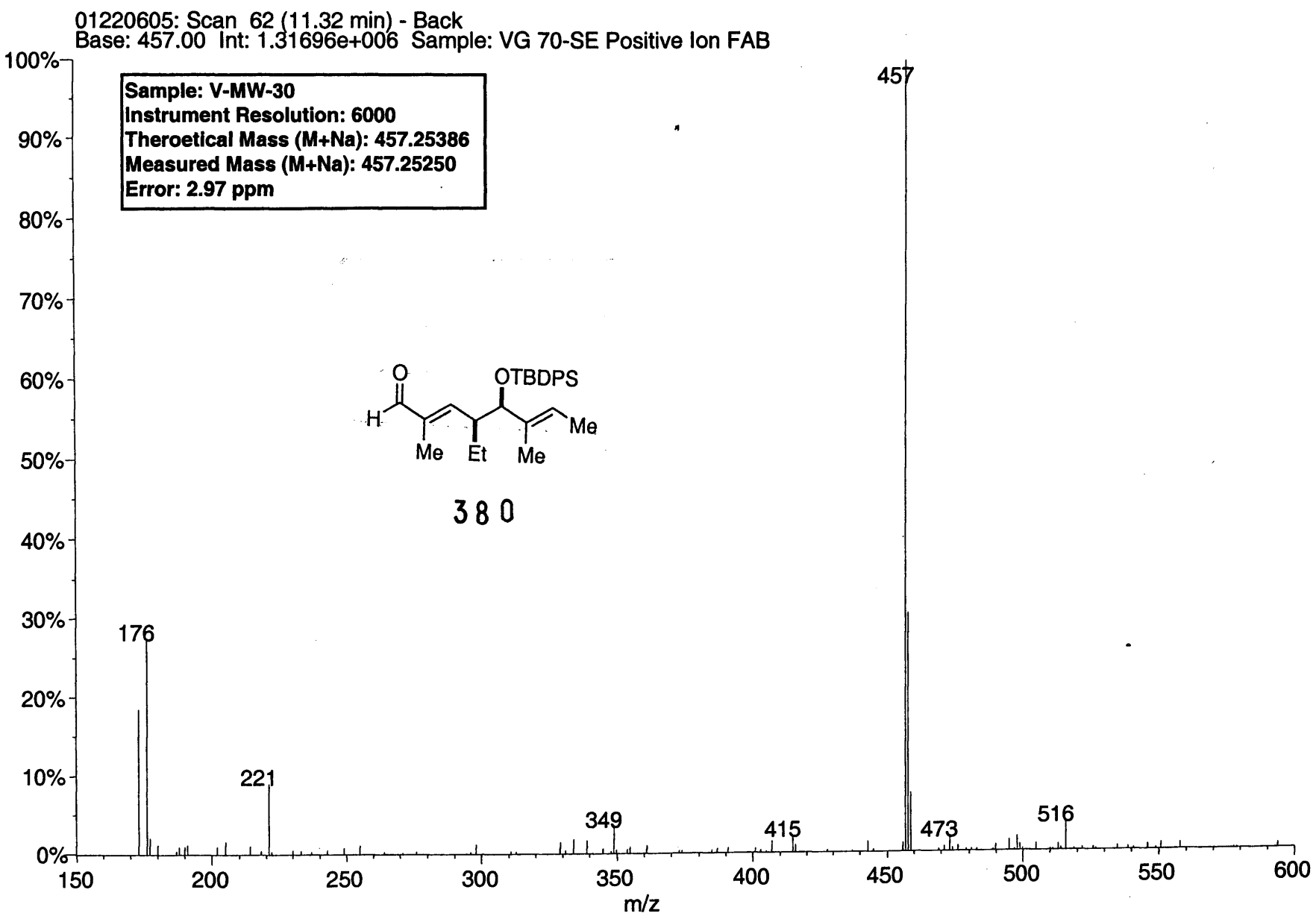
01220605: Scan 62 (11.32 min) - Back
Base: 457.00 Int: 1.31696e+006 Sample: VG 70-SE Positive Ion FAB
Sample: V-MW-30
Instrument Resolution: 6000
Theroetical Mass (M+Na): 457.25386
Measured Mass (M+Na): 457.25250
Error: 2.97 ppm
O
H
OTBDPS
Me
Me
Et
Me
380
457
176
221
349
415
473
516
100%
90%
80%
70%
60%
50%
40%
30%
20%
10%
0%
150
200
250
300
350
400
450
500
550
600
m/z

V-MW-40 ROUSH CRUDE
in CDCl3 at 298 K

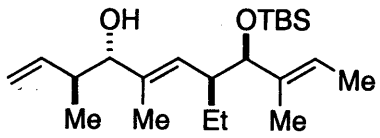

372

V-MW-40 ROUSH CRUDE (Partially Purified)
in CDCl3 at 298 K
(Expansion to show ratio)

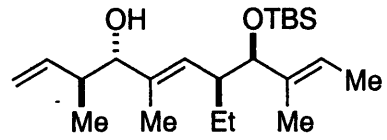

372

NMR shows that there is a 1:1 mixture
When attempting to oxidise to the sulfone
on the first attempt

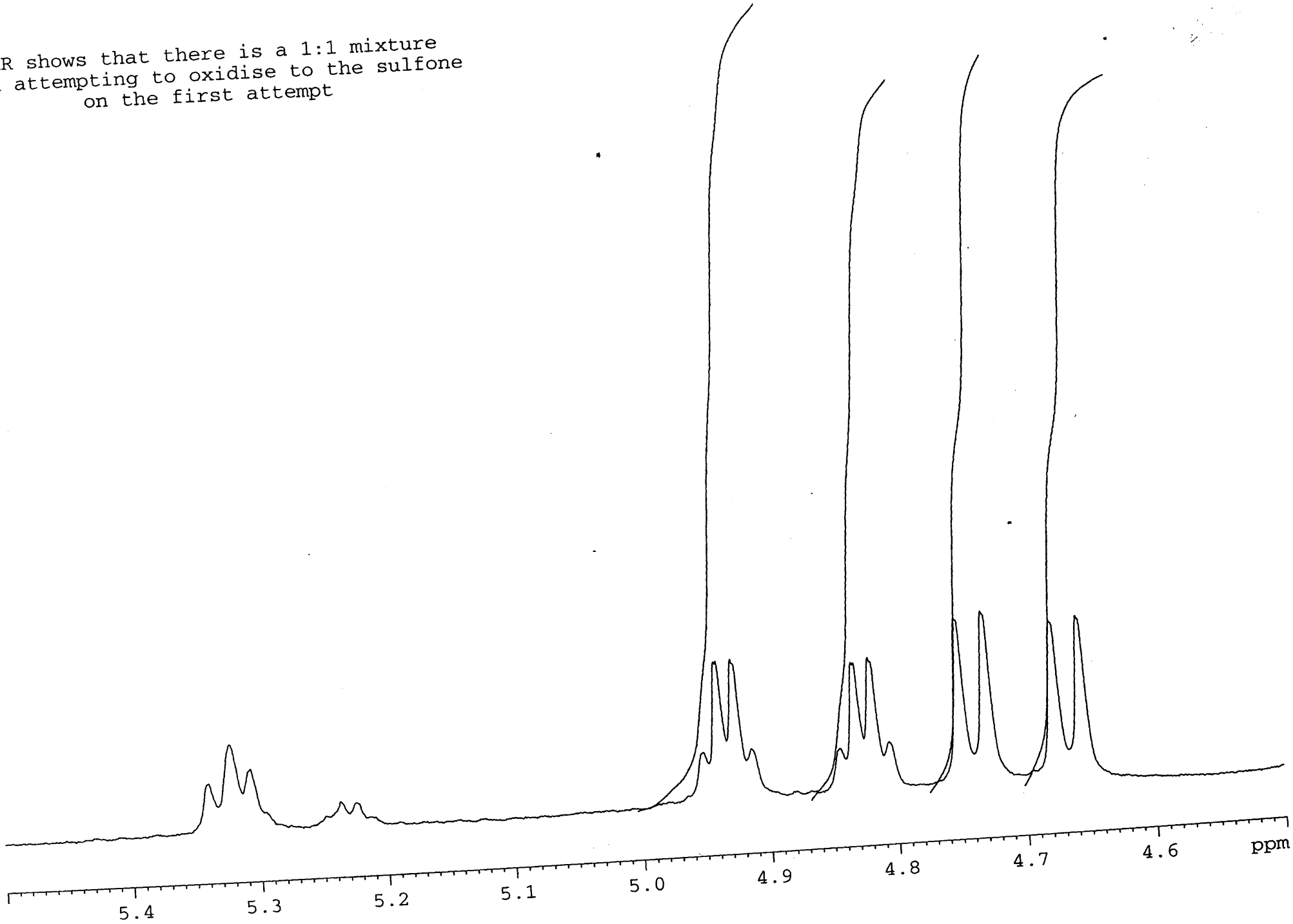

V-MW-69 in (After the second attempted oxidation-CRUDE)
CDCl3 at 298 K
Shows that the ratio has now become 2:1

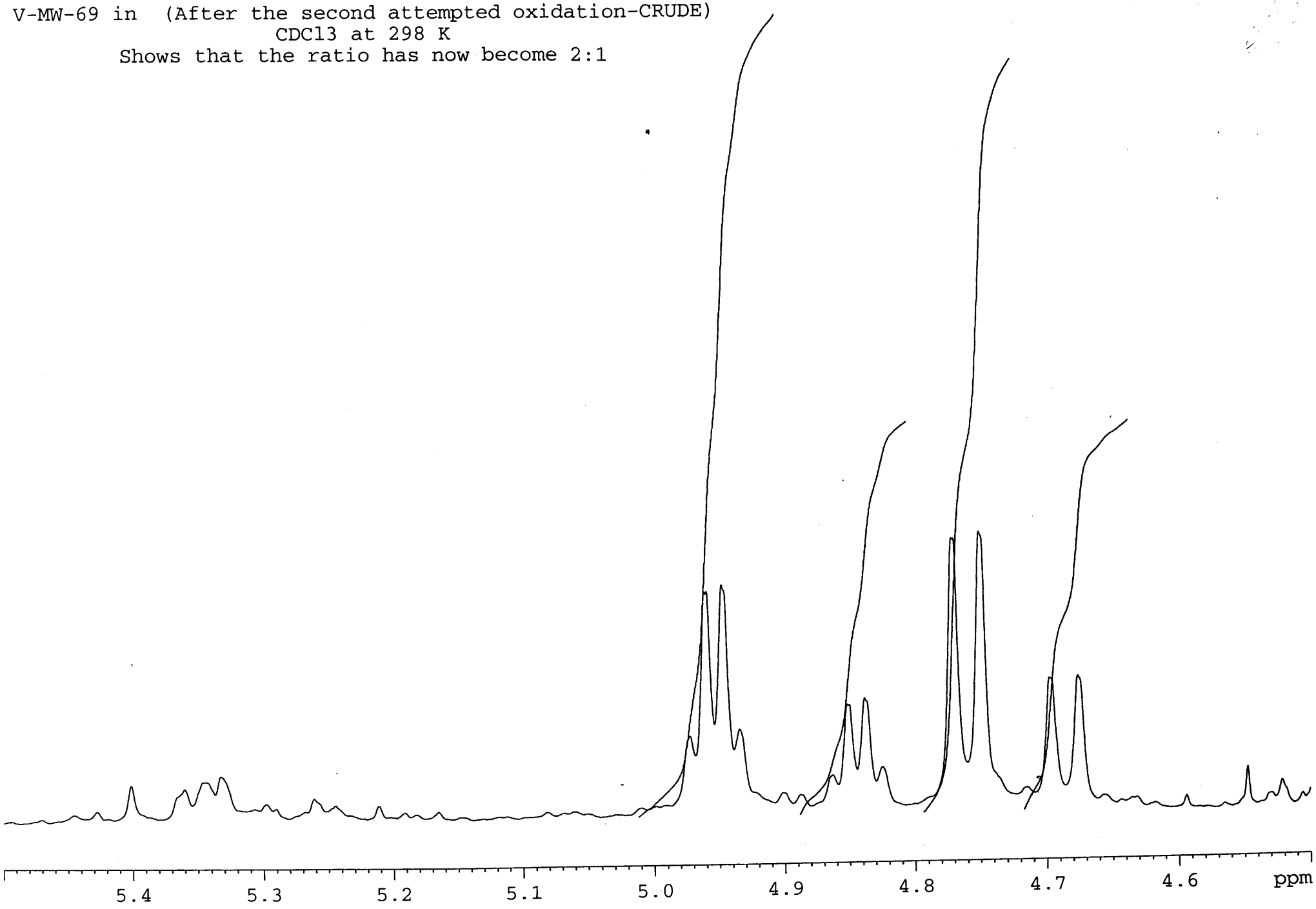

V-MW-39 in
CDCl3 at 298 K

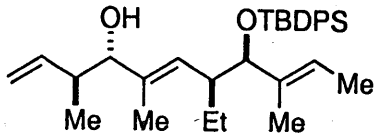

381

V-MW-39
Carbon 13 in
CDCl3 at 298 K

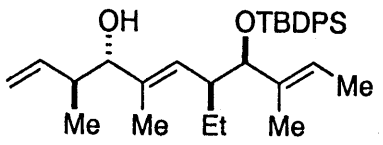

381

V-MW-39
DEPT in
CDCl3 at 298 K

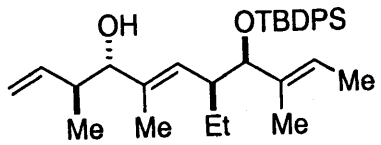

381

V-MW-39
COSY in
CDCl3 at 298 K

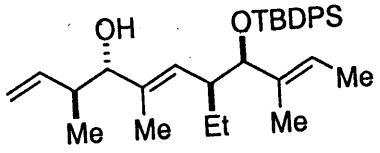

381

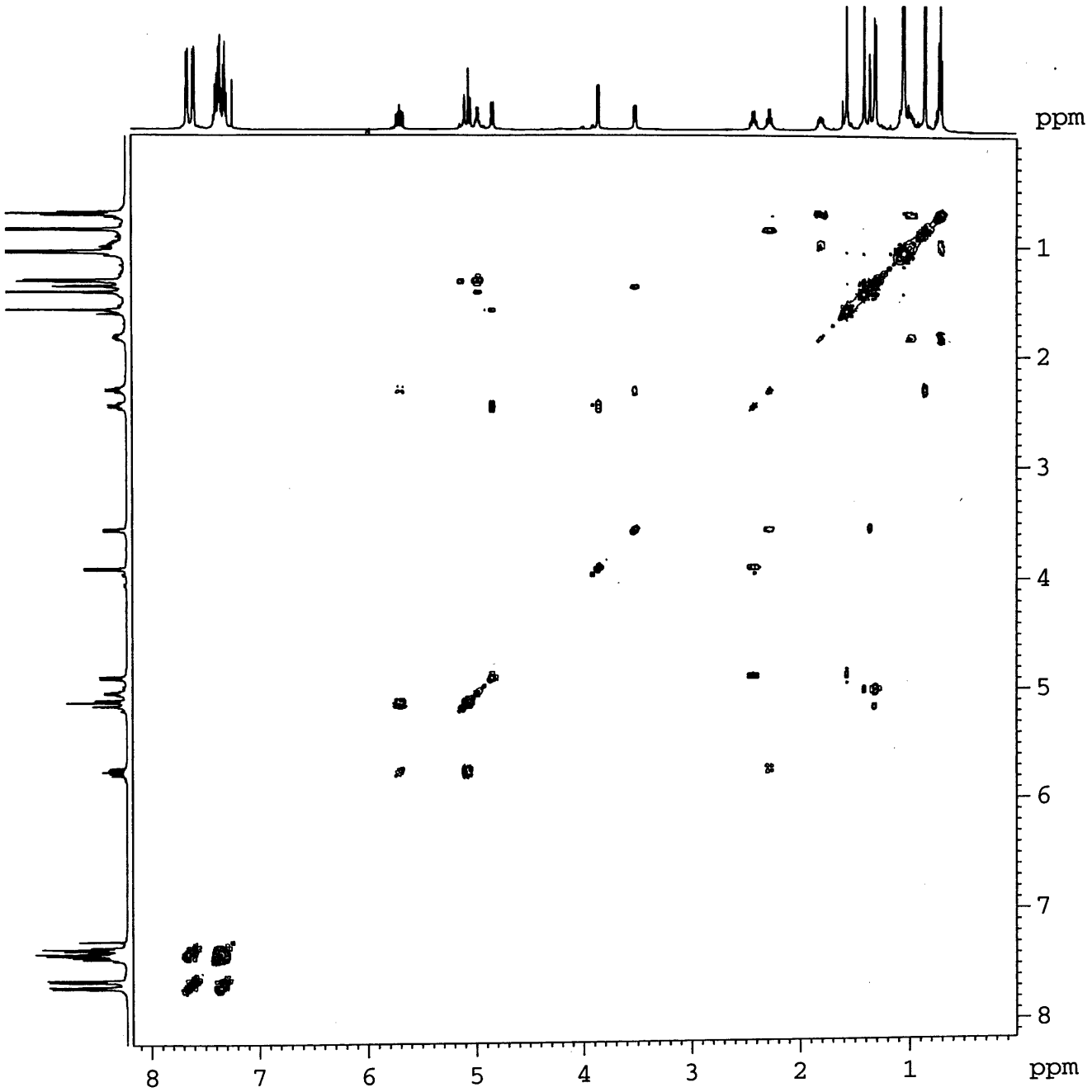

V-MW-39
HMQC in
CDCl3 at 298 K

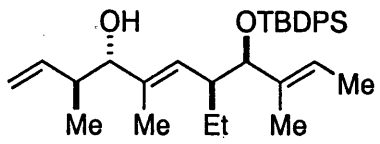

381

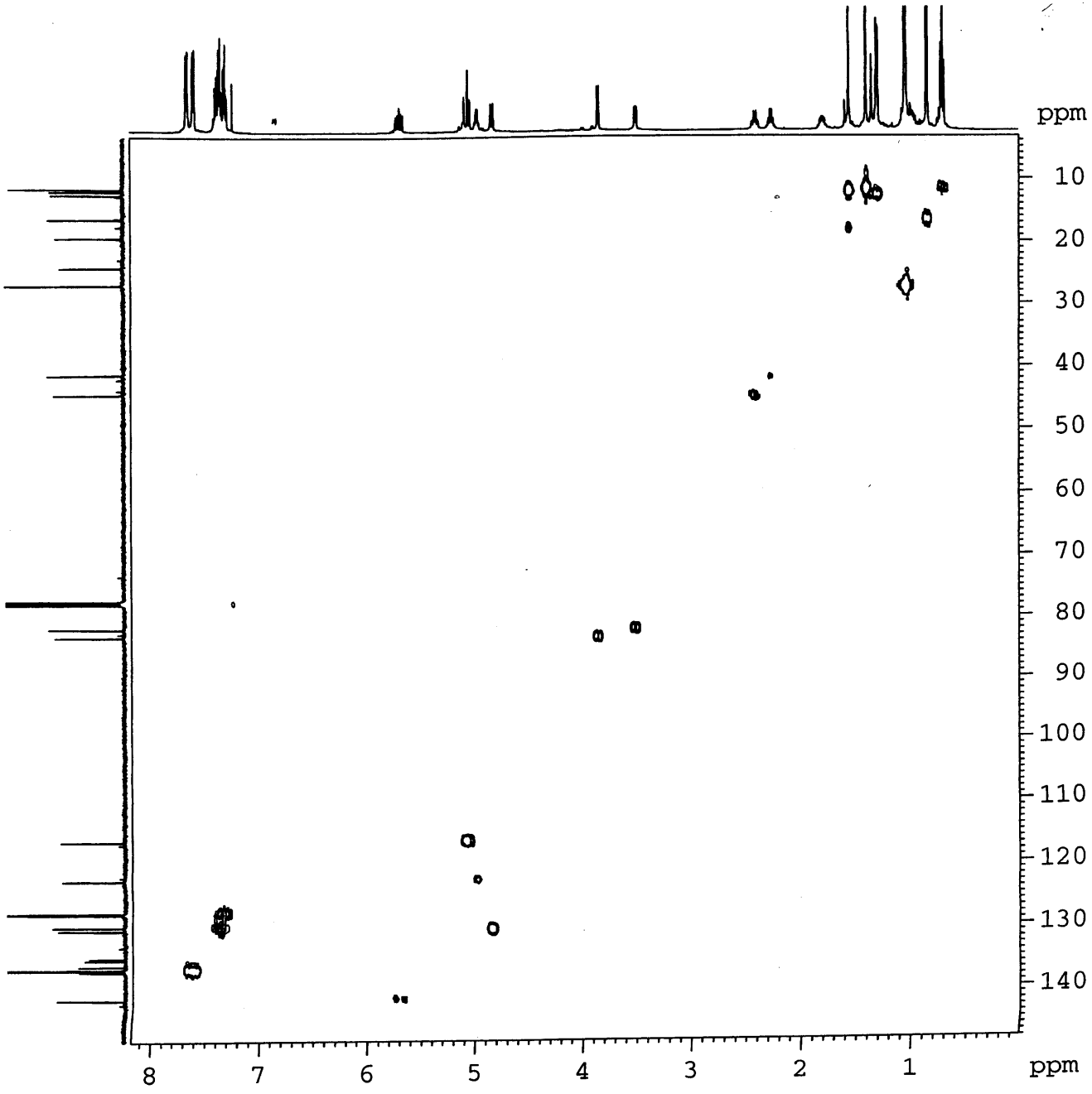

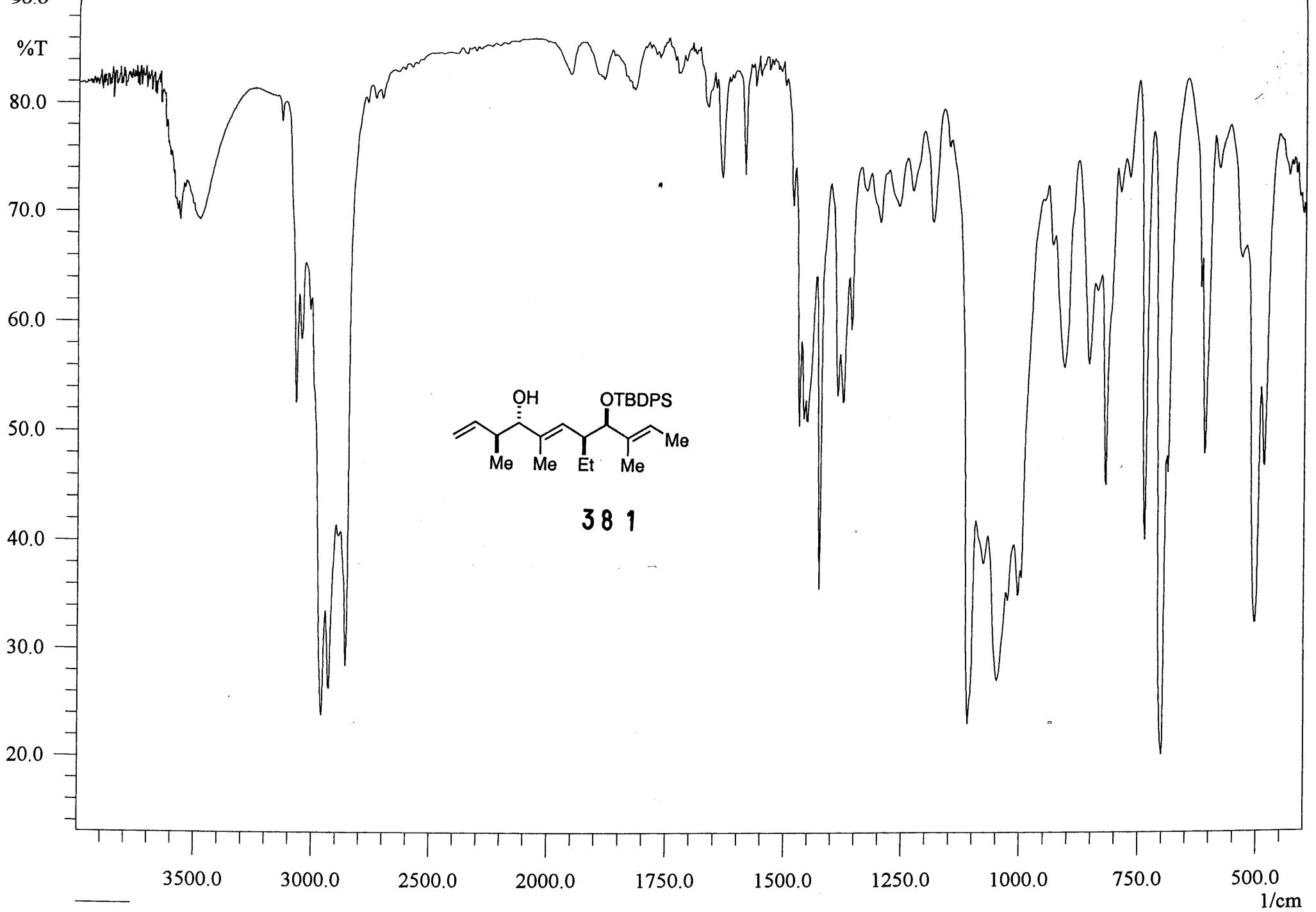
%T
80.0
70.0
60.0
50.0
40.0
30.0
20.0
OH
OTBDPS
Me
Me
Me
Et
Me
3500.0
3000.0
2500.0
2000.0
1750.0
1500.0
1250.0
1000.0
750.0
500.0
1/cm

381

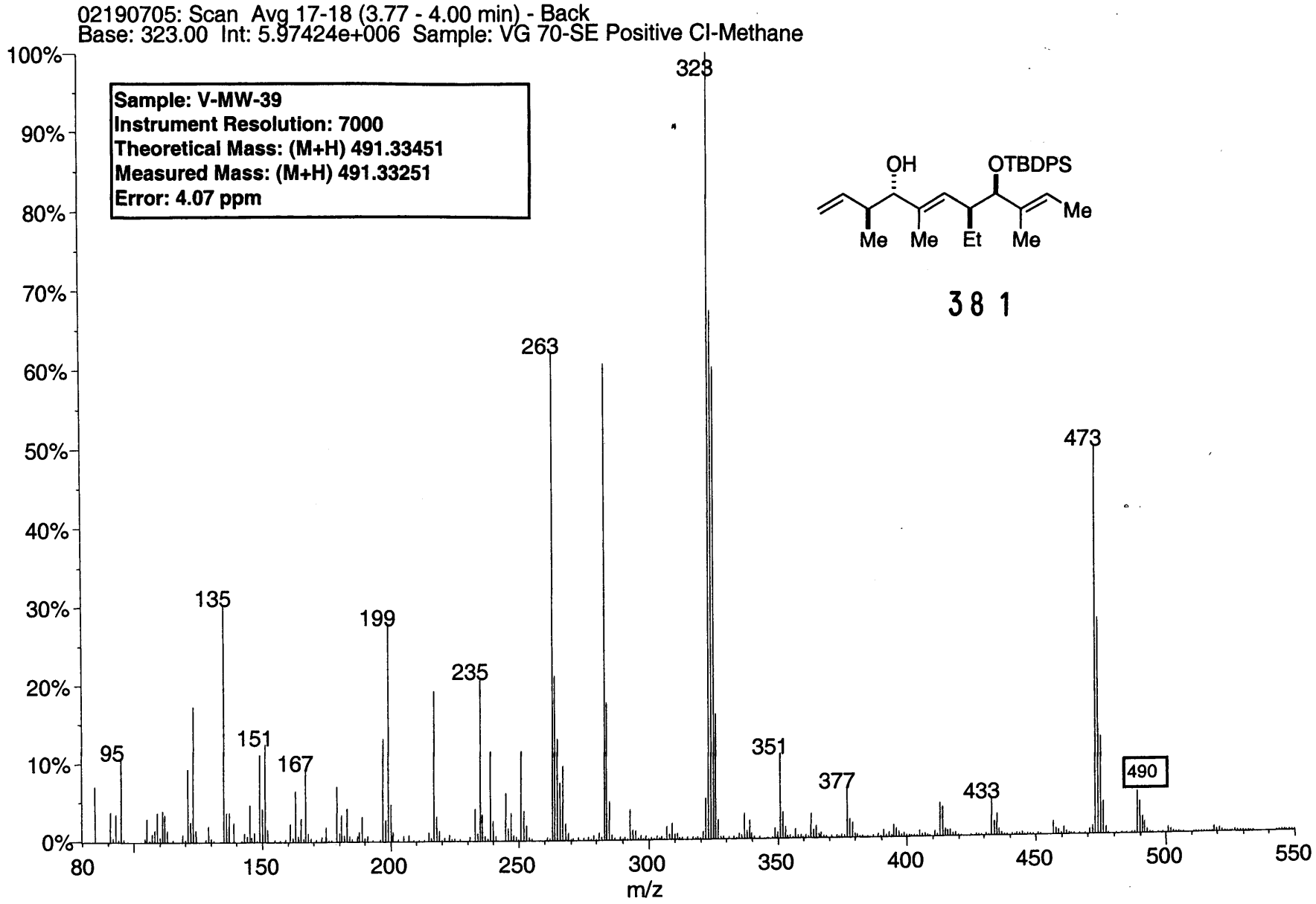
02190705: Scan Avg 17-18 (3.77 - 4.00 min) - Back
Base: 323.00 Int: 5.97424e+006 Sample: VG 70-SE Positive CI-Methane
Sample: V-MW-39
Instrument Resolution: 7000
Theoretical Mass: (M+H) 491.33451
Measured Mass: (M+H) 491.33251
Error: 4.07 ppm
OH
OTBDPS
Me
Me
Me
Et
Me
381
323
263
473
135
199
235
151
167
95
351
377
433
490
100%
90%
80%
70%
60%
50%
40%
30%
20%
10%
0%
80
150
200
250
300
350
400
450
500
550
m/z

IV-MW-186 in
CDCl3 at 298 K

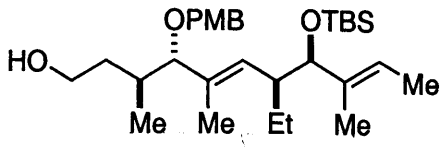

374

IV-MW-186
Carbon 13 in
CDCl3 at 298 K

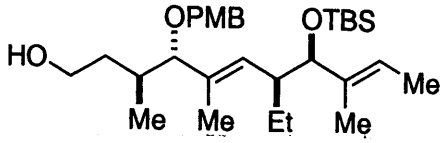

374

IV-MW-186
DEPT in
CDCl3 at 298 K

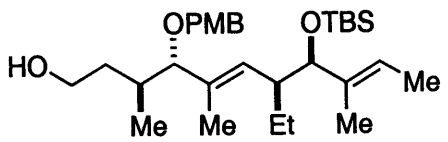

374

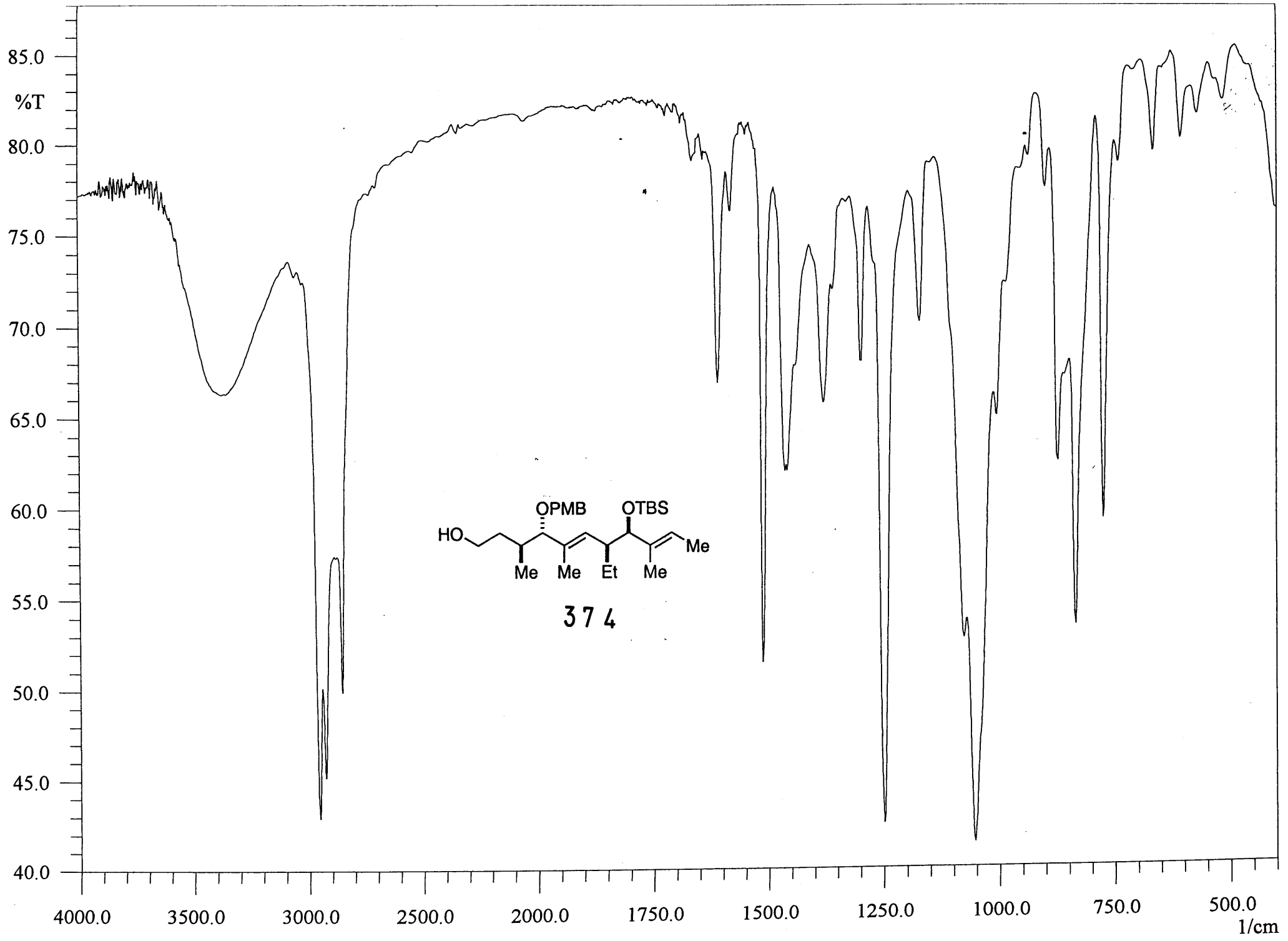
85.0
%T
80.0
75.0
70.0
65.0
60.0
55.0
50.0
45.0
40.0
4000.0
3500.0
3000.0
2500.0
2000.0
1750.0
1500.0
1250.0
1000.0
750.0
500.0
1/cm
OPMB
OTBS
HO
Me
Me
Me
Et
Me
Me

374

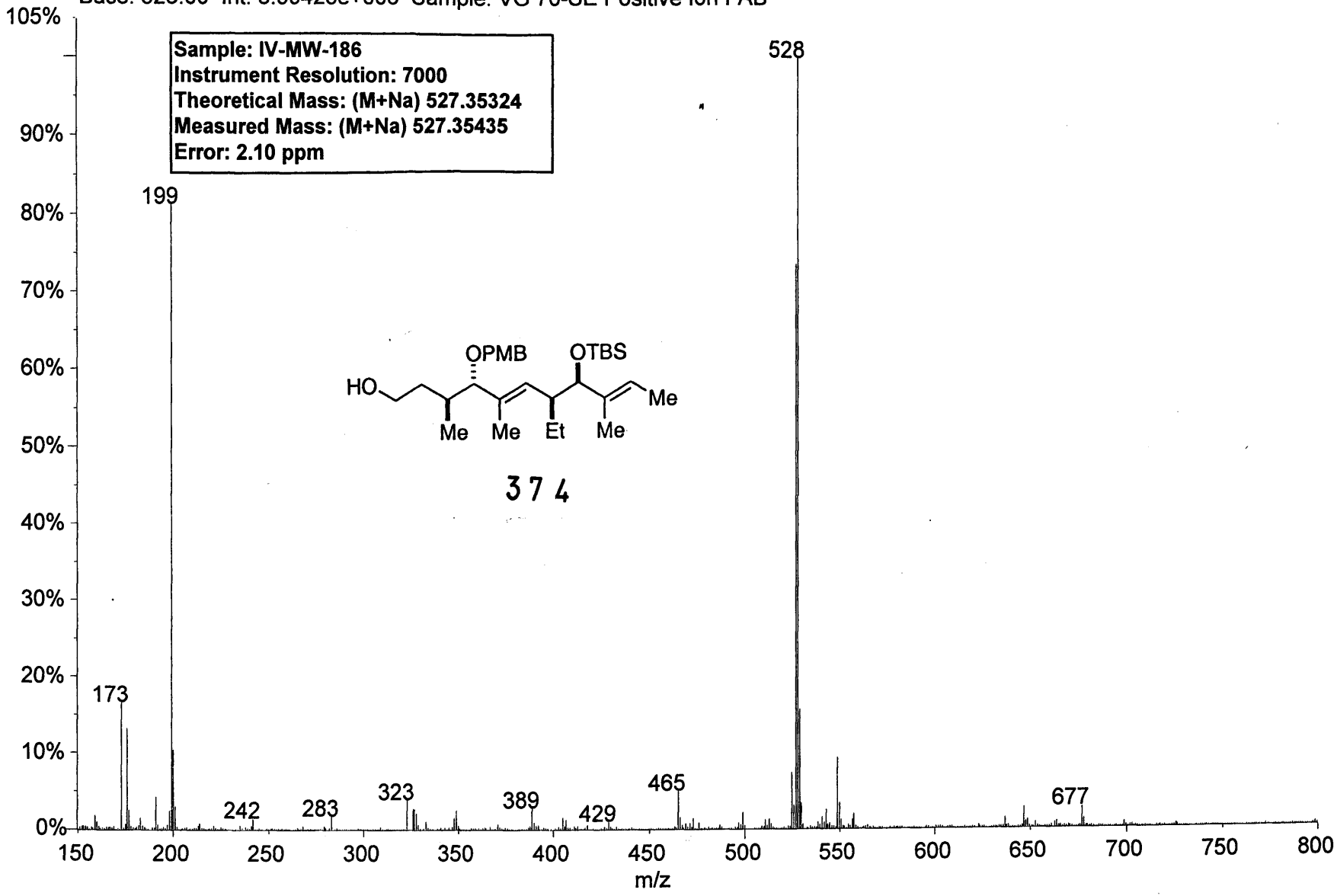
01020206: Scan Avg 9-10 (1.60 - 1.78 min) - Back
Base: 528.00 Int: 3.99423e+006 Sample: VG 70-SE Positive Ion FAB
Sample: IV-MW-186
Instrument Resolution: 7000
Theoretical Mass: (M+Na) 527.35324
Measured Mass: (M+Na) 527.35435
Error: 2.10 ppm
528
199
173
242
283
323
389
429
465
677
OPMB
OTBS
HO
Me
Me
Me
Et
Me
374
105%
90%
80%
70%
60%
50%
40%
30%
20%
10%
0%
150
200
250
300
350
400
450
500
550
600
650
700
750
800
m/z

IV-MW-190 in
CDCl3 at 298 K

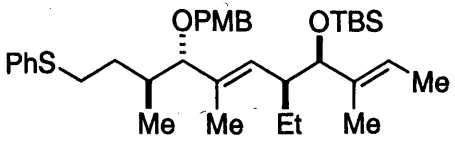

375

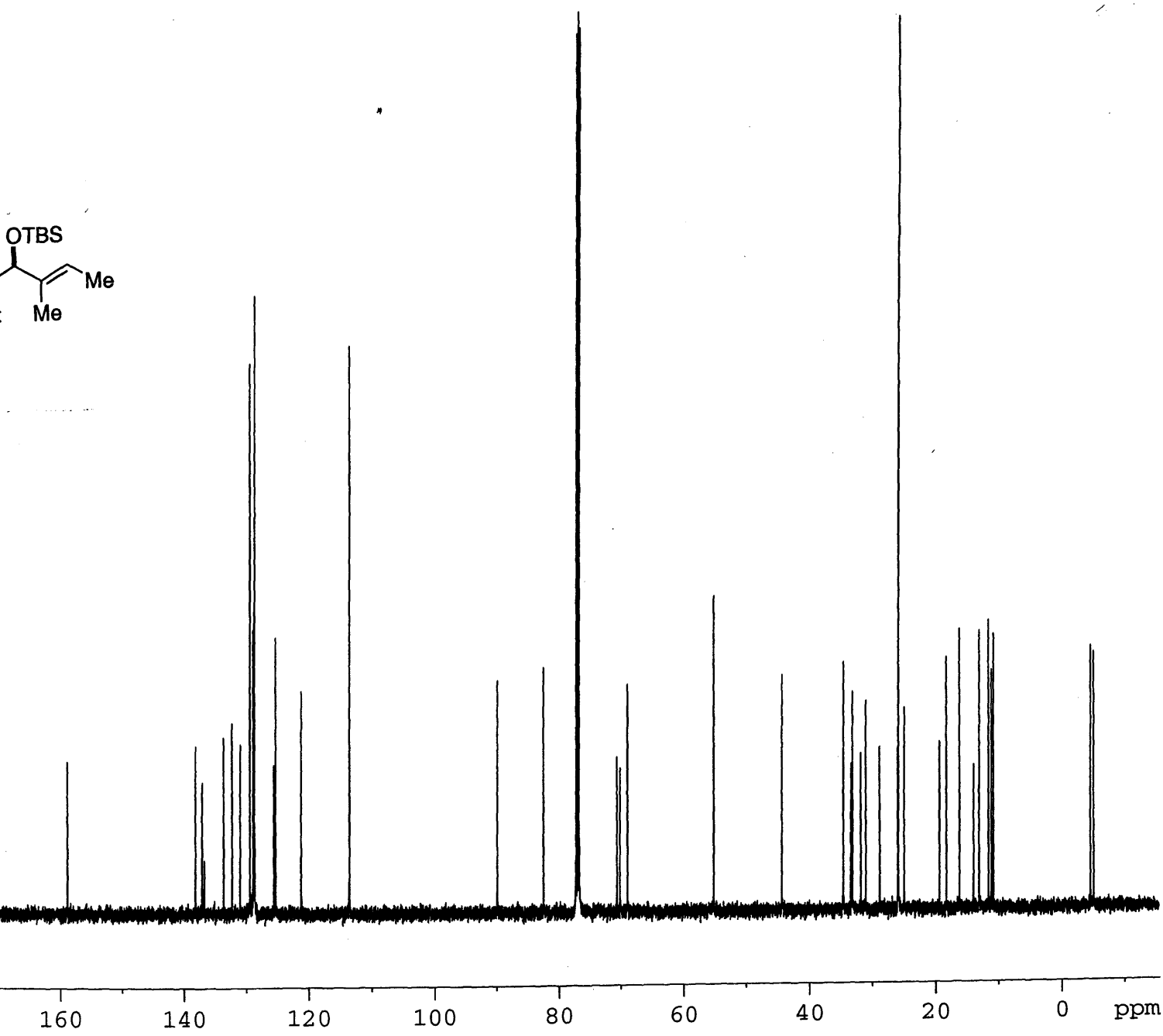
OTBS
Me
Me
160
140
120
100
80
60
40
20
0
ppm

IV-MW-190
DEPT in
CDCl3 at 298 K

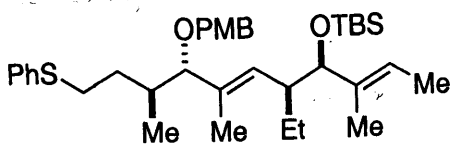

375

IV-MW-190
COSY in
CDCl3 at 298 K

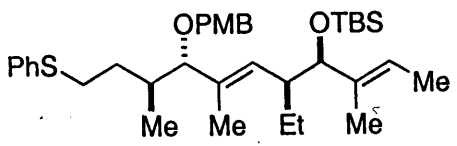

375

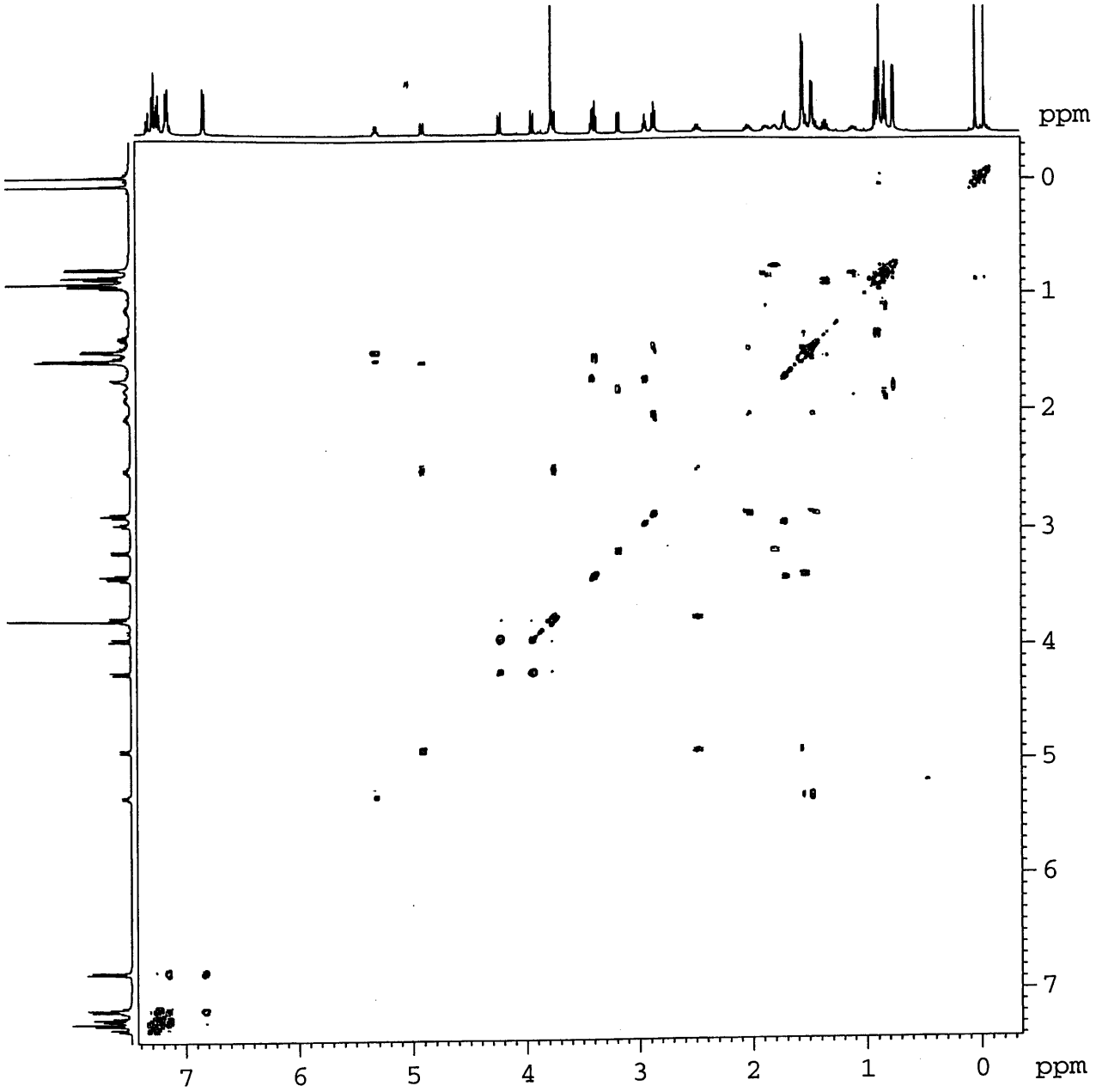

IV-MW-190
HMQC in
CDCl3 at 298 K

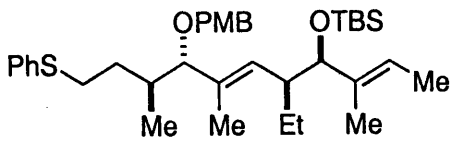

375

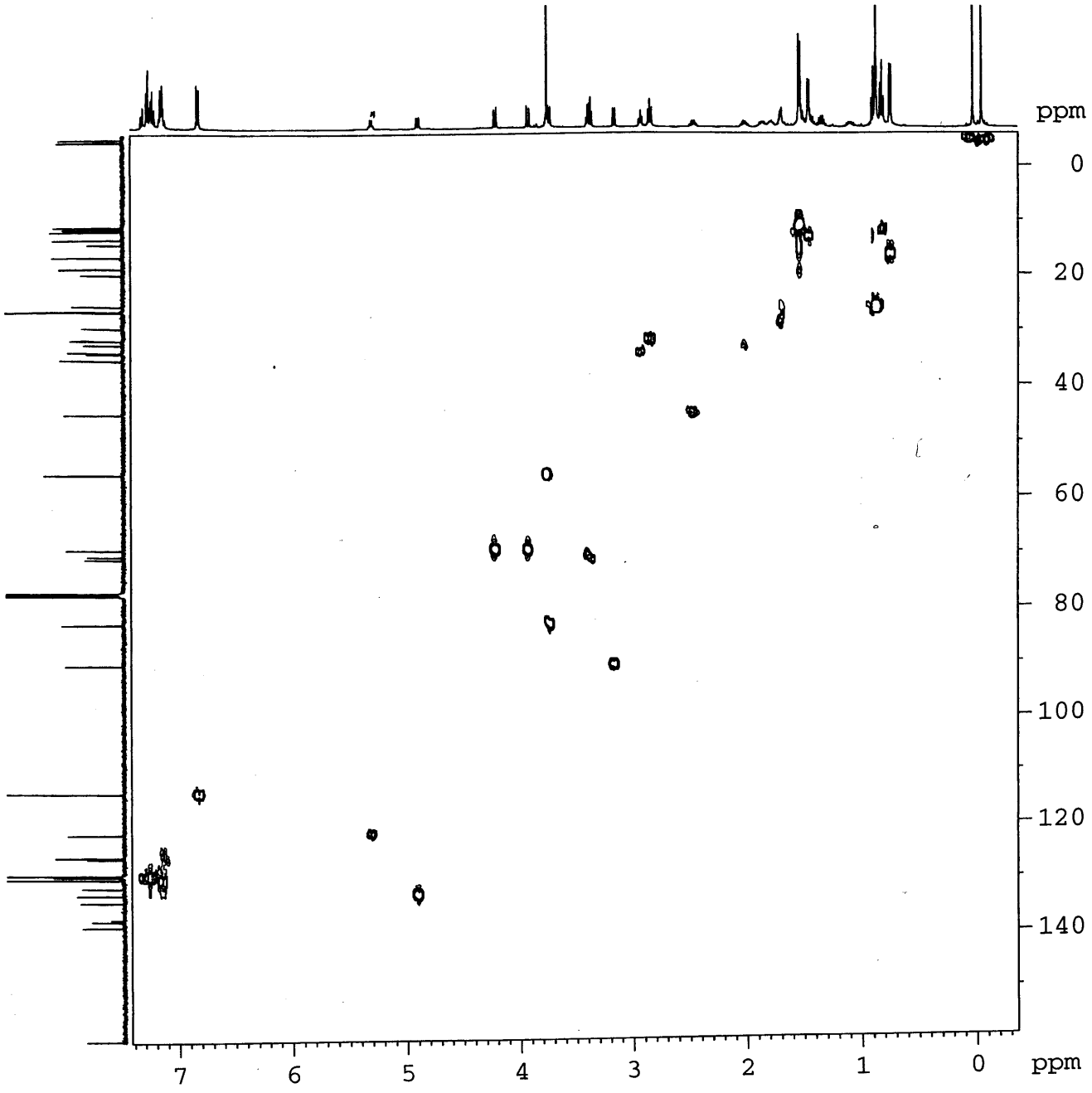

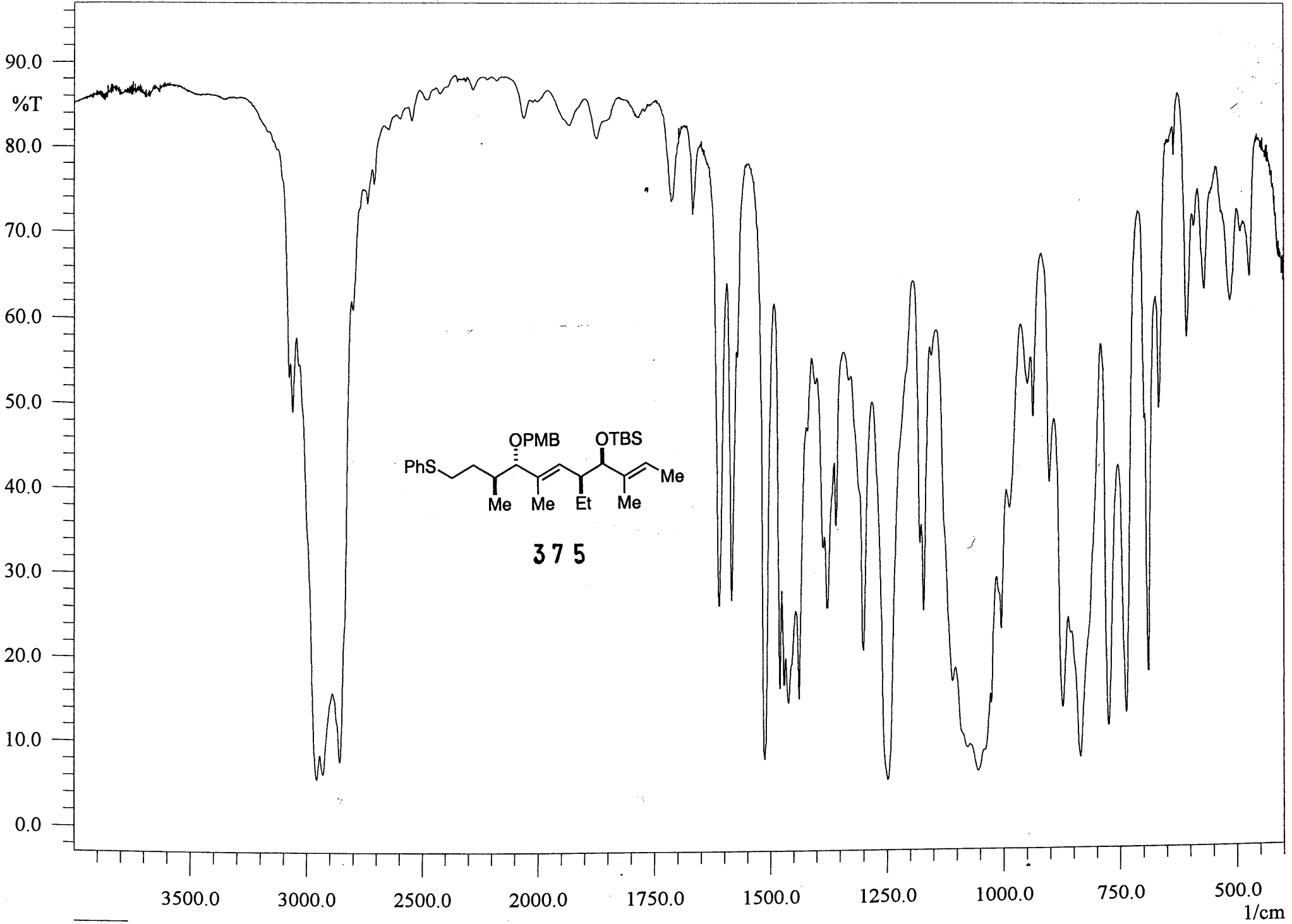
90.0
%T
80.0
70.0
60.0
50.0
40.0
30.0
20.0
10.0
0.0
3500.0
3000.0
2500.0
2000.0
1750.0
1500.0
1250.0
1000.0
750.0
500.0
1/cm
OPMB
OTBS
PhS
Me
Me
Et
Me
Me
375

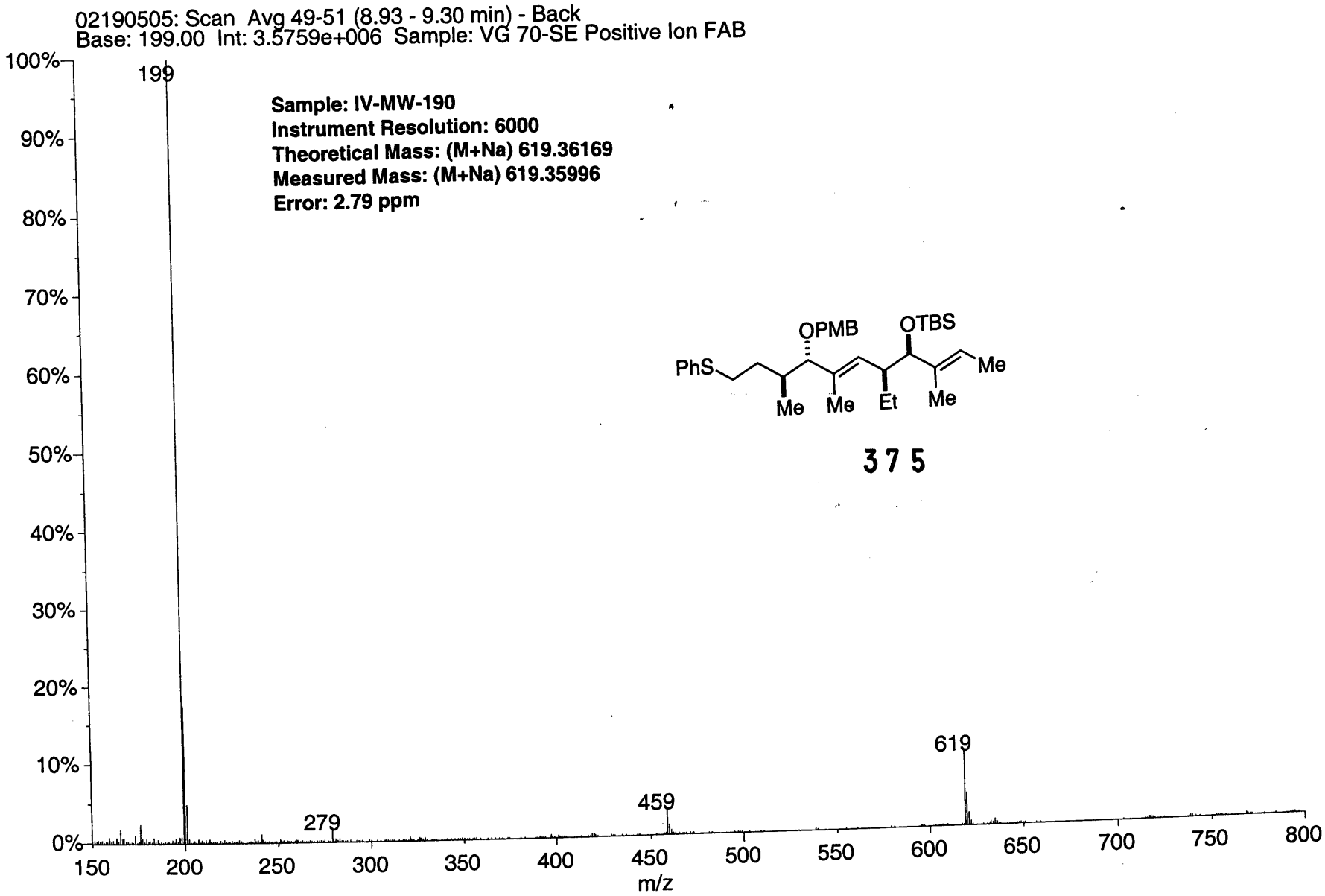
02190505: Scan Avg 49-51 (8.93 - 9.30 min) - Back
Base: 199.00 Int: 3.5759e+006 Sample: VG 70-SE Positive Ion FAB
Sample: IV-MW-190
Instrument Resolution: 6000
Theoretical Mass: (M+Na) 619.36169
Measured Mass: (M+Na) 619.35996
Error: 2.79 ppm
OPMB
OTBS
PhS
Me
Me
Me
Et
Me
Me
375
199
279
459
619
100%
90%
80%
70%
60%
50%
40%
30%
20%
10%
0%
150
200
250
300
350
400
450
500
550
600
650
700
750
800
m/z